

INFORMATION TO USERS

This manuscript has been reproduced from the microfilm master. UMI films the text directly from the original or copy submitted. Thus, some thesis and dissertation copies are in typewriter face, while others may be from any type of computer printer.

The quality of this reproduction is dependent upon the quality of the copy submitted. Broken or indistinct print, colored or poor quality illustrations and photographs, print bleedthrough, substandard margins, and improper alignment can adversely affect reproduction.

In the unlikely event that the author did not send UMI a complete manuscript and there are missing pages, these will be noted. Also, if unauthorized copyright material had to be removed, a note will indicate the deletion.

Oversize materials (e.g., maps, drawings, charts) are reproduced by sectioning the original, beginning at the upper left-hand corner and continuing from left to right in equal sections with small overlaps. Each original is also photographed in one exposure and is included in reduced form at the back of the book.

Photographs included in the original manuscript have been reproduced xerographically in this copy. Higher quality 6" x 9" black and white photographic prints are available for any photographs or illustrations appearing in this copy for an additional charge. Contact UMI directly to order.

UMI

A Bell & Howell Information Company
300 North Zeeb Road, Ann Arbor, MI 48106-1346 USA
313/761-4700 800/521-0600

Order Number 1360019

**Structural evolution of the offshore forearc basins of Peru,
including the Salaverry, Trujillo, Lima, West Pisco and East
Pisco basins**

Azalgara, Carlos, M.A.

Rice University, 1994

U·M·I
300 N. Zeeb Rd.
Ann Arbor, MI 48106

RICE UNIVERSITY

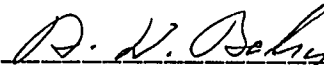
STRUCTURAL EVOLUTION OF THE OFFSHORE FOREARC BASINS OF PERU,
INCLUDING THE SALAVERRY, TRUJILLO, LIMA, WEST PISCO AND EAST
PISCO BASINS

By

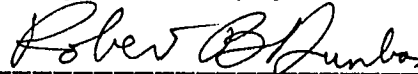
Carlos Azalgará

A THESIS SUBMITTED
IN PARTIAL FULFILLMENT OF THE
REQUIREMENTS FOR THE DEGREE
MASTER OF ARTS

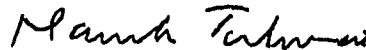
APPROVED, THESIS COMMITTEE



Albert W. Bally, Director
Geology and Geophysics



Robert B. Dunbar, Professor
Geology and Geophysics



Manik Talwani, Professor
Geology and Geophysics

Houston, Texas

August, 1993

ABSTRACT

STRUCTURAL EVOLUTION OF THE OFFSHORE FOREARC BASINS OF PERU, INCLUDING THE SALAVERRY, TRUJILLO, LIMA, WEST PISCO AND EAST PISCO BASINS

by

Carlos Azalgara

The basins of the study area were filled with the following sequences: E₀ (lower? to middle Eocene); E₁, E₂ and E₃ (fill middle Eocene half grabens); E-O (uppermost middle Eocene-Oligocene); M₁, M₂ and M₃ (lower-upper Miocene); P (uppermost Miocene-Pliocene); and, Q (Quaternary). Four compressive events occurred during Paleocene?, middle Eocene?, upper-middle to late Miocene and middle Pliocene?; and two extensional episodes took place during middle Eocene and late Pliocene. Pre-Tertiary substratum was involved in all tectonic events. The Salaverry-Trujillo High which formed during the third compressive event and the Pliocene consists of a trench-parallel open flexure and a belt of middle Eocene to upper Miocene inverted wedges. The continuous uplifting of the Salaverry-Trujillo High produced a sustained shallowing of the sea floor at the slope break zone on the western side of the high and the incision of submarine canyons.

ACKNOWLEDGEMENTS

I thank Petroperu for their permission to publish seismic and well data. I also thank Amoco Corp. for allowing me to publish Mrs. N. L. Engelhardt-Moore's paleoenvironmental study of the Ballena and Delfin wells and Professor Hisatake Okada of Yamagata University who generously provided the biostratigraphy of the Ballena and Delfin wells. His information was fundamental for the development of this study.

I want to express my gratitude to my classmates Felipe, Pete, Erika, Pablo, Gorgonio, Norio, Guillermo, Fernando, Carrie, Shengyu and Mahmoud for sharing their knowledge with me.

I am in debt to Professor Robyn Wright Dunbar, Amy Leventer and David Mucciarone for the friendly support they provided to my family and me.

Very special thanks to my good friends Antenor Aleman and Marian Allen, who were always willing to assist me and my family. Percy Alvarez, Elmer Ferro, Joan Flinch and Gabor Tari taught me the best lessons about friendship and solidarity during the time I spent far from my family, for which I will be always in debt to them.

I am grateful to Professors Hans Avé and John Oldow for their encouragement and lessons in structural geology and to Professor Peter Vail for his masterly lessons in sequence stratigraphy.

I thank Dr. Manik Talwani for his fruitful observations of this study.

I am very grateful to Professor Robert Dunbar for his encouragement, optimism, and economic support, and for his acute observations of this study and his generous effort to ease my family's life in Houston.

I had the privilege to work with Professor Albert Bally and to receive the benefit of his teachings in geology and ethics and his generous economic support. Without his patience, generosity and understanding this study would have not been completed. I always will be grateful to him.

Finally and most of all I thank my wife Ines and my children Carito and little Martin for their patience and love.

TABLE OF CONTENTS

	Page
Abstract.....	i i
Acknowledgments.....	i i i
Table of Contents.....	v
CHAPTER 1	
INTRODUCTION.....	1
1.1 Study area.....	6
1.2 Morphostructure of Peru.....	6
1.3 Previous work in the study area.....	9
1.4 Basic information.....	17
1.5 Purpose.....	19
1.6 Study method.....	19
1.7 Pre-Jurassic geologic framework.....	22
CHAPTER 2	
THE MESOZOIC-CENOZOIC ANDES OF PERU.....	25
2.1 Introduction.....	25
2.2 Early to middle Jurassic.....	26
2.3 Kimmeridgian to Paleocene.....	28
2.4 Eocene to Holocene.....	40

Page

2.5	Plutonism.....	44
2.6	Tertiary Volcanism.....	45

CHAPTER 3

	STUDY AREA STRATIGRAPHY.....	49
3.1	Introduction.....	49
3.2	Pre-Cenozoic Basement.....	52
3.21	The late Cretaceous (Sequence K).....	57
3.3	The Cenozoic.....	62
3.31	Paleocene.....	62
3.32	Eocene-Oligocene (Sequences E ₀ , E ₁ , E ₂ , E ₃ and E-O and the post-lower to middle Eocene igneous intrusive event).....	63
3.321	The lower? to middle Eocene E ₀ sequence.....	64
3.322	The post-lower to middle Eocene igneous intrusion.....	66
3.323	The syn-rift middle Eocene E ₁ , E ₂ and E ₃ sequences.....	67
3.324	The middle/upper Eocene to Oligocene E-O sequence.....	73

3.325 The Eocene-Oligocene in the Progreso, Talara and onshore Sechura and East Pisco Basins.....	75
3.33 Early-middle Miocene (M1 and M2 sequences).....	77
3.331 Early-middle Miocene in the Progreso, Talara and onshore Sechura and East Pisco Basins.....	83
3.34 Late Miocene-Pliocene (M3 and P sequences).....	85
3.341 The late Miocene-Pliocene in the Progreso, Talara and onshore Sechura and East Pisco Basins.....	92
3.35 Quaternary (Q sequence).....	93

CHAPTER 4

STRUCTURAL GEOLOGY.....	95
4.1 Introduction.....	95
4.2 The first pre-Eocene compressive event.....	96
4.3 The pre-Eocene uplift and peneplanation.....	96
4.4 The middle Eocene rifting event.....	96
4.41 Rifting phase 1.....	97
4.42 Rifting phase 2.....	98
4.43 The second middle Eocene? compressive event..	98
4.44 Rifting phase 3.....	99

4.5	The hypothetical strike-slip system.....	101
4.6	The middle Miocene syn-sedimentary extension.....	101
4.7	The third upper-middle to late Miocene compressive event.....	102
4.8	The Salaverry-Trujillo High.....	102
4.9	The upper-middle to late Miocene southern uplift and peneplanation.....	104
4.10	The fourth late? Pliocene compressive event.....	105
4.11	Latest Pliocene extension.....	107
4.12	The incision and fill of submarine canyons during middle Miocene to Pliocene.....	107
4.13	The gravitational extension at the slope.....	109
4.14	Deformation in the southern coast.....	109

CHAPTER 5

	PLATE KINEMATICS AND FOREARC EVOLUTION.....	111
5.1	The trench and the middle to lower slope zone.....	111
5.2	Current state of stress in the margin.....	115
5.3	The Cenozoic evolution of the Peruvian margin.....	116
5.31	Relationship between variations in the rate of convergence and tectonism.....	117

5.32 Relationship between variations in the direction of convergence and tectonism.....	119
5.33 Variations in the angle of subduction.....	120
5.34 Implications of this study in the evolution of the Peruvian margin.....	128
 CONCLUSIONS.....	 131
 BIBLIOGRAPHY.....	 138
 APPENDICES.....	 164
Appendix A: Nannofossils biostratigraphy of the Ballena 1X and Delfin 1X wells.....	164
Appendix B: Paleoenvironmental analyses of the Delfin 1X and Ballena 1X wells.....	168

LIST OF FIGURES, TABLES, PLATES AND PANELS

FIGURES	page
1.1 Location of the study area.....	2
1.2 Morphological zones of Peru.....	3
1.3 SW-NE regional transect at 12° S latitude.....	4
1.4 Forearc basins of Peru.....	5
1.5 Major continental shelf and upper slope basins, and the onshore-offshore structures that control their distribution.....	8
1.6 Seismic and well data.....	11
1.7 Location of seismic profile line drawings panels.....	21
 2.1 Main tectonic elements of the Peruvian Andes.....	 27
2.2 Relationship of tectonic events, magmatic pulses, and plate geodynamics in the Peruvian margin between Kimmeridgian and Paleocene times.....	29
2.3 Chronology of compressional events F1 through F6 observed in the Central Andes since late Eocene time.....	41
2.4 Miocene and Pliocene magmatic activity.....	46
2.5 Latest Pliocene and Quaternary magmatic activity.....	48
 3.1 Linear trends and forearc basins of Peru.....	 50
3.2 Zones of the study area.....	51

3.3	Correlation of Ballena well with seismic profile 3 (Panel 1).....	53
3.4	Correlation of Delfin well with seismic profile 3 (Panel 1).....	54
3.5	Geologic map of the onshore East Pisco Basin.....	56
3.6	Ballena well stratigraphic column.....	58
3.7	Delfin well stratigraphic column.....	59
3.8	Distribution of the upper Cretaceous K sequence	61
3.9	Distribution of the lower? to middle Eocene E ₀ sequence and the post-lower to middle Eocene igneous intrusives.....	65
3.10	Distribution of the middle Eocene E ₁ sequence.....	68
3.11	Distribution of the middle Eocene E ₂ sequence.....	69
3.12	Distribution of the middle Eocene E ₃ sequence	70
3.13	Distribution of the lower to middle Miocene M ₂ sequence...	79
3.14	Normal fault system developed during the lower-middle Miocene M ₂ sequence deposition.....	81
3.15	Distribution of the upper Miocene M ₃ sequence.....	86
3.16	Distribution of the uppermost Miocene-Pliocene P sequence.....	90

4.1	Middle Eocene? second compressional event.....	100
4.2	Upper middle to late Miocene third compressional event.....	103
4.3	Late? Pliocene fourth compressional event.....	106
5.1	Tectonic events and convergence rate.....	118
5.2	Hypothetical strike-slip fault system developed during the middle Eocene rifting process.....	121
5.3	Reconstructed geometry and position of the Nazca Ridge during the past 20 million years.....	125
5.4	Reconstructed geometry and position of the Nazca Ridge during the past 9 million years.....	126
TABLE 1: Drill holes in the study area.....		18

PLATES

1. Schematic chronostratigraphic cross section Onshore Sechura Basin-Trujillo Basin-Lima Basin-West Pisco Basin-Onshore East Pisco Basin.
2. Schematic chronostratigraphic cross section Lower Slope Zone-Trujillo Basin.

3. Schematic chronostratigraphic cross section Lower Slope Zone-Lima Basin-Salaverry Basin.
4. Close-up of the seismic profile line drawing 1 (Panel 1), Trujillo Basin.
5. Close-up of the seismic profile line drawing B (Panel 2), Trujillo Basin.
6. Close-up of the seismic profile line drawing 2 (Panel 1), Salaverry Basin.
7. Close-up of the seismic profile line drawing C (Panel 2), Trujillo Basin.
8. Close-up of the seismic profile line drawing 3 (Panel 1), Trujillo-Salaverry Basins.
9. Close-up of the seismic profile line drawing B (Panel 2), Trujillo Basin.
10. Close-up of the seismic profile line drawing 3 (Panel 1), Salaverry Basin.
11. Close-up of the seismic profile line drawing D (Panel 2), Salaverry Basin.
12. Close-up of the seismic profile line drawing 4 (Panel 1), Upper Slope Zone.
13. Close-up of the seismic profile line drawing 4 (Panel 1), Trujillo Basin.
14. Close-up of the seismic profile line drawing 3 (Panel 3), Lima Basin.

15. Close-up of the seismic profile 6, adjacent to the seismic profiles 3 and 4 (Panel 3), Salaverry Basin.
16. Close-up of the seismic profile line drawing B (Panel 6), West Pisco Basin.
17. Close-up of the seismic profile line drawing 1 (Panel 5), West Pisco Basin.
18. Close-up of the seismic profile line drawing 4 (Panel 5), East Pisco Basin.

PANELS

1. Line drawing of seismic profiles, Forearc region offshore Peru, north-central part of the study area, dip lines.
2. Line drawing of seismic profiles, Forearc region offshore Peru, north-central part of the study area, strike lines.
3. Line drawing of seismic profiles, Forearc region offshore Peru, south-central part of the study area, dip lines.
4. Line drawing of seismic profiles, Forearc region offshore Peru, south-central part of the study area, strike lines.
5. Line drawing of seismic profiles, Forearc region offshore Peru, southern part of the study area, dip lines.
6. Line drawing of seismic profiles, Forearc region offshore Peru, southern part of the study area, strike lines.
7. Accretionary zone-slope zone located west of the Trujillo and Lima Basins, forearc region offshore Peru.

CHAPTER 1: INTRODUCTION

The Peruvian margin, located on the Pacific border of south-central South America (Figure 1.1), is characterized by two prominent elements, the Peru-Chile Trench and the Andes Mountains (Figures 1.2 and 1.3). An SW-NE transect from the Peru-Chile Trench to the Andes (Figure 1.3) shows a relief of more than 10 km along a distance of less than 200 km. These coast-parallel features are the morphologic expression of interaction between the oceanic Nazca-Farallon plate and the continental South American plate since Liassic time (Mégard, 1987).

The Peruvian margin, bounded by the east dipping B (Benioff) and west dipping A (Ampferer) subduction zones (Figure 1.3) in the west and east respectively, shows the following main elements: the accretionary prism, 10 forearc basins, the magmatic-volcanic arc and the folded belt of the Andes.

The forearc basins are, from north to south, the Progreso (also called Tumbes Basin), Talara, Sechura, Trujillo, East Pisco, West Pisco, Moquegua and Mollendo. The forearc northern Progreso (also called Tumbes Basin), Talara and Sechura Basins extend both onshore and offshore (Figure 1.4). The Trujillo, Salaverry and Lima Basins lie entirely offshore. The West Pisco Basin is offshore whereas the adjacent East Pisco Basin is located both onshore and offshore. The

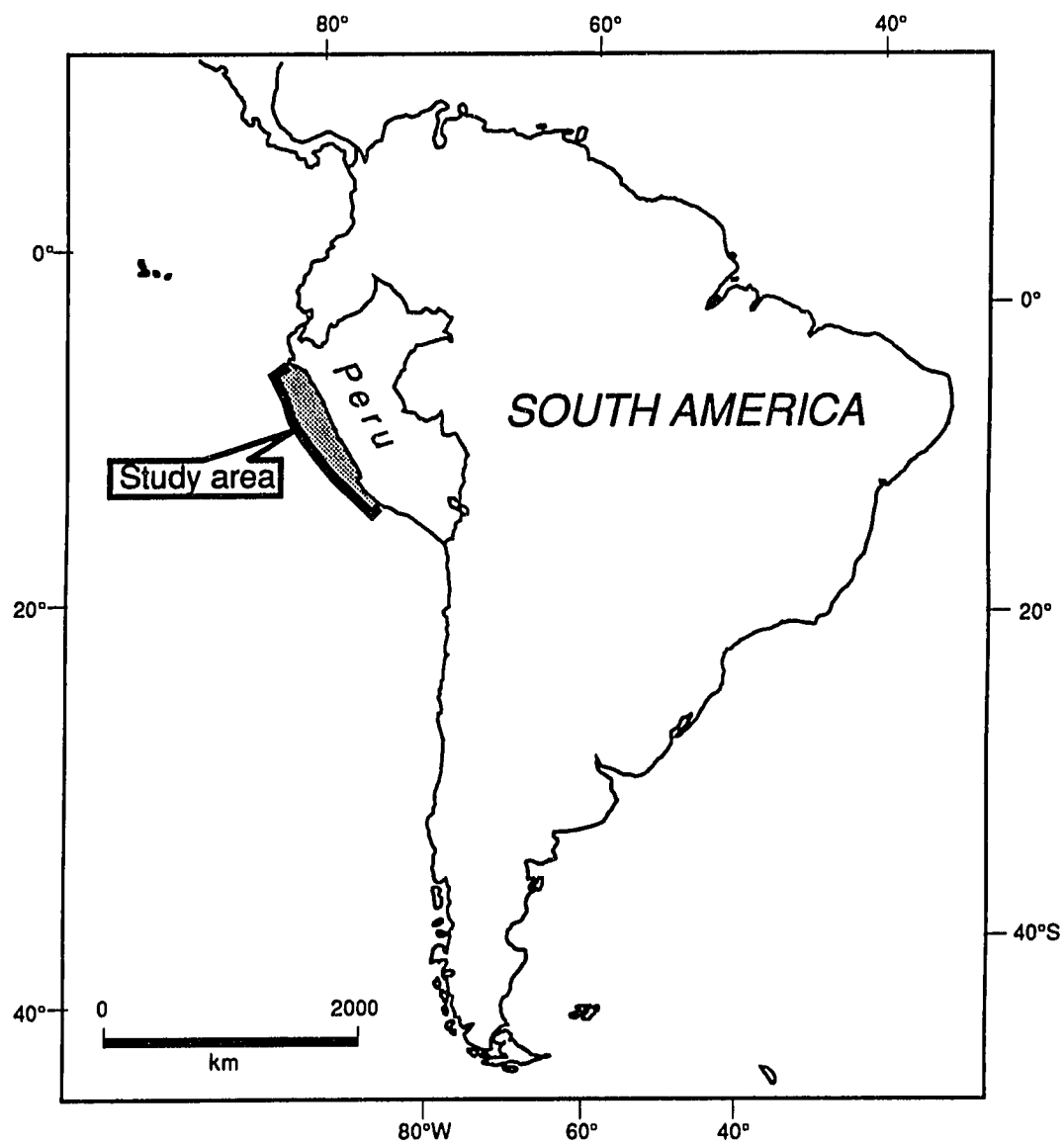


Figure 1.1 LOCATION OF THE STUDY AREA

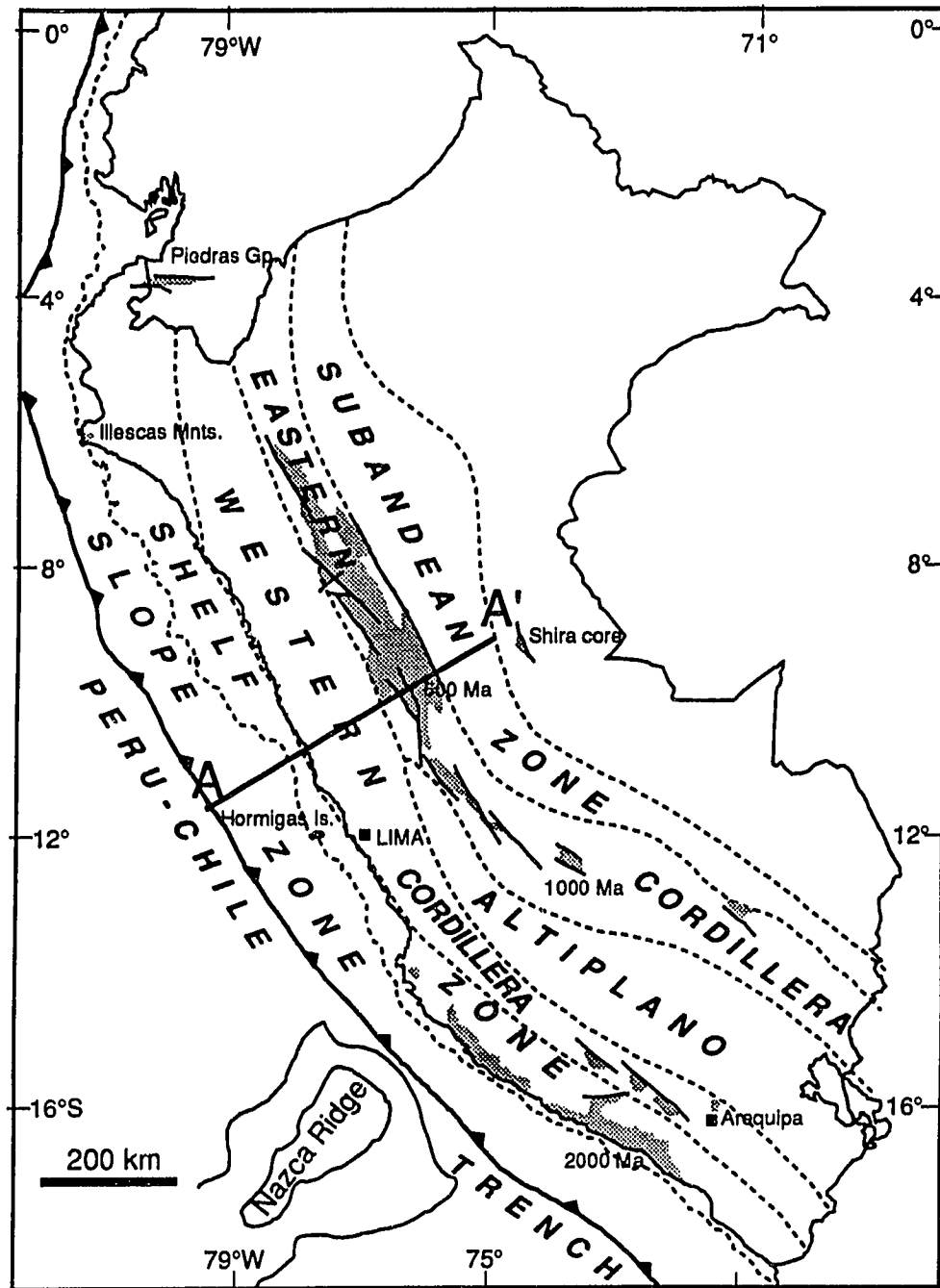
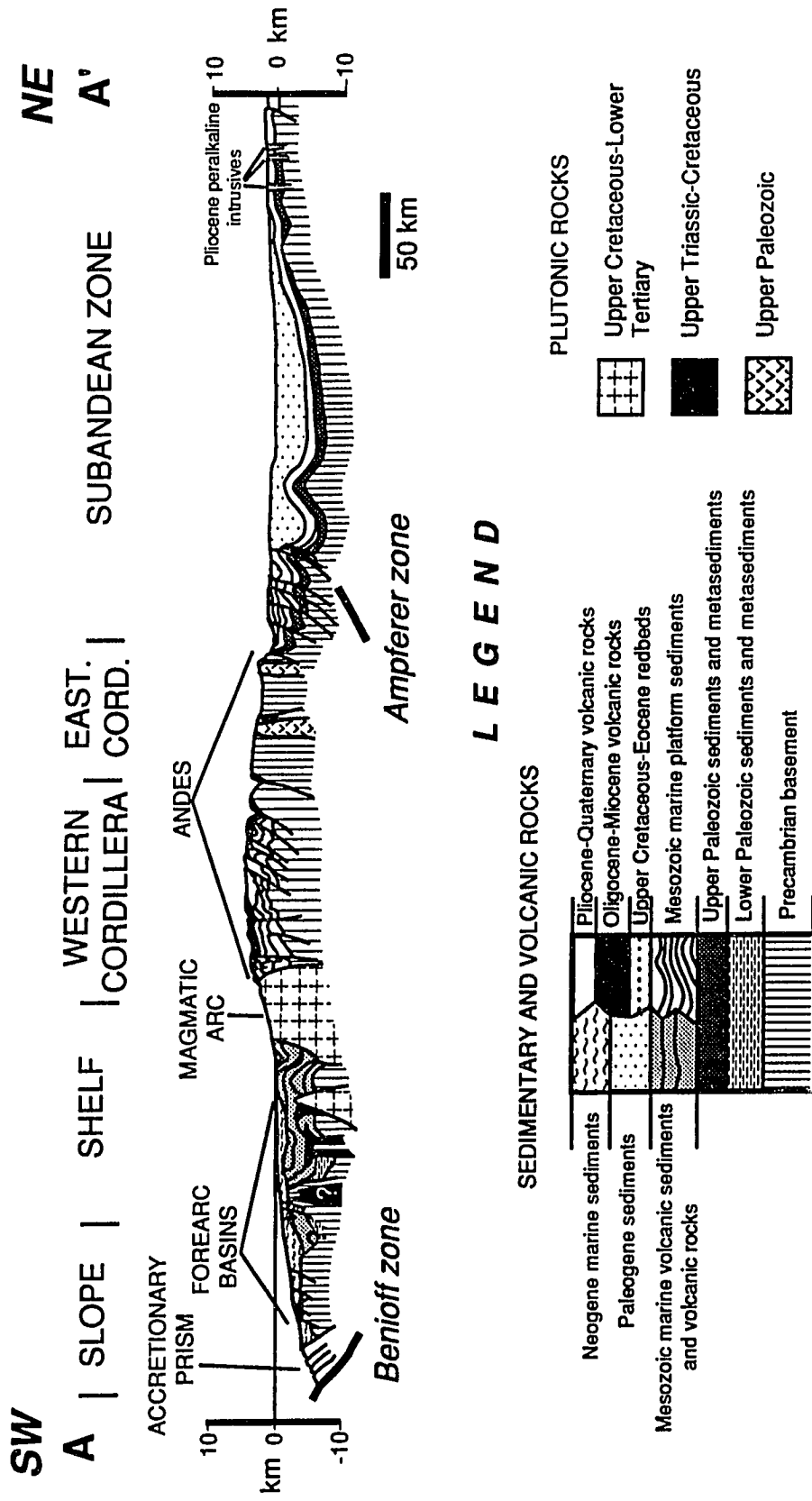


Figure 1.2 MORPHOLOGICAL ZONES OF PERU

Main Precambrian outcrops  The AA' transect is shown in Figure 1.3
After Mégard (1987)



See transect location on Figure 1.2

Figure 1.3 SW - NE REGIONAL TRANSECT AT 12° S LATITUDE

After T. Thornburg, R. Marocco, D. Davila (1985)

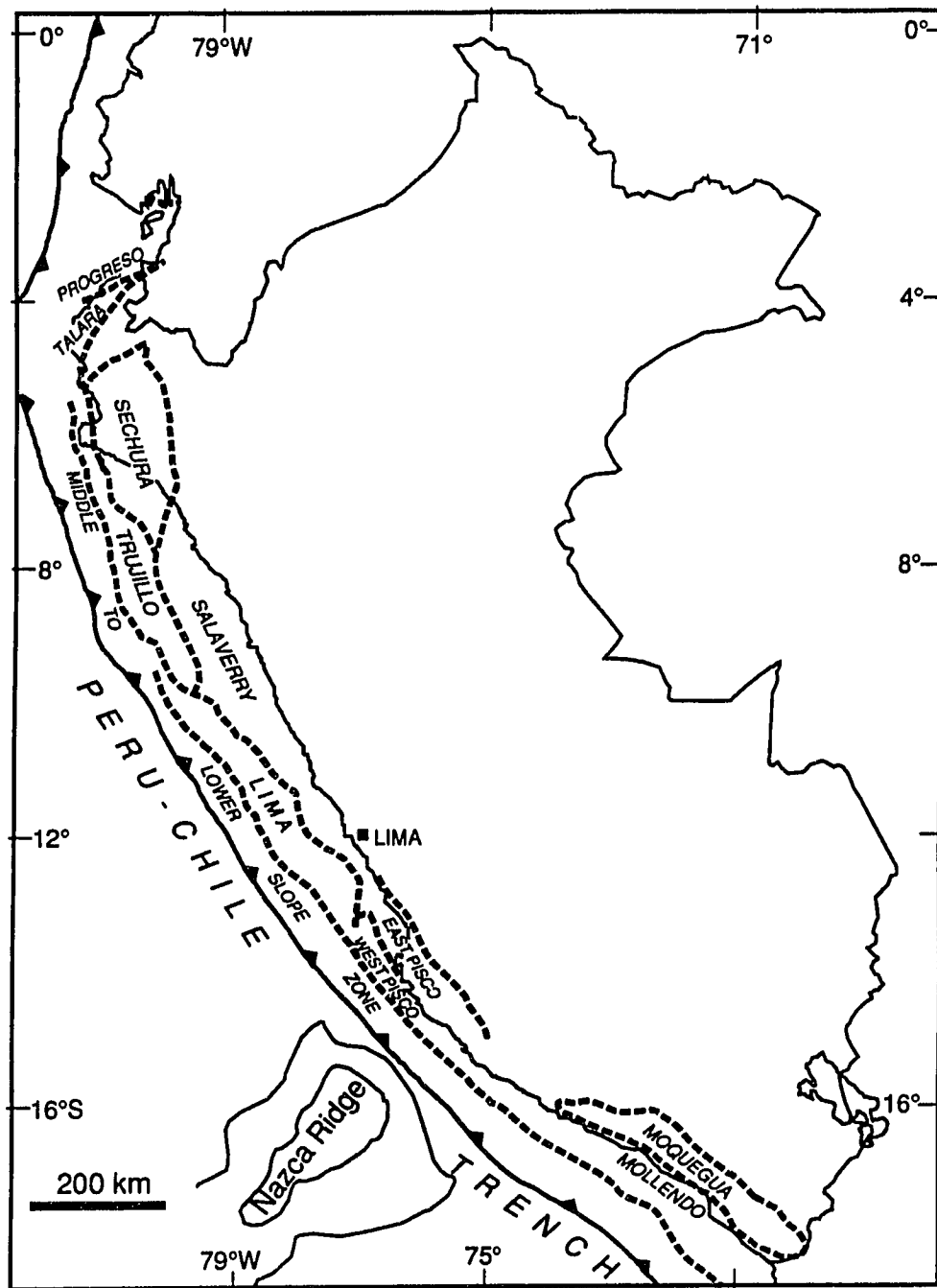


Figure 1.4 FOREARC BASINS OF PERU

After Travis et al. (1979) and Thornburg and Kulm (1981)

southern Moquegua and Mollendo Basins lie onshore and offshore respectively (Figure 1.4).

1.1 Study area

The study area extends along the offshore forearc portion between 6°S and 16°S latitude (Figures 1.1 and 1.4). This area of approximately 100,000 km² includes the southern part of the Sechura Basin, the Trujillo, Salaverry, Lima and West Pisco Basins and the western portion of East Pisco Basin.

1.2 Morphostructure of Peru

The morphology of Peru was produced during the Cenozoic evolution of the margin. There are seven subparallel northwest trending morphostructural zones (Figure 1.2): The Peru-Chile Trench, Continental Slope, Shelf, Western Cordillera, Altiplano, Eastern Cordillera and Sub-Andean Zone.

The Peru-Chile trench extends parallel to the coast, 120 to 200 km west of the Western Cordillera. Its axial depth ranges from 5.3 km in the north to 6.8 km in the south. This depth range is locally shallower at 15° S, where the trench axis shoals to about 2 km due to the intersection with the Nazca Ridge. The Continental Slope extends 60 to 130 km landward of the trench axis. Submarine

canyons dissect it only north of 7°S in a region of high rainfall on the adjacent continent. The Shelf is exposed on land north of 6°S and south of 13° 30' S, where it is about 50 to 100 km wide. It includes the Coastal Range (Figures 1.2 and 1.5), which onshore is a discontinuous string of low mountains and offshore consists of submarine basement highs, cored by a Precambrian basement to the south and Paleozoic metasediments to the north.

The Western Cordillera, where only Mesozoic and Tertiary volcanic and sedimentary rocks are exposed, reaches locally more than 6,000 m in altitude. The Altiplano consists of high plateaus that are deeply dissected by erosion; its altitude ranges from 3,800 to 4,500 m. Paleozoic metamorphic rocks crop out locally and are typically covered by Jurassic and Cretaceous strata. The Eastern Cordillera, locally rising to 6,000 m, is a vast anticlinorium characterized by open folds (Mégard, 1987). The Precambrian metamorphic basement and Paleozoic sediments crop out extensively. The Sub-Andean Zone is characterized by hills whose altitudes decrease from 2,000 m in the west to 50 m in the east. A folded and thrust faulted wedge involving Paleozoic to Pliocene sediments occupies most of the Sub-Andean Zone (Mégard, 1987).

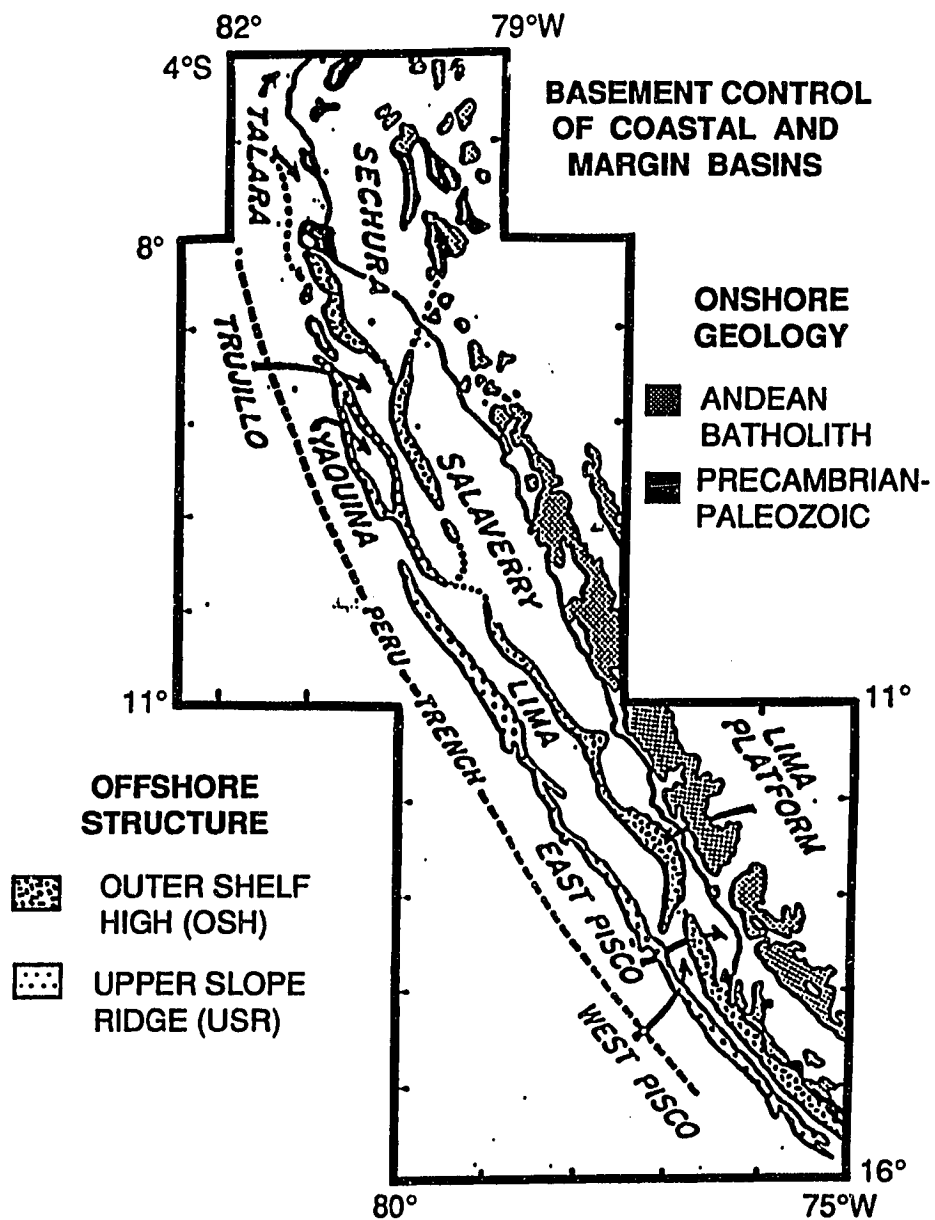


Figure 1.5 MAJOR CONTINENTAL SHELF AND UPPER SLOPE BASINS, AND THE ONSHORE - OFFSHORE STRUCTURES THAT CONTROL THEIR DISTRIBUTION

Thornburg and Kulm (1981)

1.3 Previous work in the study area

Three groups of researchers have contributed to the geologic knowledge of the Peruvian forearc: The Peruvian Government Instituto Geológico Minero y Metalúrgico (INGEMMET), the oil industry and academic institutions.

1.31 Onshore Sechura and East Pisco Basins areas

The onshore Sechura Basin, located north of the study area (Figure 1.4), was initially studied by Travis et al. (1976), Cheney et al. (1979), Caldas et al. (1980) and Ochoa (1980); later Marty (1989) redefined the stratigraphy, documented the Cenozoic biogenic sedimentation and upwelling and described its tectonic history.

Geologic understanding of the onshore East Pisco Basin, situated east of the study area, evolved during two periods: (1) From the twenties to the sixties the stratigraphy and regional geology was outlined by Lisson (1925), Steinmann (1929), Stainforth and Ruegg (1953), Petersen (1954), Newell (1956), Ruegg (1956), Rivera (1957), Mertz (1966). (2) Since the eighties the geologic knowledge notably advanced with the Balarezo et al. (1980) mapping of the Ica area (includes the East Pisco Basin); and mainly with the review and refining of the stratigraphy by Fourtanier and Macharé (1988), DeVries (1987), Davila et al. (1987), Macharé et al. (1987), Marty et

al. (1988), Dunbar and Baker (1988), Marty (1989), Stock (1989), and Dunbar et al. (1990).

In addition to establishing basin stratigraphy, other workers studied the basin tectonic and sedimentologic framework. The structural and tectonic history is summarized by Macharé (1987) and Marty (1989). Marty (1989) documented Cenozoic biogenic sedimentation and upwelling. Martin (1987) studied the secondary carbonates of the Pisco Basin. Allen and Dunbar (1988) investigated phosphate genesis. Wright and Cruzado (1988) and Stock (1989) documented some of the characteristic lithofacies found throughout the East Pisco Basin. Recently, Frantz (1993) studied the biogenic Upper Eocene-Lower Oligocene Yumaque formation of the East Pisco Basin. Dunbar et al. (1990) summarized the state of the knowledge of onshore Sechura and East Pisco Basins.

1.32 Offshore area

The earliest data in the offshore forearc south of the Talara Basin were related to the drilling of the exploratory Ballena and Delfin wells in the Trujillo Basin (Figure 1.6) by Occidental del Peru in 1971. These wells provide valuable stratigraphic information because they are the only wells drilled in the area that reached the Pre-Cenozoic basement. The Nazca Plate Project, initiated in 1972, provided dredge samples and gravimeter, magnetometer and single

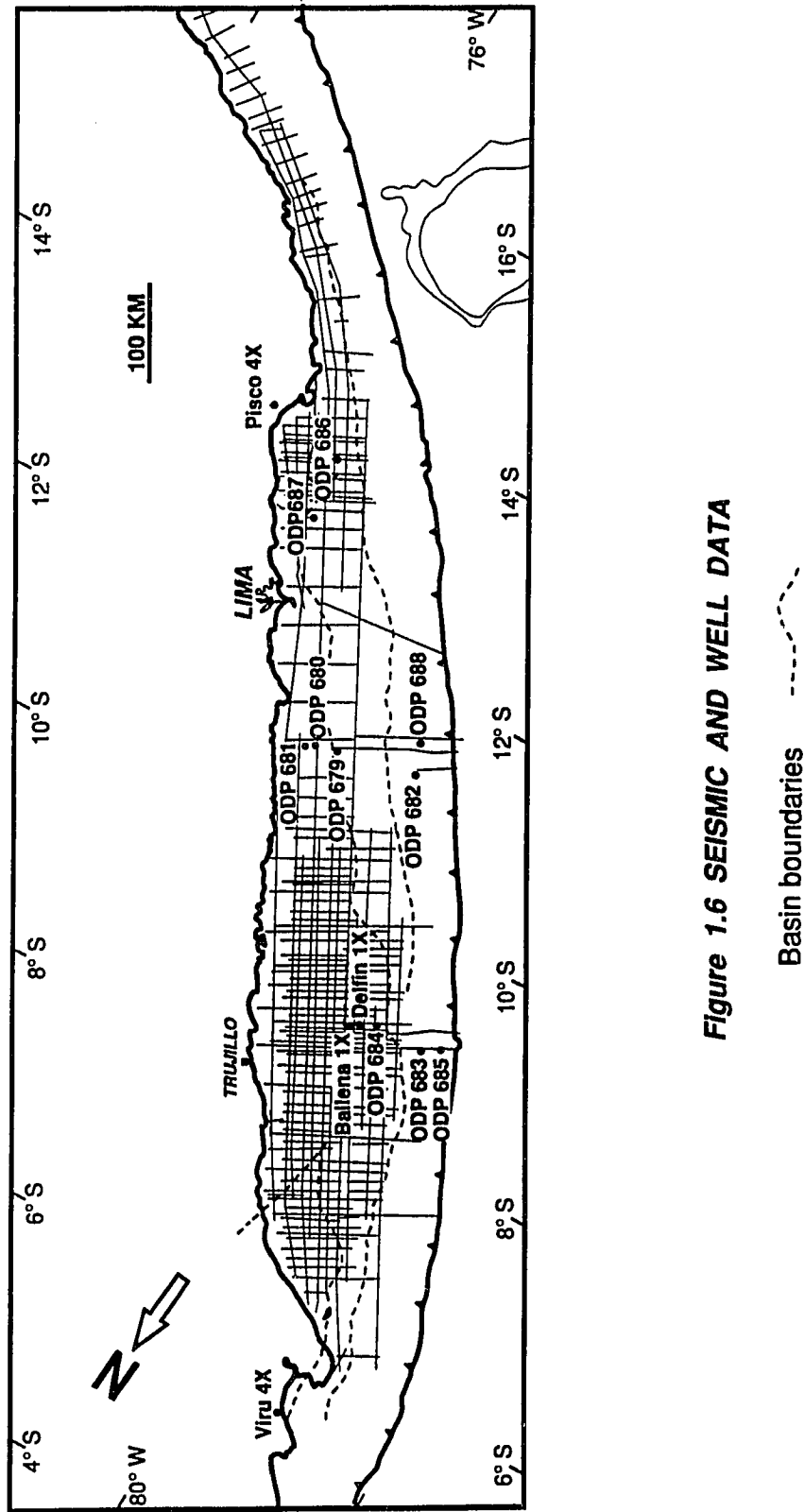


Figure 1.6 SEISMIC AND WELL DATA

and multichannel seismic data. Two extensive seismic, gravimeter and magnetometer surveys were sponsored by Petroperu, in 1973 and 1982. Seiscom-Delta Inc. in 1973 and the Compagnie Générale de Géophysique in 1982 did the geophysical surveys. In 1986, participants in Leg 112 of the Ocean Drilling Project collected additional multichannel seismic reflection profiles, reprocessed multichannel seismic lines acquired during the Nazca Plate Project, and drilled and cored 10 sites within the Peru forearc.

Nazca Plate Project results

The Nazca Plate Project was a multidisciplinary effort with focus on: (1) The regional crustal and mantle structure of the Nazca plate as a function of distance and age from the crest of the East Pacific Rise; (2) the tectonics, stratigraphy, and structure of the Peru-Chile Trench and the adjacent South American continental margin area; and (3) the processes leading to metal enrichment at the East Pacific Rise.

The project was initiated in 1972. One year later the scientific objectives of the project were reoriented, focusing on the study of mineralization at the East Pacific Rise, the convergent boundary and the continent. The new objectives related to the convergent boundary were: (1) The thickness and composition of oceanic crust and sediments just prior to subduction. (2) The degree

and composition of oceanic sediments accreted to the continent. (3) Identification of regions of accretion and consumption by their structural styles. (4) Relationship of items 1-3 to crustal structure, seismicity patterns, volcanism, and ore formation on the continent.

The main results of the Nazca Plate Project related to the continental margin are summarized as follows:

(A) Hussong et al. (1976) and Hussong and Wipperman (1981) concluded that (1) the long-term subsidence observed in the Peruvian margin at 11° 30' S latitude is due to the tectonic erosion and subsequent subduction of the continental plate material; (2) there are relatively short periods of uplift and subsidence that caused major unconformities in the sedimentary section accumulated in the slope; (3) the subducted oceanic plate is thrust, which may contribute to the vertical tectonics within the overlying continental plate.

(B) Jones (1981), combining seismic refraction and gravity information in a E-SE transect at 9°S, proposed the occurrence of a Mesozoic rock wedge with 2.65 g/cm³ density (4.55 to 5.15 km/s), which rests on Precambrian or Early Paleozoic basement and floors the Salaverry Basin Cenozoic sediments.

(C) Thornburg and Kulm (1981), Kulm et al. (1982) and Thornburg (1985) studied the area (from 6°S to 16°S latitude). These authors, using bathymetric and seismic reflection profiles, mapped two N-NW trending structural ridges (Figure 1.5), the Outer Shelf (OSH) and Upper Slope Ridge (USR), which confine two series of basins, the Slope basins located between the OSH and USR and the Shelf basins which lie between the OSH and the Andean western border. They studied (Figure 1.5) on the slope the Trujillo, Yaquina, Lima (first identified by Masias, 1976) and West Pisco Basins, and on the shelf the Salaverry Basin and offshore parts of the Sechura and East Pisco Basins. Their main conclusions were (1) the forearc shelf basins, Sechura, Salaverry and East Pisco, are floored by a block-faulted Precambrian to Paleozoic massif on which rest as much as 3 km of Cenozoic and probably Mesozoic sediments; (2) the pre-Cenozoic basement is unconformably overlain by sediments of Eocene and younger age deposited following a period of orogeny and uplift during the late Paleocene and early Eocene; (3) the shelf and Lima Basins lack an Eocene sedimentary section; (4) the Pre-Mesozoic massif experienced several pulses of uplift and subsidence during the Cenozoic. One of the most significant was a Post-Oligocene tectonic event which uplifted the Trujillo Basin area; (5) the OSH, the Trujillo Basin and the area east of the Lima Basin (Lima Platform) were uplifted and compressed (producing folds and thrust faults involving the Cenozoic sections) during Late Pliocene time. In

contrast, the Lima Basin subsided between 500 and 1100 m since Pliocene-Pleistocene time, indicating tensional stresses.

Ocean Drilling Program-Leg 112 results

Suess and von Huene et al., (1988, 1990) summarized Leg 112 results based on the drilling in the Yaquina, Trujillo and Salaverry Basins and concluded: (1) during the Early Eocene, the continental shelf extended seaward of its current position, at least to the current midslope area location; (2) a widespread Oligocene hiatus corresponds to an eastward shift of the magmatic arc and volcanism in the Western Andean Cordillera probably caused by a change in the position or configuration of the subduction zone; (3) the seaward edge of the continent subsided at least 2 km during Middle Miocene time; this subsidence suggests a subduction zone dominated by "subcrustal tectonic erosion"; (4) Cenozoic accretion began during Late Miocene time; (5) the combined effect of incremental rates of convergence and sedimentation along with the Nazca Ridge subduction at 9° S between 8.8 Ma and 7 Ma (Nur and Ben-Avraham, 1981; Cande, 1985) may have caused the change from a subduction zone dominated by tectonic erosion to a system dominated by accretion.

Ballesteros et al. (1988) reported a seismic stratigraphic study of a segment of the Lima Basin (from 11° to 11° 45' S

latitude) and the Yaquina Basin. In the Lima Basin, they recognized eleven seismic stratigraphic units. These units are: A shelfal middle Eocene sequence overlain by a middle Miocene low-energy turbiditic unit. The five following sequences consist of late Miocene sediments deposited in the shelf to shelf/slope setting. Two Pliocene sequences composed of low-energy turbidites overlay the Miocene deposits. The two uppermost sequences are Pliocene-Pleistocene and Pleistocene low-energy turbidites. The Yaquina Basin shows five sequences: middle Eocene shelf deposits at the base, overlain by two low energy turbidite packages of early Miocene-Oligocene? and middle Miocene age. The two upper sequences consist of late Miocene-Pliocene high energy turbidites capped by a late Pliocene-Quaternary low-energy turbiditic unit.

Von Huene and Lallemand (1990) proposed two mechanisms for tectonic erosion during Middle Miocene at 9° S latitude. The first mechanism is linked to subduction of the Nazca Ridge which produced uplift and breakup of the lower slope and subsequent subduction of the debris. The other mechanism consists of erosion along the base of the upper plate, which would involve intensive fragmentation of the underside of the upper plate caused by overpressured water. Small crustal fragments created in this fashion would be vulnerable to plucking by traction along the plate boundary.

Von Huene (1993, in press) correlated the Lima Basin subsidence and uplift with the geometry and subduction history of the Nazca Ridge and concluded: (1) the subsidence of the Lima Basin is coeval with the Nazca Ridge subduction; (2) the structural difference between the Trujillo and Lima Basins is due to the much smaller size (width and height) of the Nazca Ridge portion subducted under the Trujillo Basin with respect to the Ridge size segment subducted below the Lima Basin; (3) there is seismic evidence of a seaward sediment source located on the Lima Basin west flank; (4) the complex history of vertical tectonism and erosion along the Lima Basin transect can be explained by the upper plate response to the subduction of the irregularly shaped Nazca Ridge.

1.4 Basic information

The basic information for the study consists of: (1) more than 15,000 km of multichannel reflection seismic profiles which cover the approximately 100,000 km² of the study area (Figure 1.6). This seismic information was obtained in two surveys sponsored by Petroperu, performed in 1973 and 1982. Seismic line spacing is 6 to 20 km in the northern Salaverry and Trujillo Basins, 40 km in the Lima Basin and 4 to 20 km in the southern East and West Pisco Basins. Six segments of reprocessed seismic profiles (Figure 1.6) included in the ODP Leg 112 Initial Reports Volume (Suess E., von Huene R., et al., 1988) were also incorporated to include information

from the trench-accretionary complex zone. (2) Lithologic samples, electric and synthetic logs from the Delfin and Ballena (Figure 1.6) drill holes which reached pre-Cenozoic basement and are located

WELL	LOCATION	WATER DEPTH (m)	DRILLED INTERVAL (m)	OLDEST SEDIMENT RECOVERED
Ballena 1X	Trujillo	115.2	859.7	Paleoz./Prec.
Delfin 1X	Trujillo	118.6	2540.8	Paleoz./Prec.
ODP 679 A	Lima	450.0	7.0	Quaternary
ODP 679 B	Lima	461.0	107.2	Pliocene
ODP 679 C	Lima	461.0	75.5	Pliocene
ODP 679 D	Lima	450.0	245.4	Late Miocene
ODP 679 E	Lima	461.3	359.3	Mid. Miocene
ODP 680 A	Salaverry	263.0	93.8	Pleistocene
ODP 680 B	Salaverry	263.0	195.5	Early Pliocene
ODP 680 C	Salaverry	263.0	34.3	Pleistocene?
ODP 681 A	Salaverry	161.0	187.0	Pleistocene
ODP 681 B	Salaverry	161.0	143.5	Plioc./Mioc.?
ODP 681 C	Salaverry	161.0	91.4	Quaternary
ODP 682 A	Low. Slope	3799.0	436.7	Eocene
ODP 683 A	Mid. Slope	3082.3	419.2	Mid. Miocene
ODP 683 B	Mid. Slope	3082.0	488.0	Mid. Eocene
ODP 684 A	Trujillo	436.5	136.1	Mid. Miocene
ODP 684 B	Trujillo	437.0	55.0	Pliocene
ODP 684 C	Trujillo	437.0	115.0	Mid. Miocene
ODP 685 A	Low. Slope	5081.3	468.6	Early late Mio.
ODP 686 A	West Pisco	457.3	205.7	Quaternary
ODP 686 B	West Pisco	457.3	303.0	Quat./Plioc.?
ODP 687 A	Lima	17.3	207.0	Quat./Pliocen.
ODP 687 B	Lima	3.0	195.3	Quat./Pliocen.
ODP 688 A	Low. Slope	317.3	350.3	Pliocene?
ODP 688 B	Low. Slope	3830.3	360.0	NR
ODP 688 C	Low. Slope	3830.3	359.7	Quaternary
ODP 688 D	Low. Slope	3830.3	345.0	NR
ODP 688 E	Low. Slope	3830.3	779.0	Early Eocene

Table 1. DRILL HOLES IN THE STUDY AREA

toward the eastern border of the Trujillo Basin; and (3) well logs and detailed descriptions of conventional cores recovered in the ODP, Leg 112 (Figure 1.6; Table 1) were also available.

Electric logs and stratigraphic columns of the Viru 4X and Pisco 4X wells (Figure 1.6) drilled onshore in the Sechura and East Pisco Basins respectively were also made available by industry.

1.5 Purpose

The main objectives of the present study are:

(1) To define the seismic-stratigraphy of the offshore Sechura, Salaverry, Trujillo, Lima, West Pisco and East Pisco Basins, located in the Peruvian shelf and continental slope zones, between 6° and 16° S latitude (Figures 1.2 and 1.4).

(2) To reconstruct the structural evolution of these basins and to relate the structural stages to the Nazca plate subduction process.

1.6 Study method

The study was done in five phases:

(1) The rock record was subdivided and correlated, throughout the whole study area, into 11 seismic sequences bounded by unconformities or their correlative conformities which will be described in Chapter 3.

(2) Biostratigraphic and paleoenvironmental analysis on the Delfin and Ballena well cuttings were performed by Dr. H. Okada and by Mrs. N. L. Engelhardt-Moore respectively; a synthesis of their reports is included in Appendices A and B. Biostratigraphic and paleoenvironmental data of the 10 ODP wells were collected from the ODP, Leg 112 Initial Reports and Scientific Results (Suess E., von Huene R. et al., 1988, 1990). In order to date the 11 seismic sequences, the well stratigraphy was correlated with the nearest seismic profile using synthetic logs when they were available.

(3) Six regional panels of seismic profile line drawings and one panel of seismic profiles that cover most of the study area (Figure 1.7) were constructed to illustrate the distribution and structural style of the 11 sequences.

(4) To tie the stratigraphy between the offshore and adjacent onshore areas the offshore wells were correlated with industry's Viru 4X and Pisco 4X wells located onshore in the Sechura and East Pisco Basins respectively (Figure 1.6).

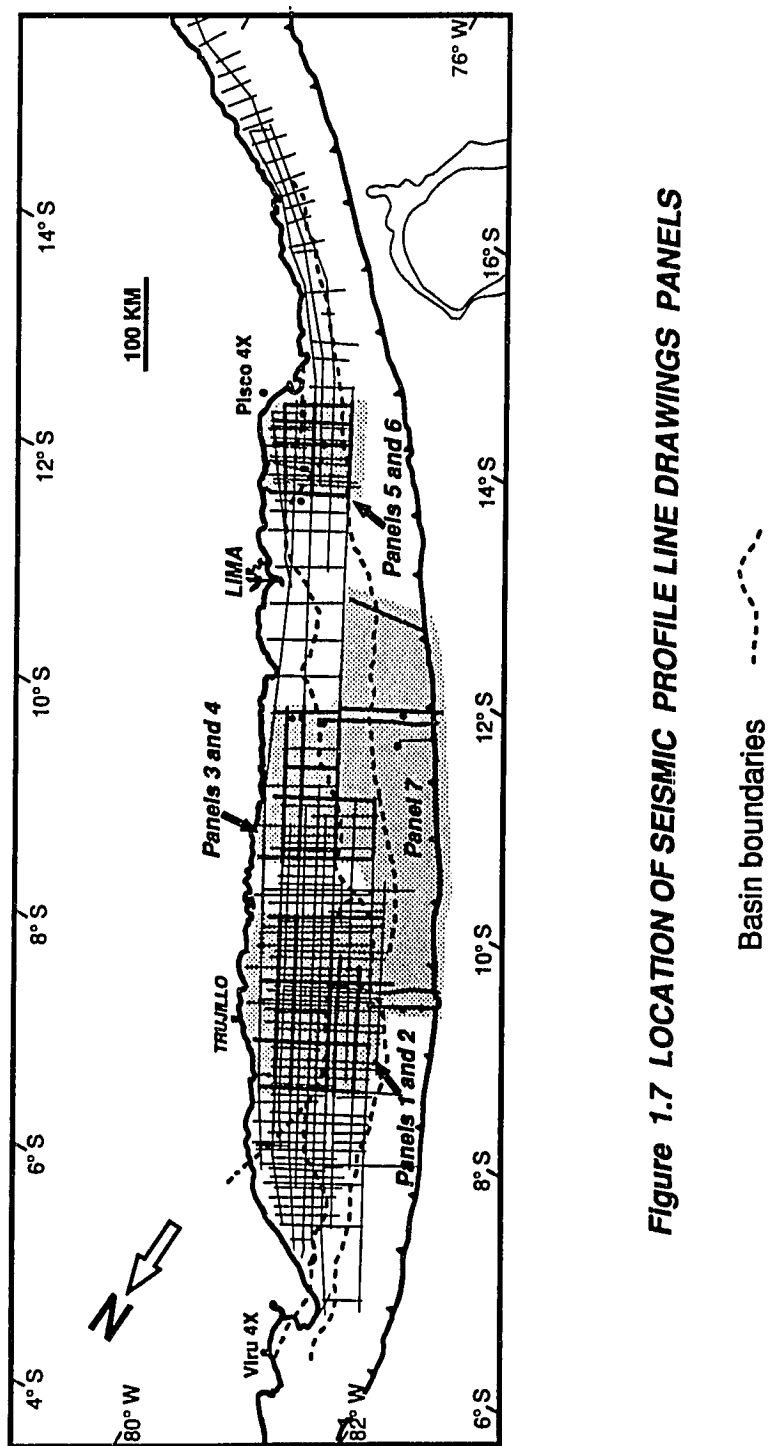


Figure 1.7 LOCATION OF SEISMIC PROFILE LINE DRAWINGS PANELS

(5) The main structural events were correlated with the Nazca (Farallon)-South American plate reconstruction of Pardo Casas and Molnar (1987).

1.7 Pre-Jurassic geologic framework

The following summary is based on the work of Mégard (1987) on the Andes evolution. Mégard (1987) described three main cycles in the pre-Jurassic geologic history of Peru.

Precambrian

The Precambrian basement, exposed in the Eastern Cordillera and along the coast, includes a series of Upper Precambrian low to medium grade metamorphic rocks, about 600 Ma old with older cores of 1.0 to 2.0 Ga. The main metamorphic core is the Arequipa massif (Mégard et al., 1971; Shackleton et al., 1979; Dalmayrac et al., 1980), (Figure 1.2) which consists of staurolite and andalusite schists and granulite-facies migmatitic gneisses. These rocks are related to a metamorphic event dated as 1,950 Ma (Dalmayrac et al., 1977). The series exposed in the Eastern Cordillera is composed of schists, quartzites, and metagraywackes intercalated with greenschist. Along the shelf zone, the metamorphic rocks of the Hormigas Islands, located 70 km west of Lima (Figure 1.2) (Kulm et al., 1981) and the Illescas Mountains of northwest Peru (Figure 1.2)

may also be of Upper Precambrian age. These Late Precambrian metamorphic rocks occur in a belt that is subparallel to the Andes.

Ordovician to Devonian sedimentation

Marine Paleozoic strata unconformably overlie late Precambrian rocks. In southern Peru and Bolivia, Paleozoic rocks accumulated in a northwest-trending basin bounded by the Brazilian shield and the Arequipa massif to the east and west respectively. Siliciclastic sedimentation was almost continuous from the middle Ordovician to the upper Devonian, reaching maximum thickness in the order of 10,000 to 15,000 m (Mégard, 1987).

Late Devonian-early Mississippian (Eo-Hercynian) folded belt

The Ordovician to Devonian strata were strongly deformed during latest Devonian or early Mississippian time (Mégard, 1967; Mégard et al., 1971; Dalmayrac et al., 1980; Martinez, 1980). This Eo-Hercynian phase produced a northwest-trending folded belt with greenschist-grade metamorphism and scarce post-tectonic granitoids (Mégard, 1987).

Mississippian to Permian sedimentation

A 1,000 to 2,000 m thick sequence of Mississippian to early Permian conglomerates, marine shales, sandstones, and carbonates rests unconformably upon the eroded folds of the Eo-Hercynian belt.

Late Permian (late Hercynian) deformation

Late Hercynian (Dalmayrac, 1980) tectonics were mainly extensional with normal faults and probably some strike-slip faults. The extensional strain of this period might be related to continental rifting (Noble et al., 1978; Dalmayrac et al., 1980). Late Permian volcanism consists of peralkaline rhyolites and sub-alkaline basalt flows. Emplacement of Permo-Triassic sub-alkaline granitoids as batholiths and stocks followed the initial period of volcanism in the Eastern Cordillera (Mégard, 1987).

CHAPTER 2: THE MESOZOIC-CENOZOIC ANDES OF PERU

2.1 INTRODUCTION

The Mesozoic-Cenozoic evolution of the Peruvian Andes began in the Liassic (Mégard, 1987), when the oceanic Farallon plate was located offshore continental South America. The Andean evolution is marked by two main periods: (1) From early Jurassic to early Cretaceous time, when strike slip and extensional tectonics dominated the margin, during oblique subduction (Pardo-Casas and Molnar, 1987; Jaillard, 1992), and (2) From late Cretaceous to the present, when compression in the back arc led to the development of the Andean folded belt and its related foredeep. During this period, a type A subduction boundary, that progressively migrates eastward incorporating younger sediments, is formed.

Andean tectonics have been described as a succession of short lived regional and synchronic phases of trench parallel folding and thrusting intercalated with periods of tectonic quiescence or extension (Steinmann, 1929; Caldas, 1983; Mégard, 1987; Sébrier and Soler, 1991; Jaillard, 1992). On the other hand the Andean foredeep evolution has not been appropriately dated and described. In the future, publication of seismic profiles from the Subandean and Low Jungle zones will help to determine whether if the so called compressional phases are indeed the spatial and temporal expression

of a continuous long-lived compressive process in which the deformation migrates toward the foreland and involves successively deeper decoupling levels.

The following summary is based on the work of Mégard (1987) on the Andes evolution; Jaillard (1992), who described the Peruvian margin tectonic and geodynamic evolution from Kimmeridgian to Paleocene time, and the synthesis of Sébrier and Soler (1991) on the tectonics and magmatism in the Peruvian Andes from late Oligocene to Present. The geographic locations of the features described in this section are shown on the morphostructural map of Peru (Figure 2.1).

2.2 EARLY TO MIDDLE JURASSIC

The Hercynian deformation preceded a widespread Norian transgression. During late Triassic, a carbonate basin occupied most of the Peruvian margin, with shallow shelf deposits to the east and deeper carbonates to the west (Loughman and Hallam 1982; Mégard, 1978). These carbonates rest unconformably on upper Permian to lower Triassic red beds.

During the Liassic: (1) In central and northern Peru, bituminous shales were deposited under restricted, relatively deep shelf conditions. (2) In central Peru tuff and ash deposits indicate

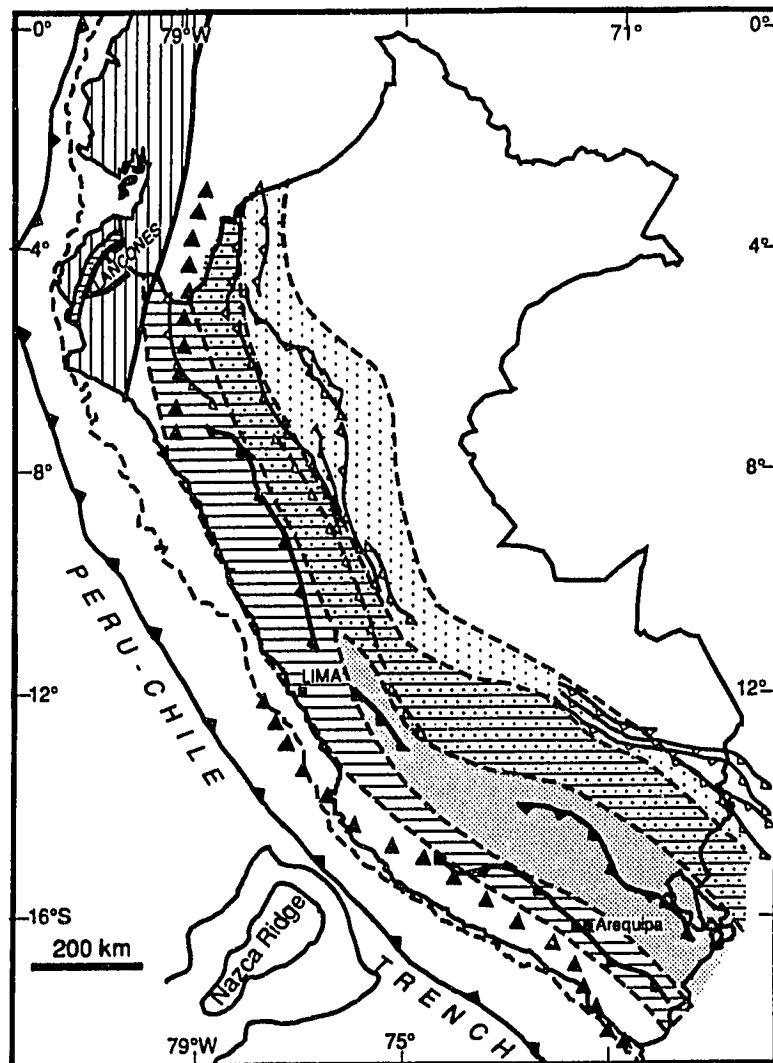

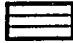

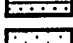
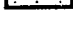


Figure 2.1 MAIN TECTONIC ELEMENTS OF THE PERUVIAN ANDES

From Mégard (1987) and Jaillard (1992)

LEGEND

MORPHOSTRUCTURAL ZONES


- Shelf and Slope 
- Western Cordillera 
- Altiplano 
- Eastern Cordillera 
- Subandean zone 


THRUSTS

Terrane accreted during the Tithonian 

Amotape Mountains 

Jurassic volcanic arc 

Late Miocene 

Late Eocene 

Late Campanian and late

Coniacian-earliest Santonian 

volcanism probably located to the west. (3) In the south, a carbonate shelf basin developed; its western boundary consisted of reefs within an andesitic volcanic belt (Jenks, 1948).

Some evidence supports extension during middle to late Liassic time (Jaillard, 1992). A NNE trending volcanic arc in northern Peru (Mourier et al., 1988) and a NW trending andesitic volcanic belt with arc-type affinity (James et al., 1975), located along the southern coast (Mégard, 1987), outline the position of the earliest volcanic arc recognized in the Peruvian margin (Figure 2.1).

2.3 KIMMERIDGIAN TO PALEOCENE

Jaillard (1992) identified three main tectonic periods that occurred between Kimmeridgian and Paleocene time:

- (1) The Kimmeridgian-Berriasian (145-130 Ma) Viru period.
- (2) The middle Cretaceous (108-95 Ma) Mochica period (Figure 2.2). Jaillard (1992) extends Mégard's (1984) Mochica phase which was initially limited to a ± 105 Ma event.
- (3) The late Cretaceous (88-73 Ma) Peruvian period (Figure 2.2).

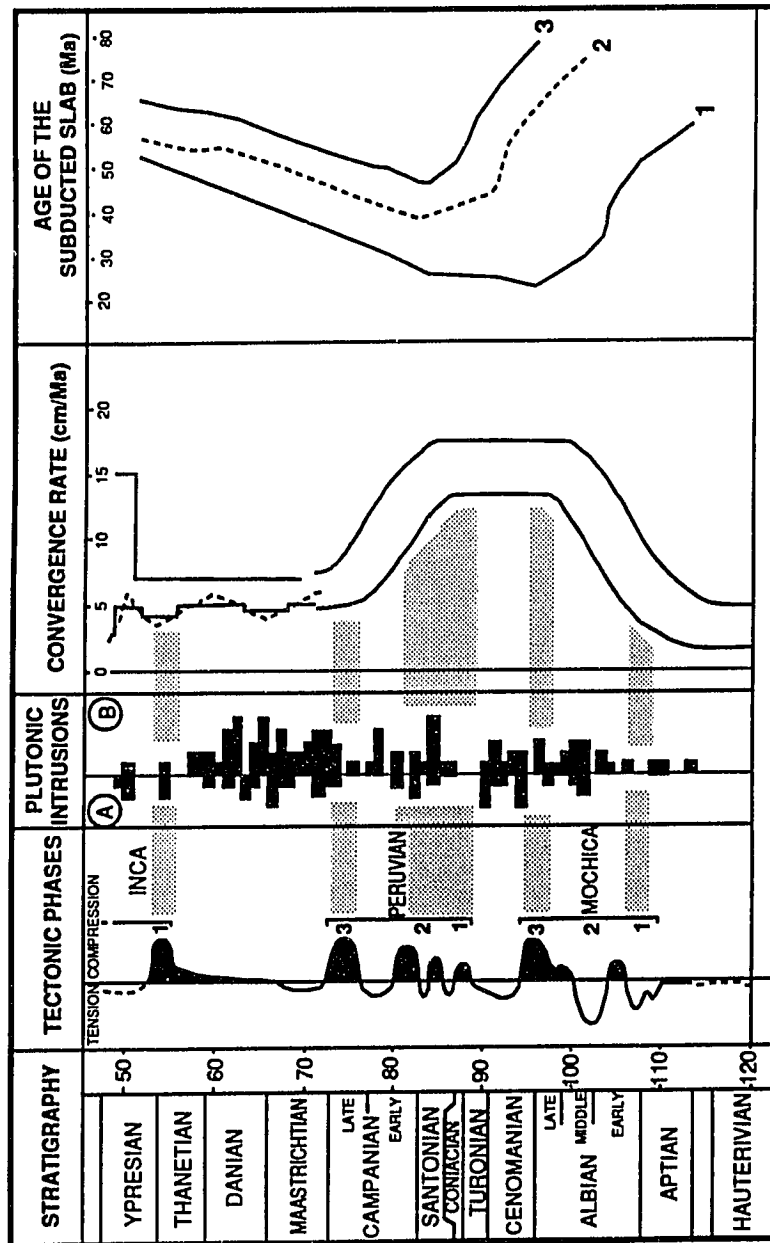


Figure 2.2 RELATIONSHIP OF TECTONIC EVENTS, MAGMATIC PULSES AND PLATE GEODYNAMICS IN THE PERUVIAN MARGIN BETWEEN KIMMERIDGIAN AND PALEOCENE TIMES

Plutonic intrusions: A in the coast of central Peru (after Soler and Bonhomme, 1990); B in the whole coastal Peru (after Beckinsale et al., 1985 and Mukasa, 1986). Convergence rate between the Farallon and the South American plates and age of the subducted slab: after Soler and Bonhomme, 1990. 1: Based on Pardo Casas and Molnar (1987) and high convergence rate during the early Cretaceous (Larson and Pitman, 1972); 2: Based on the Pilger (1981) reconstruction and high convergence rate during the early Cretaceous (Larson and Pitman, 1972); 3: Based on the Pilger (1981) reconstruction and low convergence rate during the early Cretaceous (Soler and Bonhomme, 1990).

These periods, which generally involve alternate compressive and extensional phases (Figure 2.2) with syntectonic sedimentation, are separated by periods of tectonic quiescence or relaxation.

(1) The Kimmeridgian-Berriasian (145-130 Ma) or Viru period.

This period consists of three phases: **(a) The Kimmeridgian or Viru 1 event** is interpreted as a distal response to the Argentine-Chilean "Araucan" phase. The Kimmeridgian is represented mostly by poorly-dated, discontinuous, fossil-barren, coarse-grained deposits which rest upon Callovian-Oxfordian (Mourier, 1988; Benavides, 1962; Pecho, 1981; Vicente 1981, 1989; and Olchauski, 1980) or Paleozoic to Triassic rocks (Klinck et al., 1986; Carlotto, 1989).

(b) The Tithonian Viru 2 phase is related to the collision of allochthonous terranes northwest of the margin (Figure 2.1), (Mourier et al., 1988), which will become, during the Tertiary, the substratum of the Talara and Progreso Basins. Accretion produced compression and folding in northwestern Ecuador and was associated with local extension and turbiditic deposition east of the Amotapes Mountains. In the Western Cordillera zone, an extensional back arc basin (Atherton et al., 1983, 1985) developed, accumulating hemipelagic shales interbedded with volcanics (basalts and

andesites) and volcanoclastics. In the northern Western Cordillera, a 2500 m thick package of turbidites accumulated (Jaillard and Jacay, 1989). In the southern Western Cordillera and Altiplano regions, Tithonian carbonates are overlain by fine and coarse grained siliciclastics.

(c) The Berriasian or Viru 3 phase is related to the South Atlantic rifting which probably produced a regional uplift (doming ?) in eastern Peru. Berriasian tectonism was characterized, in northwestern Peru, by the late stages of extension associated with the terrane accretion and with dextral strike-slip displacements (Jaillard and Jacay, 1989), and an uplifting over most of Peru (Jaillard et al., 1990).

Valanginian to early late Aptian

This period, characterized by an initial regional westward tilting of the South America plate (Jaillard, 1992), was followed by tectonic quiescence when a wide basin received siliciclastic fluvio-deltaic sediments supplied from the east.

(2) The late Aptian-early middle Cenomanian (108-95 Ma) or Mochica period

During Berriasian time marine sedimentation and volcanism continued on the northern coast. In the Western Cordillera this interval is probably represented by shallow marine to deltaic sandstones offset by synsedimentary normal faults (Cobbing et al., 1981, Jaillard and Jacay, 1989). Batty and Jaillard (1989), Batty et al. (1990) suggest that the southeastern region emerged during this time.

The Mochica period and the following Peruvian period probably developed during the oblique subduction of a relatively young and buoyant oceanic lithosphere, which induced a low subduction angle. There are three phases:

(a) The late Aptian-earliest Albian or Mochica 1 phase has a poorly-defined extensional character. This time is represented by shales deposited in the north-central Western Cordillera area (Myers, 1974); and farther south, by a 2500 m thick volcanic sequence. In the northern Western Cordillera zone, coarse-grained siliciclasts contain basaltic layers, whose alkaline chemical trend suggests intracontinental extension (Soler, 1989). On the southern coast a tonalite intrusive (111 Ma, Beckinsale et al., 1985) was emplaced.

(b) The early and middle Albian or Mochica 2 phase

is characterized by alternating compression and extension probably related to strike-slip displacements within the arc or back arc volcanic rocks (Jaillard,1992).

In the Lancones Basin (Figure 2.1) volcanic (basalts to rhyolites) and volcanoclastic rocks accumulated (Reyes and Caldas, 1987). Aleman (personal communication, 1993) interprets the Lancones Basin as a pull-apart basin. From the north-central Western Cordillera, Myers (1974) described a thick (2000 to 8000 m) sequence of volcanic and volcanoclastic rocks interbedded with marine shales and limestones. These dominantly basaltic and andesitic volcanic rocks show a tholeiitic trend (Soler, 1991). A local pre-middle Albian compressive event folds these rocks (Myers, 1974; Wilson, 1975). Three interpretations of this basin have been suggested: (a) a back arc, ensialic marginal basin (Atherton et al., 1983, 1985), (b) an ocean floored marginal basin (Atherton, 1990), and (c) the extensional tectonic subsidence of a volcanic arc (Soler, 1991). The central and southern coastal area shows a continuous 1000 to 2000 m thick sequence of basalts and basaltic andesites interbedded with marine sediments. Injoque (1985) and Soler (1989) interpreted these volcanic rocks as volcanic arc extrusions.

In the southwestern and northern coastal areas, plutons dated 111-99 Ma (Beckinsale et al., 1985; Clark et al., 1990) and 102 Ma (Wilson, 1975) respectively indicate early, late Aptian to middle Albian magmatism.

(c) The late Albian-early middle Cenomanian or Mochica 3 phase. This is the first major Cretaceous compressional phase on the Peruvian margin. NNW-SSE to N-S dextral wrenching displacements reported by Bussel and Pitcher (1985) in northern Peru suggest an oblique northerly to northeasterly convergence direction.

During this time volcanic sedimentation continued in the Lancones Basin, but turbidites were dominant in the western part of this basin (Morris and Aleman, 1975). The north-central Western Cordillera zone was alternately compressed and extended during late Albian to Cenomanian time (Bussel, 1983; Bussel and Pitcher, 1985). The syntectonic intrusion of gabbros and diorites preceded the emplacement of the Coastal Batholith (Cobbing et al., 1981; Pitcher et al., 1985; Soler and Bonhomme, 1990). Marine sedimentation continued until the early Cenomanian (Guevara, 1980) in the central coastal zone. After early Cenomanian time this zone was folded (Myers, 1974); Bussel and Pitcher (1985) suggested that the dominantly NW trending folds were related to dextral wrenching movements.

Synsedimentary normal faults affected limestones that accumulated in the northern Western Cordillera area during this time. Thickness variations in some areas suggest extensional conditions (Jaillard, 1987) with a WNW-ESE tensional stress (Jaillard, 1992).

To the east, the late Albian-early middle Cenomanian is represented by a westward prograding deltaic system. Along the southern coast Albian-Cenomanian volcanics are not deformed. Plutonism (monzogabbros to monzogranites) was centralized east of the East Pisco Basin (Ica, Yauca and Pisco Rivers), where Beckinsale et al. (1985) and Mukasa (1986) report dates in the range of 101 to 94 Ma . From the eastern part of the Western Cordillera to the Eastern Cordillera-Sub-Andean boundary, carbonate sedimentation prevailed. This last zone is characterized by the occurrence of large scale slumping, synsedimentary breccias and gravity slides (Audebaud, 1971, 1973; Portugal, 1974). Audebaud (1971) reported NNW-SSE trending normal faults and a WSW trending paleoslope. Jaillard (1992) pointed out the occurrence of some reverse faults which suggest NE-SW compression emphasizing the structural complexity of this area and the necessity of further studies.

The late middle Cenomanian-Turonian

During this tectonically quiescent period, turbidites were deposited in the Lancones Basin (Morris and Aleman, 1975). In the north-central Western Cordillera zone, acidic to intermediate plutons were emplaced (94-90 Ma, Mukasa, 1986; Soler and Bonhome, 1990). In the northern Western Cordillera zone, 900 m of limestones accumulated; farther east siliciclastic sedimentation prevailed. To the south, igneous intrusion ceased in the coastal area, whereas in the Eastern Cordillera region, carbonate sedimentation continued.

The Coniacian-Campanian (88-73 Ma) or Peruvian period

There are three phases of deformation in this compressive period (Figure 2.2) during which the Western Cordillera-coastal zone is uplifted and the Western Cordillera is folded.

(a) Turonian-Coniacian boundary, or Peruvian 1 phase

The Western Cordillera-coastal area was uplifted, thus isolating the western Andes from the open sea. During this phase there was no plutonic activity.

In the Lancones Basin turbiditic sedimentation persisted (Morris and Aleman, 1975). The northern coastal-Western Cordillera

area shows strike-slip faults and regional compression (Bussel and Pitcher, 1985). This period is characterized by dominantly fine-grained siliciclastics in central and eastern Peru and by fine-grained red siliciclastics and evaporites to the south.

(b) The late Coniacian-earliest Santonian (?) or Peruvian 2 phase, and the late Santonian period.

The Peruvian 2 phase is characterized by the development of foreland deposits related to thrusts produced by NE-SW compression in the southern Western Cordillera (Figure 2.1)

During this time compression along the coastal-Western Cordillera area caused uplift and the retreat of the sea from the region. In the Lancones Basin turbiditic sedimentation persisted (Morris and Aleman, 1975). Along the Western Cordillera of the northern coast, a plutonic granodioritic intrusion was emplaced between 85 and 76 Ma (Beckinsale et al., 1985; Soler and Bonhomme, 1990). The Western Cordillera zone emerged by late Santonian time. In the eastern region, fine siliciclastic sedimentation prevailed. In southwestern Peru plutonic intrusion persisted. In southernmost Peru, Clark et al. (1990) reported a 77-80 Ma (Ar-Ar) pluton.

In the southern Western Cordillera, the Santonian is represented by a sequence of marine limestones and fluvial to

lacustrine terrigenous sediments (Hosttas, 1967; Vicente, 1981; Garcia, 1978). To the southeast, shales, sands, and limestones are present (Jaillard and Sempere, 1989; Kalafatovitch, 1957; Carlotto et al., 1990).

(c) The late Campanian or Peruvian 3 phase.

In the northwest conglomerates unconformably overlie Paleozoic to Senonian rocks (Olsson, 1944, Morris and Aleman, 1975), indicating the uplift of pre-Mesozoic crystalline massifs (Olsson, 1944, Morris and Aleman, 1975) and the creation of the first late Cretaceous forearc basin to the west. In the Western Cordillera foreland deposits associated with overthrusts developed, outlining the future Western Cordillera. In southern Peru, NW trending overthrusts were associated with foreland deposits and reflected NE-SW compression. On the northern coast a pluton 73 and 70 Ma (Beckinsale et al., 1985) was emplaced.

In the Western Cordillera, undated continental red beds and fluvial and alluvial deposits may be late Campanian in age. In the east the late Campanian is represented by coarse-grained deltaic and fluvial siliciclasts. In the southeast, evidence of a short-lived marine transgression is followed by the resumption of detrital supply (Jaillard and Sempere, 1989). In the same area very thick, poorly dated red bed sequences suggest syntectonic deposition

related to thrust faults or wrenching motions (Cordova, 1986, Noblet et al., 1987, Lopez and Cordova, 1988).

Maastrichtian

In the northwestern Lancones Basin turbiditic sedimentation continued, but the adjacent forearc Talara Basin received Campanian and Maastrichtian, fine-grained, pro-delta sediments (Zuñiga and Cruzado, 1979).

Along the north-central Western Cordillera zone, plutonic intrusion resumed but shifted a few kilometers eastward (Soler and Bonhomme, 1990). In the central and eastern areas the Maastrichtian is represented by fine-grained red beds (Jenks, 1961, Mégard, 1978, Tschopp, 1953, Koch and Blissenbach, 1962). In the southern Western Cordillera, igneous intrusion and extrusion have occurred since late Maastrichtian (70-66 Ma, James et al., 1975; Beckinsale et al., 1985, Mukasa, 1986). In the Cuzco area a 4500 m thick coarse-grained, fluvial sequence accumulated (Noblet et al., 1987; Lopez and Cordova, 1988).

Paleocene

Compression during this time caused the uplift of the Western Andes. Black shales occurred in the Talara Basin. Along the coast a

plutonic intrusion occurred during early Paleocene time. In this area, Bussel and Pitcher (1985) reported high rates of strike slip displacement and regional compression. The presence of Paleocene sediments in the Western Cordillera is uncertain. In the east it is represented by fine-grained siliciclasts intercalated with evaporites and marls (Koch and Blissenbach 1962; Fyfe, 1963).

To the south, along the western border of the Western Cordillera, numerous igneous intrusions and extrusions occur (Beckinsale et al., 1985). To the east purple shales represent the Paleocene.

2.4 EOCENE TO HOLOCENE

This period records six successive phases of compression (Sébrier and Soler, 1991), (Figure 2.3) which proceeded from southwest to northeast. These are: the late Eocene or Incaic phase (Steinmann, 1929), the late Oligocene or Aymara event, the early Miocene or Quechua 1 event, the middle Miocene or Quechua 2 event, the late Miocene or Quechua 3 event and the latest Pliocene-early Pleistocene compression. Sébrier and Soler (1991) pointed out that extensional deformation between two successive compressional events reported by Mégard (1984, 1987) is restricted to areas "where topographic forces, either regional or local, were acting".

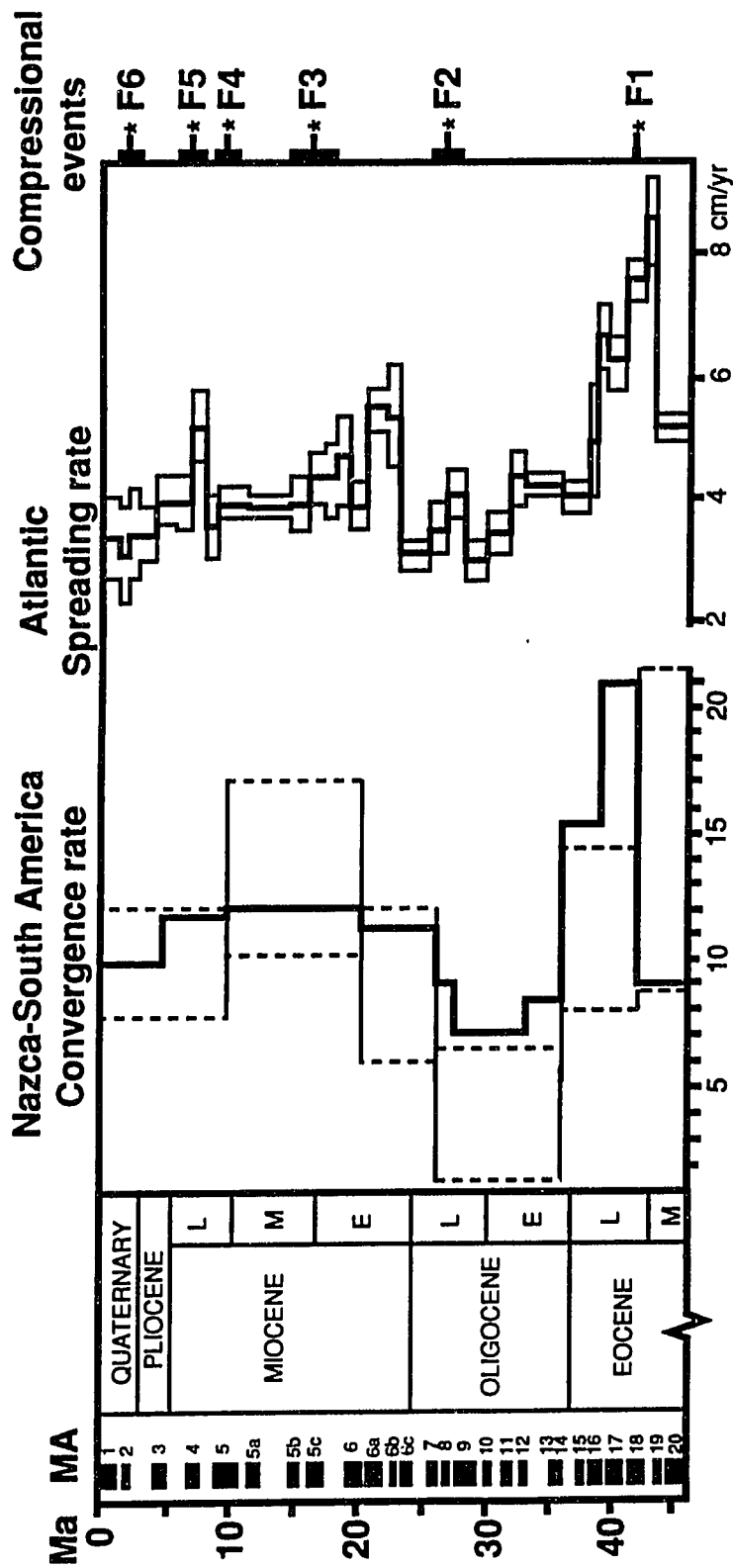


Figure 2.3. CHRONOLOGY OF COMPRESSIONAL EVENTS F1 THROUGH F6 OBSERVED IN THE CENTRAL ANDES SINCE LATE EOCENE TIME. Convergence rate between the Nazca (Farallon) and South American plates from Pilger (1983), space between dashed lines represents uncertainties on convergence rate calculated by Pardo Casas and Molnar (1987). Equatorial Atlantic western half-spreading rate from Brozena (1986). Magnetic anomalies and chrono-stratigraphy from Berggren and others (1985). Compressional events see text pages 26 and 28.

Sébrier and Soler, 1991

(1) The late Eocene or Incaic phase (Steinmann, 1929). This compressive event created the Marañon fold and thrust belt (Mégard, 1987) (Figure 2.1), which thrust the thick prism of sediments that accumulated in the northeastern part of the Western Cordillera zone to the northeast. This is the first Tertiary Andean phase of deformation. Although poorly known, a widespread unconformity overlain by coarse-grained sediments suggests the importance of this tectonic event (Jaillard, 1992). In the northern Talara Basin, lower Eocene sands and conglomerates unconformably overlie Paleocene deposits (Marsaglia and Carozzi, 1990). On the central coast a 54-50 Ma magmatic hiatus occurred (Beckinsale et al., 1985, Soler and Bonhomme, 1990). In the northern Western Cordillera, a series of conglomerates associated with a 54 Ma tuff disconformably overlies Maastrichtian red beds (Naeser et al., 1991).

In the southern coastal area, magmatism ceased by 60 Ma. In the eastern region Eocene conglomerates disconformably overlie Maastrichtian to earliest Paleocene rocks (Jaillard, 1992).

(2) The late Oligocene or Aymara event (Sébrier and Soler, 1991) has been identified along the Peruvian coast where Sébrier and Soler (1991) report a NNE-SSW trending direction of shortening.

(3) The early Miocene or Quechua 1 event (Mégard, 1973). This event has been documented in northern Peru (Mourier, 1988; Noble et al., 1990), in central Peru (Soulas, 1977; Romani, 1982; Mégard et al., 1984; Angeles, 1987) and in southern Peru (Sébrier et al., 1982, 1988). The shortening direction in central Peru is probably NE-SW (Soulas, 1977) and E-W on the southern coast (Huaman, 1985). By the end of this phase, lacustrine to fluvial sediments accumulated in the Andes as minor intercalations within dominantly volcanic units. Some elongated foredeep basins received thick sequences of sedimentary and volcanic material.

(4) The middle Miocene or Quechua 2 event has been reported in central Peru (Soulas, 1977; Romani, 1982, and Mégard et al., 1984) and in southern Peru (Huaman, 1985; Sébrier et al., 1988). The shortening direction of this event is similar to that of the Quechua 1.

(5) The late Miocene or Quechua 3 phase (Mégard, 1973) produced the sub-Andean fold and thrust belt (Figure 2.1) and folded previous foredeep deposits. In southern Peru a narrow late Miocene sub-Andean fold and thrust belt (Figure 2.1) is also present. Soulas (1977), Fornari and Vilca (1978), Mégard et al. (1984), and Huaman (1985) report an E-W direction of shortening.

(6) The latest Pliocene-early Pleistocene event. After the Quechua 3 phase of deformation, i. e. from Pliocene to Recent time, the Andes were uplifted at least 3,000 m. Folds and thrusts were produced in the Subandean zone while strike-slip faulting with localized folding are present in the High Andes and Coastal zone (Sébrier and Soler, 1991). Sébrier and Soler (1991) described two directions of shortening in the Peruvian Andes: an older E-W trending shortening direction and a younger N-S trending direction of shortening.

Pliocene extension was reported by Macharé (1987) and Huaman (1985) in the Pisco Basin and the Camana area (southern coast) respectively. Macharé (1987) documents an early Quaternary compressive event and a Quaternary to present-day extensional stress regime along the southern coast.

2.5 PLUTONISM

Plutons emplaced during the Andean Cycle underlie large areas of the Peruvian Andes (Mégard, 1987). According to Cobbing and Pitcher 1972), Myers (1975), Pitcher (1978), Cobbing et al. (1981) and Pitcher et al. (1985) the Coastal Batholith (Figure 3.1), the largest set of plutons located parallel to the coast, was formed by successive intrusions emplaced between 100 and 32 Ma (early Albian to early Oligocene). Emplacement occurred by cauldron subsidence

and associated piecemeal stoping, involving almost no deformation of host rocks. The older plutons are composed of hornblende gabbros that subsequently were intruded by large lenticular bodies of tonalites and granodiorites; granites are generally younger and commonly occur in centered complexes associated with ring dikes (Mégard, 1987). From 35 to 7 Ma, magmatic activity migrated northeastward and gave rise to small plutons of gabbroic to granodioritic composition. Miocene alkaline stocks occur in the central Eastern Cordillera and Pliocene peralkaline stocks were reported in the Amazon plain (Sébrier and Soler, 1991), (Figure 2.4).

2.6 TERTIARY VOLCANISM

Tertiary synorogenic arc volcanic activity extended from the latest Cretaceous to the Recent. Tertiary magmatic arcs were centered on the Western Cordillera and Altiplano (Noble et al., 1984; McKee et al., 1982) and volcanism was exclusively terrestrial. The rocks are of intermediate and silicic composition, ranging from basic andesites to rhyolites, with andesites and dacites being the most widespread. Volcanism was very intense during late Eocene and early Oligocene (40 to 35 Ma) and again during Miocene and Pliocene (Noble, 1974; McKee and Noble, 1982). From 26 Ma to 3-5 Ma calc-alkaline magmatic activity occurred along the Western Andes and part of the Altiplano (Figure 2.4) (Sébrier and Soler, 1991). Since 3-5 Ma to the present calc-alkaline magmatism continued in the

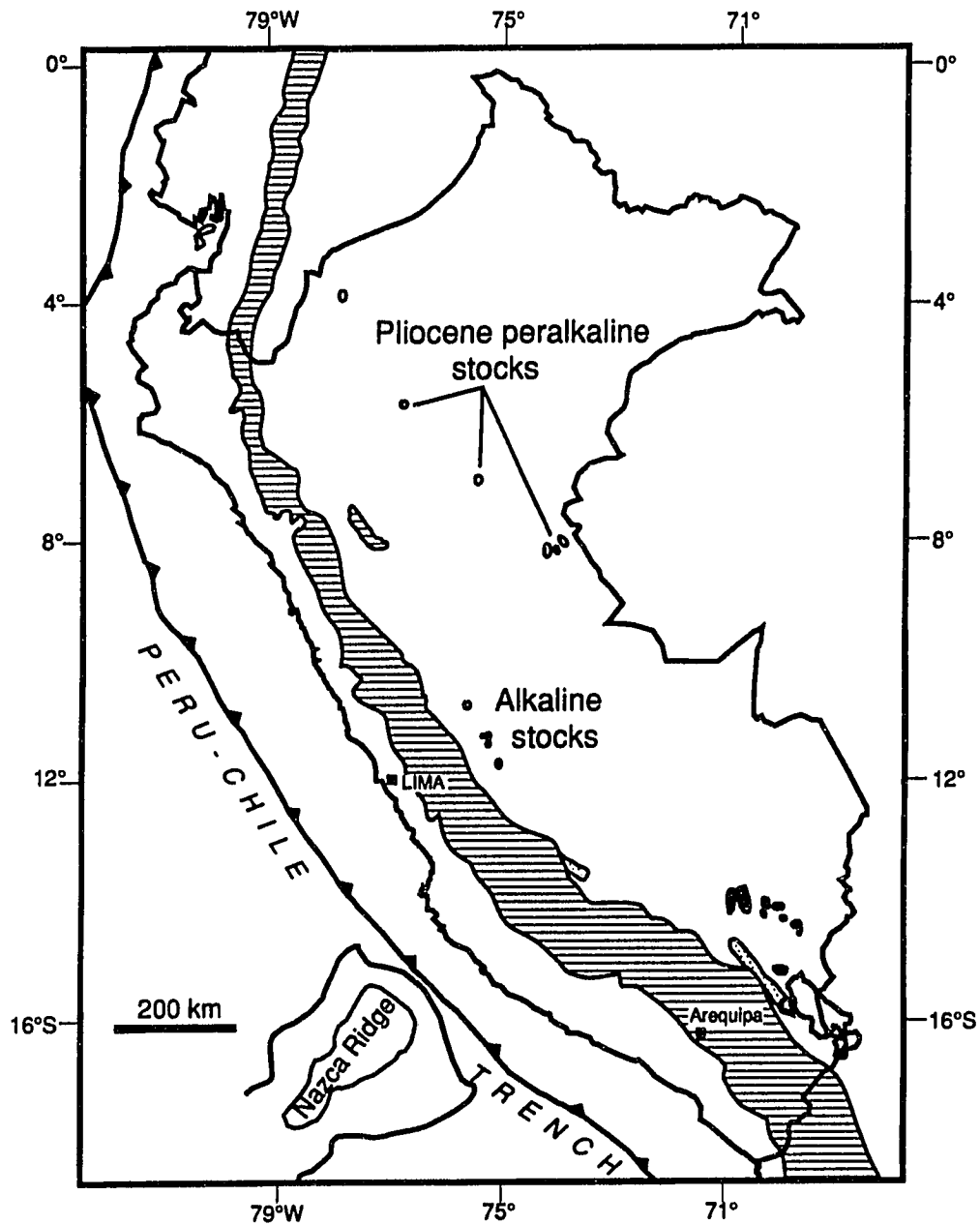
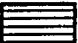




Figure 2.4 MIOCENE AND PLIOCENE MAGMATIC ACTIVITY

From Sébrier and Soler (1991)

LEGEND

Calc-alkaline arc		Shoshonitic rocks		Peraluminous felsic volcanic and plutonic rocks	
-------------------	---	-------------------	---	---	---

southern Western Cordillera only (Figure 2.5), (Noble and McKee, 1982; Sébrier and Soler, 1991). At least part of the Tertiary volcanics in the Western Cordillera are probably genetically linked to the youngest batholithic plutonics (Noble et al., 1975). Sébrier and Soler (1991) described the occurrence of Miocene to Pliocene felsic volcanics in the southern Eastern Cordillera and Miocene to Quaternary shoshonitic volcanics between the Western and Eastern Cordillera (Sébrier and Soler, 1991), (Figures 2.4 and 2.5).

Sébrier and Soler (1991) interpret that: (1) the calc-alkaline magmatism (Figure 2.4) is the normal product of the Nazca Plate subduction beneath an asthenospheric mantle wedge; (2) the occurrence of back-arc Miocene alkaline magmatism in central Peru was promoted by the increase in the convergence rate (Figures 2.3 and 2.4); (3) the Miocene to Present shoshonitic volcanism of southern Peru (Figure 2.4 and 2.5) was controlled by deep-seated faults; and (4) the peraluminous felsic intrusions of the southern Eastern Cordillera were controlled by underthrusting of the Brazilian shield under the Andes.

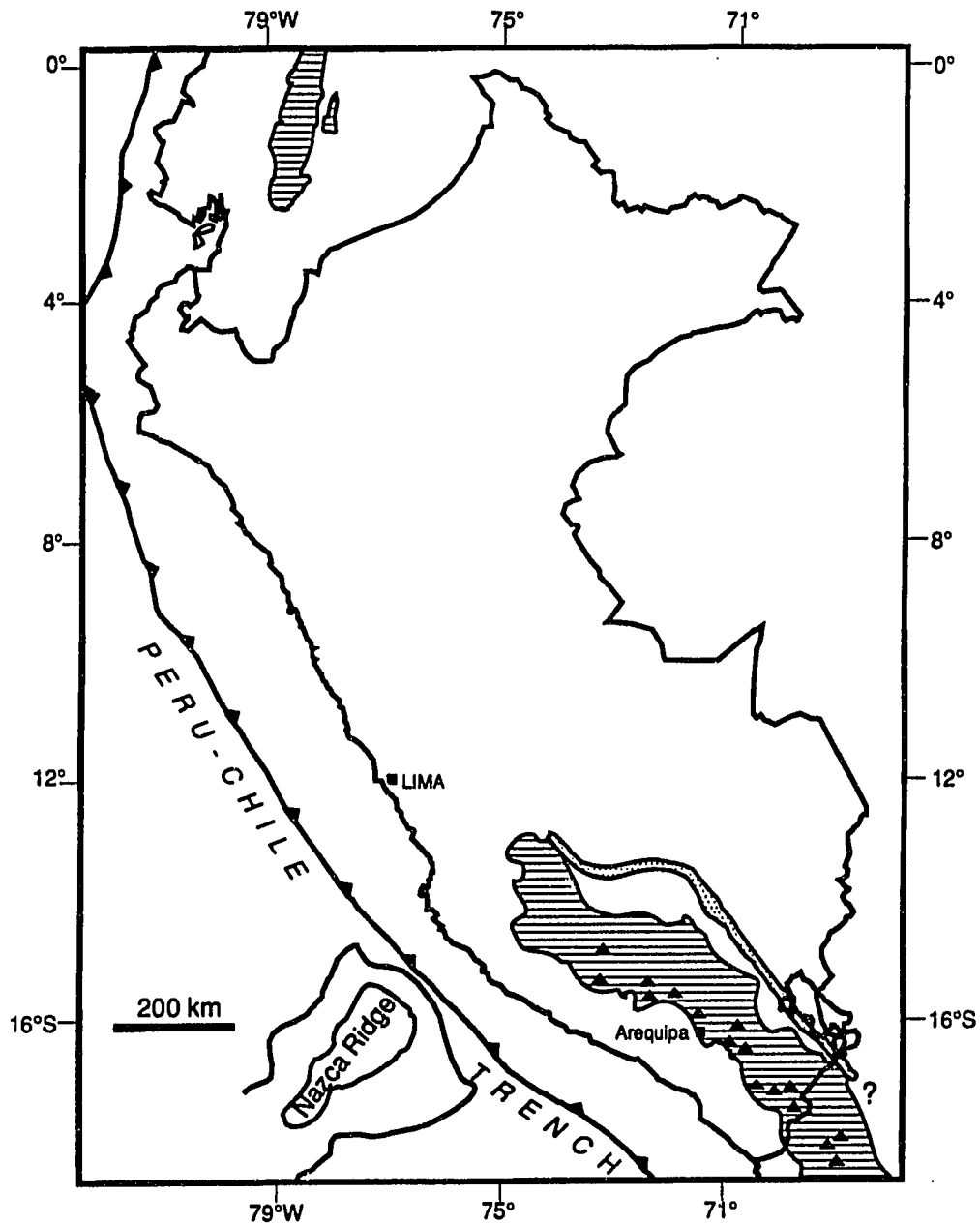


Figure 2.5 LATEST PLIOCENE AND QUATERNARY MAGMATIC ACTIVITY

From Sébrier and Soler (1991)

LEGEND

Calc-alkaline arc  Shoshonitic rocks  Active or Recent volcanoes 

CHAPTER 3: STUDY AREA STRATIGRAPHY

3.1 INTRODUCTION

The Peruvian Cenozoic forearc basins described in this study typically are filled with Eocene to Quaternary, marine, consolidated to poorly consolidated mostly fine-grained siliciclastics, biogenic sediments and minor fine-grained volcanics. These basins are floored by a deformed and heterogeneous (in age and lithology) basement ranging in age from Precambrian to Cretaceous.

The boundaries of the forearc basins are related to three topographically positive linear trends (Figure 3.1): (1) The onshore Coastal Batholith composed of arc-derived late Cretaceous to Eocene igneous rocks (Cobbing and Pitcher 1972; Noble et al., 1979), (2) the adjacent Western Cordillera (Figure 1.2) composed of deformed Mesozoic and Tertiary strata and, (3) The Coastal Range, a high area cored by Precambrian granulitic gneisses and granites and Paleozoic metasediments (Bellido and Narvaez, 1960; Cobbing et al., 1977; Caldas, 1983). Its submerged extension along central Peru is a discontinuous basement high named the Outer Shelf High (Figure 3.1) by Thornburg and Kulm (1981), even though the high does not always correspond to the shelf edge. In order to describe the forearc basins, the study area has been geographically subdivided into eight zones (Figure 3.2). These are: the Talara, Sechura, Trujillo, Salaverry,

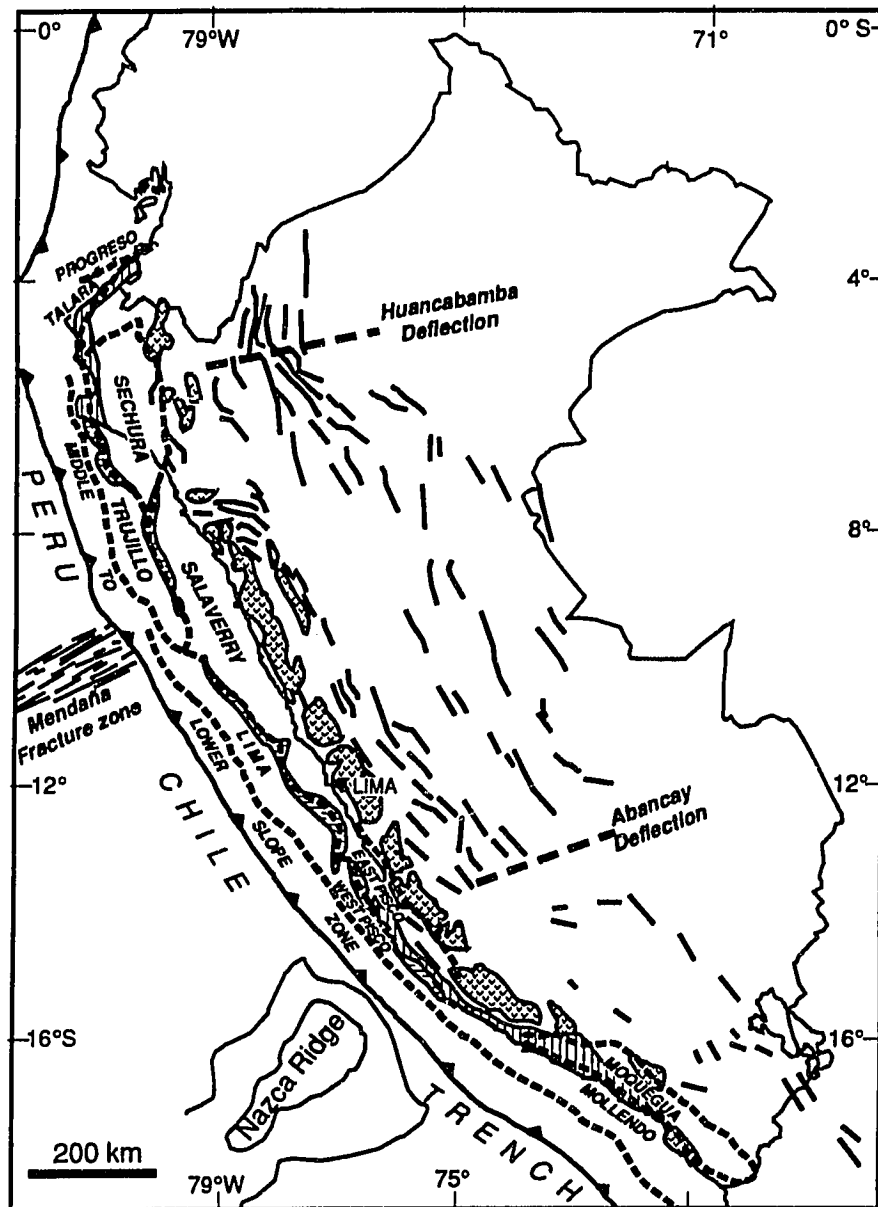
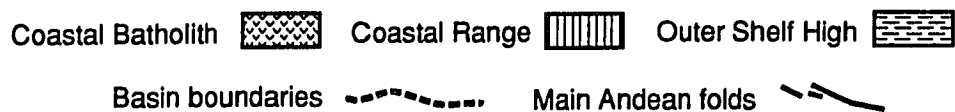


Figure 3.1 LINEAR TRENDS AND FOREARC BASINS OF PERU

After Travis (1979), Thornburg and Kulm (1981), Mégard (1987),
and Hilde and Warsi (1982)



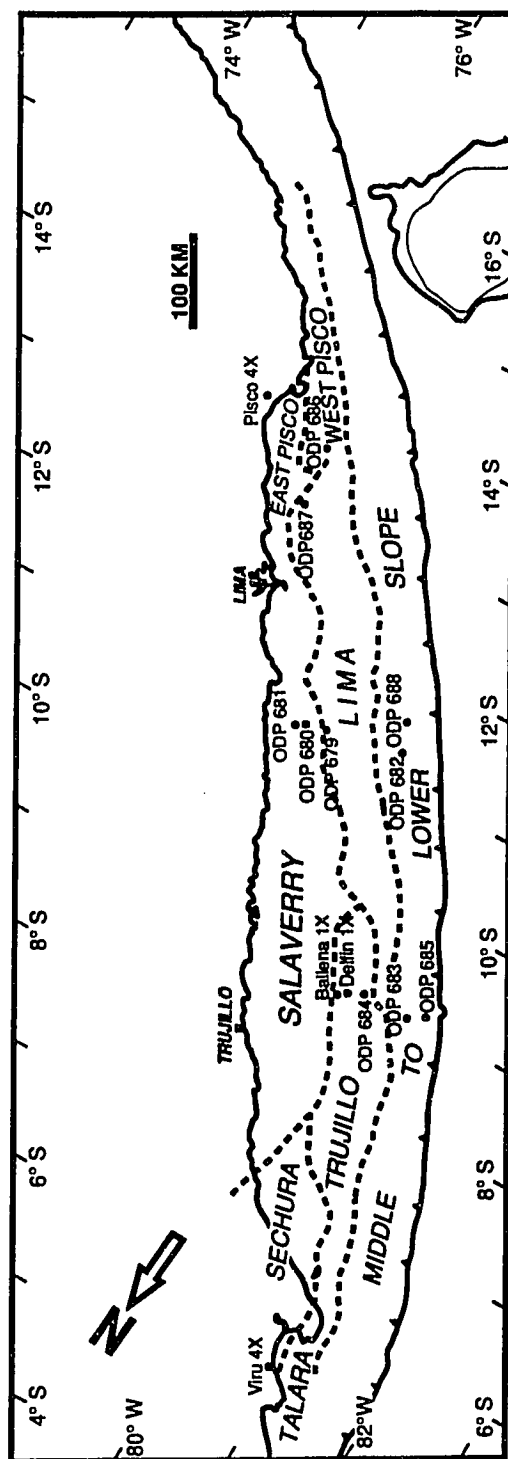


Figure 3.2 ZONES OF THE STUDY AREA

Zone boundaries - - - - -

Lima, East Pisco, West Pisco and middle-lower Slope zones. With the exception of the Yaquina Basin (Figure 3.1) which is included in the Trujillo Basin zone, I have accepted the basin boundaries proposed by Thornburg and Kulm (1981).

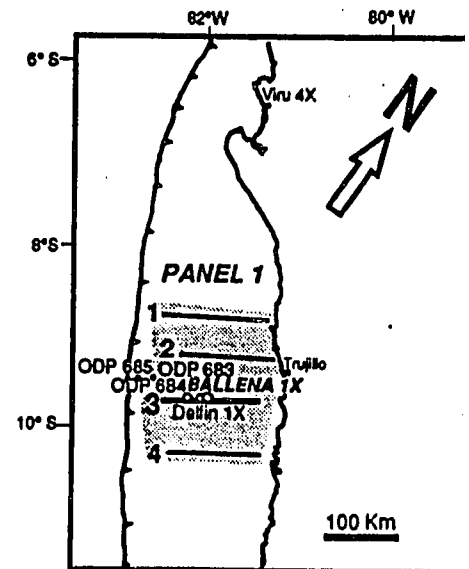
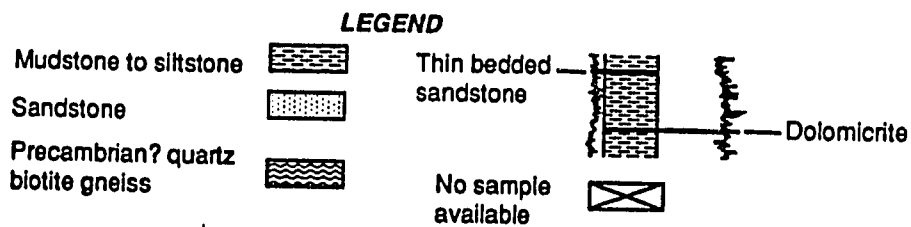
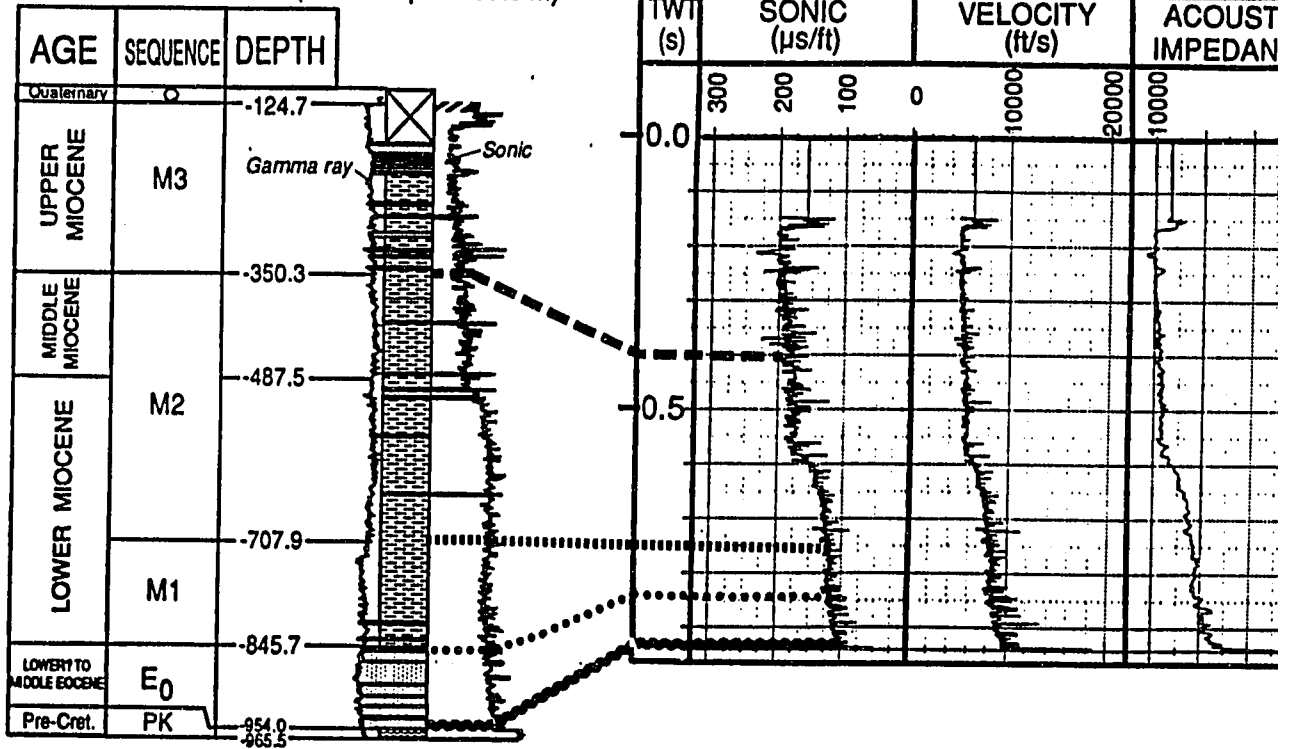
Lithologic, biostratigraphic (Okada, 1990; Appendix A; and Schrader and Cruzado, 1986) and paleoenvironmental (Engelhardt-Moore, 1991; Appendix B) studies of cuttings of the Delfin and Ballena wells, along with the detailed lithologic, biostratigraphic and paleobathymetric data provided by the Ocean Drilling Program Leg 112 (Suess E., von Huene R., et al., 1988), provide the stratigraphic basis for this study. I use synthetic logs when they are available (two examples are shown in Figures 3.3 and 3.4) and seismic reflection data to tie together these sparse points of stratigraphic control to identify and correlate the main Cenozoic stratigraphic sequences.

3.2 PRE-CENOZOIC BASEMENT

Pre-Cenozoic onshore outcrops and industry wells illustrate the basement heterogeneity everywhere along the forearc. Onshore, in the northernmost Progreso Basin (Figure 1.4), industry wells reveal that Tertiary sediments rest on gneissic rocks of pre-Paleozoic age. Cenozoic rocks of the adjacent Talara Basin are floored by Upper Cretaceous (Maastrichtian) fine-grained

BALLENA 1X

(Water depth: 105.8 m)



er depth: 105.8 m)

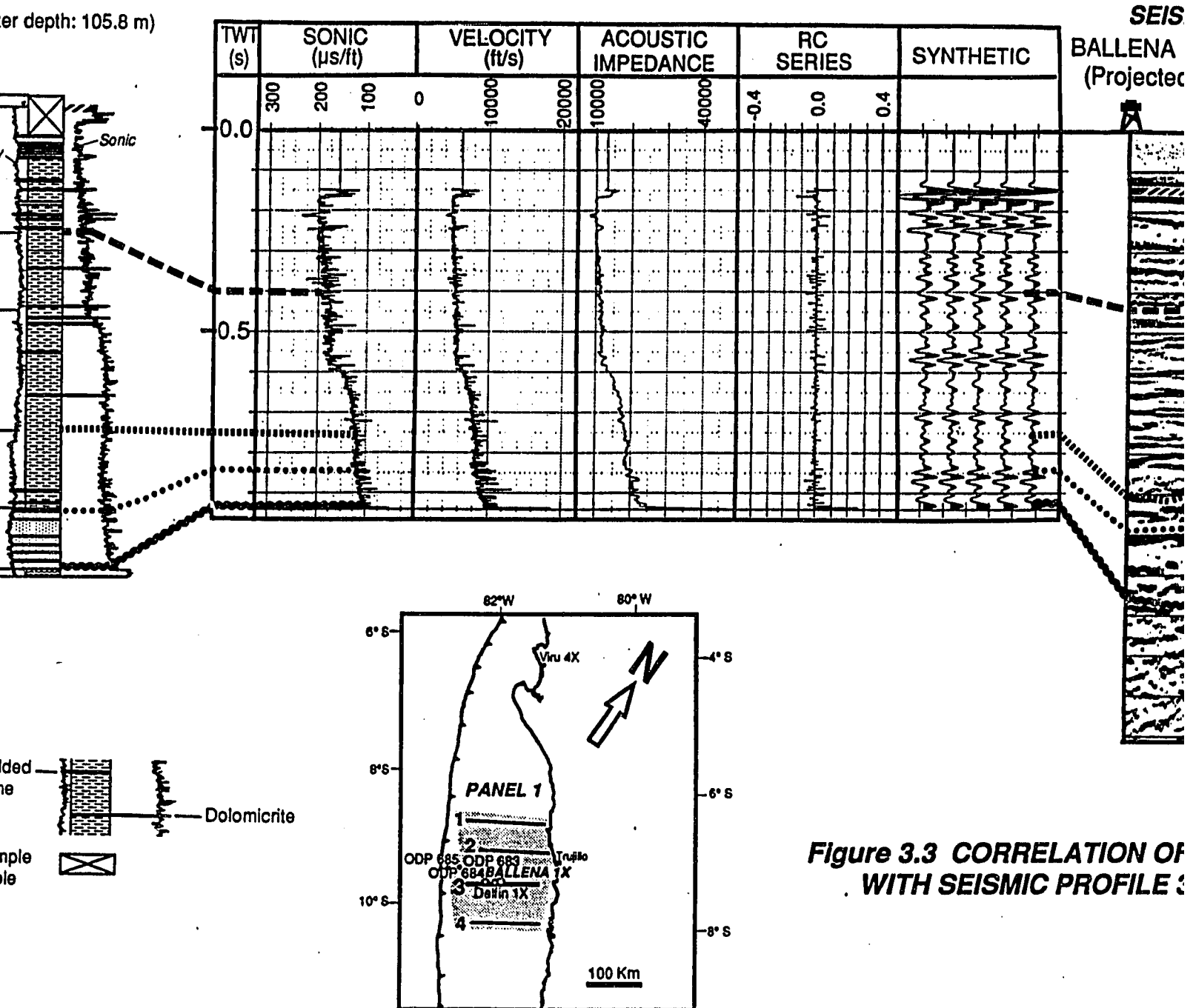
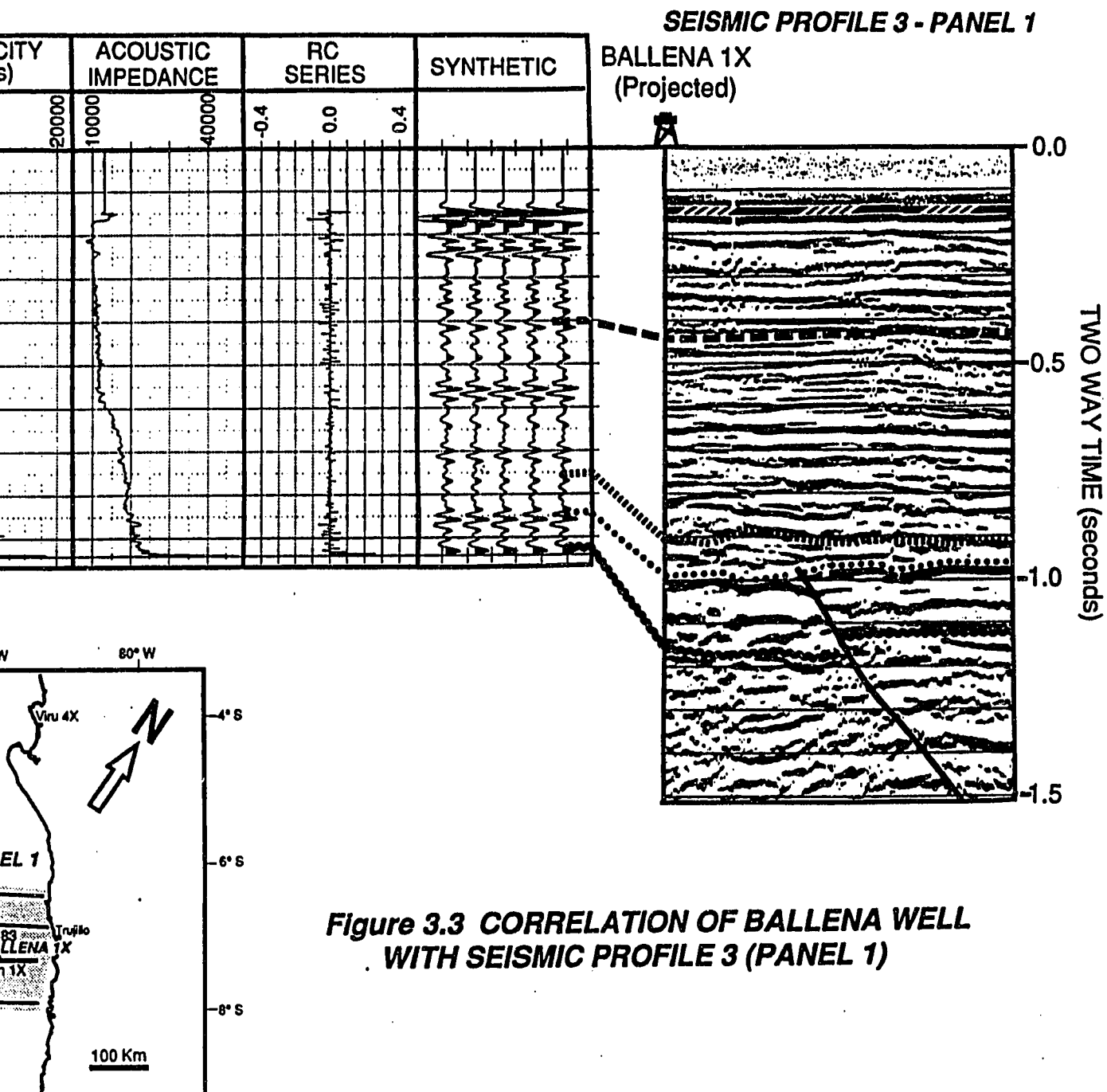


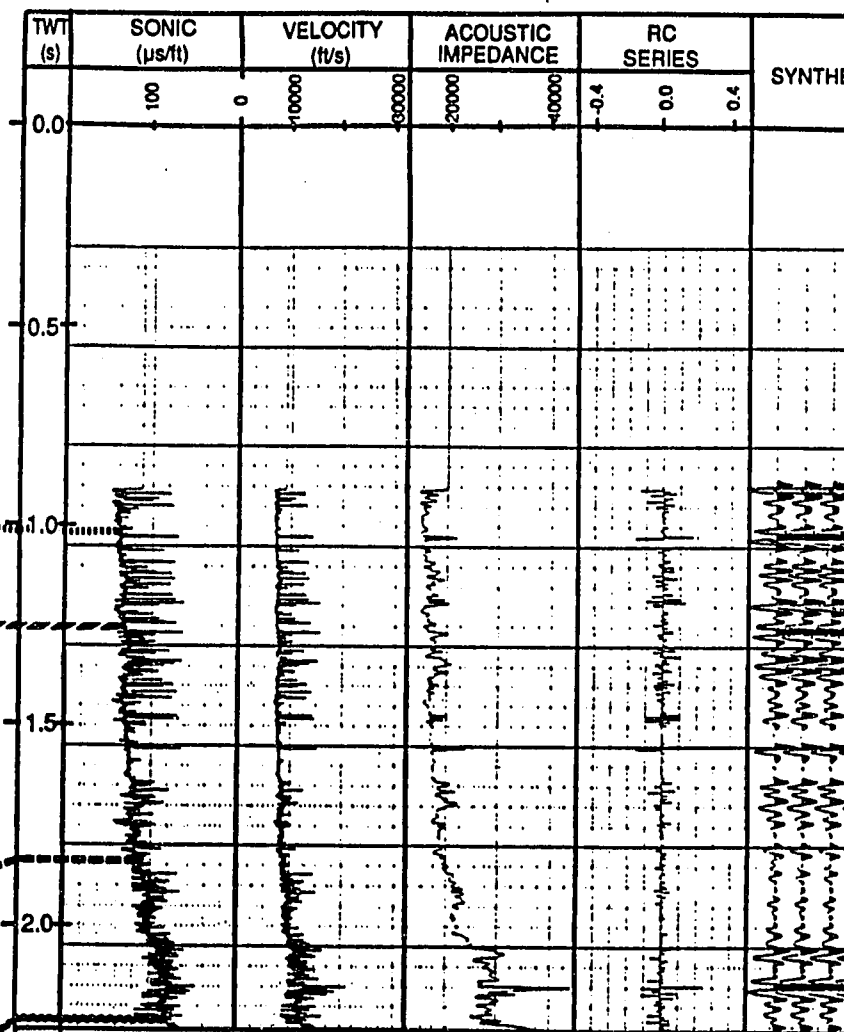
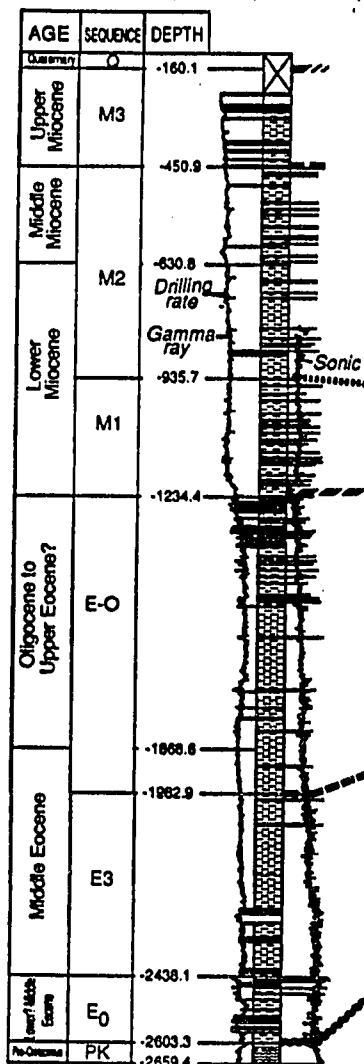
Figure 3.3 CORRELATION OF ... WITH SEISMIC PROFILE



**Figure 3.3 CORRELATION OF BALLENA WELL
WITH SEISMIC PROFILE 3 (PANEL 1)**

DELFIN 1X

(Water depth: 118.6 m)



LEGEND

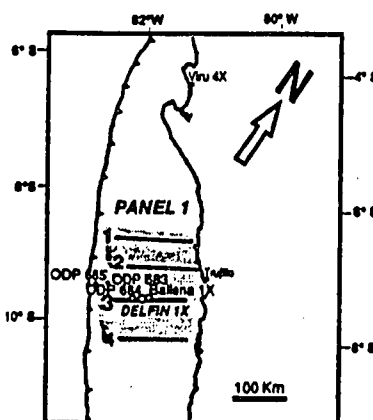
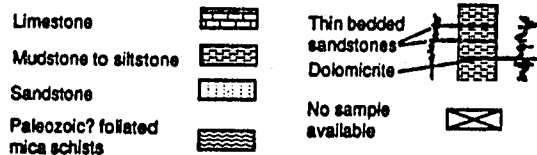
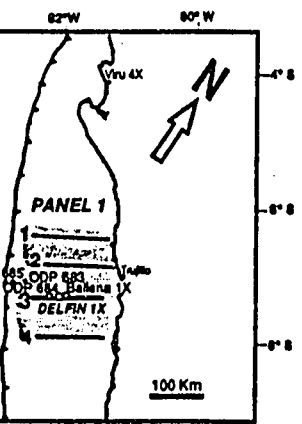
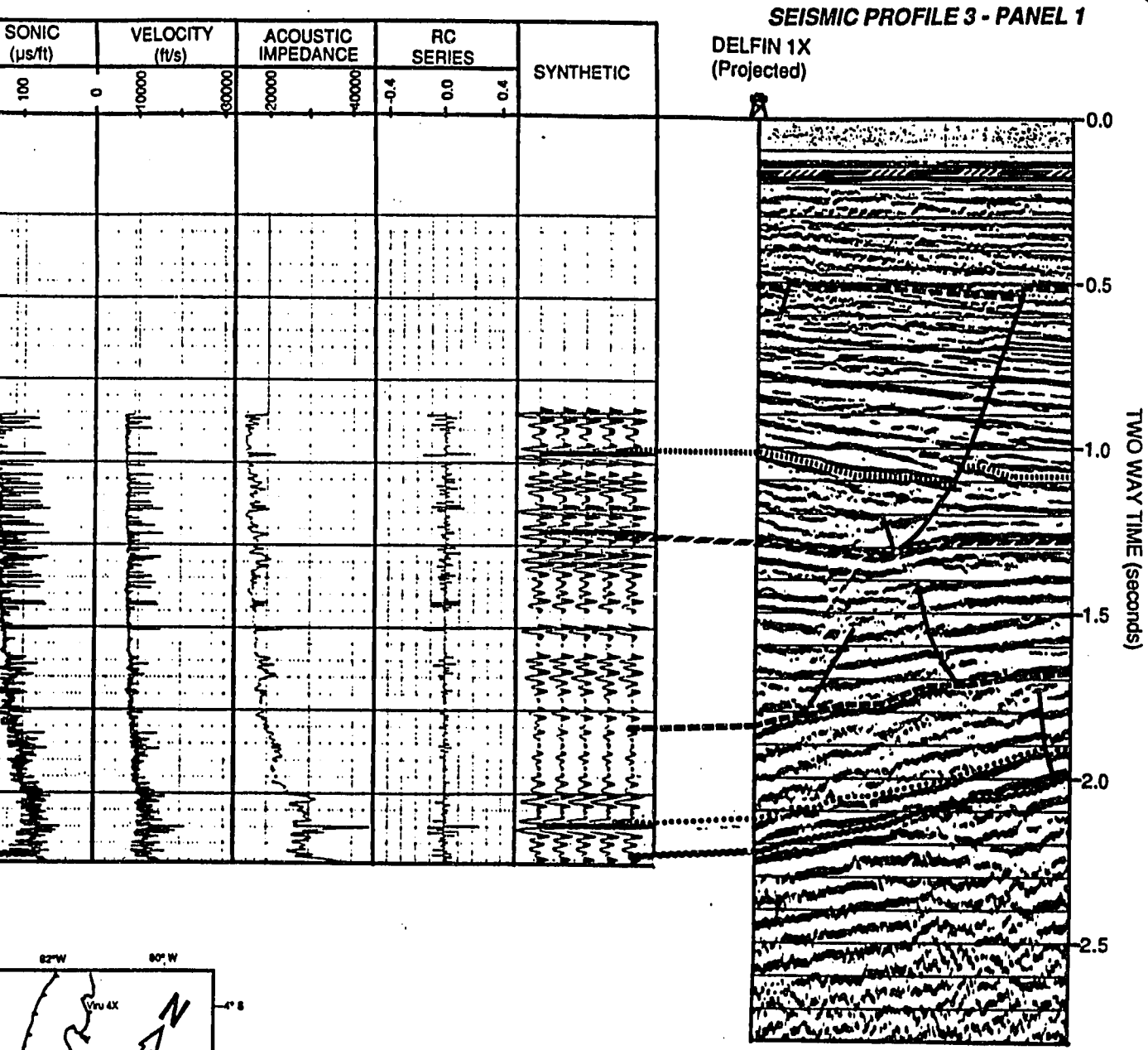


Figure 3.4 (WITH SE



**Figure 3.4 CORRELATION OF DELFIN WELL
WITH SEISMIC PROFILE 3 (PANEL 1)**

siliciclastics or else by slates and quartzites of Paleozoic (Pennsylvanian) age. In the onshore Sechura Basin segment, the basement includes Maastrichtian sediments similar to those present in the Talara Basin and Pre-Tertiary igneous rocks.

The onshore Cenozoic East Pisco Basin is bounded to the east by Mesozoic igneous rocks of the Coastal Batholith (Figure 3.1), volcanics and coarse-grained siliciclastics of the Western Andes chain and by Precambrian to Jurassic igneous, metamorphic and sedimentary rocks of the Coastal Range to the west. These rocks seem to extend below the Tertiary sediments throughout the whole area. The Pisco 4X well and a shallow stratigraphic "Core Hole" (Figure 3.5) reached quartzites and shales of probable early Cretaceous age (at -679.99 m) (Morris, 1955), and Jurassic rhyolites (at -100 m) respectively.

On the Paracas Peninsula and the adjacent San Gallan Island (Figure 3.5), the Eocene Los Chorros Fm. rests on and onlaps Carboniferous coarse siliciclastics and Precambrian igneous rocks respectively. At the Quebrada Huaricangana area (Figure 3.5), andesites and granodiorites of the Cretaceous Coastal Batholith merge with the Coastal Range which consists of Precambrian igneous and metamorphic rocks, Paleozoic limestones and quartzitic phyllites, and Jurassic siliciclastics and volcanics. Cenozoic

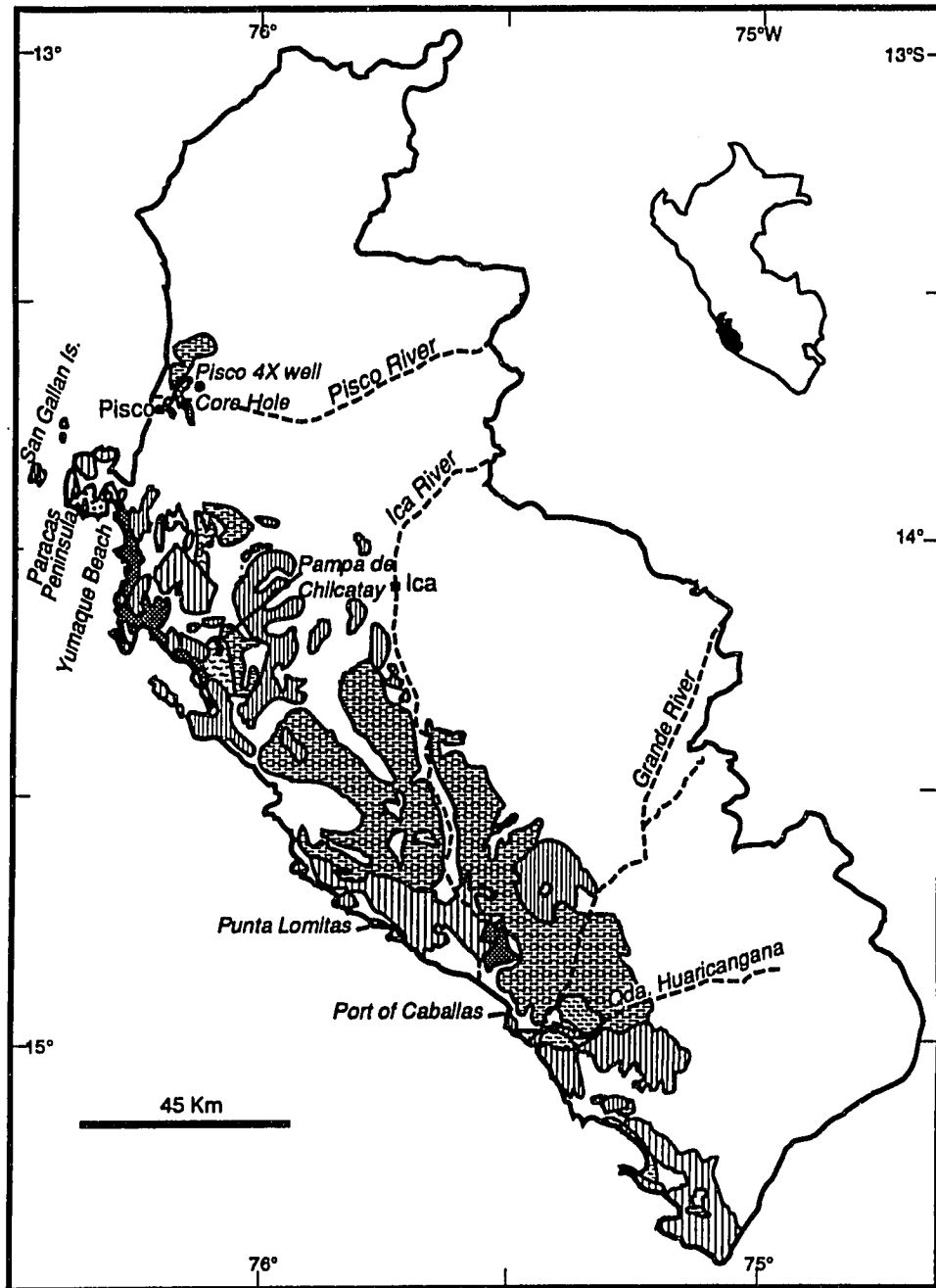
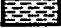






Figure 3.5 GEOLOGIC MAP OF THE ONSHORE EAST PISCO BASIN

After Dunbar et al. (1990)

- | | |
|--|--|
|  Miocene to Pliocene coarse to fine grained clastics and diatomites (Pisco): Sequence P |  Eocene clastics (Paracas): Sequence E3 |
|  Oligocene to Miocene coarse to fine grained clastics (Chilcatay): Sequences E-O, M1 and M2 |  Basement: Pre-Tertiary plutonic, volcanic, and metasedimentary rocks |
|  Eocene fine grained clastics and diatomite (Yumaque): Seq. E-O? | |

sediments rest upon and onlap these Cretaceous and older basement rocks (Stock, 1989).

On the northern Lobos de Tierra and Lobos de Afuera Islands, (Figure 1.2) outcrops of probable Paleozoic age occur (Thornburg and Kulm 1981). Kulm et al. (1981) assume that the metamorphic rocks exposed in the Hormigas Island, near 12° S latitude (Figure 1.2), are Paleozoic, while Mégard (1987) suggests that they may be Precambrian. Seismic data from areas adjacent to those islands show Tertiary strata onlapping these older rocks.

Only the Ballena 1X well, located near the boundary between the Trujillo and Salaverry Basins (Figure 3.2 and 1.5), and the Delfin 1X well, drilled in the Trujillo Basin 10 km west of the Ballena well, penetrated basement. At the Ballena (-965.5 m) and Delfin (-2659.4 m) drill sites the basement consists of quartz-biotite gneiss and foliated mica schists respectively (Figures 3.6 and 3.7). Although these rocks are not yet dated, Kulm et al. (1982) consider them to be part of the Outer Shelf High, the offshore extension of the Coastal Range, and suggest a Paleozoic-Precambrian age.

3.21 The late Cretaceous (Sequence K)

Although this study is focused on the Cenozoic forearc basins, an older unit, sequence K of probable upper Cretaceous age, has been

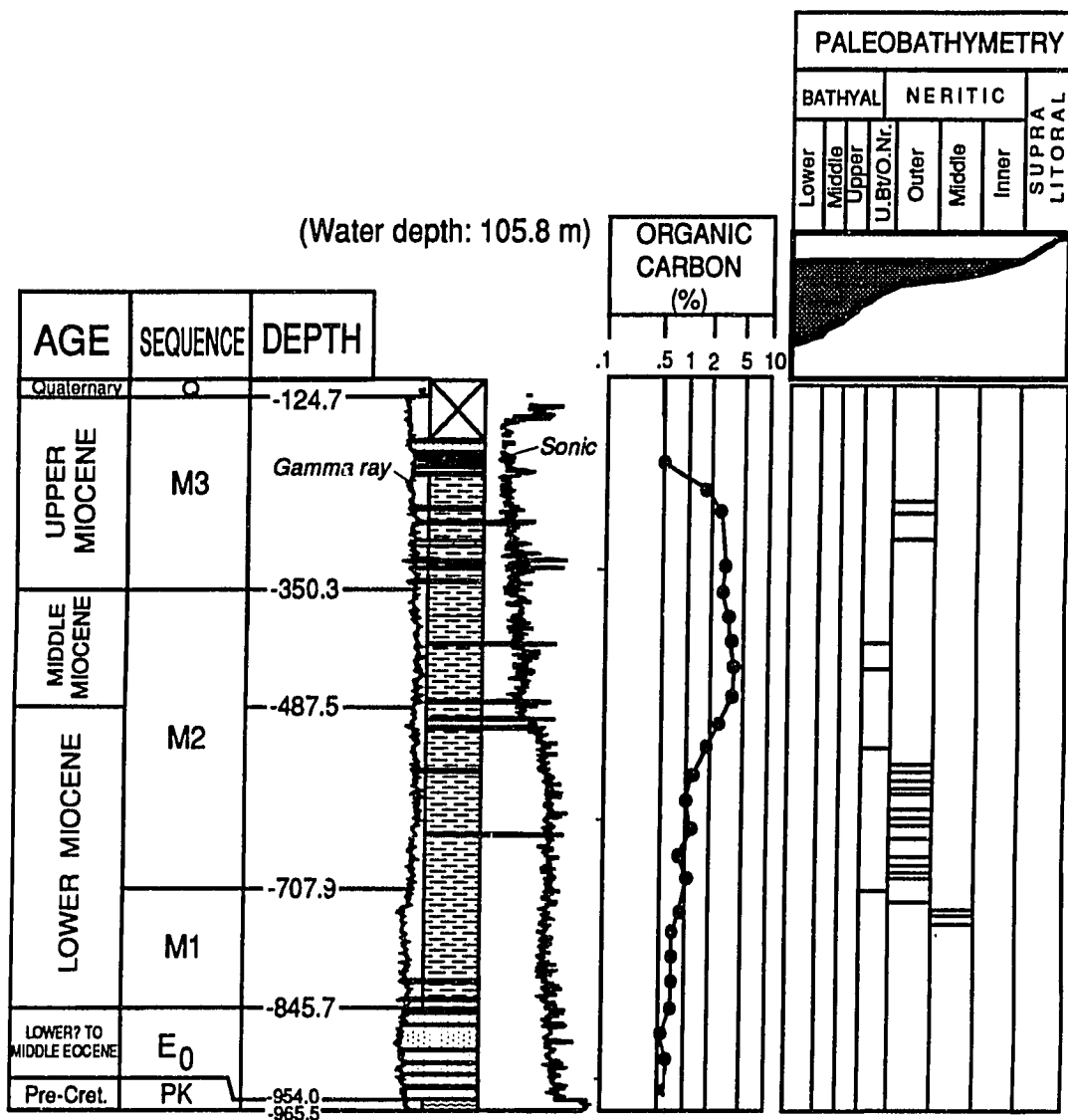
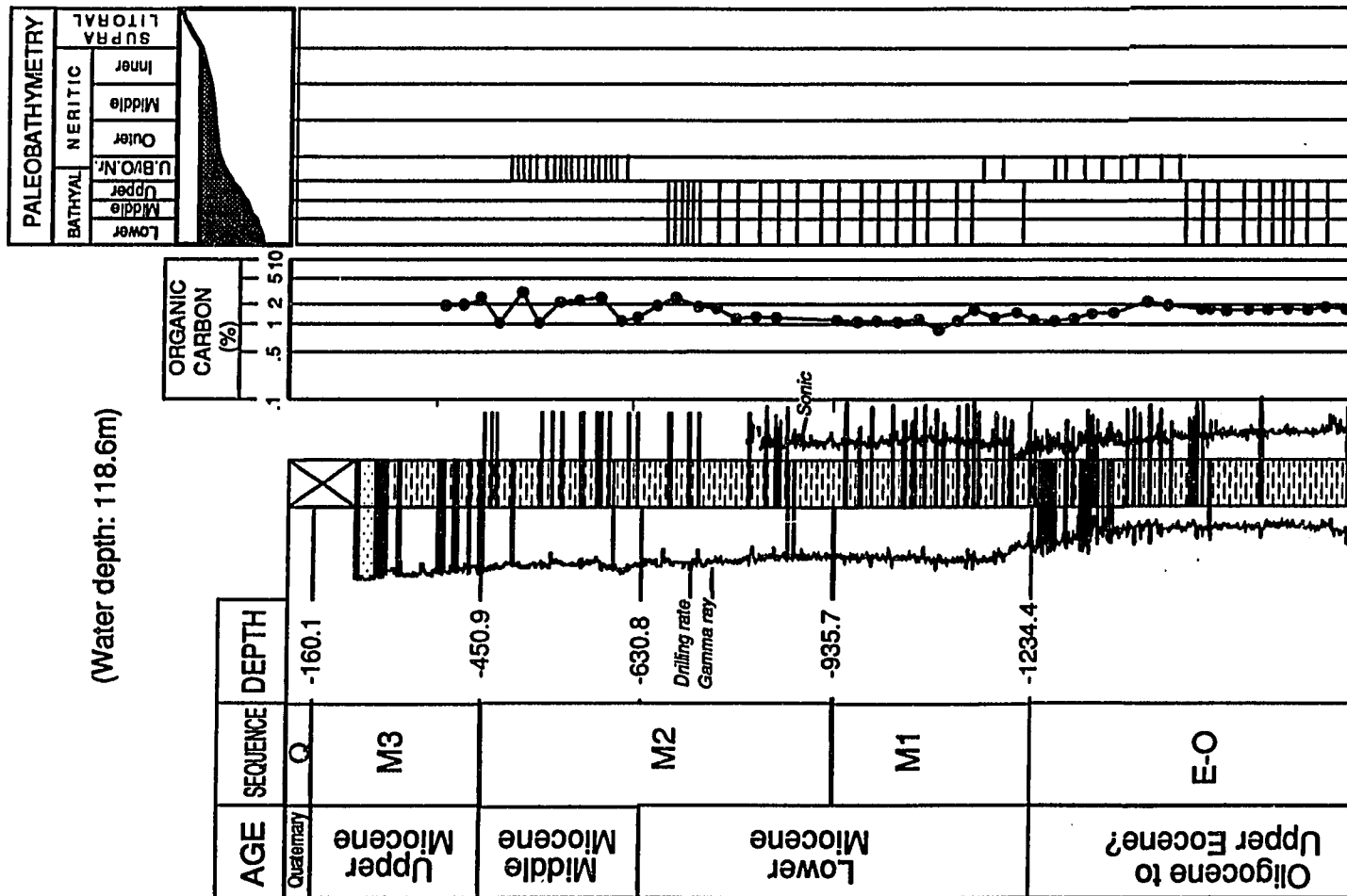


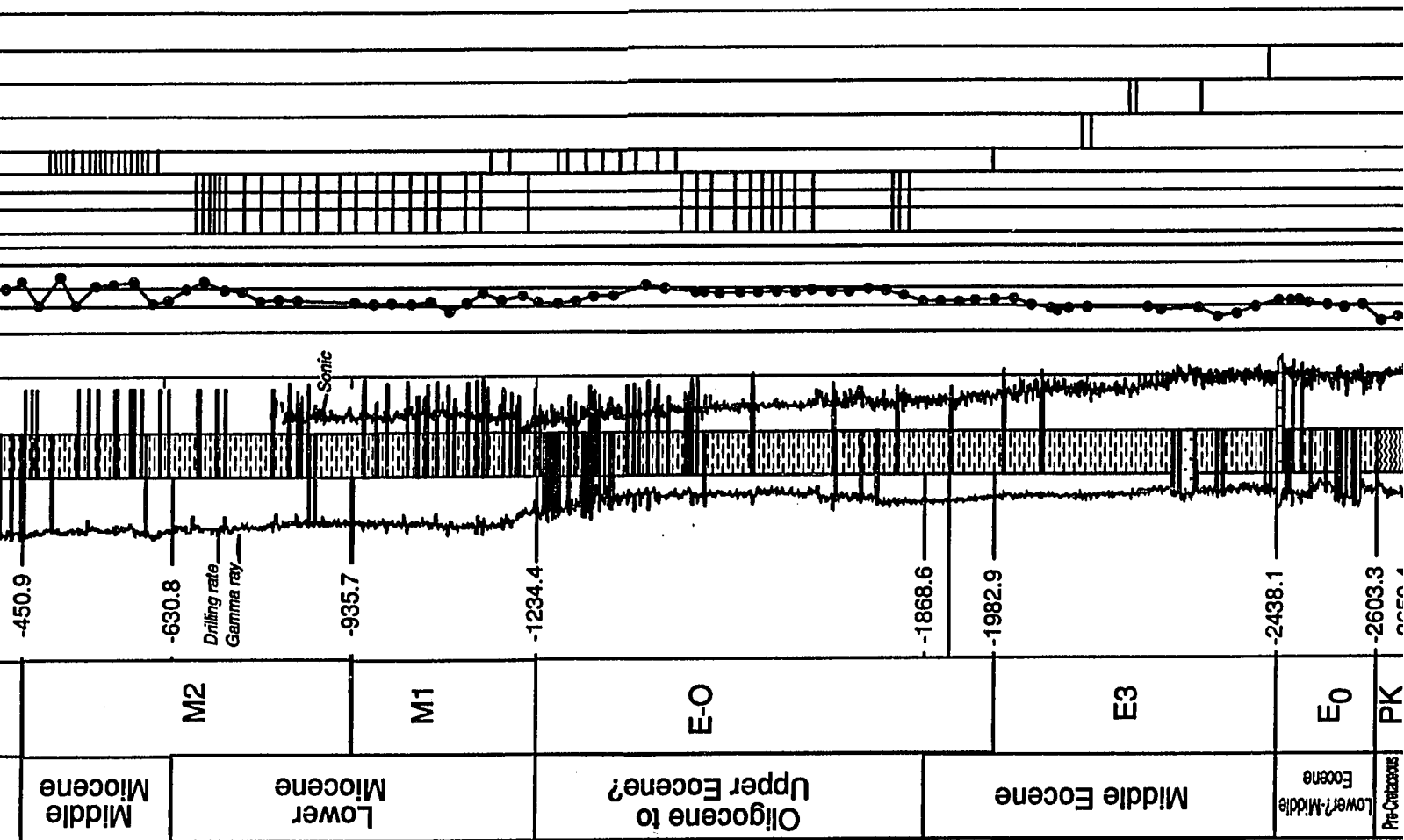
FIGURE 3.6 BALLENA WELL STRATIGRAPHIC COLUMN

LEGEND



(Water depth: 118.6m)





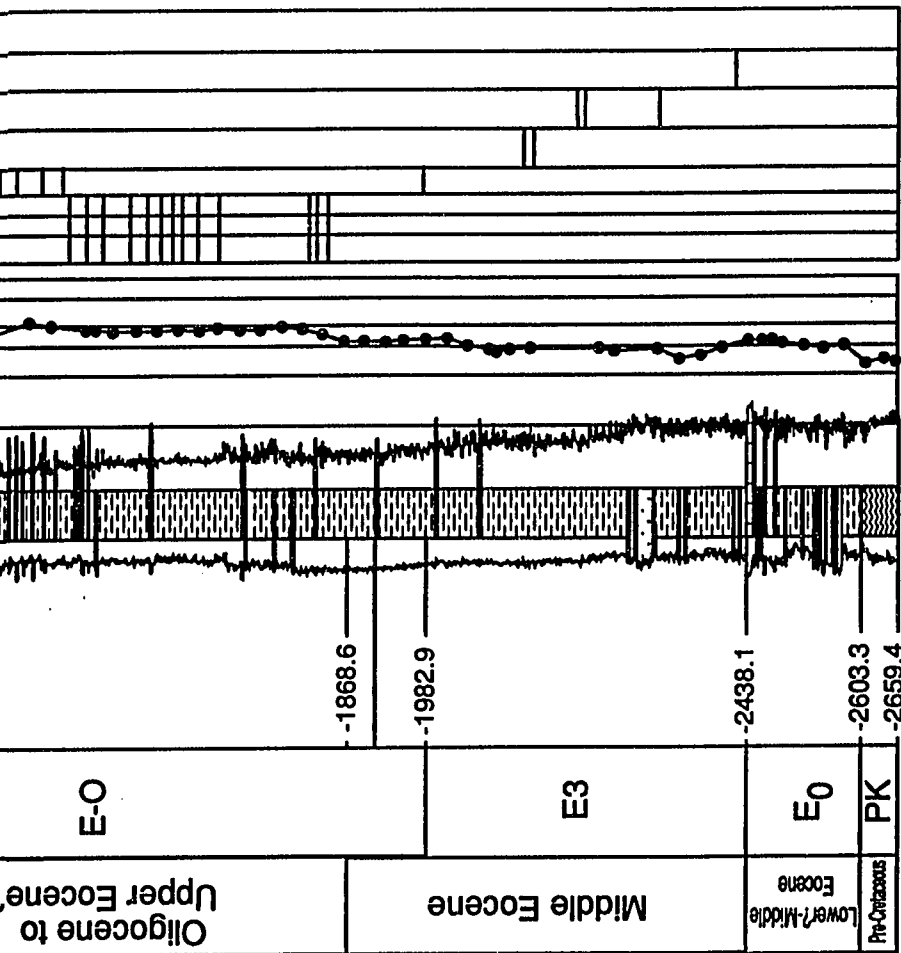
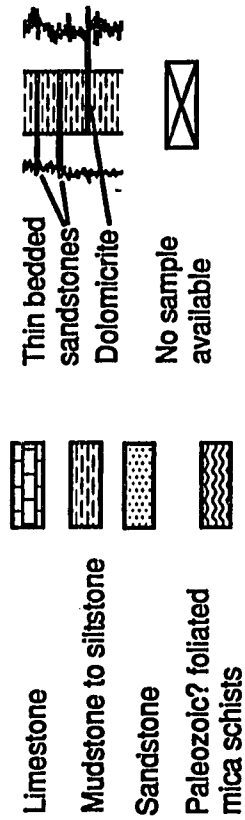


FIGURE 3.7 DELFIN WELL STRATIGRAPHIC COLUMN

LEGEND



recognized and correlated on seismic profiles (Figure 3.8, Panels 1 to 4) along the Sechura and Salaverry Basin area. Seismic correlation of the base of sequence K is difficult due to the presence of numerous multiples. Generally the base of sequence K is better defined on seismic profiles of the Compagnie Générale de Géophysique survey. It is unclear whether the K unit extends farther south to the East Pisco Basin or to the western Trujillo, Lima and West Pisco Basins.

Seismic profiles (Panels 1 to 4 and Plates 4, 6, 8, 10, 11, 13, and 15) reveal that the K sequence is a gently-folded unit which unconformably overlies the metamorphic rocks reached by the Ballena well and unconformably underlies Tertiary strata. The K sequence extends throughout the Sechura and Salaverry Basins (Figure 3.8) and reaches a maximum thickness on the order of 1,200 m (assuming an interval velocity of 3100 m/s) at the center of the Sechura Basin, thinning to the west and east.

Onshore, the Viru 4X well of the Sechura Basin penetrated 2,723 m of Maastrichtian to Campanian? (Ochoa, 1980) fine-grained siliciclastics resting on Paleozoic quartzites (Plate 1). Sequence K appears to be the offshore extension of this unit; therefore I assign a Maastrichtian to Campanian? age.

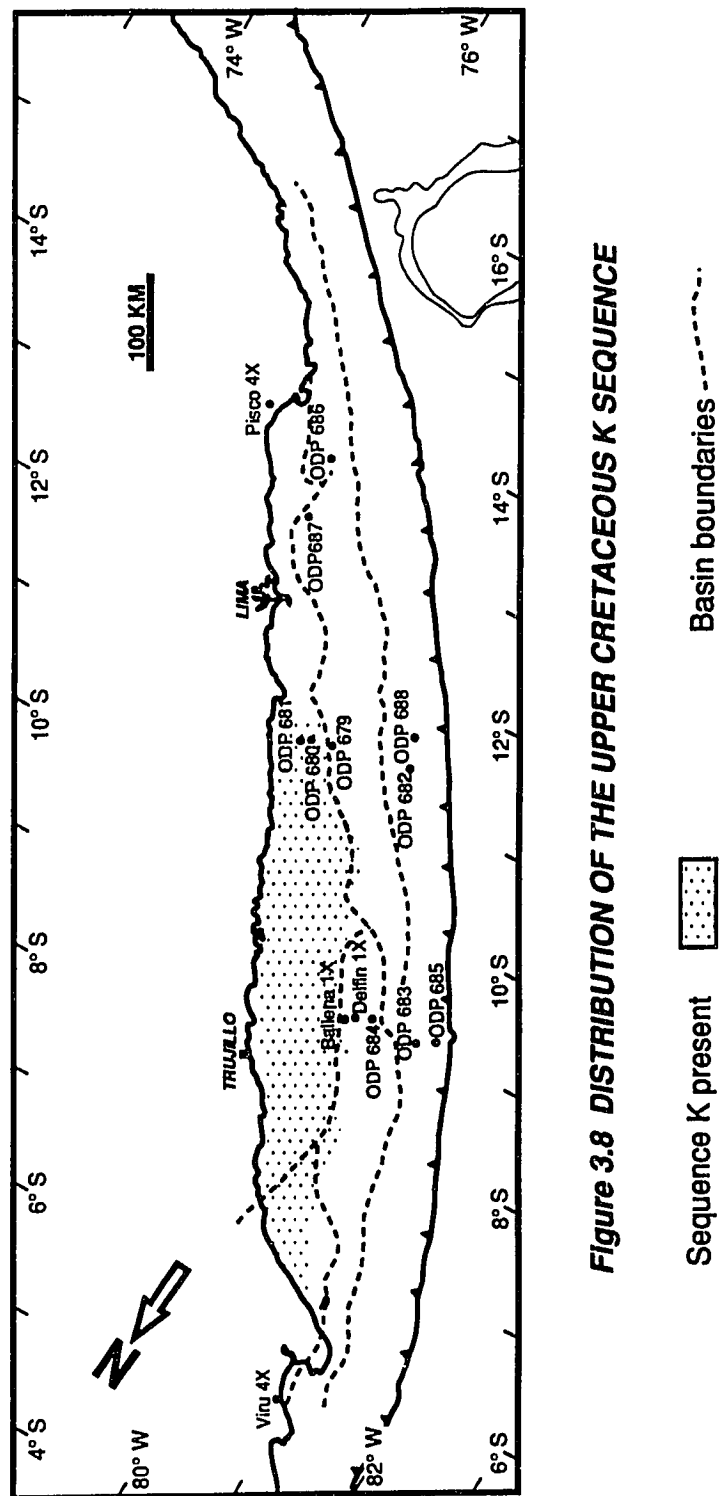


Figure 3.8 DISTRIBUTION OF THE UPPER CRETACEOUS K SEQUENCE

3.3 THE CENOZOIC

Paleocene to Eocene rocks are absent in the northernmost Progreso Basin (Figure 1.4). On the other hand, the adjacent highly oil productive Talara Basin (Figure 1.4), which shows the thickest accumulation of Eocene sediments of the whole forearc, lacks Miocene to Pliocene deposits. This Neogene section was probably removed by erosion after a regional middle-upper Miocene compression. Paleocene sediments are absent in the Sechura, Trujillo, Lima, East and West Pisco Basins. The Tertiary sediment record of these basins is characterized by a very low sand/mud ratio and is dominated by biogenic deposits, mostly accumulated under outer neritic to bathyal conditions. To the south, in the East Pisco and Moquegua Basins, the influence of volcanoclastics increases. Sedimentation in the Moquegua Basin occurred under dominantly non-marine conditions.

3.31 Paleocene

The Talara Basin (Figure 1.4) is the only Peruvian forearc basin with confirmed Paleocene sediments. About 1372 m of mostly fine-grained siliciclastics rest unconformably on Maastrichtian or Paleozoic rocks and underlie unconformably lower Eocene coarse-grained siliciclastics.

Davila et al. (1993, in press) report, east of the port of Caballas, in the Rio Grande Valley of the East Pisco Basin (Figure 3.5), the occurrence of a 100 m thick unit composed of red sandstones, siltstones and mudstones, which rests unconformably on pre-Tertiary basement. This unit, named Caballas Fm. by Caldas (1980), was tentatively dated by Davila et al. (1993, in press) as Paleocene-Eocene. Because the age of this unit is based solely on benthic foraminifera, further paleontological studies may be desirable.

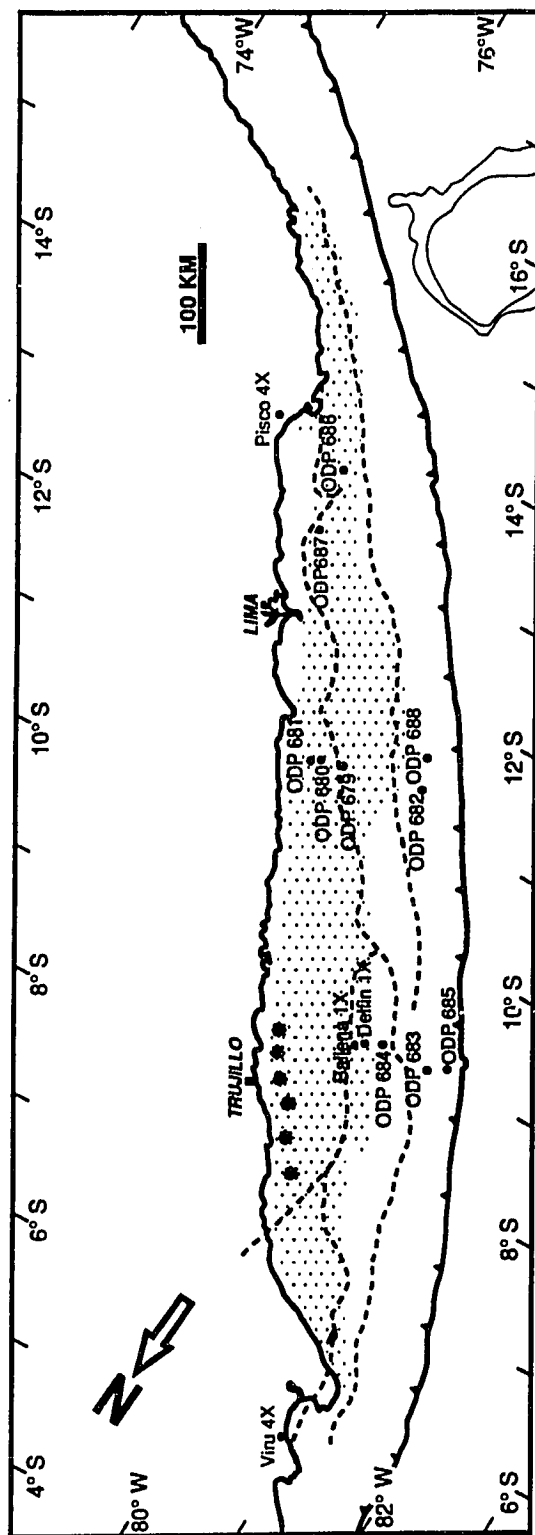
3.32 Eocene-Oligocene (Sequences E₀, E₁, E₂, E₃ and E-O and the post-lower to middle Eocene igneous intrusive event)

Units E₀, E₁ to E₃ and E-O are 3rd order sequences (0.5 to 5 Ma cycles) deposited under three different eustatic, paleogeographic and tectonic regimes. The widespread, coarse-grained lower? to middle Eocene E₀ sequence accumulated in a period of tectonic quiescence. The middle Eocene E₁, E₂ and E₃ sequences represent three pulses of a regional rifting event. Finally, the middle/upper Eocene to Oligocene E-O sequence, deposited during the post-rift phase, is characterized by tectonic quiescence and the onset of an upwelling system and biogenic sedimentation.

3.321 The lower? to middle Eocene E₀ sequence

During the early? to middle Eocene one of the most conspicuous, uniform (in thickness) and widespread units, the E₀ sequence, was deposited. Figure 3.9 shows the area through which this unit has been correlated, and Plates 4 to 16 illustrate its most characteristic seismic expression. This unit, which unconformably overlies Cretaceous or older basement rocks and unconformably underlies rifted middle Eocene sediments and younger strata, was penetrated by the Ballena and Delfin wells (Figures 3.6, 3.7 and Plate 2). Sequence E₀ is 108.2 m thick in the Ballena drill site and consists of coarse to very coarse-grained sandstones. At the Delfin well its thickness increases to 165.2 m and it is composed of a 39 m thick coarse to fine-grained sandstone at the base underlying 96.2 m of marine mudstones and siltstones capped by a 30 m thick light brown biosparite. All these characteristics suggest that the E₀ unit was deposited during a period of tectonic quiescence with global eustasy as the main factor controlling the sea level fluctuations. On the other hand, rainfall and an efficient regional system of sediment supply (probably fluvial) may have characterized the source area.

The coarse-grained lithology of the E₀ sequence prevented H. Okada (see Appendix A) from dating this sequence at the Ballena well. Sample cuttings taken at -2510.4 m in the Delfin well were



**Figure 3.9 DISTRIBUTION OF THE LOWER TO MIDDLE EOCENE E_0 SEQUENCE
AND THE POST-LOWER TO MIDDLE EOCENE IGNEOUS INTRUSIVES**

Sequence E_0 present Igneous intrusive Basin boundaries-----

tentatively assigned to the middle Eocene Okada-Burky CP-13 zone (Appendix A). In this study, I assume that sequence E₀ age is lower to middle Eocene.

At ODP site 688 drill site in the slope zone west of the central part of Lima Basin (Figure 3.2 and Plate 3), the E₀ sequence consists of siltstones, sandstones and mudstones deposited in the inner neritic to middle bathyal bathymetric range. This section contains scarce radiolarians, and diatoms are absent.

3.322 The post-lower to middle Eocene igneous intrusion

Seismic profiles reveal the presence of bodies that intrude the K and E₀ sequences (Panel 1, eastern side of seismic profile 2), (Plate 6). These 1.2 to 2 km wide bodies are aligned parallel to the current coast line, close to the northeastern Salaverry Basin border (Figure 3.9). I interpret these as igneous intrusions. Note that evaporite deposits have never been reported either in the Progreso, Talara and Sechura Basins or in the adjacent coastal region. It is uncertain whether the intrusion occurred before or after E₁, E₂ and E₃ deposition.

3.323 The syn-rift middle Eocene E1, E2 and E3 sequences

During middle Eocene time a regional rifting event affected large segments of the study area. The direction of extension was E-W to ESE-WNW, and the main structural elements were: (1) A N-S to NNE-SSW trending master fault system that formed half graben boundaries. (2) An E-W to ESE-WNW trending transfer fault system (Figures 3.10, 3.11 and 3.12), and (3) A hypothetical trench-parallel, strike slip system, separating the extended zones from the non-extended zones. The structural characteristics of this event will be discussed in Chapter 4.

The rifting process developed in three pulses represented by the E1, E2 and E3 sequences (Figures 3.10, 3.11 and 3.12). Unfortunately the E1 and E2 sequences were not penetrated by any of the holes drilled in the area, but they are recognized on seismic profiles. The E3 unit was penetrated by the Delfin well.

The E1 sequence

This unit filled a half graben system located in the Trujillo and West Pisco Basins (Figure 3.10). Although geographically more restricted than the E3 sequence, the E1 unit is the thickest (about 4980 m assuming a velocity interval of 4150 m/s) (Panel 1, seismic

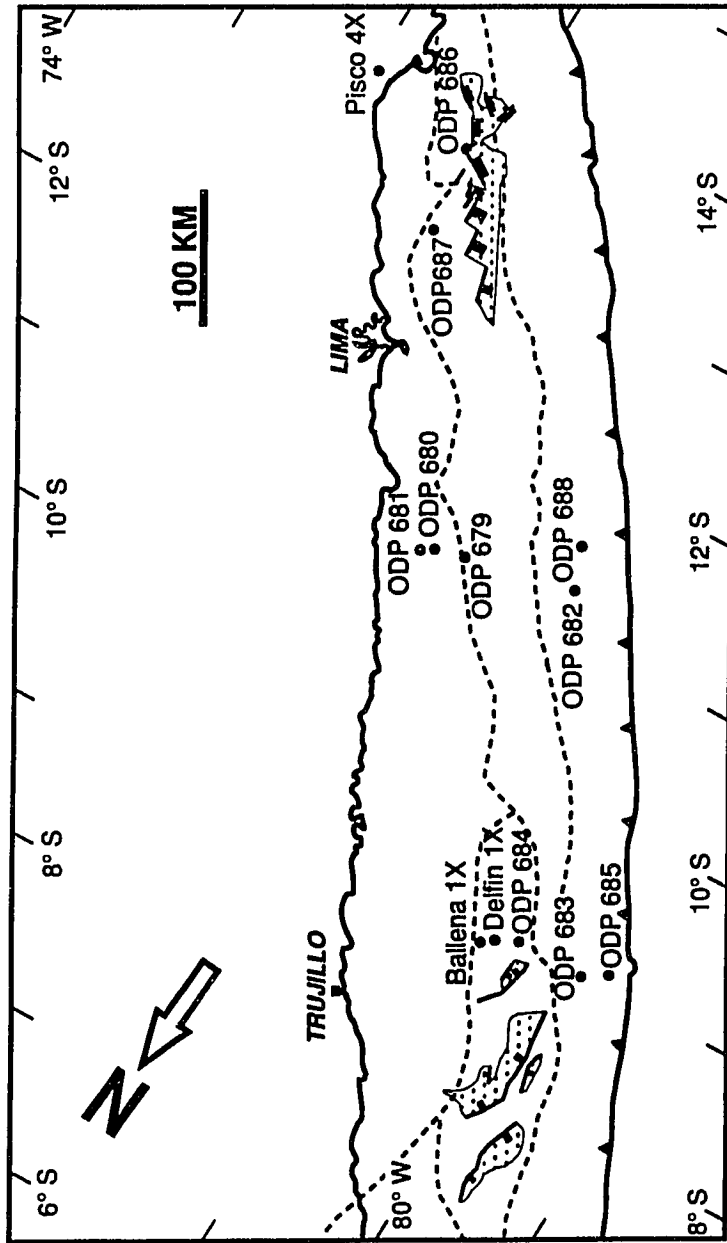
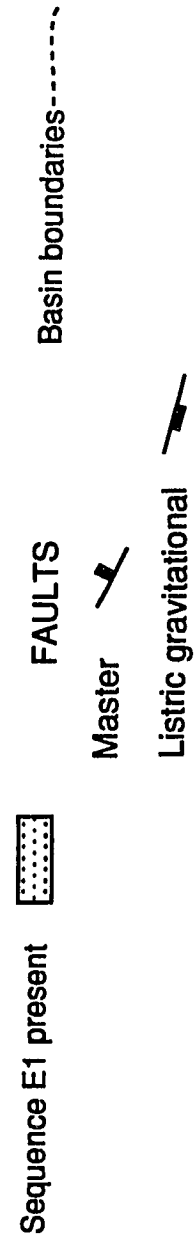


Figure 3.10 DISTRIBUTION OF THE MIDDLE EOCENE E1 SEQUENCE



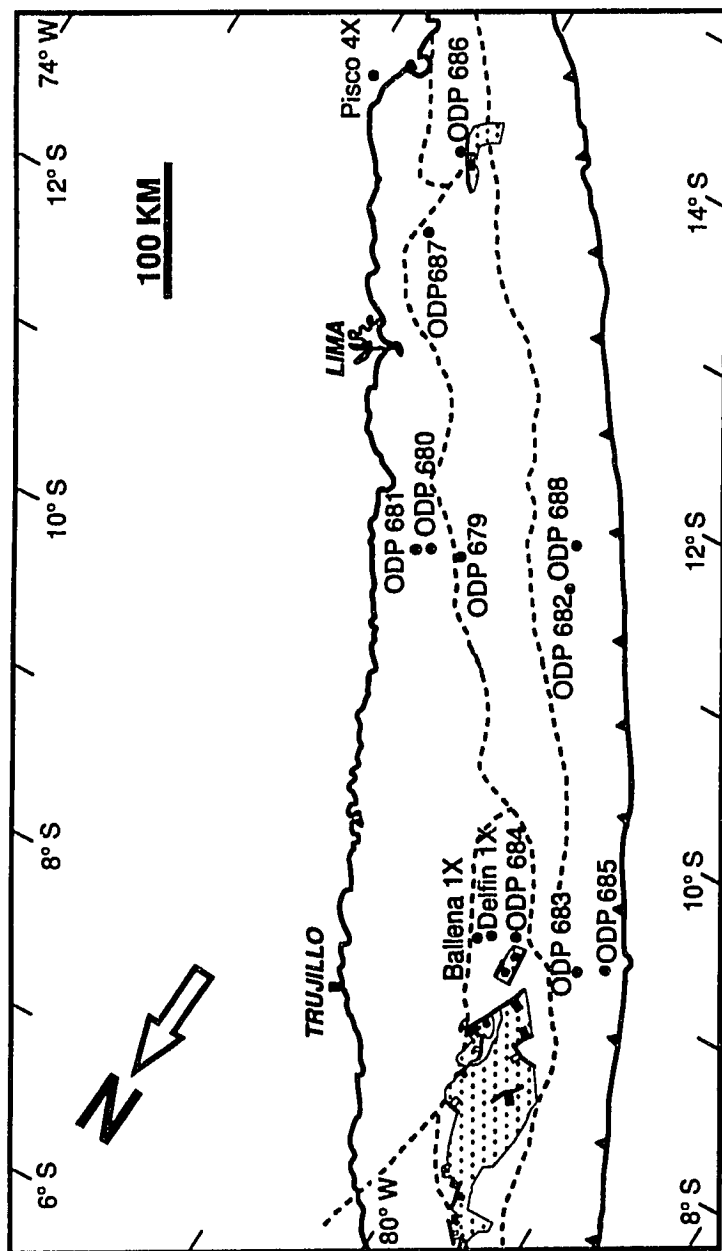
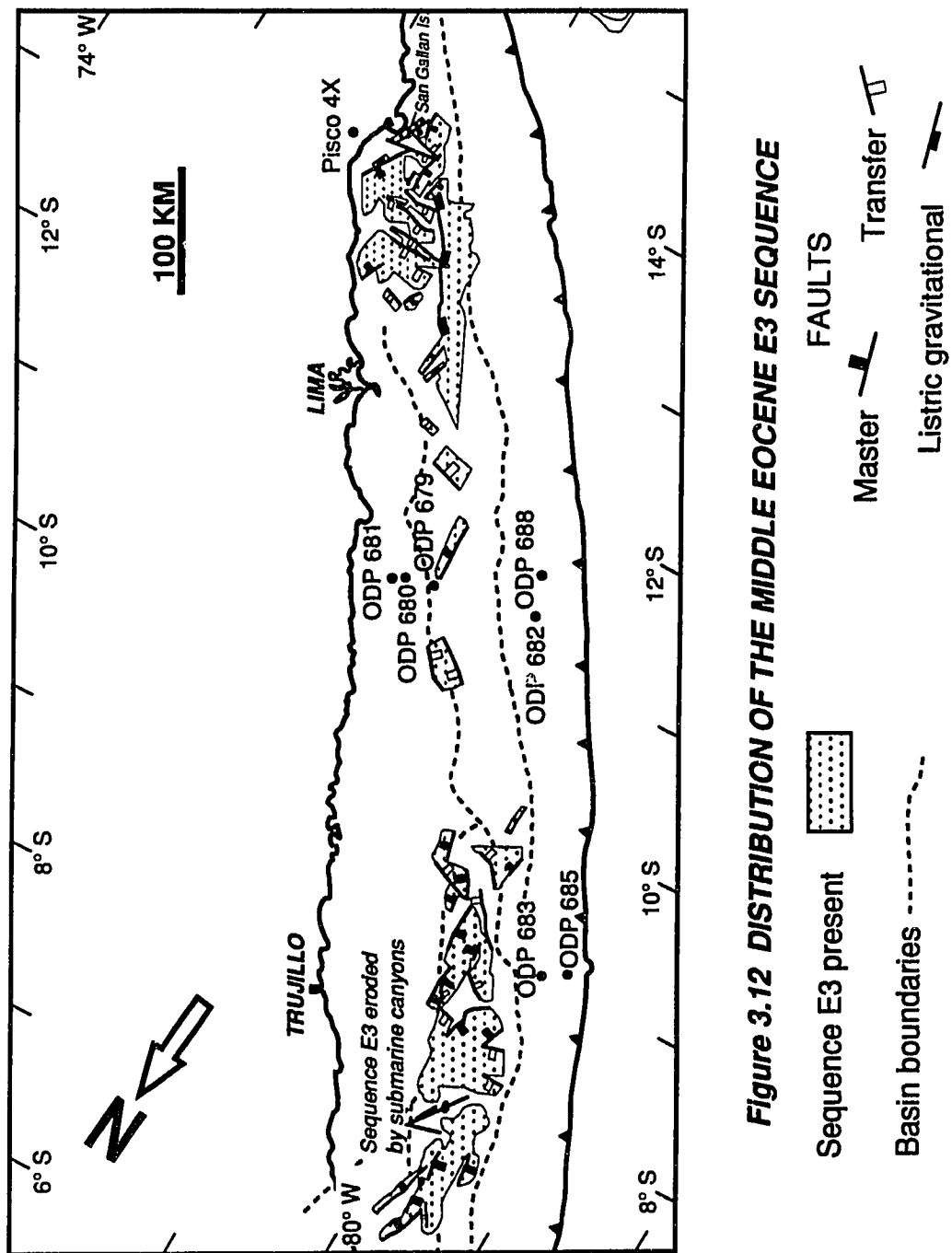


Figure 3.11 DISTRIBUTION OF THE MIDDLE EOCENE E2 SEQUENCE





profile 1 and Plate 4) of all the syn-rift sequences. On the other hand, the internal divergence of reflectors reveals that the depositional rate was higher or equal to the rate of faulting.

The E2 sequence

This sequence represents the second pulse of rifting and occurs in the Trujillo Basin (Panels 1 and 2, Plate 5) and in a more restricted fashion in the West Pisco Basin (Figure 3.11). This unit is similar to the E1 sequence. The maximum thickness of 1200 m (calculated with a velocity interval of 5000 m/s) occurs in a half graben located in the middle part of the Trujillo Basin (Panel 2, Profile C).

The E3 sequence

The E3 sequence filled half grabens created during the third and last pulse of rifting, which extended the Trujillo and East Pisco Basins and part of the Sechura, Lima and West Pisco Basins (Figure 3.12, Plates 4, 5, 7, 8, 9, 13, 14, 16, and 17). The Delfin well penetrated the E3 sequence where it consists of 419.8 m of calcareous silty mudstones interbedded with siltstones and a 35.4 m thick package of very coarse to coarse glauconitic sandstone located in the middle-lower part of the section (Figure 3.7). Okada (Appendix A) analyzed cuttings collected from the lower (-2327.4 m), middle

(-2144.5 m) and upper (-2007.3 m) parts of the sequence (Figure 3.7), assigning them to the middle Eocene CP-14a to 13c, CP-14a and CP-14a zones respectively. Paleobathymetric data (Engelhardt-Moore, Appendix B) reveal the transgressive character of unit E3 representing inner neritic conditions at the base and an outer neritic bathymetry at the top (Figure 3.7).

The prominent half graben system present in the offshore East Pisco Basin and eastern part of the West Pisco Basin (Panel 6, Figure 3.12, Plate 16) very likely corresponds to the E3 sequence. On the adjacent Paracas Peninsula and San Gallan Island (Figure 3.5) the onshore extension of the E3 sequence appears to be part of a 700 m thick section of nearshore and inner shelf bioclastic conglomerates, sandstones and mudstones (Los Chorros formation) of Middle to Upper Eocene age, resting on rocks of the pre-Cenozoic basement (Dunbar et al., 1989).

At the western part of the West Pisco Basin, the structural style of the E3 sequence as well as that of the underlying E1 and E2 sequences change to a trench parallel, listric normal fault system, dipping to the west (Figures 3.10 to 3.12, Plate 17). The origin of these segments of the E1, E2 and E3 units, which seem to represent deep syntectonic deposition at the slope, will be treated in the next chapter.

The ODP 682 and 683 wells, located in the slope zone, west of the Lima and Trujillo Basins respectively, penetrated middle to upper bathyal fine-grained sediments of middle Eocene age before reaching total depths. The wedge-shaped unit, whose top corresponds to the 32 m thick middle Eocene section cut by the ODP 683, suggests the occurrence of a half graben of the E3 sequence at this location (Plate 2 and Panel 7).

3.324 The middle/upper Eocene to Oligocene E-O sequence

This post-rift unit has been correlated offshore, along the Trujillo Basin and western border of the Sechura Basin (Panels 1 and 2, Plates 4, 5, 7, 8, and 9), and parts of the Lima Basin. The E-O sequence was not deposited in the Salaverry Basin and only small remnants were preserved in the East Pisco Basin because of uplifting and erosion that occurred during the late Miocene time in that area.

Okada H. (Appendix A) analyzed several cuttings from the 748.4 m thick interval that overlies the E3 sequence in the Delfin well (Figure 3.7). All samples were barren of nannofossils, except two located at -1751.5 m and -1361.3 m, which were assigned to the late middle Eocene CP-14b zone and to the early to late Oligocene CP-19a? zone respectively.

The Delfin well encountered a 748.4 m thick section of the E-O sequence. This unit is composed of calcareous mudstones interbedded with thin, micritic limestones and dolomicrites, which underlie a 125.6 m sequence of turbiditic sandstones interbedded with calcareous, glauconitic claystones (Figure 3.7). The E-O unit is regressive at the Delfin well drill site as shown by paleobathymetric data which indicate that lower to upper bathyal sediments shallow upward to upper bathyal-outer neritic deposits (Figure 3.7).

The upper 459.7 m of the lower fine-grained unit contain radiolarians (Engelhardt-Moore, Appendix B), are rich in amorphous kerogen (Bolaños, 1986) and show a relatively high organic carbon content (2-3.5 %), (Figure 3.7). These characteristics suggest that cold water upwelling was effective during the upper Eocene-Oligocene in this area, a situation which correlates well with similar upper Eocene-Oligocene deposits described onshore in the Sechura and East Pisco Basins (Marty, 1989 and Dunbar et al., 1990).

In the slope zone, west of the Lima Basin, the ODP 682 well cut 91 m of Oligocene to middle Miocene brecciated mudstones.

3.325 The Eocene-Oligocene in the Progreso, Talara and onshore Sechura and East Pisco Basins

Outcrops and industry drill holes reveal that the Eocene to Oligocene sedimentary record in the northern Progreso and Talara Basins is characterized by relatively high sedimentation rates, the occurrence of coarse grained-siliciclastics and, in contrast with southern basins, the absence of biogenic rocks.

Progreso and Talara Basins

Eocene sediments are absent in the Progreso Basin, but the Oligocene is represented by more than 1980 m of syntectonically deposited deltaic to fluvial mudstones and sandstones (Delfaud et al., 1985) that fill downthrown blocks (limited by listric normal faults, Sanz, 1991).

Delfaud et al. (1985) recognized three major periods in Talara Basin evolution: (1) An active subsidence phase, during which a thick upper Cretaceous-lower Eocene series consisting of coarse and fine grained siliciclastics was deposited in shallow marine to continental environment. (2) A deep turbidite depositional phase suddenly initiated in the middle Eocene. The sediments accumulated during this phase prograded from the southern part of the Amotapes Mountains (Figure 2.1) and consist of turbiditic mudstones and

sandstones whose main distal bodies trend N-S. (3) The third phase, initiated in early Oligocene, completes the basin opening and marks the resumption of shallow coastal and continental deposition (Delfaud et al., 1985).

The sediments accumulated during the first and second phases represent, in the Talara Basin, the E₀ and E₁ to E₃ sequences respectively (Delfaud et al., 1985). It is noteworthy that, during the middle Eocene (second phase), the paleogeographic and oceanographic conditions in the north were very different from those prevailing in the study area. In the Talara Basin, the occurrence of rainfall, fluvio-deltaic sedimentation, and perhaps warm ocean water allowed the accumulation of thicker sedimentary sequences and prevented biogenic deposition; whereas farther south, cold water and associated dry conditions inhibited the influx of large amounts of terrigenous sediments into the basins and promoted biogenic sedimentation.

Onshore Sechura Basin

Industry well data and outcrops indicate that the E-O sequence is present onshore in the Sechura Basin, where it is represented by 300 m to 900 m of upper Eocene calcareous sandstones and shales (Verdun Formation), overlain by calcareous sandstones and diatomaceous shales (Chira Formation) (Caldas et al., 1980).

Samples of this late Eocene biogenic unit that outcrops on the sea cliffs at Bayovar show a high content of radiolarians (Dunbar et al., 1990). Lower to middle Eocene and Oligocene sediments seem to be absent in the Sechura Basin.

Onshore East Pisco Basin

The E3 sequence is represented in the Paracas Peninsula area by part of a 700 m thick, shallowing-upward succession of middle to upper Eocene shallow marine, bioclastic conglomerates, sandstones and mudstones (Los Chorros fm., Dunbar et al., 1990). On the other hand, the more than 150 m of the upper Eocene Yumaque fm. (Dunbar et al., 1990), which outcrop along the Yumaque Beach (Figure 3.5) represent the E-O sequence. At this location, the Yumaque formation consists of marine mudstones, phosphatic shales, diatoms, porcellanites, and cherts (Dunbar et al., 1990). The E-O unit is also present near Salinas de Otuma and Punta Lomitas (Figure 3.5), where Fourtanier and Macharé (1988) reported upper Eocene-lower Oligocene diatomaceous sediments.

3.33 Early-middle Miocene (M1 and M2 sequences)

The early to middle Miocene is characterized by a regional transgression initiated with the deposition of the geographically restricted M1 sequence in the earliest Miocene, followed by the

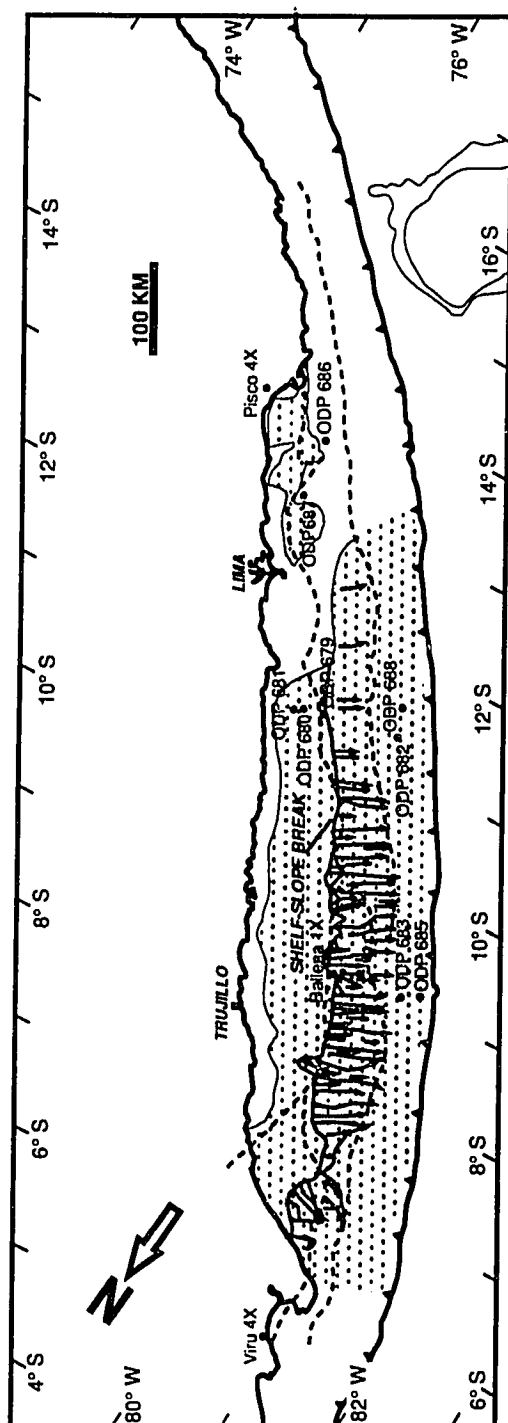
sedimentation of the widespread lower to middle Miocene M2 sequence.

The lowermost Miocene M1 sequence

The geographic distribution of the M1 unit (Panels 1,2, 5, 6; Plates 4, 5, 7, 8, 9, 12, and 16) is restricted to the Trujillo Basin, part of the Lima Basin, the East Pisco Basin, and the slope zone. Okada assigned an early Miocene age (CN 3-1 zones, Appendix A) to a Delfin well sample located at -1234.4 m. The M1 sequence is represented in the Ballena well by 137.8 m of siltstones and mudstones (Figure 3.6). Paleobathymetric data show that the upper part of this section is transgressive, with middle neritic to outer neritic deposits at the base of the interval and upper bathyal sediments at the top (Figure 3.6), (Engelhardt-Moore, Appendix B). In the Delfin well drill site the M1 unit consists of 298.8 m of silty mudstones interbedded with thin brown dolomicrites deposited in the lower to upper bathyal bathymetric range (Figure 3.7).

The lower to middle Miocene M2 sequence

The M2 sequence is present in the Sechura, Salaverry, Trujillo, and Lima Basins and part of the East Pisco Basin and the slope zone (Figure 3.13). The dip-oriented seismic profiles illustrate the eastward back-stepping at the base of this sequence (Panels 1 and 3;



Sequence M2 present

Submarine canyon axis

Basin boundaries-----

Plate 8). The M2 unit was deposited in two main areas bounded by a narrow NW-SE trending shelf-slope break zone (Figure 3.13). Shelfal sedimentation prevailed in the eastern area, whereas a very active process of submarine canyon cut and fill took place in the west (Figure 3.13 and Panels 2 and 4, Plates 4, 5, 7, and 9). In this western area the M2 sequence is also affected by two types of normal faults: (1) a synsedimentary fault system that involves the pre-Tertiary basement (Figure 3.14 and Plate 8) and (2) a listric normal fault system whose detachment surface does not affect the pre-Eocene basement (Plate 12). These fault systems, along with the causes and characteristics of the canyon system, will be discussed in Chapter 4.

H. Okada (Appendix A) analyzed four samples of the M2 sequence, three collected from the Delfin well and one from the Ballena well. The Delfin well samples, located at -803 m, -601.8 m, and -479.9 m (Figure 3.7), were assigned to the late early Miocene CN-3 zone, to the middle Miocene CN-5? zone and to the late to middle Miocene CN 9-5b zones respectively. The Ballena well sample (-549.1 m) (Figure 3.6) was assigned to the early Miocene CN 3-1 zones. Schrader and Cruzado (1986) analyzed the diatoms in three samples from the Ballena well, located at -489 m, -382.3 m and -351.8 m, and assigned respective ages in the range of 17.8-16.4 Ma, 13.5-14.2 Ma and 10.2-11.2 Ma.

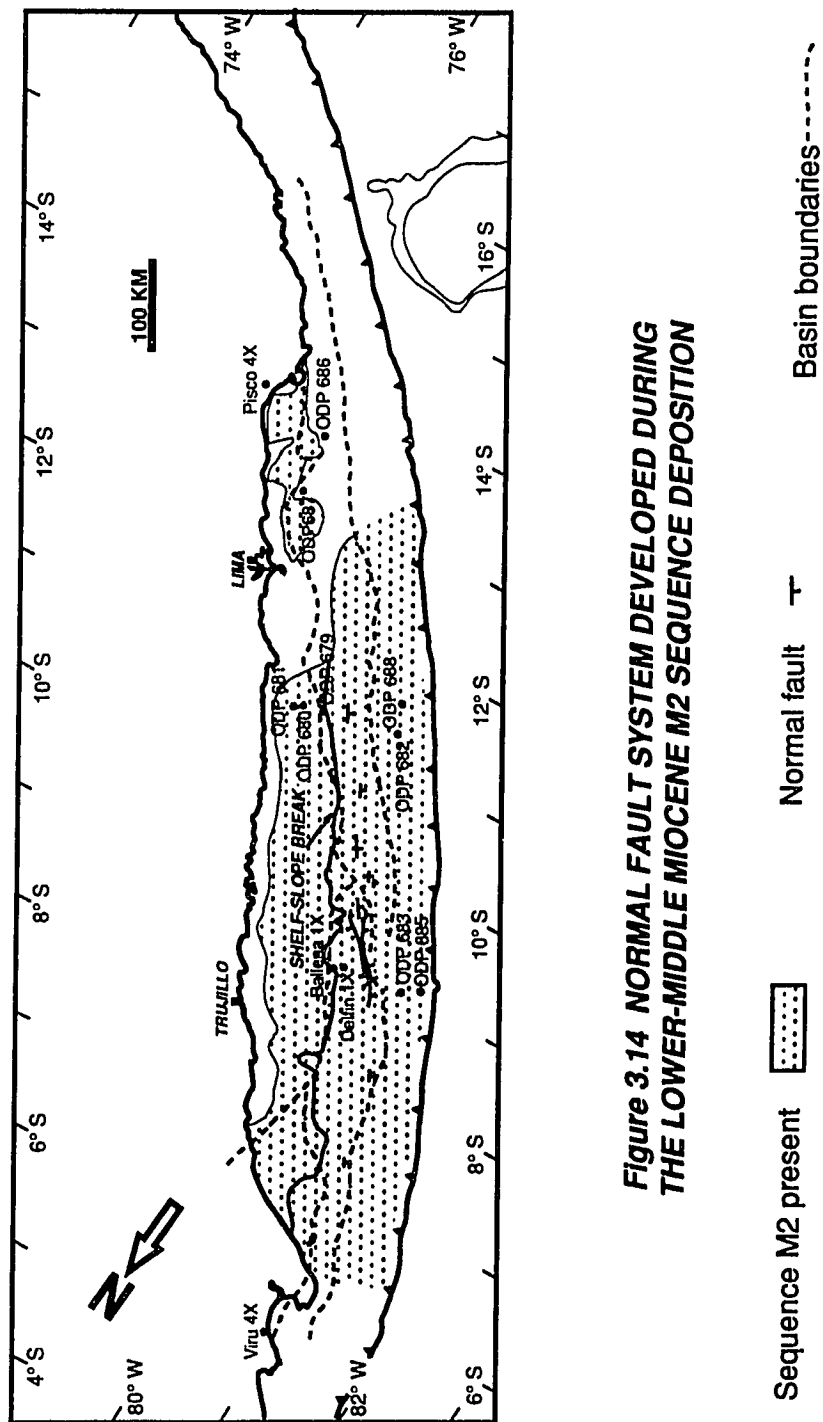


Figure 3.14 NORMAL FAULT SYSTEM DEVELOPED DURING THE LOWER-MIDDLE MIOCENE M2 SEQUENCE DEPOSITION

Both the Delfin and the Ballena wells were drilled in the western deeper area dominated by cut and fill features of submarine canyons (Figure 3.13). The section of the M2 unit encountered in the Ballena well consists of a 357.6 m thick transgressive succession of outer neritic microfossiliferous siltstones which grade upward to mudstones and claystones deposited in an upper bathyal-outer neritic setting (Figure 3.6), (Engelhardt-Moore, Appendix B). The M2 sequence is represented in the Delfin well by 484.8 m of claystones interbedded with thin brown dolomicrites. The lower half of the section consists of lower to upper bathyal glauconitic deposits, whereas the upper part accumulated in the upper bathyal-outer neritic setting. (Figure 3.7).

The M2 sequence is also represented by the lowermost 107.3 m penetrated by the ODP 679 well (Plate 3) which consist of middle Miocene dolomitic claystones overlain by siltstones. The paleobathymetry of the lower 9.3 m is upper to middle bathyal (Suess E., von Huene R., et al., 1988). At the ODP site 683, located on the slope zone west of the Trujillo Basin, the M2 unit is 219 m thick and consists of lower to middle bathyal diatomaceous mudstones (Plate 2). Also on the slope zone, but west of the Lima Basin, ODP sites 682 and 688 (Plate 3) include 112 m and 142 m respectively of the M2 sequence. In this location, the M2 unit is composed of diatomaceous mudstones accumulated in the upper to lower bathyal

bathymetric range. The remarkable lack of coarse-grained sediments in the submarine canyon fill (sections penetrated by the Delfin and Ballena wells and probably the ODP 679 well), along with the occurrence of a relatively high organic carbon content (>2%) and amorphous kerogen (Bolaños, 1986) in the upper part of the M2 sequence in the Ballena and Delfin wells (Figures 3.6 and 3.7), and the presence of diatomaceous mudstones in the slope zone (ODP 682, 683 and 688), suggests the lack of an efficient system of sediment transport from the continent.

3.331 Early-middle Miocene in the Progreso, Talara and onshore Sechura and East Pisco Basins

The Progreso Basin contains about 1128 m of lower to upper Miocene which consist of 762 m of coarse-grained deep sea fan deposits (Zorritos formation), (Leon, 1983) and 366 m of basinal marls (Leon, 1983). The Talara Basin lacks Miocene sediments.

In the Sechura Basin, industry well data and outcrops indicate that the early-middle Miocene is represented by three lithologic units: (1) The 300 m thick lower Miocene Mancora and Heath Formations, which consist of sandstones interbedded with shales and diatomaceous shales, (2) The Montera Formation, composed of sandstones interbedded with bioclastic limestones that unconformably overlie the Heath Formation, (3) The middle to upper

Miocene lower Zapallal Formation, which is an upward-fining sequence with sandy mudstones at the base and diatomites at the top. (Caldas et al., 1980).

The Cenozoic section penetrated by the Pisco 4X well, located 13 km NE of Pisco (Figure 1.6), consists of 37 m of Quaternary sediments, 390 m of diatomaceous shales, 357 m of shales interbedded with siltstones, and a lower section consisting of 43 m of bentonitic shales and siltstones which overlie 91.5 m of bioclastic sandstones and conglomerates (Plate 1). Ashworth (1955) reported the presence of Nonionella S-1 in the fine-grained 43 m thick interval. Because this species occurs in the Montera formation only (Ashworth,1955), which represents the M2 sequence in the onshore Sechura Basin, I consider that this fine-grained interval along with the underlying coarse-grained barren section and the overlying 357 m of non-diatomaceous shales and siltstones correspond to the M2, M1 and E-O sequences (Plate 1).

At the Pampa de Chilcatay (Figure 3.5) in the East Pisco Basin, De Vries (1988) described a 200 m thick unit composed of uppermost Oligocene-early middle Miocene siltstones and sandstones with interbedded diatomaceous intervals, named the Chilcatay Formation (E-O to M2 sequences). According to Fourtanier and Macharé (1988) and Dunbar et al. (1989) this basin lacks Neogene sediments older than middle Miocene.

3.34 Late Miocene-Pliocene (M3 and P sequences)

The late Miocene-Pliocene period began with a late-middle Miocene compressional event. This deformation produced: (1) The uplift and subaerial exposure of the Trujillo-Salaverry Sechura boundary area which I will name Salaverry-Trujillo High. (2) The uplift and erosion of the M2 sequence in the Lima and the West Pisco Basins and part of the onshore East Pisco Basin. (3) The creation of a trench-parallel folded belt in the Salaverry Basin. (4) The syntectonic deposition of the upper Miocene M3 sequence. At the end of this compressive episode, the widespread P sequence was accumulated during the late Miocene-Pliocene.

The upper Miocene M3 sequence

The M3 sequence was deposited syntectonically during the upper Miocene compression and uplift of the Salaverry-Trujillo High (Figure 3.15, Plates 4 to 15), which emerged by the latest Miocene, isolating the Salaverry and Sechura Basins from the Trujillo Basin. This unit extends through the Salaverry, the Trujillo, and part of the Lima Basin and the middle-lower slope zone.

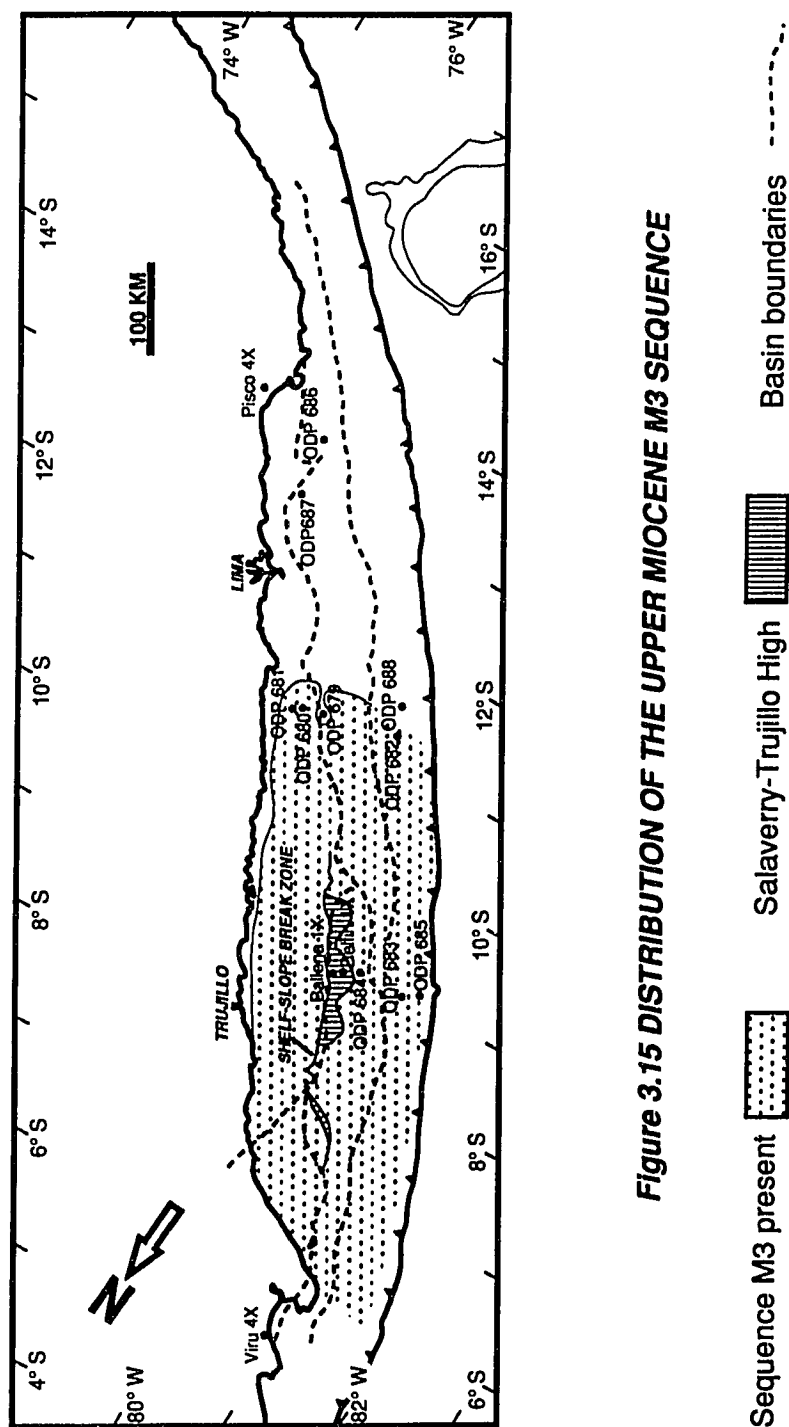


Figure 3.15 DISTRIBUTION OF THE UPPER MIOCENE M3 SEQUENCE

As with the underlying M2 unit, the M3 sequence shows two different depositional settings separated in the lower part of the section by the shelf-slope break zone and by the Salaverry-Trujillo High in the upper part (Figures 3.15). West of the Salaverry-Trujillo High, the M3 sequence was deposited through a complex process of submarine canyons cutting and filling, whereas shelf sedimentation prevailed to the east (Plates 4 to 15).

The M3 sequence was penetrated in the Trujillo Basin by the Ballena (225.6 m), Delfin (290.9 m), and the ODP 684 (more than 80.1 m) wells; and by the ODP 682 (87 m), ODP 685 (more than 265.6 m) and ODP 688 (41 m) wells in the slope zone (Plates 2 and 3). Okada (Appendix A) analyzed cuttings from the Ballena well, collected at -335.7 m and -223.8, and assigned ages of middle Miocene (CN-5?) and early Pliocene-middle Miocene (CN 11-5b) respectively (Figure 3.6). On the other hand, Schrader and Cruzado (1986), working with diatoms, dated a sample taken at -263.4 m as late Miocene (7.65-8.8 Ma) (Figure 3.6). Two samples from the Delfin well, located at -361 m and -266.5 m, were assigned by Okada (Appendix A) to late Miocene CN-9 and the early Pliocene-Late Miocene CN 11-9 zones respectively (Figure 3.7). Even though these data suggest that the M2 unit age should be upper Miocene to lower Pliocene, I have restricted the age of this unit to the early-upper Miocene in order to keep a consistent regional chronostratigraphic

framework among all the stratigraphic points of control (wells) of the study area and the onshore stratigraphy.

In the Ballena well, the M3 unit rests on upper bathyal-outer neritic mudstones of the M2 sequence and consists of 134.2 m of outer neritic mudstones interbedded with thin sandstones, overlain by 41.1 m of very fine to coarse bioclastic sandstones (Figures 3.6 and Plate 2). This coarsening upward sedimentary succession records the uplift, subaerial exposure and erosion of the Salaverry-Trujillo High. There were no samples available from the upper 50.3 m of the M3 sequence. The Delfin well encountered a M3 sequence section similar to that of the Ballena well, which is composed of 186 m of mudstones interbedded with thin sandstones capped by 45.7 m of poorly consolidated coarse-grained bioclastic sandstones (Figure 3.7). There were no samples available from the upper 59.1 m of the section. The ODP Site 684 well on the west side of the Salaverry-Trujillo High (Figure 3.14) penetrated 100.1 m of middle to upper bathyal calcareous, diatomaceous muds of the M3 unit.

On the middle-lower slope zone, ODP Site 685, located west of the Trujillo Basin, penetrated a thick section of the M3 unit composed of lower bathyal diatomaceous mudstones (Plate 2); ODP Sites 682 and 688, drilled west of the Lima Basin, penetrated lower bathyal to outer neritic diatomaceous mudstones and diatomaceous siltstones respectively.

The uppermost Miocene-Pliocene P sequence

The P sequence is absent in the Ballena and Delfin wells (Figure 3.16), but it was penetrated at ODP Sites 679 (184 m), 680 (more than 122.5 m), 681 (19? m), 682 (65 m), 683 (237? m), 684 (41 m), 687 (more than 104 m), and 688 (72 m) (Plates 1 to 3).

In the Lima Basin, at ODP 679 Site, the P sequence unconformably rests upon the M2 sequence and consists of 147 m of diatomaceous siltstones and 35 m of upper bathyal glauconitic, diatomaceous mudstones separated by a thin unit of sandstone. At Site 680, located east of Site 679 (Plate 3), the P sequence is represented by sandy, diatomaceous mudstones, diatomaceous mudstones and silty sandstones. A thin conglomeratic unit deposited in an outer neritic setting occurs near the top.

ODP Site 687, drilled in the Lima Basin, near the Lima-East Pisco Basin boundary, penetrated 104 m of the P unit (Plate 1). The P sequence consists of upper bathyal-outer neritic diatomaceous mudstones and siltstones interbedded with thin dolomites before reaching a total depth of -513.8 m. The P sequence is represented in the slope zone (ODP Sites 682, 683, and 688) by diatomaceous mudstones deposited in a lower bathyal setting.

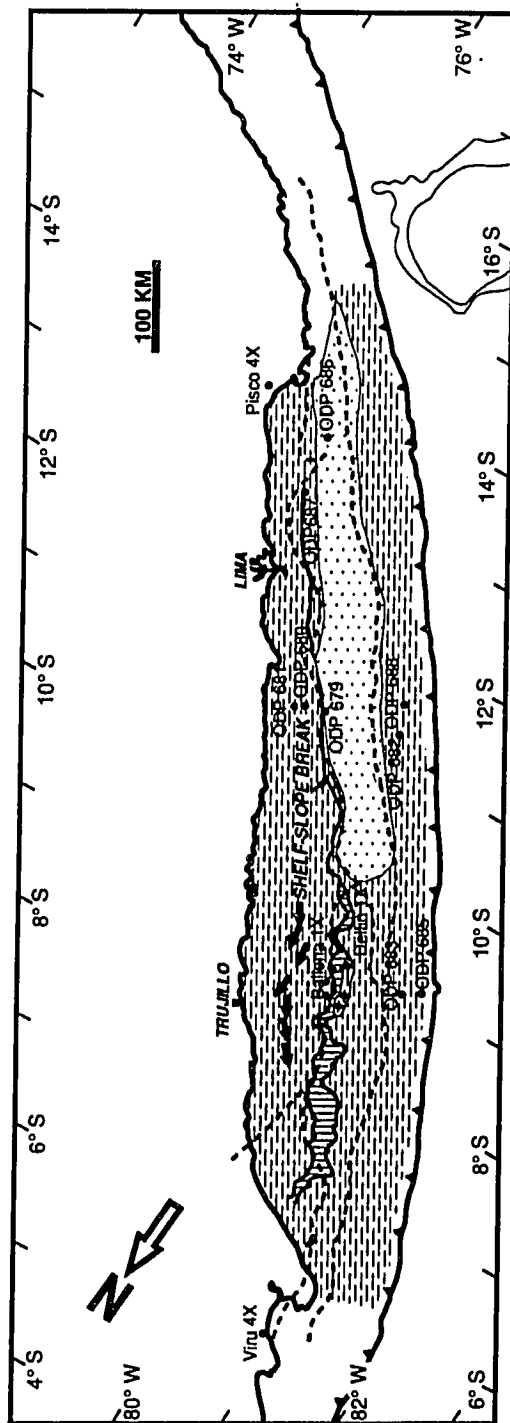
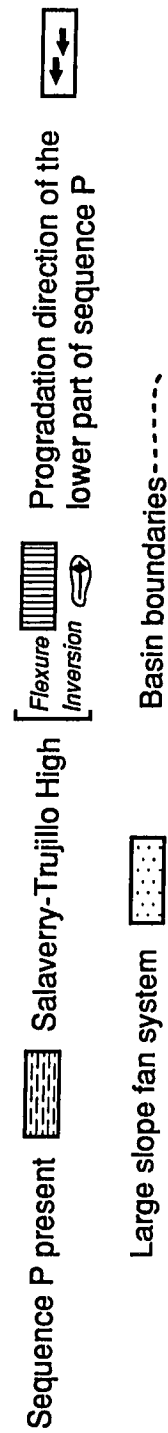


Figure 3.16 DISTRIBUTION OF THE UPPERMOST MIOCENE-PLIOCENE P SEQUENCE



Seismic and well data reveal the important influence of the Salaverry-Trujillo High during the P unit deposition. The high defined three depositional areas (Figure 3.16): (1) One shallow **internal basin** to the east coincident with the Sechura Basin and the northern portion of the Salaverry Basin, (2) A **deep basin** to the west of the Salaverry-Trujillo High, and (3) An **open basin** located south of the high, which embraced the rest of the study area.

There were two fillings in the northern internal basin: (1) The first was progradational, (Panel 2, Profile B, Plate 11, and Figure 3.16), with a northward direction of progradation. The clinoforms of this phase, shown in Panel 2, Profile B and Plate 11, probably represent a northerly prograding fluviodeltaic system. (2) During the second phase which was aggradational, the sediment transport system was more complex and local erosion and sediment redeposition were common (Panel 1).

At the same time, the slope zone and the Trujillo Basin were subjected to a cut and fill process of submarine canyon similar to that described in the M2 and the M3 sequences, having the Salaverry-Trujillo High as the main sediment source area.

On the other hand, the southern open basin was divided by a NW-SE trending shelf-slope break zone (approximately coincident

with the Salaverry-Lima and Salaverry-East Pisco boundaries) into an eastern relatively shallow neritic area and a western deep bathyal zone (Figure 3.16, Plates 14 to 18). The P sequence is represented by a large slope fan system accumulated from the Lima Basin to the West Pisco Basin (Figure 3.16, Panel 3, Profile 4 and Panel 7).

3.341 The late Miocene-Pliocene in the Progreso, Talara and onshore Sechura and East Pisco Basins

In the northern Progreso Basin, the late Miocene-Pliocene is represented by about 2140 m of coarse-grained siliciclastics of the Tumbes formation (Upper Miocene) and the Mal Pelo formation (Pliocene) (Sanz, 1991) was deposited in a fluvio-deltaic setting (Leon, 1983). The Talara Basin lacks Miocene-Pliocene sediments.

In the Sechura Basin, upper Miocene diatomaceous and phosphatic deposits of the Upper Zapallal formation unconformably rest on gently folded strata of the Lower Zapallal formation (Marty, 1989). The Pliocene-Pleistocene continental deposits of the Miramar and Hornillos formations unconformably overlie the Upper Zapallal formation (Dunbar et al., 1990).

Marty (1989) and Dunbar et al. (1990) describe a widely variable uppermost middle Miocene to lower Pliocene unit named the

Pisco Formation. Along the Pisco River, near the Pisco 4X well drill site (Figure 3.5), the Pisco formation is folded and consists of about 500 m of uppermost middle Miocene to lower Pliocene diatomite and diatomaceous mudstone (Dunbar et al., 1988). The Pisco 4X well penetrated 390 m of diatomaceous shale, which overlies the M2 sequence and represent the P sequence at the Pisco 4X drill site (Plate 1).

3.35 Quaternary (Q sequence)

During late Pliocene-Quaternary time the whole region subsided, the Salaverry-Trujillo High was submerged and a relatively thin sequence of muds and sands accumulated in the Salaverry and East Pisco zones, whereas in the southern West Pisco Basin and in some parts of the slope zone, thick slope fan deposits were deposited (Plates 1 to 3, and Panels 1 to 6).

All the wells drilled in the study area penetrated the Q sequence. There were no available samples of this interval from the Ballena and Delfin wells. The ODP 681 (168 m) and ODP 687 (103m) wells, drilled in the Salaverry and the Lima Basins respectively (Plate 3), penetrated sandstones, thin conglomerates and diatomaceous siltstones interbedded with thin dolomicrites deposited in the inner neritic-upper bathyal bathymetric range.

ODP Site 684 (15 m) located in the Trujillo Basin, and the ODP Site 679 (68 m) and 680 (53 m), drilled in the Lima Basin, penetrated a Q sequence section consisting of diatomaceous muds deposited in the outer neritic-upper bathyal bathymetric setting (Plates 1 to 3). ODP Site 686 (more than 303 m), located in the West Pisco Basin, encountered a transgressive sequence of outer neritic diatomaceous muds interbedded with dolomites, capped by upper bathyal siltstones interbedded with sandstones before reaching a total depth of 749.8.8 m (Plate 3, Panel 7).

The Q sequence is represented in the slope by lower bathyal dolomitic diatomaceous muds recovered in cores of ODP Sites 682 (48 m), 683, 685 (203 m), ODP 688 (337 m) (Plates 2 and 3, Panel 7).

CHAPTER 4: STRUCTURAL GEOLOGY

4.1 INTRODUCTION

The study area was affected by four compressive events and two main extensional episodes. Compression occurred during the late Cretaceous-Paleocene?, middle Eocene, late Miocene, and middle Pliocene?. Extension took place during the middle Eocene and late Pliocene. The middle Eocene extension was a synsedimentary rifting process. In all these tectonic episodes, the pre-Tertiary substratum was involved. The lack of resolution of seismic profiles below the pre-Cenozoic interface precluded the study of a pre-lower Eocene extensional episode that offsets the K sequence (Panels 1 and 2, Plate 4).

The Salaverry-Trujillo High was formed during early Miocene to Pliocene time; this uplift may have been an important contributing factor to the creation of the large submarine canyon systems that affect the M2, M3 and P sequences on the western side of the Salaverry-Trujillo High. A system of synsedimentary normal faults that involve the pre-Cenozoic basement developed in the Lima Basin and the Trujillo-Lima Basins boundary during the M2 sequence deposition. Gravity-induced listric normal faults with shallow detachment zones affect sediments of the M1, M2, M3 and P sequences.

4.2 The first pre-Eocene compressive event

This compressive episode, which occurred before the deposition of the lower-middle Eocene E₀ sequence, is poorly defined on the seismic profiles. It was identified in the Salaverry and Trujillo Basins where flat-lying strata of the E₀ sequence overlie folded strata of the K sequence (Plates 8, 10, and 11). It was not possible to map the structures of this event.

4.3 The pre-Eocene uplift and peneplanation

The lack of relief of the K to E₀ sequence interface (Panels 2 to 6) suggests that the region was uplifted and peneplaned after the deposition of the K sequence.

4.4 The middle Eocene rifting event

During the middle Eocene, a regional rifting event affected large segments of the study area. The direction of extension was E-W to ESE-WNW, and the main structural elements were: (1) A N-S to NNE-SSW trending master fault system that formed the half graben boundaries. (2) An E-W to ESE-WNW trending left-lateral transfer fault system (Figures 3.10, 3.11, and 3.12). The faults of this system are normal faults with a relatively larger oblique displacement

component with respect to the dip displacement component. The dip of this system is less than expected (i. e. values close to 90°); in fact the dips are similar to the master fault system (Panels 5 and 6, Plate 16). For this reason it is difficult to differentiate both systems on a two-dimensional section only. (3) A hypothetical trench-subparallel, right-lateral strike slip system, separating the extended zones from the non-extended zones.

The rifting process developed in three pulses represented by the E1, E2 and E3 sequences (Figures 3.10 to 3.12). The rifting process was shortly interrupted by a compression produced after the deposition of the E2 sequence. Divergence of the reflectors contained inside the half grabens, depicted in seismic profiles, indicates a rate of extension in balance with the sediment supply rate (Plates 4 and 16).

4.41 Rifting phase 1

During this phase the Trujillo and West Pisco Basins were extended (Figure 3.10, Plate 4). In the Trujillo Basin, adjacent half grabens show a change in the polarity of the faults (Figure 3.10) which is uncommon among the half grabens produced during the rifting process in this area.

4.42 Rifting phase 2

This phase mostly affected the Trujillo Basin (Figure 3.11, Panels 1 and 2, Plate 5). The half grabens of phase 2, which do not exhibit a change in polarity, are wider than those of the previous phase 1 (Figures 3.10 and 3.11).

4.43 The second middle Eocene? compressive event

Seismic profiles suggest the occurrence of a middle Eocene? compressive event (Figure 5.2) that interrupted the rifting process, folded and thrust-faulted strata of the K and E₀ sequences (Figure 4.1, Plates 5, 7, 12, and 15) and produced a slight inversion of the previously formed half grabens. It is unclear if this event occurred before or after the deposition of the E₃ sequence. The later reactivation of some of the structures produced during this episode complicates a more accurate dating of this event. The mini-inversion shown by a half graben filled with sediments of the E₂ sequence which underlies undeformed strata of the E₃ sequence on the central part of the Trujillo Basin (Panel 2, Plate 5) suggests that this compression took place before the E₃ sequence deposition (middle Eocene time).

The main structures produced during this episode are asymmetric folds and thrust faults which can be traced for 6 to 20

km (Figure 4.1). The predominant trend of these structures is NW-SE and the dip is mostly ENE; a subordinate E-W trending system which dips S and N occurs in the north of the study area (Figure 4.1). The maximum shortening produced during this episode occurs in the eastern Salaverry Basin zone where seismic profiles depict apparent displacements up to 5 km (Plate 15).

4.44 Rifting phase 3

During the last pulse of Eocene rifting the Trujillo and East Pisco Basins and part of the Sechura, Lima and West Pisco Basins (Figure 3.12) were extended. The offset along two transfer faults located in the Trujillo Basin is 8 and 16 km (Figure 3.12). There are very few cases where the polarity of the half grabens changes.

In the western part of the West Pisco Basin, the structural styles of the E1, E2 and E3 sequences change to trench-parallel, listric normal fault systems which dip to the west (Figures 3.10 and 3.12, Plate 17). This structural regime suggests gravity-induced extension in a slope setting. It is unclear if the listric normal faults involve the pre-Eocene basement or not. This change in structural style may also indicate a change in the pre-Eocene substratum, from the more rigid basement of the eastern part of the basin, to a more incompetent basement underlying the western portion.

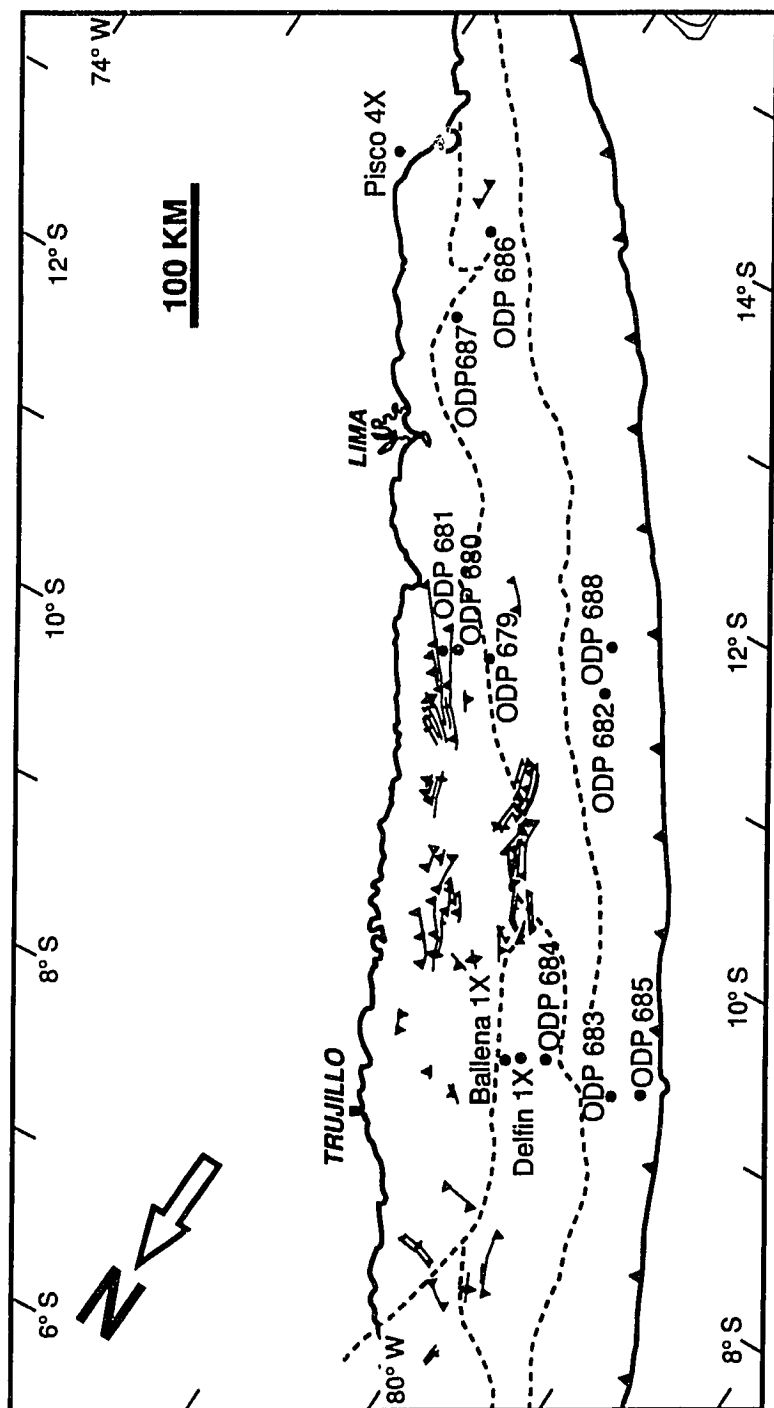


Figure 4.1 MIDDLE EOCENE? SECOND COMPRESSIONAL EVENT

Anticline axis \times Syncline axis \vee Monocline fold axis \sim
 Thrust \blacktriangle Basin boundaries $---$

4.5 The hypothetical strike-slip system

A trench-parallel strike-slip fault located on the eastern border of the middle slope is suggested by the following: (1) The master and transfer faults stop against this zone (Figure 5.2). (2) The geometric and kinematic relationships among the normal fault system with this hypothetical strike-slip zone are very similar to those reported in numerous examples of wrench tectonics (Wilcox et al., 1973; Dibblee, Jr., 1977; Reading, 1980; Spörli K. B.; 1980; and Worrall, 1991) and clay models (Harding, 1974; Wilcox et al., 1973). The plate tectonic reconstruction of Pardo Casas and Molnar (1987) suggests right-lateral displacement and will be discussed in Chapter 5.

4.6 The middle Miocene syn-sedimentary extension

Along the Lima Basin, the Trujillo-Lima Basins boundary and the Trujillo Basin-Middle Slope boundary the M3 sequence is offset by discontinuous synsedimentary normal faults that involve the pre-Cenozoic basement (Figure 3.14, Panels 1 and 3; and Plate 8). These faults which seem to be gravitationally induced are trench-parallel and predominantly dip to the trench (Figure 3.14).

4.7 The third upper-middle to late Miocene compressive event

After deposition of the E-O and M1 sequences and the lower part of the M2 sequence the Trujillo, the Salaverry and the Lima Basins were compressed again during the upper-middle to late Miocene (Figure 5.2) leading to (1) the reactivation of some of the structures formed during the second compressive episode, (2) the formation of trench-parallel folds in the Salaverry Basin and the Trujillo-Middle slope zone boundary (Figure 4.2). Deformation produced in this episode was mild. Folds which can be traced along strike for 15 to 40 km are asymmetric and the axial planes and thrusts strike NNW-SSE and dip to the east and west (Figure 4.2).

During this event the uplifting of the Salaverry-Trujillo High continued and the M3 sequence was syntectonically deposited.

4.8 The Salaverry-Trujillo High

The Salaverry-Trujillo High is a trench-parallel trending open flexure which extends about 370 km along the Trujillo-Sechura and Trujillo-Salaverry boundaries (Figure 3.16, Panel 1, Plate 13). A 60 km long western portion of the high, located about the Ballena and Delfin wells (Figure 3.16), is a set of trench-parallel anticlines which involves strata of the E3, E-O, M1, M2 and M3 sequences (Panel

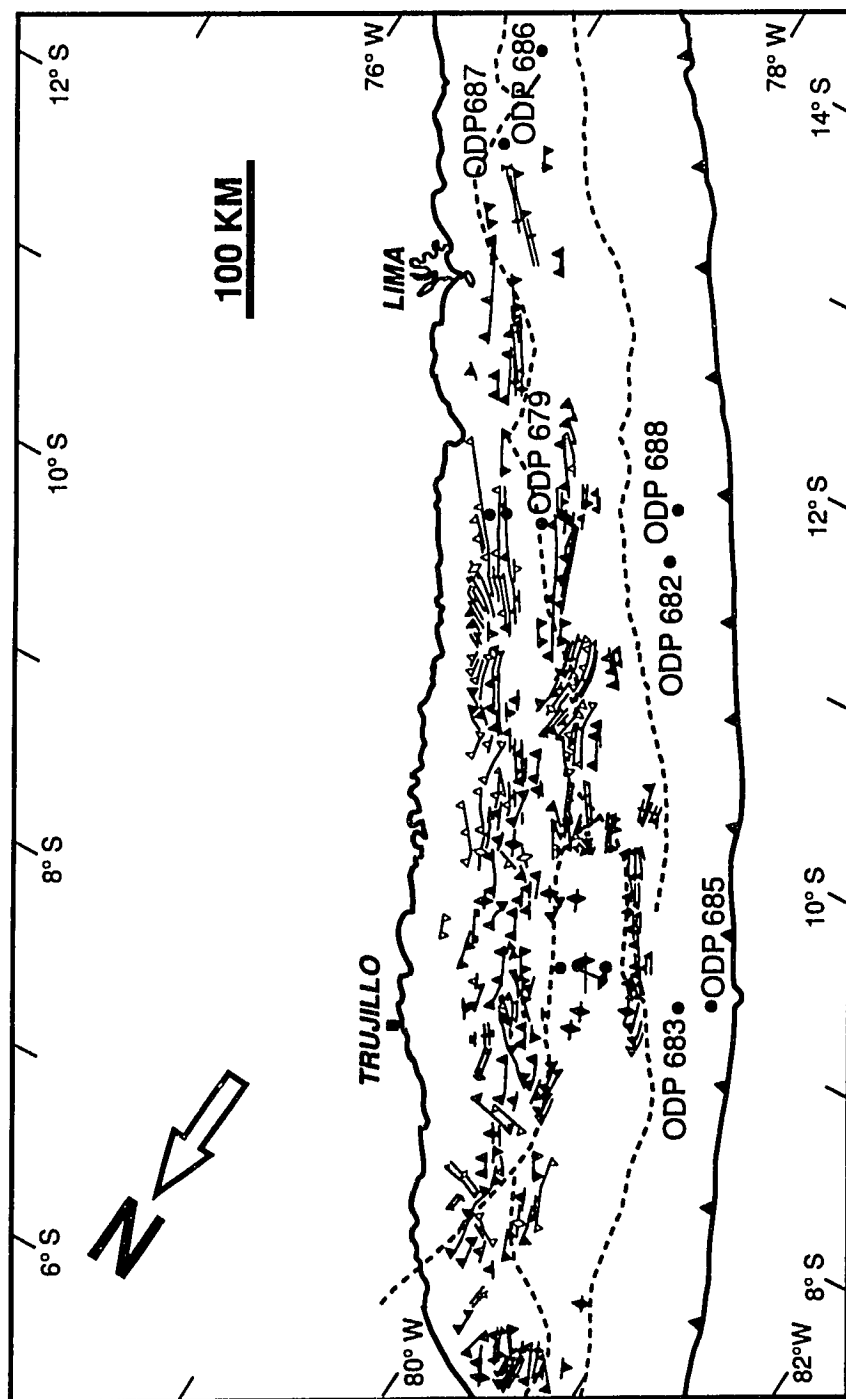


Figure 4.2 UPPER MIDDLE TO LATE MIOCENE THIRD COMPRESSIONAL EVENT

Thrust Anticline axis Syncline axis Monocline fold axis

Structures of the Second Compressive Event reactivated Basin boundaries-----

1, Plate 8). The divergence of the westward dipping reflectors contained in the upper part of the M2 sequence, at the western side of the Salaverry-Trujillo High (Plate 13), indicates that this feature became uplifted by the end of the Middle Miocene. Similar divergence in the internal reflectors of the M3 and P sequences at both sides of the high (Panels 1 and 2, Plates 4, 8, and 13) suggests that the uplifting process was continuous from the late Miocene to the Pliocene. The formation of this high was, therefore, coeval with the third compressive event. The set of anticlines which form the 60 km long western part of the high north of the Ballena and Delfin wells (Figure 3.16) are the structural inversion of middle Eocene to upper Miocene sediments produced during late Miocene, by the end of the third compressive event (Plate 8).

4.9 The upper-middle to late Miocene southern uplift and peneplanation

During the late Miocene compression and coeval with the first stage of the Salaverry-Trujillo High uplifting process, the offshore East Pisco Basin, the West Pisco Basin and the southern part of the Lima Basin were also uplifted and probably peneplaned. The uplift was more pronounced in the west (southern Lima Basin and West Pisco Basin) where a thicker section was eroded and a very conspicuous unconformity was created (Panels 3 to 6, Plates 16 and 18). In the West Pisco Basin the M2 sequence was completely eroded

and sediments of the uppermost Miocene-Pliocene P sequence rest directly upon Eocene strata (Plate 17). During the latest Miocene the area south of the Salaverry-Trujillo High subsided, whereas the Salaverry-Trujillo High uplifting continued.

4.10 The fourth late? Pliocene compressive event

This compressive episode affected the East and West Pisco Basins (Figure 5.2) producing trench-oblique N-S trending thrusts and folds in the East Pisco Basin and NW trending thrusts in the West Pisco Basins (Figure 4.3). In both basins the folds are asymmetric (Panel 5, Plate 18); the thrusts and fold axial surfaces of the East Pisco Basin dip predominantly W, while those of the West Pisco Basin dip NE. Seismic profiles show evidence of late Pliocene syntectonic sedimentation during thrust fault development (Panel 5, Plate 18).

Onshore, near Pisco (Figures 3.5, 4.3 and 5.2), east vergent monoclinical folds of marine Pliocene sediments described by Petersen (1954), Newell (1956), Ruegg (1956), Soulas (1977) and Macharé (1987) represent the fourth compressional event. The influence of this compressive episode in the geometry and paleobathymetry of the onshore East Pisco Basin was pointed out by DeVries (1988) who recognized a complex facies distribution pattern due to the presence of active highs during the Pliocene.

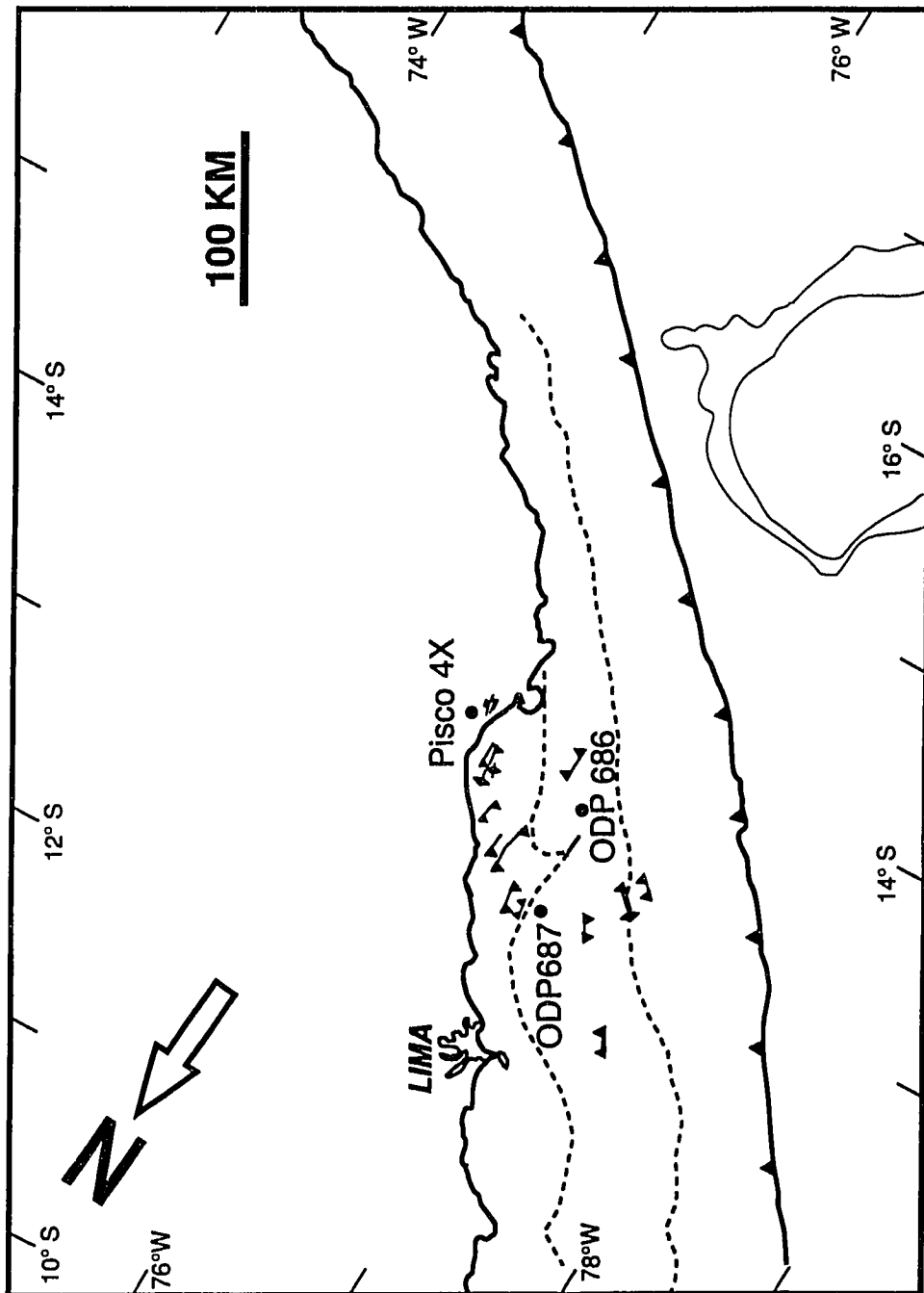


Figure 4.3 LATE? PLIOCENE FOURTH COMPRESSIONAL EVENT

Thrust  Anticline axis  Syncline axis  Monocline fold axis  Basin boundaries 

4.11 Latest Pliocene extension

The last extensional episode occurred during the latest Pliocene. It is mostly characterized by high-angle synsedimentary normal faults whose trend is quite variable (Panels 1 to 6). The most prominent set of faults representing this event are faults of the rifting system which were reactivated during the latest Pliocene (Plates 4, 8, 13, 14, and 16). The synsedimentary nature of this phenomenon may have also affected the facies distribution during the P sequence deposition.

4.12 The incision and fill of submarine canyons during Middle Miocene to Pliocene

The submarine canyon systems present along the steep western side of the Trujillo-Salaverry High and part of the Lima-Salaverry boundary zone in the M2, M3 and P sequences are spectacular features more than 1s deep and 14 km wide (Plates 4, 5, 7, and 9). These features generally consist of narrow canyons in the canyon head zone, which merge downstream to form a wide canyon toward the base of the paleoslope. The predominant trend of the canyon thalwegs is perpendicular to the trench. The canyon incision progressed landward through time.

Carlson and Karl (1988) described the development of recent large submarine canyons in the Bering Sea and concluded that some of the most important events that contribute to the incision of canyons are the sea level lowstands during the Cenozoic glacial stages.

On the other hand, Bouma et al. (1989) proposed a conceptual sea-level-driven depositional model for the late Pleistocene fanlobes (channel-overbank systems) of the Mississippi Fan; according to this model, the submarine canyon and upper fan channels form during initial lowering of sea level.

The continuous uplift of the Salaverry-Trujillo High during deposition of the M3 and P sequences (upper Middle Miocene to Pliocene time) produced a sustained and very localized shallowing of the sea floor at the slope-shelf break zone on the western side of the Salaverry-Trujillo High. This process may have promoted the incision of the submarine canyon systems and their development as the uplift continued.

As pointed out by Carlson and Karl (1988) and Bouma et al. (1989) for the Bering sea and the Mississippi Fan canyon systems respectively, slumping and sliding may have been the main mechanisms responsible for excavating and shaping the canyons of the M2, M3 and P sequences. It is also possible that the seismic

activity of the margin may have contributed to the canyon development by triggering the slumps and slides.

4.13 The gravitational extension at the slope

Sediments of the M1 to P sequences located on a paleoslope setting were commonly affected by gravitationally-induced listric normal faults with shallow detachment zones and dip downslope (Panel 1, 3, 5 and 7; Plates 12 and 13).

4.14 Deformation in the southern coast.

Macharé (1987) provided a structural analysis of the coastal area. Six (F1 to F6) short-lived compressional events occurred, ie during the late Eocene (by 42 Ma), the late Oligocene (by 26-28 Ma), the early Miocene (by 15-17 Ma), the middle Miocene (by 10 Ma), the late Miocene (by 7 Ma), and the early Quaternary (by 2 Ma).

The second and third compressional episodes recognized in this study correlate well with Macharé's F1 and F5 events respectively; and the fourth late? Pliocene compression may be his early Quaternary F6 event. Macharé (1987) pointed out that the occurrence of the F3 and F4 events is dubious.

Macharé (1987) also described three extensional episodes. The first one consists of syn-sedimentary normal faults that affect late Eocene sediments of the Paracas Fm. near Puerto Caballas (Figure 3.5). A second extensional event offsets, also syntectonically, upper Pliocene sediments. Both episodes have a NE-SW trending stretching direction (Macharé, 1987).

Normal faults of the last extension offset Quaternary sediments and have N-S trending tensional axes (Macharé, 1987).

There is a lack of synchronism between my middle Eocene rifting event and Macharé's late Eocene extension. It is possible that the age of the coarse-grained Paracas Fm is older than that assigned by Macharé. On the other hand, the NE-SW stretching direction is similar to that of the rifting event. The Pliocene extension identified in this study correlates well with Macharé's second extensional event.

CHAPTER 5: PLATE KINEMATICS AND FOREARC EVOLUTION

Before addressing the relationship between plate kinematics and the evolution of the forearc, I include a brief description of the trench-slope zones and a summary of the current state of stress in the margin.

5.1 The trench and the middle to lower slope zone

The description of the accretionary wedge is limited to two narrow transects (Figure 1.7, Panel 7). The northern transect is located west of the Trujillo Basin and has the CDP-2 and Peru 5 seismic profiles. The southern transect, located west of the Lima Basin, includes the Peru 14, CDP-1 and Shell 1017 seismic lines.

The middle to upper slope boundary is located about 25 to 85 km east of the trench axis (Panel 7), while the lower to middle slope boundary occurs 13 to 42 km east of the trench axis (Thornburg, 1985; Moore and Taylor, 1988). The CDP-2, Peru 5, Peru 14, CDP-1 and Shell 1017 seismic dip profiles (Figure 1.7 and Panel 7) illustrate the trench-slope zone, west of the Trujillo Basin (CDP-2 and Peru 5) and the Lima Basin (Peru 14, CDP-1 and Shell 1017).

The main elements of the lower to middle slope are the subducted oceanic slab, the trench, the accretionary complex and the

most distal Cenozoic sequences underlain by a pre-Cenozoic continental basement or else by a pre-Cenozoic accretionary complex.

The subducted oceanic plate

The subducted oceanic slab is well displayed on all seismic profiles and can be traced at least 26 km east of the trench axis below the accretionary prism and the middle slope (Panel 7).

Along the trench, the Nazca Plate is younger in the north than in the south; thus it is 33 to 36 Ma north of the Mendaña Fracture Zone (Figure 3.1), 41 Ma at 12° S latitude, and 44 Ma south of the Nazca Ridge. In the northern transect about 100 m of hemipelagic sediments cover the Nazca Plate. Normal faults affect the flexured portion of the oceanic plate adjacent to the trench (Panel 7). A half graben within the subducted portion of the oceanic plate, first described by Moore and Taylor (1988), is shown on the CDP-2 profile (Panel 7).

The trench

On the northern Peru 5 profile, the trench is 3 km wide and contains 350 to 400 ms of flat-lying trench sediments (Moore and Taylor, 1986). Kulm et al. (1981) describe turbiditic silt and sand

interlayered with muds from cores recovered in this area. On the Peru 14 line, the trench axis is 2 km wide and contains about 400 to 500 m of turbiditic sediments (Moore and Taylor, 1988).

The accretionary prism

All seismic profiles show the presence of a relatively small Cenozoic accretionary complex with east-dipping imbricates (Panel 7). The CDP-2 line best illustrates the accretionary wedge. Seismic profile CDP-2 depicts imbricated trench deposits that have been scraped off the oceanic crust (Panel 7).

It seems that the sediment flux into the trench was not sufficient to create a well-developed accretionary prism. The main cause for the restricted sediment supply probably was a dry climate in the onshore region, which precluded the development of an efficient source for sediments.

The Peru 14 line shows, at the lower slope, a pre-Cenozoic accretionary complex underlying Cenozoic sediments; I do not know whether this pre-Cenozoic accretionary wedge extends to the middle and upper slope. The lack of seismic resolution and the absence of deeper wells in this portion of the margin do not permit to answer this question.

The middle-upper slope boundary

On the CDP-2 line and probably the Peru 5 profile, the upper and middle slope zones are separated by a prominent east-dipping thrust fault which offsets the sea floor and the pre-Cenozoic basement. It is unclear whether a similar structure occurs on the southern profiles where no offset of the sea floor is observed.

On the lower and middle slope of the northern lines (CDP-2 and Peru 5), strata of the uppermost Q sequence unconformably rest with angular unconformity on top of east-dipping imbricates of the M3 and M2 sequences. Some of the faults of the imbricate system offset the Q sequence and the sea floor (Panel 7).

On the southern lines (Peru 14, CDP-1 and Shell 1017), the Cenozoic sediments display different depositional and structural styles. The E3, M2 and M3 sequences were deposited in a complex system of submarine canyons which are particularly well defined on the Shell 1017 line. The Q sequence and probably the P sequence unconformably cover the older strata. The Peru 14 line shows, on the lower slope zone, west-dipping thrusts with a shallow detachment involving the Q and P ? sequences.

Hydrate reflectors

Seismic profiles Peru 14, CDP-1 and Shell 1017 show discontinuous sea floor parallel hydrate reflectors along the landward part of the lower slope (Panel 7).

Upper slope fan systems

On the northern lines the upper slope zone contains a slope fan system corresponding to the M2, M3, and M1? sequences. These deposits are folded and, in part, offset by listric normal faults with shallow detachment surfaces; normal faults that involve the Pre-Cenozoic basement also occur. In contrast the southern lines exhibit a large undeformed slope fan system belonging to the P sequence which unconformably rests on top of the M2 sequence.

5.2 Current state of stress in the margin

Current seismic activity indicates that trench-orthogonal compression occurs along the forearc and the Subandean Zone (Sébrier and Soler, 1991). In the forearc, focal depths range from 20 to 40 km and are located at the continental-oceanic plates interface (Suarez et al., 1982); whereas, in the Subandean belt, the focal depth ranges from 10 to 30 km (Suarez et al., 1982). In the Eastern

Cordillera of Central Peru active thrust faults have also been reported (Suarez et al., 1982).

Longitudinal, i.e. N-S trending, extension is indicated by an E-W trending normal fault system which occurs along the Altiplano-Eastern Cordillera boundary, the Western Andes and, in the south, at the Forearc-Western Cordillera boundary (Sébrier et al., 1985, 1988).

In the southern Western Andes, 100 km north of Arequipa (Figure 3.1), calc-alkaline volcanism is coeval with Recent E-W trending normal faults (Sébrier and Soler, 1991). In the Cuzco area, along the Altiplano-Eastern Andes boundary, an E-W to NW-SE trending fault zone has been the locus of several destructive shallow earthquakes. Quaternary and Recent volcanic centers with shoshonitic affinities occur along the fault zone. This suggests that an E-W trending Andean normal fault system controls the current magmatic activity (Sébrier and Soler, 1991).

5.3 The Cenozoic evolution of the Peruvian margin

The Cenozoic history of the Peruvian forearc is dominated by the subduction of the Nazca Plate. Important parameters that affect the subduction regime and consequently forearc tectonics are: (1) variations in relative rates of convergence and

subduction; (2) variations in the direction of convergence; (3) variations in the angle of subduction.

5.31 Relationship between variations in the rate of convergence and tectonism

Convergence rate direction at the Peru-Chile trench has varied through time. Pardo-Casas and Molnar (1987) calculated the variation in the rate and direction of convergence at the latitude of central Peru based on plate reconstructions. These authors reported a close correlation between periods of rapid plate convergence (>100 mm/a) and the two most recent phases of intense Andean tectonic activity recognized in Peru (Steinmann's (1929) late Eocene Incaic and the Mio-Pliocene Quechua phases). In contrast, periods between 70 and 50 Ma (Maastrichtian to middle Eocene) and between 36 and 26 Ma (Oligocene) were characterized by slow convergence (50 to 55 ± 30 mm/a) and correlate with periods of quiescent tectonic activity.

The average rates of convergence as a function of time calculated by Pardo-Casas and Molnar (1987) show the following relationship with the tectonic events recognized in the study area (Figure 5.1): (1) The first compressive event, with its poorly constrained age, may correspond to the increase in the convergence rate which occurred during the middle Paleocene. (2) The rifting

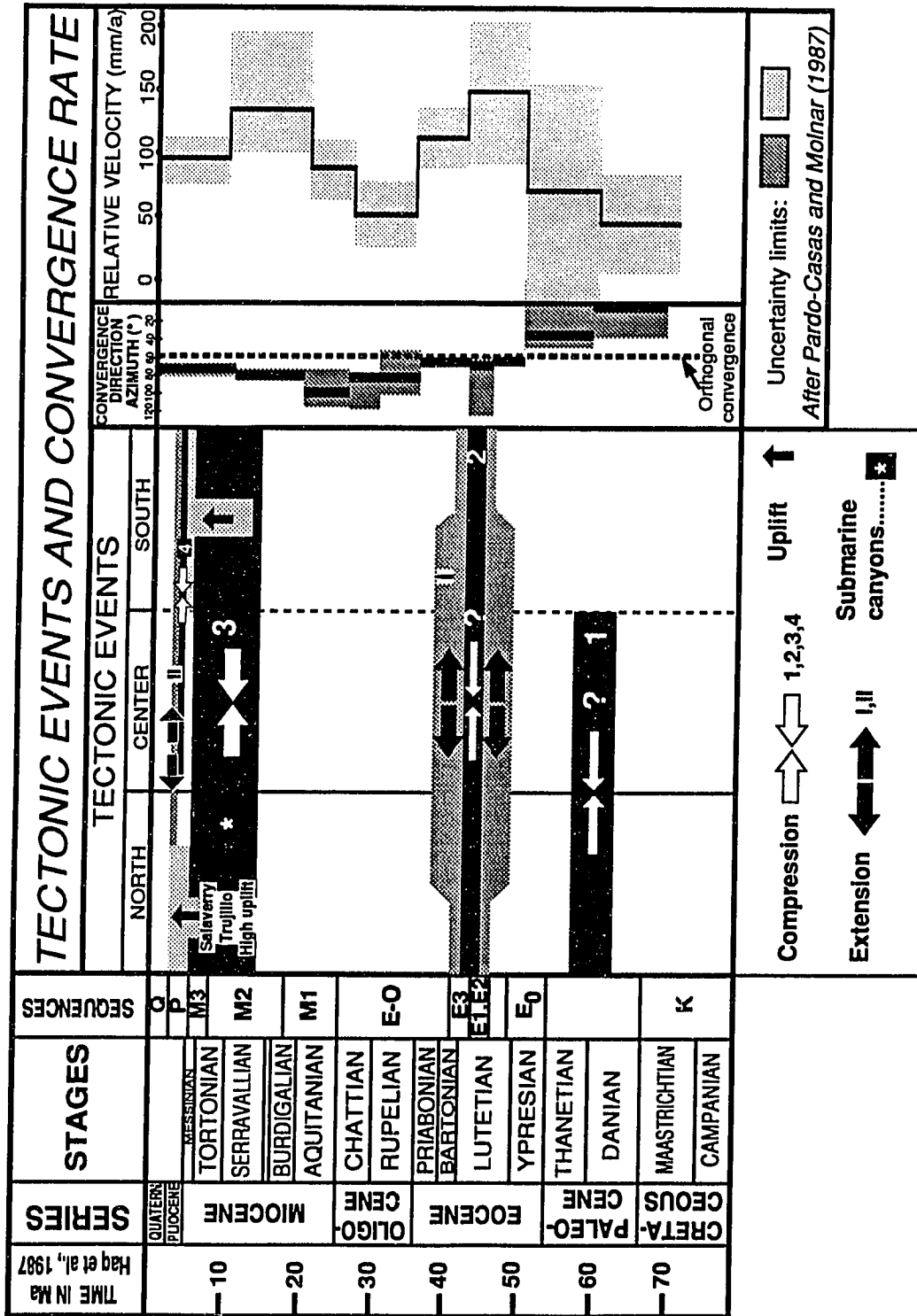


Figure 5.1 TECTONIC EVENTS AND CONVERGENCE RATE

episode and the second compressive event correlate well with a prominent peak in the convergence rate curve during the middle Eocene. (3) The third compressive event occurred during a period of negative acceleration of the convergence rate. (4) There was no variation in the convergence rate during the fourth compressive episode and the Pliocene second extensional event (5.1). I will discuss later the probable relationship of the last compressional episode with the Nazca Ridge subduction.

5.32 Relationship between variations in the direction of convergence and tectonism

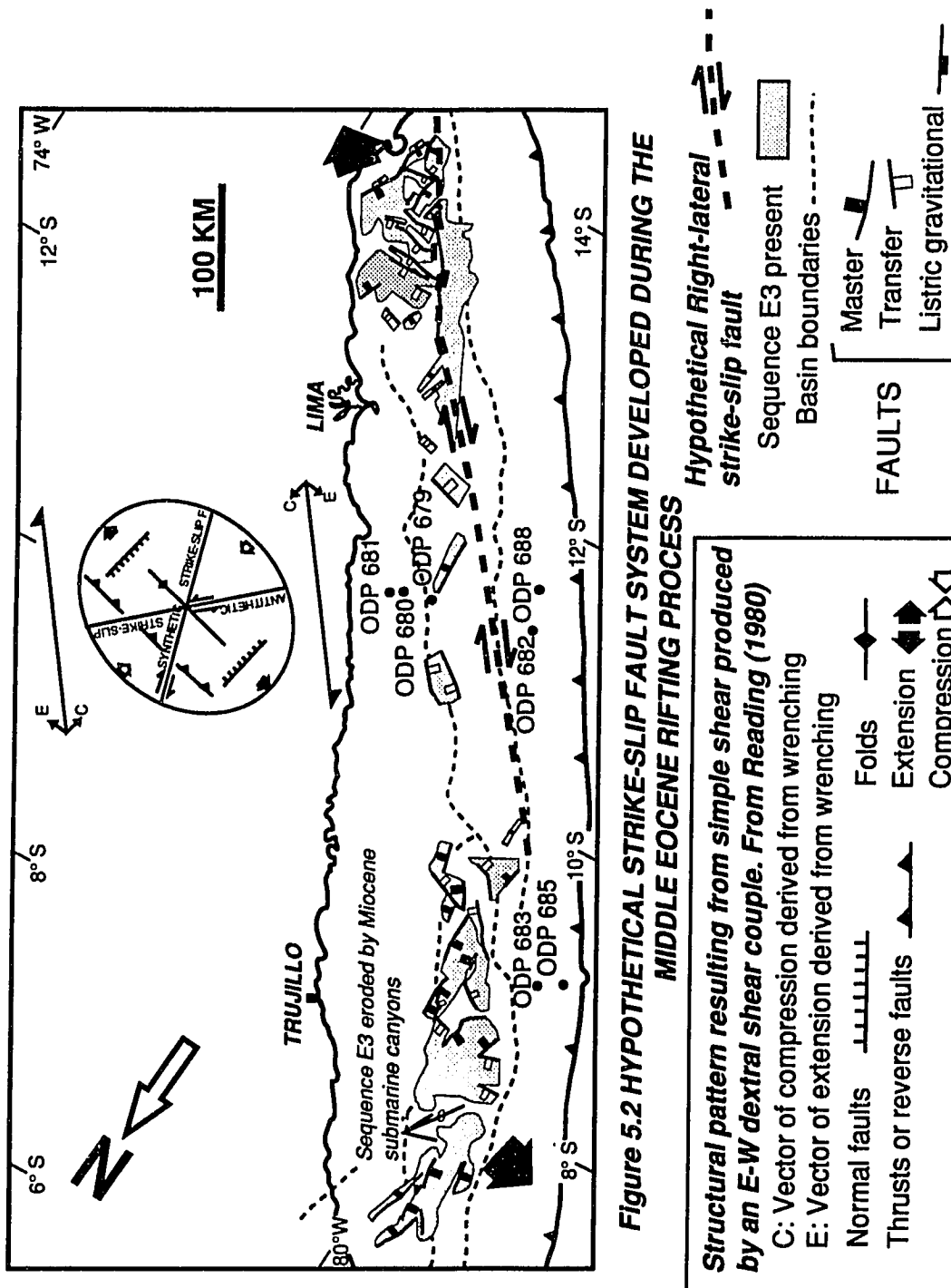
Pardo-Casas and Molnar (1987) reported that between 59 and 49.5 Ma (upper Paleocene to lower Eocene time, or the time of the anomalies 25 and 21 respectively), the direction of convergence of the Nazca Plate with respect to South America was NE, oblique to the interplate boundary. The direction of convergence changed to predominantly E-W (orthogonal to the interplate boundary) convergence after 49.5 Ma (Figure 5.1).

According to Pardo Casas and Molnar (1987), the oblique convergence ended before middle Eocene, but the large uncertainties in plate motion reconstruction reported by these authors open the possibility to extend the oblique convergence until middle Eocene. If this is the case, the occurrence of NE trending oblique convergence

during middle Eocene suggests the possibility that the strain in the upper plate may have been resolved into components normal and parallel to the trench as postulated by Fitch (1972) and Walcott (1978). This would have led to the development of a major right lateral strike-slip fault system parallel to the trench axis (Figure 5.2). Possible locations of a strike-slip zone in the study area are (1) the Lima Basin-middle slope zone boundary where the master and transfer faults abruptly stop (Figures 1.4 and 5.2), and (2) the trench parallel zone in the West Pisco Basin through which the structural style of the Eocene sediments changes from that of the rifting system to a trench parallel listric normal fault system (Figures 1.4 and 5.2, Panel 5). The geometric and kinematic relationships among the master and transfer fault systems with this hypothetical strike-slip zone are similar to wrench tectonics examples reported by Wilcox et al. (1973), Dibblee Jr. (1977), Reading (1980), Spörli (1980) and Worrall (1991) and clay models described by Harding (1974), Wilcox et al. (1973) and Reading (1980) (Figure 5.2).

5.33 Variations in the angle of subduction

The angle of subduction is mainly controlled by (1) the age of the subducted slab, (2) lithospheric discontinuities, and (3) the presence of buoyant aseismic ridges and plateaus.



5.331 Nazca Plate age

When a relatively young (less than 50 Ma) lithosphere is subducted, the buoyancy created by its thermal state tends to reduce the subduction angle (Molnar and Atwater, 1978). It is uncertain whether a relatively young oceanic plate underlaid the forearc during all the Cenozoic.

5.332 Lithospheric discontinuities

The presence of trench oblique lithospheric discontinuities on both the oceanic and/or the continental plate may separate zones with different angles of subduction.

The Huancabamba and Abancay deflections are angular bends in the Andes (Figure 3.1). Mitouard et al. (1990) reported a post-Oligocene clockwise rotation ($\sim 25^\circ$) north of the Huancabamba deflection and a synchronous counterclockwise rotation ($\sim 20^\circ$) south of the deflection, based on paleomagnetic data. The origin of the Abancay deflection has not yet been addressed.

Studies of earthquake hypocenter distribution indicate that the Nazca Plate is subducted beneath South America at moderate angles (25° to 30°) along the segment of the Peruvian margin south of the

Abancay deflection (Figure 3.1) (Isacks and Molnar, 1971; Stauder, 1973, 1975; Barazangi and Isacks, 1976, 1979; Isacks and Barazangi, 1977). This region shows, onshore, a chain of Quaternary volcanoes trending parallel to the trench (Figure 2.5). Quaternary volcanoes are absent along northern and central Peru between the Huancabamba and Abancay deflections, where the subduction angle is very low ($<10^\circ$). Barazangi and Isacks (1976) attributed the absence of volcanism in this region to the displacement of the wedge of partially melted asthenosphere by the very low angle of the subducting lithosphere and the consequent direct superposition of two lithospheric plates.

The Mendaña Fracture Zone is an oceanic fracture zone located on the Nazca Plate off Peru. It trends approximately N 65° E and intersects the Peru-Chile Trench between $9^\circ 40'$ S and $10^\circ 35'$ S latitude (Huchon and Bourgeois, 1990), (Figure 3.1). It is 100 km at their junction with the trench and 50 km wide 400 km seaward of the trench and consists of a series of N 65° E trending parallel ridges and troughs. Hilde and Warsi (1982) postulated that the Mendaña Fracture Zone is the locus of an active spreading center that propagates seaward. Huchon and Bourgeois (1990) reported that new oceanic crust has formed since about 3.5 Ma and that the westward rifting velocity of propagation is 10 cm/a.

5.333 The Nazca Ridge

Aseismic ridges and plateaus are topographic high areas with less density than the surrounding oceanic lithosphere; their relatively high buoyancy tends to reduce the subduction angle when they are subducted. Shallow subduction angles along northern and central Peru may be caused by the oblique subduction of the aseismic Nazca Ridge (Pilger, 1981). Pilger (1981) proposed a reconstruction of the Nazca Ridge drifting and subduction history assuming: (1) a common site of origin for the Nazca and Tuamotu Ridges at the Pacific-Farallon spreading center; and (2) a symmetrical configuration for the Tuamotu and Nazca Ridges. According to his reconstruction, the Nazca Ridge intersected the Peru-Chile trench at 5° S at approximately 9 Ma (late Miocene time) and moved southward as it was subducted (Figure 5.3). The Nazca Ridge is presently being subducted beneath the South America Plate in southern Peru (Figures 5.3 and 5.4) at the latitude of the Pisco Basin (16° S). The Nazca Ridge subducted portion consists of three segments (Pilger, 1981); the older one trends parallel to the trench, whereas the other two are trench-oblique (Figures 5.3 and 5.4).

Marty et al. (1987) interpreted that an 8 Ma deformation event recorded in the Sechura Basin of northern Peru was produced by the local subduction of the Nazca Ridge. The deformation described by Marty et al. (1987) is similar to the third compressive event of this

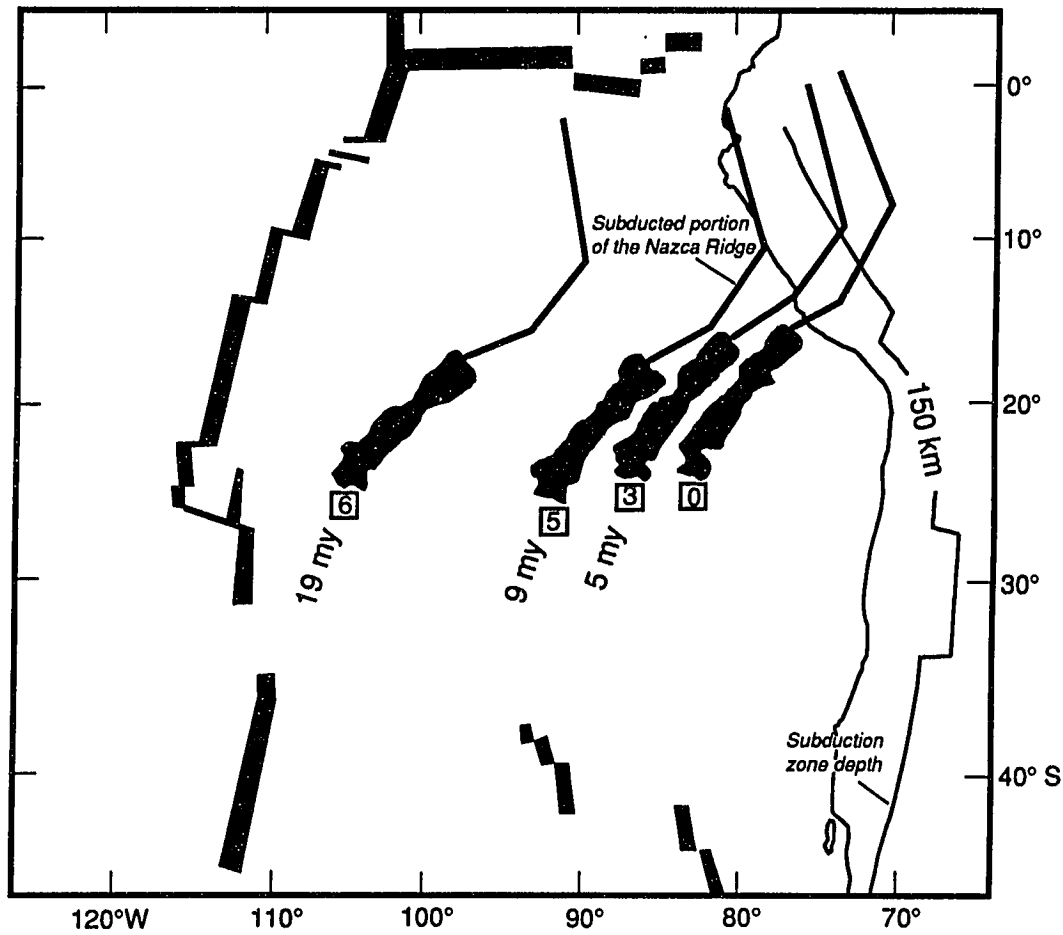


Figure 5.3 RECONSTRUCTED GEOMETRY AND POSITION OF THE NAZCA RIDGE DURING THE PAST 20 MILLION YEARS

Anomalies: 0 3 5 6

Pilger (1981)

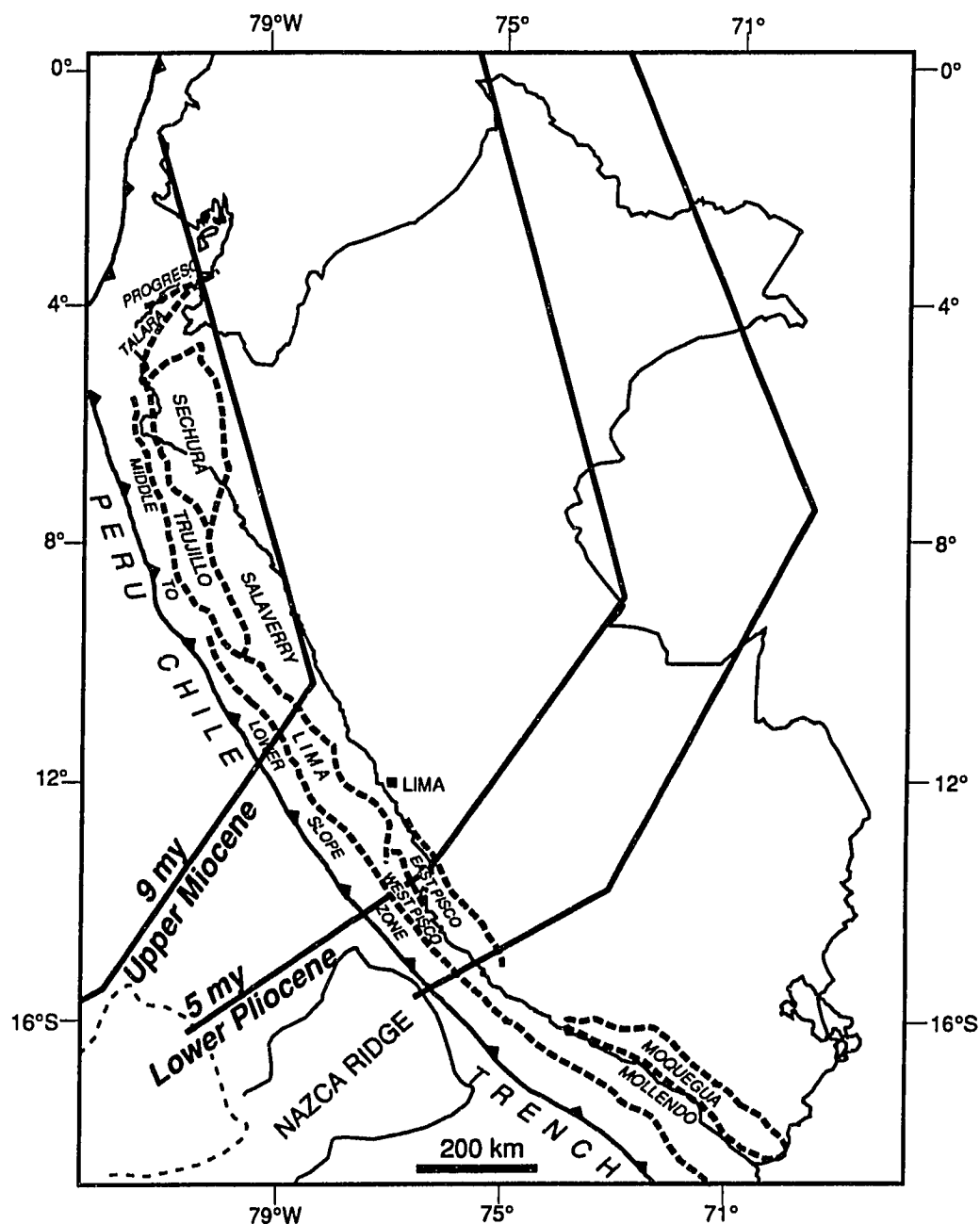


Figure 5.4 RECONSTRUCTED GEOMETRY AND POSITION OF THE NAZCA RIDGE DURING THE PAST 9 MILLION YEARS

Subducted portion
of the Nazca Ridge

from Pilger (1981)

study. Marty's et al. interpretation is attractive because it explains compression during a period of decreasing rate of convergence (Figure 5.2). On the other hand, the Nazca Ridge subduction below the Trujillo Basin during the middle Miocene (Figures 5.3 and 5.4) coincided with the initiation of the Salaverry-Trujillo uplift and the development of submarine canyons which suggests that the Nazca Ridge subduction was the cause of these processes.

The northerly prograding clinoforms of the sequence P which filled the northern part of the Salaverry Basin (Figure 3.16) during the late Miocene indicate the existence of a high located at the center of the basin. Pilger's reconstruction shows that one of the trench-oblique segments of the Nazca Ridge was subducted below the central part of the Salaverry Basin during the late Miocene (Figure 5.4); this suggests that the oblique subduction of this segment of the Nazca Ridge may have caused the local uplift of the Salaverry Basin central portion, thus defining the paleocurrent pattern during the deposition of the lower part of the P unit.

Although Pilger's reconstruction helps to explain the origin of some important tectonic features of the forearc there are other important questions that relate to the timing of subduction and the geometry of the ridge, i. e. (1) Why were the uplifts of the Salaverry-Trujillo High, the Lima Basin, the West Pisco and the East Pisco Basins coeval if the Nazca Ridge was not synchronically

subducted below all these zones?. (2) Why did the Salaverry-Trujillo High uplift and the canyon cut and fill process continued long after the passage of the ridge?.

The last Pliocene compressive event, which was restricted to the East and West Pisco Basins, seems to be related to the passage of the subducted Nazca Ridge (Figures 4.3 and 5.4).

5.34 Implications of this study in the evolution of the Peruvian margin

This study documents the Cenozoic evolution of a large portion of the Peruvian forearc which contains the offshore Sechura, Trujillo, Salaverry, Lima, East Pisco and West Pisco Basins. The oldest Tertiary sediments are Lower? to middle Eocene coarse grained siliciclasts of the widespread sequence E₀ which unconformably rest on top of a heterogeneous basement consisting of upper Cretaceous? and older rocks. During the middle Eocene the forearc region was extended (trench parallel extension) through a rifting process in which sequences E₁ to E₃ were deposited, filling half grabens in all but the Salaverry Basin. The occurrence of this event has not yet been reported in the backarc, but it seems indeed that this region was continuously compressed since at least the late Cretaceous.

The presence of trench-parallel extension in the forearc and coeval trench-orthogonal compression in the backarc is possible under an oblique convergence regime; in this case the strain in the upper plate can be resolved into components normal (compressional in the backarc) and parallel (extensional in the forearc) to the trench (Fitch, 1972). The boundary of these two structural zones would be a trench-parallel strike-slip fault system located along the forearc and particularly along the western boundary of the magmatic arc. This is a favorable zone for a high-angle detachment due to the lithologic contrast between the host rock and the intrusives. Although plate reconstruction (Pardo Casas and Molnar, 1987) indicates that the northeast oblique convergence of the Nazca (Farallon) with respect to South America ended in the early Eocene, these authors admit that the largest uncertainties in their plate reconstruction are related to the calculation of the direction of convergence (Pardo Casas and Molnar, 1987); therefore it is possible that the northeasterly oblique convergence may have extended until the middle Eocene. The fault pattern displayed by the middle Eocene extension strongly suggests the occurrence of a right-lateral strike-slip fault system which is consistent with the northeasterly oblique convergence described by Pardo Casas and Molnar (1987). The onshore presence of a middle Eocene strike-slip fault system, particularly along the western boundary of the magmatic arc, must be investigated in order to confirm this hypothesis.

Since the late Eocene to the present the offshore Sechura, Salaverry, Trujillo, Lima, East Pisco and West Pisco Basins received fine grained siliciclastics, biogenic sediments and minor fine grained volcanics (sequences E-O, M1, M2, M3, P and Q) which reflect dry weather and the lack of an efficient system of sediment transport in the onshore area, and recurrent upwelling conditions in the ocean. The low rate of sediment flux into the trench precluded the creation of a well-developed accretionary prism. During this period, characterized by trench-orthogonal convergence, the backarc was strongly folded and thrust, creating the main features of the Andes. Meanwhile the forearc basins were mildly folded and thrust. The Miocene to the Present deformation in the forearc seems to be influenced by the oblique subduction of the Nazca Ridge although a complete understanding of its relationship with the margin tectonics is still pending.

CONCLUSIONS

Stratigraphy

1. A Cretaceous? sequence and ten Cenozoic sequences filled the basins of the study area. These are: (1) the Maastrichtian to Campanian? K sequence, (2) the lower? to middle Eocene E₀ sequence, (3) the middle Eocene E₁ sequence, (4) the middle Eocene E₂ sequence, (5) the middle Eocene E₃ sequence, (6) the uppermost middle Eocene to Oligocene E-O sequence, (7) the lowermost Miocene M₁ sequence, (8) the lower to middle Miocene M₂ sequence, (9) the upper Miocene M₃ sequence, (10) the uppermost Miocene-Pliocene P sequence and, (11) the Quaternary Q sequence.
2. The widespread E₀ sequence was deposited during a period of tectonic quiescence.
3. A small chain of small coast-parallel igneous bodies intruded the E₀ sequence during middle or late Eocene?.
4. The E₁, E₂ and E₃ sequences are half graben fills representing three pulses of a rifting process that affected large segments of the study area.

5. The rifting process was interrupted by a compressive episode that took place after the second pulse of rifting.
6. After the rifting event the study area lacked an efficient system of sediment transport from the continent, thus the sedimentary record mostly consists of fine-grained sediments. The main cause for the restricted sediment supply probably was the dry climate in the onshore region. It seems that the sediment flux into the trench was not adequate to create a well-developed accretionary prism.
7. The post-rifting E-O sequence was deposited along the Trujillo Basin and the western border of the Sechura Basin, in parts of the Lima and East Pisco Basins. Cold water upwelling was effective during the E-O unit deposition.
8. The M1 and M2 sequences represent an early to middle Miocene regional transgression. The M2 sequence was deposited in two main areas bounded by a narrow trench-parallel shelf-slope break zone. Shelf sedimentation prevailed in the eastern area, whereas cutting and filling associated with submarine canyons took place in the west.
9. The M3 sequence was syntectonically deposited during a late Miocene compressive event. During this time the Salaverry-Trujillo High emerged and provided sediments to the Salaverry and Trujillo

Basins. The canyon cutting and filling continued west of the Salaverry-Trujillo High.

10. During the latest Miocene to the Pliocene, east of the emerged Trujillo-Salaverry High an interior shallow basin was formed, whereas in the west the submarine canyon cutting and filling continued. The P sequence was deposited in these settings. The interior basin was filled by a northerly prograding phase followed by an aggradational phase. Farther south, in the Lima Basin a trench-parallel slope-shelf break zone divided an eastern zone with shelfal deposits from a western area which received large fan slope deposits.

11. In the Quaternary the Salaverry-Trujillo High was submerged.

Structural Geology

12. The study area was affected by four compressive events and two extensional episodes. The compressions occurred during Paleocene?, middle Eocene?, upper-middle to late Miocene and middle Pliocene?. The extensions took place during middle Eocene and late Pliocene. Pre-Tertiary substratum was involved in all the tectonic events.

13. The deformation of the first compressive episode occurred during the Paleocene?, is mild, and is poorly defined in seismic profiles of the Salaverry and Trujillo Basins.

14. Prior to the deposition of the lower to middle Eocene E₀ sequence the region was peneplaned.

15. The direction of extension during the basement-involved rifting process was E-W to ESE-WNW, and the main structural elements were: (1) A N-S to NNE-SSW trending master fault system that formed the half graben boundaries. (2) An E-W to ESE-WNW trending left-lateral transfer fault system. (3) A hypothetical trench-parallel, right-lateral strike-slip system.

16. The rifting process developed in three pulses represented by the E₁, E₂ and E₃ sequences. The rifting process was interrupted by a short-lived compression that took place after the deposition of the E₂ sequence. During rifting phase 1, the Trujillo and West Pisco Basins were extended. Phase 2 affected the Trujillo Basin. During the last pulse of rifting, the Trujillo and East Pisco Basins and part of the Sechura, Lima and West Pisco Basins were extended.

17. In the western part of the West Pisco Basin, the E₁, E₂ and E₃ sequences are affected by a trench-parallel listric normal faults

system. This structural style suggests gravity-induced extension in a slope setting.

18. The middle Eocene second compression interrupted the rifting process after the E2 sequence deposition, produced folds and thrusts in strata of the K and E₀ sequences and a very mild inversion in some of the half grabens of the E2 sequence. A predominant NW-SE trending fold-thrust system occurred along the Sechura, Lima, Salaverry and West Pisco Basins.

19. The Salaverry-Trujillo High which began to form by the end of middle Miocene and proceeded until Pliocene is a 370 long, trench-parallel open flexure and, in part, a 60 km long, trench-parallel belt of anticlines. These anticlines are the structural inversion of middle Eocene to upper Miocene wedges (E3 to M3 sequences), and originated during the third compressive event.

20. The third (late Miocene) compressive event produced: (1) the reactivation of structures formed during the second compression; (2) the formation of a trench-parallel trending folded belt in the Salaverry Basin, (3) syntectonic deposition of the M3 sequence, (4) the structural inversion of middle Eocene to upper Miocene deposits and, (5) differential uplift and erosion in the West Pisco Basin and southern Lima Basin, where a conspicuous unconformity was created.

21. The fourth (late? Pliocene) compression affected the East and West Pisco Basins producing in the East Pisco Basin trench-oblique N-S trending folds and a mild-half graben inversion. E-W trending thrusts were formed in the West Pisco Basin.

22. The second extensional episode (late Pliocene) is characterized by the reactivation of faults formed during the first extensional event.

23. The continuous uplift of the Salaverry-Trujillo High during the deposition of the M2, M3 and P sequences produced a sustained and very localized shallowing of the sea floor at the slope break zone on the western side of the high and the incision of submarine canyons.

24. Gravity-induced listric normal faults with shallow detachment zones affect sediments of the M1, M2, M3 and P sequences.

Plate kinematics and forearc tectonics

25. The middle Eocene extensional rifting episode and the second compressive event correlate well with a prominent positive peak in the convergence rate curve.

26. An unexpected coincidence between the occurrence of the third compressive event and an interval of negative acceleration in the convergence rate is observed.

27. There is no correlation between the rate of convergence, the fourth compressive episode and the second extensional event.

28. The fourth compressive event, which is restricted to the East and West Pisco Basins, seems to be related to the passage of the subducted Nazca Ridge during late Pliocene through Pleistocene.

BIBLIOGRAPHY

Allen M. R., and Dunbar R. B., 1988. Phosphatic Sediments in the Pisco Basin. In Dunbar R. B. and Baker P. A. (eds.): Cenozoic Geology of the Pisco Basin, IGCP #156. Guidebook to Field Workshop, May 1988, Lima, p. 109-124.

Angeles C., 1987. Les chevauchements de la Cordillère Occidentale par 12° 15' S (Andes du Pérou Central) [Ph. D. thesis]: Montpellier Université des Sciences et Techniques du Languedoc, 184 p.

Ashworth E. T., 1955. Memorandum of Correlation Pisco 4x. Petroperu internal report, unpublished.

Atherton M. P., Pitcher W. S., and Warden V., 1983. The Mesozoic marginal Basin of central Peru. *Nature* 305, p. 303-306.

Atherton M. P., Sanderson L. M., Warden V., McCourt W. J., 1985. The volcanic cover; Chemical composition and the origin of the magmas of the Calipuy Group, in Pitcher W. S., Atherton M. P. Cobbing E. J., and Beckinsale R. D., eds. *Magmatism at a plate edge; The Peruvian Andes*: Glasgow, Blackie, p. 273-284.

Atherton M. P., 1990. The Coastal Batholith of Peru: the product of rapid recycling of "new" crust formed within rifted continental margin. *Geological Journal*, 25, p. 337-349, London.

Audebaud E., 1971. Mise au point sur la stratigraphie et la tectonique des calcaires cénomaniens du Sud-Est péruvien

(formation Ayavacas). R. C. Acad. Sciences Paris, (D), 272, p. 1059-1062.

Audebaud E., 1973. Geologia de los cuadrangulos de Ocongate y Sicuani. Bol. Inst. Geol. Min. Metal., 25, 72 p., Lima.

Balarezo E. P. R., Samame B., and Morales A. B., 1980. Sinopsis explicativa del mapa del Departamento de Ica: Instituto Geologico Minero y Metalurgico, Boletin Serie F, N° 2. Lima, Peru, 27 p.

Ballesteros M. W., Moore G. F., Taylor B. and Ruppert S., 1988. Seismic Stratigraphic Framework of the Lima and Yaquina Forearc basins, Peru. In Suess E., von Huene R., et al., Proc. ODP, Init. Repts., 112: College Station, TX (Ocean Drilling Program), p. 77-90.

Bally A. W., and Snelson S., 1980. Realms of subsidence. In Miall A. D. (ed.): Facts and principles of world petroleum occurrence. Canadian Society of Petroleum Geologists, Memoir 6, p. 1-94.

Bally A. W., 1983. (ed.): Seismic Expression of Structural styles, Volume 3. Tectonics of Compressional Provinces/Strike Slip Tectonics. Studies in Geology Series #15. The American Association of Petroleum Geologists.

Bally A. W. and Oldow J. S., 1984. Plate tectonics, structural styles, and the evolution of sedimentary basins. Rice University, Houston, 238 p.

Barazangi M., Isacks B. L., 1976. Spatial distribution of earthquakes and subduction of the Nazca Plate beneath South America. Geology, 4, p. 686-692.

Barazangi M., Isacks B. L., 1979. Subduction of the Nazca Plate beneath Peru: Evidence from spatial distribution of earthquakes. Roy. Astron. Soc. Geophys. Jour., 57, p. 537-555.

Batty M. and Jaillard E., 1989. La sedimentacion Neocomiana (Jurásico terminal-Aptiano en el Sur del Perú, in: Contribuciones de los simposios sobre el Cretáceo de América Latina, A: Eventos y registro sedimentario, p. 75-88, Buenos Aires.

Batty M., Carlotto V., Jacay J., Jaillard E., 1990. The Kimmeridgian (?) -early Valanginian tectonic events on the Peruvian margin. Internat. Symp. on Andean Geodynamics, Grenoble 1990, ORSTOM (ed)., p. 265-268.

Bellido E. and Narvaez S., 1960. Geología del Cuadrángulo de Atico. Comisión Carta Geológica Nacional, 59 p.

Benavides V., 1962. Estratigrafía pre-Terciaria de la región de Arequipa. Bol. Soc. Geol. Perú, v. 38, p. 5-63.

Beckinsale R. D., Sanchez-Fernandez A. W., Brook M., Cobbing E. J., Taylor W. P., and Moore N. D., 1985. Rb-Sr whole-rock isochron and K-Ar age determinations for the Coastal Batholith of Peru. Pitcher, Atherton, Cobbing, Beckinsale. Magmatism at a Plate Edge, The Peruvian Andes. Halsted Press, John Wiley and Sons Inc., New York, p. 177-207.

Bolaños R., 1986. Evaluación geológica y posibilidades petrolíferas de la cuenca Terciaria Salaverry-Trujillo. Petroperu internal report. 51 p.

Bouma A. H., Coleman J. M., Stetling Ch. E. and Kohl B., 1989. Influence of Relative Sea Level Changes on the construction of the Mississippi Fan. *Geo-Marine Letters*, v. 9, p. 161-170.

Bourgeois J., Pautot G., Bandy W., Boinet T., Chotin P., Huchon P., Mercier de Lepinay B., Monge F., Monlau J., Pelletier B., Sosson M., and von Huene R., 1986. Regime tectonique de la marge andine convergente du Pérou (Campagne SEAPERC du N.O. Jean-Charcot, juillet 1986). *C. R. Acad. Sci. Paris*, 303, p. 1599-1604.

Bussel M. A., 1983. Timing of tectonic and magmatic events in the Central Andes of Peru. *J. Geol. Soc. London*, v. 40, p. 279-286.

Bussel M. A., Pitcher W. S., 1985. The structural control of batholith emplacement. In: Pitcher M. P., Cobbing E. J., Beckinsale R. D. eds.: *Magmatism at a Plate Edge: the Peruvian Andes*. Blackie Halsted Press, London, p. 167-176.

Caldas J., 1980. Geologic map of the Rio Grande and Cerro Huaricangana areas, in: Balarezo V. E., Samame V. M., and Morales A. B.: *Sinopsis explicativa del mapa del Departamento de Ica*: Instituto Geologico, Minero y Metalurgico, Boletin Serie F, N° 2, Lima.

Caldas J., Palacios O., Pecho V., and Vela C., 1980. Geologia de los Cuadrangulos de: Bayovar, Sechura, La Redonda, Pta. La Negra, Lobos de Tierra, Las Salinas y Morrope. Instituto Geologico, Minero y Metalurgico, Boletin Serie A, N° 32, Lima, Peru, 78 p.

Caldas J., 1983. Tectonic evolution of the Peruvian Andes: in Cabré R. S. J. (ed.), *Geodynamics of the Eastern Pacific Region*,

Caribbean and Scotia Arcs, Geodynamics Series, American Geophysical Union, 9, p. 77-82.

Cande S. C., 1985. Nazca-South American Plate interactions since 50 my b. P. to Present. In Hussong D. M., Dang S. P., Kulm L. D. Couch R. W., and Hilde T. W. C. (eds.), Atlas of the Ocean Margin Program, Peru Continental Margin, Region VI: Woods Hole (Marine Science International), 14.

Carlotto V., 1989. Formacion Huambutio: Nueva unidad estratigrafica, marcador del evento tectonico-sedimentario infraneocomiano. First Workshop sobre el Cretaceo en el Peru, Lima 1989, p. 5 (abstract).

Carlotto V., Jurado J., Miranda C., Carlier G., Jaillard E., 1990. Evolucion tectonica sedimentaria de la formacion Yuncaypata (Aptiano superior?-Campaniano). Second Workshop sobre el Cretaceo en el Peru, Lima, 4 p.

Carlson P. R. and Karl H. A., 1988. Development of large submarine canyons in the Bering Sea, indicated by morphologic, seismic, and sedimentologic characteristics. Geological Society of America Bulletin, v. 100, p. 1594-1615.

Cheney T. M., McClellan G. H., and Montgomery E. S., 1979. Sechura phosphate deposits, their stratigraphy, origin and composition: Economic Geology, v. 74, p. 232-259.

Clark A. H., Farrar E., Kontak D. J., Langridge R. J., Arenas M. J., France L. J., Mc Bride S. L., Woodman P. L., Wasteneys H. A., Sandeman H. A., Douglas D. A., 1990. Geologic and Geochronologic Constraints on

the Metallogenic Evolution of the Andes of Southeastern Peru. *Econ. Geology*, 85, p. 1520-1583, Lancaster.

Cobbing E. J., and Pitcher W. S., 1972. The Coastal batholith of central Peru. *Geol. Soc. London Jour.* 128, p. 421-460.

Cobbing E. J., Ozard J. M., and Snelling N. J., 1977. Reconnaissance geochronology of the crystalline basement rocks of the Coastal Cordillera of Southern Peru. *Geol. Soc. America Bull.* 88, p. 241-246.

Cobbing E. J., Pitcher W. S., Wilson J. J., Baldock J. W., Taylor W. P., Mc Court W., Snelling N. J., 1981. The Geology of the Western Cordillera of Northern Peru. *Inst. Geol. Sciences London, Overseas Mem.*, 5, 143 p.

Cordova A., 1986. Estudio estratigrafico y sedimentologico de las rocas del Cretaceo medio y superior en el pongo de Rentema, rio Mara  n, departamento de Amazonas. [thesis] Univ. Nac. May. San Marcos, Lima, 105 p.

Coulbourn W. T., and Moberly R., 1977. Structural evidence for the evolution of forearc basins off South America. *Can. J. Earth Science*, 14, p. 102-116.

Cross T. A., Pilger R. H., 1982. Controls of subduction geometry, location of magmatic arcs, and tectonics of arc and back-arc regions. *Geological Society of America Bulletin*, v. 93, p. 545-562.

Dalmayrac B., Lancelot J. R., and Leyreloup A., 1977. Two-billion year granulites in the Lata Precambrian metamorphic basement along the southern Peruvian coast. *Science* 198, p. 49-51.

Dalmayrac B., Laubacher G., and Marocco R., 1980. Géologie des Andes péruviennes: Caracteres généraux de l'évolution géologique des Andes péruviennes. ORSTOM Trav. Doc. 122, 501 p.

Davila D., Torres A., Sanchez W., Rodriguez U., Escalante A., Bustamante D. and others, 1987. Litoestratigrafia y sedimentologia del Terciario del Rio Grande-Palpa: Resumenes del VI Congreso Peruano de Geologia, p. 88.

Davila D., Sanchez A., Villavicencio E. and Torres J., 1993. Cenozoic stratigraphy of the Rio Grande Valley, Pisco Basin, Peru, in press.

Delfaud J., Marocco R., Mégard F., Cordova E., and Leon I., 1985. Peculiarities of the sedimentary filling of Talara-Tumbes basins on the North Peruvian active margin. 6th European Regional Meeting of Sedimentology I. A. S. Lleida.

DeVries T. J., 1987. Cenozoic Molluscan biostratigraphy of southern Peru: New data from the Pisco Basin, in Barron J. A. and Blueford J. R. (eds.), Abstract volume, Fourth international Congress on Pacific Neogene Stratigraphy, p. 17-18.

DeVries T. J., 1988. Paleoenvironments of the Pisco Basin. In: Dunbar R. B. and Baker P. A. (eds.): Cenozoic Geology of the Pisco Basin, IGCP #156. Guidebook to Field Workshop, May 1988, Lima, p. 41-50.

Dibblee Jr. T. W., 1977. Strike-Slip Tectonics of the San Andreas Fault and its Role in Cenozoic Basin Evolvment. Late

Mesozoic and Cenozoic Sedimentation and tectonics in California: San Joaquin Geological Society, p. 26-38.

Dunbar R. B. and Baker P. A. (eds.), 1988. Cenozoic Geology of the Pisco Basin, IGCP #156. Guidebook to Field Workshop, May 1988, Lima, 253 p.

Dunbar R. B., Marty R. C., and Baker P. A., 1990. Cenozoic marine sedimentation in the Sechura and Pisco Basins, Peru. *Palaeoceanography, Palaeoclimatology, Palaeoecology* special issue: Pacific Neogene Event Stratigraphy and Paleooceanographic History, Tsuchi R. (ed.), v. 77, p. 235-261.

Fitch T. J., 1972. Plate convergence, transcurrent faults, and internal deformation adjacent to southeast Asia and the western Pacific. *Journal Geophys. Res.*, v. 77, p. 4432-4461.

Fornari M., Vilca C., 1978. Mineralización argentífera asociada al volcanismo cenozoico de la faja Puquio-Cailloma, in *Anales del IV congreso peruano de geología*, Lima: Boletín de la Sociedad Geológica del Perú, N° 60, p. 101-128.

Fourtanier E., and Macharé J., 1988. Late Eocene to Pliocene marine diatoms from Peru, in F. E. Round (ed.): *Proceedings of the Ninth International Diatom Symposium*, Bristol U. K., Biopress Ltd., Bristol, p. 151-163.

Frantz E., 1993. Sedimentological and geochemical study of the late Eocene to early Oligocene Yumaque formation, East Pisco Basin, Peru. [M. A. thesis] Rice University, Houston.

Fyfe D., 1963. Estudio estratigrafico del Pozo Yurimaguas 2-1, Loreto, Peru. Bol. Soc. Geol. Peru, 37, p. 27-36.

Garcia W., 1978. Geologia de los cuadrangulos de Puquina, Omate, Huaitire, Mazo Cruz y Pizacoma. Bol. Inst. Geol. Min. Metal., (A), 29, 33 p. Lima.

Guevara C., 1980. El grupo Casma del Peru Central entre Trujillo y Mala. Bol. Soc. Geol. Peru, 49, p. 25-52.

Harding, 1974. Petroleum Traps Associated with Wrench Faults. The American Association of Petroleum Geologists Bulletin, v. 58, N° 7, p. 1290-1304.

Hilde T. W. C. and Warsi W. E. K., 1982. Subduction induced Rifting of the Nazca Plate along the Mendaña Fracture Zone, Eos, Trans. AGU, 63, 444.

Hosttas E., 1967. Estudio Geologico del tunel terminal entre Huambo y Querque. Thesis Univ. Nac. San Agustin Arequipa, 107 p.

Huaman D., 1985. Évolution tectonique cénozoïque et neotectonique du piedmont Pacifique dans la region d'Arequipa (Andes du Sud Pérou), [Ph. D. thesis]: Orsay, University of Paris, 220 p.

Huchon P. and Bourgois J., 1990. Subduction-induced Fragmentation of the Nazca Plate off Peru: Mendana Fracture Zone and Trujillo Trough Revisited. Journal of Geophysical Research, v. 95, N° B6, p. 8419-8436.

Hussong D. M., Edwards P. B., Johnson S. H. Campbell J. F., and Sutton, 1976. Crustal structure of the Peru-Chile trench : 8° - 12° S

latitude, in: Sutton G. H., Manghnani M. H. and Moberly R. (Eds.). The Geophysics of the Pacific Ocean Basin and its' Margin (Wollard Volume). Monogr. Am. Geophys. Union, 19, 71-86.

Hussong D. M., Wipperman L. K., 1981. Vertical movement and tectonic erosion of the continental wall of the Peru-Chile Trench near 11° 30' S latitude, in Kulm L. D., Dymond J., Dasch E. J., and Hussong D. M. (eds.), Nazca Plate: Crustal Formation and Andean Convergence. Geological Society of America Memoir 154, p. 509-524.

Injoque J., 1985. Geochemistry of the Cu-Fe amphibole skarn deposits of the Peruvian central coast. [Ph. D. thesis] Univ. Nottingham, 392 p., unpublished.

Isacks B. L., and Molnar P., 1971. Distribution of stresses in the descending lithosphere from a global survey of focal-mechanism solutions of mantle earthquakes: Reviews of Geophysics and Space Physics, v. 9, p. 103-174.

Isacks B. L. and Barazangi M., 1977. Geometry of Benioff Zones: Lateral segmentation and downwards bending of the subducted lithosphere, in Talwani M., and Pitman W. C. III, Island arcs, deep sea trenches and back-arc basins, Maurice Ewing Series, v. 1: American Geophysical Union, p. 99-114.

Jaillard E., 1987. Sedimentary evolution of an active margin during middle an upper Cretaceous times: the North Peruvian margin from late Aptian up to Senonian. Geol. Rundsch., 76, 677-697, Stuttgart.

Jaillard E. and Jacay J., 1989. Les "couches Chicama" du Nord du Pérou: Colmatage d' un bassin né d'une collision oblique au Tithonique. C. R. Acad. Sciences Paris, (II), 308, p. 1459-1465.

Jaillard E. and Sempere T., 1989. Cretaceous sequence stratigraphy of Peru and Bolivia. In: Contribuciones de los Simposios sobre el Cretacico de America Latina. A: Eventos y registro sedimentario, 1-27, Buenos Aires.

Jaillard E., Soler P., Carlier G., Mourier T., 1990. Geodynamic evolution of the northern and central Andes during early to middle Mesozoic times: a Tethyan model. J. Geol. Soc. London, 147, 1009-1022.

Jaillard E., 1992. Tectonic and geodynamic evolution of the Peruvian margin between Kimmeridgian and Paleocene times. In Salfity J. A. (ed.): Cretaceous tectonics in the Andes. Earth evolution Sciences-International Monograph series, Vieweg Publishing, Wiesbaden, in press.

James D. E., Brooks C., Cuyubamba A., 1975. Early evolution of the Central Andean tectonic arc. Carnegie Inst. Yearbook, 74, 247-250.

Jenks W. F., 1948. Geologia de la hoja de Arequipa al 200,000. Peru Inst. Geol. Bol. 9, 104 p.

Jenks W. F., 1961. Triassic to Tertiary stratigraphy near Cerro de Pasco, Peru. Geol. Soc. Am. Bull., 62, p. 203-219.

Jones P. R., 1981. Crustal structures of the Peru continental margin and adjacent Nazca plate, 9° S latitude, in Kulm L. D., Dymond

J., Dasch E. J., and Hussong D. M. (eds.), Nazca Plate: Crustal Formation and Andean Convergence. Geological Society of America Memoir 154, p. 423-443.

Kalafatovitch C., 1957. Edad de las calizas de la Formacion Yuncaypata, Cuzco. Bol. Soc. Geol. Peru, 32, p. 125-139, Lima.

Klinck B. A., Ellison R. A., Hawkins M. P., 1986. The geology of the Cordillera occidental and Altiplano, West of the Lake Titicaca, Southern Peru. Inst. Geol. Min. Metal., Preliminary report, 353 p., Lima.

Koch E., Blissenbach E., 1962. Las Capas Rojas del Cretaceo Superior-Terciario en la region del curso medio del rio Ucayali, Oriente del Peru. Bol. Soc. Geol. Peru, 39, p. 7-141, Lima.

Kulm L. D., Prince R. A., French W., Johnson S., and Masias A., 1981. Crustal structure and tectonics of the central Peru continental margin and trench. In Kulm L. D., Dymond J., Dash E. J., and Hussong D. M. (eds.), Nazca Plate: Crustal Formation and Andean Convergence. Geol. Soc. Am. Mem., 154, p. 445-468.

Kulm L. D., Miller J., and von Huene R., 1987. The Peru continental margin Record Section 2. In von Huene R. (ed.). Seismic images of modern convergent margins. Tulsa (AAPG Studies in Geology Series), 26.

Kulm L. D., Resig J. M., Thornburg T. M. and Schrader H. J., 1982. Cenozoic structure, stratigraphy and tectonics of the central Peru forearc. In Leggett J. K. (ed.). Trench Forearc Geology: Sedimentation

and Tectonics on Modern and Ancient Active Plate Margins, Geological Society Special Publication N° 10, London, p. 151-169.

Kulm L. D., Thornburg T. M., Schrader H., Masias A., Resig J., Johnson L. 1981. Late Cenozoic carbonates on the Peru continental margin: Lithostratigraphy, biostratigraphy, and tectonic history, p. 469-508.

Leon I., 1983. Analyse séquentielle et évolution dynamique du Bassin Tumbes dans la région nord-ouest du Pérou. D. E. A. de Géologie des matières premières minérales et énergétiques. Université de Pau.

Lisson C. K., 1925. Algunos fosiles de Peru: Boletin Sociedad Geologica del Peru, v. 1, p. 547-563.

Lopez R., Cordova E., 1988. Estratigrafia y sedimentacion de la serie continental "Capas Rojas" (Maastrichtiano-Paleoceno) entre Cuzco y Ccorao. Bol. Soc. Geol. Peru, 78, p. 149-164, Lima.

Loughmann D. L., Hallam A., 1982. A facies analysis of the Pucara group (Norian to Toarcian carbonates, organic-rich shales and phosphates) of Central and Northern Peru. Sedimentary Geology, 32, p. 161-194.

Macharé J. and Fourtanier E., 1987. Datation des formations tertiaires du bassin de Pisco (Pérou) a partir d' associations de diatomées: Comptes Rendus de l' Academie des Sciences, Paris.

Macharé J., 1987. La Marge Continentale du Pérou: Regimes Tectoniques et Sedimentaires Cénozoïques de L' Avant-Arc des Andes [Docteur en Sciences thesis]. Université de Paris Sud. 385 p.

Marocco R., Delfaud J., Lavenu A., 1985. Ambiente deposicional de una cuenca continental intramontañosa Andina: El Grupo Moquegua (Sur del Peru) Primeros resultados. Bol. Sociedad Geologica del Peru, N° 75, p. 73-90.

Marsaglia K. M., Carozzi A. V., 1990. Depositional environment, sand provenance, and diagenesis of the Basal Salina Formation (lower Eocene), Northwestern Peru. J. South American Earth Sci., 3, p. 253-267.

Martin J. B., 1987. Geochemistry of organic dolomites in the Pisco Basin of Peru [M. S. thesis]: Durham, N. C., Duke University, 208 p.

Martinez C., 1980. Structure et évolution de la chaîne hercynienne et de la chaîne andina dans le Nord de la Cordillere des Andes de Bolivie. Paris, Office de Recherche Scientifique et Technique d'Outre Mer Memoir 119, 352 p.

Marty R., Dunbar R., Martin J., Baker P., 1988. Late Eocene diatomite from the Peruvian coastal desert: Coastal upwelling in the eastern Pacific and Pacific circulation before the terminal Eocene event. In Dunbar R. B. and Baker P. A. (eds.), 1988. Cenozoic Geology of the Pisco Basin, IGCP #156. Guidebook to Field Workshop, May 1988, Lima, p. 63-78.

Marty R., 1989. Stratigraphy and Chemical Sedimentology of Cenozoic Biogenic Sediments from the Pisco and Sechura Basins, Peru [Ph. D. thesis]. Rice University, Houston.

Masias J. A., 1976. Morphology, shallow structure and evolution of the Peruvian continental margin 6° to 18° S. [M. S. thesis]. Corvallis, Oregon State University, 92 p.

McKee E. H., and Noble D. C., 1982. Miocene volcanism and deformation in the Western Cordillera and high plateaus of south-central Peru. *Geol. Soc. America Bull.* 93, p. 622-657.

Mégard F., 1967. Commentaire d'une coupe schématique a travers les Andes centrales de Pérou. *Rév. Géog. phys. Géol. dyn., Sér.* 2, 9, p. 335-345.

Mégard F., 1973. Etude géologique d'une transversale des Andes au niveau du Pérou central. [Sc. D. thesis] unpublished, Univ. Montpellier.

Mégard F., 1984. The Andean orogenic period and its major structures in central and northern Peru. *Geol. Soc. London Jour.* 141, p. 893-900.

Mégard F., 1987. Structure and evolution of the Peruvian Andes. In Schaer J. and Rodgers J. (eds.). *The Anatomy of Mountain Ranges*, p. 179-210.

Mégard F., Dalmayrac B., Laubacher G., Marocco R., Martinez C., Paredes J., and Tomasi P., 1971. La chaîne hercynienne au Pérou et en Bolivie: Premiers résultats. *ORSTOM Cah., Sér. géol.*, 3, p. 5-43.

Mégard F., Noble D. C., McKee E. H., and Bellon H., 1984. Multiple pulses of Neogene compressive deformation in the Ayacucho intermontane Basin, Andes of central Peru. *Geological Society of America Bulletin*, v. 95, p. 1108-1117.

Mertz D., 1966. Micropaläontologische und sedimentologische Untersuchung der Pisco Formation Sudperus: *Palaeontographica*, Abt. B, Bd. 118, 1-51.

Mitouard P., Kissel C., Laj C., 1990. Post-Oligocene rotations in southern Ecuador and northern Peru and the formation of the Huancabamba deflection in the Andean Cordillera. *Earth and Planetary Science Letters*, 98, p. 329-339.

Molnar P., and Atwater T., 1978. Interarc spreading and Cordilleran tectonics as alternates related to the age of subducted oceanic lithosphere: *Earth and Planetary Science Letters*, v. 41, p. 330-340.

Moore G. F., and Taylor B., 1988. Structure of the Peru Forearc from multichannel seismic-reflection data. In Suess E., von Huene R., et al. *Proc. ODP, Init. Repts.*, 112: College Station, TX (Ocean Drilling Program), p. 71-76.

Morris R. C., 1955. Report on Wildcat well Pisco 4X. Petroperu internal report, unpublished.

Morris R. C. and Aleman A., 1975. Sedimentation and tectonics of middle Cretaceous Copa Sombrero formation in northwest Peru. *Bol. Soc. Geol. Peru*, v. 48, p. 49-64.

Mourier T., 1988. La transition entre Andes marginales et Andes cordillérraines a ophiolites. Evolution sédimentaire, magmatique et structurale du relai de Huancabamba (3°-8° S, Nord Pérou-Sud Equateur). [Dr. thesis], Univ. Paris XI, 275 p.

Mourier T., Laj C., Mégard F., Roperch P., Mitouard P., and Farfan Medrano A., 1988. An accreted continental terrane in northwestern Peru. *Earth and Planetary Science Letters*, 88, p. 1-11.

Mourier T., Mégard F., Pardo A., Reyes L., 1988. L'évolution mésozoïque des Andes de Huancabamba (3°-8° S) et l'hypothèse de l'accrétion du microcontinent Amotape-Tahuin. *Bull. Soc. Geol. France*, (8), 4, p. 69-79.

Mukasa S. B., 1986. Zircon U-Pb ages of superunits in the Coastal Batholith of Peru: Implications for magmatic and tectonic processes. *Geol. Soc. Am. Bull.*, 97, p. 241-254.

Myers J. S., 1974. Cretaceous Stratigraphy and Structure, Western Andes of Peru Between Latitudes 10°-10° 30'. *The American Association of Petroleum Geologists Bulletin*, v. 58, N° 3, p. 474-487.

Myers J. S., 1975. Cauldron subsidence and fluidization: Mechanisms of intrusion of the Coastal Batholith of Peru into its own volcanic ejecta. *Geol. Soc. America Bull.* 86, p. 1209-1220.

Naeser C. W., Crochet J., Jaillard E., Laubacher G., Mourier T., Sigé B., 1991. Tertiary Fission-Track ages from the Bagua syncline (Northern Peru). Stratigraphic and tectonic implications. *Journal of South American Earth Sciences*, in press.

Newell N. D., 1956. Reconocimiento geológico de la region Pisco-Nazca: *Bol. Soc. Geol. Peru*, 30, p. 261-295.

Noble D. C., McKee E. G., Farrar E., and Petersen U., 1974. Episodic Cenozoic volcanism and tectonism in Andes of Peru: *Earth Planetary Science Letters*, 21, p. 213-220.

Noble et al, 1984. Rare-element enriched S-type ash-flow tuffs containing phenocrysts of muscovite, andalusite, and sillimanite, southeastern Peru. *Geology*, v. 12, p. 35-39.

Noble D. C., Silberman M. L., Mégard F., and Bowman H. R., 1978. Comendite (peralkaline rhyolite) and basalt in the Mitu Group, Peru: Evidence for Permian-Triassic lithospheric extension in the central Andes. *U. S. Geol. Surv. Jour. Res.* 6, p. 453-457.

Noble D. C., Farrar E., and Cobbing E. J., 1979. The Nazca Group of south-central Peru: Age, source, and regional volcanic and tectonic significance. *Earth Planet. Sci. Lett.* 45, p. 80-86.

Noble D. C., and McKee E. H., 1982. Nevado Portuqueza volcanic center, central Peru: A Pliocene central volcanic-collapse caldera complex with associated silver mineralization. *Econ. Geology* 77, p. 1893-1900.

Noble D. C., McKee E. H., Mourier T., Mégard F., 1990. Cenozoic stratigraphy, magmatic activity, compressive deformation, and uplift in Northern Peru. *Geol. Soc. Am. Bull.*, 102, p. 1105-1113.

Noblet C., Marocco R., Delfaud J., 1987. Analyse sédimentologique des "Couches Rouges" du bassin intramontagneux de Sicuani (Sud du Pérou). *Bull. Inst. Fr. Et. And.*, 16, p. 55-78, Lima.

Nur A., and Ben-Avraham Z., 1981. Consumption of aseismic ridges and volcanic gaps in South America. In Kulm L. D., Dymond J.,

Dash E. J., and Hussong D. M. (eds.) Nazca Plate: Crustal Formation and Andean Convergence, Geological Society of America, Memoir 154, 729-740.

Ochoa A., 1980. Evaluacion hidrocarburifera de la cuenca Sechura. Boletin Sociedad Geologica Peru, 67, p. 133-154.

Olchowski L. E., 1980. Geologia de los cuadrangulos de Jaqui, Coracora, Chala y Chaparra. Bol. Inst. Geol. Min. Metal., (A), 34, 71 p., Lima.

Okada H., and Burky D., 1980. Supplementary modification and introduction of code numbers to the low-latitude coccolith biostratigraphic zonation (Burky, 1973 and 1975). Mar. Micropaleontol., 5, p. 321-325.

Olsson A. A., 1944. Contributions to the Paleontology of Northern Peru. Part VII: The Cretaceous of the Paita region. Bull. Am. Paleont., 28, 113 p.

Pardo Casas F. and Molnar P. 1987. Relative motion of the Nazca (Farallon) and South American plates since Late Cretaceous time. Tectonics, vol. 6, N° 3, p. 233-248.

Pecho V., 1981. Geologia de los cuadrangulos de Chalhuanca, Antabamba y Santo Tomas. Bol. Inst. Geol. Min. Metal., (A), 35, 67 p. Lima.

Petersen G., 1954. Informe preliminar sobre la geologia de la faja costera del Departamento de Ica: Boletin Tecnico Empresa Petrolera Fiscal, v. 1, Lima, Peru, p. 33-61.

Pilger R. H., 1981. Plate reconstructions, aseismic ridges, and low angle subduction beneath the Andes. GSA Bulletin, v. 92, p. 448-456.

Pitcher W. S., 1978. The anatomy of a batholith. Geol. Soc. London Jour. 135, p. 157-182.

Pitcher W. S., Atherton M. P., Cobbing E. J., Beckinsale R. D. (eds.); 1985. Magmatism at a Plate Edge, The Peruvian Andes. Halsted Press, John Wiley and Sons Inc., New York, 328 p.

Portugal J., 1974. Mesozoic and Cenozoic Stratigraphy and Tectonic events of Puno-Santa Lucia Area, Department of Puno, Peru. Am. Assoc. Petrol. Geol. Bull., 58, p. 982-999.

Reading H. G., 1980. Characteristics and recognition of strike-slip fault systems. Special Publication Number 4 of the International Association of Sedimentologists. In Ballance P. F. and Reading H. G. (eds.), Blackwell Scientific Publications Oxford, London, Edinburgh, Boston Melbourne, p. 7-26.

Rivera R., 1957. Moluscos fosiles de la formacion Paracas, Departamento de Ica. Boletin de la Sociedad Geologica del Peru, v. 32, p. 165-219.

Reyes L., Caldas J., 1987. Geologia de los cuadrangulos de Las Playas, La Tina, Las Lomas, Ayabaca, San Antonio, Chulucanas, Morropon, Huancabamba, Olmos y Pomahuaca. Bol. Inst. Geol. Min. Metal., (A), 39, 83 p., Lima.

Rodriguez R., Cabré R., and Mercado A., 1976. Geometry of the Nazca Plate and its Geodynamic implications. In Sutton G., Manghnani

M., and Moberly (eds.): The Geophysics of the Pacific Ocean Basin and its Margin: Monograph American Geophysical Union, N° 19, p. 87-103.

Romani M., 1982. Géologie de la région minière Uchuchacua-Hacienda Otuto, Pérou. [Thesis third cycle] Univ. Grenoble, 176 p.

Ruegg W., 1956. Geologie zwischen Cañete-San Juan 13° 00'-15° 24' Sudperu: Geologische Rundschau, v. 45, p. 775-858.

Sanz V. R., 1991. Geologia del departamento de Tumbes. VII Congreso Peruano de Geologia, Lima, p. 367-371.

Scholl D. W., von Huene R., Vallier T. L., Howell D. G., 1980. Sedimentary masses and concepts about tectonic processes at underthrust ocean margins. *Geology*, vol. 8, p. 564-568.

Schrader H. and Cruzado Castañeda J. C., 1990. The Ballena and Delfin wells off Central Peru: Revised ages. In Suess E., von Huene R. et al., Proc. ODP, Sci. Results, 112: College Station, TX (Ocean Drilling Program), p. 209-215.

Sébrier M., Marocco R., and Macharé J., 1982. Évolution tectonique du piedmont Pacifique et ses relations avec la Cordillere des Andes du Pérou central et meridional. Toulouse, Montagnes et Piedmonts, *Revue de Géographie Physique du Sud-Ouest*, p. 49-70.

Sébrier M. Mercier J. L., Mégard F., Laubacher G., and Carey-Gailhardis E., 1985. Quaternary normal and reverse faulting and the state of stress in central Andes of southern Peru. *Tectonics*, v. 4, p. 739-780.

Sébrier M., Lavenu A., Fornari M., and Soulas J. P., 1988. Tectonic and uplift in central Andes, Perú, Bolivia, northern Chile, from Eocene to Present. *Geodynamique*, v. 3, p. 85-106.

Sébrier M. and Soler P., 1991. Tectonics and magmatism in the Peruvian Andes from late Oligocene time to the Present. In Harmon R. S., and Rapela C. W. (eds.) *Andean Magmatism and its tectonic setting*: Geological Society of America, Special Paper 265, p. 259-278.

Shackleton R. M., Ries A. C., Coward M. P., and Cobbold P. R., 1979. Structure, metamorphism and geochronology of the Arequipa massif of coastal Peru. *Geol. Soc. London Jour.* 136, p. 195-214.

Shepherd G. L., and Moberly R. 1981. Coastal structure of the continental margin, northwest Peru and southwest Ecuador, in Kulm L. D., Dymond J., Dasch E. J., and Hussong D. M. (eds.), *Nazca Plate, Crustal Formation and Andean Convergence*. Geological Society of America Memoir 154, p. 351-391.

Soler P., 1989. Petrography and Geochemistry of lower Cretaceous alkali basalts from the High Plateaus of central Peru and their tectonic significance. *Zbl. Geol. Palaont.*, p. 1053-1064, Stuttgart.

Soler P. and Bonhomme M., 1990. Relations of magmatic activity to plate dynamics in Central Peru from late Cretaceous to Present. In Kay S., Rapela C. eds.: *Plutonism from Antarctica to Alaska*. *Geol. Soc. Am. Memoir* 241, p. 173-192.

Soler P., 1991. El volcanismo Casma: cuenca marginal abortada o arco en ambiente distensivo?. VII Cong. peruano Geol., Lima, 4 p.

Soulas J. P., 1977. Les phases tectoniques andines du Tertiaire superieur, resultats d'un transversale Pisco-Ayacucho, Pérou Central. Paris, Comptes Rendus de l'Academie des Sciences, serie D, p. 2207-2210.

Soulas J. P., 1978. Las fases tectonicas del Terciario superior en el Peru, corte Ayacucho-Pisco. Boletin de la Sociedad Geologica del Peru, 57/58, p. 59-72.

Spörli K. B., 1980. New Zealand and oblique-slip margins: Tectonic development up to and during the Cainozoic. Special Publication Number 4 of the International Association of Sedimentologists. In Ballance P. F. and Reading H. G. (eds.), Blackwell Scientific Publications Oxford, London, Edinburgh, Boston Melbourne, p. 147-170.

Stainforth R., and Ruegg W., 1953. Mid-Oligocene transgression in southern Peru: AAPG Bulletin, v. 37, p. 568-569.

Stauder W., 1973. Mechanism and spatial distribution of Chilean earthquakes with relation to the subduction of the ocean plate. Journal of Geophysical Research, v. 78, p. 5003-5061.

Stauder W., 1975. Subduction of the Nazca Plate under Peru as evidenced by focal mechanisms and by seismicity. Journal of Geophysical Research, v. 81, p. 1053-1064.

Steinmann G., 1929. Geologie von Peru, Carl Winter ed., Heidelberg, 448 p.

Stock C. E., 1989. Tertiary Geology of the Quebrada Huaricangana Area, East Pisco basin, Southern Peru: Late Paleogene to Neogene transgressive sedimentation within a forearc basin. [M. A. thesis]. Rice University, Houston. 166 p.

Suarez G., Molnar P., and Burchfiel B. C., 1983. Seismicity, fault plane solutions, depth of faulting, and active tectonics of the Andes of Peru, Ecuador, and Southern Colombia. *Journal of Geophysical Research*, v. 88, N° B12, p. 10403-10428.

Suess E., von Huene R., et al., 1988. Proc. ODP, Init. Repts., 112: College Station, TX (Ocean Drilling Program).

Suess E., von Huene R., et al., 1990. Proc. ODP, Sci. Results, 112: College Station, TX (Ocean Drilling Program).

Thornburg T. and Kulm L. D., 1981. Sedimentary basins of the Peru continental margin: Structure, stratigraphy and Cenozoic tectonics from 6° to 16° S latitude, in Kulm L. D., Dymond J., Dasch E. J., and Hussong D. M. (eds.), *Nazca Plate: Crustal Formation and Andean Convergence*. Geological Society of America Memoir 154, p. 393-422.

Thornburg T. 1985. Seismic stratigraphy of Peru forearc basins. In Hussong D. M. et al. (eds.): *Atlas of the Ocean Margin Drilling Program, Peru Continental Margin, Region VI: Woods Hole (Marine Science International)*.

Travis, R. B. , 1953, La Brea-Pariñas oil field, northwestern Peru: *American Association of Petroleum Geologists Bulletin* , v. 37, p. 2093-2118.

Travis R. B., Gonzales G., and Pardo A., 1976. Hydrocarbon Potential of Coastal Basins of Peru. In Halbouty M., Maher J. and Lian H. M. (eds.), Circum-Pacific energy and mineral resources. American Association of Petroleum Geologists, Memoir 25, p. 331-338.

Tschopp H. J., 1953. Oil exploration in the Oriente of Ecuador. Am. Assoc. Petrol. Geol. Bull., 37, 2303-2347.

Vicente J. C., 1981. Elementos de la estratigrafia mesozoica sur-peruana, in W. Volkheimer, E. Musacchio (eds.): Cuencas sedimentarias del Jurasico y Cretacico de America del Sur, 1, 319-351, Buenos Aires.

Vicente J. C., 1989. Early late Cretaceous overthrusting in the Western Cordillera of Peru, in: G. E. Ericksen, M. T. Canas Pinochet, J. A. Reinemund (eds.): Geology of the Andes and its relations to energy and mineral resources. Circum-Pacific Council for Energy and Mineral Resources, Earth Science Series, 11,p. 91-117, Houston, Texas.

von Huene R., Lallemand S. 1990. Tectonic erosion along the Japan and Peru convergent margins. Geological Society of America Bulletin, v. 102, p. 704-720.

von Huene R., 1991. The sedimentary structure and tectonic history of Lima Basin, an offshore contemporary of Pisco Basin. In press.

Walcott R. I., 1978. Geodatic strains and large earthquakes in the axial tectonic belt of North Island, New Zealand. Journal Geopys. Res., v. 83, p. 4419-4429.

Warsi W. E. K., Hilde T. W. C. and Searle R. C., 1983. Convergence structures of the Peru Trench between 10° S and 14° S. In Hilde, T. W. C. and Uyeda S (eds.), *Convergence and Subduction. Tectonophysics*, 99, p. 313-329.

Wilcox et al., 1973. Basic Wrench Tectonics. *The American Association of Petroleum Geologists Bulletin*, v. 57, N° 1, p. 74-96.

Wilson P. A., 1975. K-Ar age studies in Peru with special reference to the emplacement of the Coastal Batholith. [Ph. D. thesis], Univ. Liverpool, unpublished.

Worrall, D. M., 1991. Tectonic History of the Bering Sea and the Evolution of Tertiary Strike-Slip Basins of the Bering Shelf. *Geological Society of America, Special Paper 257*, 120 p.

Wright R., and Cruzado R., 1988. Cenozoic nearshore clastic deposits of the Pisco Basin. In: Dunbar R. B. and Baker P. A. (eds.): *Cenozoic Geology of the Pisco Basin, IGCP #156. Guidebook to Field Workshop*, May 1988, Lima, p. 51-61.

Zuñiga, F., and Travis, R. B., 1975, The geology of the coast and continental margin of Peru [abs]: *EOS (American Geophysical Union Transactions)*, v. 56, p. 911.

Zuñiga F., Cruzado J., 1979. Bioestratigrafia del Noroeste Peruano. *Bol. Soc. Geol. Peru*, 60, 219-232, Lima.

APPENDICES

Appendix A: Nannofossils biostratigraphy of the Ballena 1X and Delfin 1X wells. By Hisatake Okada, Yamagata University, 1990.

Ocurrence of Calcareous Nannofossils in Ballena 1X Well

SAMPLE NUMBER	B1	B1.1	B1.2	B2	B2.1	B3	B4
SAMPLE DEPTH (mbsl)	223.8	336.6	550	604.9	659.8	705.5	806.1
ABUNDANCE-PRESERVATION	AM	AM	FM	B	B	B	R-
ETCHING/OVERGROWTH	0/2	0/1	1/1				
Braarudosphaera bigelowii	F	R	-				-
Calcidiscus leptoporus	F	-	-				-
Calcidiscus macintyreii	R	-	-				-
Coccolithus miopelagicus	-	-	F				-
Coccolithus pelagicus	A	F	C				+
Cyclargolithus floridanus	-	-	F				-
Dictyococcites perplexa	A	A	C				+
Dictyococcites productus	-	A	-				-
Discoaster adamanteus	-	R	F				-
Discoaster deflandrei	-	-	C				-
Discoaster intercalaris	-	-	-				-
Discoaster cf. musculus	-	R	-				-
Discoaster spp.	-	R	-				-
Helicosphaera ampliapertura	-	-	R				-
Helicosphaera californiana	-	F	-				-
Helicosphaera carteri	F	R	F				-
Helicosphaera mediterranea	-	-	F				-
Helicosphaera sp.	-	F	F				-
Pontosphaera multipora	-	-	R				-
Reticulifenestra gelida	A	A	-				-
Reticulifenestra haqil	-	F	C				-
Reticulifenestra minuta	A	A	A				-
Reticulifenestra minutula	-	F	-				-
Reticulifenestra pseudoumbilica	C	C	-				-
Reticulifenestra spp.	-	-	A				-
Sphenolithus compactus	-	R	F				+
Sphenolithus moriformis	-	R	F				-
Sphenolithus neobabes	F	-	-				-
Umbilicosphaera sp.	C	-	F				-
OKADA -BURKY ZONATION (CN-)	11-5b	5?	3-1				?

A= abundant (more than 10% of assemblage); C= common (more than 1% less than 10%); F= few (less than 1%); R= rare (less than 0.1%). For overall abundance: A= abundant; C= common; F= few; R= rare. Reworked specimens: c= common; f= few; r= rare. G= good; M= moderate; P= poor. 1= slight; 2= moderate; 3= strong.

Occurrence of Calcareous Nannofossils in Delfin 1X Well. Samples D1 to D6.

SAMPLE NUMBER	D1	D2	D3	D3.1	D3.2	D4	D4.1	D5	D6
SAMPLE DEPTH (mbsl)	266.5	361	479.9	601.8	803.0	937.2	1001.2	1089.6	1223.8
ABUNDANCE-PRESERVATION	R-	FM	FM	AM	CM	R-	R-	R-	CM
ETCHING/OVERGROWTH		1/1	1/1	0/1	1/0				0/1
<i>Calcidiscus leptoporus</i>	-	C	-	-	-	-	-	-	-
<i>Calcidiscus macintyreii</i>	-	F	-	-	-	-	-	-	-
<i>Coccolithus miopelagicus</i>	-	-	-	-	C	-	-	-	F
<i>Coccolithus pelagicus</i>	+	A	A	C	A	+	+	-	A
<i>Cyclargolithus floridanus</i>	-	-	-	-	R	+	+	+	C
<i>Dictyococclites perplexa</i>	+	C	C	-	-	+	+	-	-
<i>Dictyococclites productus</i>	-	C	C	A	A	-	-	-	A
<i>Discoaster adamanteus</i>	-	-	-	-	F	-	-	-	R
<i>Discoaster deflandrei</i>	-	-	-	-	C	-	-	-	C
<i>Discoaster intercalaris</i>	+	-	-	-	F	-	-	-	-
<i>Discoaster cf. musicus</i>	-	-	-	-	F	-	-	-	-
<i>Discoaster quinqueramus</i>	-	F	-	-	-	-	-	-	-
<i>Discoaster variabilis</i>	-	-	-	-	F	-	-	-	-
<i>Discoaster</i> spp.	-	-	F	-	-	-	-	-	F
<i>Helicosphaera ampliaperta</i>	-	-	-	-	C	-	-	-	-
<i>Helicosphaera carteri</i>	-	F	F	F	C	-	-	-	R
<i>Helicosphaera euphratis</i>	-	-	-	-	-	-	-	-	F
<i>Helicosphaera mediterranea</i>	-	-	-	-	-	-	-	-	F
<i>Helicosphaera</i> sp.	-	-	-	R	-	-	-	-	-
<i>Pontosphaera multipora</i>	-	-	-	-	F	-	-	-	-
<i>Reticulofenestra gelida</i>	+	A	A	A	-	-	-	-	-
<i>Reticulofenestra haqii</i>	+	A	A	A	A	-	+	+	-
<i>Reticulofenestra minuta</i>	-	-	-	C	-	-	-	-	A
<i>Reticulofenestra minutula</i>	-	-	-	C	C	-	-	-	C
<i>Reticulofenestra pseudumbilica</i>	+	A	A	A	-	-	-	-	-
<i>Reticulofenestra</i> spp.	-	-	-	-	A	+	+	-	C
<i>Sphenolithus compactus</i>	-	-	-	-	C	-	-	-	F
<i>Sphenolithus cf. heteromorphus</i>	-	-	-	-	R	-	-	-	-
<i>Sphenolithus moriformis</i>	-	-	-	-	F	-	-	-	C
<i>Triquetrorhabdulus cf. carinatus</i>	-	-	-	-	-	-	-	-	R
OKADA-BURKY ZONATION (CN-)	11-9	9	9-5b	5?	3	?	?	?	3-1

A= abundant (more than 10% of assemblage); C= common (more than 1% less than 10%); F= few (less than 1%); R= rare (less than 0.1%). For overall abundance: A= abundant; C= common; F= few; R= rare. Reworked specimens: c= common; f= few; r= rare. G= good; M= moderate; P= poor. 1= slight; 2= moderate; 3= strong.

Occurrence of Calcareous Nannofossils in Delfin 1X Well (Samples D7 to D17).

SAMPLE NUMBER	D7	D7.1	D8	D9	D10	D11	D12	D13	D14	D15	D16	D17
SAMPLE DEPTH (mbsl)	1479.9	1543.9	1604.9	1714.6	1870.1	2007.3	2144.5	2263.4	2327.4	2400.6	2464.6	2510.4
ABUNDANCE-PRESERVATION	RM	R	B	B	RM	QM	RM	R	RM	B	B	R
ETCHING/OVERGROWTH	0/1				0/1	0/1	0/1		0/1			
<i>Braardosphaera bigelowii</i>	-	-	-	-	F	F	F	-	-	-	-	-
<i>Chiasmolithus consuetus</i>	-	-	-	-	-	F	F	-	C	-	-	+
<i>Chiasmolithus expansus</i>	-	-	-	-	-	-	R	-	-	-	-	-
<i>Chiasmolithus grandis</i>	-	-	-	-	-	F	-	-	C	-	-	-
<i>Chiasmolithus solitus</i>	-	-	-	-	f	F	F	-	C	-	-	-
<i>Chiasmolithus</i> sp.	-	-	-	-	-	-	-	+	C	-	-	+
<i>Coccolithus eopelagicus</i>	-	-	-	-	-	F	-	-	-	-	-	-
<i>Coccolithus miopelagicus</i>	F	-	-	-	-	-	-	-	-	-	-	-
<i>Coccolithus pelagicus</i>	A	+	-	-	A	C	A	+	A	-	+	-
<i>Cribrocentrum reticulatum</i>	-	-	-	-	F	-	-	-	-	-	-	-
<i>Cruciplacolithus</i> aff. <i>staurion</i>	-	-	-	-	-	-	-	-	R	-	-	-
<i>Cruciplacolithus</i> spp.	-	-	-	-	-	F	-	-	F	-	-	-
<i>Cyclargolithus floridanus</i>	A	+	-	-	A	-	C	+	F	-	-	-
<i>Dictyococclites bisectus</i>	C	-	-	-	F	-	-	-	-	-	-	-
<i>Dictyococclites scrippsae</i>	F	-	-	-	C	-	-	-	-	-	-	-
<i>Discoaster barbadensis</i>	-	-	-	-	F	F	-	-	-	-	-	-
<i>Discoaster bifax</i>	-	-	-	-	-	-	-	-	R	-	-	-
<i>Discoaster dellandrei</i>	-	-	-	-	F	-	-	-	-	-	-	-
<i>Discoaster germanicus</i>	-	-	-	-	-	-	-	-	F	-	+	-
<i>Discoaster salpanensis</i>	-	-	-	-	-	-	-	-	F	-	-	-
<i>Ericsonia formosa</i>	-	-	-	-	F	F	F	+	C	-	-	+
<i>Helicosphaera bramlettel</i>	-	-	-	-	F	-	-	-	-	-	-	-
<i>Helicosphaera dinesenii</i>	-	-	-	-	-	-	-	-	R	-	-	-
<i>Helicosphaera lophota</i>	-	-	-	-	C	F	F	-	F	-	-	-
<i>Helicosphaera recta</i>	F	-	-	-	-	-	-	-	-	-	-	-

(Continue in next page)

Occurrence of Calcareous Nannofossils in Delfin 1X Well. Samples D7 to D17.

SAMPLE NUMBER	D7	D7.1	D8	D9	D10	D11	D12	D13	D14	D15	D16	D17
SAMPLE DEPTH (mbsl)	1479.9	1543.9	1604.9	1714.6	1870.1	2007.3	2144.5	2263.4	2327.4	2400.6	2464.6	2510.4
ABUNDANCE-PRESERVATION	RM	R-	B-	B-	RM	QM	RM	R-	RM	B	B	R-
ETCHING/OVERGROWTH	0/1				0/1	0/1	0/1		0/1			
<i>Helicosphaera salebrosa</i>	-	-			-	-	R	-	-			-
<i>Helicosphaera seminulum</i>	-	-			-	C	C	+	F			+
<i>Helicosphaera wilcoxii</i>	-	-			F	-	-	-	-			-
<i>Lanternithus minutus</i>	-	-			-	-	-	-	F			-
<i>Lithostromation simplex</i>	-	-			-	F	C	+	-			-
<i>Micrantholithus altus</i>	-	-			F	F	F	-	-			-
<i>Pedinocyclus larvalis</i>	-	-			-	-	-	-	-			+
<i>Pemina angulata</i>	-	-			-	F	F	-	C			-
<i>Pemina basquensis</i>	-	-			A	A	A	+	A			+
<i>Pemina concinnus</i>	-	-			-	F	F	-	-			-
<i>Pemina papillatum</i>	-	-			-	R	-	-	-			-
<i>Pontosphaera enormis</i>	-	-			-	-	-	+	C			+
<i>Pontosphaera inconspicua</i>	-	-			-	C	-	-	-			-
<i>Pontosphaera multipora</i>	-	-			-	F	C	+	F			-
<i>Reticulofenestra hilla</i>	-	-			F	-	-	-	-			-
<i>Reticulofenestra samodurovi</i>	-	-			C	C	C	-	C			-
<i>Reticulofenestra umbilica</i>	-	-			C	-	R	-	-			-
<i>Reticulofenestra</i> spp.	A	+			A	A	A	+	A			+
<i>Sphenolithus dissimilis</i>	F	-			-	-	-	-	-			-
<i>Sphenolithus distentus</i>	F	-			-	-	-	-	-			-
<i>Sphenolithus furcatolithoides</i>	-	-			-	R	-	-	-			-
<i>Sphenolithus moriformis</i>	C	-			C	C	C	-	-			-
<i>Sphenolithus predistentus</i>	F	-			-	-	-	-	-			-
<i>Sphenolithus radians</i>	-	-			-	F	-	-	-			-
<i>Transversopontis pulcheroides</i>	-	-			-	F	F	-	-			-
<i>Zygrhabdolithus bijugatus</i>	-	-			F	F	-	-	-			-
OKADA-BURKY ZONATION (CP-)	19A?	?			14b	14a	14a	?	14a-13c			13?

Appendix B: Paleoenvironmental analyses of the Delfin 1X and Ballena 1X wells. By N. L. Engelhardt-Moore, 1990.

STRATIGRAPHY - DELFIN-1

IN UNDIFFERENTIATED UPPER MIOCENE/LOWER PLIOCENE (CN9 - CN11)

INTERVAL: 750 ft - 1210 ft

Interval Top and Age Based on: the presence of *Reticulofenestra pseudoumbilica* (CN9-CN11) at 900 ft.

Paleoenvironment: Indeterminate - probably outer shelf or deeper, + 300 ft.

Lithology: Fine to coarse sand and siltstone interbedded with calcite. Below 1040 ft, sand interbedded with dolomitised micritic brown limestone.

Nannofossils: The only sample examined in this interval was at 900 ft. Only rare upper Miocene or lower Pliocene forms were noted. Dr. Okada assigned the age range based on the occurrence of *R. pseudoumbilica*. Reworking was noted.

Planktonic Foraminifera: No in situ forms were noted. At 750 ft, these reworked Eocene species *Pseudohastigerina micra*, *Globorotalia cocoaensis*, and *Acarinina cf. primitiva* occur.

Benthonic Foraminifera: Benthic occurrence is very poor. At 750 ft and 810 ft, the assemblages were dominated by reworked specimens of varying preservation which include *Valvulineria*

venezuelana, *Trochammina* spp., *Cibicides* spp., *Bulimina* spp. and *Uvigerina* spp. Dark red casts of costate *Bulimina* cf. *charapotoensis* were rare. Two specimens each of *Hanzawaia* cf. *concentrica* at 750 ft and *Lenticulina* sp. at 810 ft were possibly *in situ*. Otherwise, scattered, mostly single specimens were noted with no definitive *in situ* forms.

Other Fossils: Rare, worn shell and coral fragments were noted at the top of the interval. Also notable was undifferentiated "organic debris".

Remarks: The lack of preserved fossils, the high clastic content, and the occurrence of authigenic limestone along with rare shell fragments suggests that deposition was rapid with transportation of shallow water sediments into deep water. The presence of authigenic limestone which forms off the Peruvian coast during cold water upwelling supports this interpretation. The environmental setting probably was outer shelf or deeper. Today, the Delfin-1 is situated on the upper slope. During the upper Miocene/lower Pliocene, this site was probably infilled with shallow marine sediments.

FIRST UNDIFFERENTIATED MIDDLE TO UPPER MIOCENE (CN5? - CN9)

INTERVAL: 1210 ft - 2570 ft

Interval Top based on: The presence of *R. pseudoumbilica* (CN9-CN11) with the first appearance of *Discoaster quinquaramus* (CN9) at 1210 ft.

Paleoenvironment: Probably Upper Bathyal, 600 - 1500 ft.

Lithology: Fine sandstone/siltstone interbedded with dolomitised limestone. Below 1510 ft, less sandstone; limestone interbedded with mudstone and sandstone/siltstone with calcite streaks. Abundant glauconite at 2210 ft.

Nannofossils: Nannofossils are common. Three samples were examined in this interval. *D. quinquaramus* occurs only at 1210 ft. It restricts the age to late upper Miocene. However, the floral assemblages below, without *D. quinquaramus*, suggest the lower part of this interval is middle to upper Miocene (CN5-CN9). A middle Miocene age at 2130 ft is supported by the diatom zonal range of *Coscinodiscus lewisianus* through *Craspedodiscus coscinodiscus* (Schrader and Castaneda, 1990).

Planktonic Foraminifera: Planktonics are very rare with only sporadic nondiagnostic globigerinids noted. At 2390 ft, a questionable specimen of the lower Miocene species *Catapsydrax dissimilis* was noted.

Benthonic Foraminifera: Benthics are infrequent to 1450 ft. Below, they increase in abundance with the first upper Miocene species, *Buliminella ecuadorana*, being noted. The fauna is similar to that described from the upper Miocene of Ecuador and many species are also known from the middle and upper Miocene of California. Other forms include *Buliminella cf. elegantissima*, *Buliminella curta*, *Bolivina cf. marginata*, *Globobulimina cf. affinis*, *Cassidulina cf. delicata*, *Bolivinaopsis sp.*, *Fursenkoina schreibersiana* and *Fursenkoina cf. acuta*. At 1740 ft and just below were *Amphimorphina cf. amchitkaensis*, *Bulimina uvigerinaformis*, *Gyroldina venezuelana*, *Pseudoparrella cf. exigua*, *Uvigerina peregrina*, *Cancris cf. palmarealensis*, *Bulimina charapotoensis* and *Bolivina dispar* with the first appearances of these genera: *Bolivina*, *Lenticulina*, and *Cibicides*. Below the glauconite at 2210 ft, many new, possibly older, deep water species first appear including *Buliminella subfusiformis*, *Oridorsalis umbonatus*, *Ecuadorota cf. bristowi*, *Uvigerina cf. schwageri*, *Epistominella smithi* and *Globocassidulina subglobosa* with *Transversigerina transversa* and *Cancris cf. oblonga* at 2360 ft. At 2480 ft, these forms first appear; *Cibicidoides cf. floridanus*, *Cibicidoides cf. subtenuissimus*, *Plectofrondicularia cf. californica*, *Valvulineria cf. robusta*, and *Chilostomella* spp.. Several of these species are known from the lower and basal middle Miocene of Ecuador.

Other Fossils: Diatoms are rare with an increase at 1780 ft.

Remarks: Between 1210 ft - 1310 ft, the interval is barren except for nannofossils. Clastic and organic debris dominate. At 1330 ft, the first small rare benthics occur. Below 1450 ft, a change, marked by an increase in diversity, is simultaneous with the first mudstone. The fauna improves as clastics decrease and deteriorates with the occurrence of limestone. At 1740 ft, the first upper bathyal fossils appear. Below the glauconitic horizon, a distinct bathyal fauna is developed. This interval shows a shallowing upward sequence above the glauconite which is supported by an increase in clastics. Below the glauconite, deep open marine conditions existed. It is uncertain if this lower section is lower Miocene in age.

FIRST LOWER MIOCENE NOTED (CN1 - CN3)

INTERVAL: 2570 ft - 4800 ft

Interval top and age based on: The first occurrences of several benthic forams at 2570 ft, *Catapsydrax dissimilis* at 2690 ft, and these nannofossils; *Discoaster deflandrei* (CP19-CN3), *Discoaster variabilis* (CN3-CN11.25), and *Helicosphaera ampliaperta* (CP19.75-CN3) at 2660 ft, with *Triquetrorhabdulus cf. carinatus* (CP18.5-CN1.3) at 4040 ft.

Paleoenvironment: Middle to Upper Bathyal, 600 - 4000 ft.

Lithology: Brown mudstone interbedded with dolomitised micritic limestone with fine siltstone and streaks of calcite. Coarse sand at 4100 ft.

Nannofossils: Five samples were examined. Only at 2660 ft and 4040 ft were significant forms recovered. At 2660 ft, a high diversity flora with *D. deflandrei*, *D. variabilis* and *H. ampliaperta* first appears. Only *D. deflandrei* occurs below. Other forms include *Cyclicargolithus floridanus* and *Sphenolithus cf. heteromorphus*. The three samples between 2660 ft and 4040 ft were basically barren. This interval is dominated by carbonate, so no age determinations could be made. The sample at 4040 ft, contained a diverse flora including the species at 2660 ft and three new forms. Of significance is the first appearance of *Triquetrorhabdulus cf. carinatus*. This is an early lower Miocene species. Dr. Okada assigned a late lower Miocene age to 2660 ft and a range of early lower to late lower Miocene to 4040 ft.

Planktonic Foraminifera: Planktonics are rare. At 2570 ft, a rare fauna consisting of *Globigerinoides immaturus*, *Globorotalia mayeri* and indeterminate globigerinids was noted. At 2690 ft, *Catapsydrax dissimilis* s.s. (P17-N6) first appears, supporting a lower Miocene age. At 3080 ft, other species noted include *Globorotalia continuosa*, *Globigerina bulloides* and *Globigerinoides trilocularis*. Below 3200 ft., planktonic occurrence is again sporadic with a notable break at 4010 ft which includes *Globigerina praebulloides*. Below, planktonics are very rare.

Benthonic Foraminifera: At 2570 ft a significant faunal break was noted. The abundant high diversity fauna suggests a major change which probably represents the lower Miocene. Nannofossils just below are lower Miocene. These species first appear; *Bulimina cf. pupoides*, *Bulimina subacuminata*, *Uvigerina rugosa*, *Sphaeroidina bulloides*, *Oridorsalis tener*, *Cibicides cf. matanzaensis*, *Cibicides ungerianus*, *Melonis pompilioides*, *Pullenia subcarinata*, *Ammobaculites nummus*, *Bolivina cf. churchi*, *Nonionella cf. miocenica*, *Pseudoparrella cf. relizensis*, *Gyroidina altiformis* and *Cyclammina* sp. At 2690 ft, more new species occur; *Cibicidoides cf. wuellerstorfi* and *Ecuadorotia bristowi* with *Uvigerina charapotoensis*, *Pseudoparrella cf. subperuviana*, *Bolivina cf. directa*, *Valvulineria cf. venezuelana*, *Rectuvigerina mayi*, *Rectuvigerina multicostata* and *Bulimina cf. ovata* just below. Many are known from the lower Miocene of Ecuador and California. In Ecuador, *E. bristowi* and *R. mayi* are restricted to the lower Miocene with *V. venezuelana* and *T. transversa* restricted to the basal middle and lower Miocene. At 4010 ft another break which includes *Siphonodosaria cf. advena*, *Cibicidoides cf. trincherasensis*, *Globobulimina cf. pacifica*, *Brizalina cf. pozonensis* and *Oolina globosa* was noted. No age significance can be tied to this horizon.

Other Fossils: Diatoms are rare with occasional fish teeth, otoliths and pellets.

Remarks: This interval is lower Miocene. It is uncertain based on benthic evidence alone, if the section above 2570 ft up to 2210 ft is also lower Miocene. In the lower Miocene, deposition at this site occurred in a bathyal setting.

IN MIDDLE OLIGOCENE (CP19A?)

INTERVAL: 4820 ft - 5810 ft

Interval Top and Age Based on: The occurrence of these nannofossils *Sphenolithus distentus* (CP16-CP19A), *Sphenolithus predistentus* (CP13.5-CP18?) and *Helicosphaera recta* (CP18-CP19) at 4880 ft along with the first radiolarians at 4820 ft.

Paleoenvironment: Middle - Upper Bathyal, 600 - 4000 ft

Lithology: Interbedded siltstone and calcareous brown mudstone with brown calcite marking the base. Brown limestone is probably cave.

Nannofossils: Four samples were examined. Only the sample at 4880 ft contained a good flora. The others were essentially barren. Dr. Okada assigned CP19A? based on the occurrence of *S. distentus*, *S. predistentus* and *H. recta*. These species are Oligocene in age and have been reported from the middle Oligocene of Ecuador. Their first occurrence appears to be within the Oligocene.

Planktonic Foraminifera: None.

Benthonic Foraminifera: At 4820 ft, the fauna shows little change with the only new species, *Trochammina cf. pacifica* at 5000 ft and *Cyclammina* sp.2 at 5200 ft. However, at 5320 ft several species first appear which include *Gyroidina planata*, *Gyroidina planulata*, *Uvigerina cf. auberiana*, and *Sigmomorphina pseudoschencki* with *Lenticulina abulotensis* just below. This fauna appears to be Oligocene, since *S. pseudoschencki* is only known from the Oligocene of Ecuador. At 5530 ft, the fauna with *Melonis affinis* and *Ammobaculites cf. stratherensis* is still bathyal. However, below this depth between 5630 ft and 5810 ft, the interval is unzoned due to abundant calcite.

Other Fossils: At 4820 ft, common radiolarians first appear. This possibly coincides with the top of the Oligocene because the nannofossils at 4880 ft are Oligocene in age. Only nondiagnostic spherical spumellarian *actinommids* were noted.

Remarks: The middle Oligocene is first noted at 4820 ft. However, there is some question as to whether it ranges higher. The foram break at 4010 ft shows no age evidence and the nannofossils

were not examined between 4040 ft and 4880 ft. The first Oligocene could occur anywhere within this interval, even at the noted foram break. However, the first appearance of radiolarians with diagnostic nannos definitely places the Oligocene at 4820 ft. At 5630 ft, abundant calcite marks the transition between the Oligocene and Eocene. This boundary represents a major hiatus. Below 5810 ft., samples were not examined until 5920 ft. The presence of radiolarians indicates cold water upwelling played a significant part in the faunal configuration and that water temperature could have been controlled by a proto Peru current during the Oligocene.

IN MIDDLE EOCENE (CP14B)

INTERVAL: 5920 ft - 8270 ft

Interval Top and Age Based on: The occurrence of *Globigerina pomeroli* (?P11-P17) at 5920 ft and *Morozovella densa* (P8.25-P14) at 6010 ft with a middle Eocene (CP14B) nannofossil flora at 6160 ft.

Paleoenvironment: Inner Shelf to possibly Upper Bathyal, 60 ft to 1500 ft.

Lithology: Interbedded limestone, mudstone and siltstone. Below 7210 ft, gray and brown micaceous mudstone dominates with coarse sandstone at 7600 ft. Calcite is rare.

Nannofossils: Eight samples were examined in this interval. At 6160 ft, a common diverse flora was noted with these key species; *Chiasmolithus solitus* (CP8.5-CP14.5), *Helicosphaera lophota* (CP9-CP14.3), *Reticulofenestra umbilica* (CP13-CP16), and *Reticulofenestra hillae* (CP13.75-CP16). Dr. Okada dated the sample as late middle Eocene (CP14B). At 6610 ft, the flora is slightly older, middle Eocene (CP14A) with the first appearances of *Helicosphaera seminulum* (CP9.5-CP14) and *Chiasmolithus grandis* (CP10-CP14). At 7660 ft, the flora suggests an older middle Eocene age. The last sample at 8260 ft had a very poor flora and was questionably dated as middle Eocene.

Planktonic Foraminifera: Planktonics are again very rare. However, the presence of *Globigerina pomeroli* at 5920 ft and *Morozovella densa* at 6010 ft dates this interval as middle Eocene (P14). This is supported by the occurrence of *Truncorotaloides rohri* (P8.5-P14) at 6450 ft and the nannofossils at 6160 ft.

Benthonic Foraminifera: Deep water benthic forams are common at the top of the interval. At 5920 ft, *Discorbis cf. samanica* first appears with *Gyroidina cf. altispira*, *Gyroidina cf. girardana*, *Bulimina microcostata*, *Bulimina cf. instabilis*, *Ceratobulimina* sp., *Allomorphina* sp. and *Dentalina* spp. just below. At 6460 ft, these species occur; *Gyroidina cf. chirana*, *Bulimina cf. brevis*, *Bulimina cf. peruviana* and *Uvigerina cf. mantaensis*. Many of these forms show affinities to the Eocene Chira

fauna of Peru. At 6940 ft, a faunal break with *Buliminella cf. peruviana* suggests an outer shelf environment with bathyal forms disappearing. The fauna at 7210 ft appears to be middle neritic. Below, there is a distinct shallower break in the last sample at 7960 ft. The fauna is dominated by abundant *Nonion aff. pizzarensis* typical of an inner shelf setting.

Other Fossils: Radiolarians are common. Significantly at 5920 ft, the spumellarians are *Phacodiscids* (a flat form) not *Actinommids* (a spherical form). This change coincides with the middle Eocene as demonstrated by the forams and nannos. Rare *Spongodiscids* (a triangular form) were also noted with pyritized diatoms frequent at 6010 ft. At 6940 ft, a change occurs and the first ostracods appear; *Cythereis aff. montgomeryensis*, *Cythereis aff. suttoni*, *Buntonia* sp. and *Bythocypris* sp. This break suggests a shallower horizon. At 7960 ft, the last sample examined, *Cytherella symmetrica* first appears with shell fragments. All these forms show affinities to Eocene species of the Gulf of Mexico.

Remarks: The lower portion of this well shows a distinct deepening during the Eocene from inner shelf to bathyal conditions. The abundance of radiolarians suggests that cold water upwelling was in effect off the Peruvian shelf during the middle Eocene. Above, deep marine lower Oligocene sediments rest unconformably on marine Eocene sediments. This upper Eocene hiatus suggests that either nondeposition and/or erosion were the active processes at that time possibly due to ongoing tectonic activity.

STRATIGRAPHY - BALLENA-1

IN UNDIFFERENTIATED UPPER MIOCENE/LOWER PLIOCENE (CN5B - CN11)

INTERVAL: 760 ft - 1130 ft

Interval Top and Age Based on: The occurrence of *Reticulofenestra pseudoumbilica* (CN9 - CN11), *Sphenolithus neoabies* (CN10? - CN11) and their associated flora at 760 ft.

Paleoenvironment: Outer neritic, 300 - 600 ft.

Lithology: Siltstone to coarse sandstone interbedded with calcareous brown limestone. Shells with rare coral fragments at the top of the interval.

Nannofossils: Based on the common occurrence of *R. pseudoumbilica*, some specimens of *S. neoabies* and the associated flora, Dr. Okada assigned an age of upper Miocene or lower Pliocene (CN5b - CN11) to the sample at 760 ft. This is supported by the reported upper Miocene age at

890 ft based on the diatom zone, *Coscinodiscus yabei* (Schrader and Castaneda, 1990). Reworked Eocene species were noted.

Planktonic Foraminifera: Planktonics are extremely rare and consist of nondiagnostic globigerinid forms with one specimen of *Orbulina suturalis* at 820 ft and one specimen of *Globorotalia cf. praescitula* at 950 ft. Their presence suggests an age of middle Miocene or younger.

Benthonic Foraminifera: Many species noted in this interval are known from the middle and upper Miocene of California. The fauna also shows strong affinities to the upper Miocene/Pliocene faunas of the Manabi Basin, coastal Ecuador. These species include *Buliminella cf. subfusiformis*, *Buliminella curta*, *Buliminella ecuadorana*, *Bulimina charapotoensis*, *Hanzawaia cf. concentrica*, *Fursenkoina cf. bramelette*, *Nonion cf. pizzarensis*, *Virgulina gunteri* and *Valvulineria cf. miocenica*. Many of these forms occur in the Delfin-1 within the Miocene. The assemblage, dominated by genera such as *Nonion*, *Buliminella*, *Bulimina*, *Valvulineria*, and *Cibicides*, is indicative of an outer shelf environment with no bathyally restricted species noted.

Other Fossils: At 820 ft and 850 ft some shell and rare coral fragments were noted. Their presence appears to be the result of transport. Also notable were otoliths and rare radiolarians (*phacodiscids*).

Remarks: The age of this interval is probably upper Miocene, but more evidence is needed to be certain. The occurrence of a high abundance low diversity nanno flora, a low diversity shallow water benthic fauna and no planktonics suggests a shelf setting for this interval during deposition. The occurrence of reworked Eocene nannofossils indicates that downslope transport was prevalent. As in the Delfin-1, the presence of authigenic limestone supports upwelling of cold water had a major influence on faunal abundance and preservation.

FIRST MIDDLE MIOCENE NOTED (CN5?)

INTERVAL: 1130 ft - 1480 ft

Interval Top and Age Based on: The occurrence of *Helicosphaera californiana* (CN3-CN5) and the associated flora at 1130 ft.

Paleoenvironment: Outer neritic - upper bathyal, 300 - 1500 ft.

Lithology: Micritic brown dolomitised limestone interbedded with silty limestone and fine to medium quartz sandstone.

Nannofossils: The only sample examined for nannofossils in this interval was at 1130 ft. It contained an abundant fairly diverse flora of middle and upper Miocene species. The presence of *H. californiana* and the lack of any lower Miocene indicators, resulted in Dr. Okada's middle Miocene age assignment. This is supported by the reported middle Miocene diatom zone, *Craspedodiscus coscinodiscus* at 1180 ft (Schrader and Castaneda, 1990). This interval also contained rare reworked Eocene species.

Planktonic Foraminifera: Planktonics are extremely rare. One specimen of *Globigerina praebulloides* and three small specimens of *Globigerinoides trilobus* were noted at 1390 ft. These are long-ranging nondiagnostic forms. No other planktonics were noted.

Benthonic Foraminifera: The benthic fauna shows an increase of diversity within this interval. Many of the forms previously noted continue to be prevalent. First occurrences at 1300 ft include *Siphonodosaria advena*, *Buliminella subfusiformis*, *Bulimina cf. murifica*, *Uvigerina cf. californica*, *Uvigerina cf. Parva*, *Valvulineria cf. robusta*, *Bolivinaopsis* sp. and *Baggatella* sp. At 1390 ft these species were first noted: *Uvigerina peregrina*, *Bolivina cf. marginata* and *Bolivina cf. cochei*. As noted previously, many of these species are known from the Miocene of California and Ecuador. The faunal assemblage also shows an affinity to the Agua Salada Formation of Venezuela. Many of these forms also occur in the middle to upper Miocene interval of the Delfin-1.

Other Fossils: None

Remarks: The increase in nannofossil and foram diversity along with some deeper water forms suggests a possible upper bathyal setting at the time of deposition. The dominance of *Bolivinas*, *Buliminas* and *Baggatella* suggests an apparent oxygen deficiency which could be accounted for by the intersection of an upper bathyal oxygen minimum with the continental slope (Whittaker, 1988). This interval does not show evidence of extremely deep water which supports its middle Miocene age based on deeper lower Miocene facies in the region. This is shown to be true to the north off Ecuador.

FIRST LOWER MIOCENE (CN1-CN3)

INTERVAL: 1480 ft - 2710 ft

Interval Top and Age Base on: The occurrence of *Praeorbulina glomerosa* (N7-N8.5) at 1480 ft. and the nannofossil assemblage at 1830 ft.

Paleoenvironment: ? Middle Neritic to Upper Bathyal, 180 ft to 1500 ft.

Lithology: Dolomitised limestone interbedded with sandstone, siltstone and calcareous mudstone. Below 1860 ft, clastic material increases. At 2250 ft, sandstone is interbedded with silty limestone and mudstone and layers of iron nodules occur. At 2520 ft, casing cement is abundant.

Nannofossils: Based on the common occurrence of *Discoaster deflandrei* (CP18-CN3), rare *Helicosphaera ampliaperta* (CP19.75-CN3), *Helicosphaera mediterranea* (CP19.6-CN3.5) and the associated flora at 1830 ft, Dr. Okada assigned a lower Miocene age (CN1-CN3). This age is also supported at 1630 ft, where a lower Miocene age is suggested by the diatom zone, *Denticulopsis nicobarica* (Schrader and Castaneda, 1990). This agrees with the foram data. Four other samples examined were barren and therefore not useful in age determination. Also notable at 1830 ft, were reworked Eocene species.

Planktonic Foraminifera: The occurrence of two specimens of *P. glomerosa* at 1480 ft indicates a restricted age of top lower Miocene or basal middle Miocene (N7-N8.5). At 1920 ft, *Catapsydrax dissimilis* (P17-N6) supports a lower Miocene age. Otherwise, planktonic occurrence continues to be very poor with rare globigerinids persisting to 2430 ft.

Benthonic Foraminifera: There is a slight change in the fauna at 1480 ft. This is evident as an increase in diversity and abundance. New species include *Baggina robusta*, *Pseudononion cf. obductus*, *Uvigerina cf. ornata*, *Brizalina cf. granti*, *Brizalina cf. pozonensis*, *Bolivina cf. rankini*, *Cibicidoides cf. floridanus*, *Gyroidina venezuelana*, *Cassidulina cf. laevigata* and *Nodosaria cf. franki*. The fauna is representative of an upper bathyal environment. At 1800 ft, more new species were noted. They include *Amphimorphina cf. amchitkaensis*, *Nodosaria stainforthi*, *Bulimina cf. rostrata*, *Brizalina maculata*, *Bolivina brevior*, *Sphaeroidina cf. variabilis* and *Bolivina floridana*. Other species first noted below 1890 ft and above 1950 ft were *Trochammina sp.*, *Bulimina cf. ovata* and *Nonionella cf. miocenica*. Below 1950 ft, the fauna decreases in abundance and diversity.

Other Fossils: Rare radiolarians (*phacodiscids*), fish otoliths and pyritized diatoms occur sporadically below 1480 ft. At 1980 ft and 2310 ft, pellets are common and below 1980 ft, "bone fragments" occur. All faunal elements disappear below 2430 ft.

Remarks: This interval is marked by a rich, diverse upper bathyal fauna between 1480 ft and 1860 ft. Below, the fauna shows a distinct decrease in abundance and diversity. This coincides with poorer preservation and a lower diversity dominated by *Valvulineria cf. miocenica* which suggests a shallower outer shelf setting for the lower part of the interval. This change marks an increase in clastics indicative of a dynamic shelf setting. As a whole, the interval shows a deepening upward

sequence. Above this interval, the well shows an apparent swallowing upward sequence. At 2520 ft, cement dilutes the fauna so that from this depth to the last sample at 2710 ft, the interval is unzoned.

LITHOLOGIC DISCUSSION

Dark brown dense, aphanitic carbonates (dolomicrite, lime micrite and calcareous mudstone) were the most prevalent lithologies noted in both wells. Organic-rich mudstones derived from coastal upwelling make up the bulk of the sediment. These sediments accumulate on the outer shelf and upper slope which is seaward of the high-productivity surface waters of the inner shelf. The carbonates form by the cementation of porous upwelling sediments in the subsurface diagenetic environment in association with biogenic decomposition of organic carbon. This process transforms an initial organic-rich mud into an authigenic carbonate. The delicate microfossils, organic matter and high sediment rates impart a high primary porosity to the muds which are subsequently infilled by carbonate cement. The composition of the diagenetic carbonates varies from calcite to dolomite.

The high influx of organic carbon to the seafloor beneath upwelling zones exhausts the oxygen content of the bottom waters through aerobic oxidization. This process allows some of the influx to be preserved and buried in the sediment. Bioturbation is suppressed because anoxic environments are not conducive to benthic colonization. Periodic increases in circulation winnow the mud and increase the oxygen content of the bottom waters.

Finally, benthic foraminifera are not well known off Peru. The primary factors that affect benthic foram assemblages are water mass, currents, eustacy, upwelling with consequent high primary productivity, low oxygen, diagenesis, phosphatization, downslope transport and vertical tectonic displacement. Several of these factors played an important role during sedimentation in foram preservation within these two wells. In areas where upwelling is pervasive, the most abundant and common biogenic components are diatom frustules and organic matter. Sponge spicules, silicoflagellates, and radiolarians usually occur, and nannoplankton are occasionally seen. However, calcareous microfossils are rare. The absence of planktonic forams in both wells is suspected to be caused by low oxygen conditions that form during upwelling. The diminished benthic foram assemblages coincide with the occurrence of carbonate. This observation is consistent with the fact that the authigenic formation of dolomitic sediments is destructive to foram tests (Suess and von Huene, *et al.*, 1990).

N. L. ENGELHARDT-MOORE

PLEASE NOTE:

Oversize maps and charts are filmed in sections in the following manner:

LEFT TO RIGHT, TOP TO BOTTOM, WITH SMALL OVERLAPS

The following map or chart has been refilmed in its entirety at the end of this dissertation (not available on microfiche). A xerographic reproduction has been provided for paper copies and is inserted into the inside of the back cover.

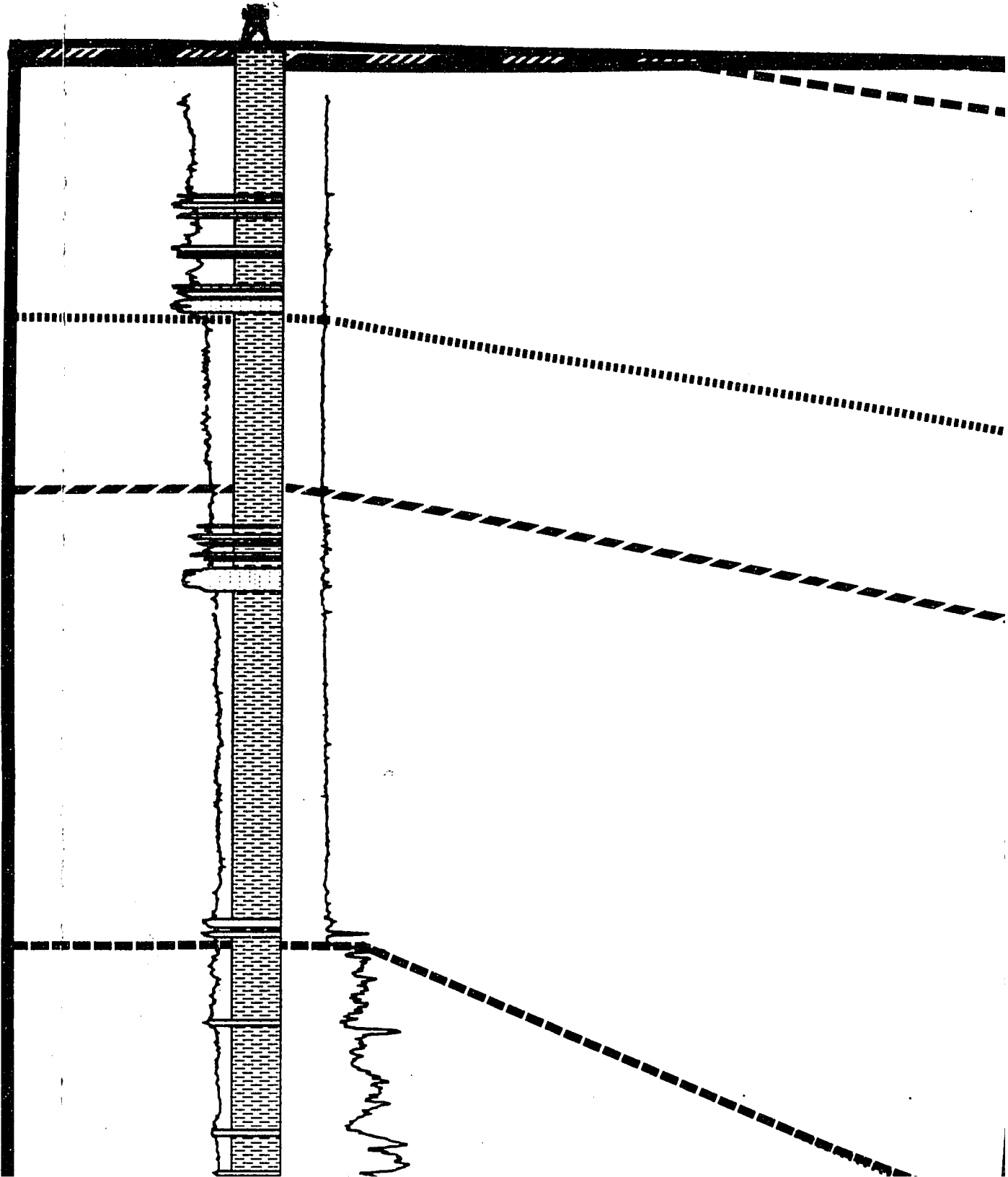
Black and white photographic prints (17" x 23") are available for an additional charge.

UMI

NNW

VIRU 4X

70 m





M3

M2

M1

E-O

Delfin 1

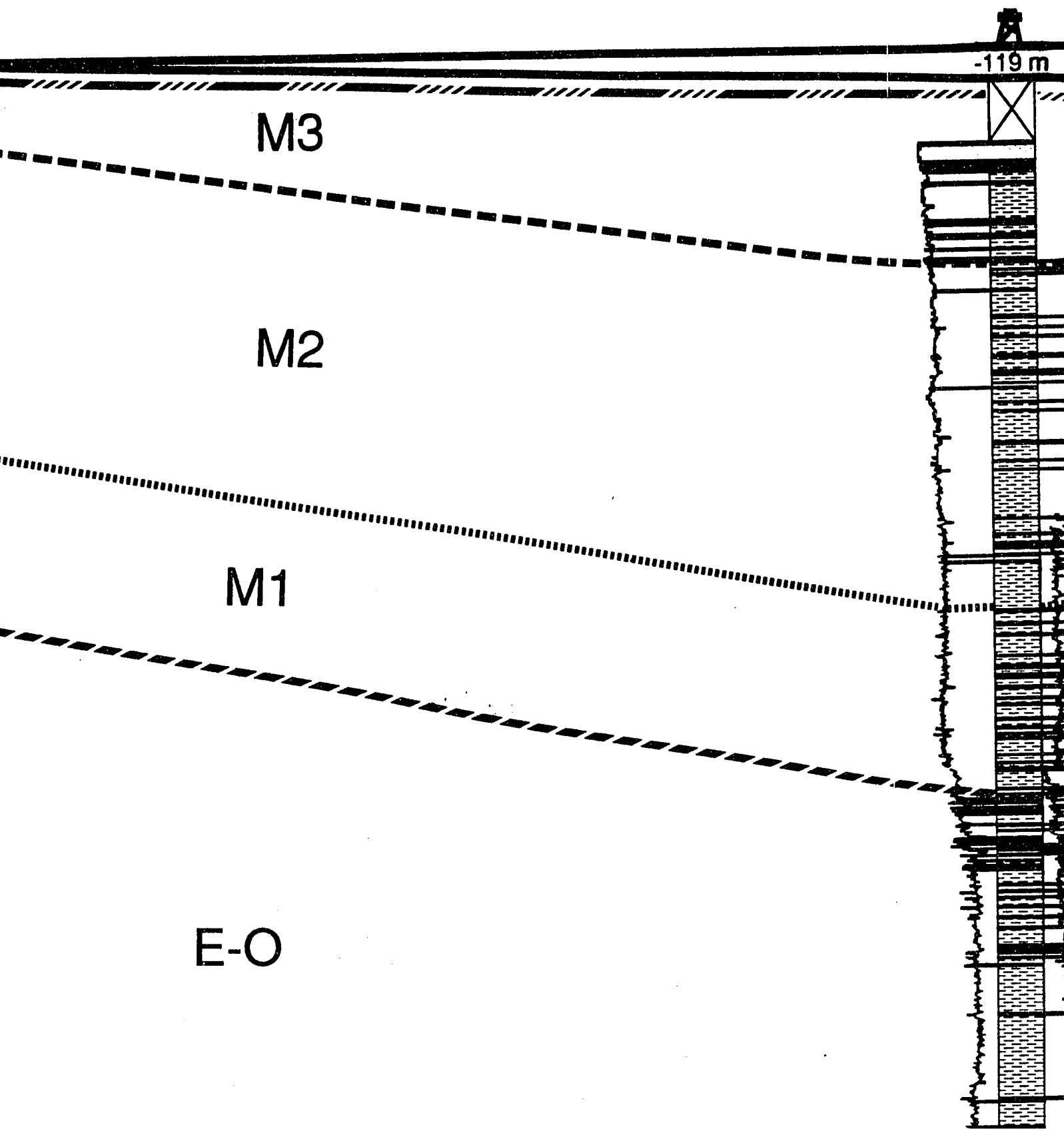
-119 m

M3

M2

M1

E-O



Delfin 1X

-119 m

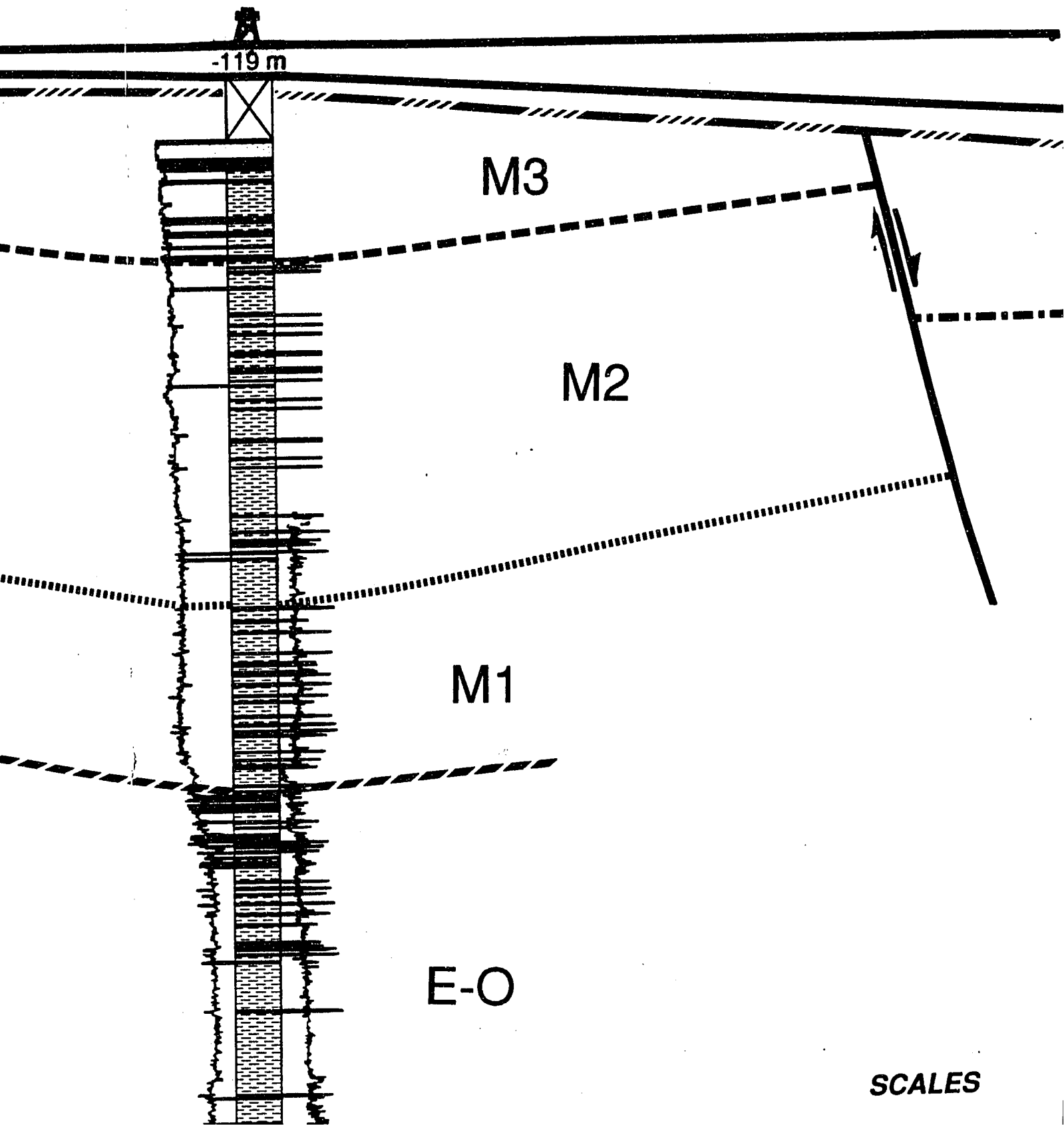
M3

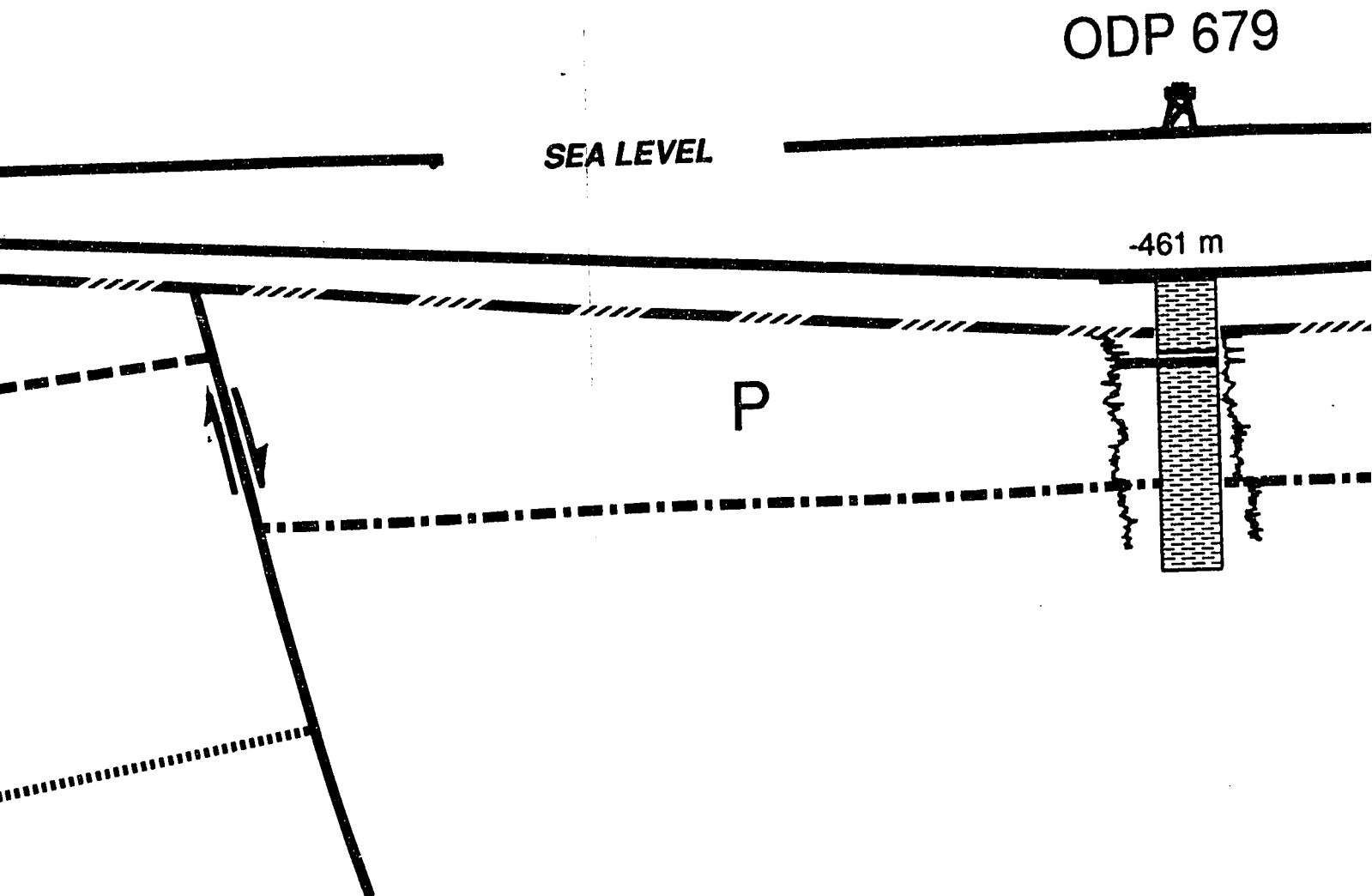
M2

M1

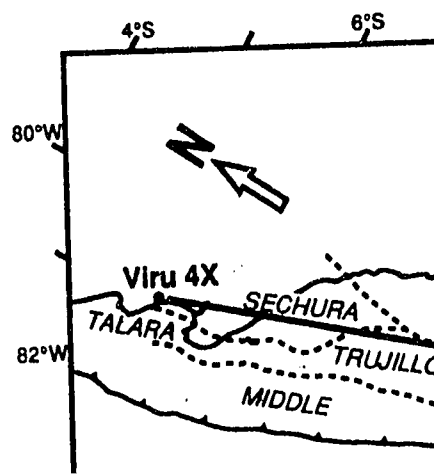
E-O

SCALES

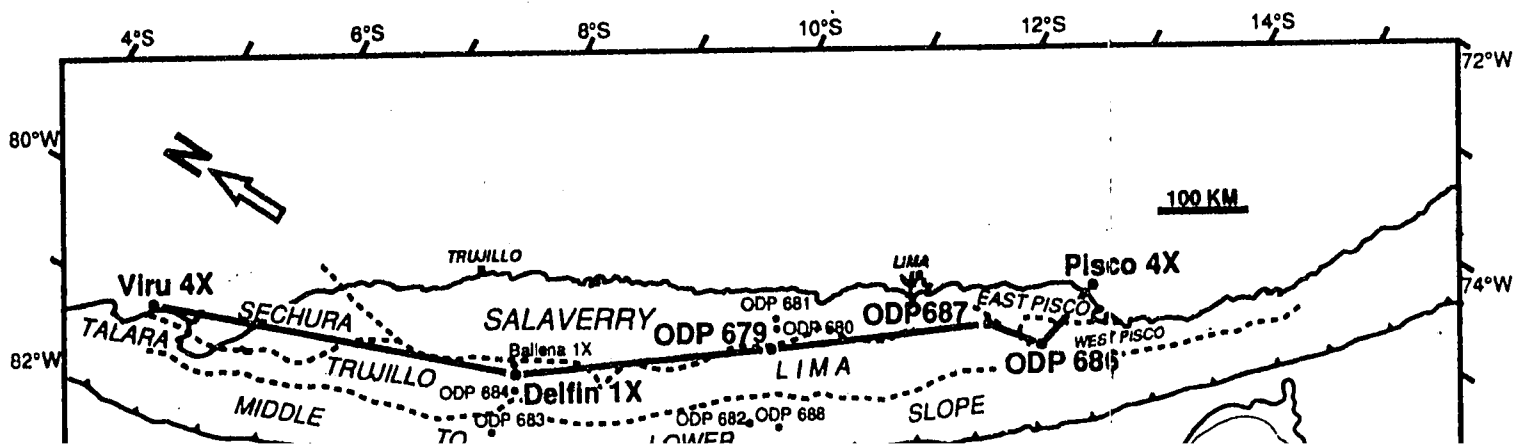
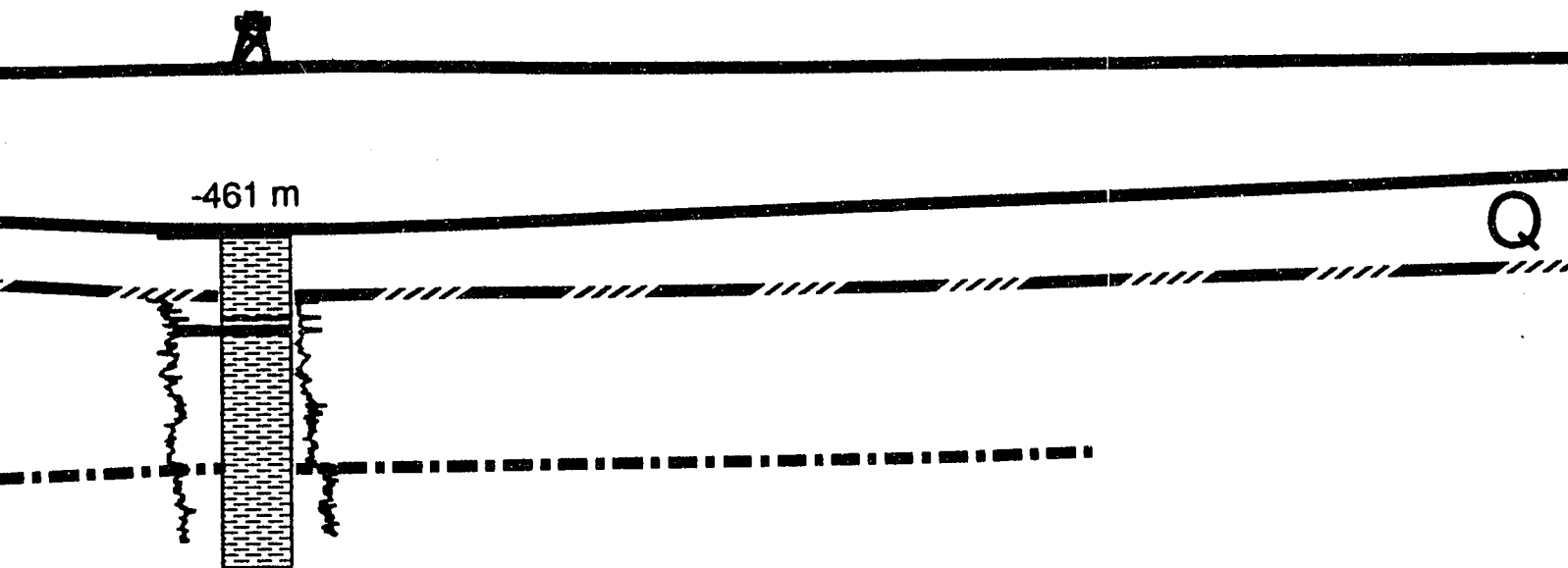




SCALES



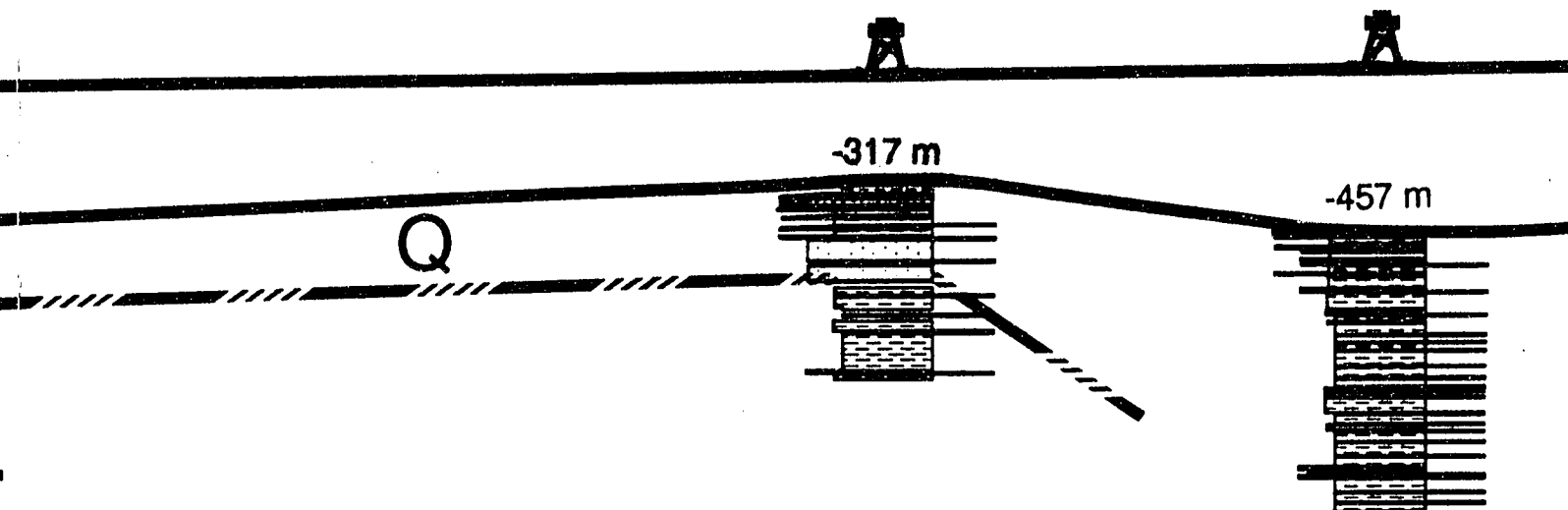
ODP 679



N
a
t
i
o
n
a
l
S
c
i
e
n
c
e
M
u
s
e
u
m

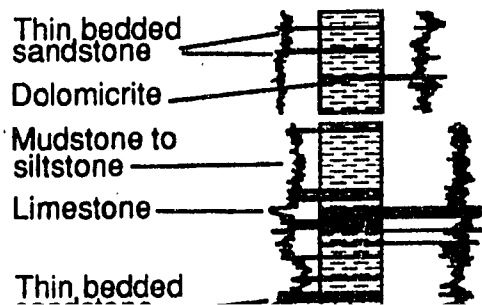
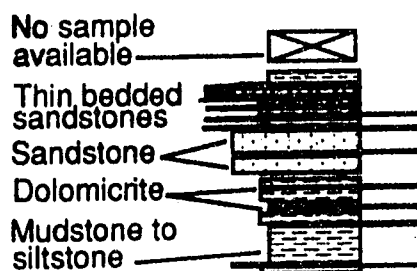
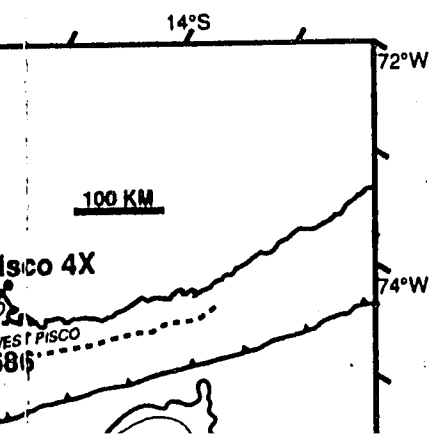
ODP 687

ODP 686



M2

L E G E N D



S

SSE

ODP 686

PISCO 4X

115 m

-457 m

Q

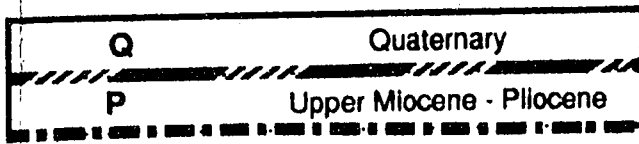
P

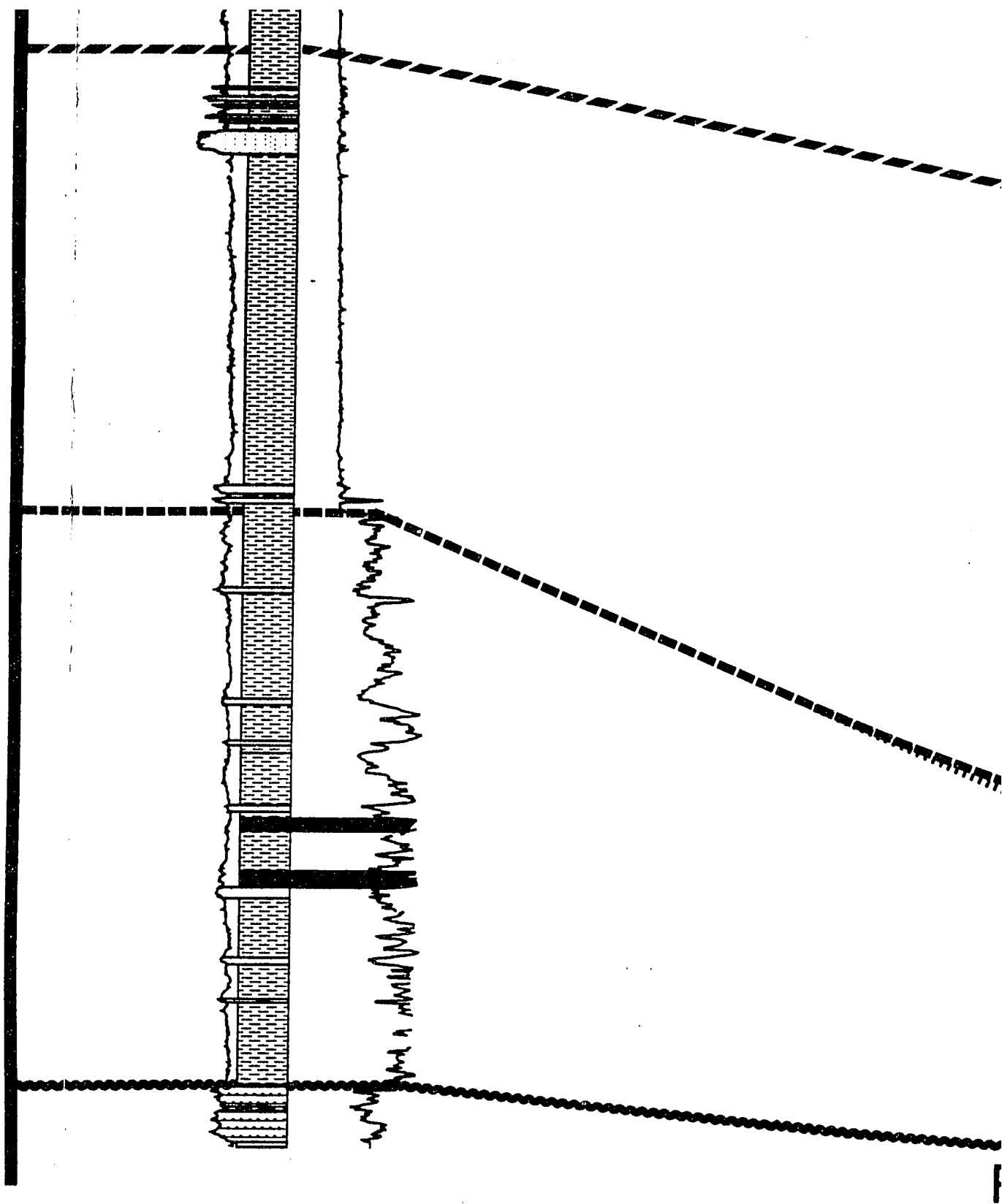
M2 M1 E-O

K

E N D

SEQUENCE AGE







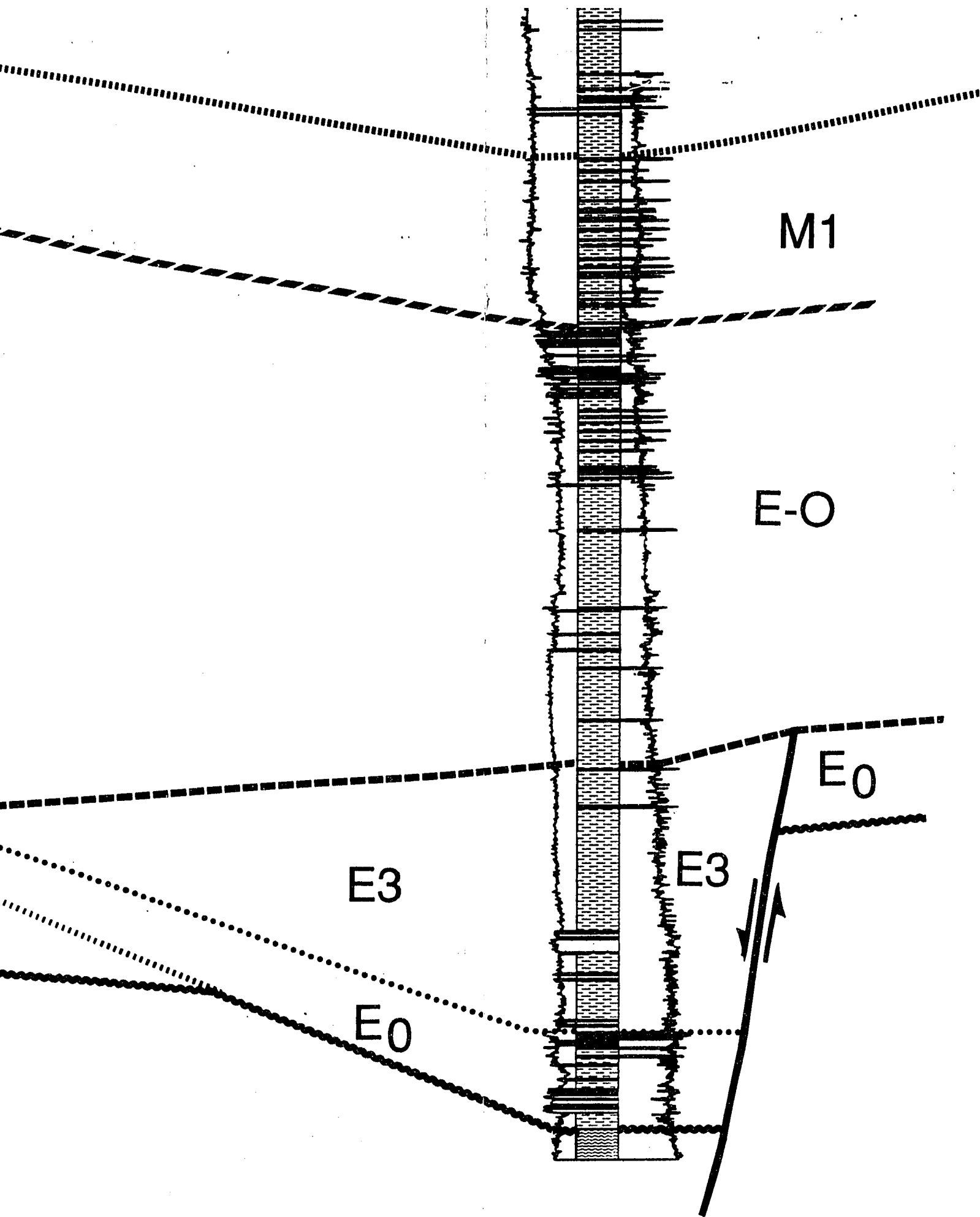
A diagram consisting of four regions separated by lines of different styles. The regions are labeled M1, E-O, K, and PK. The lines are: a dotted line at the top, a dashed line below it, a solid line below that, and a wavy line at the bottom. The labels are placed in the center of each region.

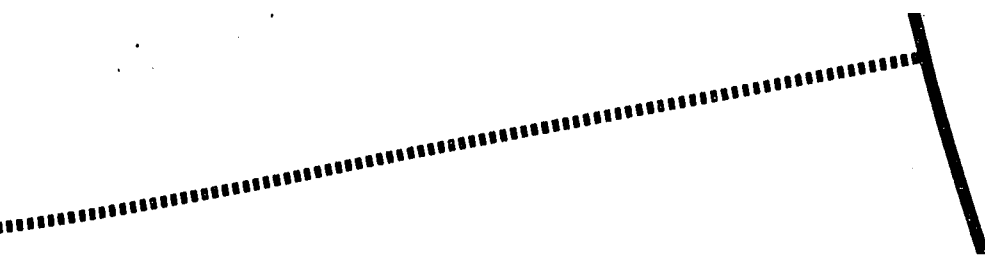
M1

E-O

K

PK



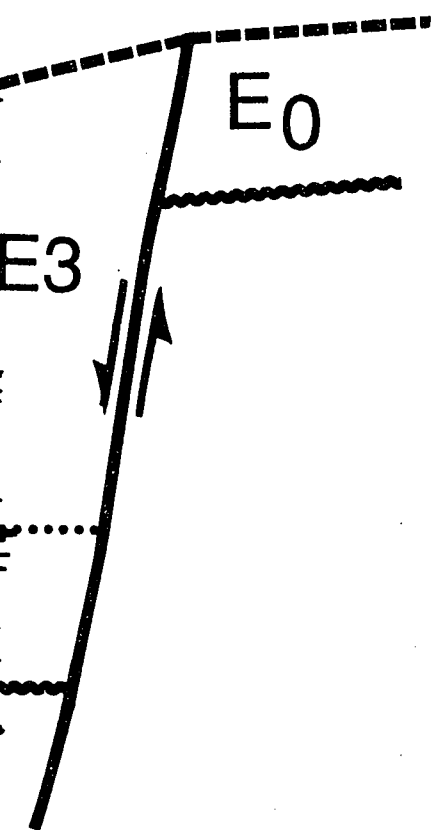


M1



E-O

SCALES



Sea level

500 m

Sea bottom

500 m

100 km



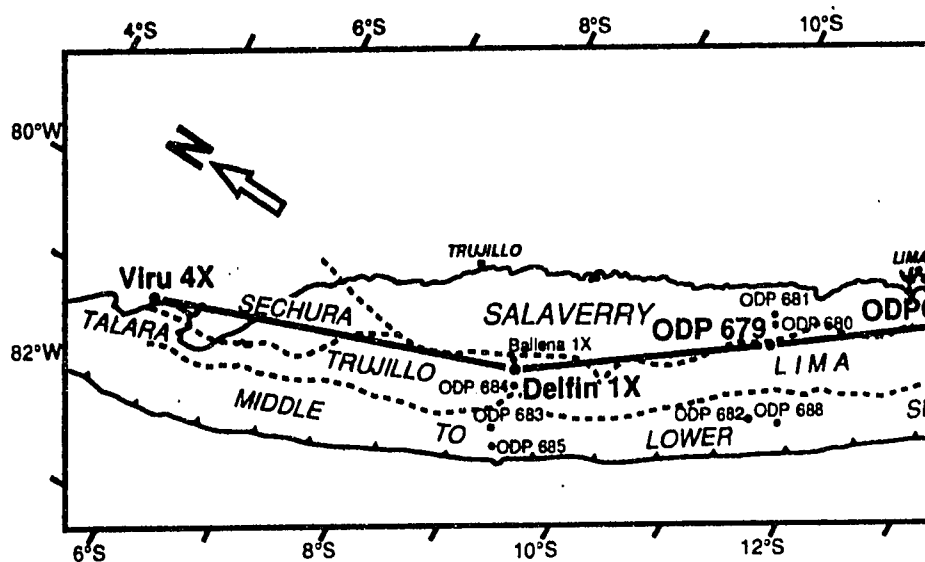
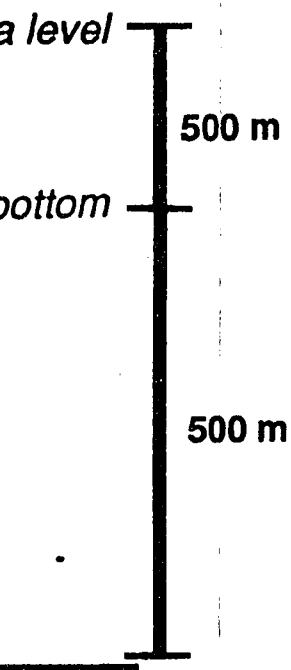


Plate 1

**SCHEMATIC CHRONOSTRATIGRAPHIC CORRELATION
ONSHORE SECHURA BASIN-TRUJILLO BASIN
WEST PISCO BASIN-ONSHORE E**

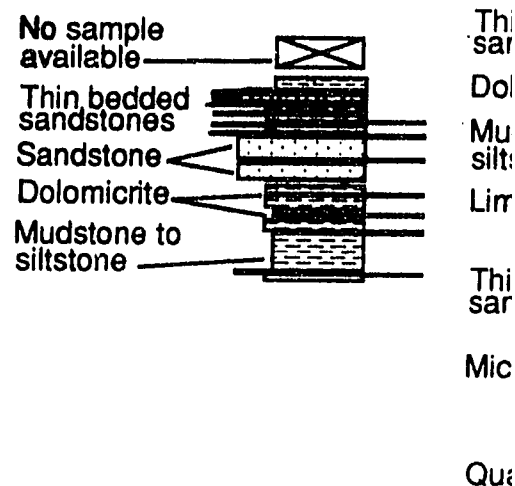
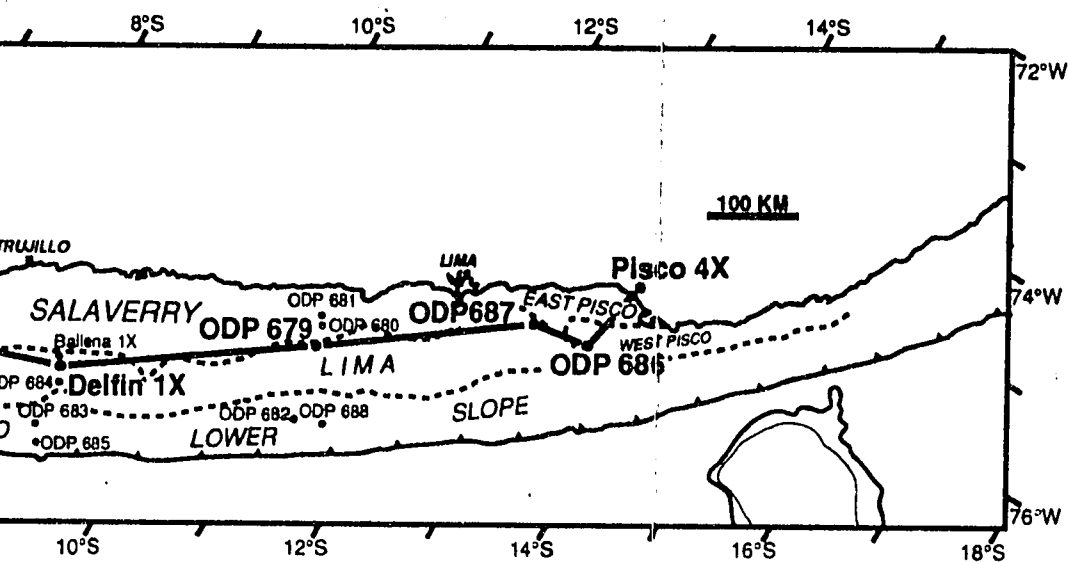
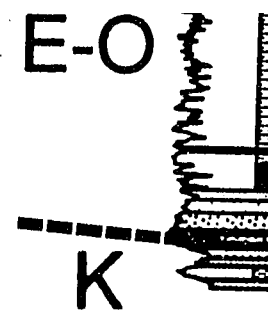


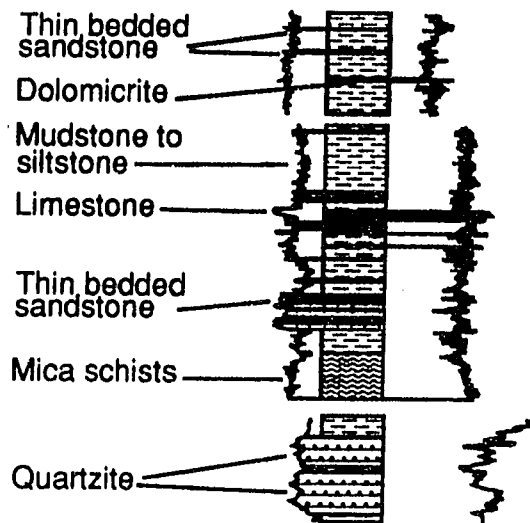
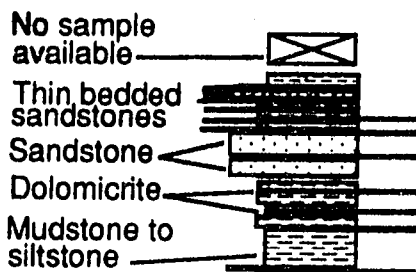
Plate 1

**ONOSTRATIGRAPHIC CROSS SECTION
RA BASIN-TRUJILLO BASIN-LIMA BASIN-
SIN-ONSHORE EAST PISCO BASIN**

M2 M1 E-O



L E G E N D

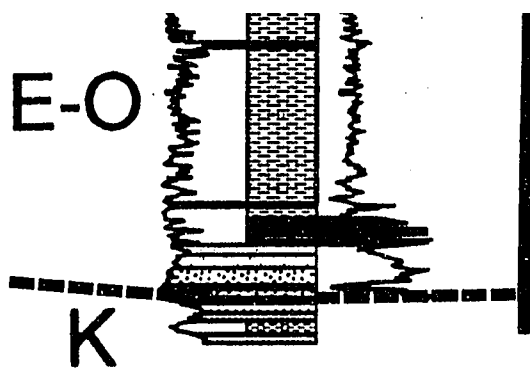


SEQUENCE A

Q	Quater
P	Upper Miocer
M 3	Upper M
M 2	Middle - Low
M 1	Lower M
E-O	Uppermost mi to Oligo
E 3	Middle E
E 2	Middle E
E 1	Middle E
E ₀	Lower ? - Mid
K	Cretace
PK	Pre-Cretaceou

ON
SIN-

M2 M1 E-O



E N D

SEQUENCE A G E

Q	Quaternary
P	Upper Miocene - Pliocene
M 3	Upper Miocene
M 2	Middle - Lower Miocene
M 1	Lower Miocene
E-O	Uppermost middle Eocene to Oligocene
E 3	Middle Eocene
E 2	Middle Eocene
E 1	Middle Eocene
E ₀	Lower ? - Middle Eocene
K	Cretaceous ?
PK	Pre-Cretaceous Basement

PLEASE NOTE:

Oversize maps and charts are filmed in sections in the following manner:

LEFT TO RIGHT, TOP TO BOTTOM, WITH SMALL OVERLAPS

The following map or chart has been refilmed in its entirety at the end of this dissertation (not available on microfiche). A xerographic reproduction has been provided for paper copies and is inserted into the inside of the back cover.

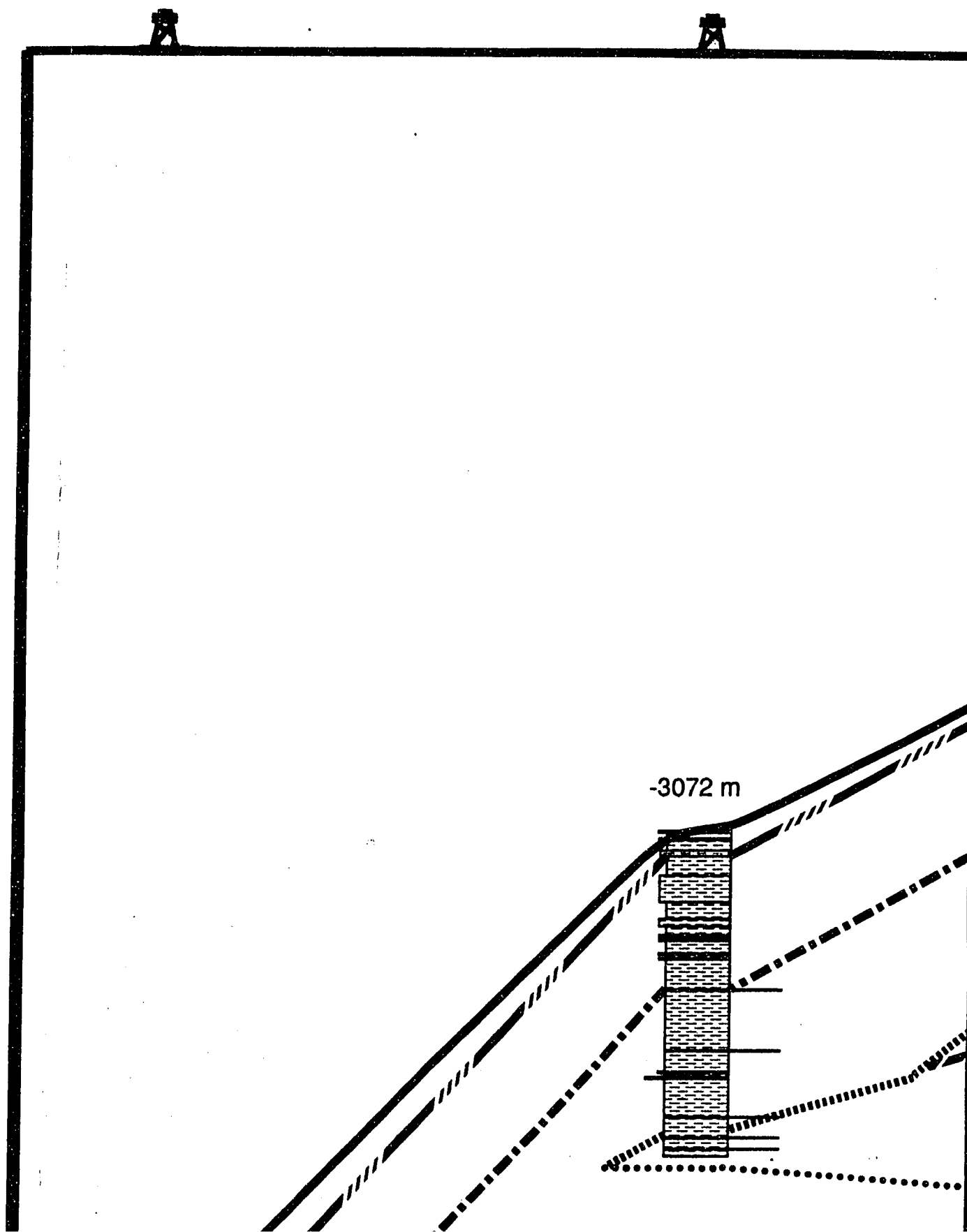
Black and white photographic prints (17" x 23") are available for an additional charge.

UMI

WSW

ODP 685

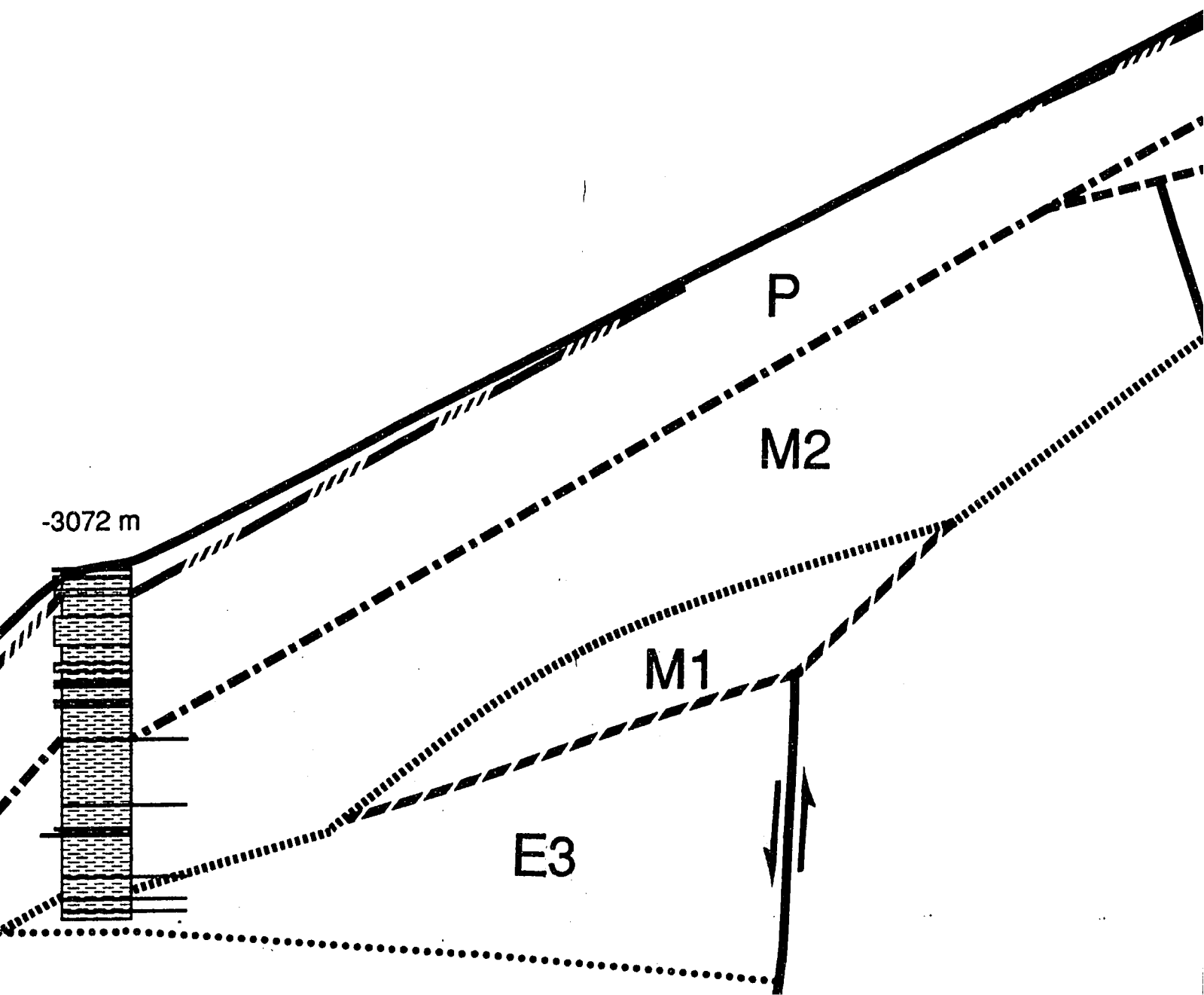
ODP 683



ODP 683

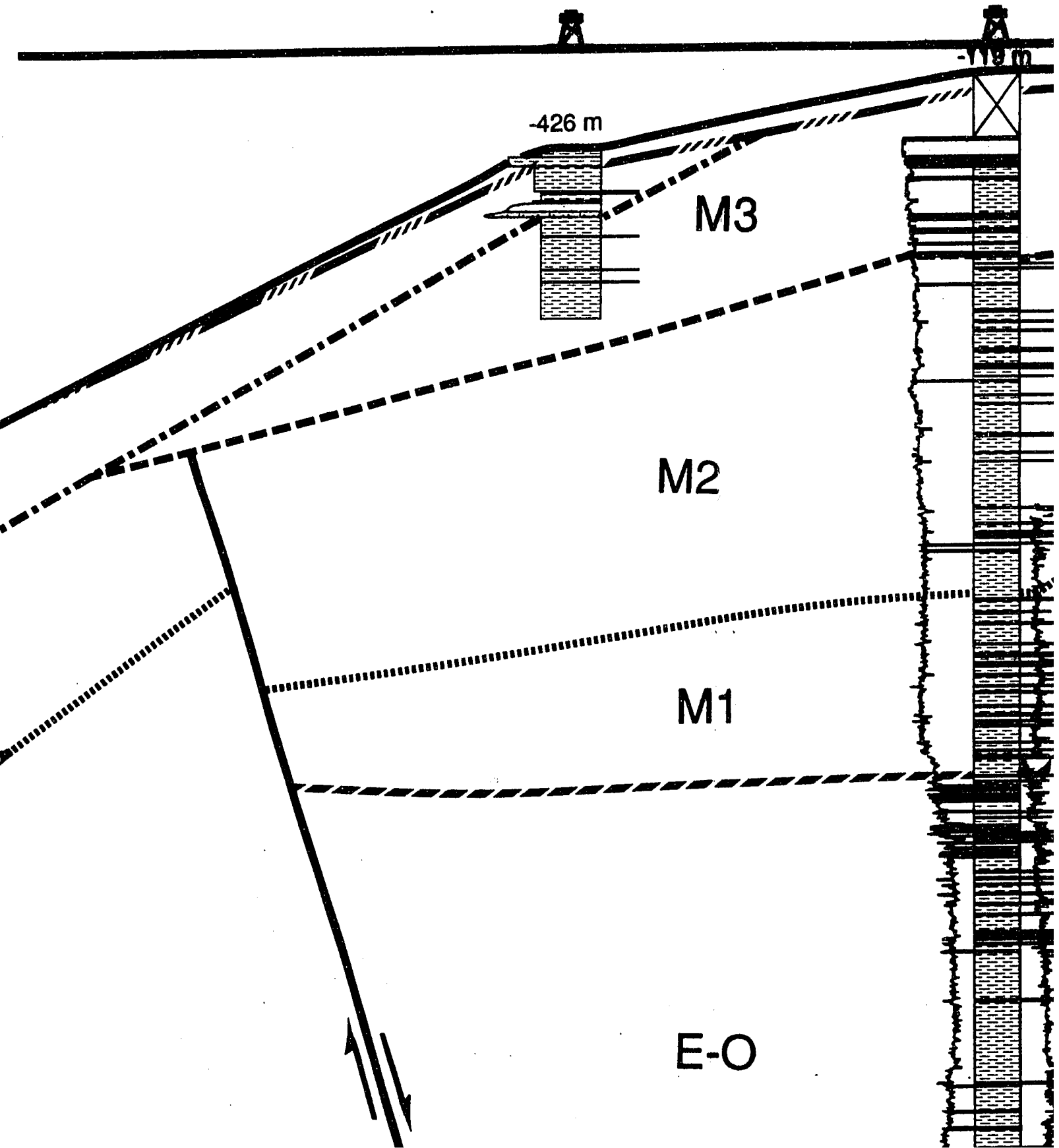


SEA LEVEL



ODP 684

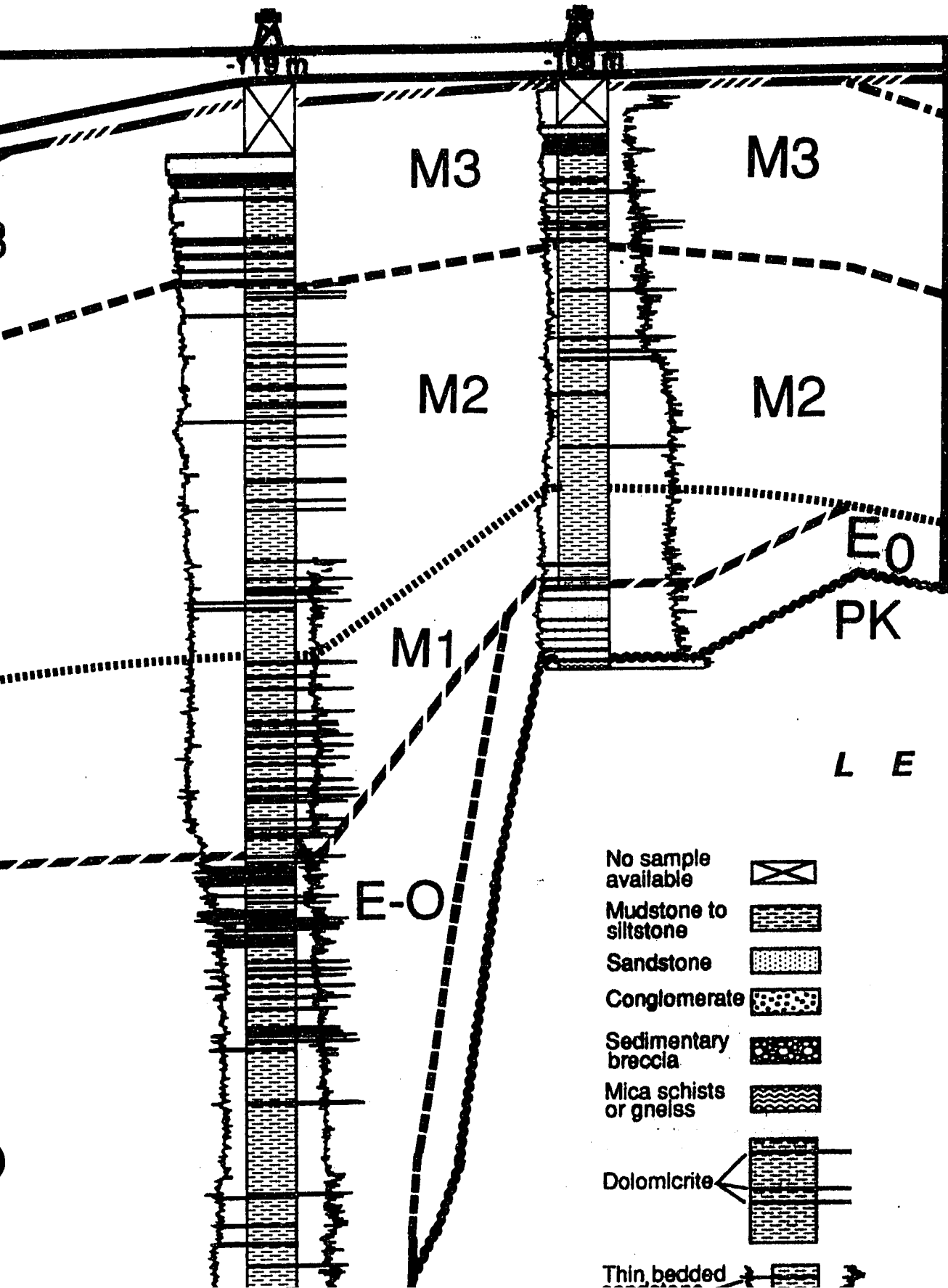
Delfin 1



ENE

Delfin 1X

Ballena 1X



LEGEND

SEQUENCE

No sample available



Mudstone to siltstone



Sandstone



Conglomerate



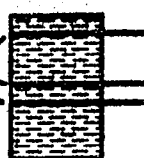
Sedimentary breccia



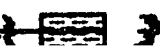
Mica schists or gneiss



Dolomiticrite



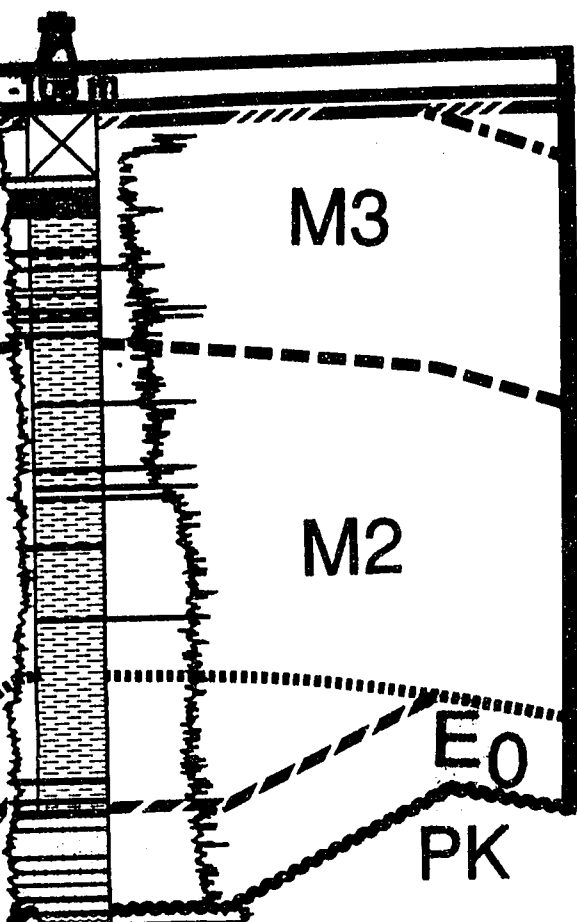
Thin bedded









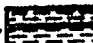
Q
P
M 3
M 2
M 1
E-O
E 3
E 2
E 1
E ₀

ENE

lena 1X

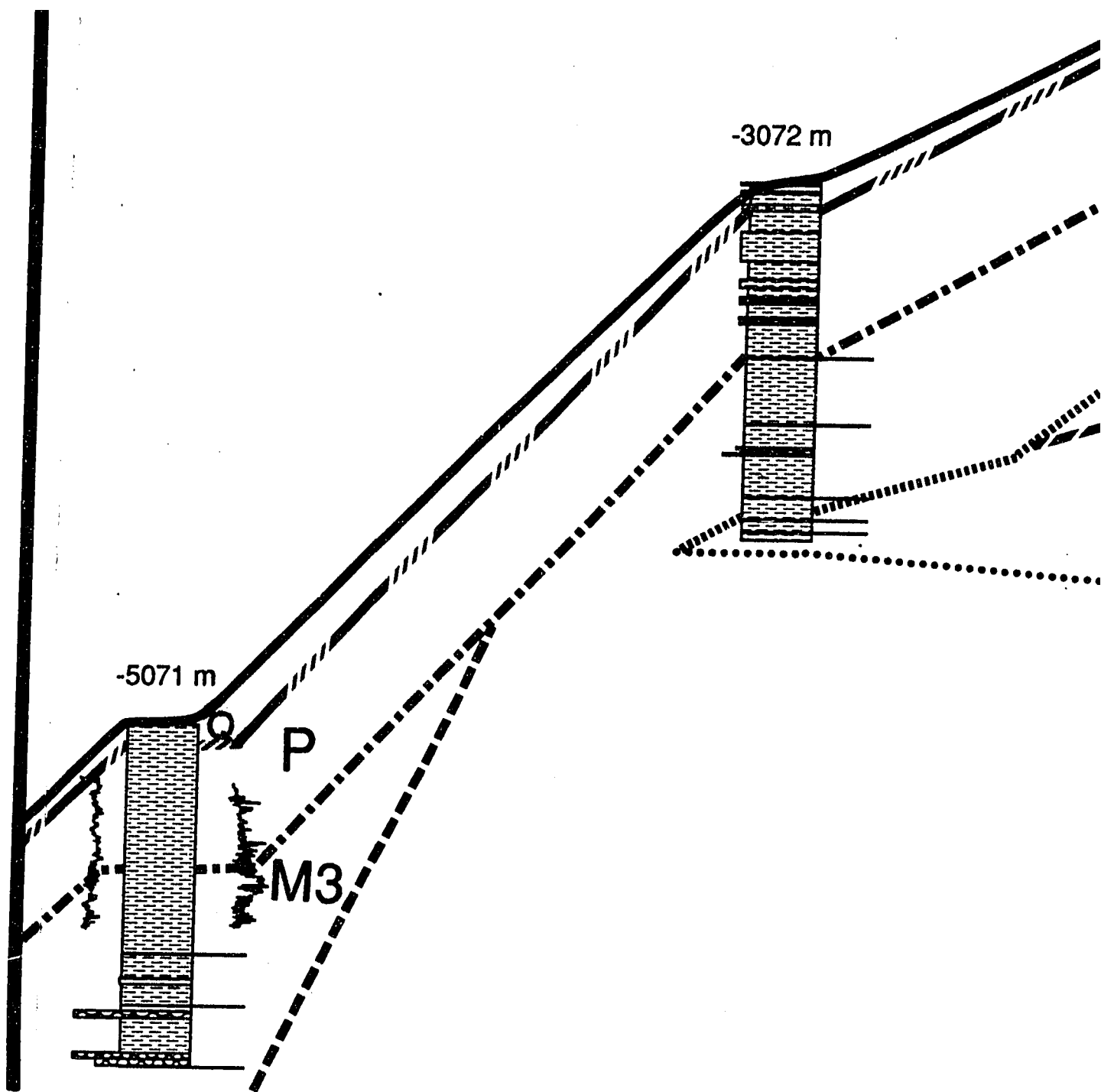


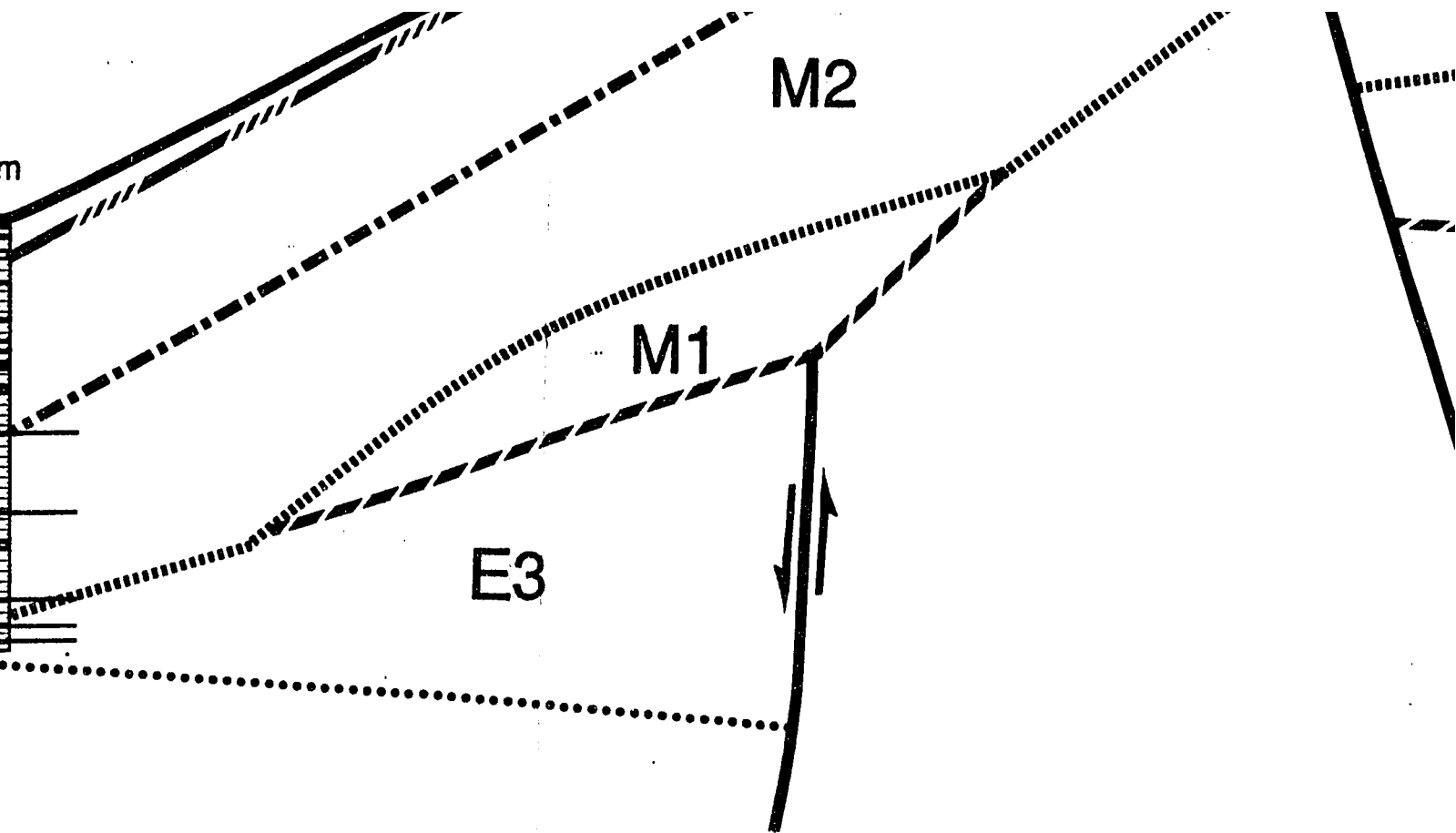
LEGEND

- No sample available 
- Mudstone to siltstone 
- Sandstone 
- Conglomerate 
- Sedimentary breccia 
- Mica schists or gneiss 
- Dolomicrite 

SEQUENCE AGE

Q	Quaternary
P	Upper Miocene - Pliocene
M 3	Upper Miocene
M 2	Middle - Lower Miocene
M 1	Lower Miocene
E-O	Uppermost middle Eocene to Oligocene
E 3	Middle Eocene
E 2	Middle Eocene
E 1	Middle Eocene





SCALES

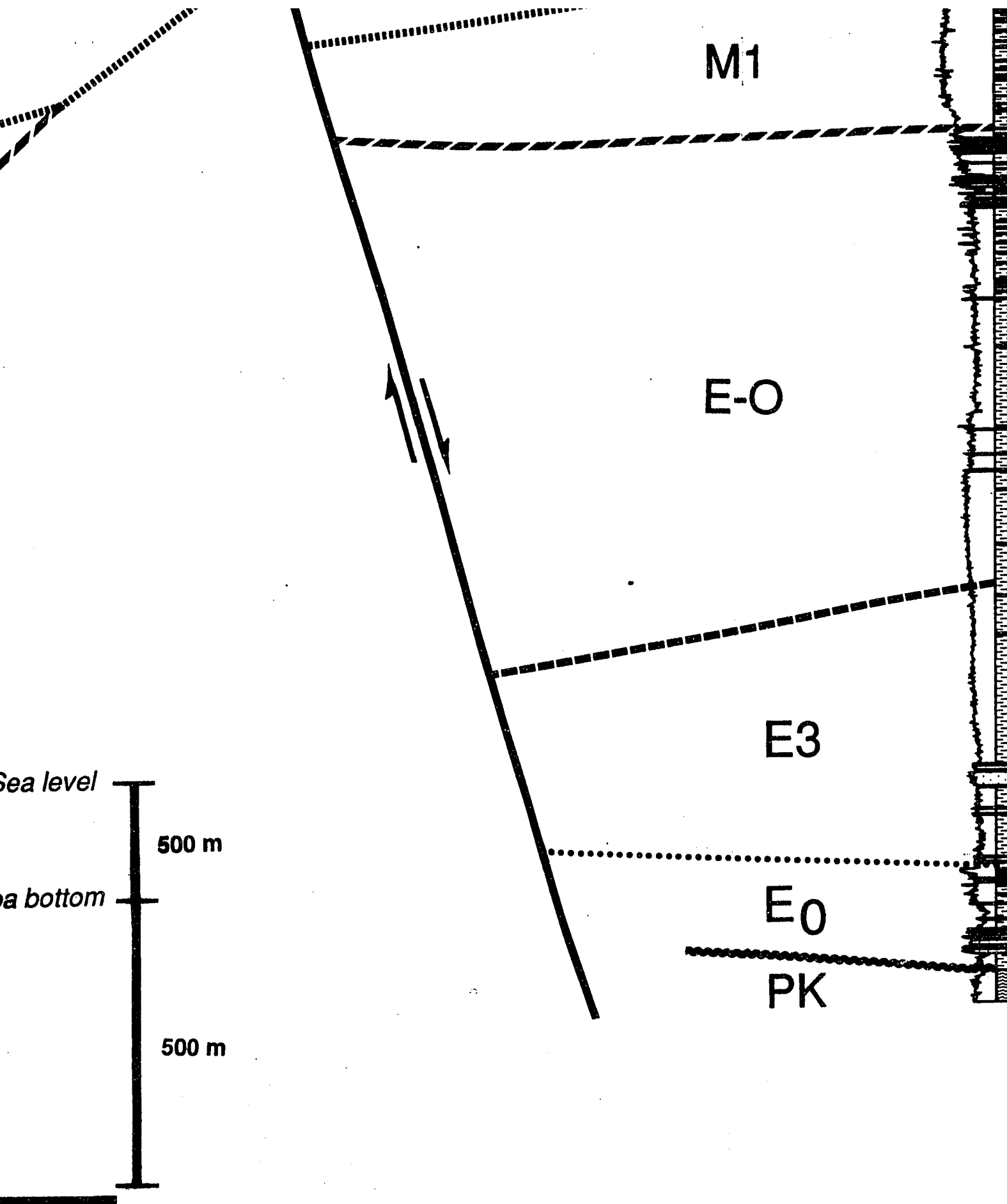
Sea level

500 m

Sea bottom

500 m

20 km



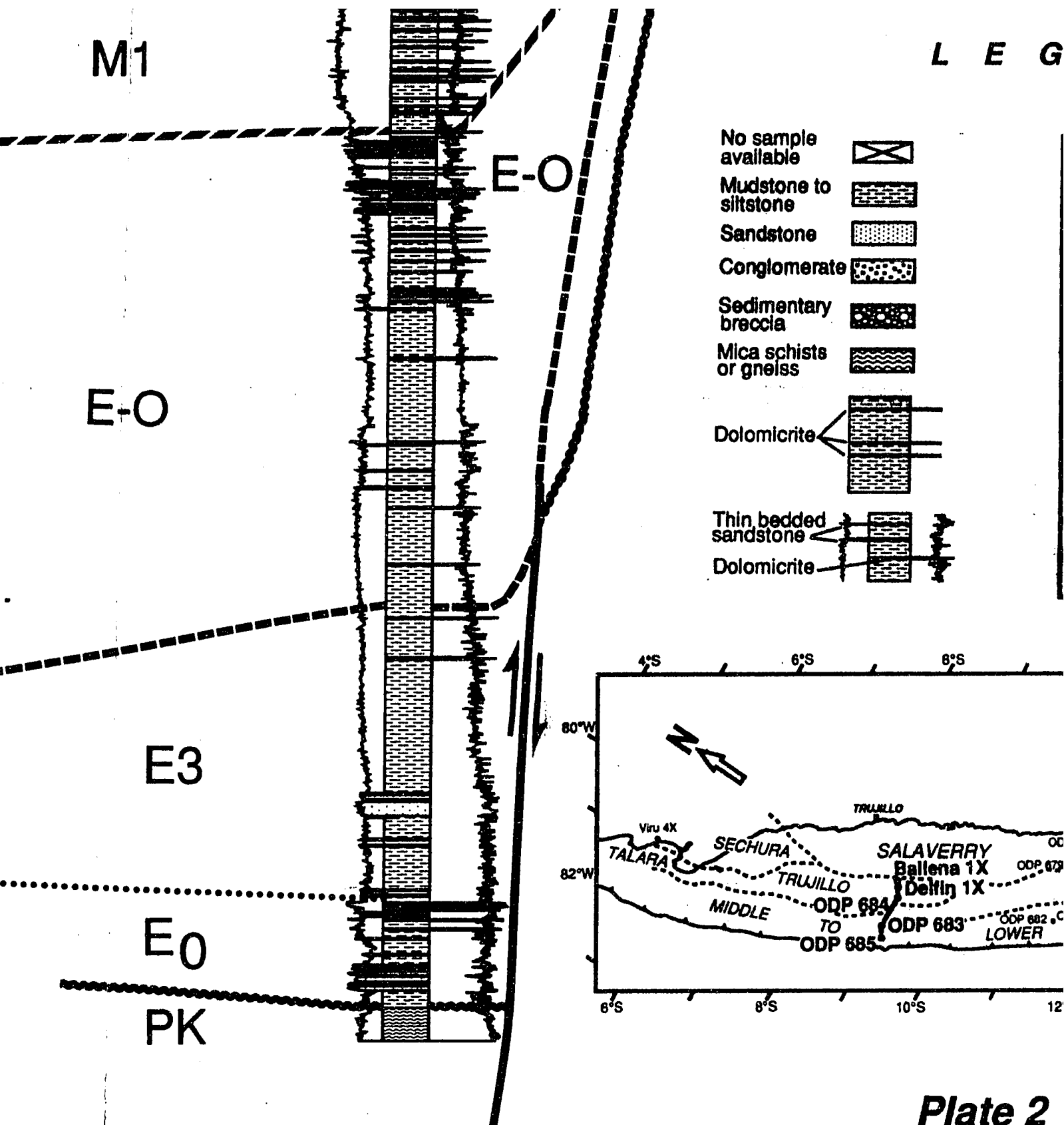


Plate 2
SCHEMATIC CHRONOSTRATIGRAPHIC
LOWER SLOPE ZONE-

Plate 2
CHRONOSTRATIGRAPHIC CROSS SECTION
FOR SLOPE ZONE-TRUJILLO BASIN

PLEASE NOTE:

Oversize maps and charts are filmed in sections in the following manner:

LEFT TO RIGHT, TOP TO BOTTOM, WITH SMALL OVERLAPS

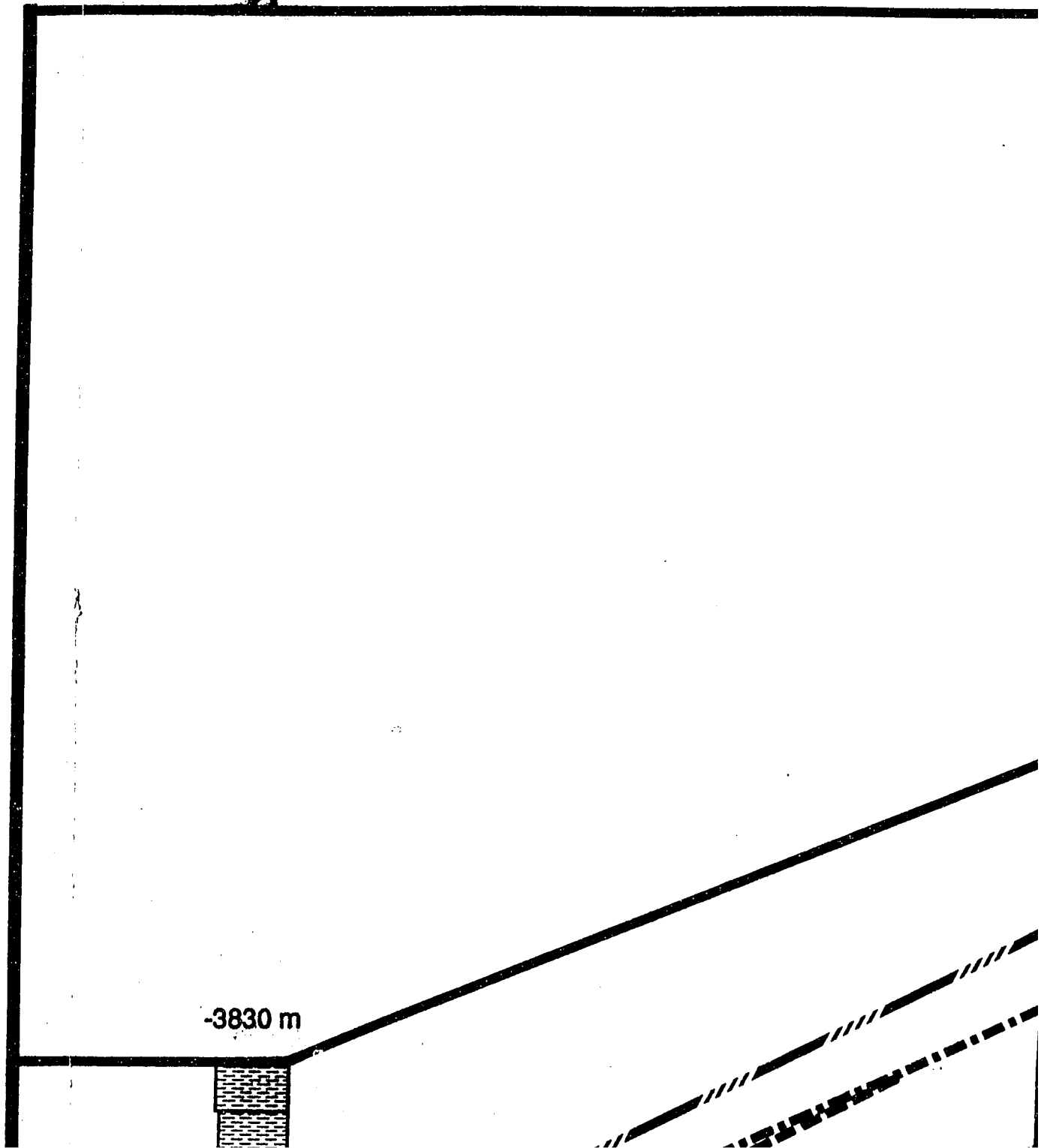
The following map or chart has been refilmed in its entirety at the end of this dissertation (not available on microfiche). A xerographic reproduction has been provided for paper copies and is inserted into the inside of the back cover.

Black and white photographic prints (17" x 23") are available for an additional charge.

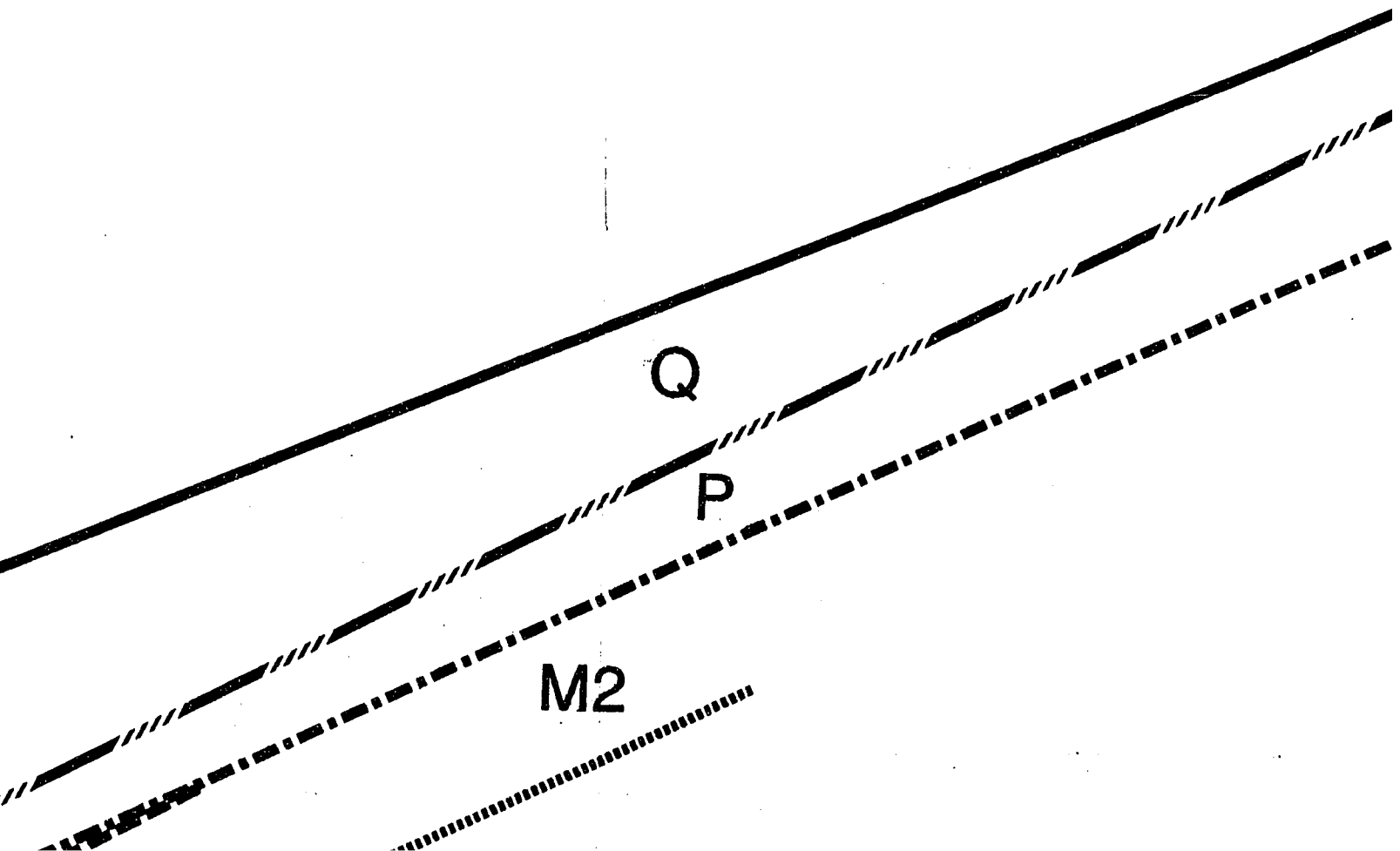
UMI

WSW

ODP 688



SEA LEVEL



ODP 679



-461 m



SCALES

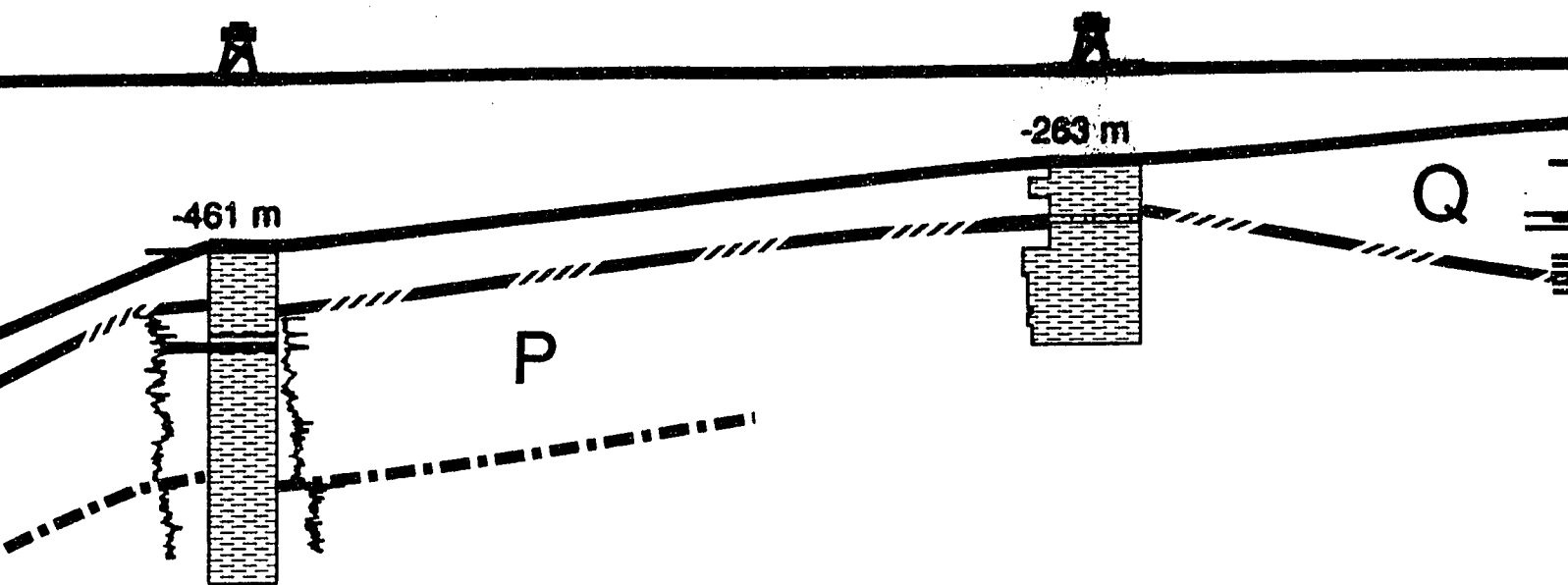
Sea level

Sea bottom

ODP 679

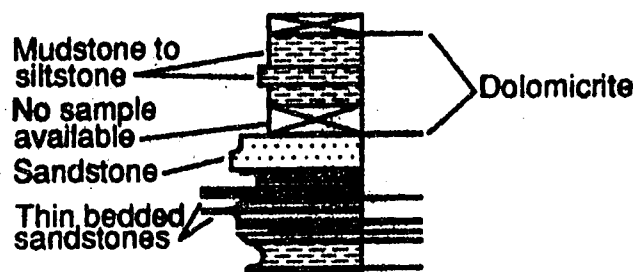
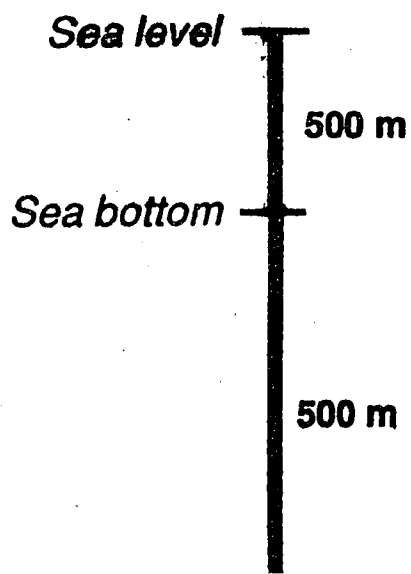
ODP 680

Ol



L E G E N D

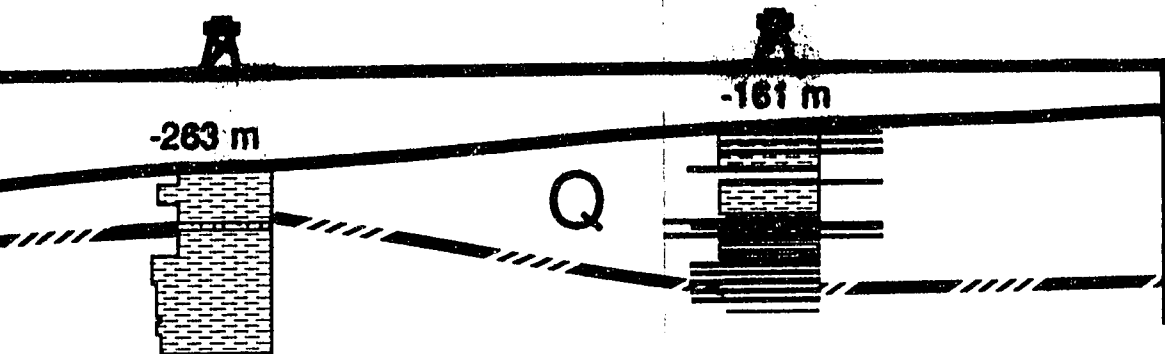
SCALES



ENE

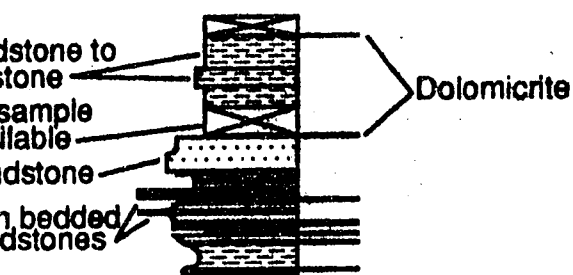
ODP 680

ODP 681

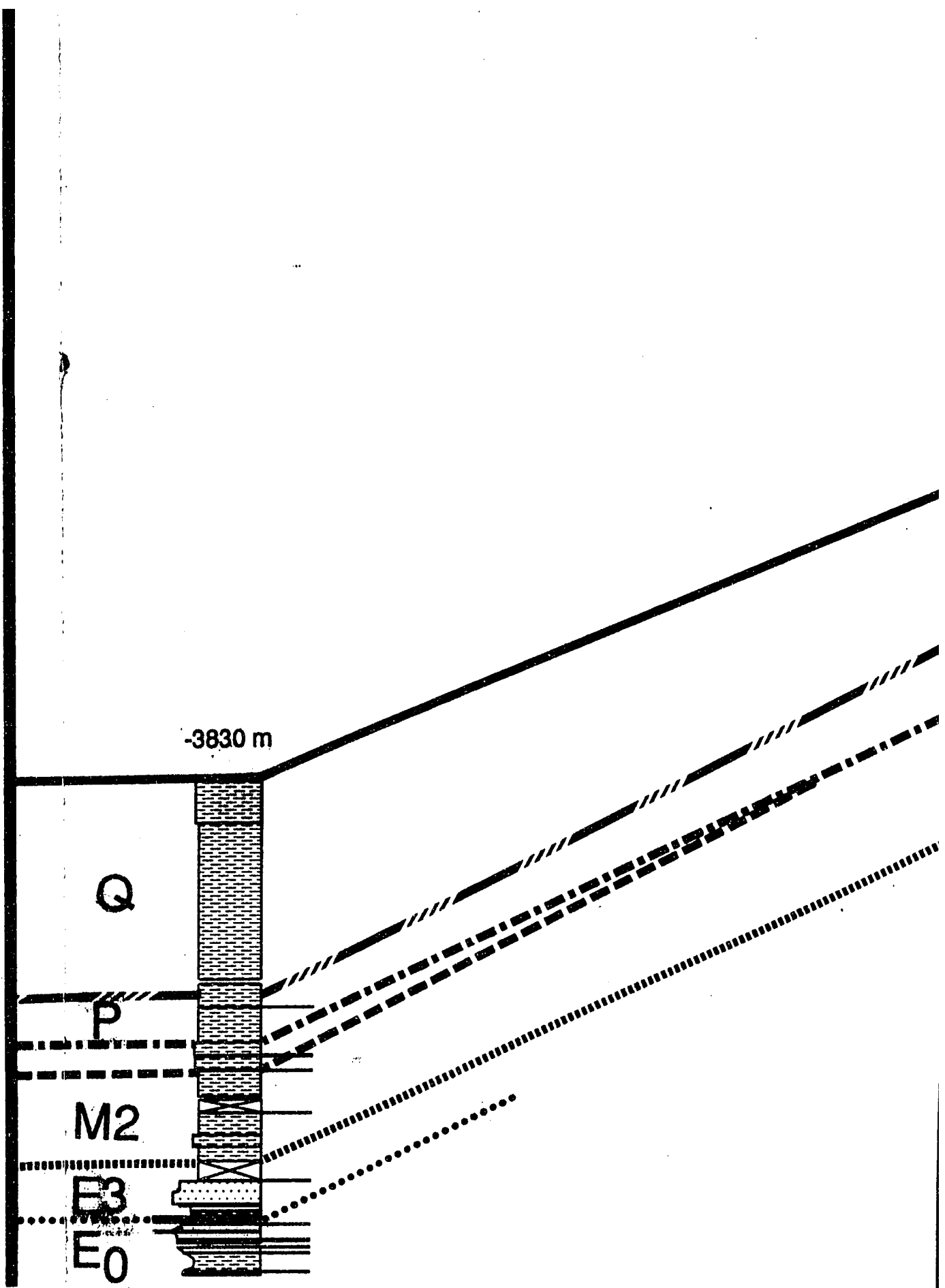


L E G E N D

SEQUENCE AGE



Q	Quaternary
P	Upper Miocene - Pliocene
M 3	Upper Miocene
M 2	Middle - Lower Miocene
M 1	Lower Miocene
E-O	Uppermost middle Eocene to Oligocene
E 3	Middle Eocene
E 2	Middle Eocene
E 1	Middle Eocene
E ₀	Lower ? - Middle Eocene
K	Cretaceous ?
PK	Pre-Cretaceous Basement



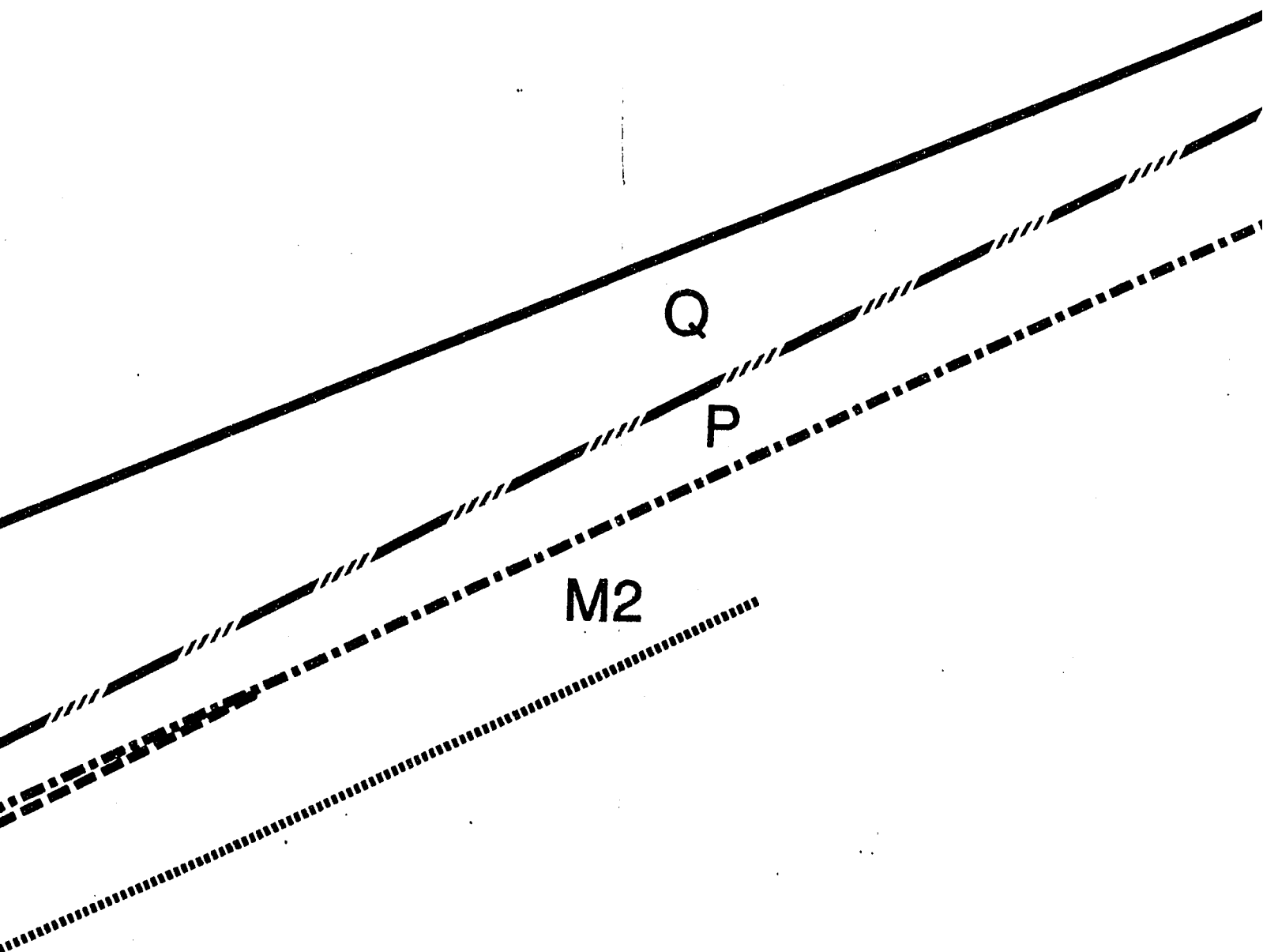
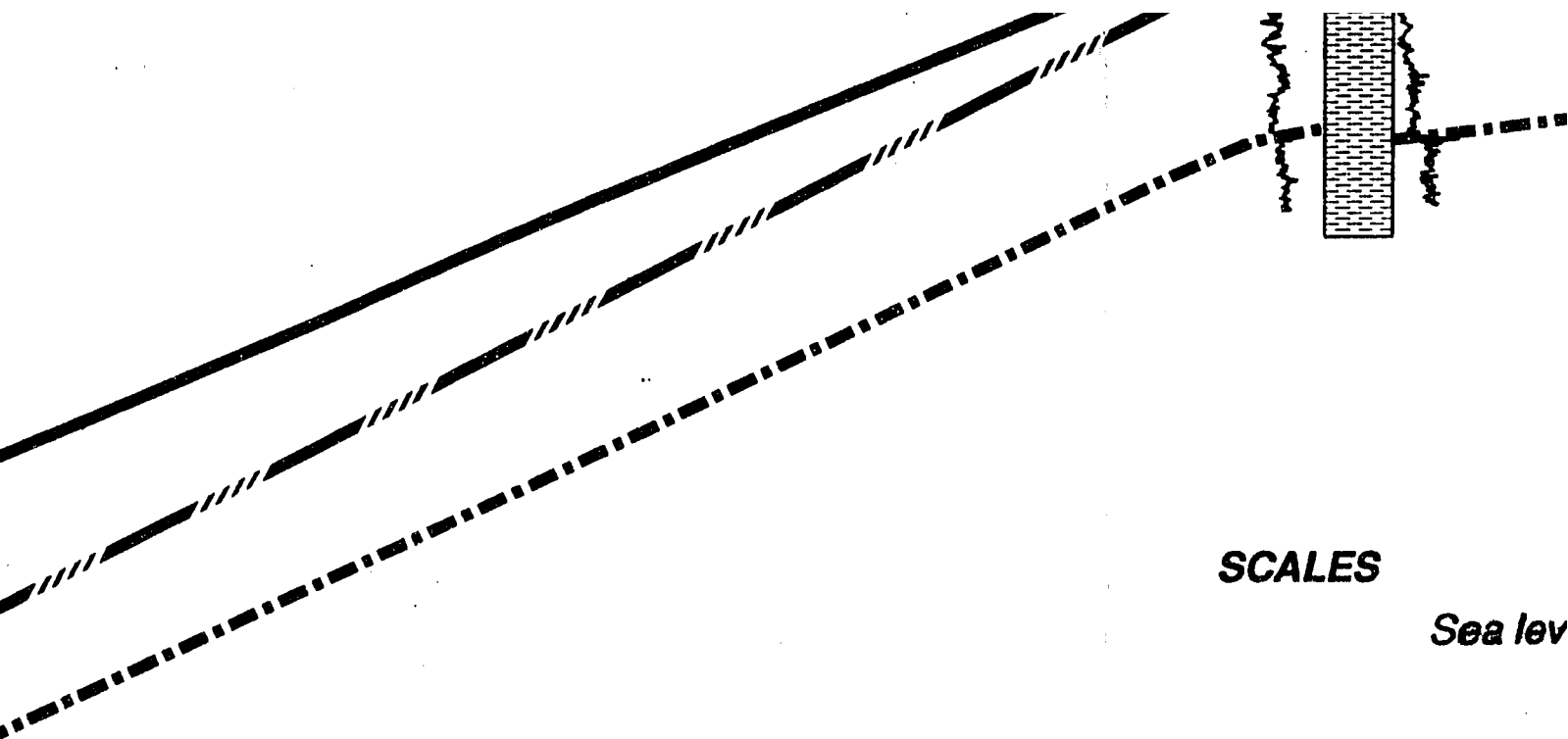


Plate
SCHEMATIC CHRONOSTRA
LOWER SLOPE ZONE-LIMA



SCALES

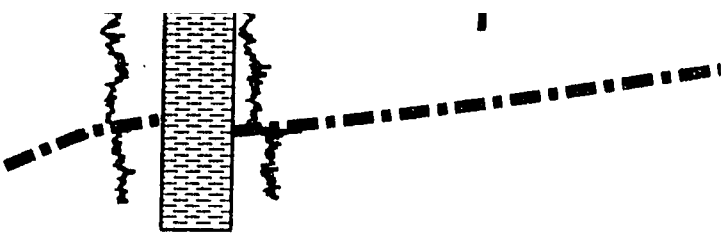
Sea lev

Sea botto

20 km

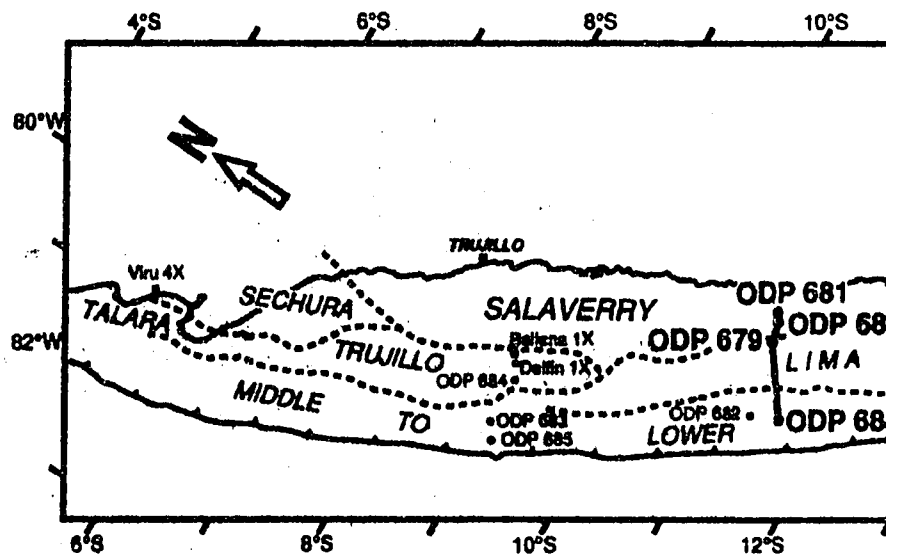
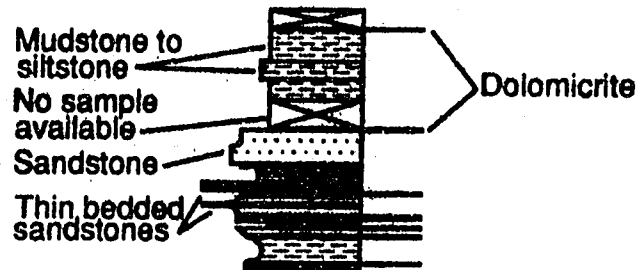
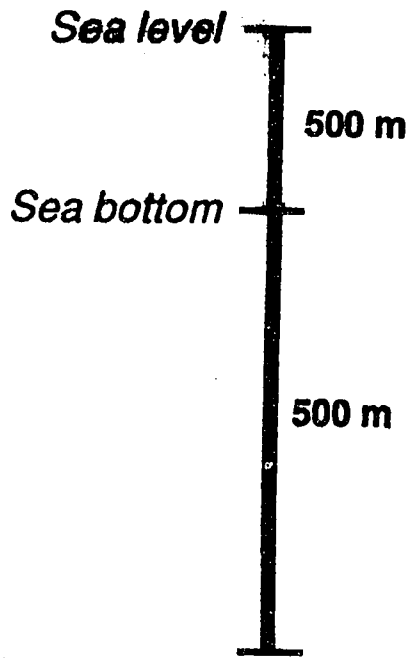
Plate 3

**CHRONOSTRATIGRAPHIC CROSS SECTION
E ZONE-LIMA BASIN-SALAVERRY BASIN**



L E G E N D

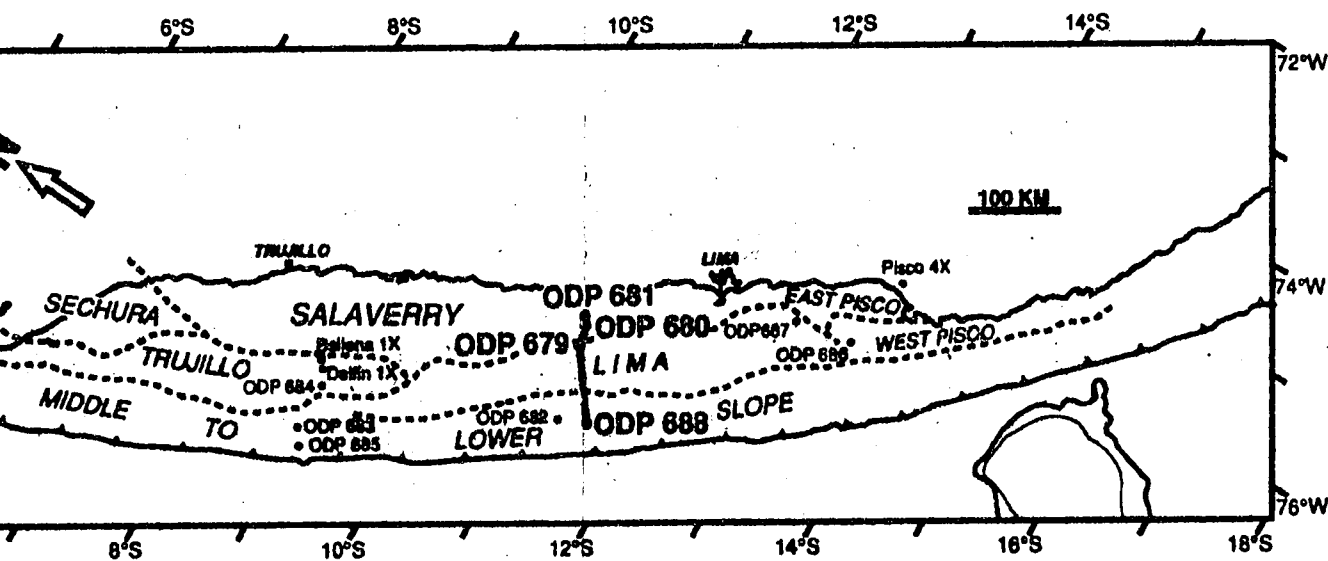
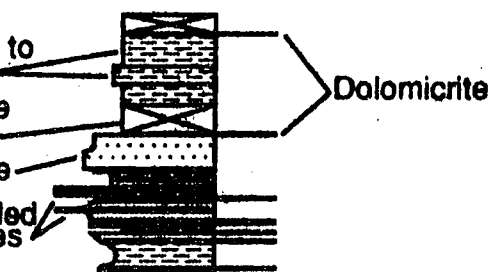
SCALES

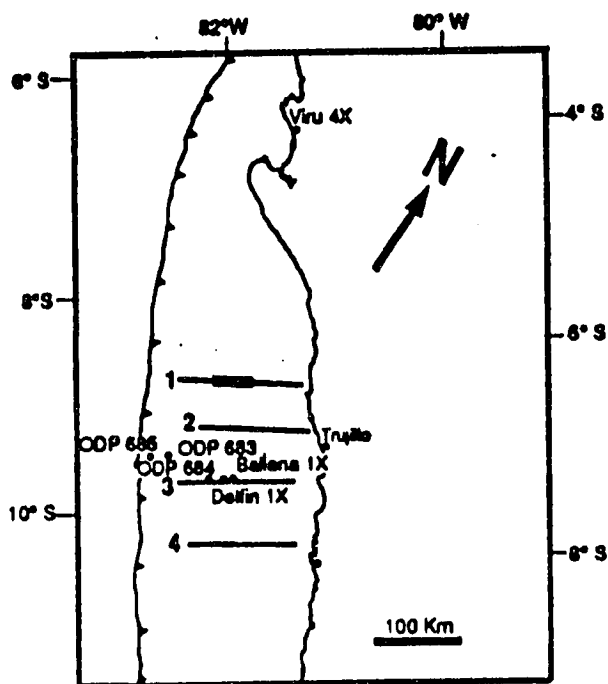


LEGEND

SEQUENCE AGE

Q	Quaternary
P	Upper Miocene - Pliocene
M 3	Upper Miocene
M 2	Middle - Lower Miocene
M 1	Lower Miocene
E-O	Uppermost middle Eocene to Oligocene
E 3	Middle Eocene
E 2	Middle Eocene
E 1	Middle Eocene
E ₀	Lower ? - Middle Eocene
K	Cretaceous ?
PK	Pre-Cretaceous Basement





L E G E N D

S E Q U E N C E A G E

Q	Quaternary
P	Upper Miocene - Pliocene
M 3	Upper Miocene
M 2	Middle - Lower Miocene
M 1	Lower Miocene
E-O	Uppermost middle Eocene to Oligocene
E 3	Middle Eocene
E 2	Middle Eocene
E 1	Middle Eocene
E ₀	Lower ? - Middle Eocene
K	Cretaceous ?
PK	Pre-Cretaceous Basement

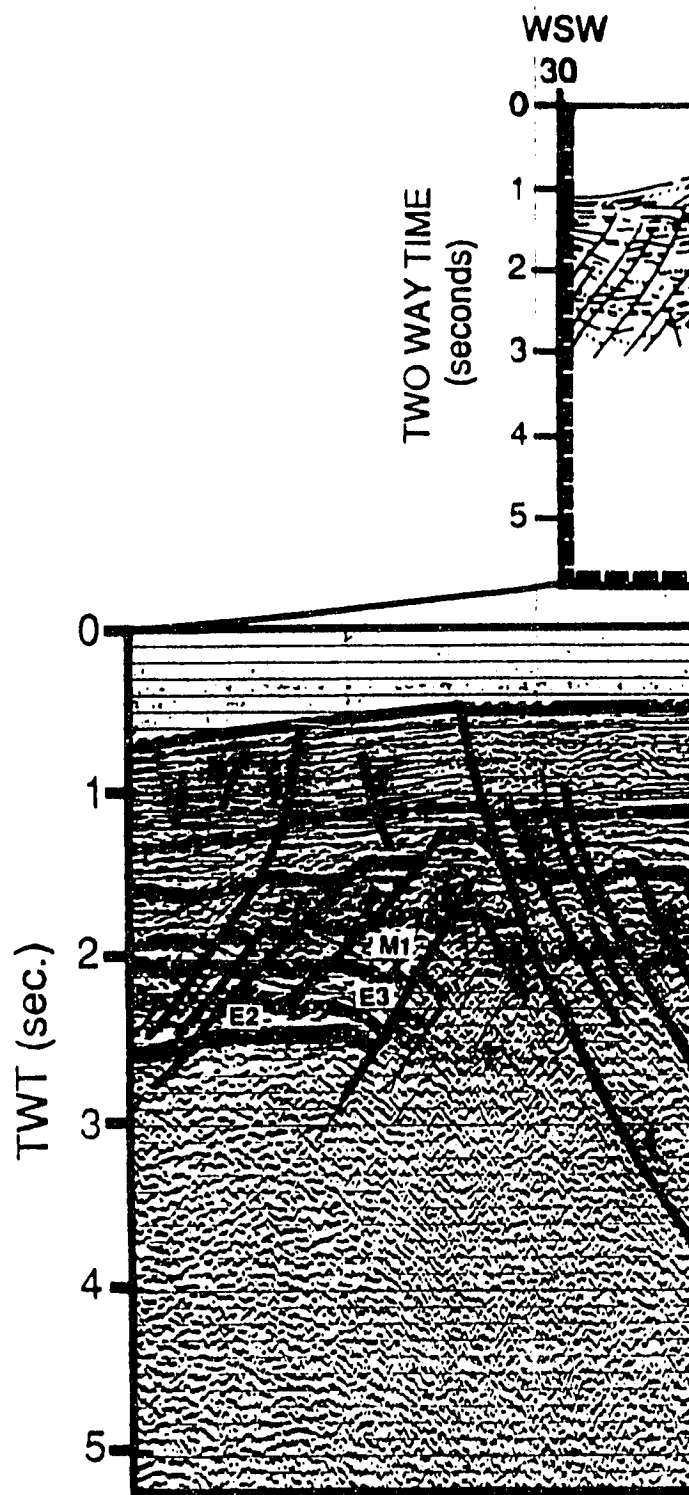
Normal fault

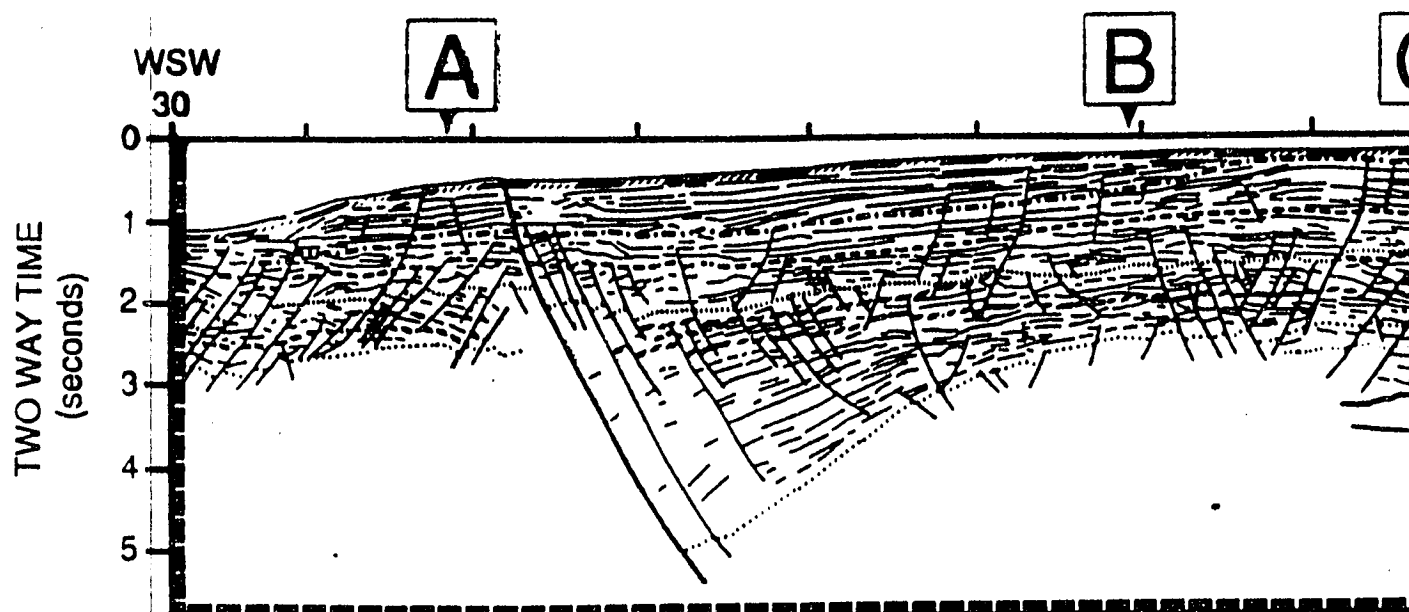


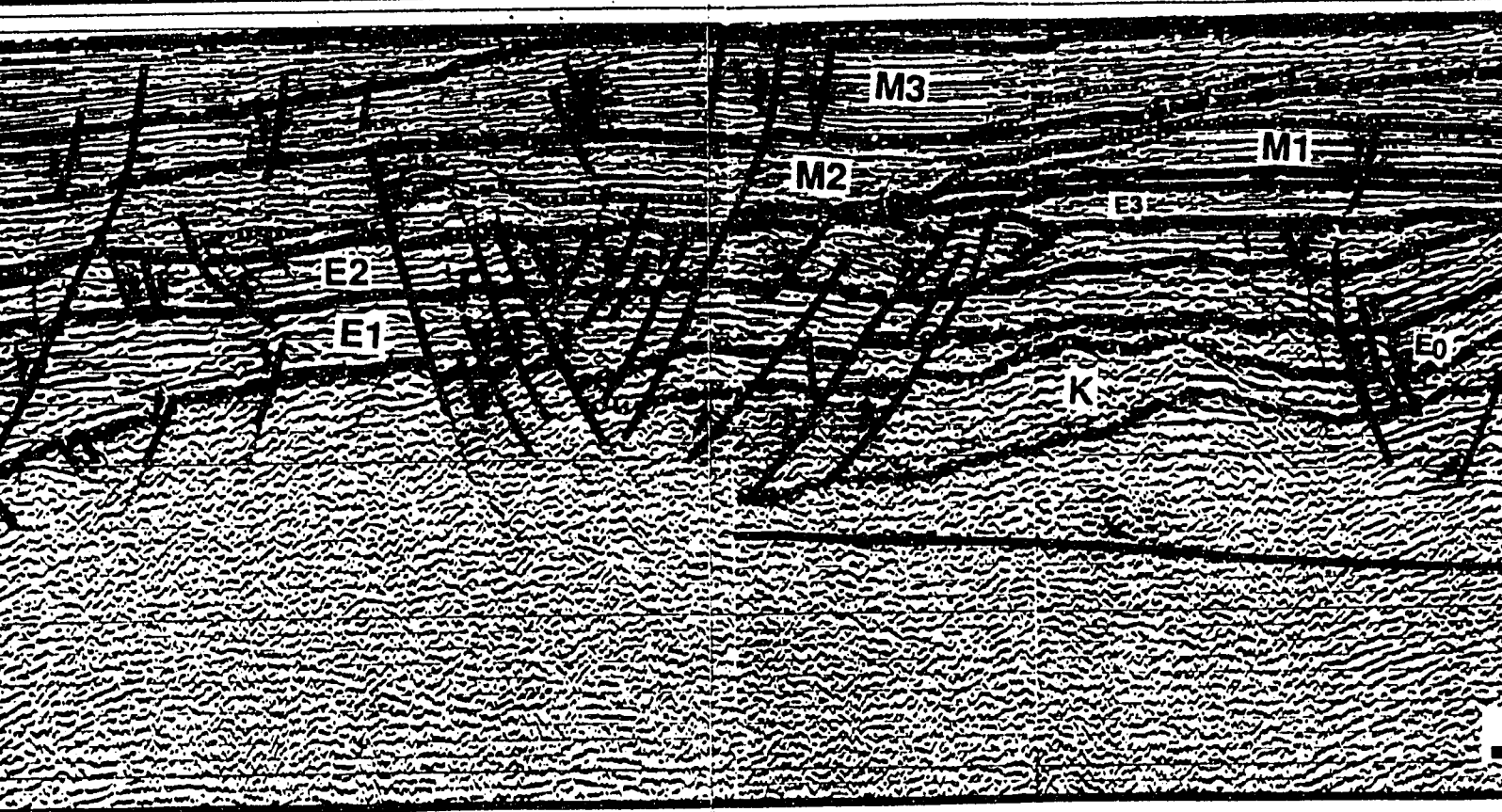
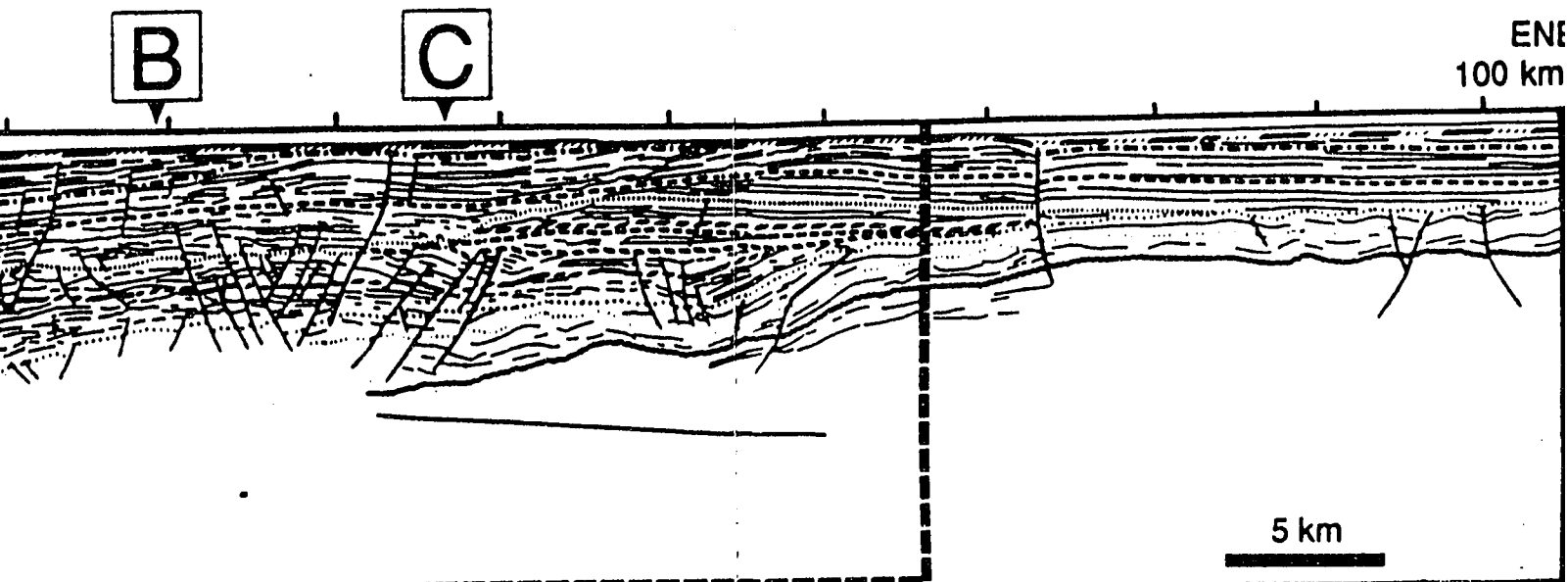
Reverse fault

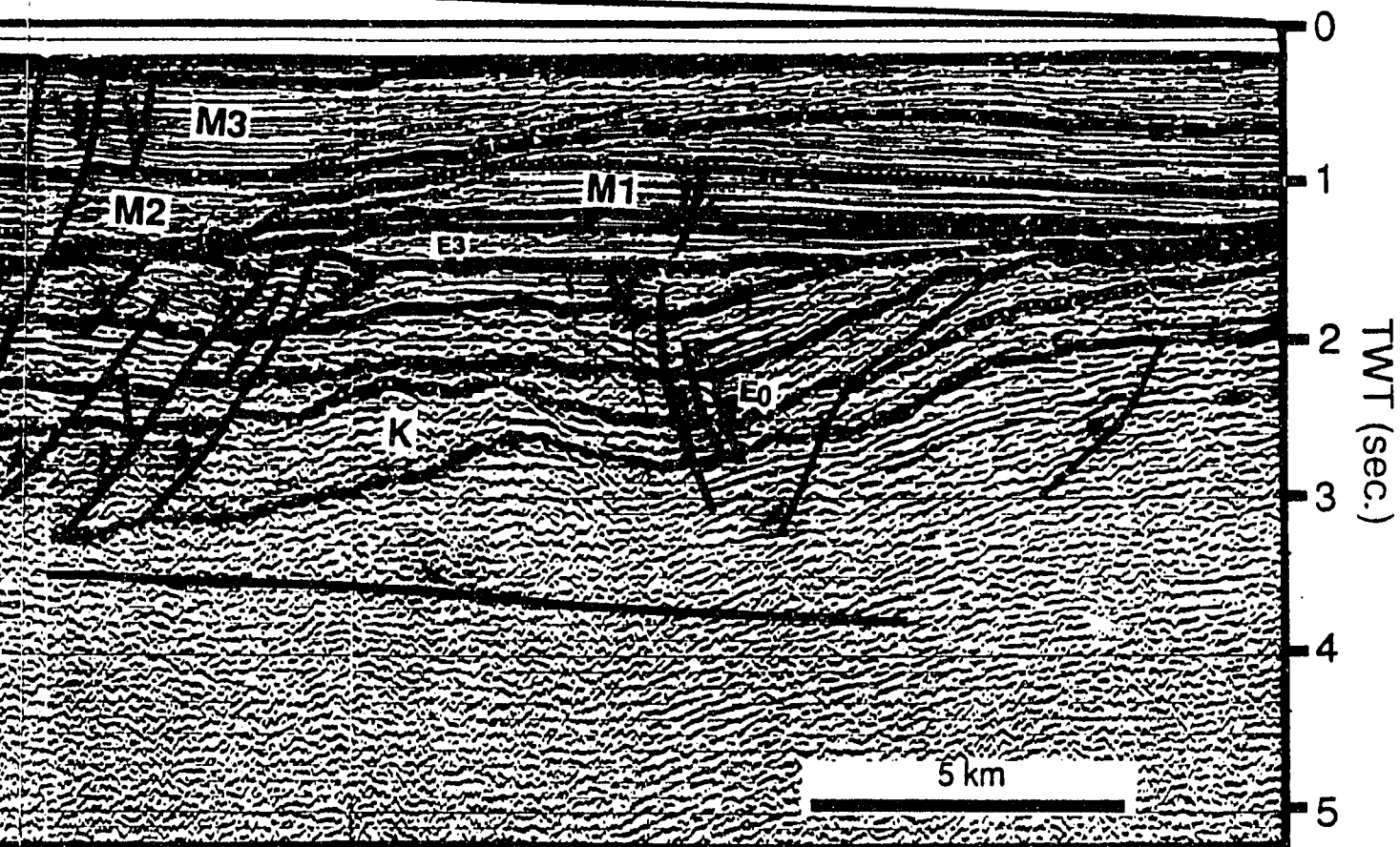
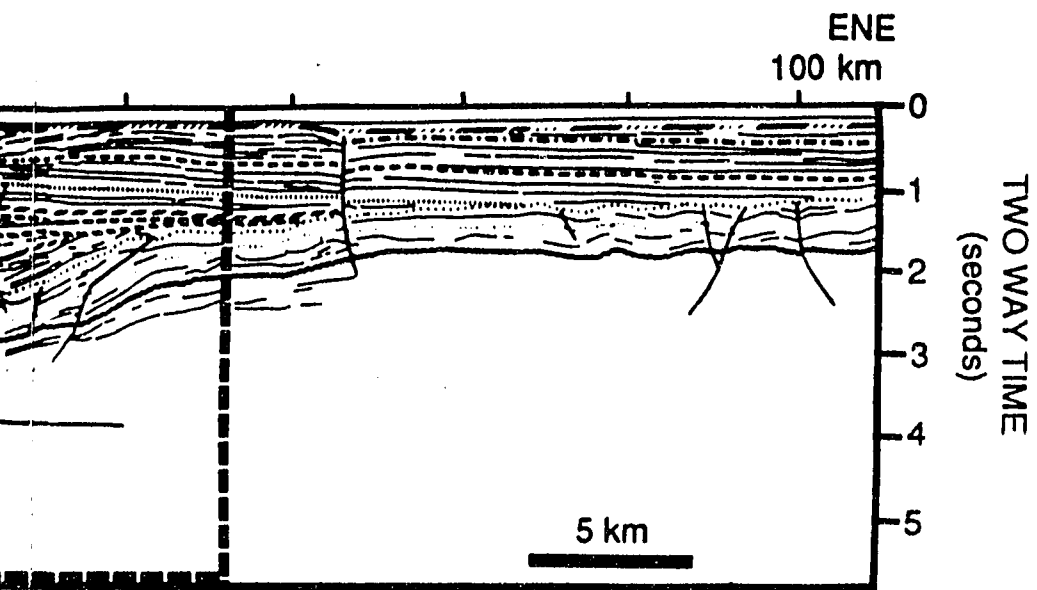


Base of submarine canyon





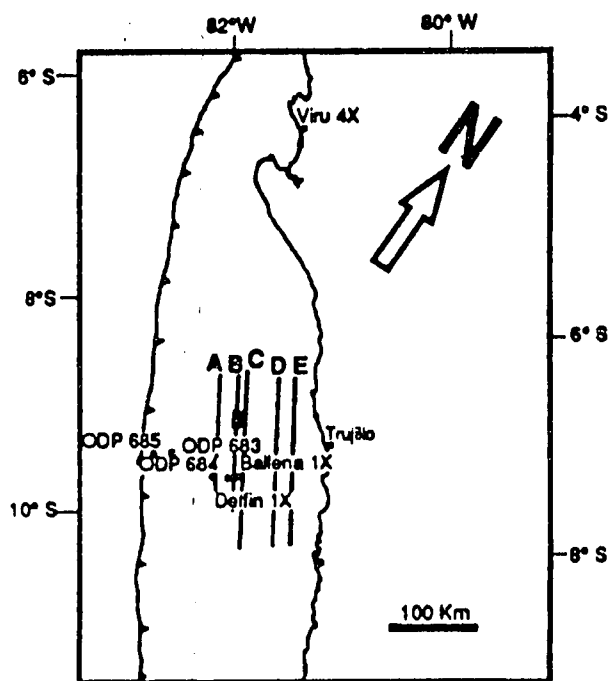




**PLATE 4 . CLOSE UP OF THE SEISMIC PROFILE LINE DRAWING 1
(PANEL 1), TRUJILLO BASIN.**

All the stratigraphic sequences are shown on this plate. The lack of seismic resolution prevents the correlation of sequences K and E₀ in the half western part of the seismic profile. The subhorizontal fault that occurs below the K sequence strikes parallel to the seismic profile and dips NW and was produced within the context of the pre-lower Eocene-post-Cretaceous extension. The large half graben filled with sediments of the E₁ sequence is bounded by a master fault (to the left) which was inactive during the deposition of the other synrift E₂ and E₃ units. Systems of synthetic and antithetic normal faults related to the master fault involve the basement. The divergence of the half graben seismic reflectors indicates a balance between the rate of faulting and the rate of sedimentation. This plate also illustrates the western part of the Salaverry-Trujillo High where the M₂ and M₃ units filled submarine canyons. The base of the sequence M₂ is a profound canyon excavated into the M₁, E-O and E₃ units. The eastern part of the seismic profile was emerged during the P sequence deposition. The master fault was reactivated during the late Pliocene extension. Two systems of normal faults with shallow detachment surfaces offset the E₂ to P units.

TWT (sec.)



L E G E N D

S E Q U E N C E A G E

Q	Quaternary
P	Upper Miocene - Pliocene
M3	Upper Miocene
M2	Middle - Lower Miocene
M1	Lower Miocene
E-O	Uppermost middle Eocene to Oligocene
E3	Middle Eocene
E2	Middle Eocene
E1	Middle Eocene
E ₀	Lower ? - Middle Eocene
K	Cretaceous ?
PK	Pre-Cretaceous Basement

Normal fault

Base of submarine canyon

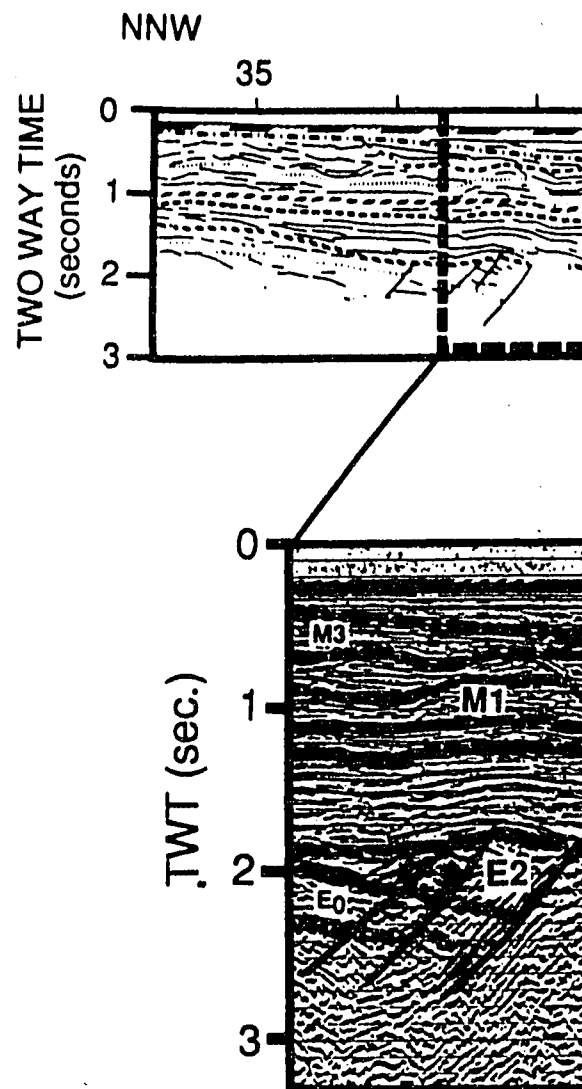


PLATE 5. CLOSE UP OF TH.
At the center a half graben of whereas the master fault of tl sequence was inactive during onlap the folded top of the ur middle Eocene; the small ar inversion produced by this con M3, and P; the base of the M: M1 and E-O units.

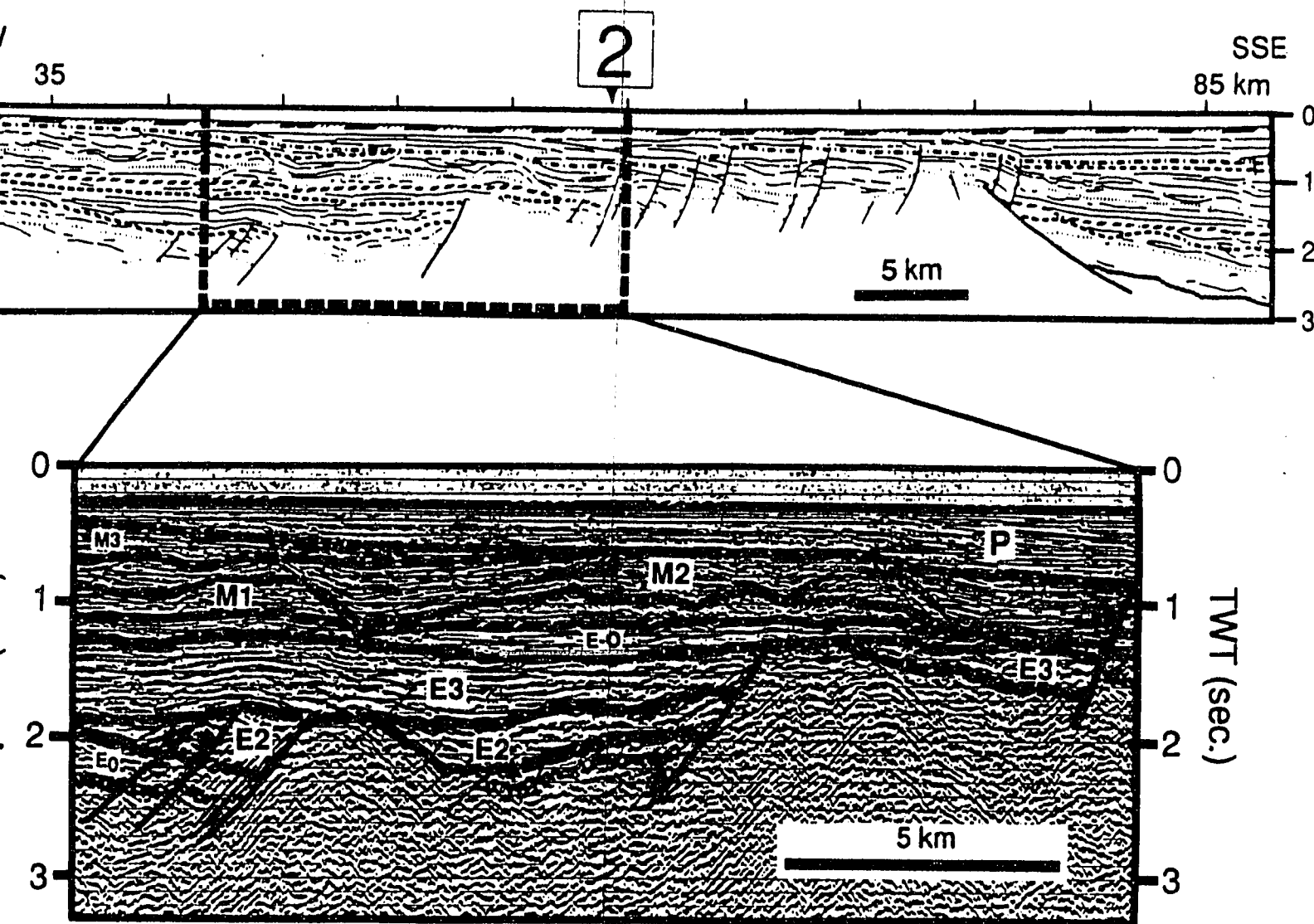
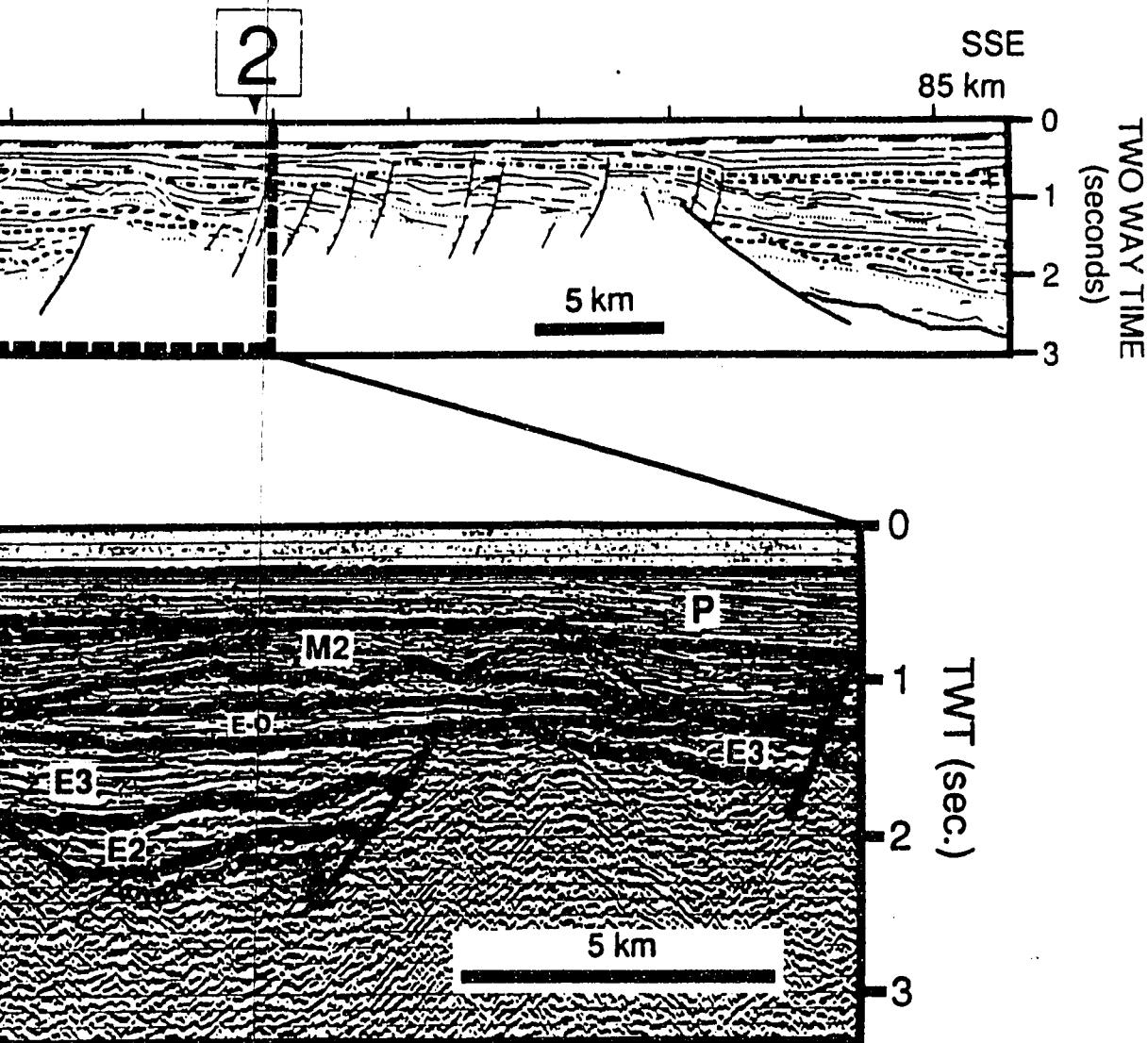
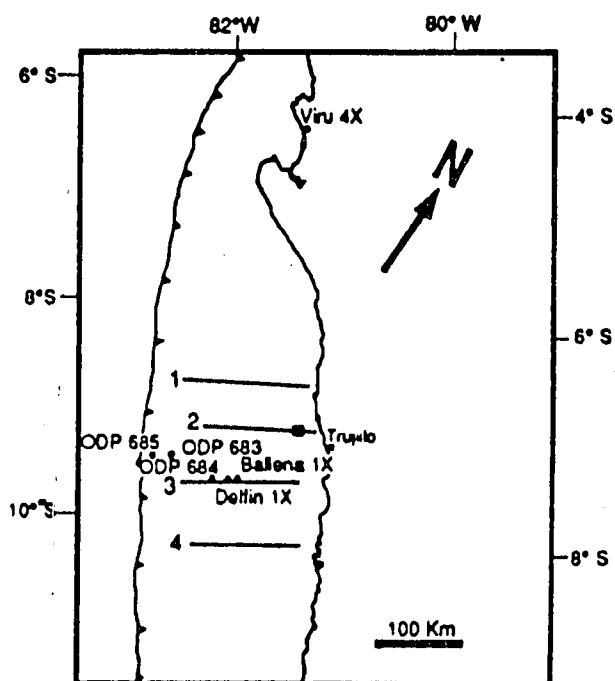


FIGURE 5. CLOSE UP OF THE SEISMIC PROFILE LINE DRAWING B (PANEL 2), TRUJILLO BASIN
 In the center a half graben of the E2 sequence shares the master fault with an overlying E3 half graben. To the left, the master fault of the adjacent half graben (at the left) also filled with sediments of the E2 sequence was inactive during the deposition of the E3 unit. At the center, reflectors of the E3 unit on the folded top of the underlying E2 sequence, this relationship dates the second compression as the Eocene; the small anticline of the E2 unit adjacent to the master fault suggests a minor compression produced by this compressive event. Submarine canyon systems are present in sequences M2, M1, and P; the base of the M2 sequence is a prominent submarine canyon which locally has eroded the E2 and E-O units.



SEISMIC PROFILE LINE DRAWING B (PANEL 2), TRUJILLO BASIN

The E2 sequence shares the master fault with an overlying E3 half graben. The adjacent half graben (at the left) also filled with sediments of the E2 deposition of the E3 unit. At the center, reflectors of the E3 unit within the E2 sequence, this relationship dates the second compression as post-E3. The presence of the E2 unit adjacent to the master fault suggests a compressive event. Submarine canyon systems are present in sequences M2, and P. Sequence P is a prominent submarine canyon which locally has eroded the



LEGEND **SEQUENCE AGE**

Q	Quaternary
P	Upper Miocene - Pliocene
M 3	Upper Miocene
M 2	Middle - Lower Miocene
M 1	Lower Miocene
E-O	Uppermost middle Eocene to Oligocene
E 3	Middle Eocene
E 2	Middle Eocene
E 1	Middle Eocene
E ₀	Lower ? - Middle Eocene
K	Cretaceous ?
PK	Pre-Cretaceous Basement

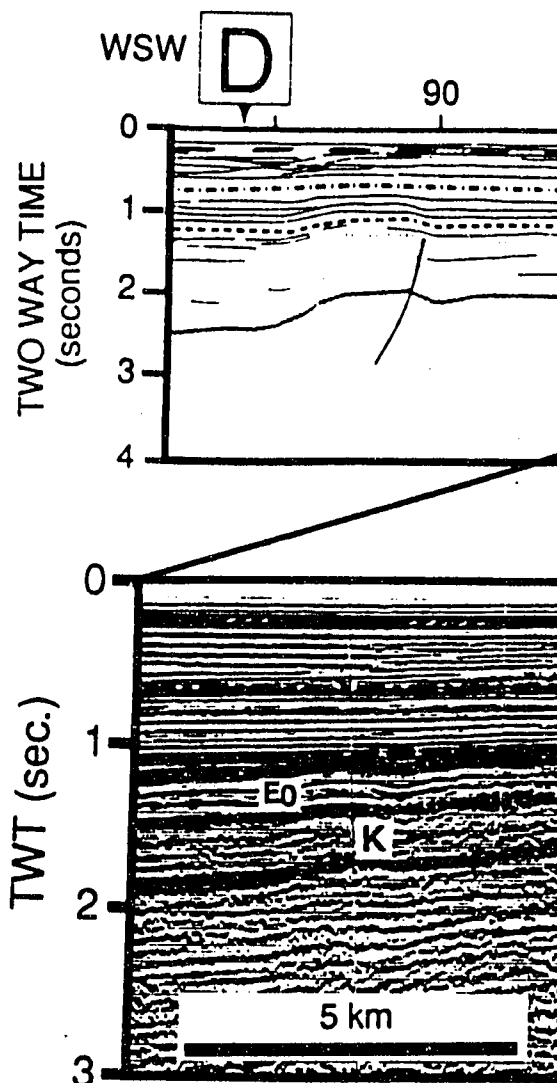
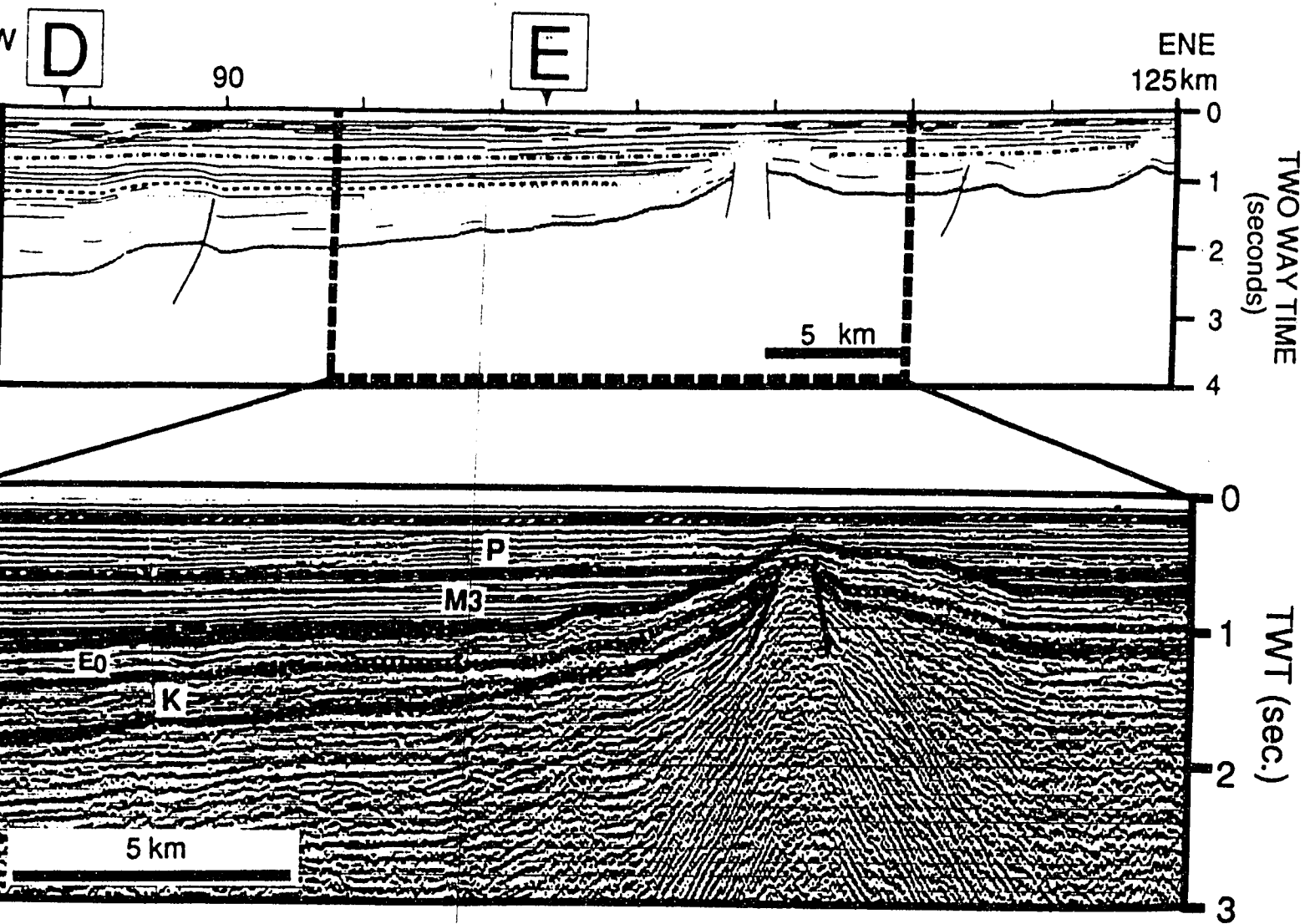
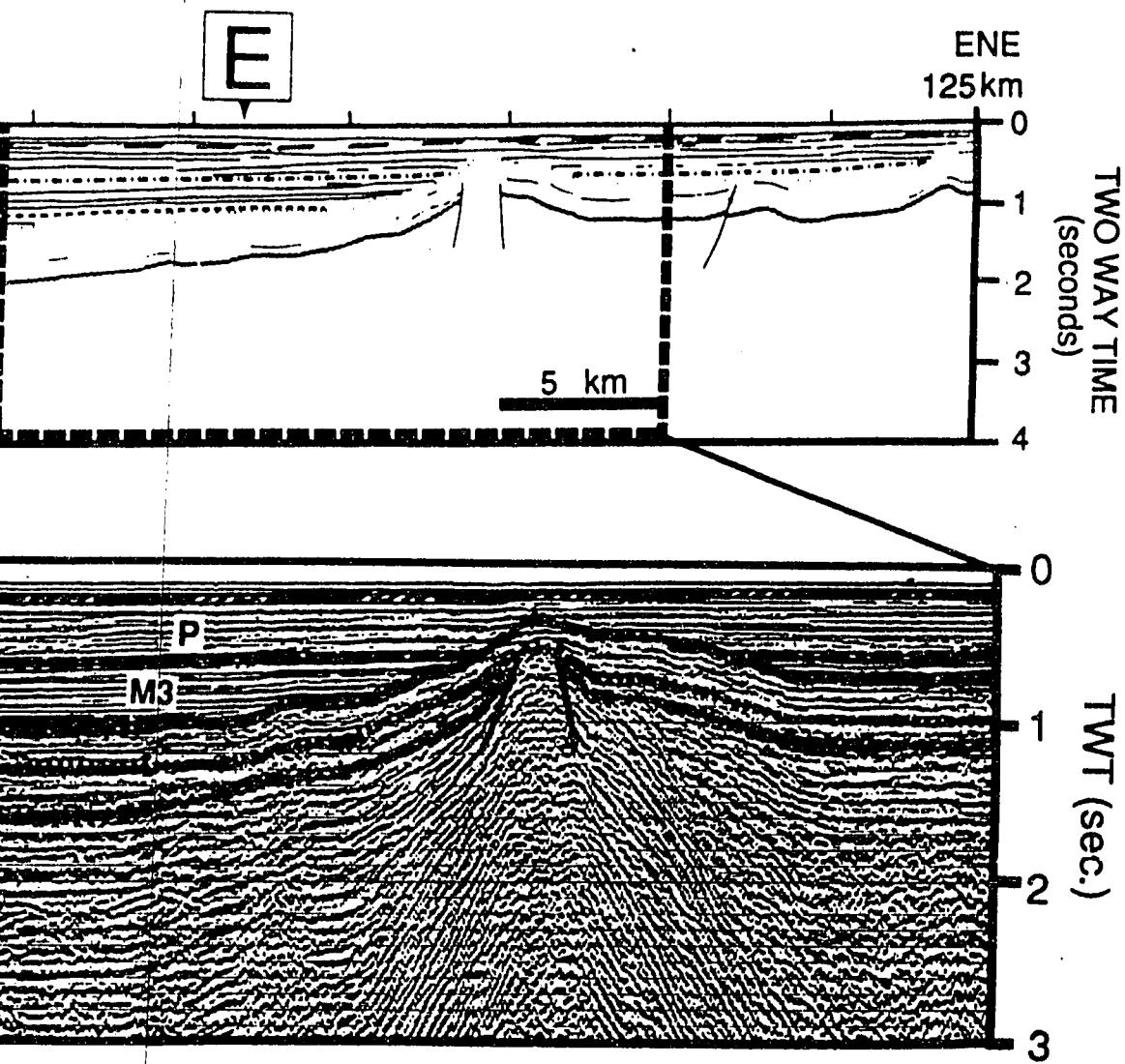


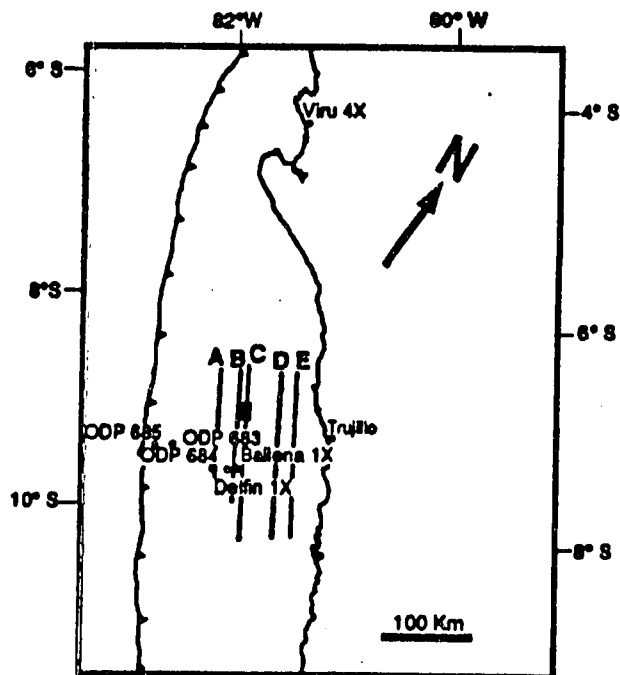
PLATE 6. CLOSE UP OF THE SE
Sequences K and E₀ were intrude
of shelfal M3 and P units onlap the



6. CLOSE UP OF THE SEISMIC PROFILE LINE DRAWING 2 (PANEL 1), SALAVERRY BASIN
 es K and E0 were intruded by an igneous body which created a local uplift. Flat laying reflectors
 l M3 and P units onlap the top of the uplifted E0 sequence.



SEISMIC PROFILE LINE DRAWING 2 (PANEL 1), SALAVERRY BASIN
 ed by an igneous body which created a local uplift. Flat laying reflectors
 top of the uplifted E₀ sequence.



L E G E N D

S E Q U E N C E A G E

Q	Quaternary
P	Upper Miocene - Pliocene
M 3	Upper Miocene
M 2	Middle - Lower Miocene
M 1	Lower Miocene
E-O	Uppermost middle Eocene to Oligocene
E 3	Middle Eocene
E 2	Middle Eocene
E 1	Middle Eocene
E ₀	Lower ? - Middle Eocene
K	Cretaceous ?
PK	Pre-Cretaceous Basement

Normal fault

Reverse fault

Base of submarine canyon

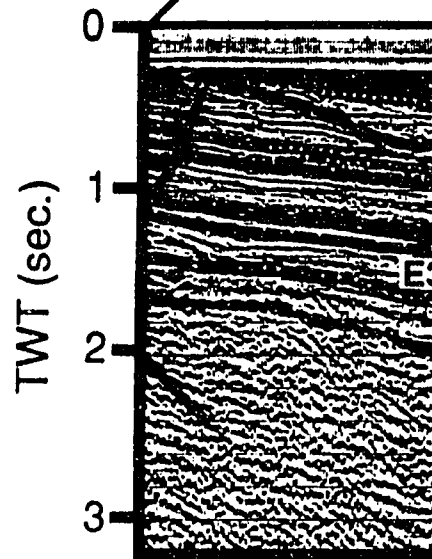
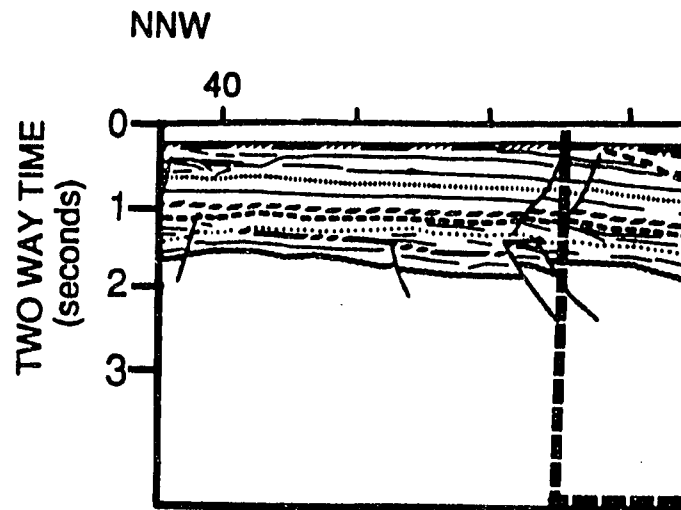


PLATE 7. CLOSE UP OF THE
The sequence E₀ which underlies the second middle Eocene (E2) and P sequences are characterized by

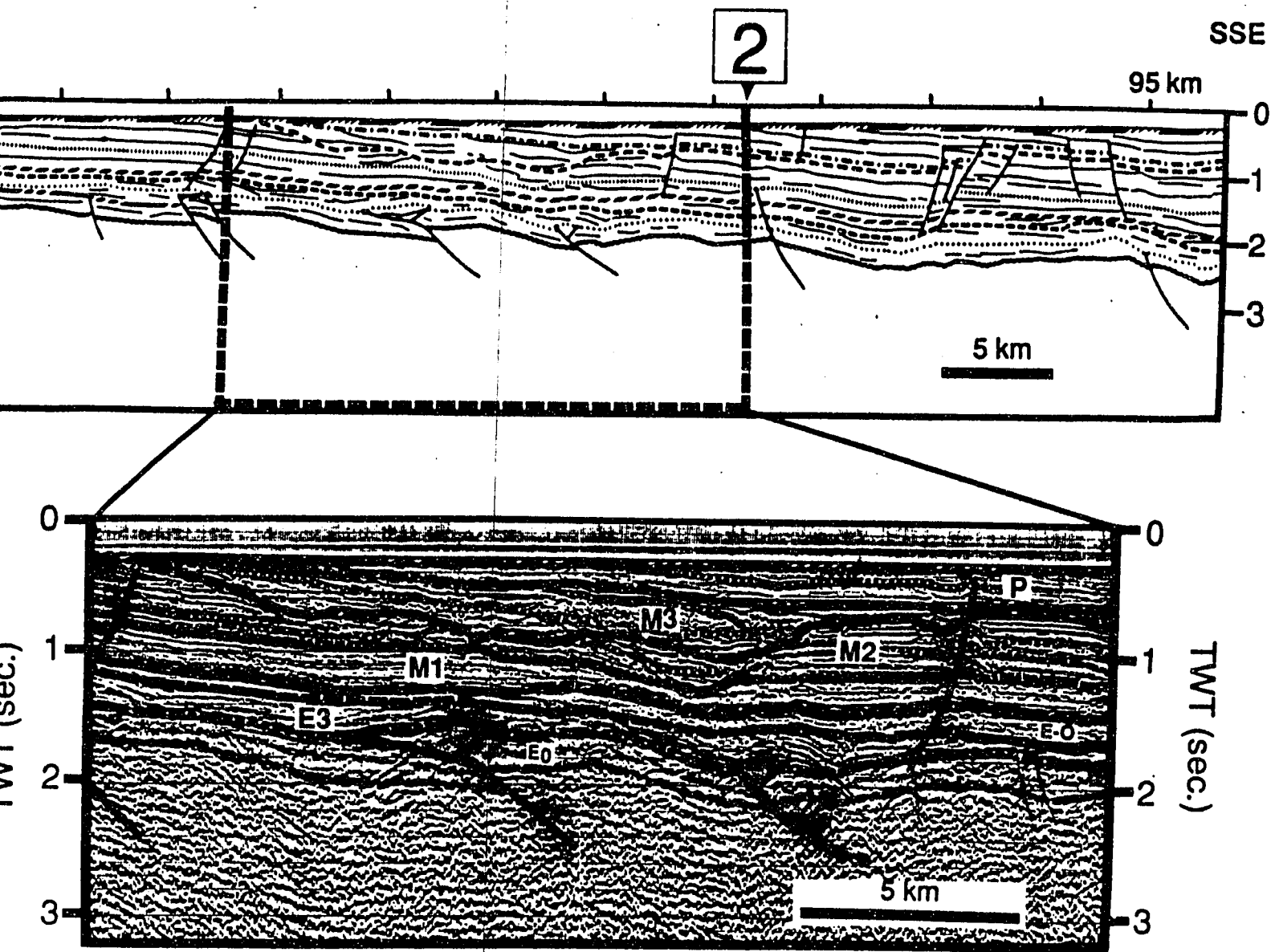
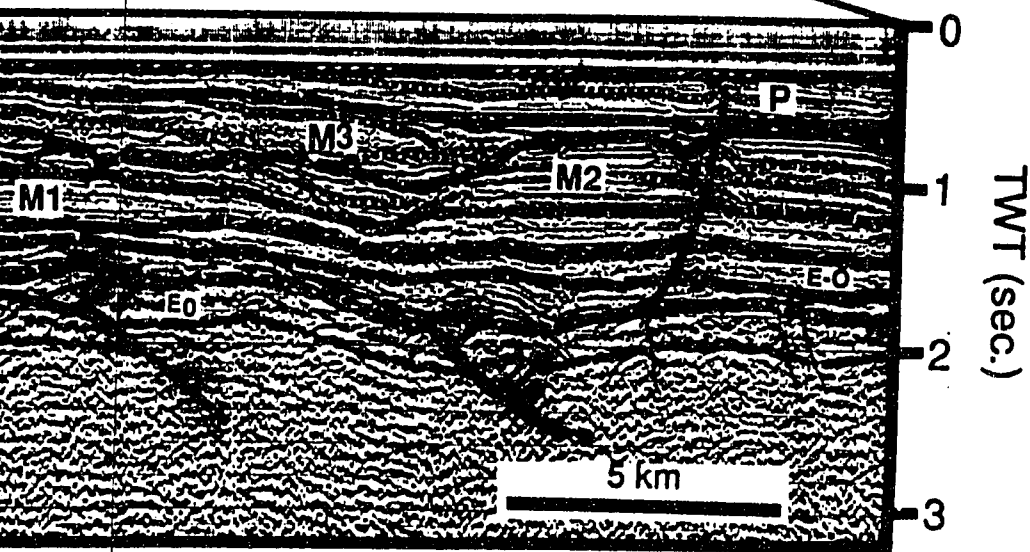
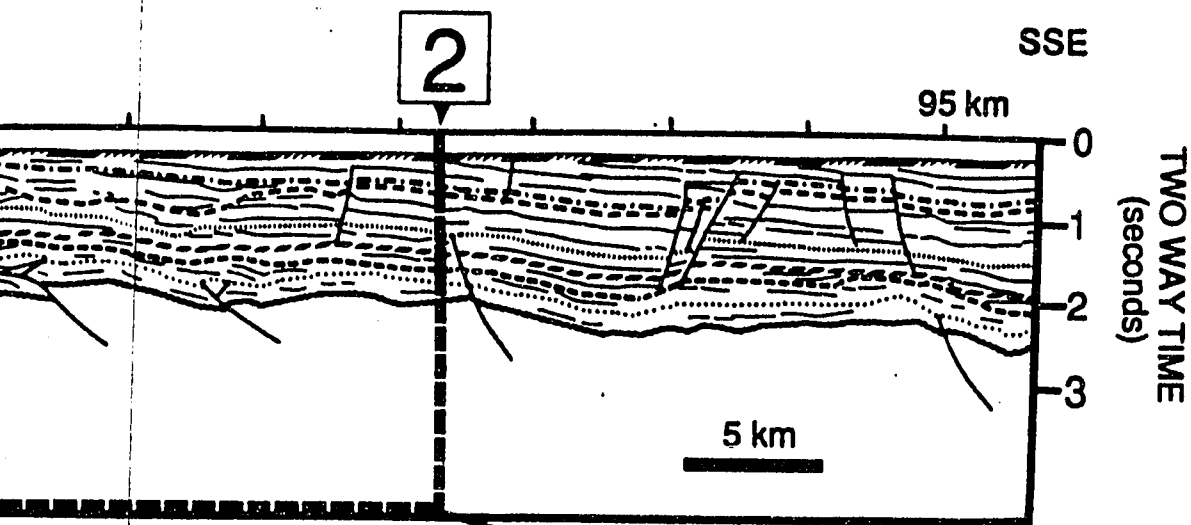
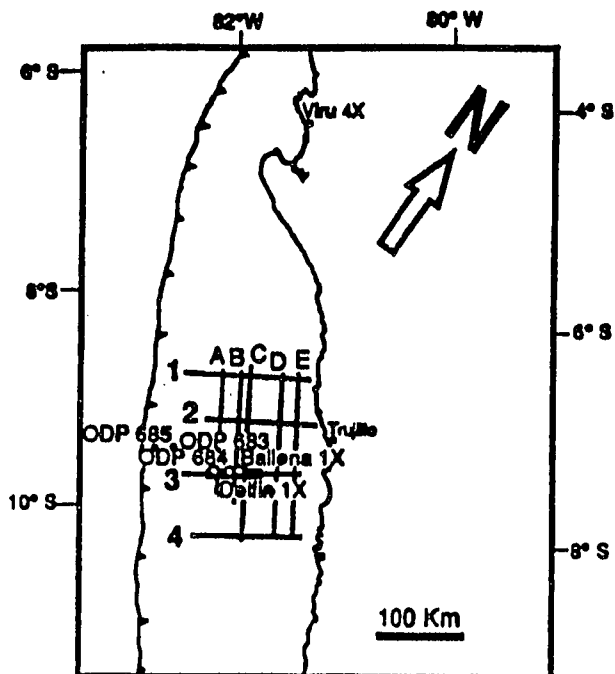


FIGURE 7. CLOSE UP OF THE SEISMIC PROFILE LINE DRAWING C. (PANEL 2), TRUJILLO BASIN
 The sequence E₀ which unconformably rests on Pre-Cretaceous basement was folded and thrust during the second middle Eocene compression. The submarine canyons filled with sediments of the M₃, M₂, and P sequences are characteristic of this area located west of the Salaverry-Trujillo High.



SEISMIC PROFILE LINE DRAWING C. (PANEL 2), TRUJILLO BASIN
 The profile shows a complex structure with folds and faults. The layers are labeled M1, M2, M3, E0, and P. The profile is oriented SSE. The vertical axis represents Two Way Time in seconds, and the horizontal axis represents distance in kilometers.



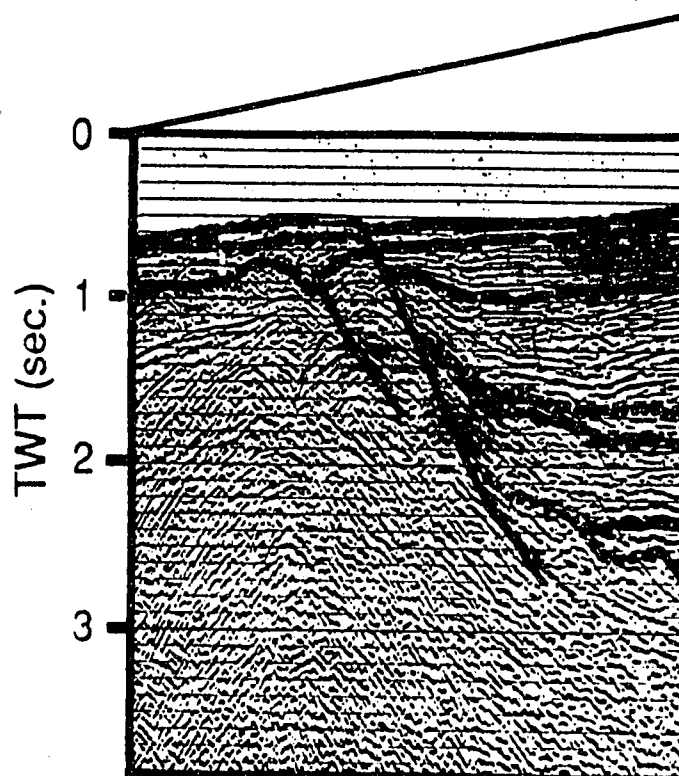
L E G E N D

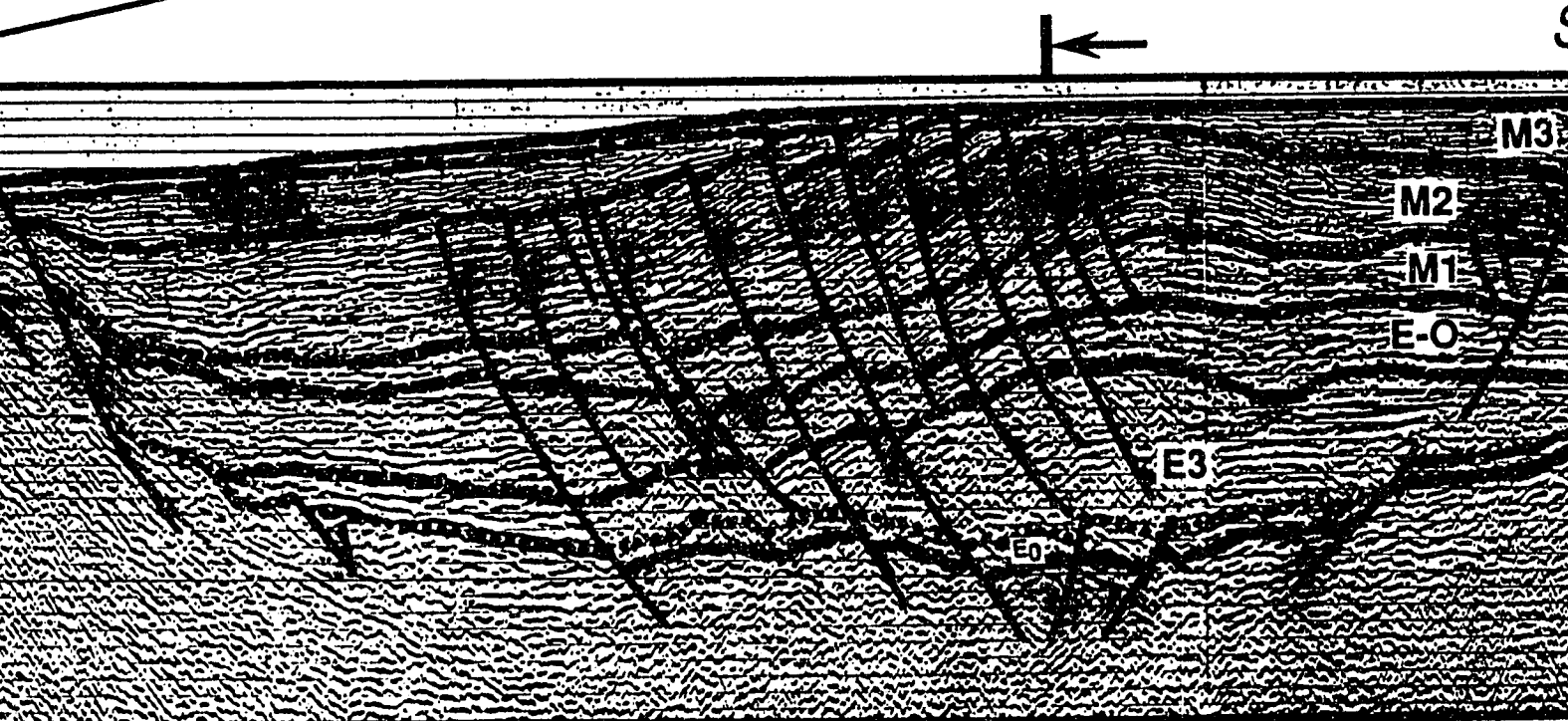
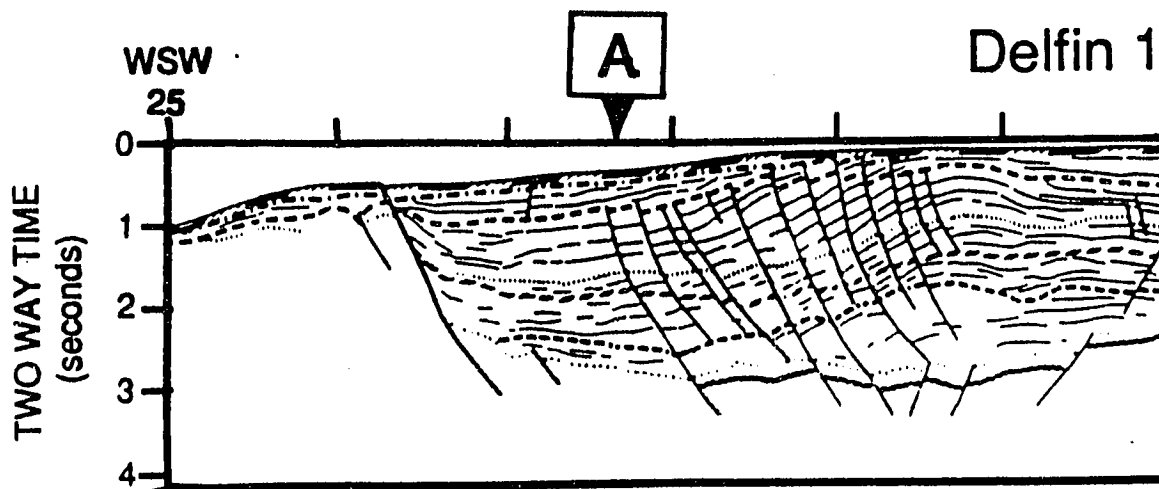
S E Q U E N C E A G E

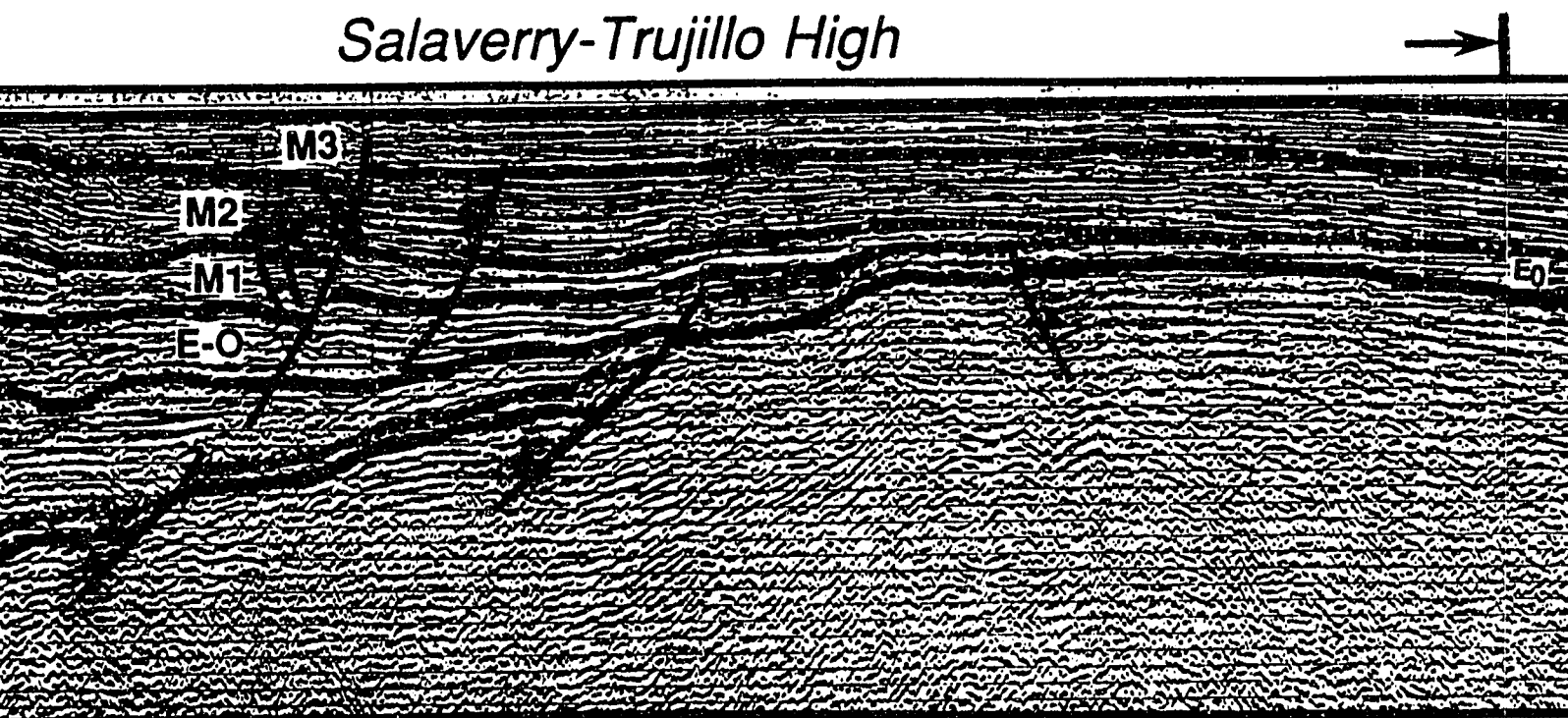
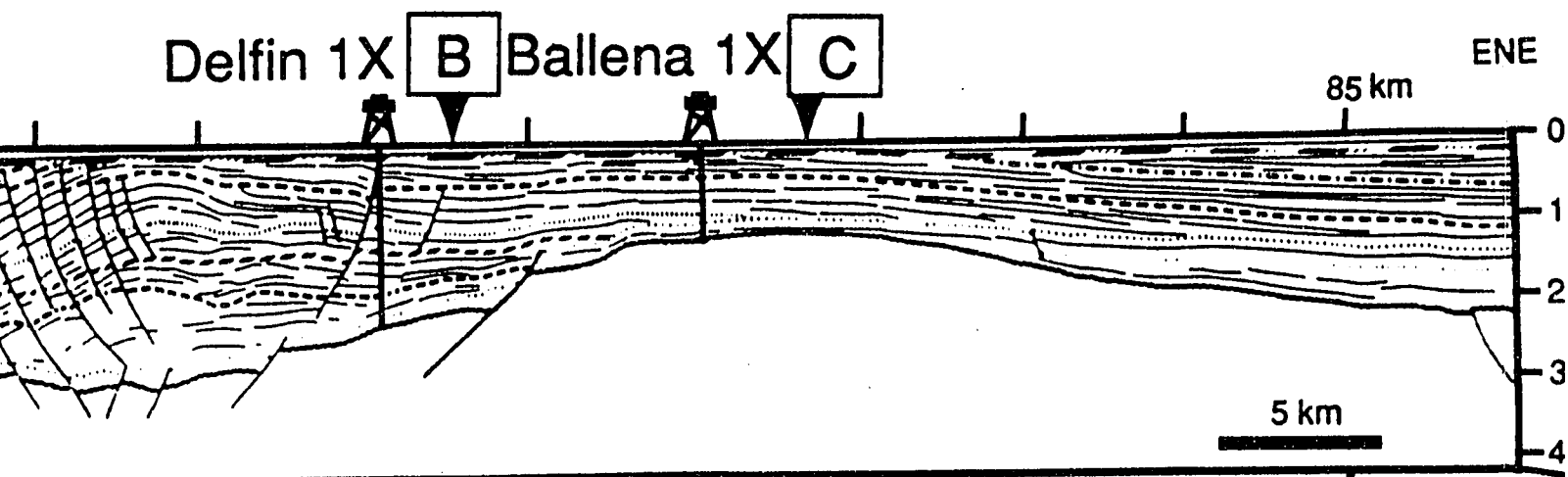
Q	Quaternary
P	Upper Miocene - Pliocene
M 3	Upper Miocene
M 2	Middle - Lower Miocene
M 1	Lower Miocene
E-O	Uppermost middle Eocene to Oligocene
E 3	Middle Eocene
E 2	Middle Eocene
E 1	Middle Eocene
E ₀	Lower ? - Middle Eocene
K	Cretaceous ?
PK	Pre-Cretaceous Basement

Normal fault

Reverse fault

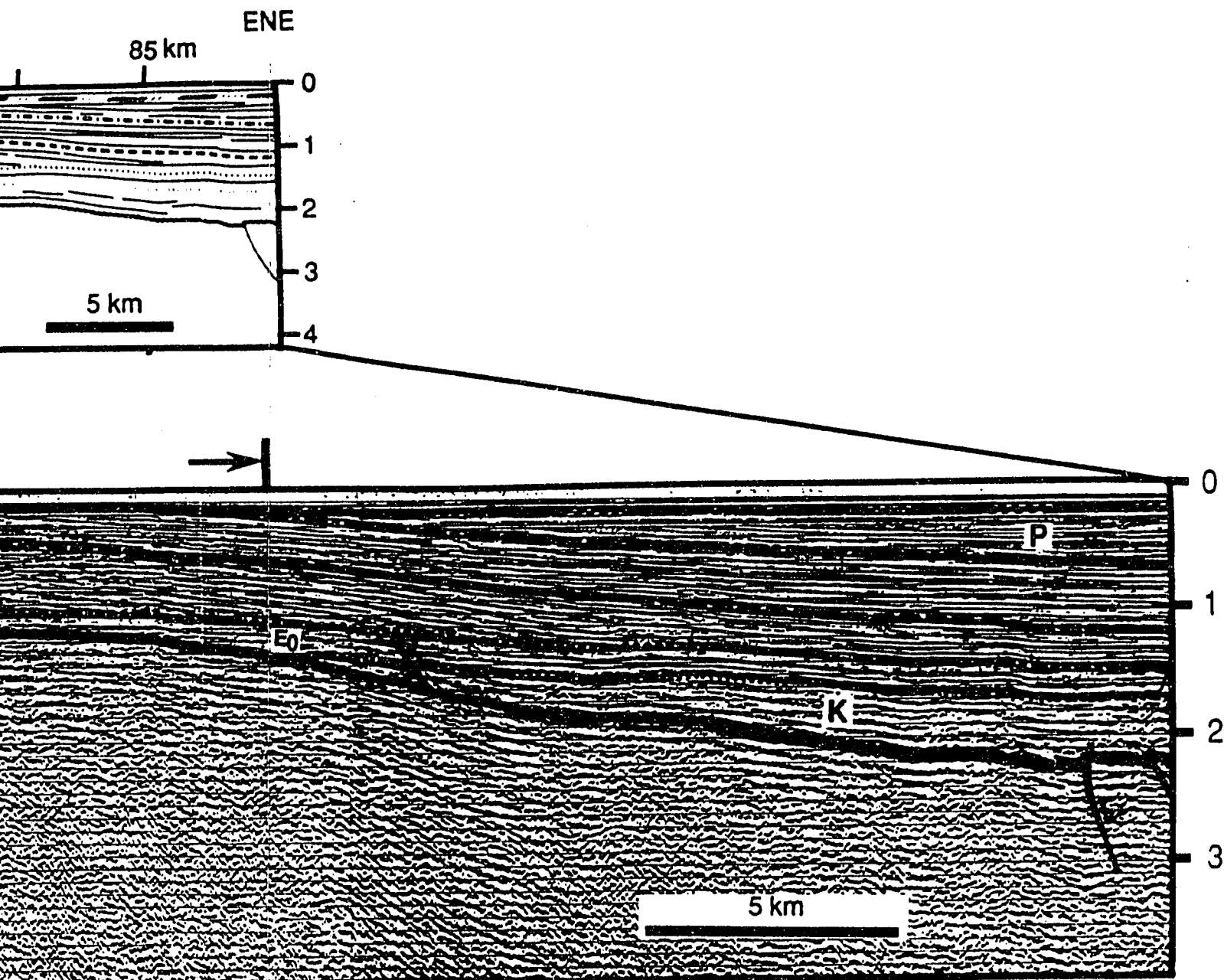




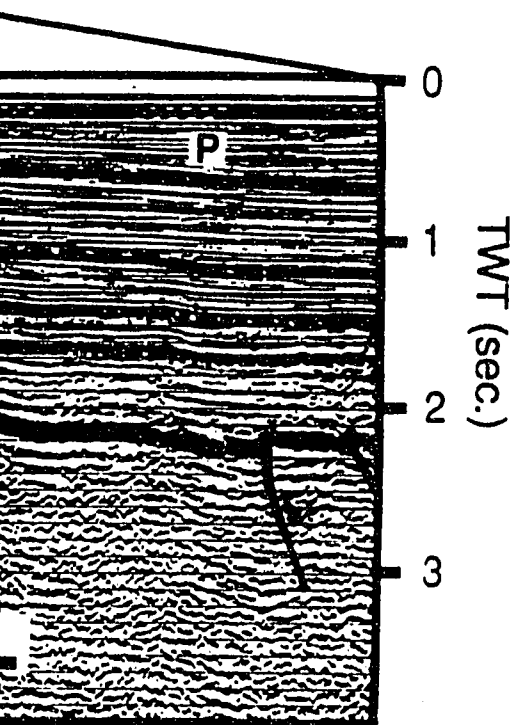


1

2



**PLATE 8. CLOSE UP OF THE SEISMIC PROFILE LINE D
(PANEL 1), SALAVERRY-TRUJILLO BASINS**

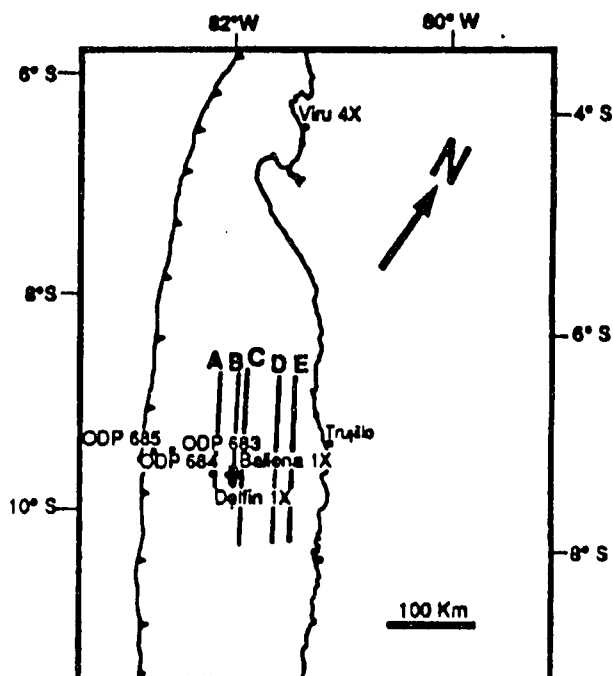


The sequence K thins toward the Salaverry-Trujillo is offset by two thrusts developed during Paleocene? compression. At the Salaverry-Trujillo E0 unit is offset by the master normal fault of a filled with sediments of the E3 sequence. The c sequences E-O and M1 is restricted to the T (western part of the Salaverry-Trujillo High). stepping onlap toward the ENE displayed by the M2 units illustrates the transgressive nature sequences. The uplift of the Salaverry-Trujillo tilted the M2 sequence portion located east of Sequences E-O, M1 and M2 are bounded to the basement-involved syn-sedimentary normal fault active until the deposition of the M2 sequence reactivated during the Recent. The anticline located western side of the Salaverry-Trujillo High, where sediments of the E3, E-O, M1, M2 and M3 sequences the best examples of the inversion produced during upper-middle to late Miocene compression. Some of the post-folding (late Miocene-Pliocene) is a fault system that offset E3, E-O, M1, M2 and M3 from the basement. The thinning of the M3 unit Salaverry-Trujillo High indicates that the uplift was active during the deposition of this sequence (Miocene). The absence of the P unit at the high symmetric distribution (to both sides of the high) that the Salaverry-Trujillo High was emerged during sequence deposition (late Miocene-Pliocene time).

**PLATE 8. CLOSE UP OF THE SEISMIC PROFILE LINE DRAWING 3
(PANEL 1), SALAVERRY-TRUJILLO BASINS**

The sequence K thins toward the Salaverry-Trujillo High and is offset by two thrusts developed during the first Paleocene? compression. At the Salaverry-Trujillo High the E₀ unit is offset by the master normal fault of a half graben filled with sediments of the E₃ sequence. The occurrence of sequences E-O and M₁ is restricted to the Trujillo Basin (western part of the Salaverry-Trujillo High). The back-stepping onlap toward the ENE displayed by the E-O, M₁ and M₂ units illustrates the transgressive nature of these sequences. The uplift of the Salaverry-Trujillo High has tilted the M₂ sequence portion located east of the high. Sequences E-O, M₁ and M₂ are bounded to the left by a basement-involved syn-sedimentary normal fault which was active until the deposition of the M₂ sequence, and was reactivated during the Recent. The anticline located at the western side of the Salaverry-Trujillo High, which involves sediments of the E₃, E-O, M₁, M₂ and M₃ sequences, is one of the best examples of the inversion produced during the third upper-middle to late Miocene compression. Some of the faults of the post-folding (late Miocene-Pliocene) listric normal fault system that offset E₃, E-O, M₁, M₂ and M₃ units involve the basement. The thinning of the M₃ unit toward the Salaverry-Trujillo High indicates that the uplifting process was active during the deposition of this sequence (the late Miocene). The absence of the P unit at the high and its symmetric distribution (to both sides of the high) indicates that the Salaverry-Trujillo High was emerged during the P sequence deposition (late Miocene-Pliocene time).

TWT (sec.)



LEGEND **SEQUENCE AGE**

Q	Quaternary
P	Upper Miocene - Pliocene
M 3	Upper Miocene
M 2	Middle - Lower Miocene
M 1	Lower Miocene
E-O	Uppermost middle Eocene to Oligocene
E 3	Middle Eocene
E 2	Middle Eocene
E 1	Middle Eocene
E ₀	Lower ? - Middle Eocene
K	Cretaceous ?
PK	Pre-Cretaceous Basement

Normal fault

Base of submarine canyon

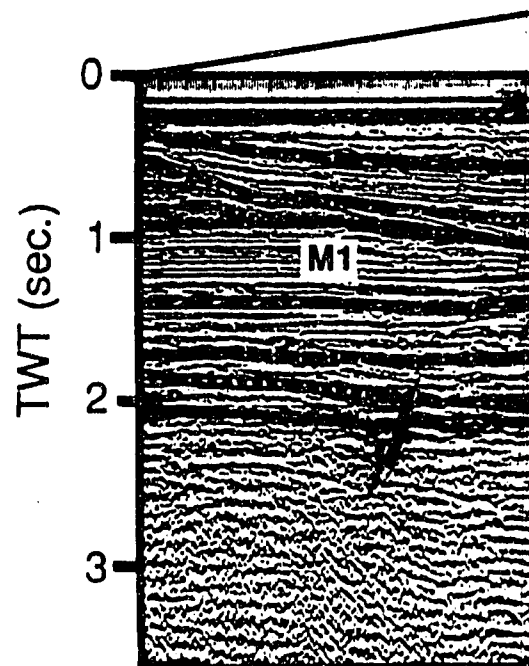
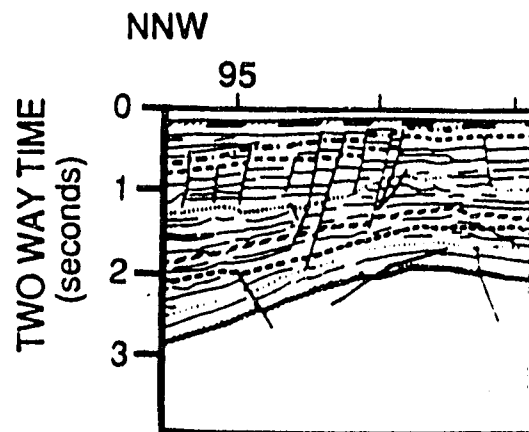


PLATE 9. CLOSE UP OF THE SE
 The sequence E₀ is offset by a n
 unit. This seismic profile is locate
 filled submarine canyons. The M1
 the middle-early Miocene.

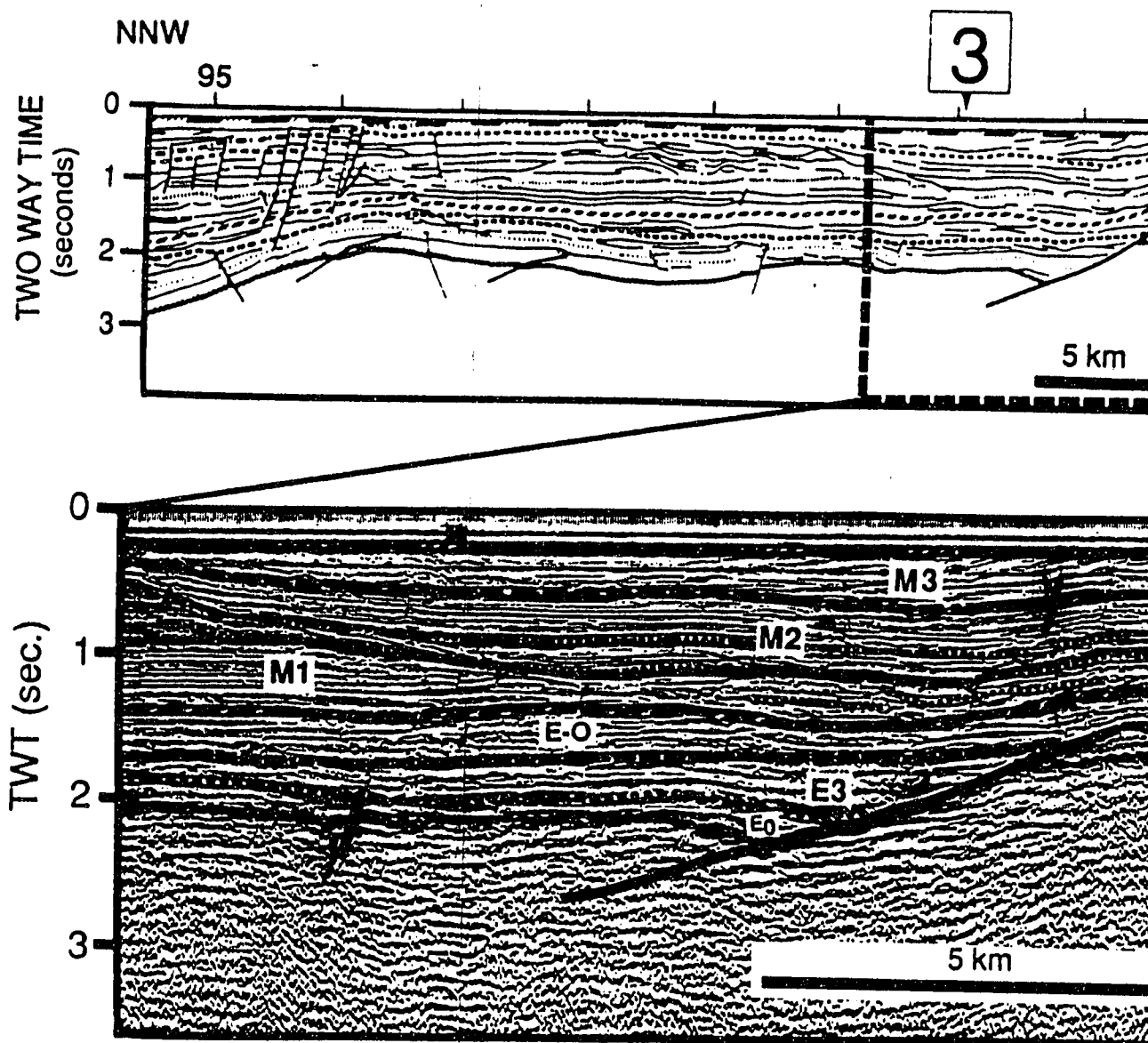


PLATE 9. CLOSE UP OF THE SEISMIC PROFILE LINE DRAWING B (PANEL 2), T
 The sequence E₀ is offset by a master normal fault of a half graben filled with sedi
 unit. This seismic profile is located west of the Salaverry-Trujillo High where the M
 filled submarine canyons. The M₁ unit was partially eroded by a prominent canyon
 the middle-early Miocene.

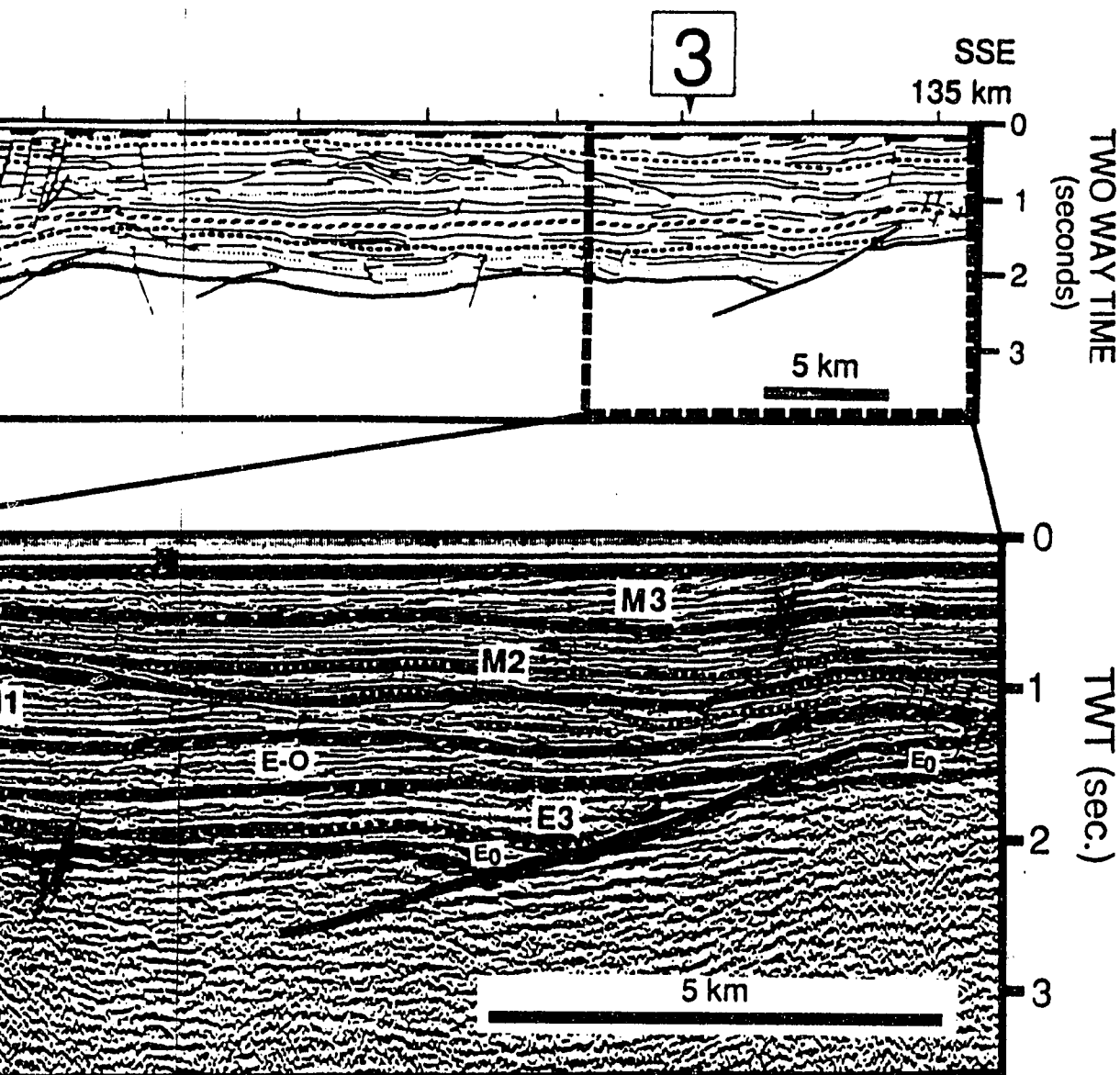
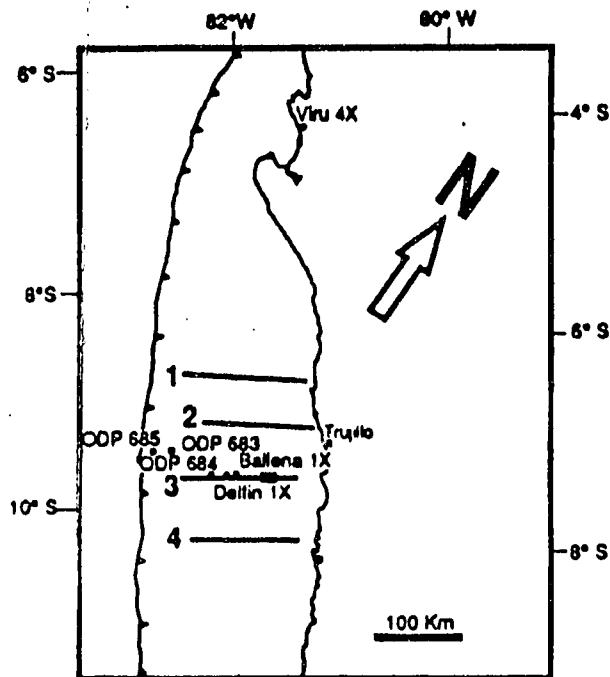


FIGURE 1. SEISMIC PROFILE LINE DRAWING B (PANEL 2), TRUJILLO BASIN
 The profile is offset by a master normal fault of a half graben filled with sediments of the E3
 profile is located west of the Salaverry-Trujillo High where the M2 and M3 units
 are present. The M1 unit was partially eroded by a prominent canyon excavated during
 the Eocene.



LEGEND **SEQUENCE AGE**

Q	Quaternary
P	Upper Miocene - Pliocene
M 3	Upper Miocene
M 2	Middle - Lower Miocene
M 1	Lower Miocene
E-O	Uppermost middle Eocene to Oligocene
E 3	Middle Eocene
E 2	Middle Eocene
E 1	Middle Eocene
E ₀	Lower ? - Middle Eocene
K	Cretaceous ?
PK	Pre-Cretaceous Basement

Reverse fault

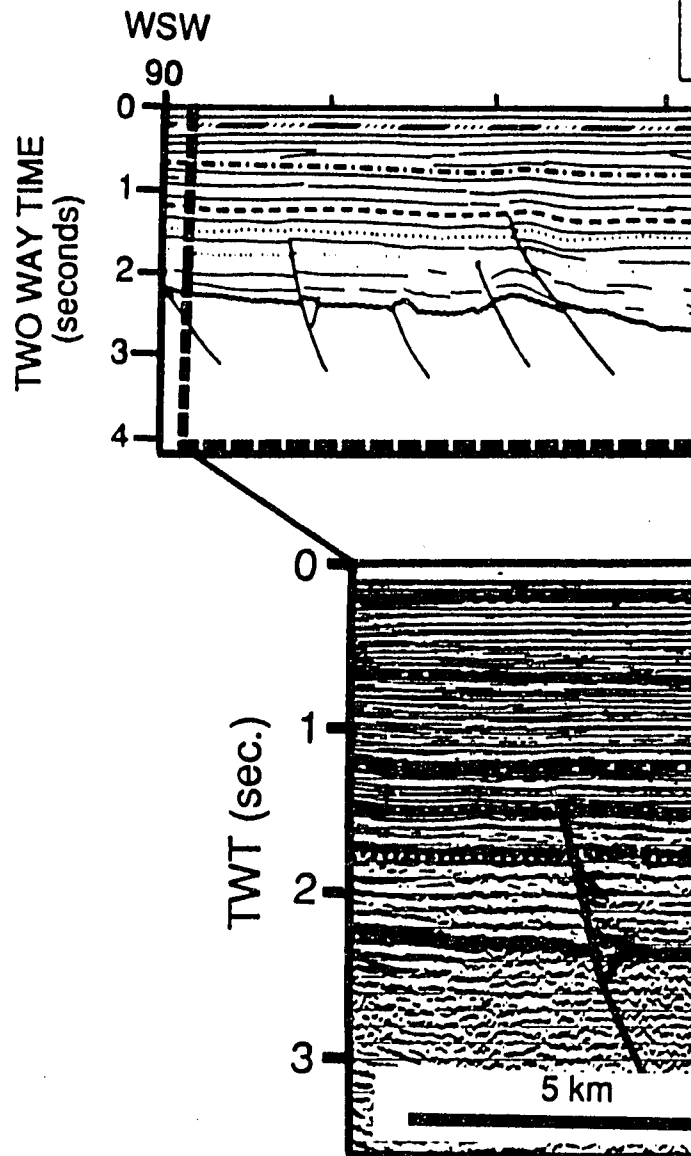


PLATE 10. CLOSE UP OF THE
The thrust and anticline that involve correspond to the first Paleocene sequences K, E₀, M2 and M3 (to compression).

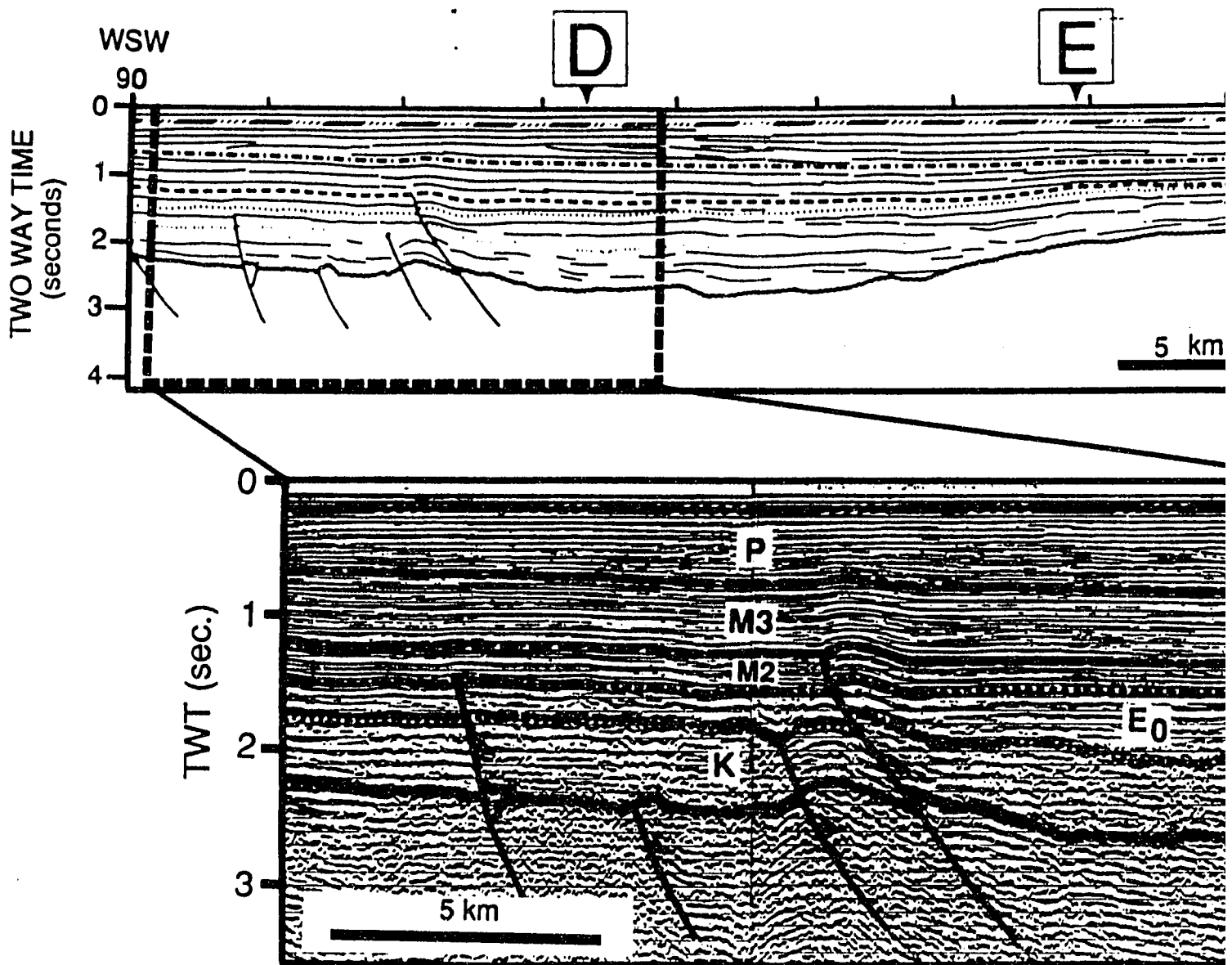
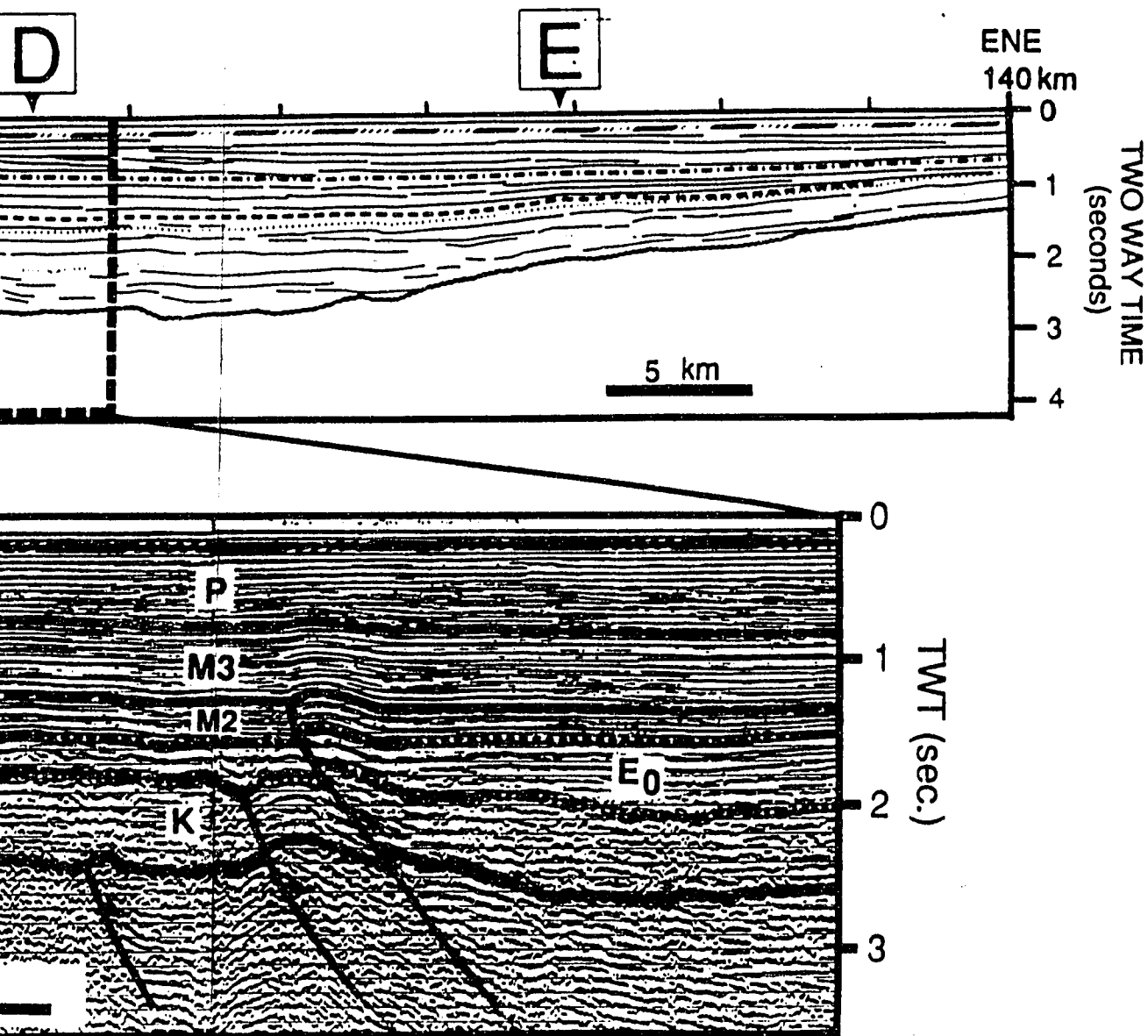
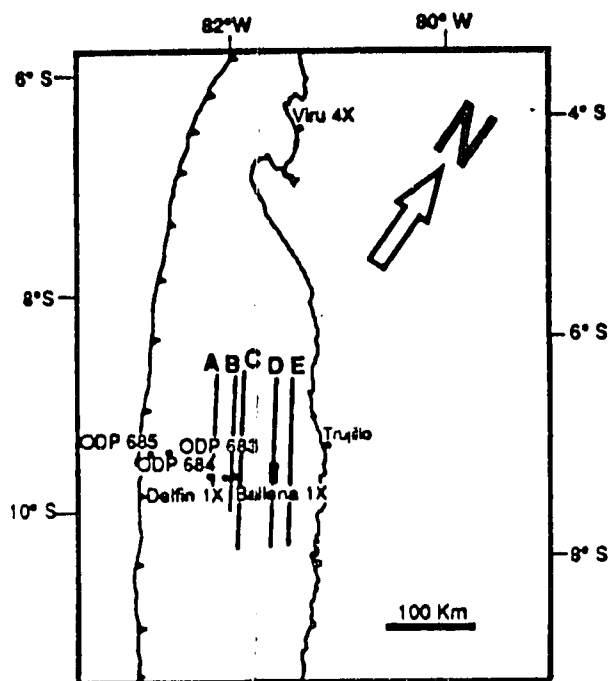


PLATE 10. CLOSE UP OF THE SEISMIC PROFILE LINE DRAWING 3 (PANEL1) SA
 The thrust and anticline that involves the sequence K and the base of the E₀ unit (correspond to the first Paleocene? compressive event; whereas the thrust and an sequences K, E₀, M2 and M3 (to the right) were developed during the third upper-mid compression.



SEISMIC PROFILE LINE DRAWING 3 (PANEL1) SALAVERRY BASIN
 involves the sequence K and the base of the E₀ unit (at the center) may
 be? compressive event; whereas the thrust and anticline that affects
 to the right) were developed during the third upper-middle to late Miocene



LEGEND **SEQUENCE AGE**

Q	Quaternary
P	Upper Miocene - Pliocene
M 3	Upper Miocene
M 2	Middle - Lower Miocene
M 1	Lower Miocene
E-O	Uppermost middle Eocene to Oligocene
E 3	Middle Eocene
E 2	Middle Eocene
E 1	Middle Eocene
E ₀	Lower ? - Middle Eocene
K	Cretaceous ?
PK	Pre-Cretaceous Basement

Reverse fault

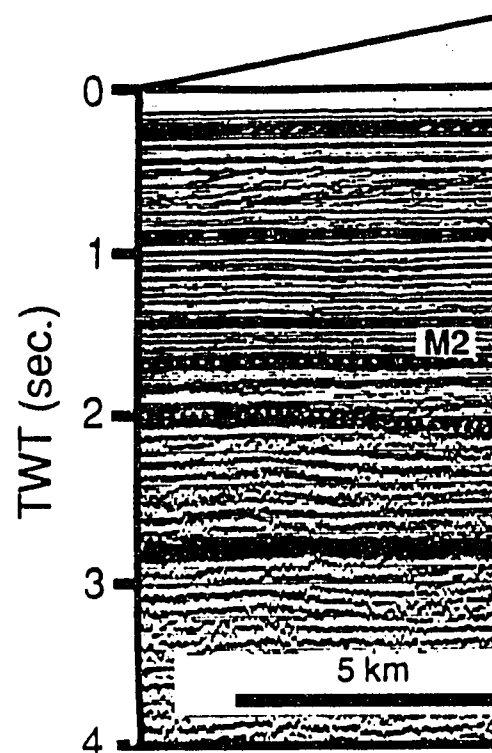
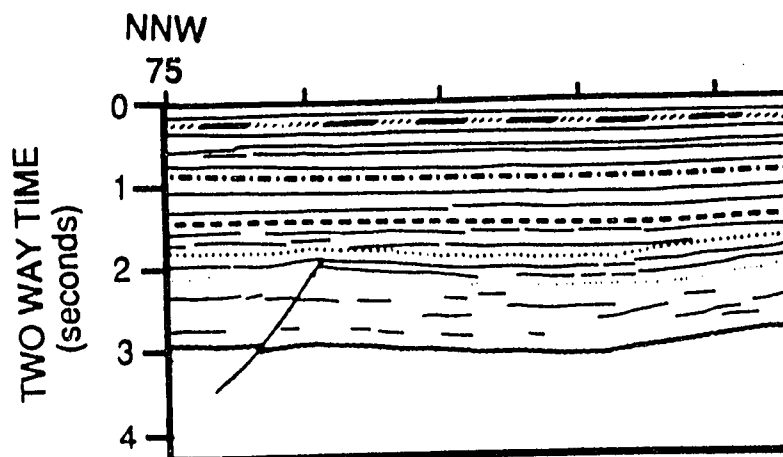


PLATE 11 CLOSE UP OF THE S
 The base of the K sequence is compression. The sequence P s developed in the interior basin Miocene-Pliocene.

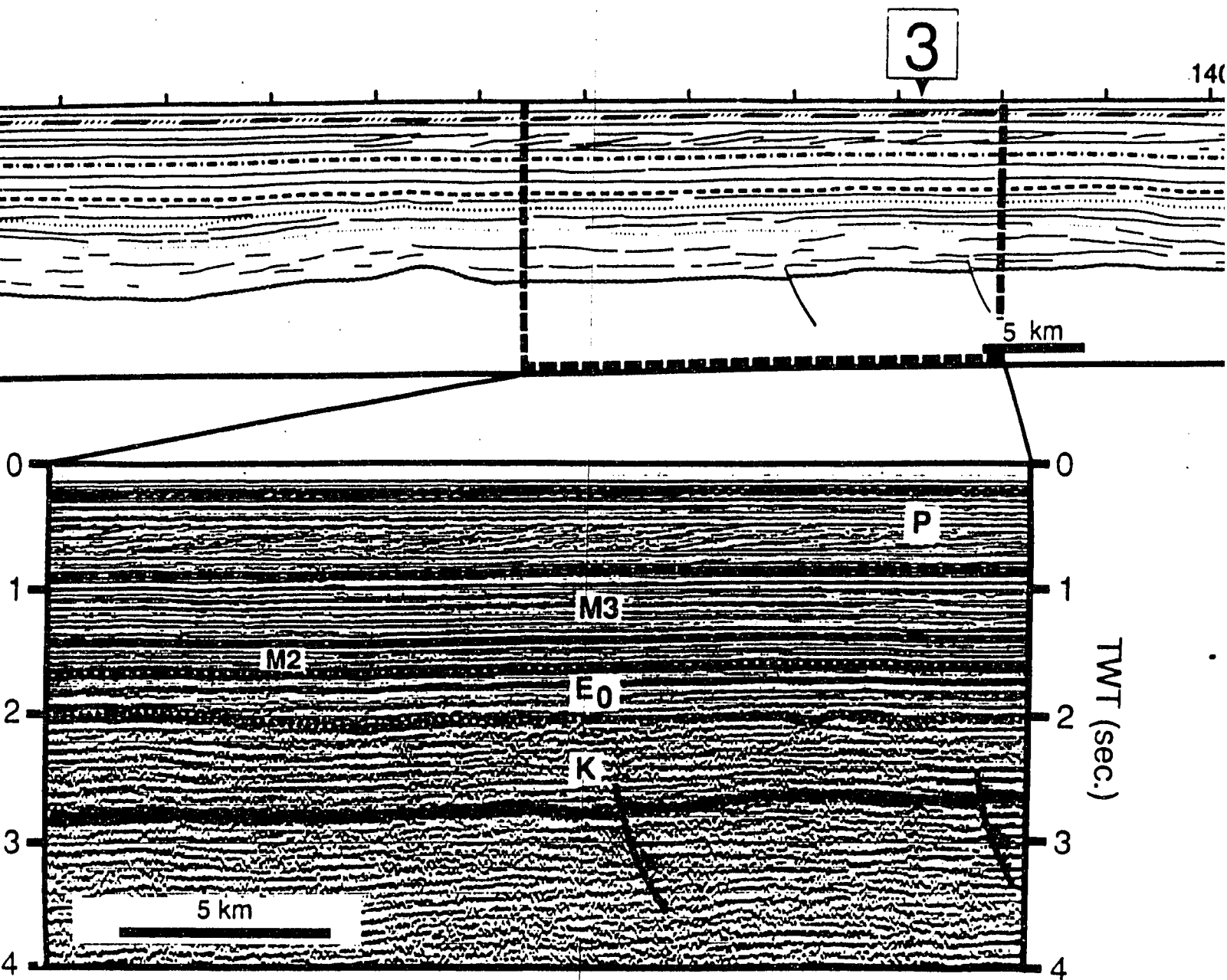
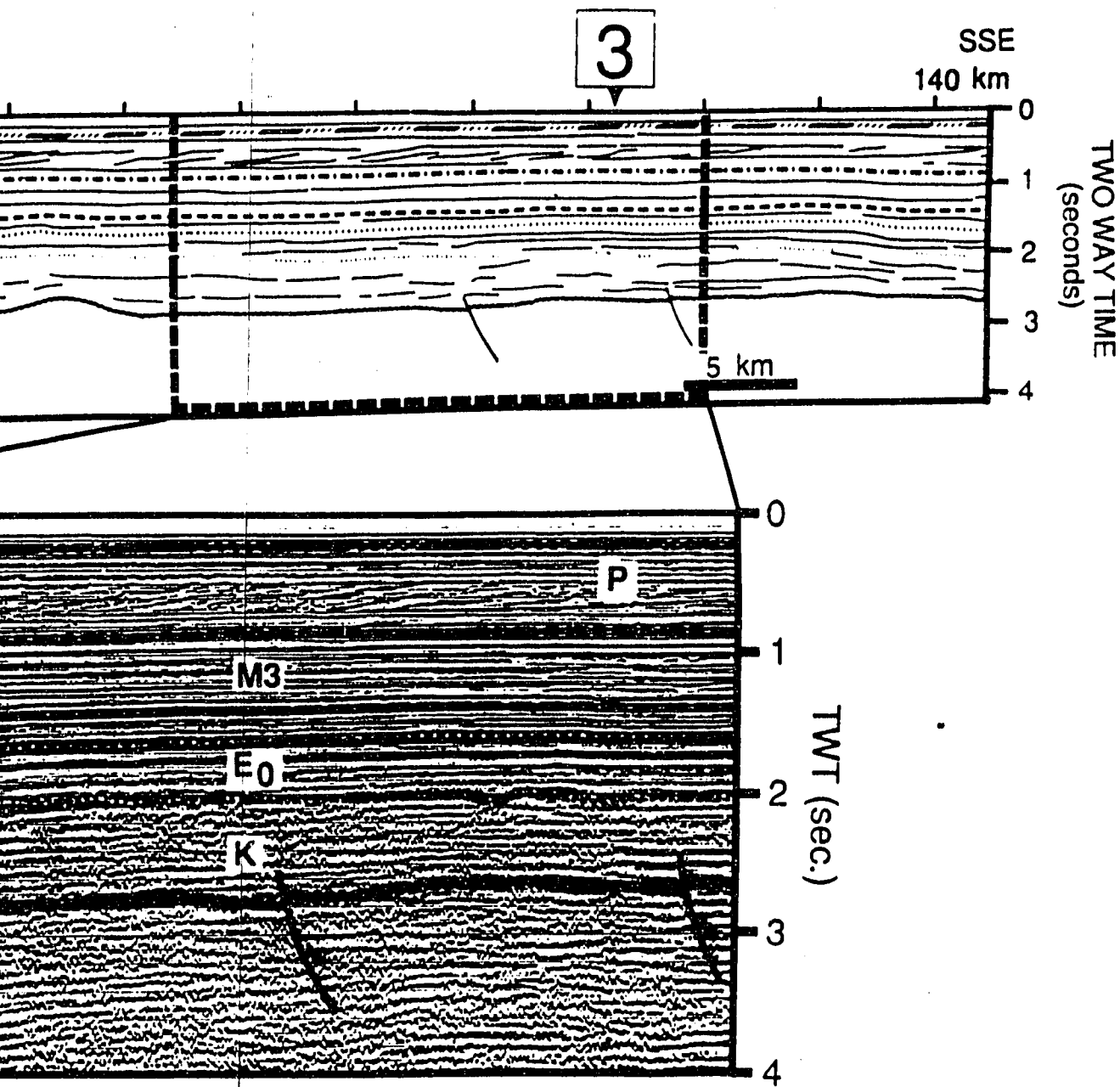
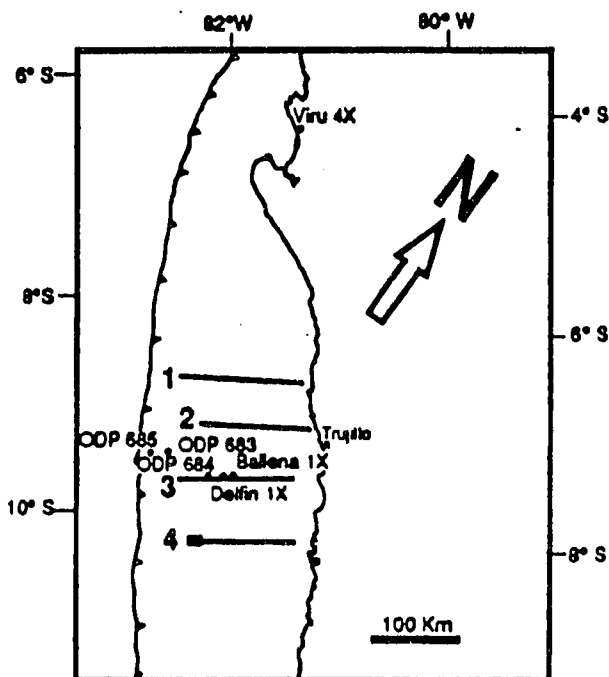


FIGURE 11 CLOSE UP OF THE SEISMIC PROFILE LINE DRAWING D (PANEL 2), SALAVERRY BASIN
 The base of the K sequence is offset by a thrust probably developed during the first Paleocene? session. The sequence P shows northerly prograding clinoforms which suggest a deltaic system developed in the interior basin (located east of the emerged Salaverry-Trujillo High) during the late Paleocene.



SEISMIC PROFILE LINE DRAWING D (PANEL 2), SALAVERRY BASIN
 offset by a thrust probably developed during the first Paleocene?
 is northerly prograding clinoforms which suggest a deltaic system
 located east of the emerged Salaverry-Trujillo High) during the late



L E G E N D

S E Q U E N C E A G E

Q	Quaternary
P	Upper Miocene - Pliocene
M 3	Upper Miocene
M 2	Middle - Lower Miocene
M 1	Lower Miocene
E-O	Uppermost middle Eocene to Oligocene
E 3	Middle Eocene
E 2	Middle Eocene
E 1	Middle Eocene
E ₀	Lower ? - Middle Eocene
K	Cretaceous ?
PK	Pre-Cretaceous Basement

Normal fault

Reverse fault

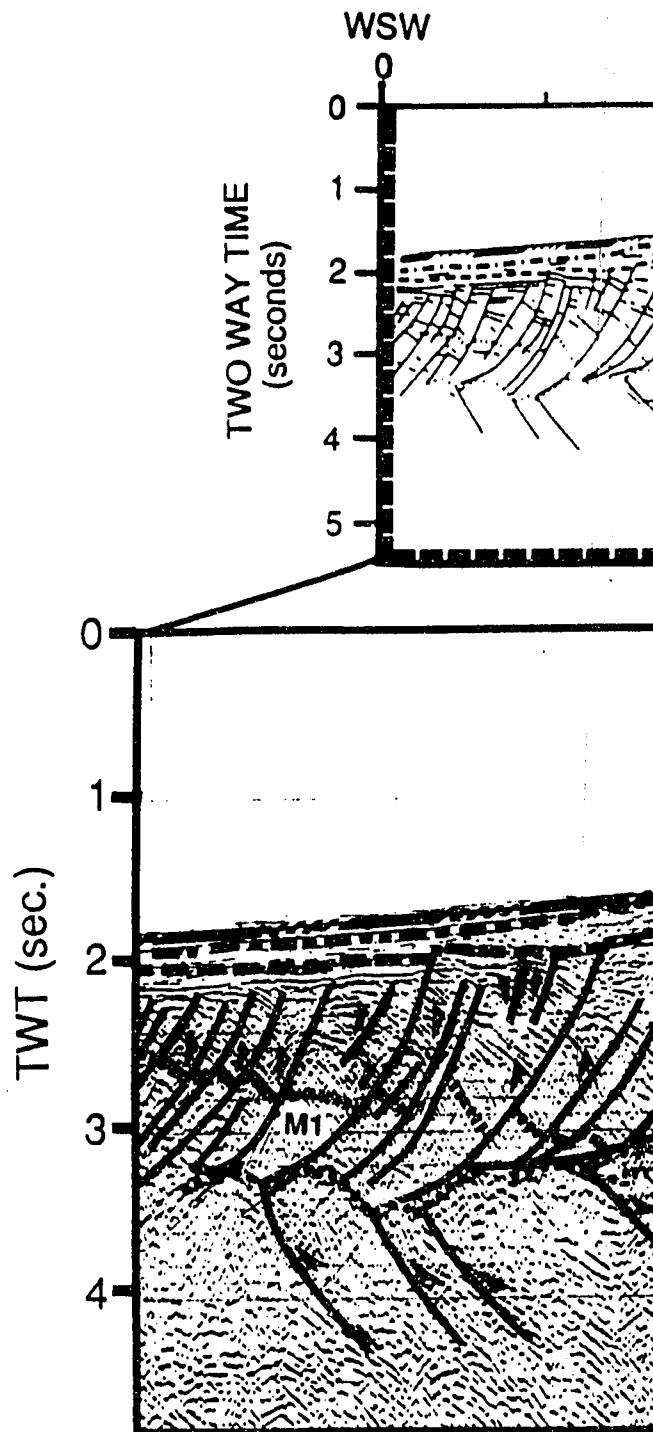


PLATE 12 CLOSE UP OF THE SEISMIC PROFILE

The sequence E₀ was folded and thrust due to the two fault systems. The sequences M1, M2, and M3 are offset by two systems of fault surfaces which dip to the WSW and ENE, respectively. The sequences P and Q and the sea floor are also offset by these fault systems.

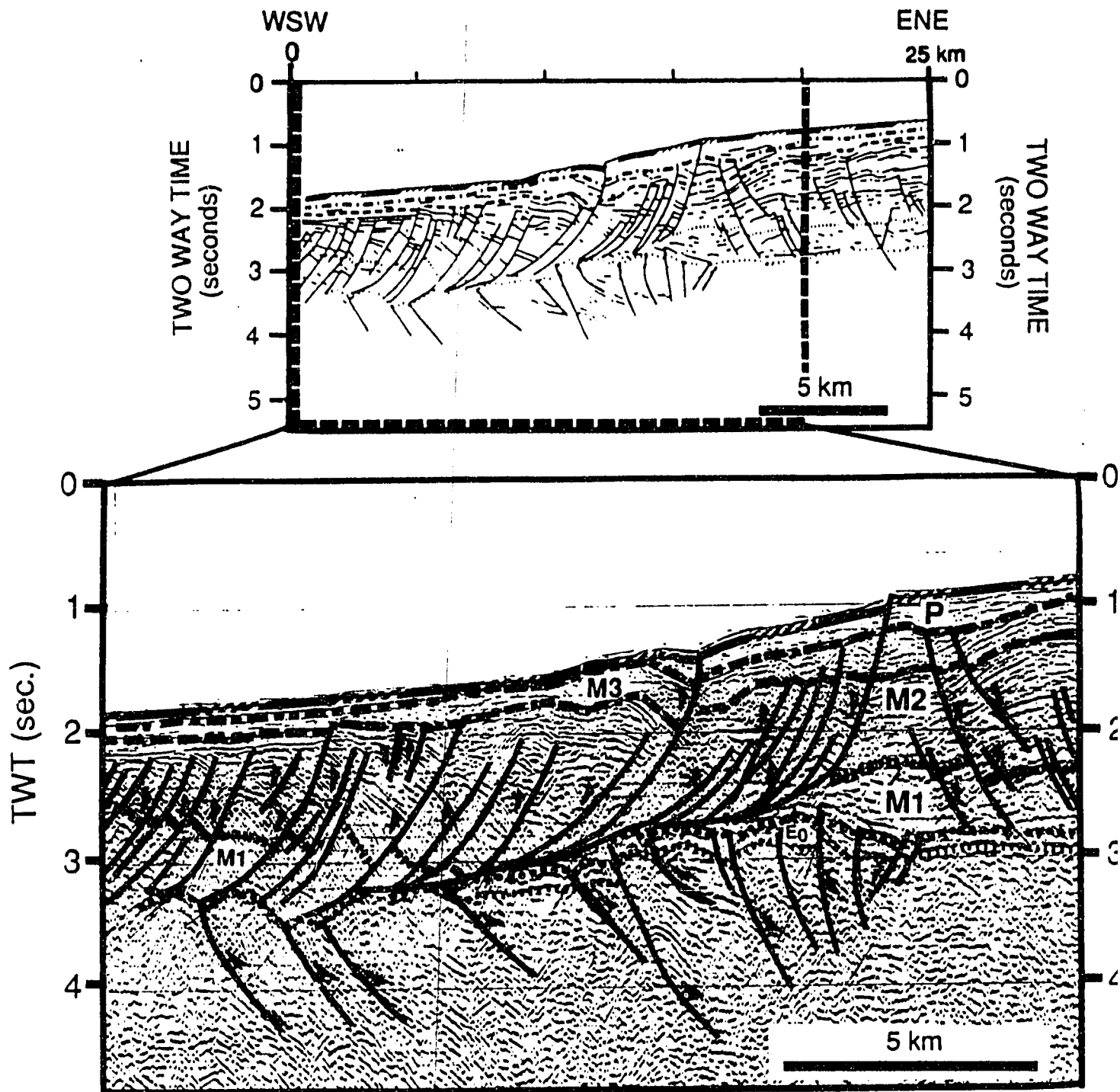
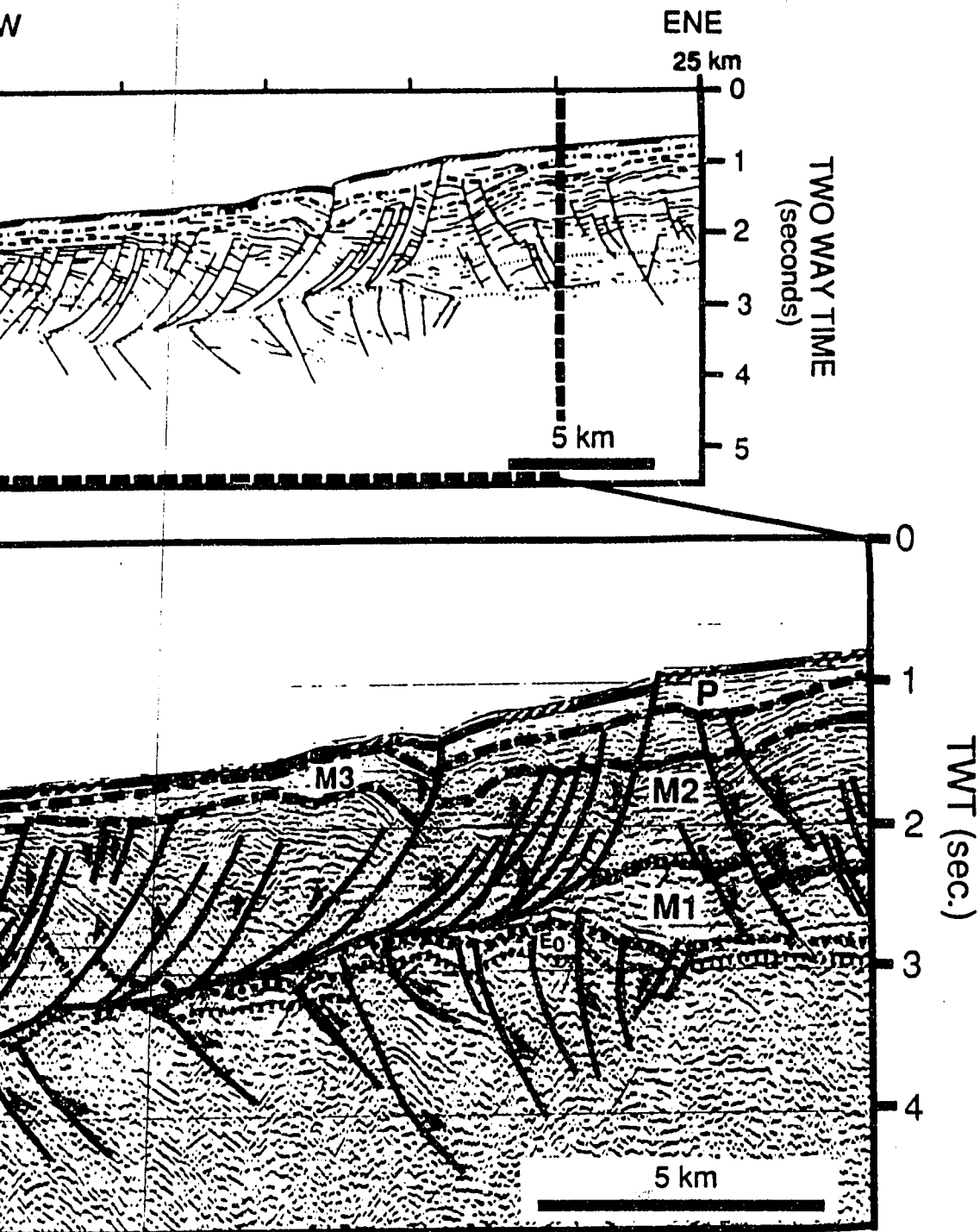
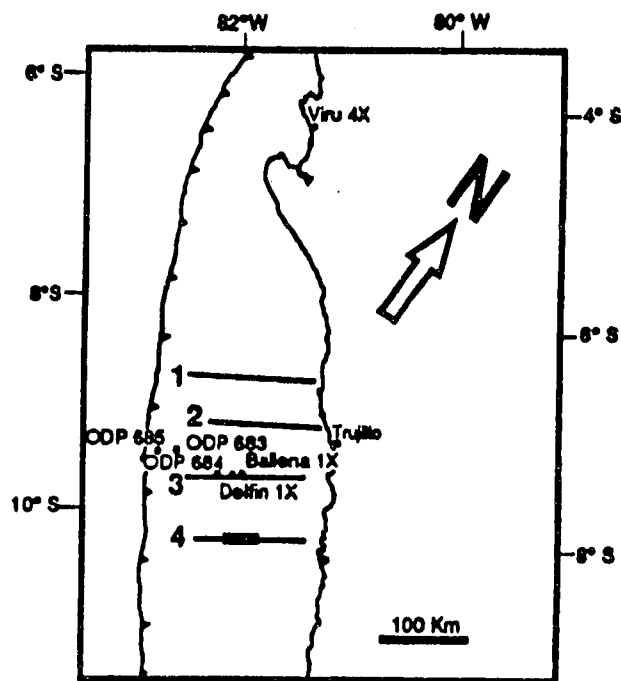


PLATE 12 CLOSE UP OF THE SEISMIC PROFILE LINE DRAWING 4 (PANEL 1), UPPER SLOPE
 The sequence E₀ was folded and thrust during the Middle Eocene second compressive event. Se M1, M2, and M3 are offset by two systems of gravitational listric normal faults with shallow detachment surfaces which dip to the WSW and ENE, some of these faults were reactivated during the Rec offset sequences P and Q and the sea floor.



THE SEISMIC PROFILE LINE DRAWING 4 (PANEL 1), UPPER SLOPE ZONE
 and thrust during the Middle Eocene second compressive event. Sequences
 by two systems of gravitational listric normal faults with shallow detachment
 VSW and ENE, some of these faults were reactivated during the Recent and
 and the sea floor.



L E G E N D **SEQUENCE A G E**

Q	Quaternary
P	Upper Miocene - Pliocene
M 3	Upper Miocene
M 2	Middle - Lower Miocene
M 1	Lower Miocene
E-O	Uppermost middle Eocene to Oligocene
E 3	Middle Eocene
E 2	Middle Eocene
E 1	Middle Eocene
E ₀	Lower ? - Middle Eocene
K	Cretaceous ?
PK	Pre-Cretaceous Basement

Normal fault

Reverse fault

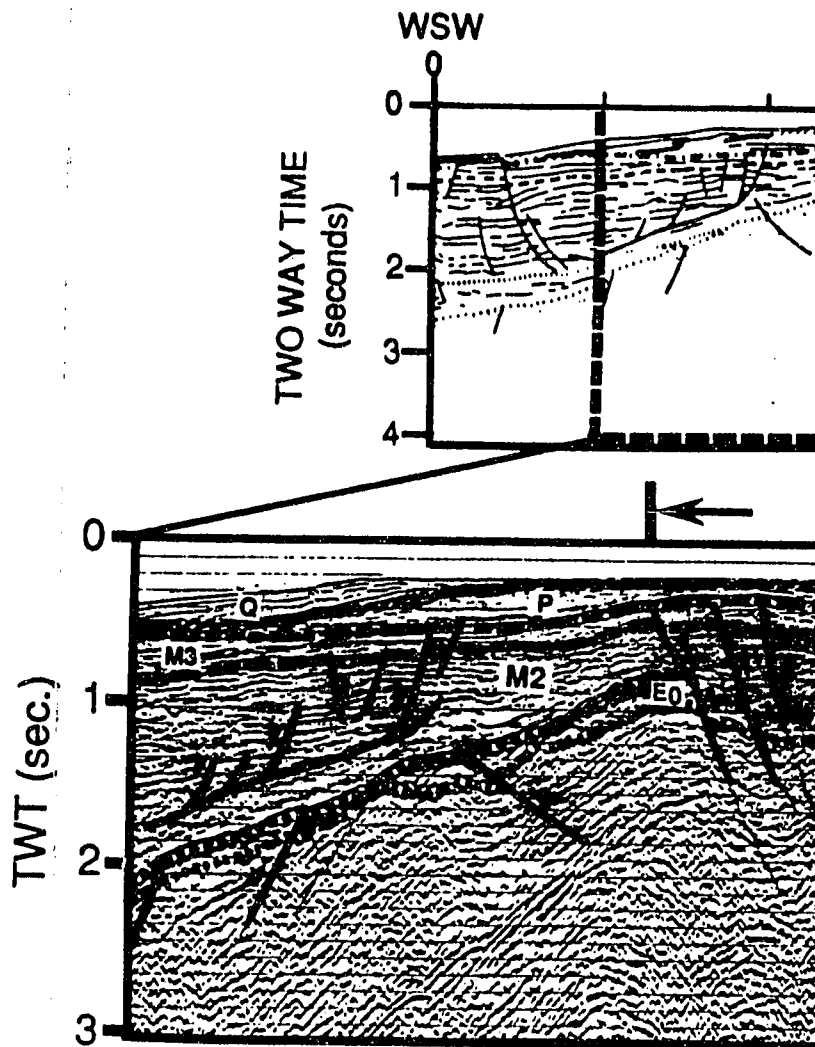
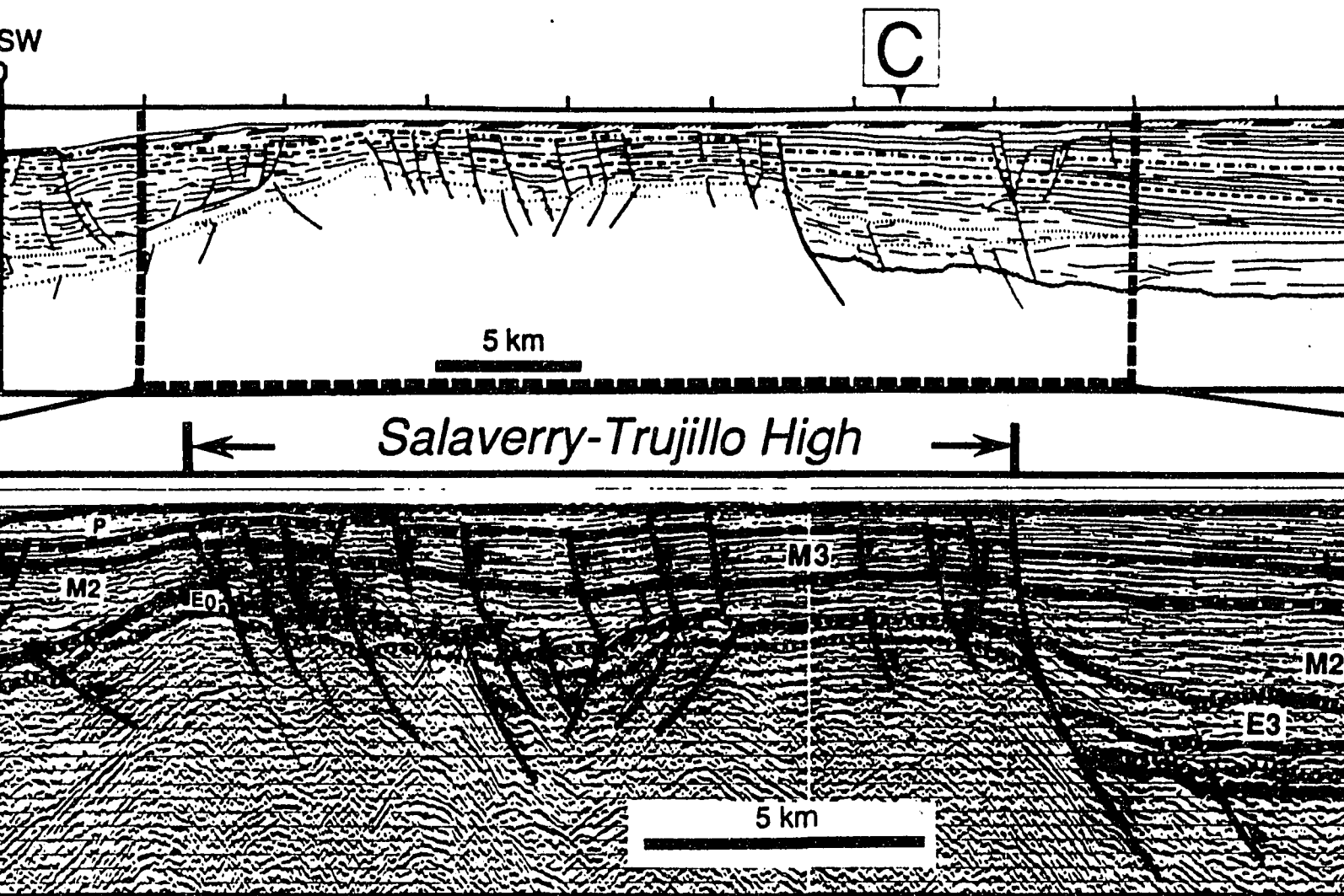


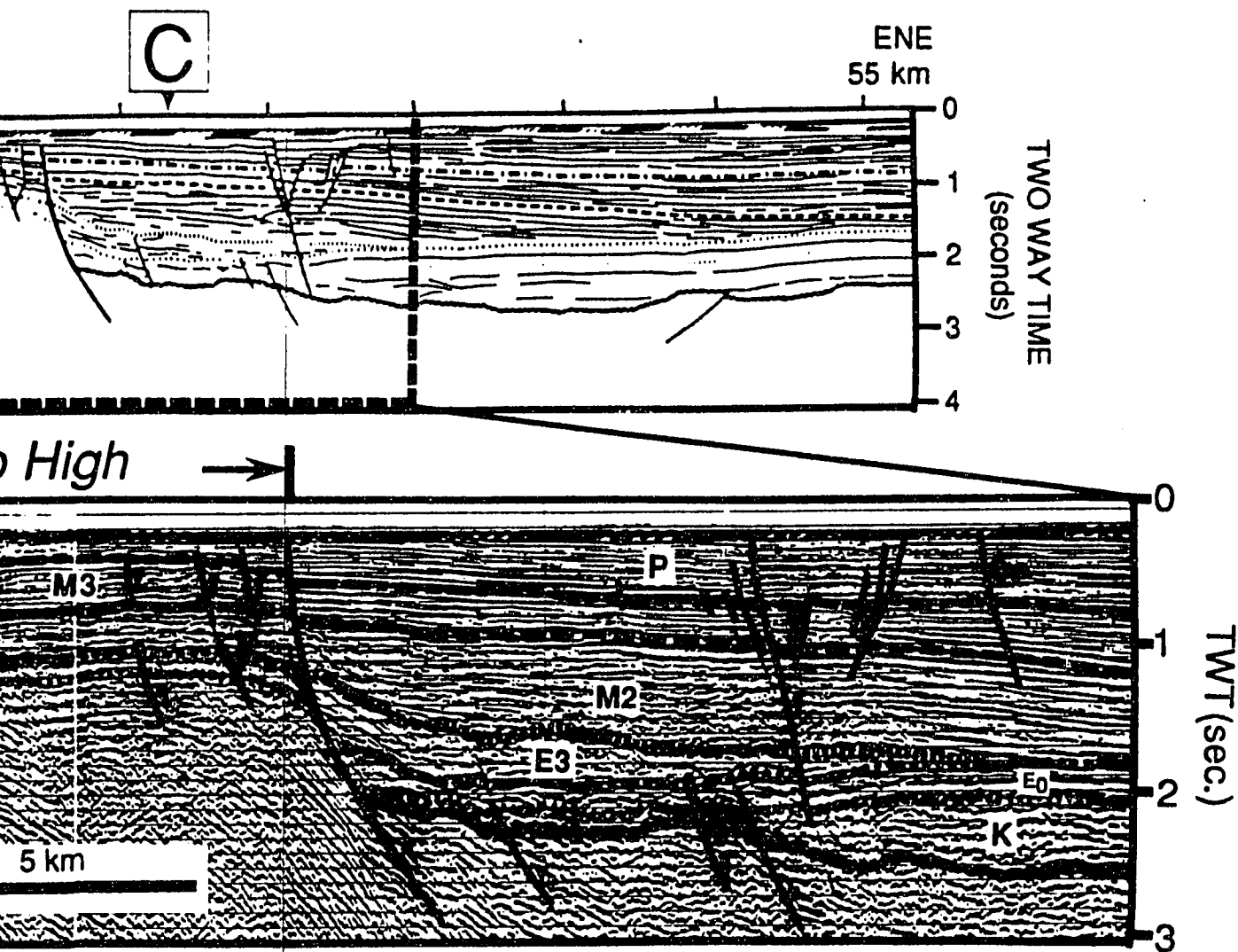
PLATE 13. CLOSE UP OF THE SEISMIC (PANEL 1) SALAVERRY-TRUJILLO HIGH
 A transfer fault of the middle Eocene rift the Salaverry-Trujillo High marks the west offsets the E₀ unit, and bounds a half gr the E3 sequence. The M2 sequence onlaps and E3 units west and east of the Salave this unit thins towards the high which ir during the M2 unit deposition (middle to



SE UP OF THE SEISMIC PROFILE LINE DRAWING 4 LAVERRY-TRUJILLO HIGH

of the middle Eocene rifting which is located east of
ujillo High marks the western limit of the K sequence,
unit, and bounds a half graben filled with sediments of
. The M2 sequence onlaps the top of the underlying E0
west and east of the Salaverry-Trujillo High respectively;
towards the high which indicates that it was uplifted
unit deposition (middle to early Miocene time); similar

relationships involve units M3 and P w
of the Salaverry-Trujillo High until th
offset the E0 unit were developed during
Miocene compression. The transfer fa
late Pliocene second extensional episode
offset by two normal fault systems w
Cenozoic basement. The left part of
gravitational listric normal fault with
that involves the M2, M3 and P units.



relationships involve units M3 and P which illustrate the uplift history of the Salaverry-Trujillo High until the Pliocene. The thrusts that offset the E₀ unit were developed during the third upper-middle to late Miocene compression. The transfer fault was reactivated during the late Pliocene second extensional episode. Sequences M2, M3 and P are offset by two normal fault systems which do not involve the pre-Cenozoic basement. The left part of the seismic profile shows a gravitational listric normal fault with shallow detachment surface that involves the M2, M3 and P units.

LEGEND **SEQUENCE AGE**

Q	Quaternary
P	Upper Miocene - Pliocene
M3	Upper Miocene
M2	Middle - Lower Miocene
M1	Lower Miocene
E-O	Uppermost middle Eocene to Oligocene
E3	Middle Eocene
E2	Middle Eocene
E1	Middle Eocene
E ₀	Lower ? - Middle Eocene
K	Cretaceous ?
PK	Pre-Cretaceous Basement

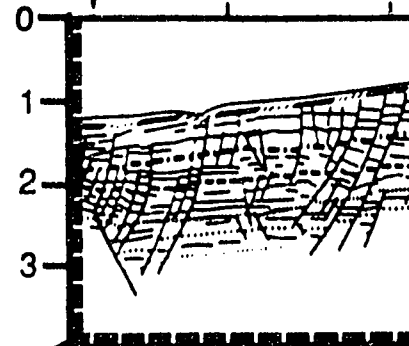
Normal fault

WSW

B

5

TWO WAY TIME
(seconds)



TWT (sec.)

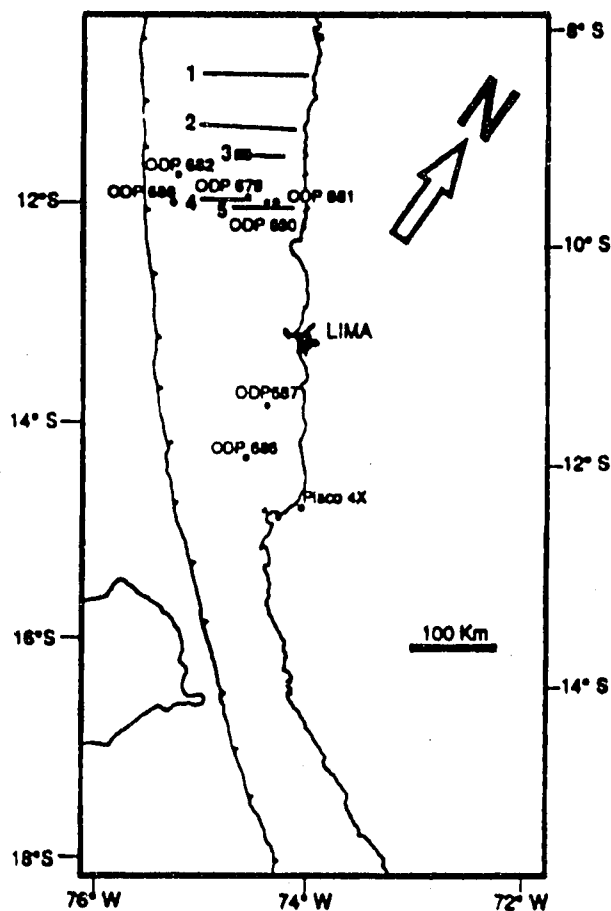
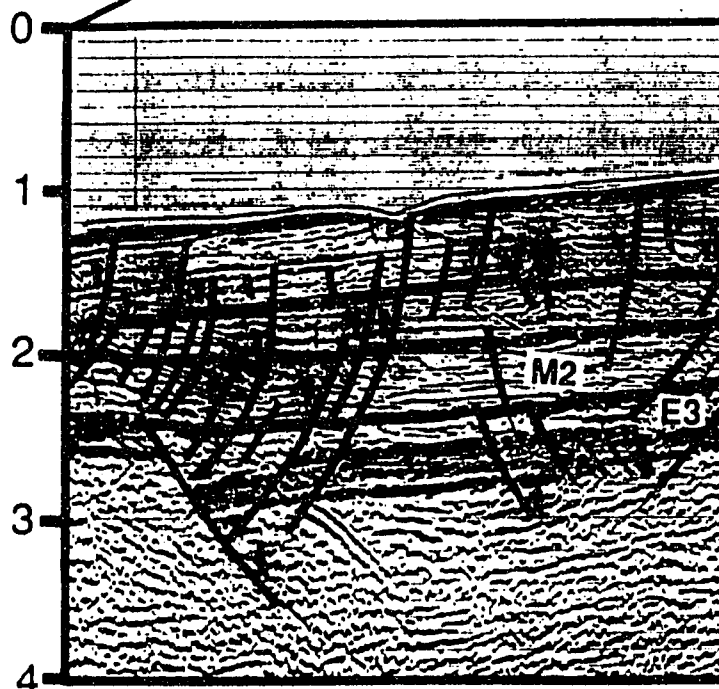
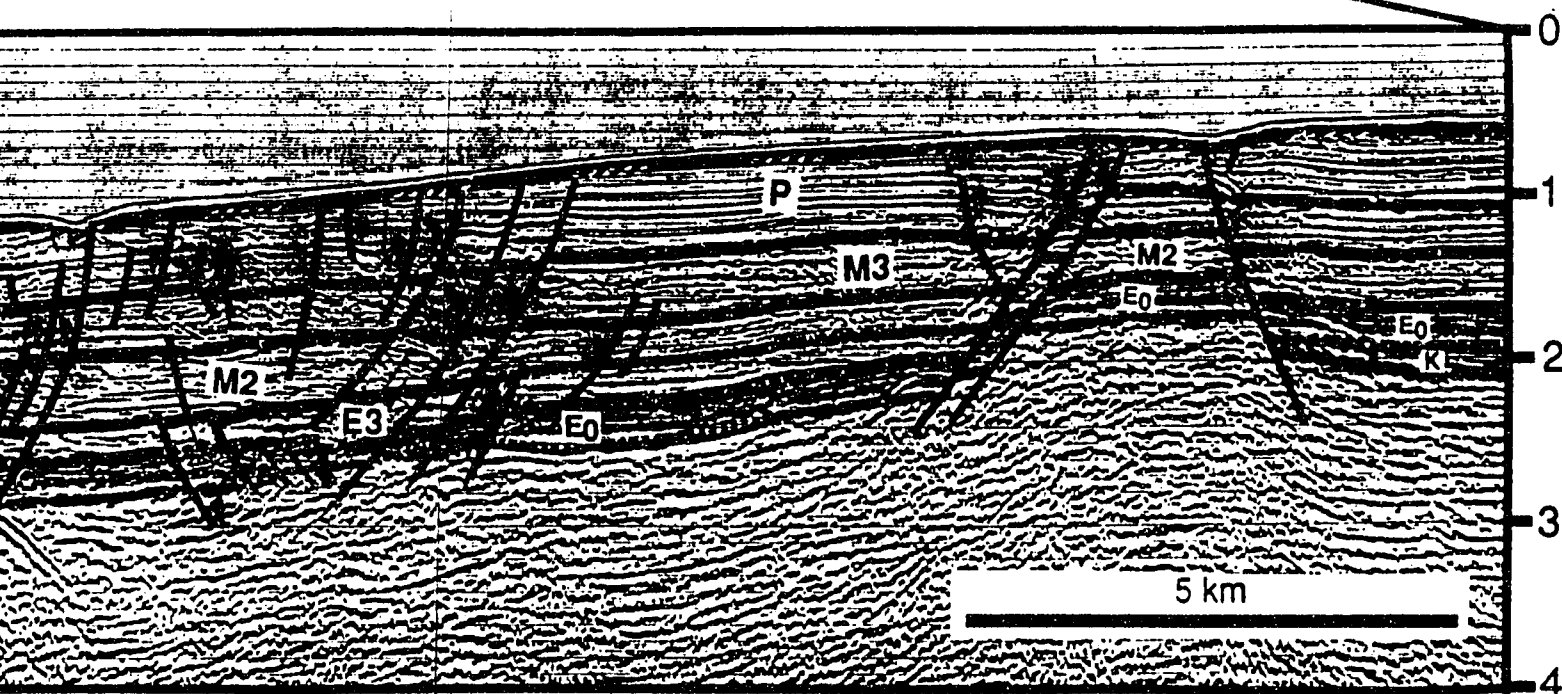
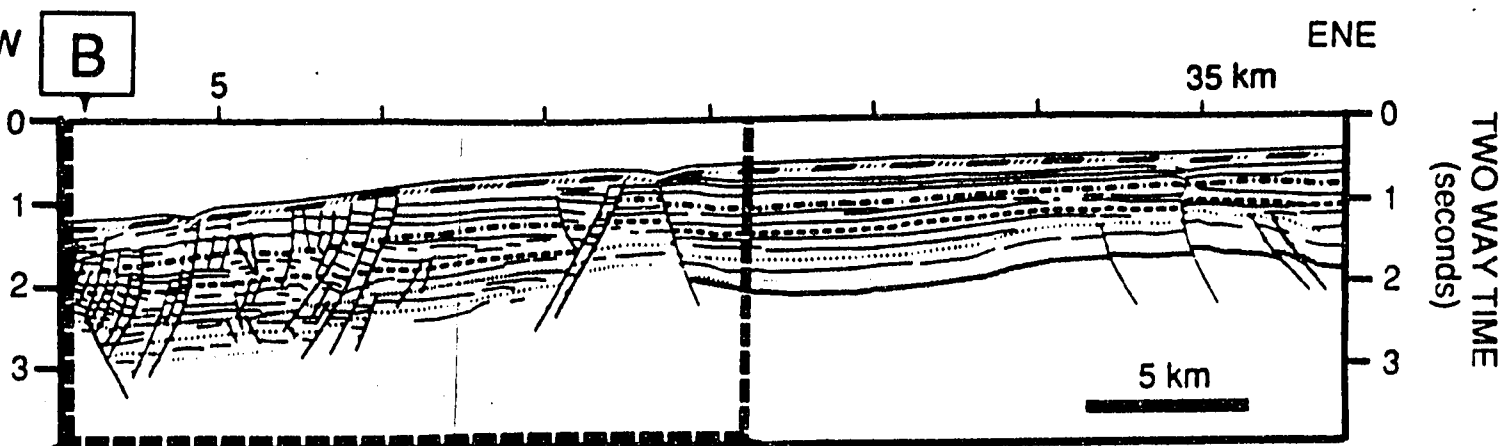


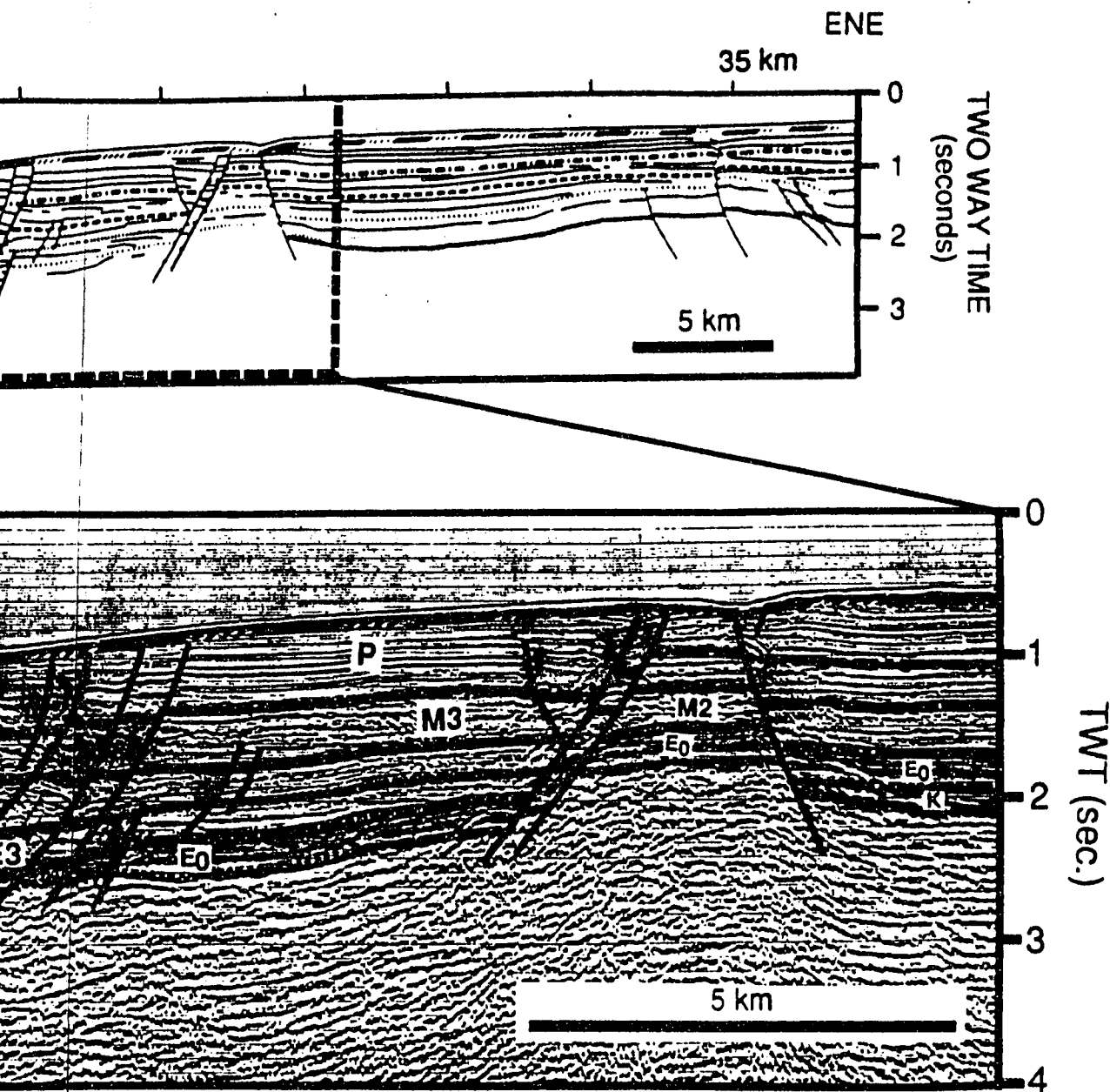
PLATE 14. CLOSE UP OF THE SEI

A half graben of the E3 sequence transfer system (right). Synthetic fault offset the pre-Cenozoic and early Miocene, the Pliocene and during the late Pliocene extension which does not involve the pre



CLOSE UP OF THE SEISMIC PROFILE LINE DRAWING 3 (PANEL 3), LIMA BASIN

ben of the E3 sequence is bounded by a master fault (left) and faults of the system (right). Synthetic and antithetic fault systems related to the master at the pre-Cenozoic basement and were reactivated during the middle to ene, the Pliocene and the Recent. The transfer faults were also reactivated late Pliocene extension; by the same time a listric normal fault system s not involve the pre-Cenozoic basement was developed.

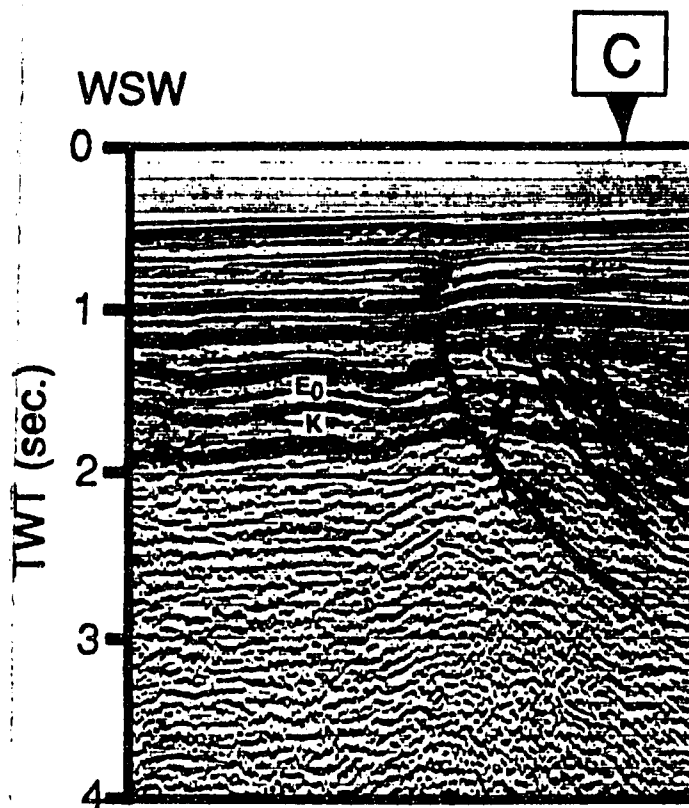
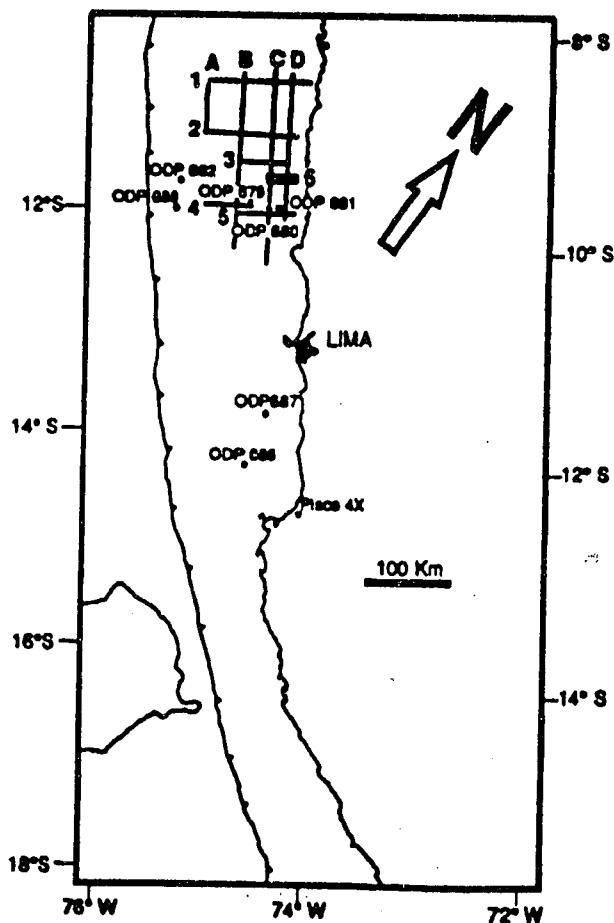


SEISMIC PROFILE LINE DRAWING 3 (PANEL 3), LIMA BASIN

ence is bounded by a master fault (left) and faults of the
 hetic and antithetic fault systems related to the master
 c basement and were reactivated during the middle to
 and the Recent. The transfer faults were also reactivated
 ension; by the same time a listric normal fault system
 pre-Cenozoic basement was developed.

L E G E N D **SEQUENCE A G E**

Q	Quaternary
P	Upper Miocene - Pliocene
M 3	Upper Miocene
M 2	Middle - Lower Miocene
M 1	Lower Miocene
E-O	Uppermost middle Eocene to Oligocene
E 3	Middle Eocene
E 2	Middle Eocene
E 1	Middle Eocene
E₀	Lower ? - Middle Eocene
K	Cretaceous ?
PK	Pre-Cretaceous Basement



Reverse fault

PLATE 15. SEI:
This profile is not
during the secor
Miocene compr
originated during
during the fourth

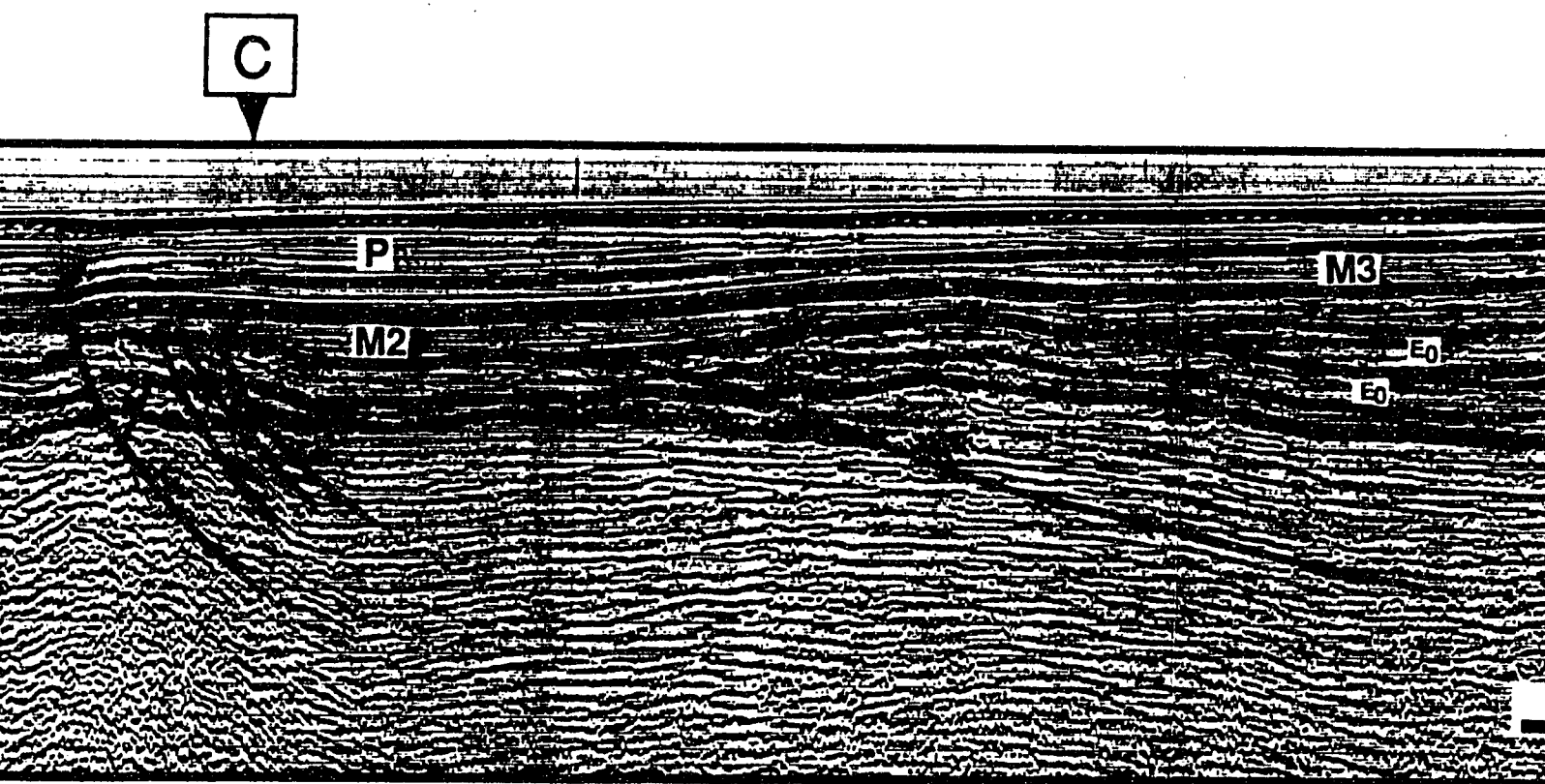
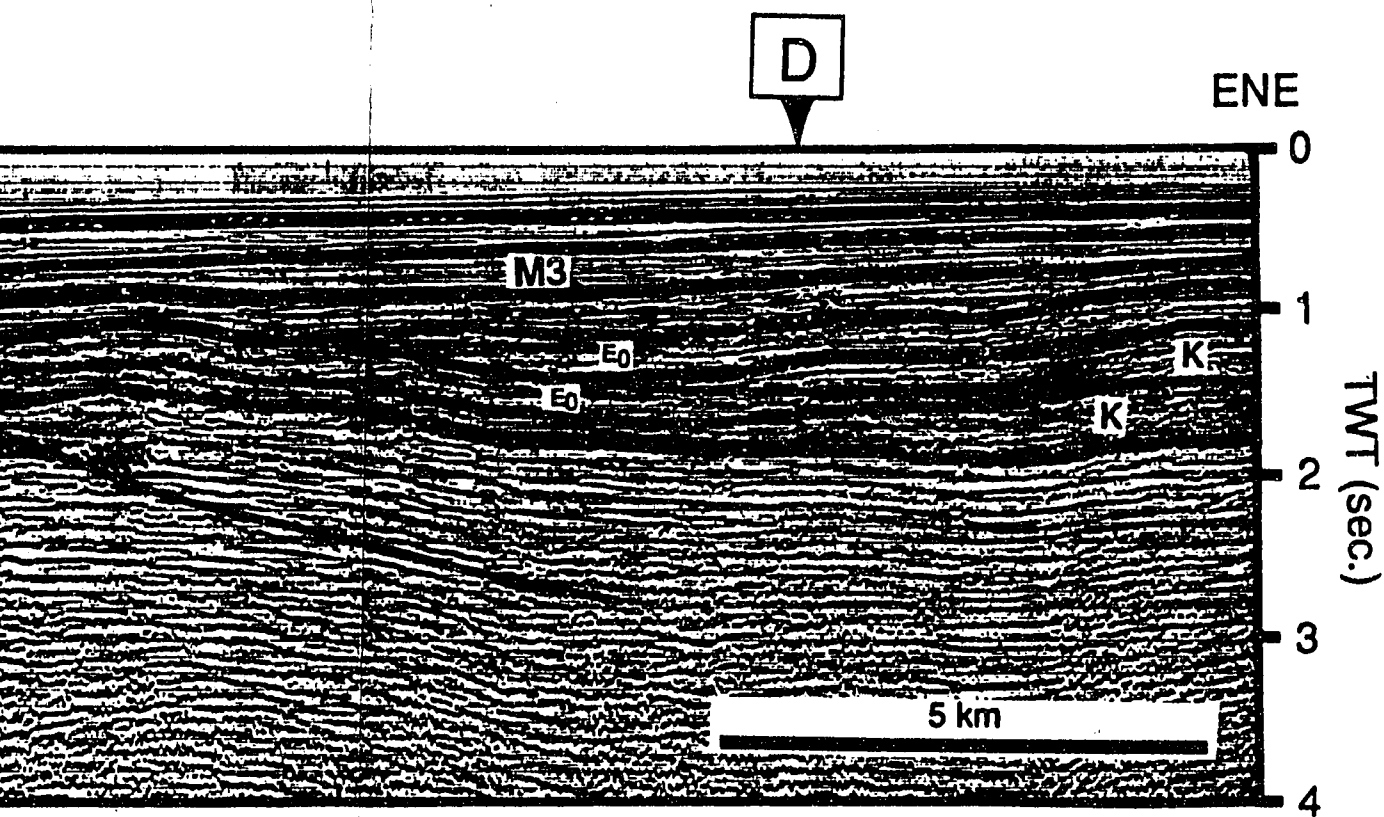


PLATE 15. SEISMIC PROFILE 6 ADJACENT TO THE SEISMIC PROFILE 3 (PANEL 3), SALAVE. This profile is not included in Panel 3. The thrusts and anticlines that affect the K and E₀ sequences during the second middle Eocene compression and were later reactivated during the third upper-Miocene compressive episode as indicates the minor folding of the M2 and M3 units. The thru originated during the third compression. The small back-thrust that affects the P unit (to the left) during the fourth late? Pliocene compressive event.



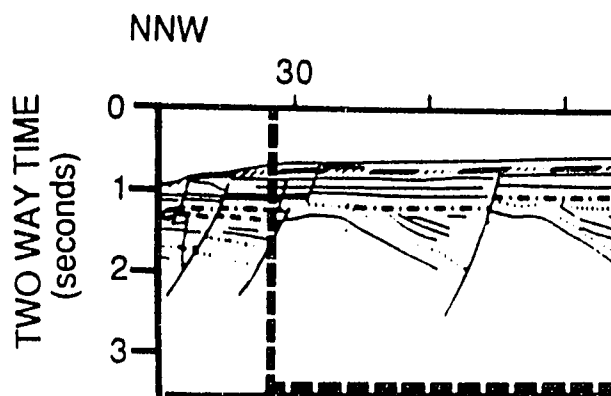
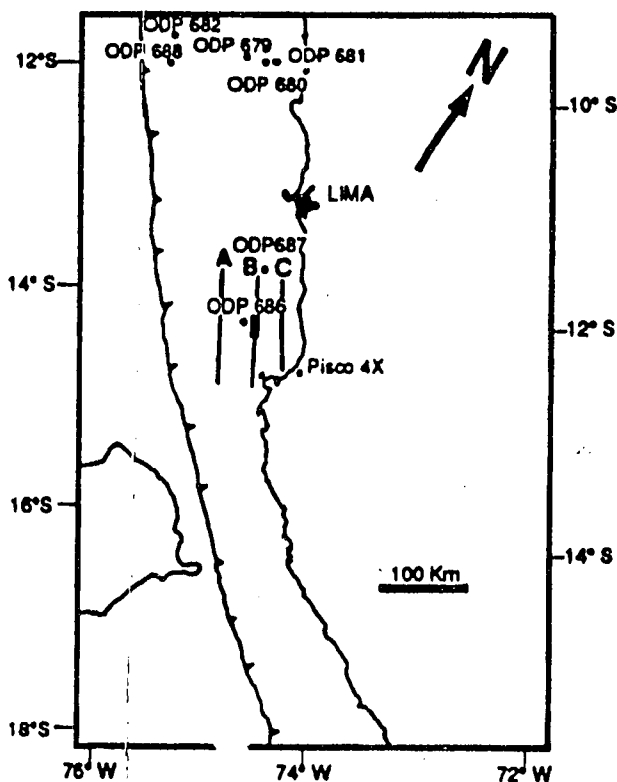
THE SEISMIC PROFILE 3 (PANEL 3), SALAVERRY BASIN

and anticlines that affect the K and E₀ sequences were produced and were later reactivated during the third upper-middle to late minor folding of the M₂ and M₃ units. The thrusts at the left back-thrust that affects the P unit (to the left) was produced

L E G E N D **SEQUENCE AGE**

Q	Quaternary
P	Upper Miocene - Pliocene
M2	Middle - Lower Miocene
M1	Lower Miocene
E-O	Uppermost middle Eocene to Oligocene
E3	Middle Eocene
E2	Middle Eocene
E1	Middle Eocene
E ₀	Lower ? - Middle Eocene
K	Cretaceous ?
PK	Pre-Cretaceous Basement

The upper Miocene M3 sequence was not deposited in this area. Sequences M2, M1 and E-O are not differentiated.



Normal fault

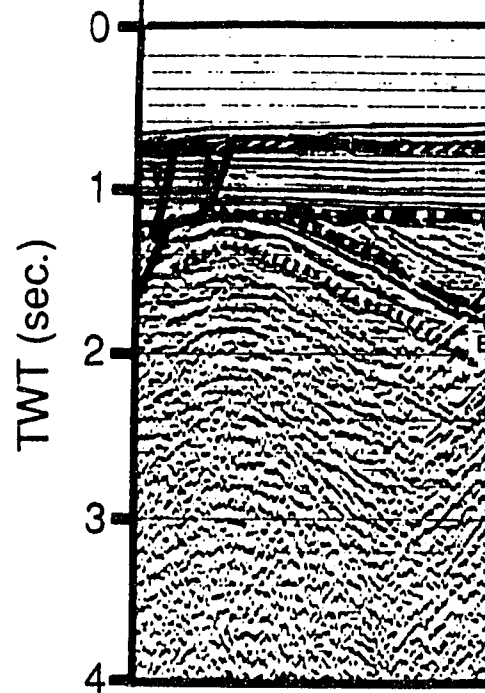


PLATE 16 CLOSE UP OF THE
Two half grabens filled with sediments of the transfer system (right). Sequence event. A prominent angular unconformity sequence P is also offset by the fault. This fault involves the base of the sequence

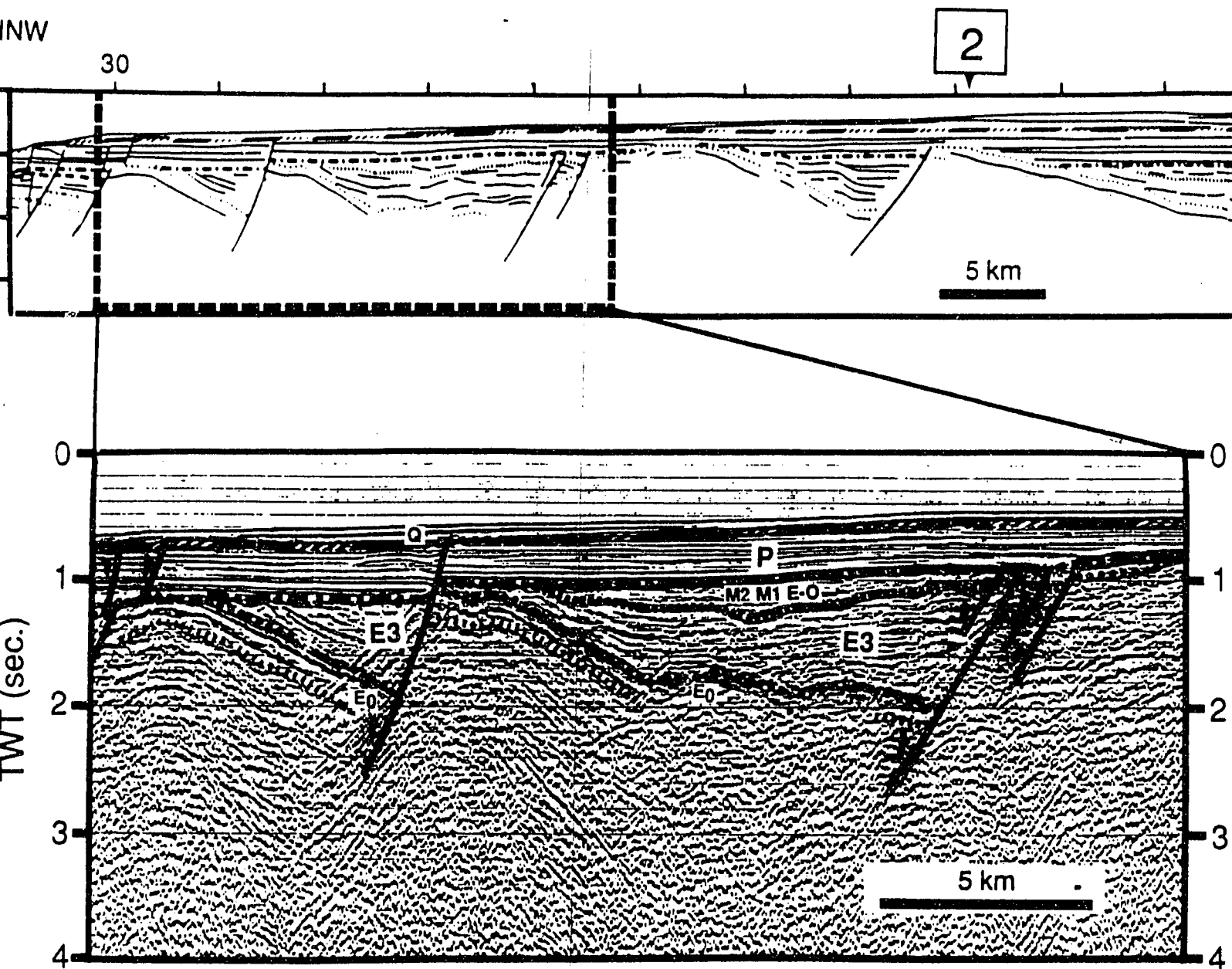
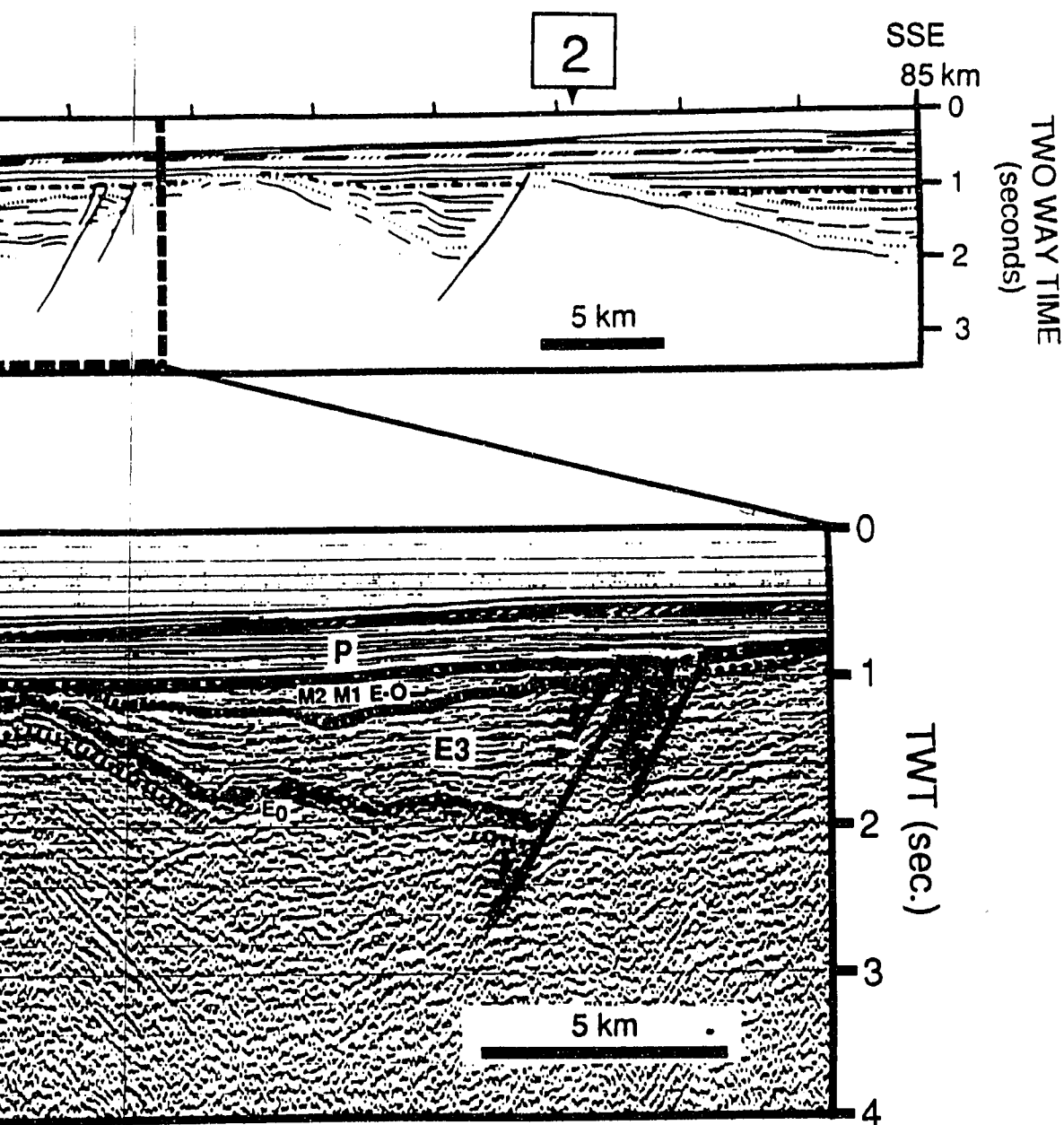


PLATE 16 CLOSE UP OF THE SEISMIC PROFILE LINE DRAWING B (PANEL 6), WEST PISCO BASIN
 Two half grabens filled with sediments of the E3 sequence are bounded by a master normal fault (left) and a transfer system fault (right). Sequences E0, E3 and M2 were folded during the third late Miocene compressional event. A prominent angular unconformity separates the sequence P from the underlying E0, E3 and M2 units. Sequence P is also offset by the master fault which was reactivated during the Pliocene; further reactivation of the fault involves the base of the sequence Q.



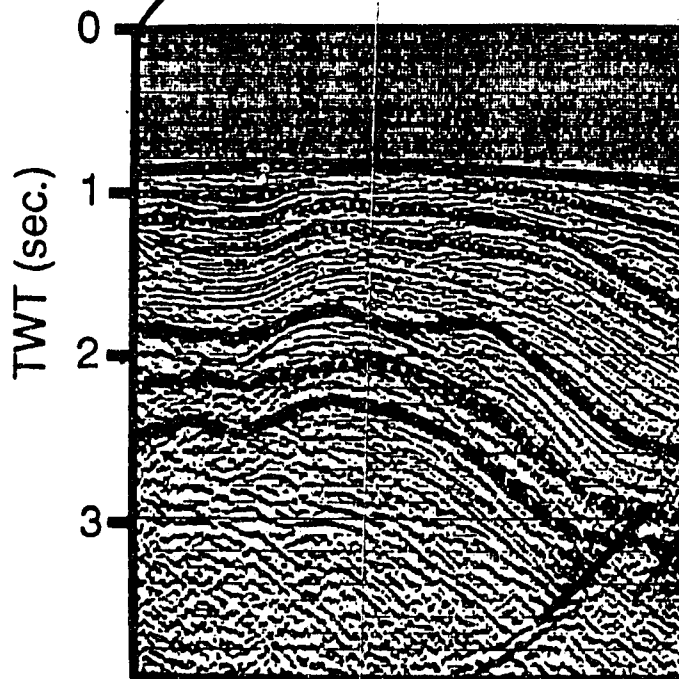
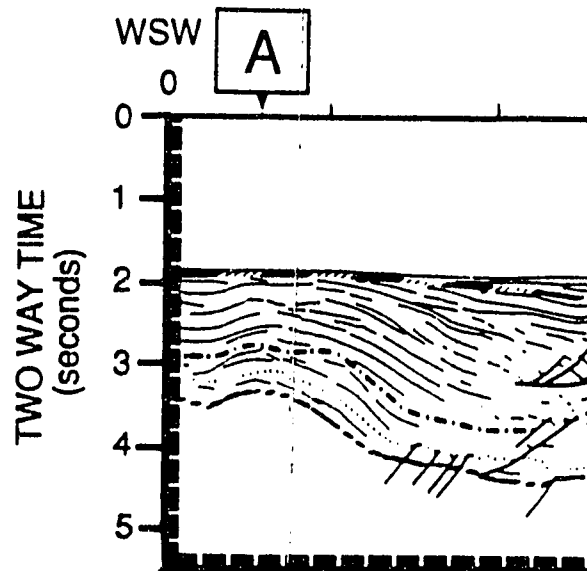
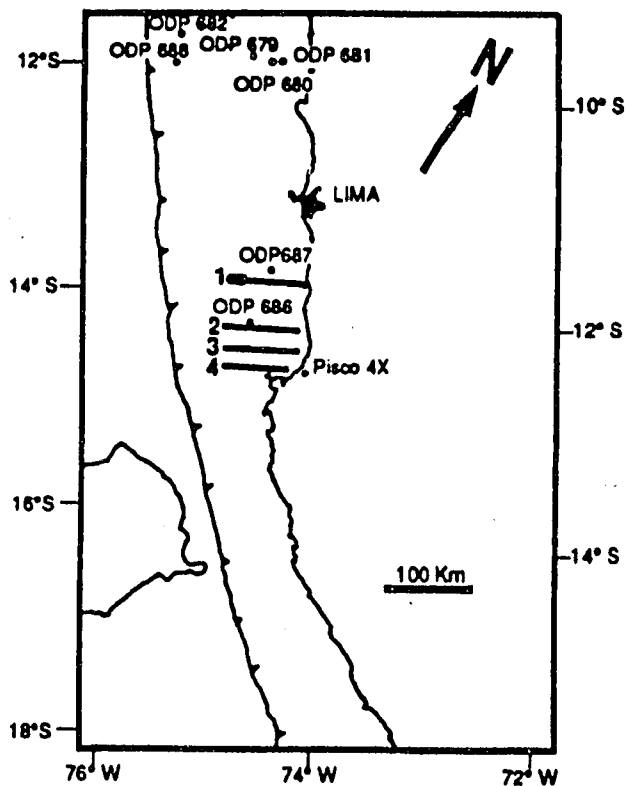
SEISMIC PROFILE LINE DRAWING B (PANEL 6), WEST PISCO BASIN

The E3 sequence are bounded by a master normal fault (left) and faults E0, E3 and M2 were folded during the third late Miocene compressive separates the sequence P from the underlying E0, E3 and M2 units. The fault which was reactivated during the Pliocene; further reactivation of Q.

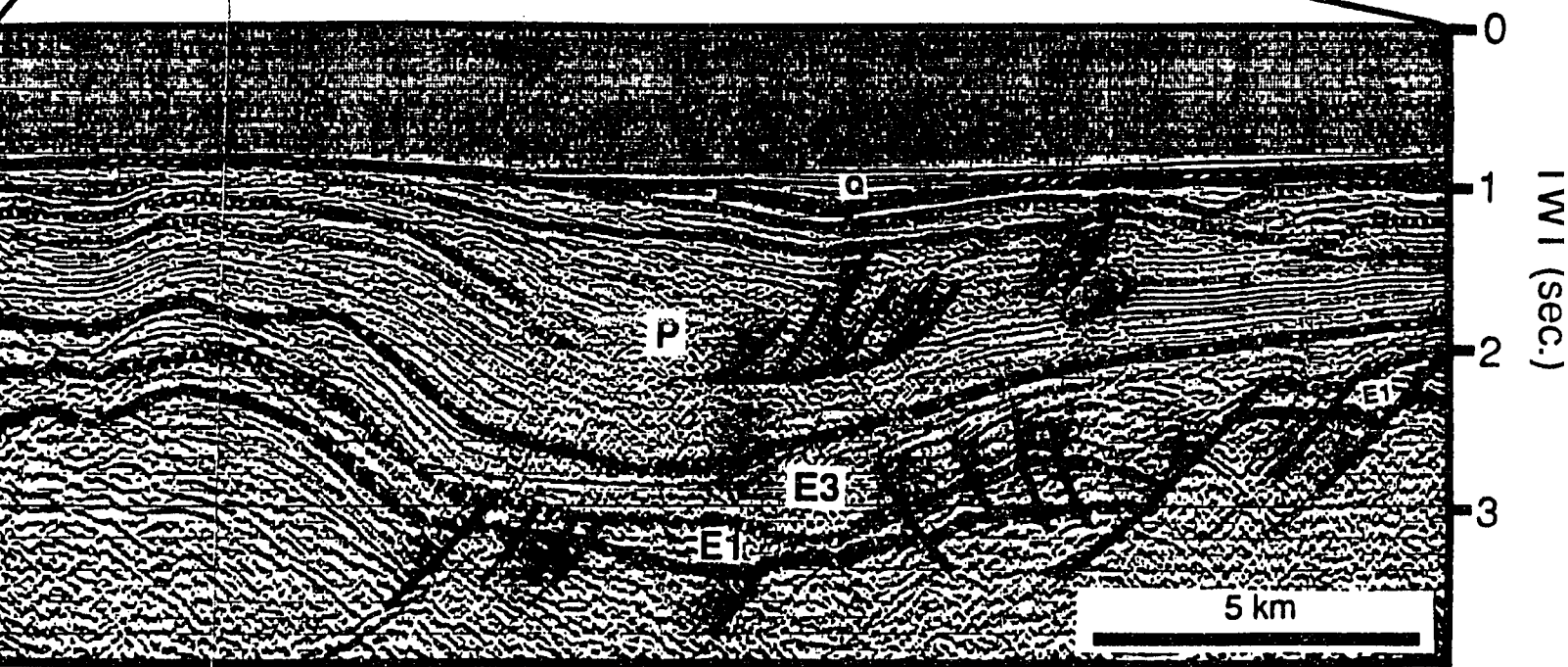
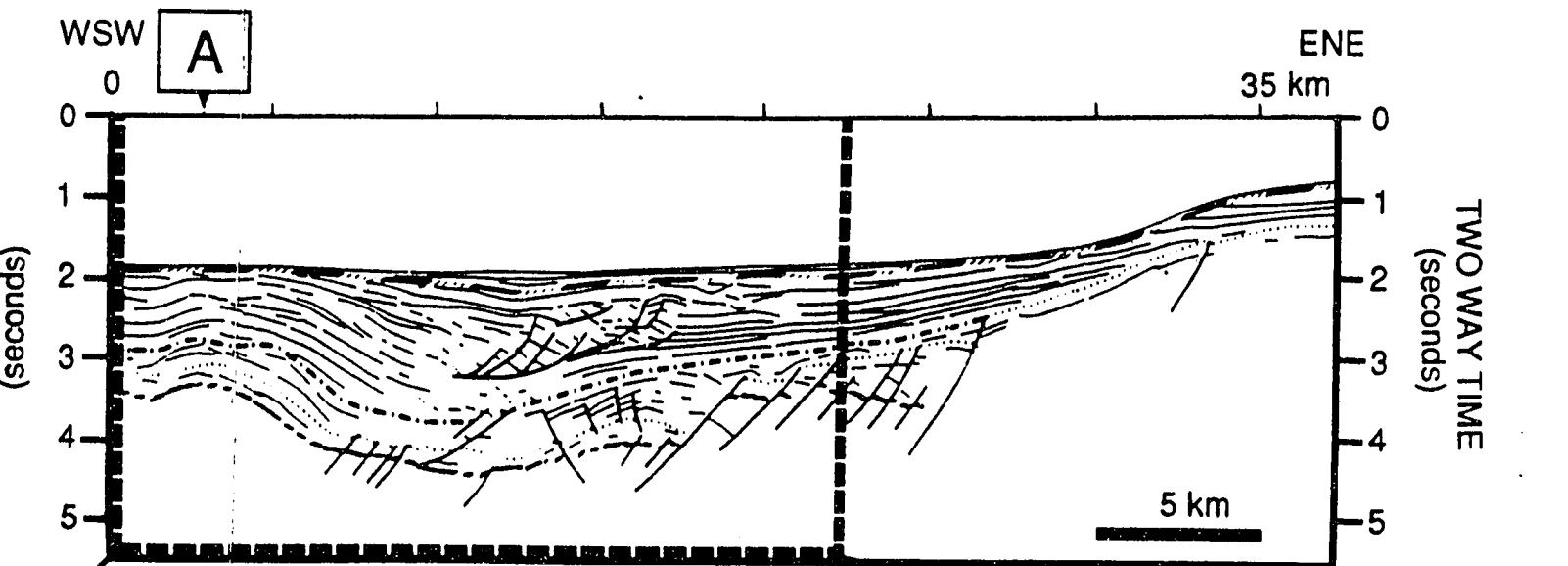
L E G E N D **SEQUENCE A G E**

Q	Quaternary
P	Upper Miocene - Pliocene
M 2	Middle - Lower Miocene
M 1	Lower Miocene
E-O	Uppermost middle Eocene to Oligocene
E 3	Middle Eocene
E 2	Middle Eocene
E 1	Middle Eocene
E ₀	Lower ? - Middle Eocene
K	Cretaceous ?
PK	Pre-Cretaceous Basement

The upper Miocene M3 sequence was not deposited in this area. Sequences M2, M1 and E-O are not differentiated.



Normal fault

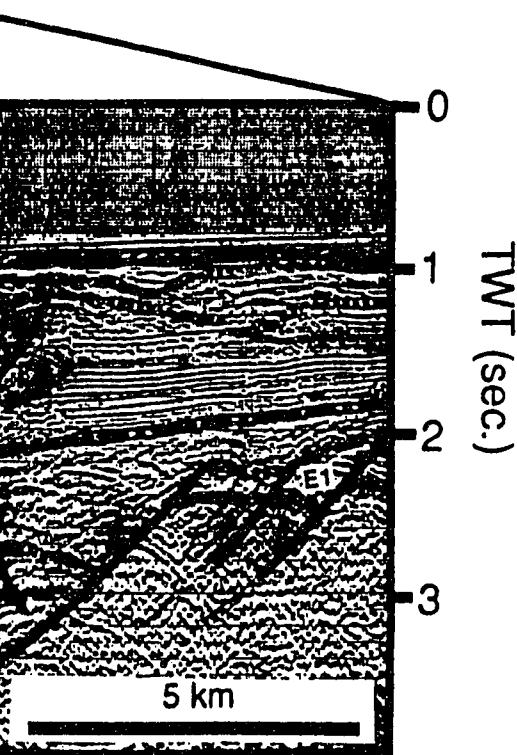
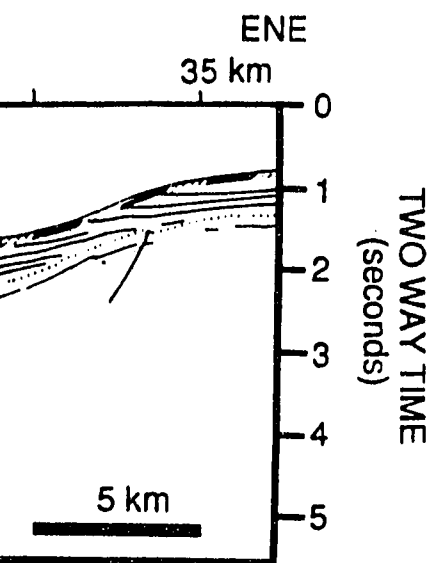


Normal fault



Base of submarine canyon





**PLATE 17. CLOSE UP OF THE SEISMIC PROFILE LINE DI
(PANEL 5), WEST PISCO BASIN**

Sequences E1 and E3 fill a half graben bounded to the ENE normal fault that involves the Pre-Cenozoic basement. The s which unconformably overlies the E3 unit, consists of stacked deposits locally offset by listric normal faults with detachment zone. Sequences E-O, M1, M2 and M3 were eroded upper-middle to upper Miocene regional uplift. E1, E3 and P folded during the fourth late? Pliocene compressive event. flat laying deposits of the sequence Q unconformably rest on sequence P.

**PLATE 17. CLOSE UP OF THE SEISMIC PROFILE LINE DRAWING 1
(PANEL 5), WEST PISCO BASIN**

Sequences E1 and E3 fill a half graben bounded to the ENE by a listric normal fault that involves the Pre-Cenozoic basement. The sequence P, which unconformably overlies the E3 unit, consists of stacked slope fan deposits locally offset by listric normal faults with a shallow detachment zone. Sequences E-O, M1, M2 and M3 were eroded during the upper-middle to upper Miocene regional uplift. E1, E3 and P units were folded during the fourth late? Pliocene compressive event. Quaternary flat laying deposits of the sequence Q unconformably rest on top of the sequence P.

TWT (sec.)

L E G E N D **SEQUENCE A G E**

Q	Quaternary
P	Upper Miocene - Pliocene
M2	Middle - Lower Miocene
M1	Lower Miocene
E-O	Uppermost middle Eocene to Oligocene
E3	Middle Eocene
E2	Middle Eocene
E1	Middle Eocene
E0	Lower ? - Middle Eocene
K	Cretaceous ?
PK	Pre-Cretaceous Basement

The upper Miocene M3 sequence was not deposited in this area. Sequences M2, M1 and E-O are not differentiated.

Normal fault

Reverse fault

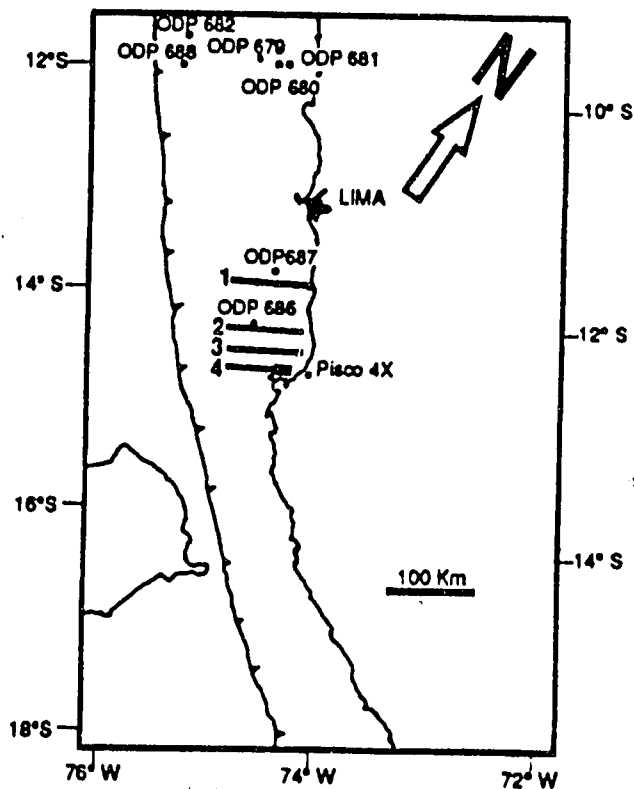
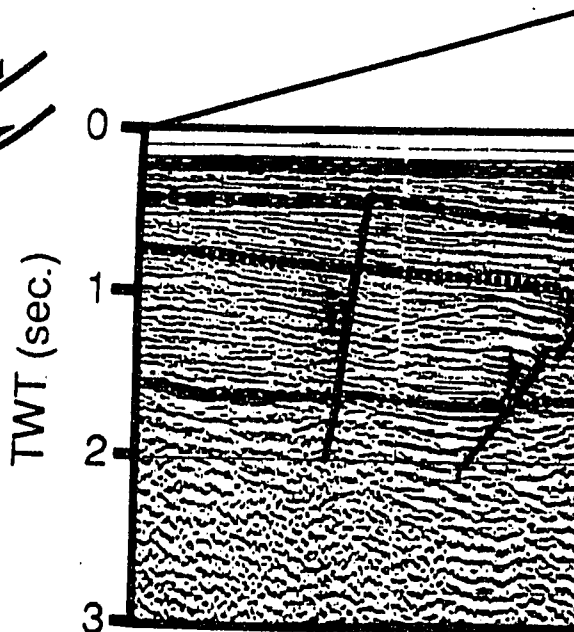
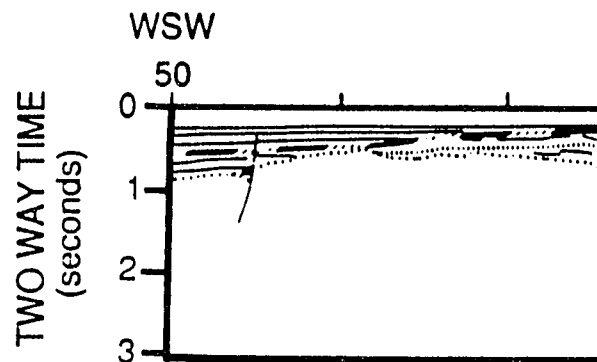
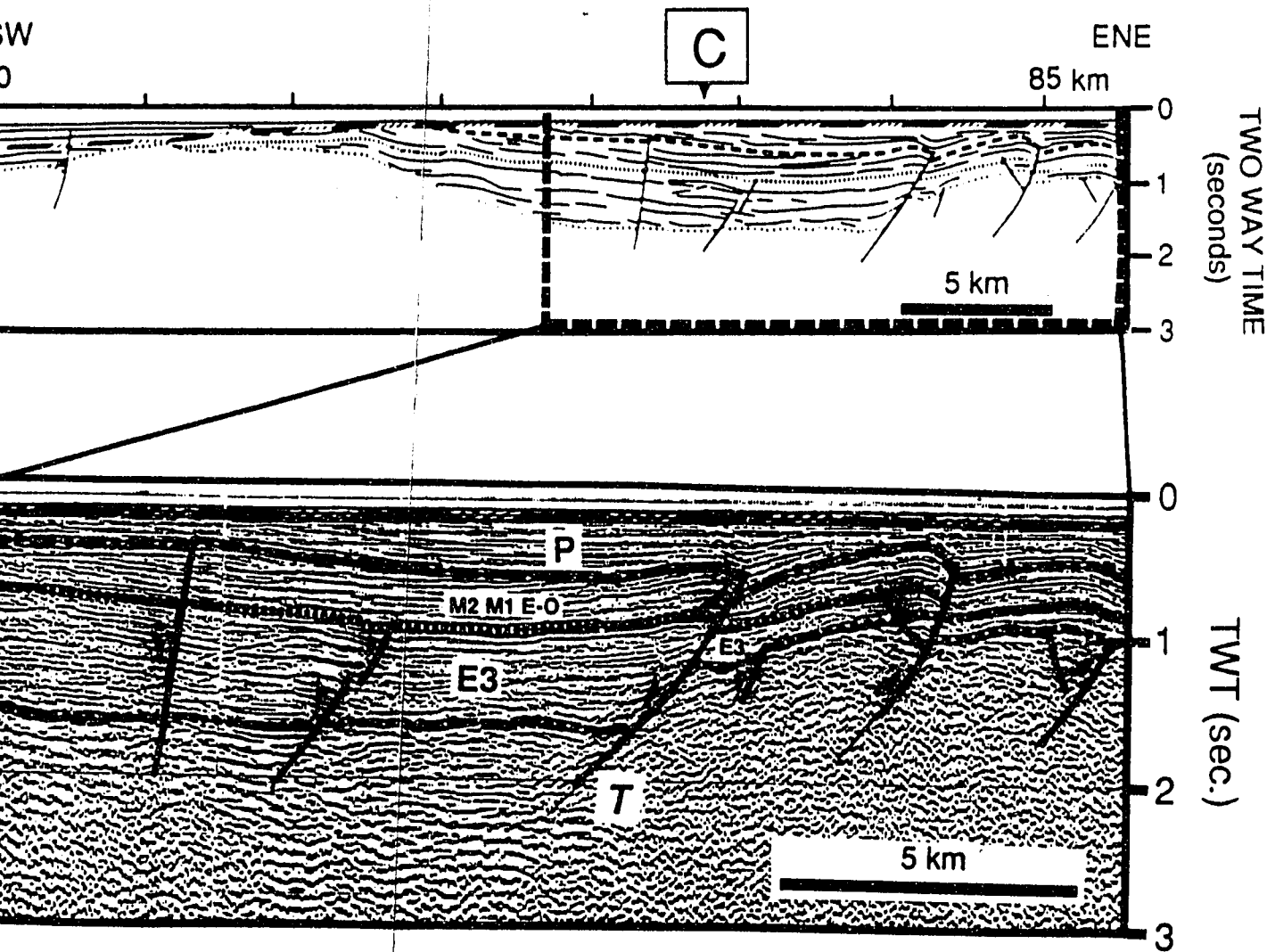


PLATE 18. CLOSE UP OF THE SEISMIC
A half graben of the E3 sequence that is fourth middle Pliocene? compression. The by wedges of the sequence P bounded by



CLOSE UP OF THE SEISMIC PROFILE LINE DRAWING 4 (PANEL 5), EAST PISCO BASIN
 of the E3 sequence that is bounded by a transfer fault (T) was slightly inverted during the Pliocene? compression. The compression was coeval with the P unit deposition as indicated the sequence P bounded by thrust faults.

PLEASE NOTE:

Oversize maps and charts are filmed in sections in the following manner:

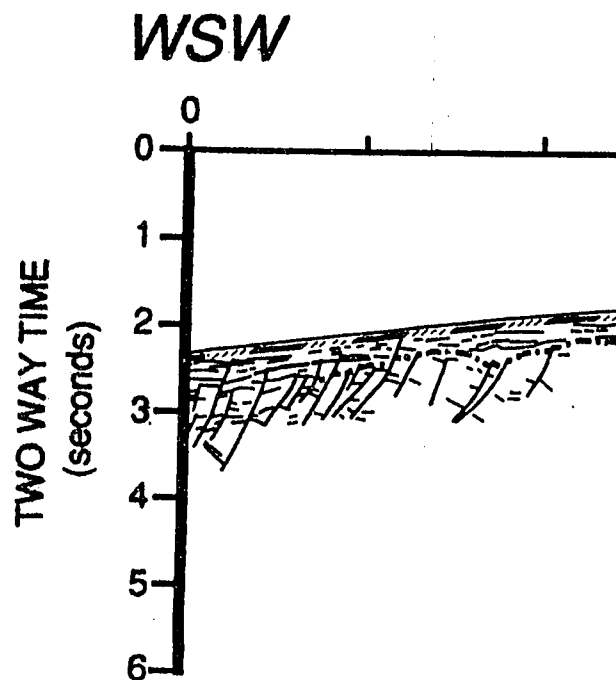
LEFT TO RIGHT, TOP TO BOTTOM, WITH SMALL OVERLAPS

The following map or chart has been refilmed in its entirety at the end of this dissertation (not available on microfiche). A xerographic reproduction has been provided for paper copies and is inserted into the inside of the back cover.

Black and white photographic prints (17" x 23") are available for an additional charge.

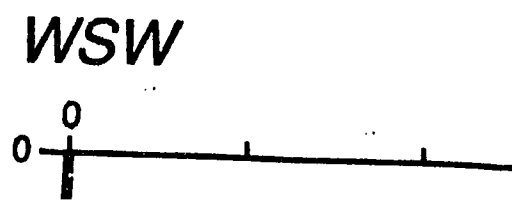
UMI

Profile 1



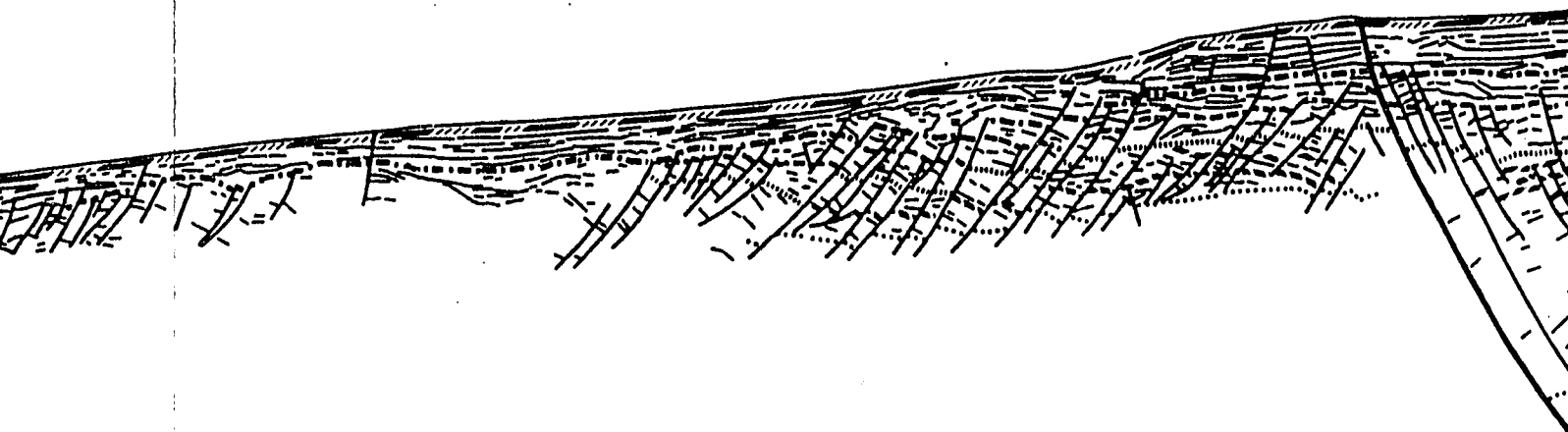
Prof

Profile 3



V

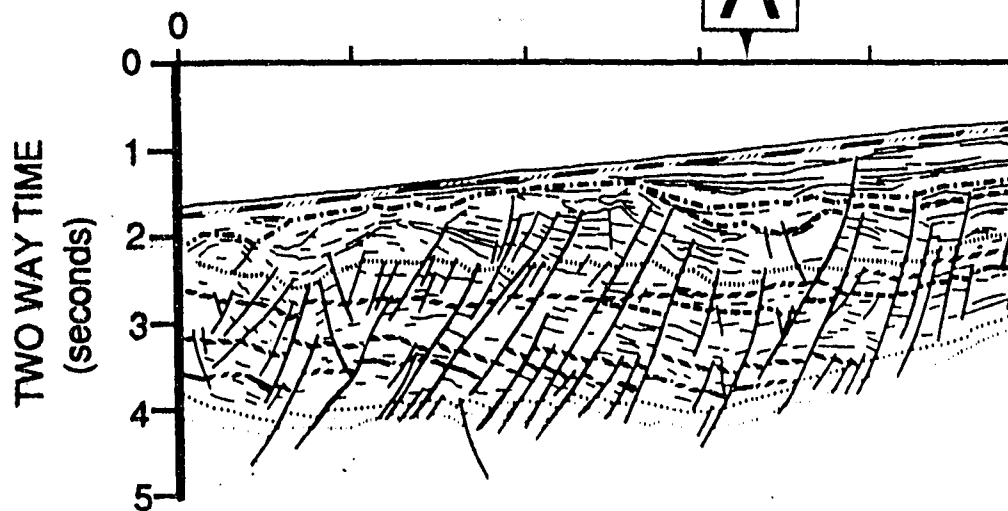
A



Profile 2

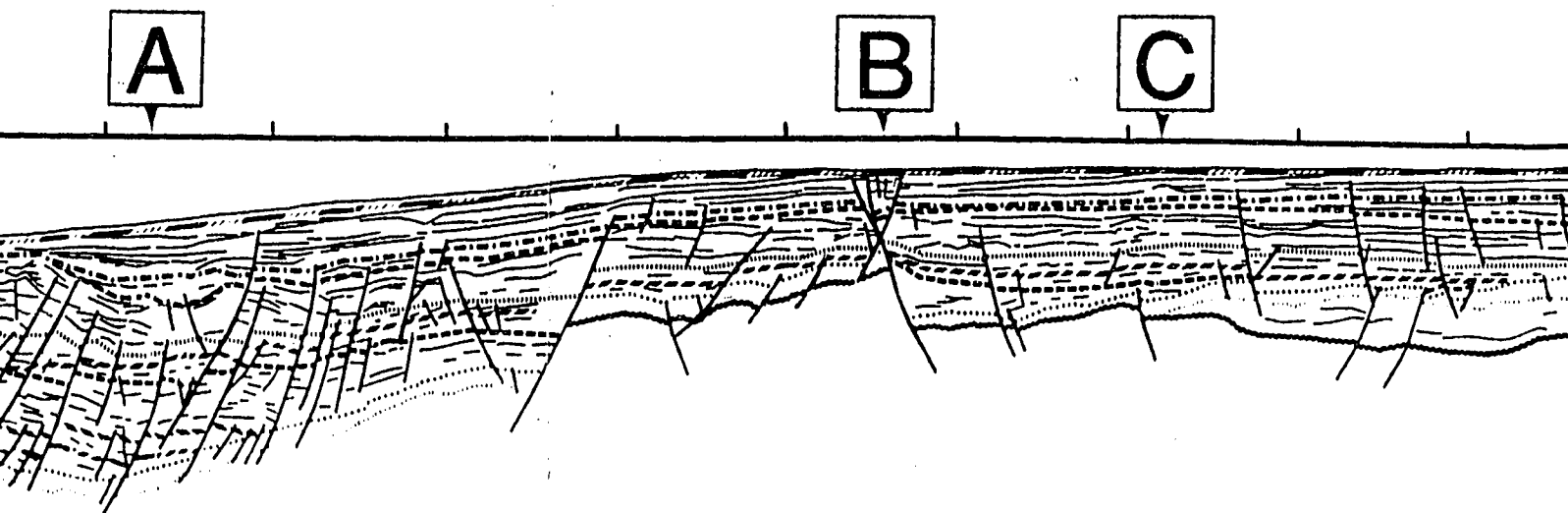
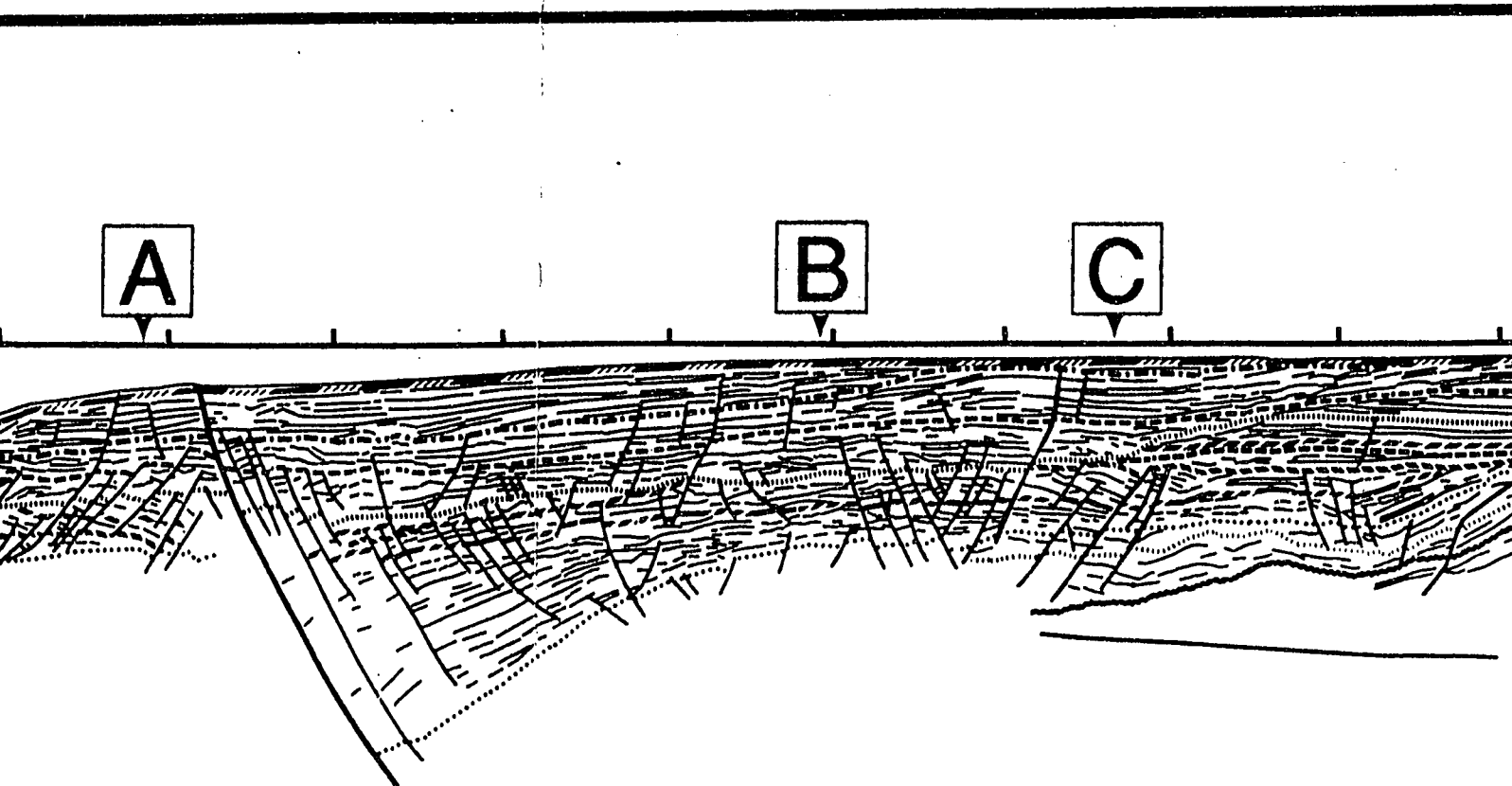
WSW

A



W

A



A

Delfin 1X

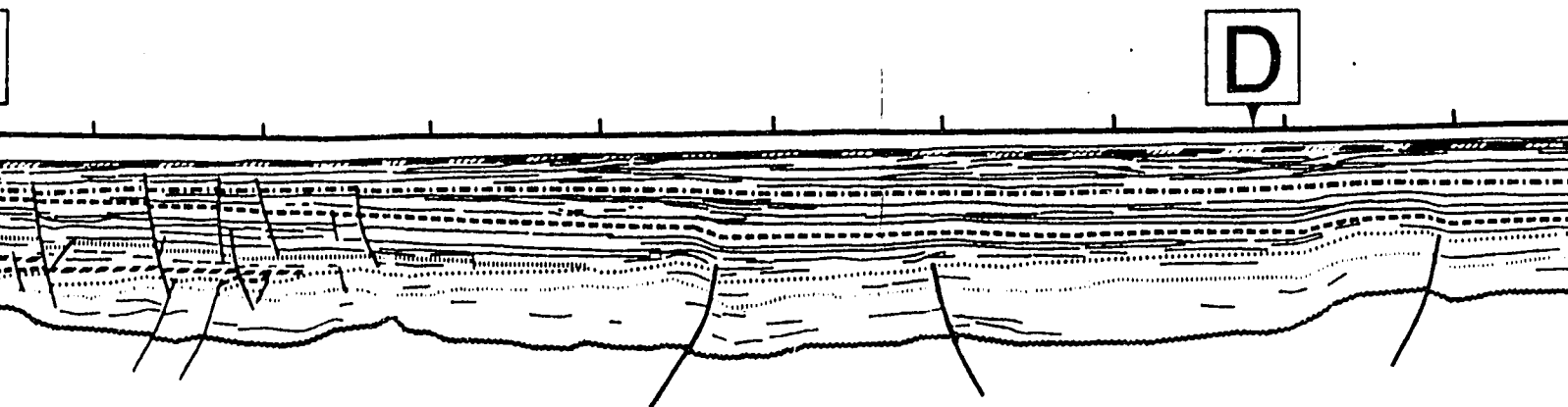
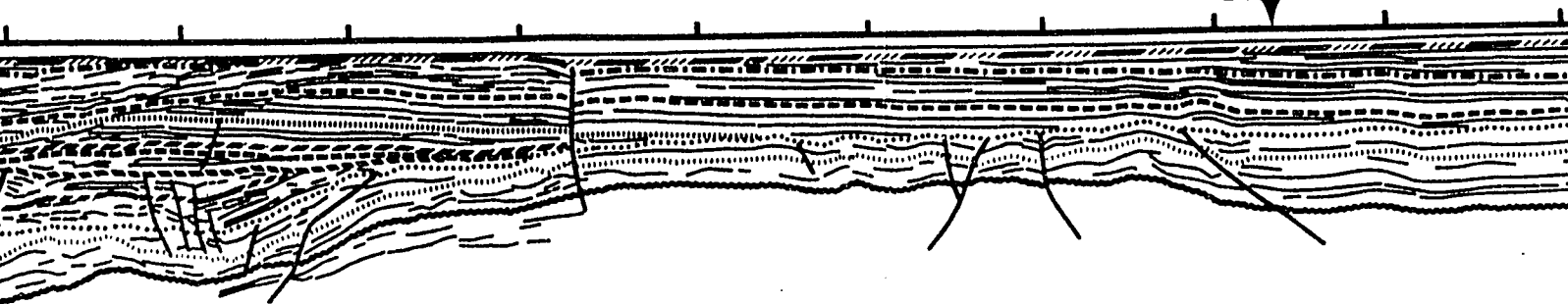


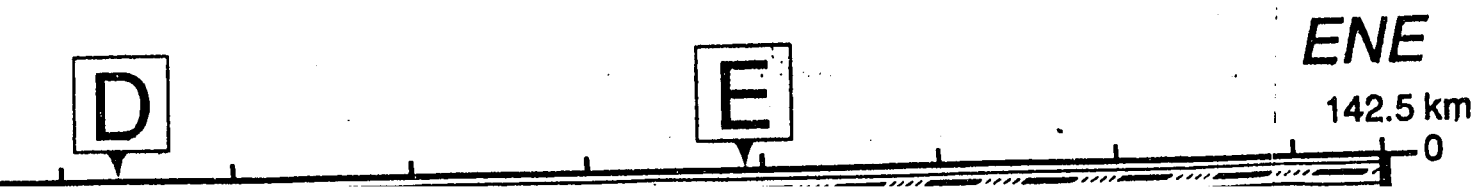
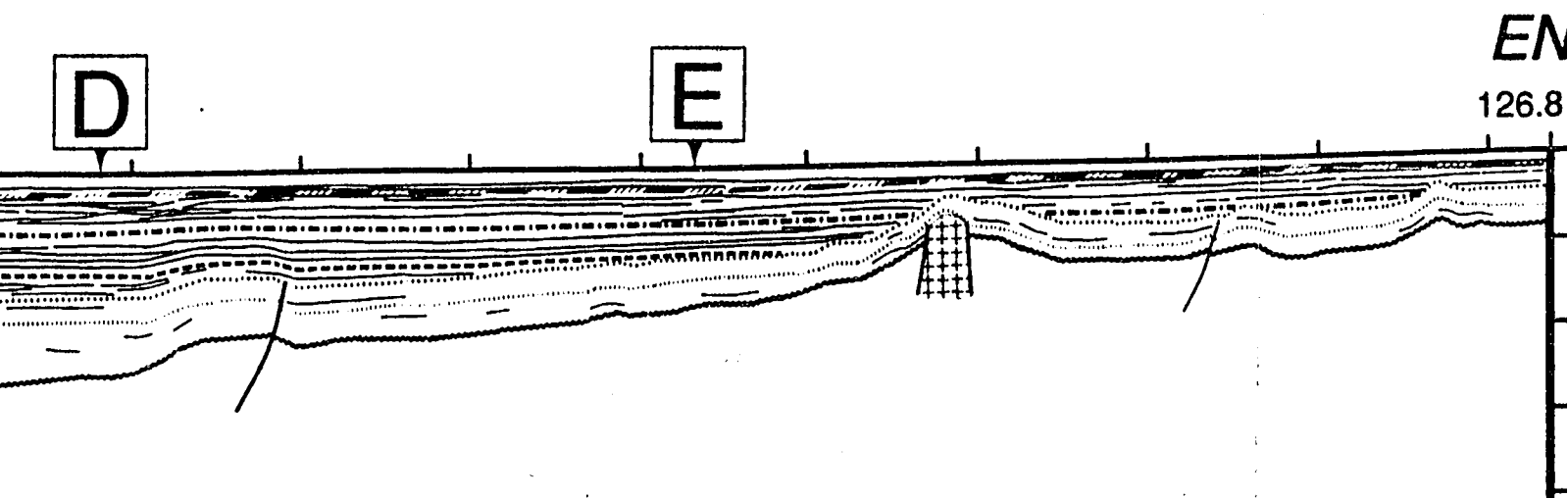
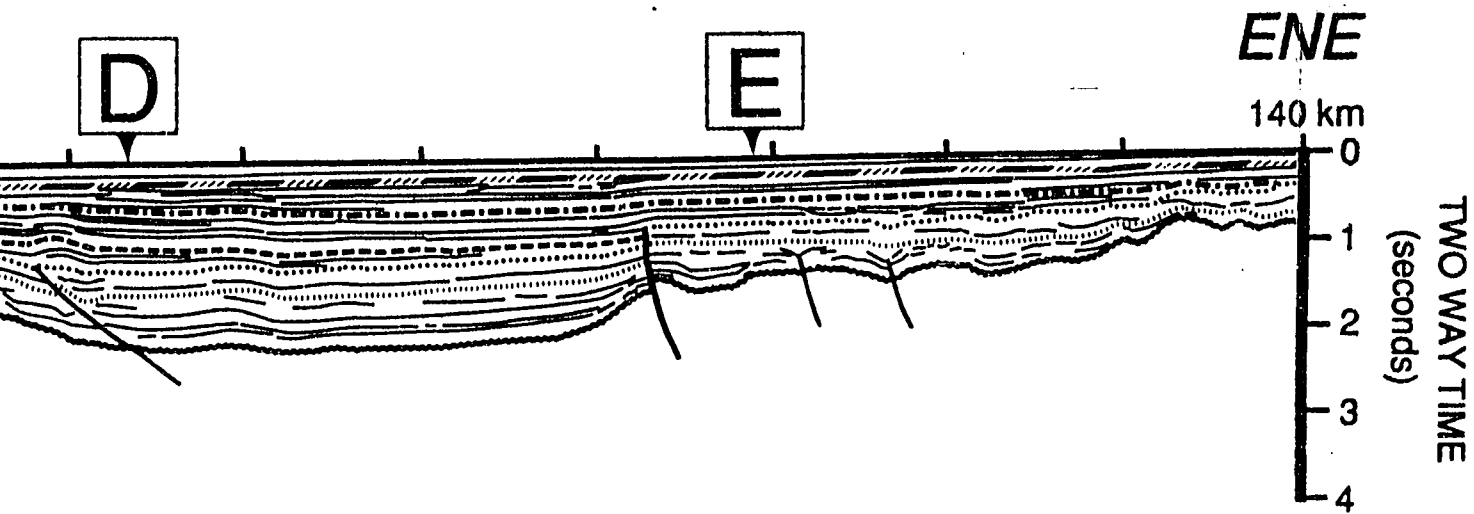
B

Ballena 1X



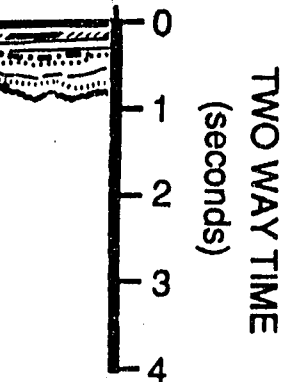
C





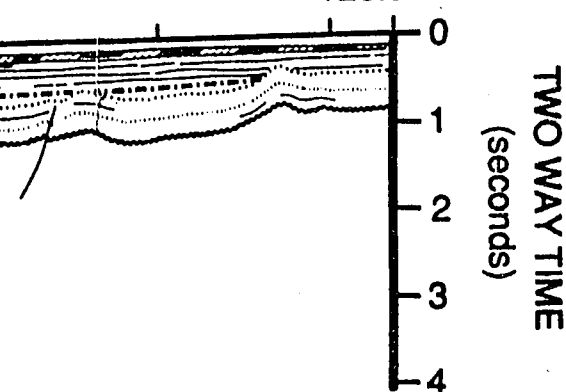
ENE

140 km



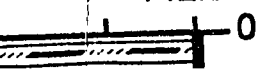
ENE

126.8 km



ENE

142.5 km



L E G

SEQUENCE

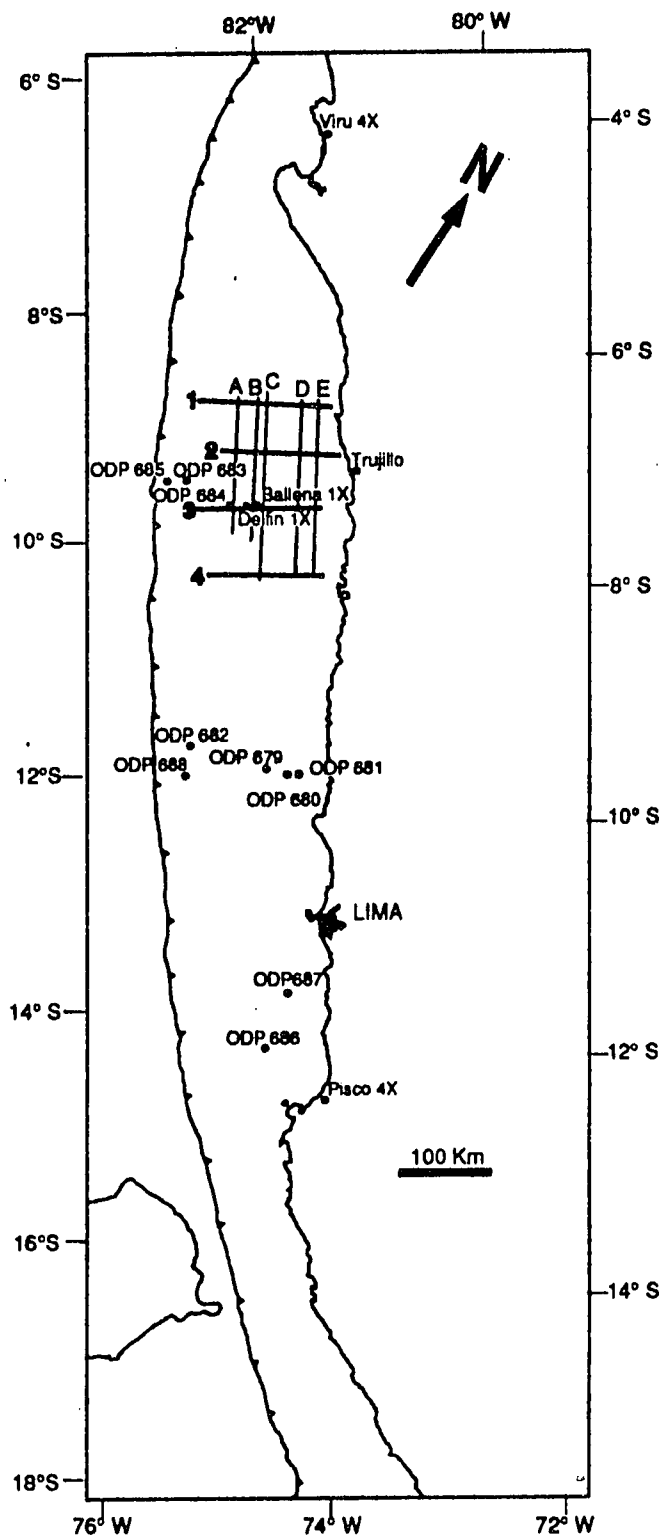
Q	
P	Up
M 3	
M 2	M
M 1	
E-O	Up
E 3	
E 2	
E 1	
E ₀	Lo
K	
PK	Pre

Post-lower to middle Eocene lg

L E G E N D **SEQUENCE A G E**

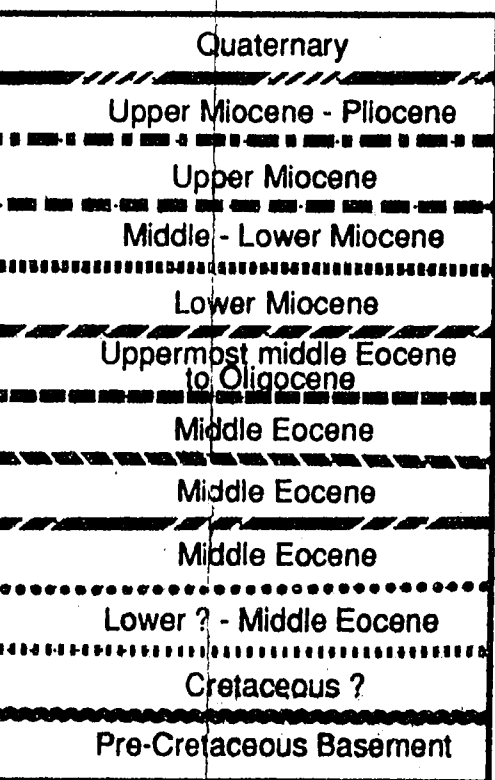
Q	Quaternary
P	Upper Miocene - Pliocene
M 3	Upper Miocene
M 2	Middle - Lower Miocene
M 1	Lower Miocene
E-O	Uppermost middle Eocene to Oligocene
E 3	Middle Eocene
E 2	Middle Eocene
E 1	Middle Eocene
E₀	Lower ? - Middle Eocene
K	Cretaceous ?
PK	Pre-Cretaceous Basement

er to middle Eocene igneous intrusive

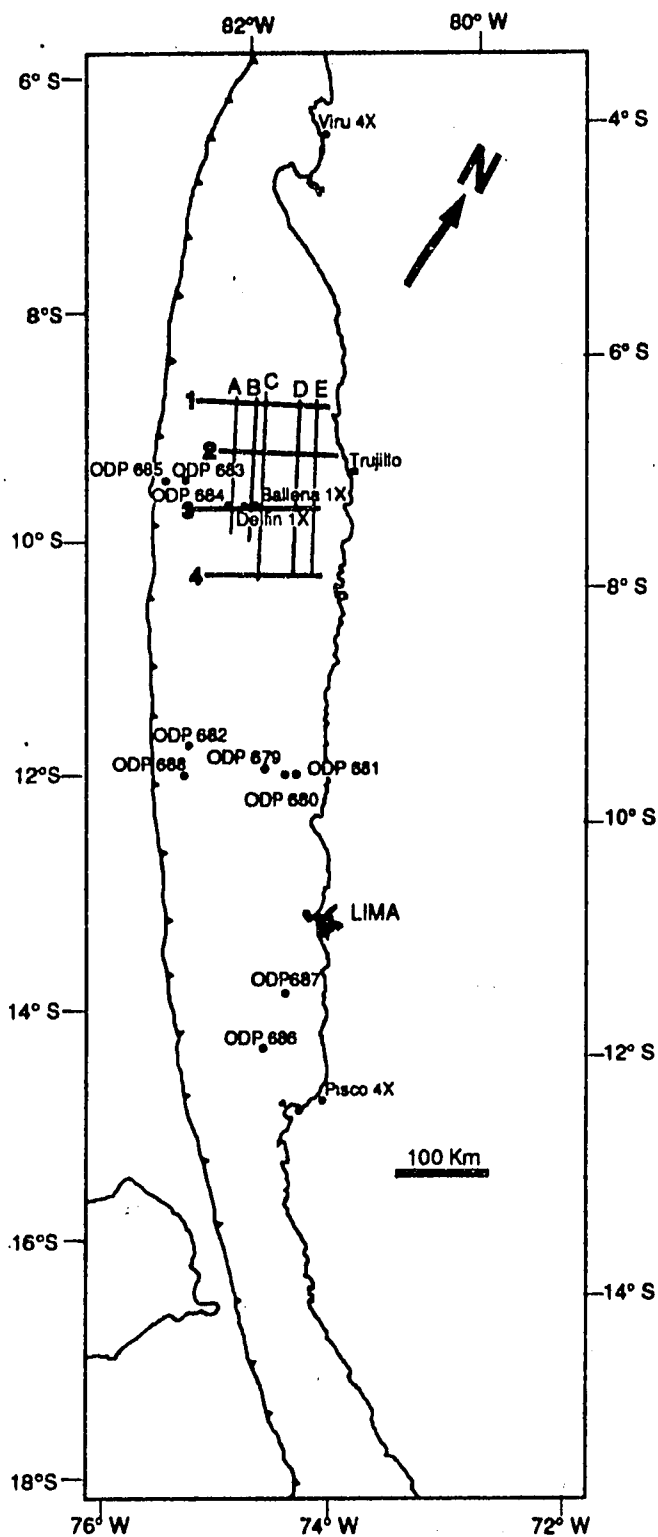


LEGEND

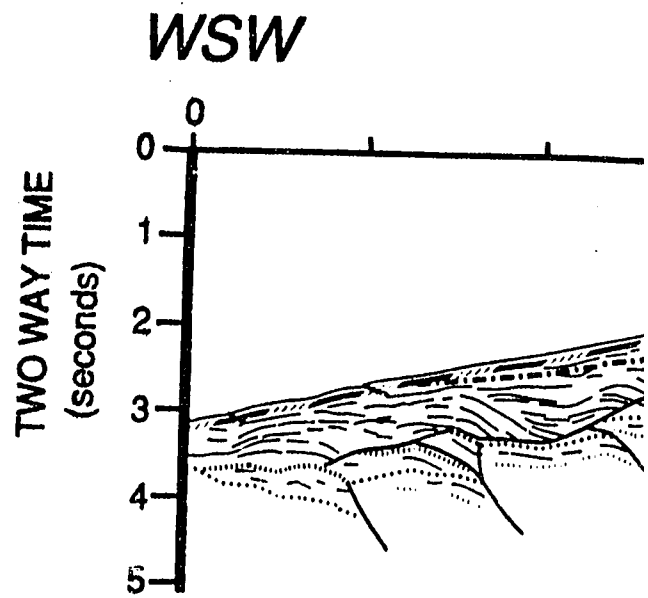
AGE



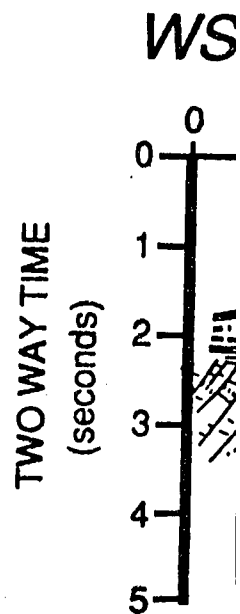
ocene Igneous Intrusive

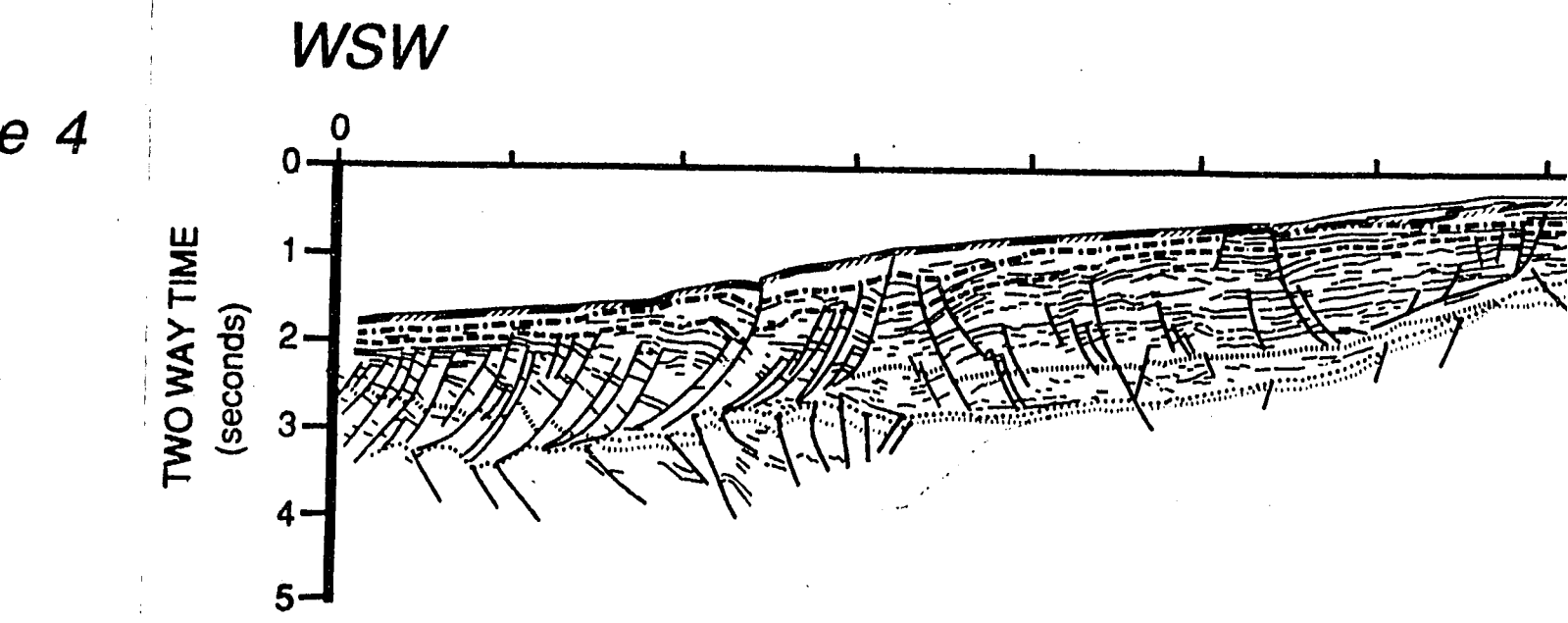
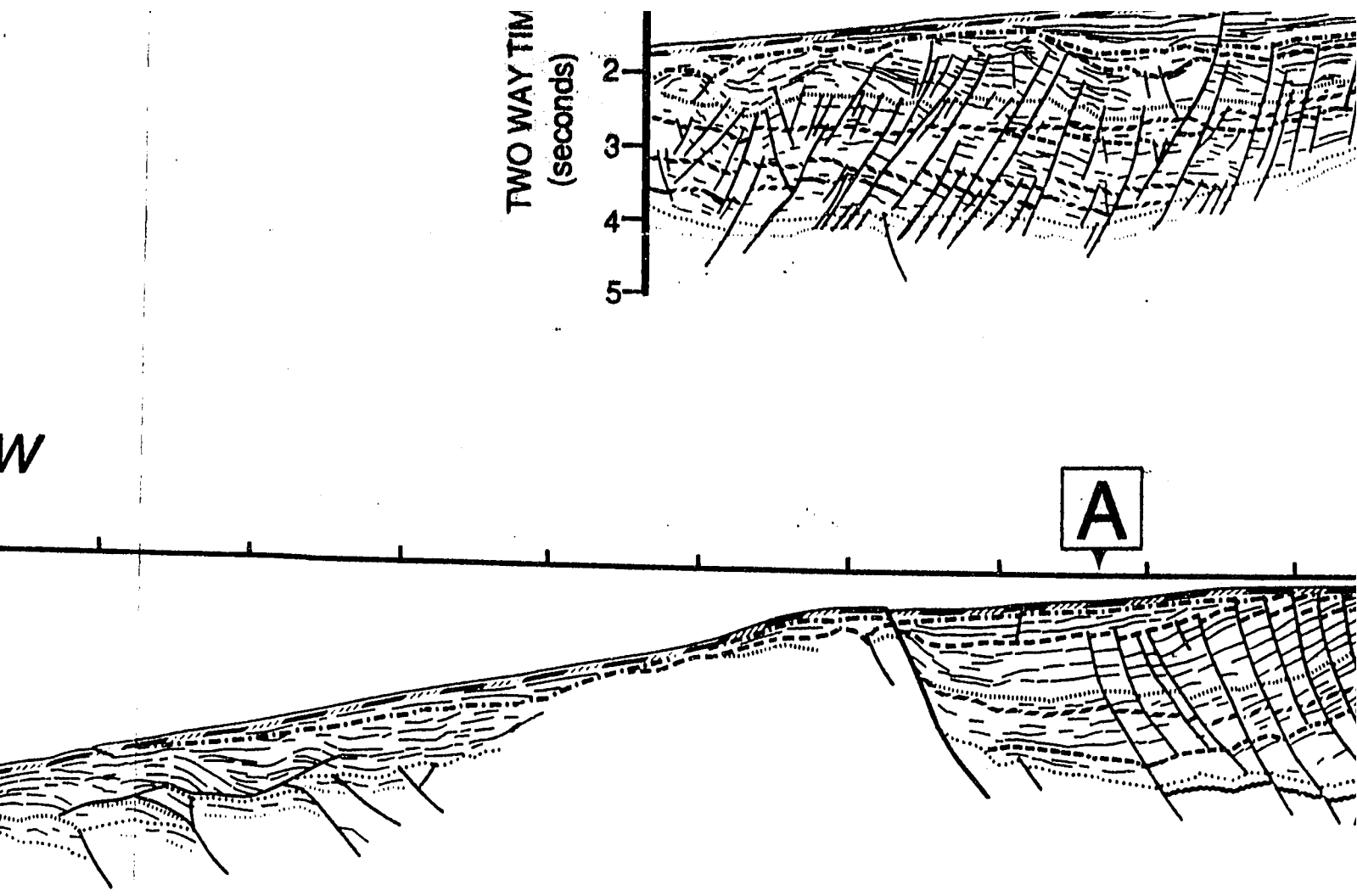


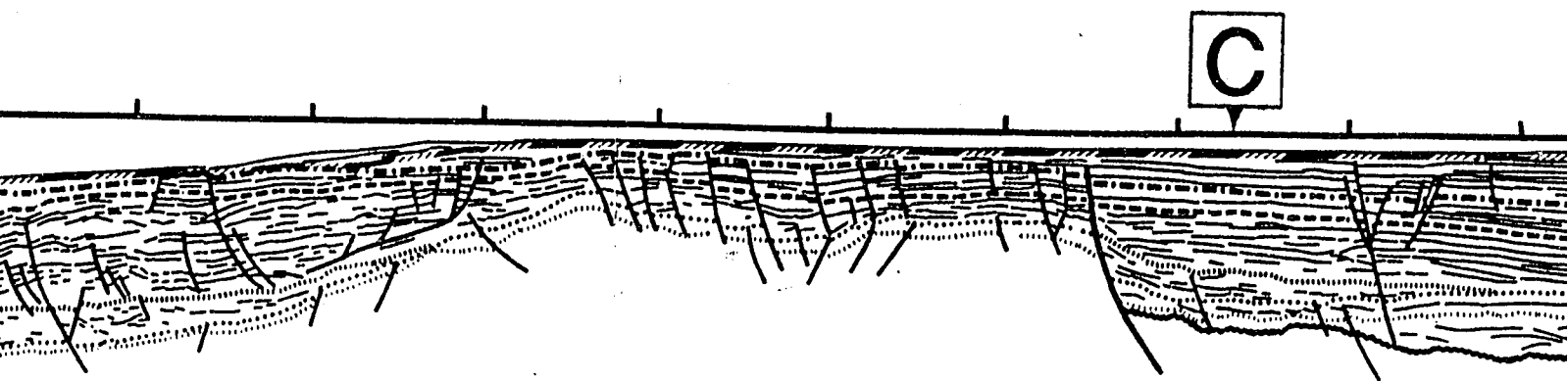
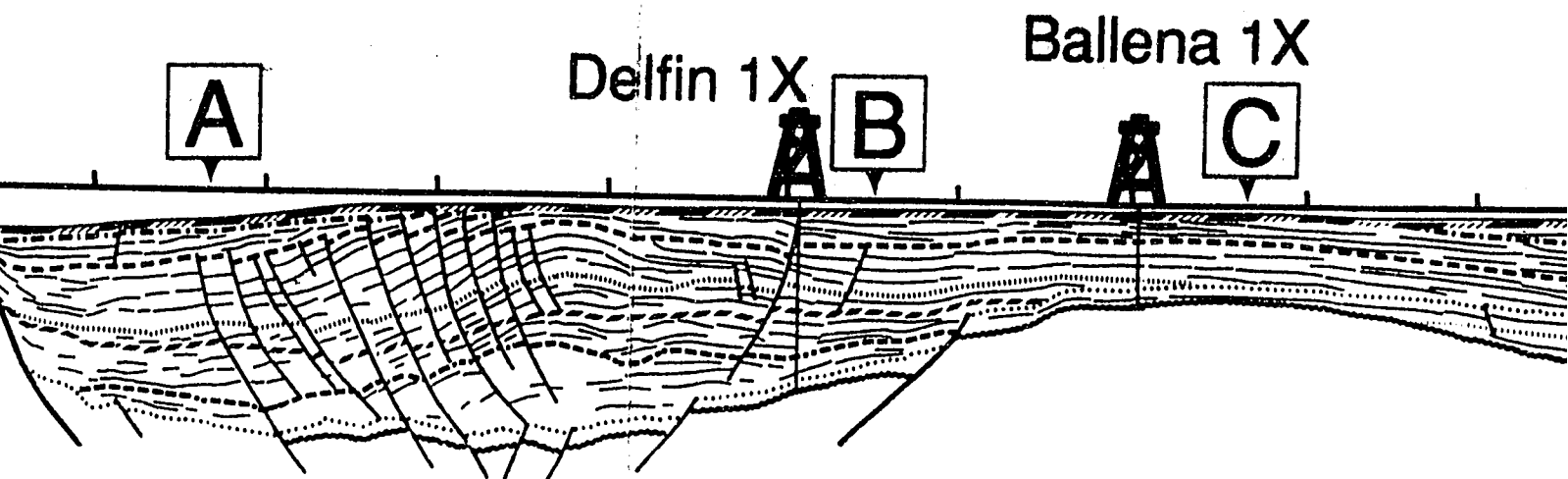
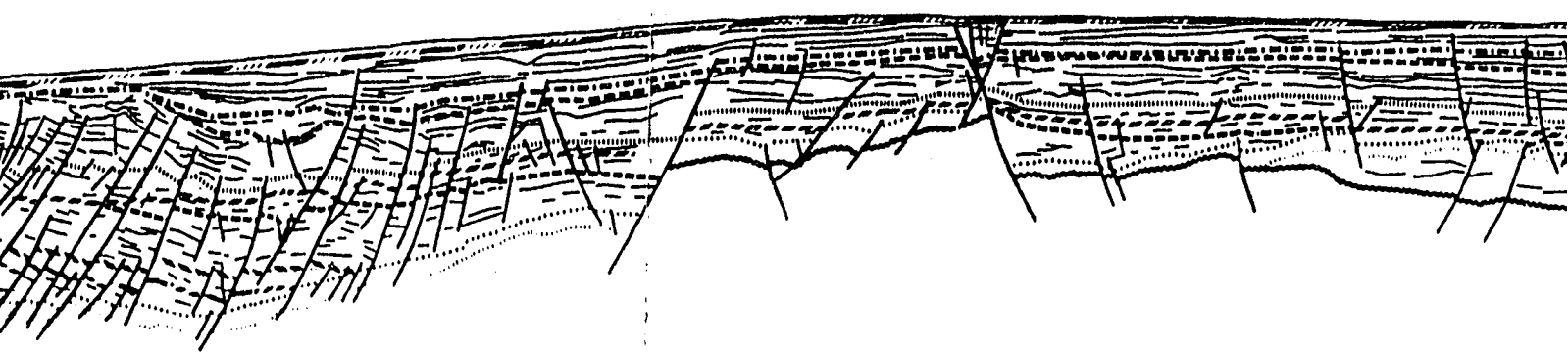
Profile 3



Profile 4

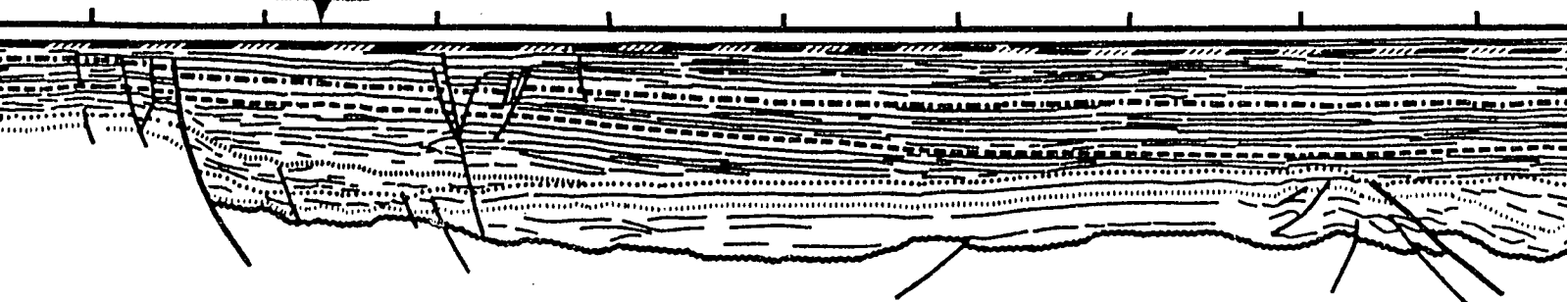
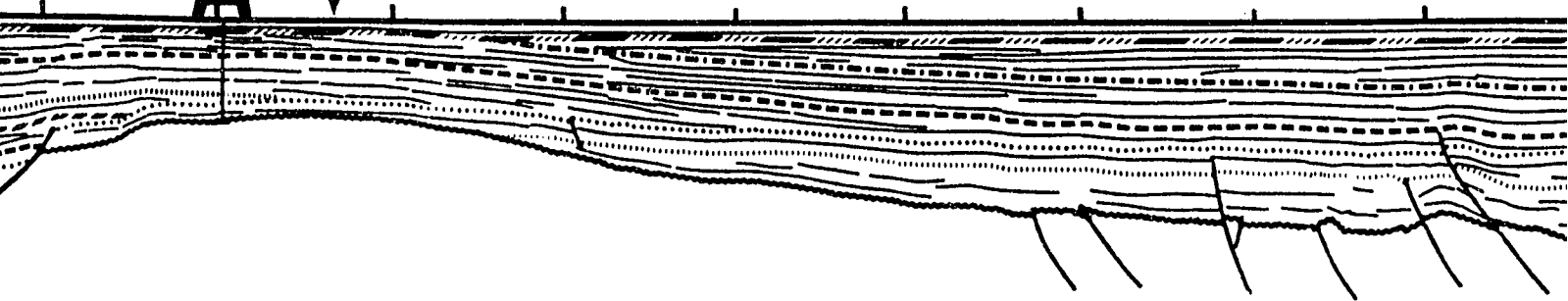


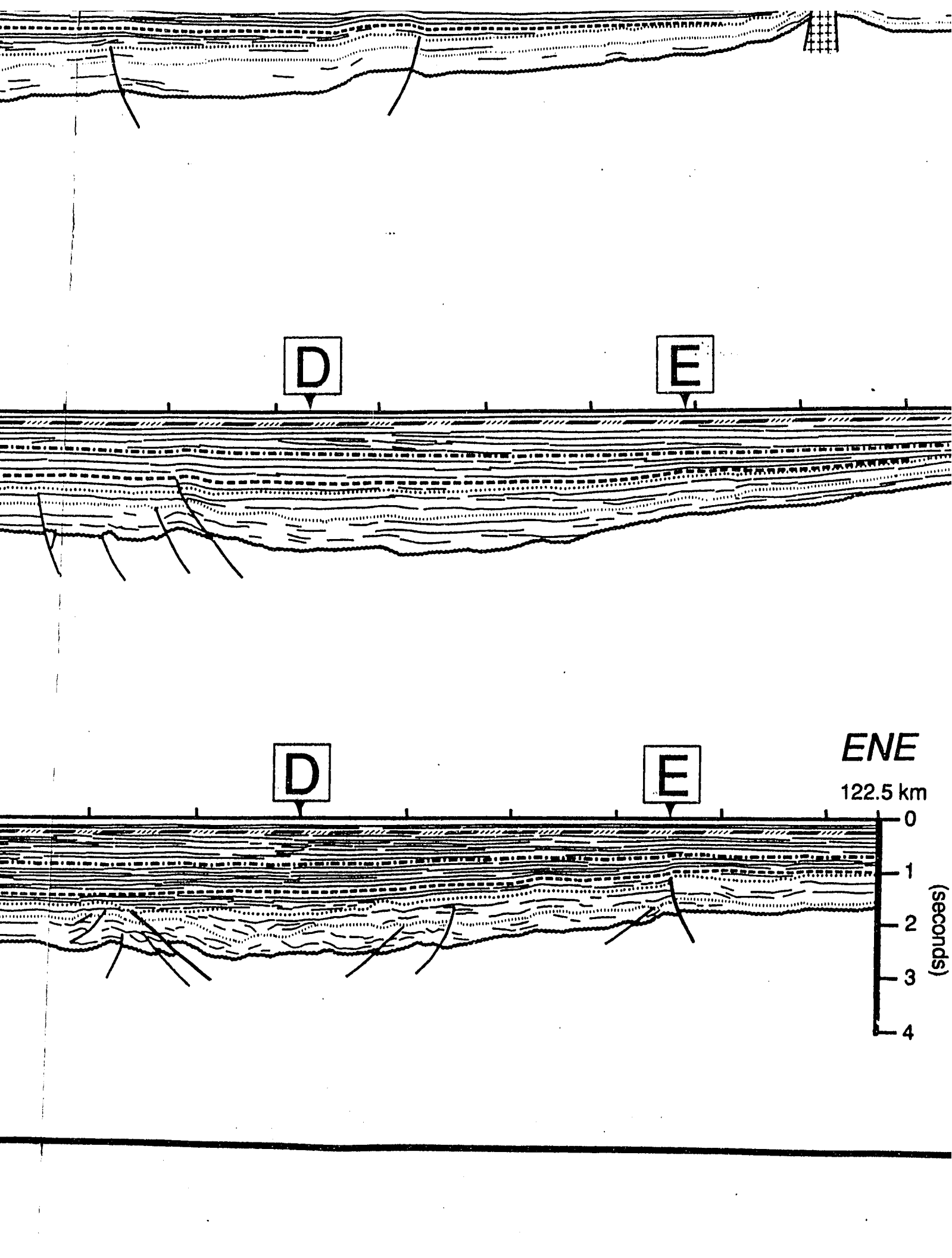


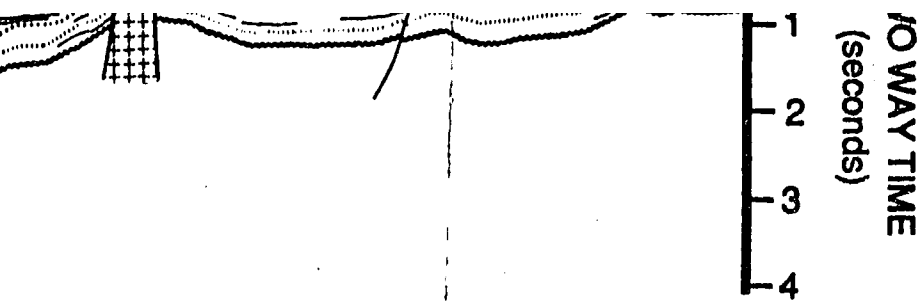




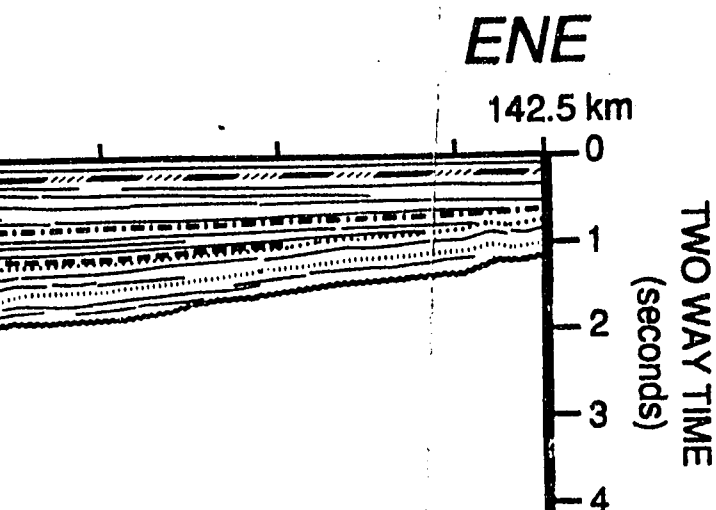
Ballena 1X



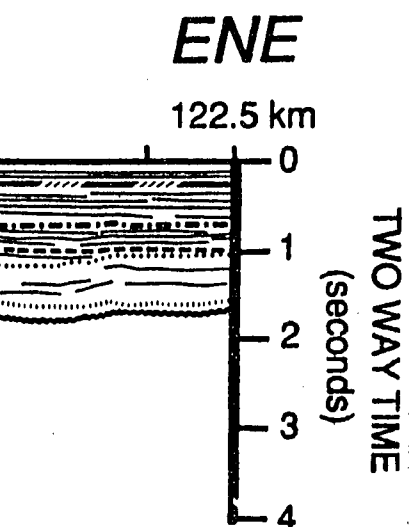




Post-lower

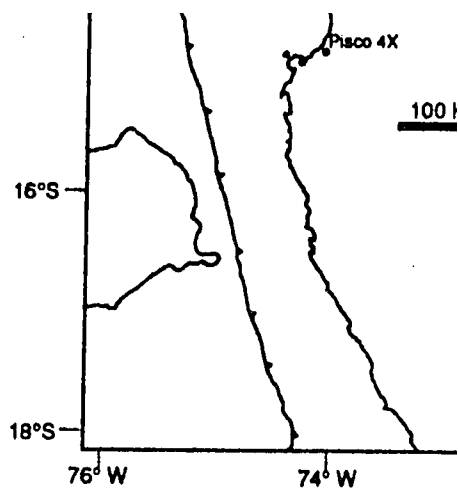
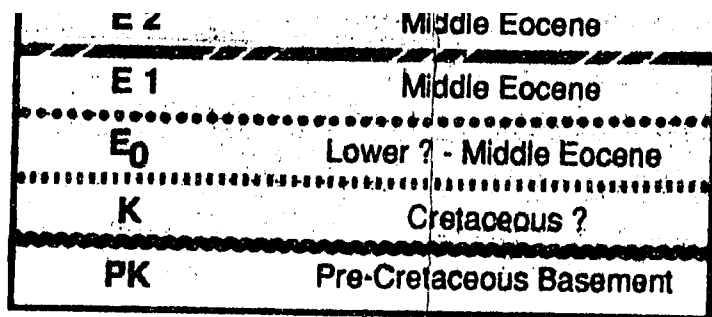


LINE DRAWING FOREARC R NORTH CENT

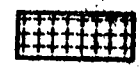


PANE

0

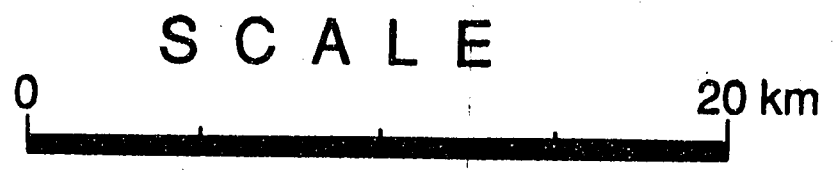


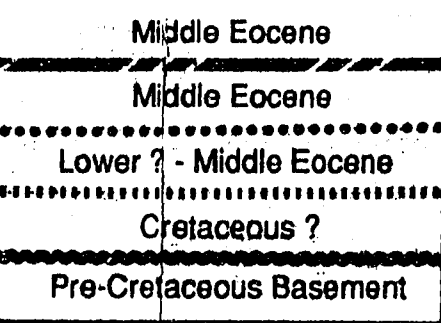
Post-lower to middle Eocene Igneous Intrusive



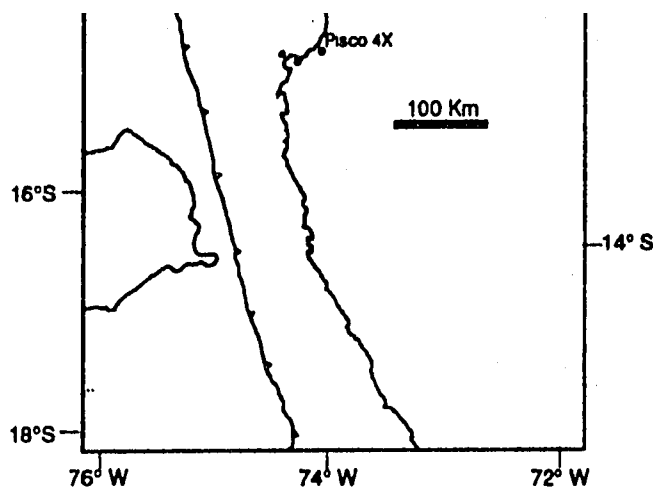
DRAWING OF SEISMIC PROFILES EARC REGION OFFSHORE PERU CENTRAL PART OF STUDY AREA

PANEL 1 - DIP LINES





ene Igneous intrusive



SEISMIC PROFILES OFFSHORE PERU PART OF STUDY AREA

DIP LINES

SCALE

20 km



PLEASE NOTE:

Oversize maps and charts are filmed in sections in the following manner:

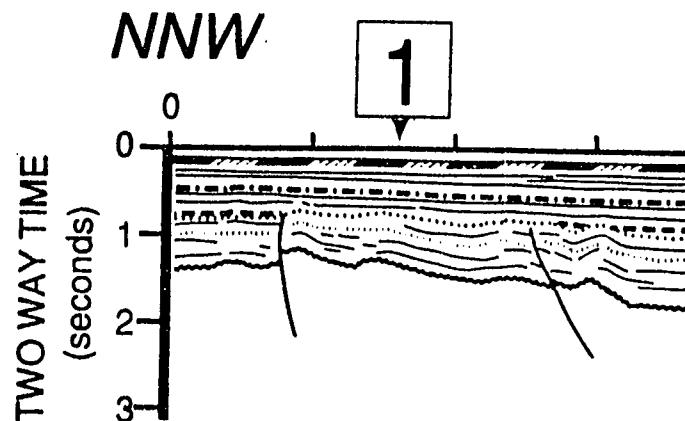
LEFT TO RIGHT, TOP TO BOTTOM, WITH SMALL OVERLAPS

The following map or chart has been refilmed in its entirety at the end of this dissertation (not available on microfiche). A xerographic reproduction has been provided for paper copies and is inserted into the inside of the back cover.

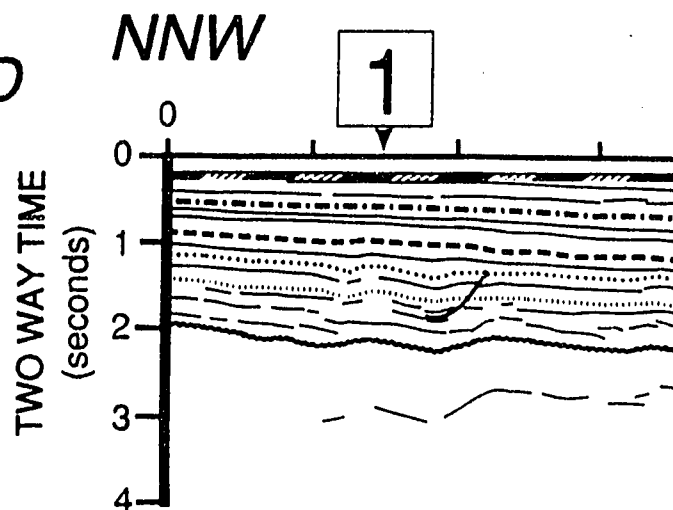
Black and white photographic prints (17" x 23") are available for an additional charge.

UMI

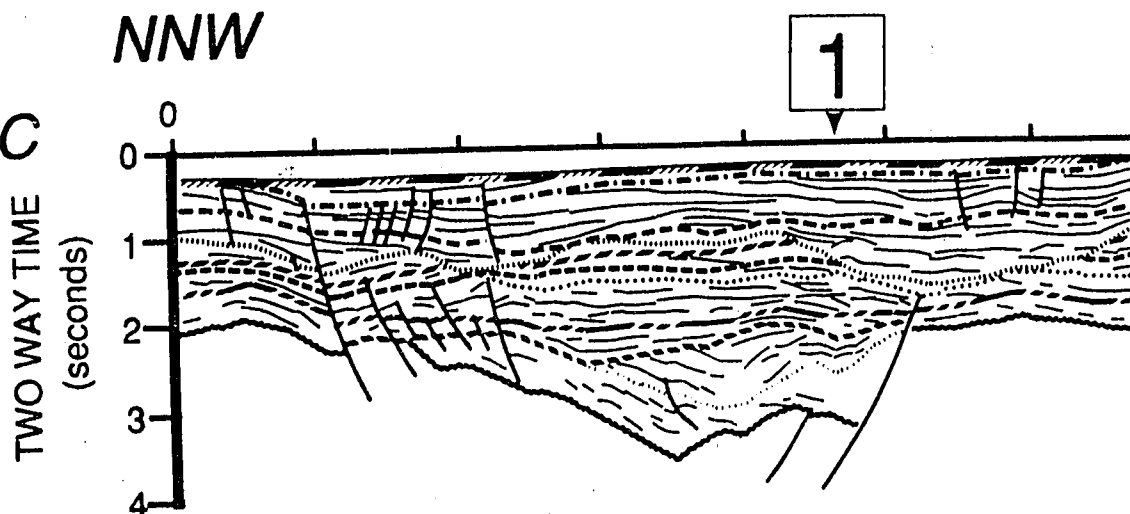
Profile E



Profile D



Profile C

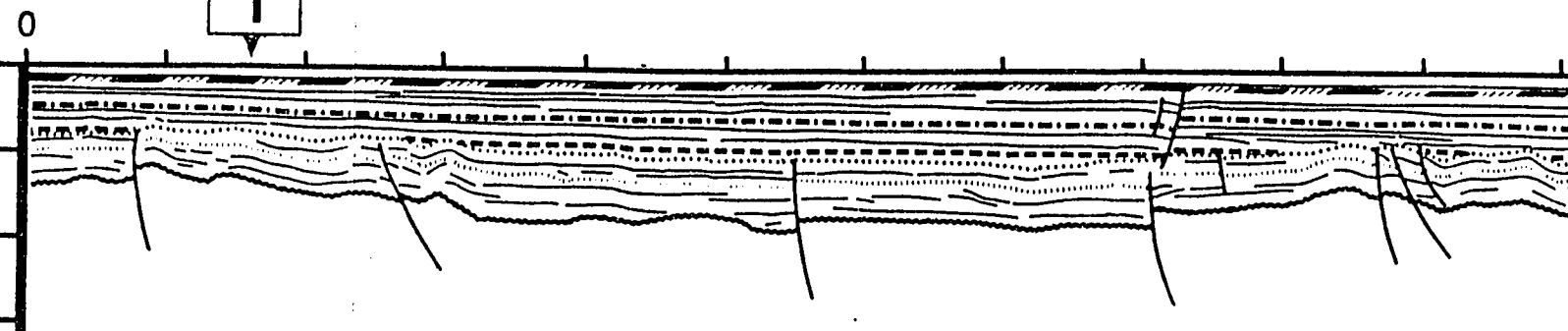


Profile B



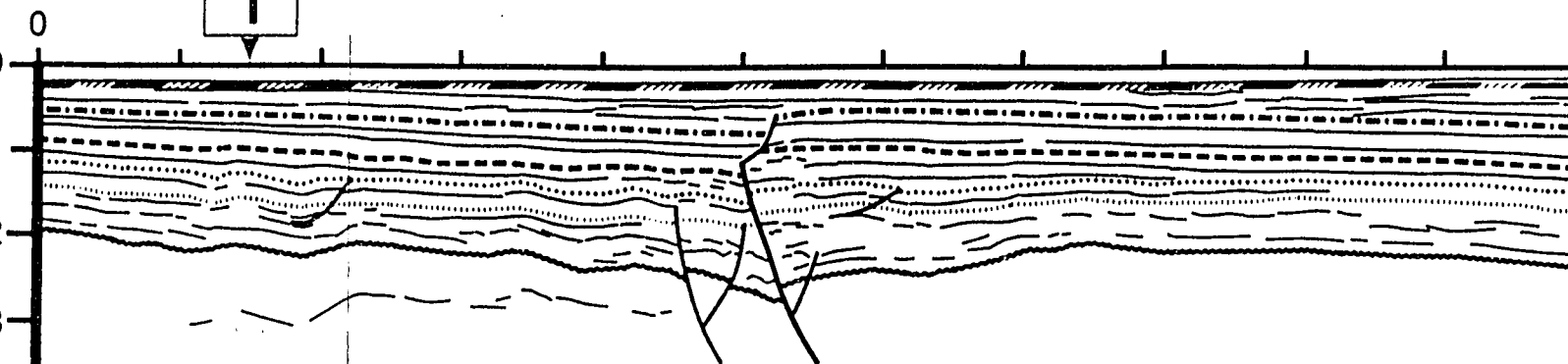
INW

1

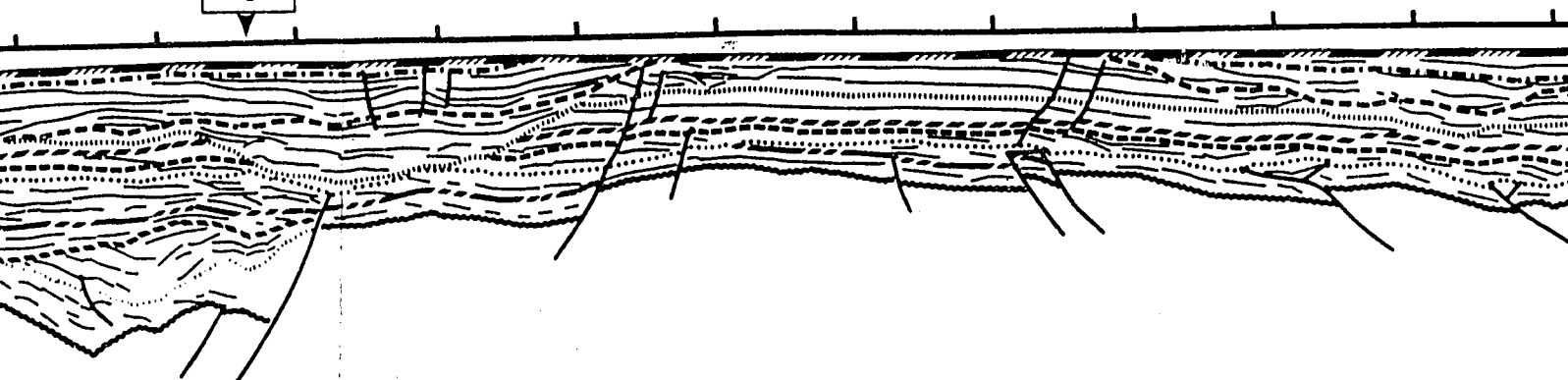


VNW

1

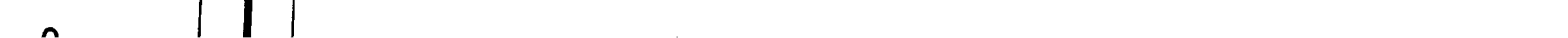


1

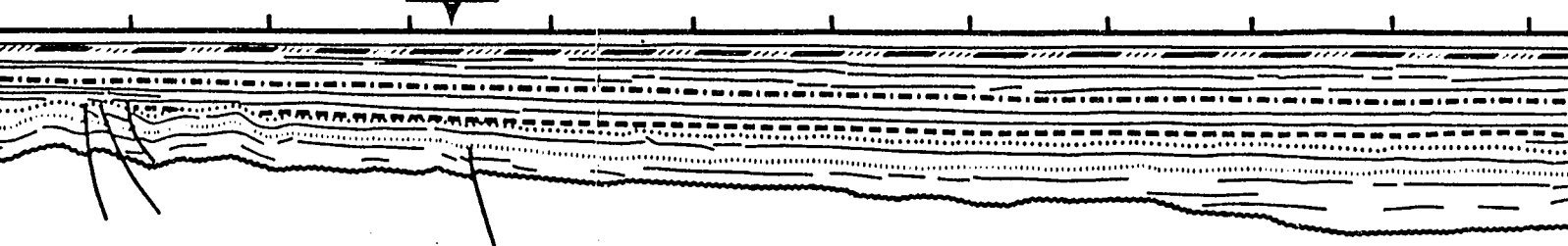


VNW

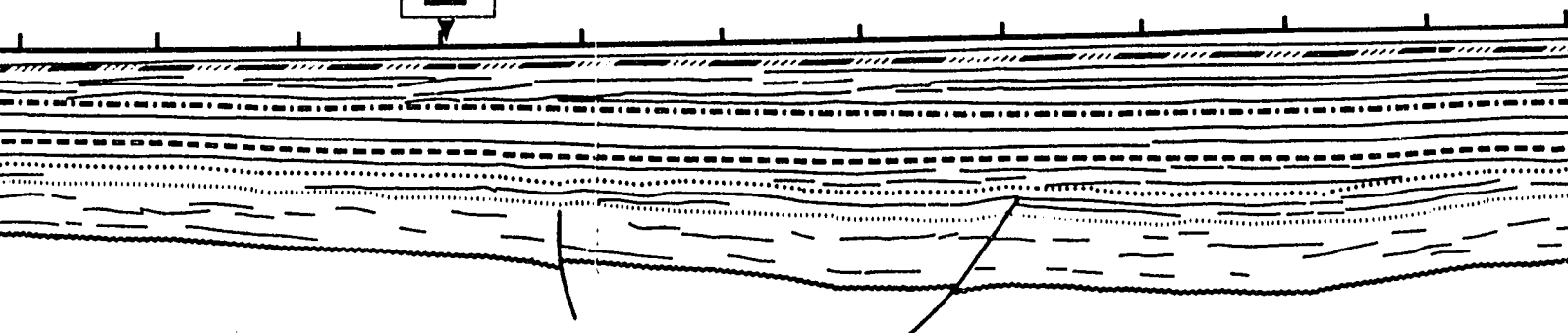
1



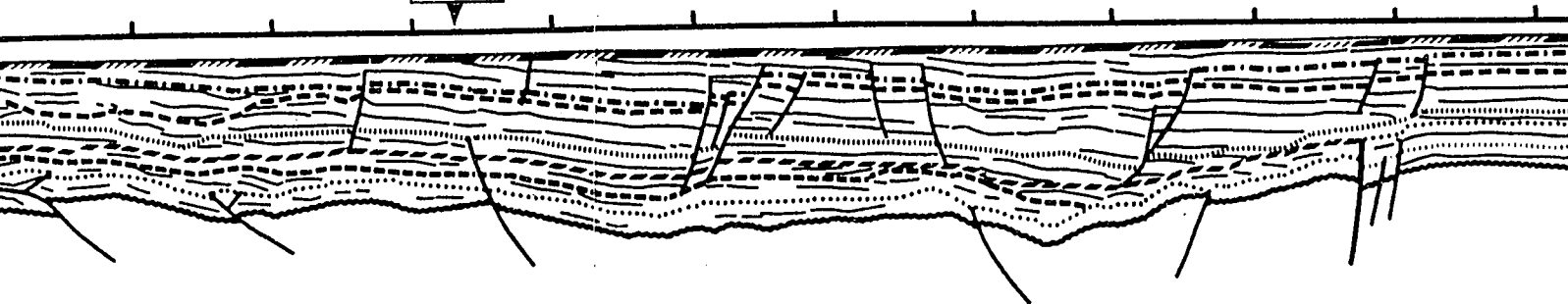
2



2

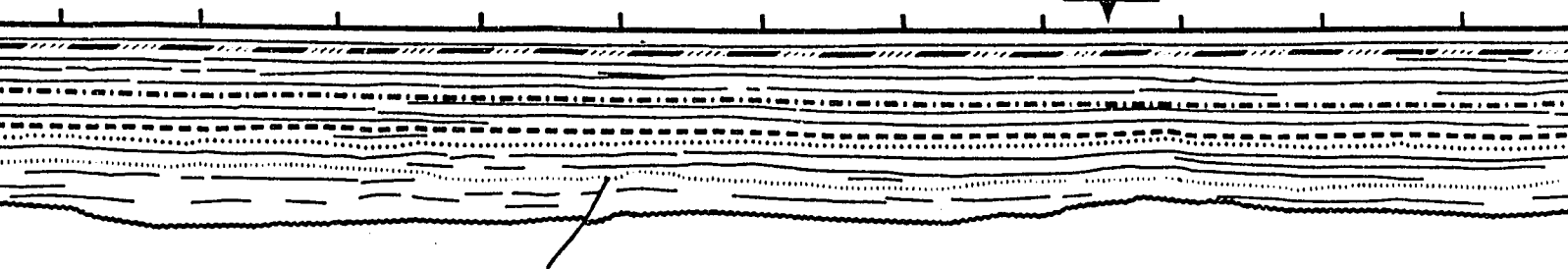


2

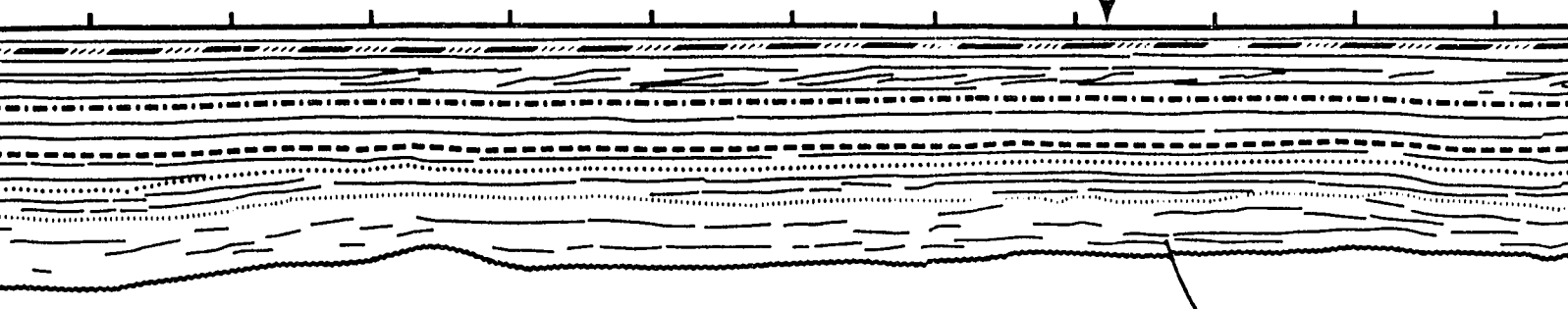


2

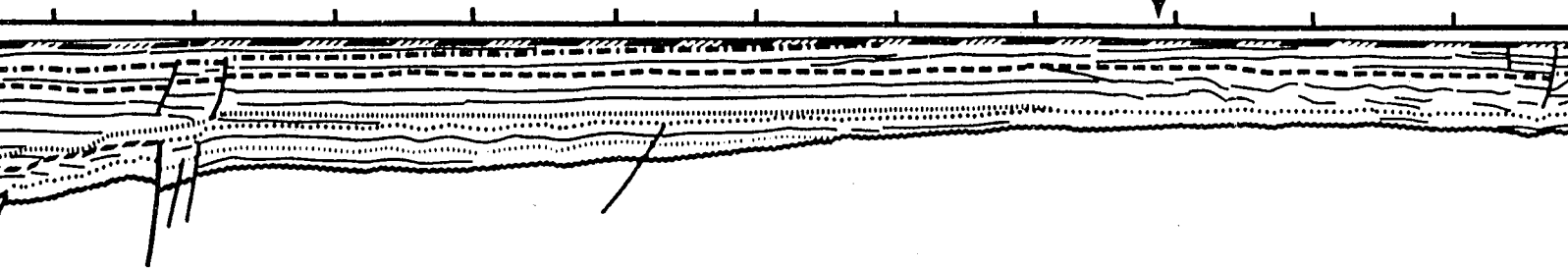
3



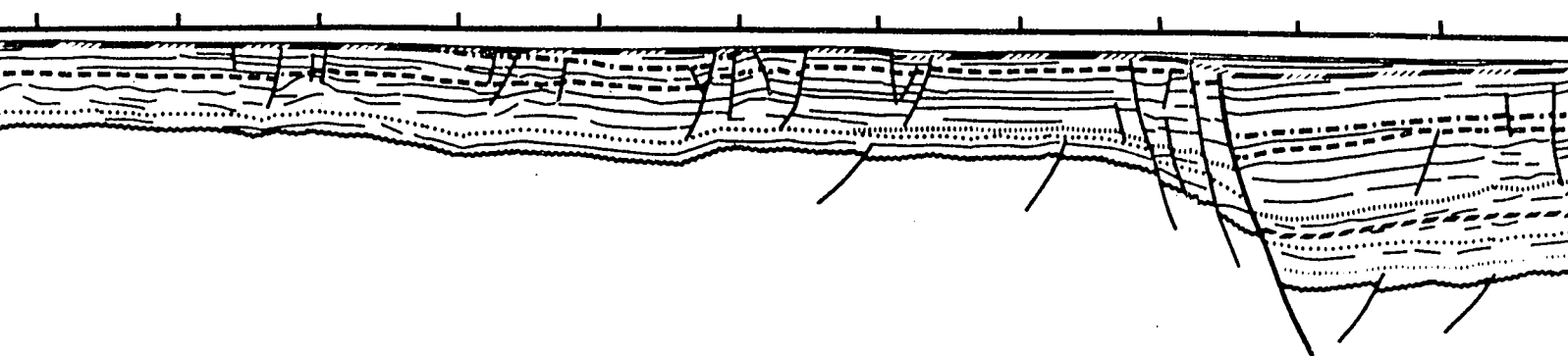
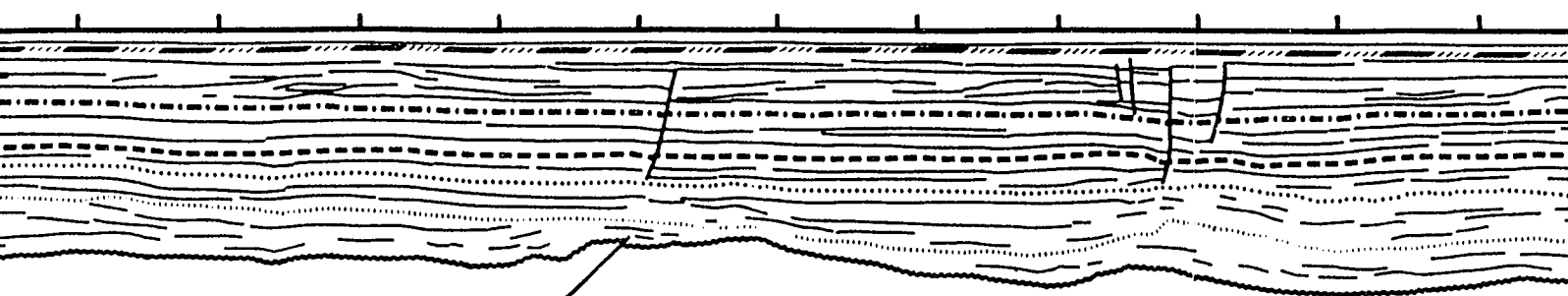
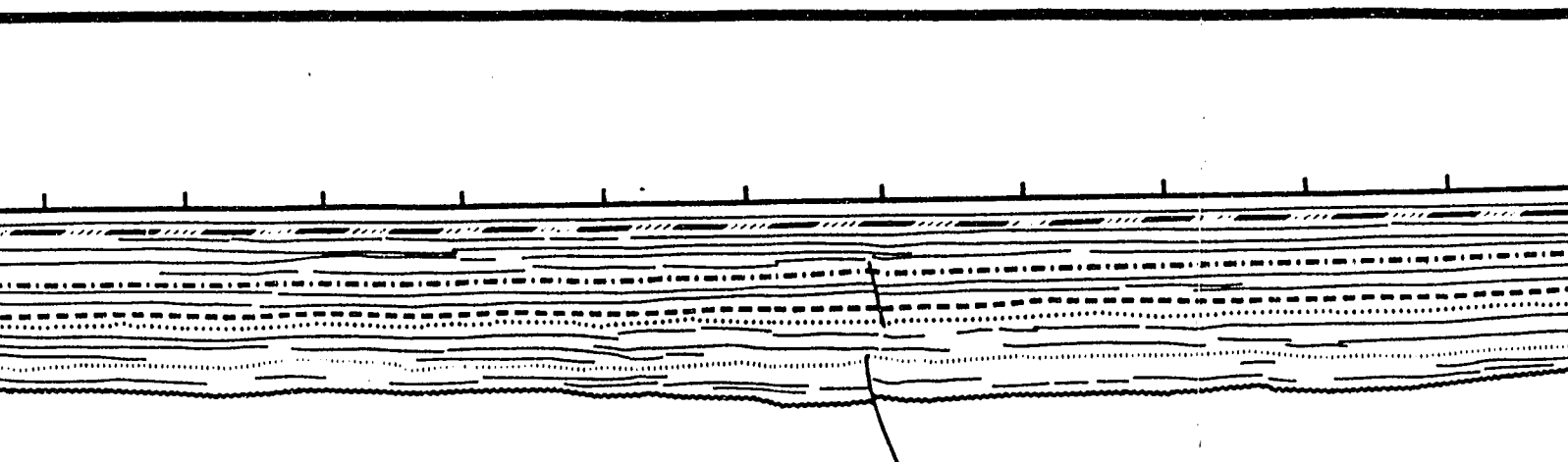
3



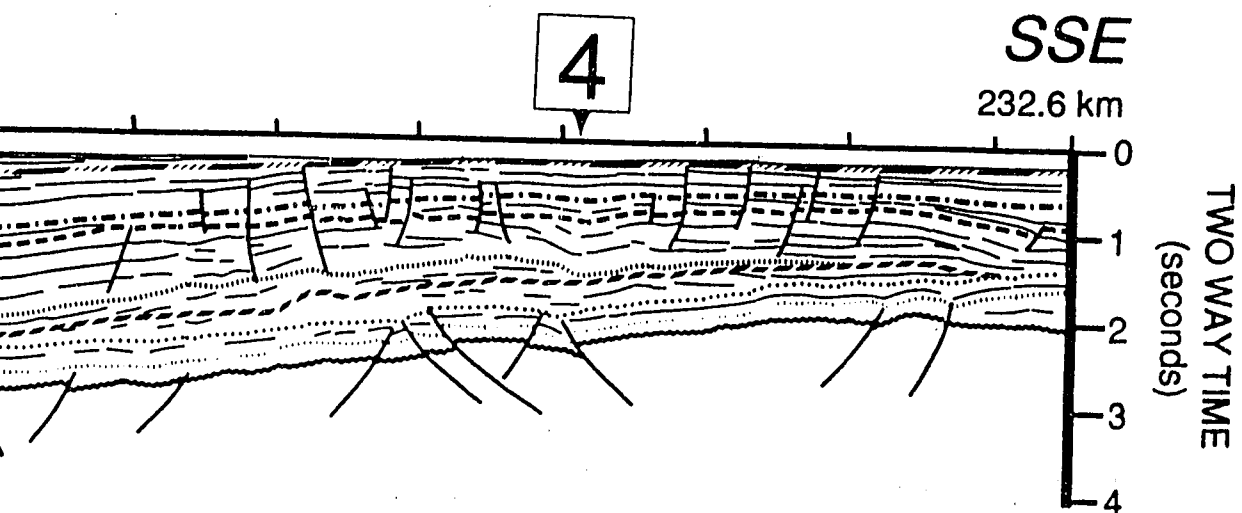
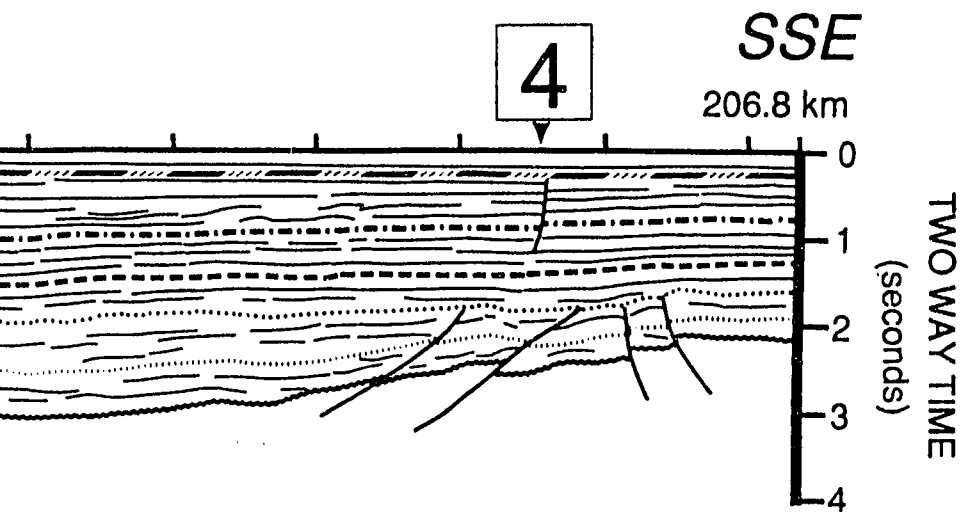
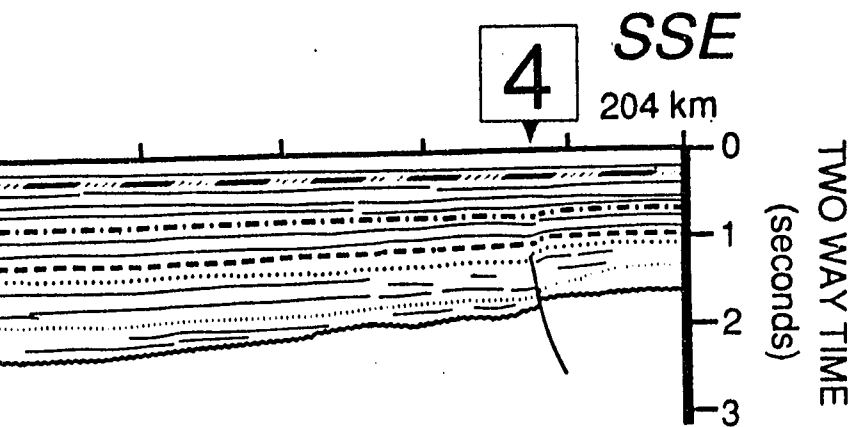
3



3



SSE
155 km

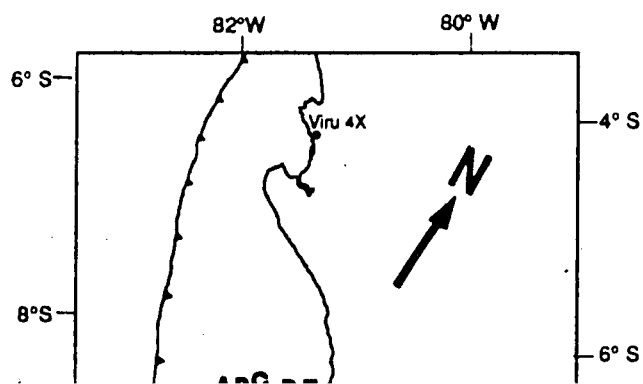


0

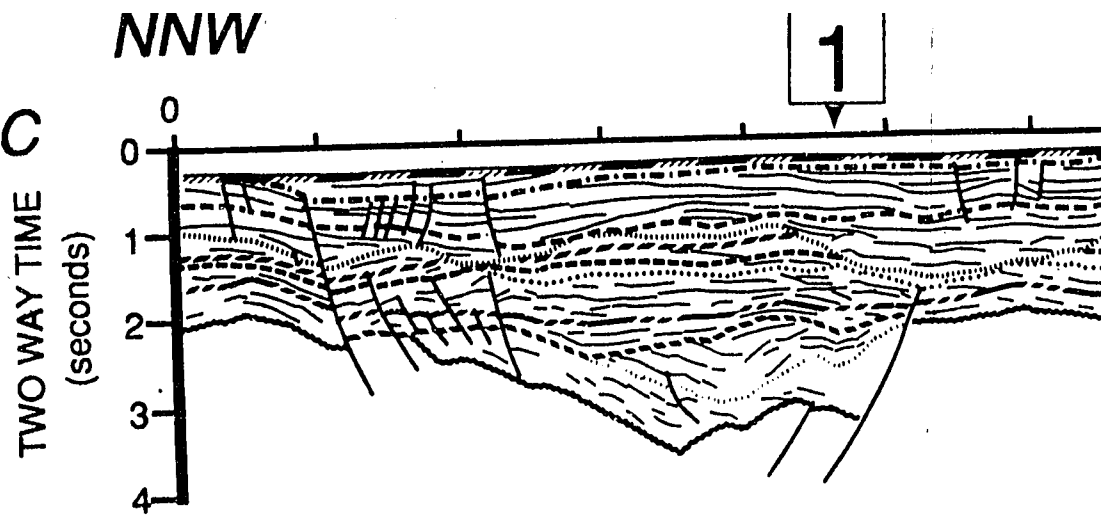
L E G E N D **SEQUENCE A G E**

Q	Quaternary
P	Upper Miocene - Pliocene
M 3	Upper Miocene
M 2	Middle - Lower Miocene
M 1	Lower Miocene
E-O	Uppermost middle Eocene to Oligocene
E 3	Middle Eocene
E 2	Middle Eocene
E 1	Middle Eocene
E₀	Lower ? - Middle Eocene
K	Cretaceous ?
PK	Pre-Cretaceous Basement

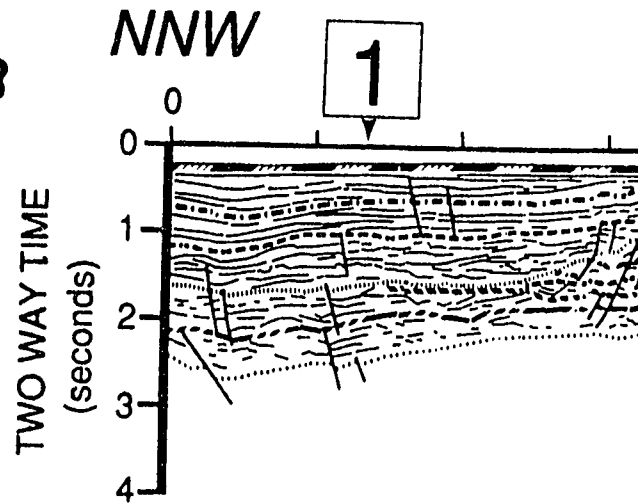
S C A L E



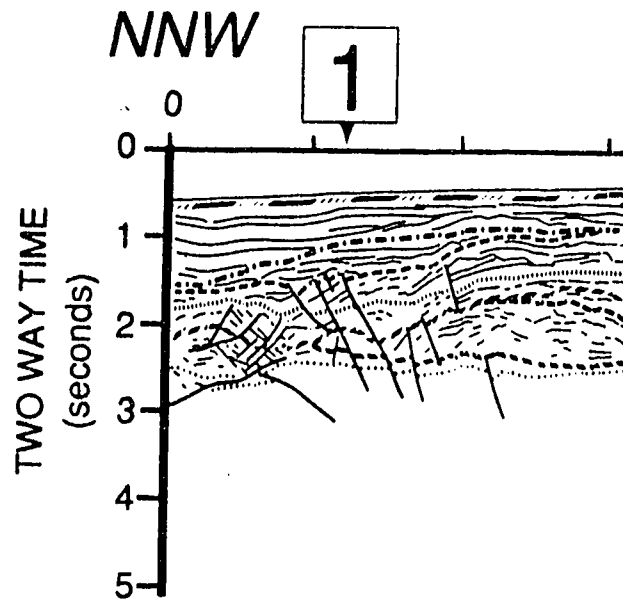
Profile C

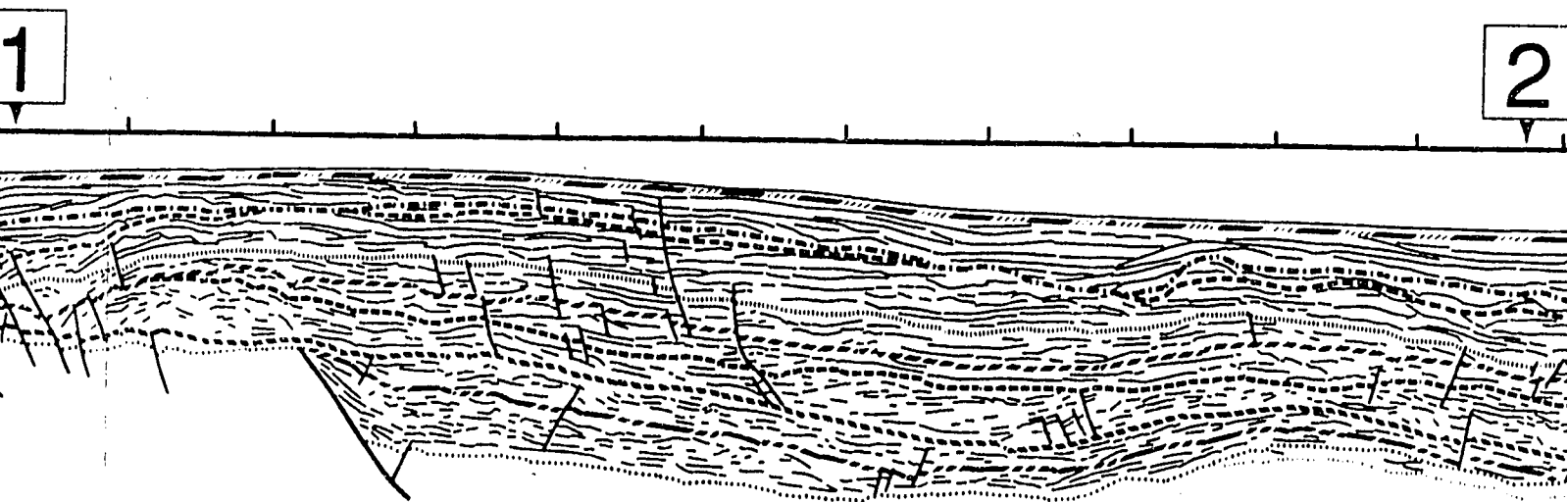
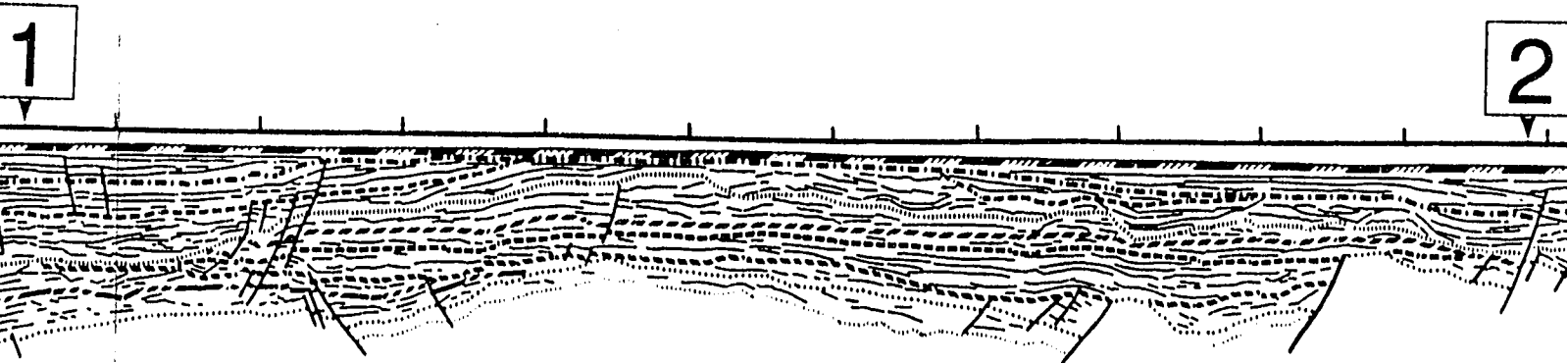
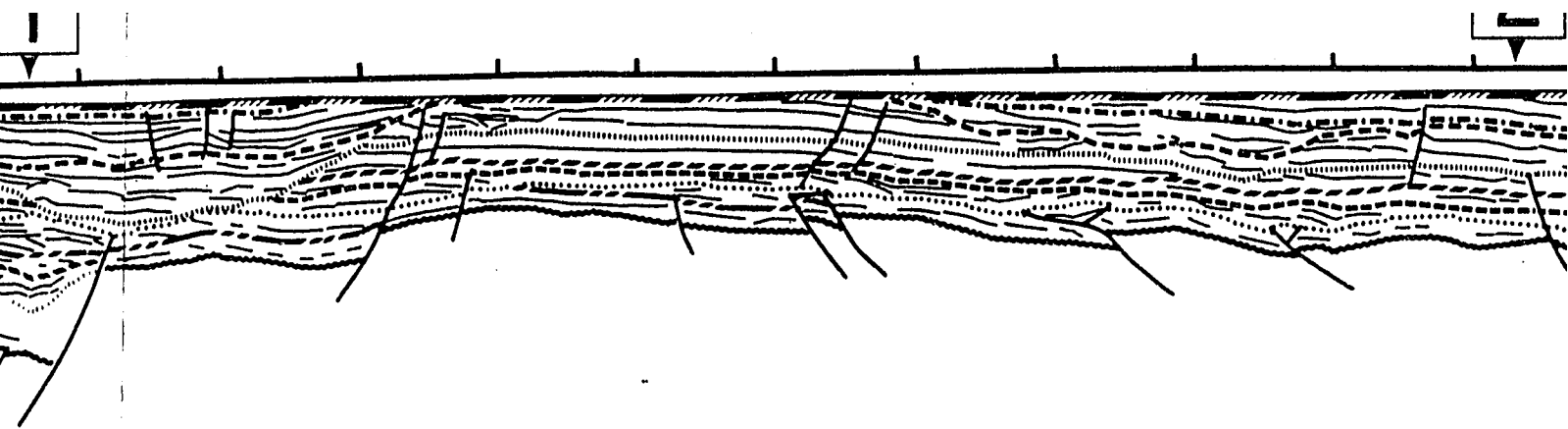


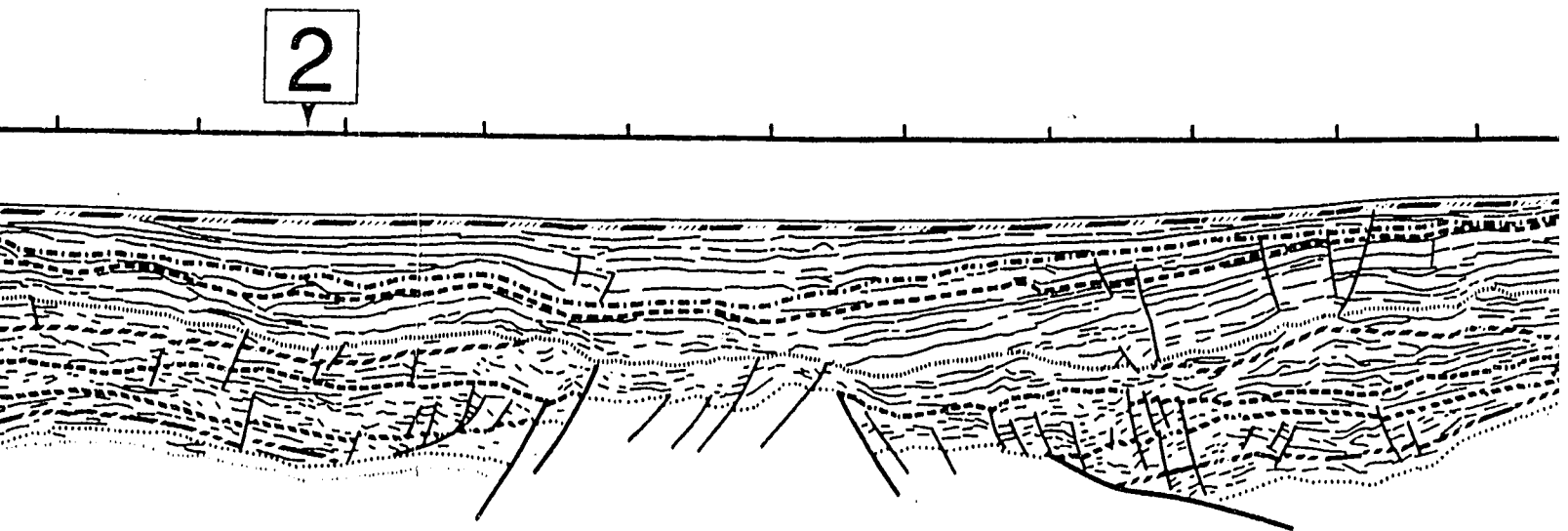
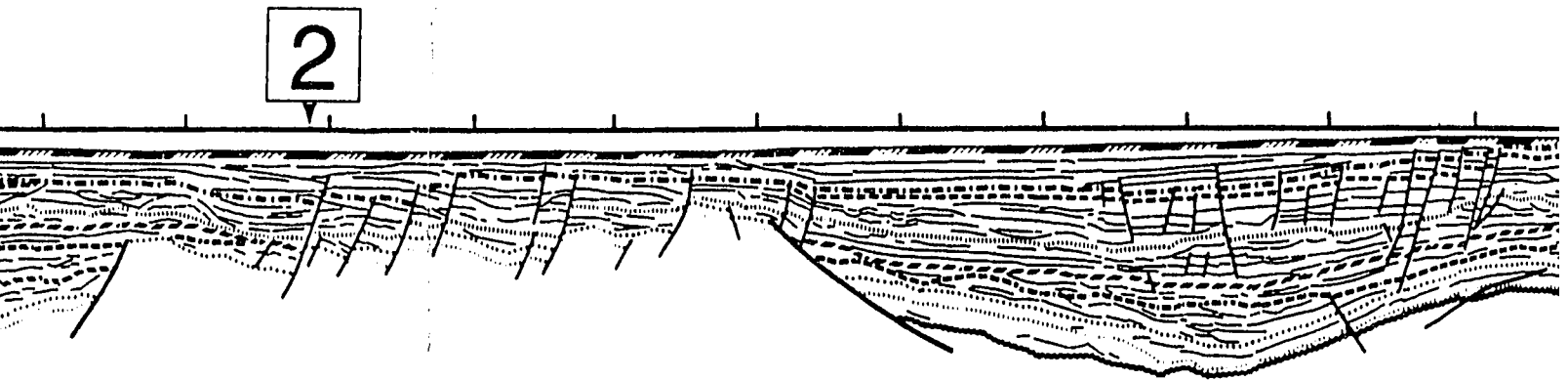
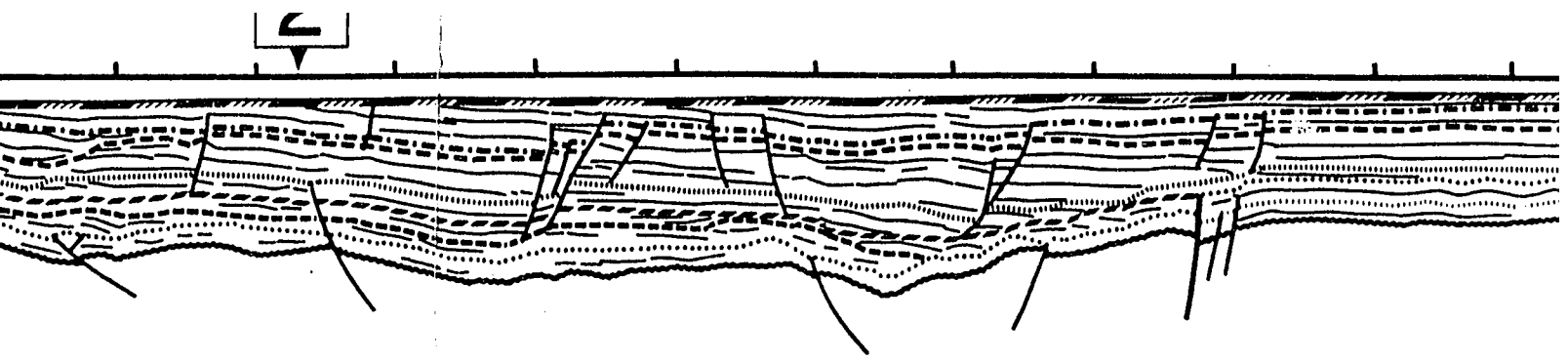
Profile B

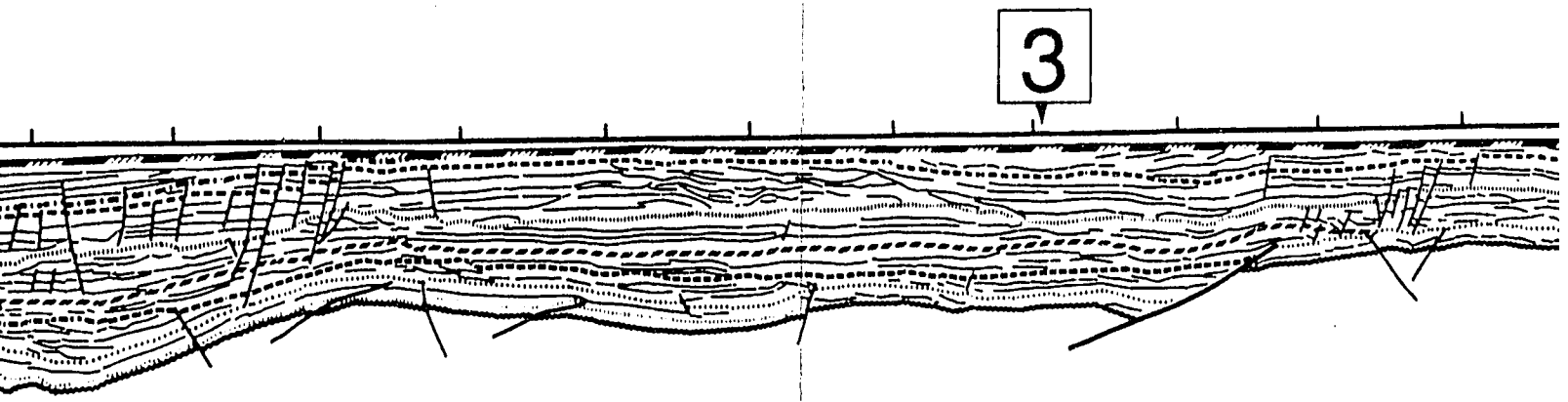
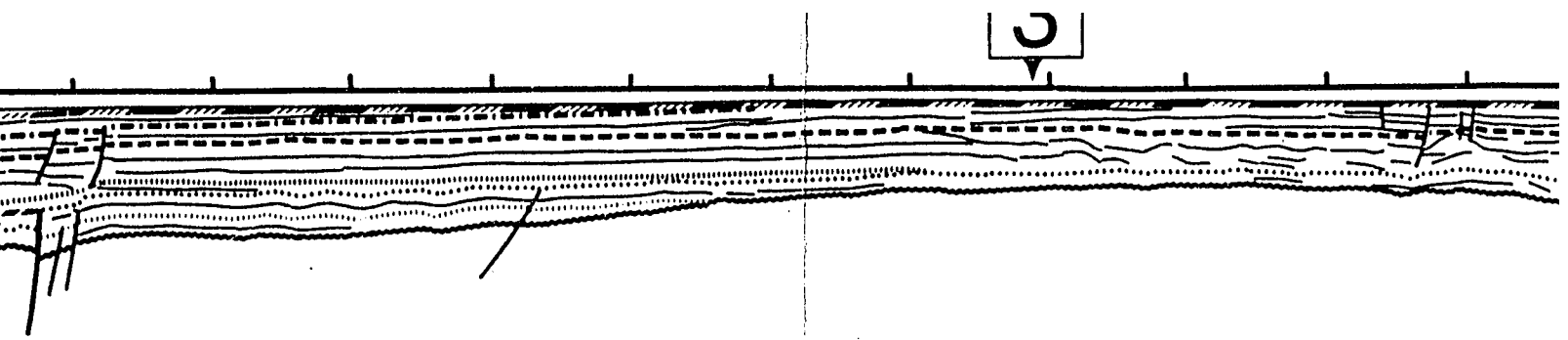


Profile A

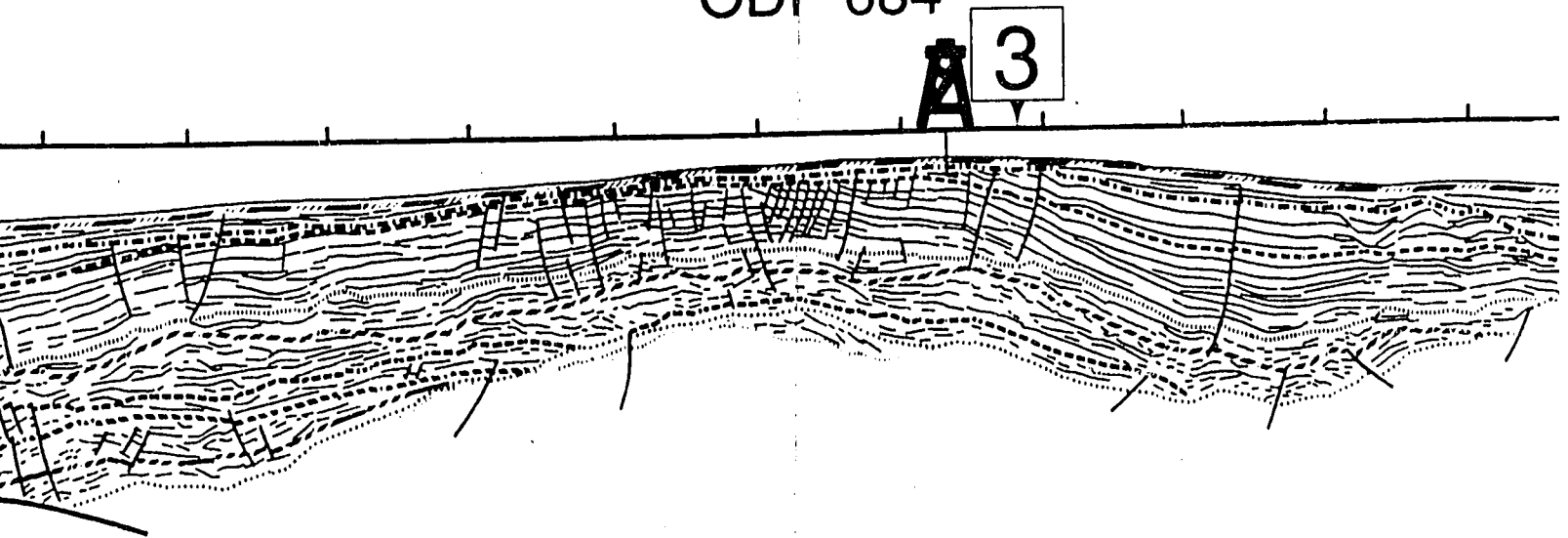


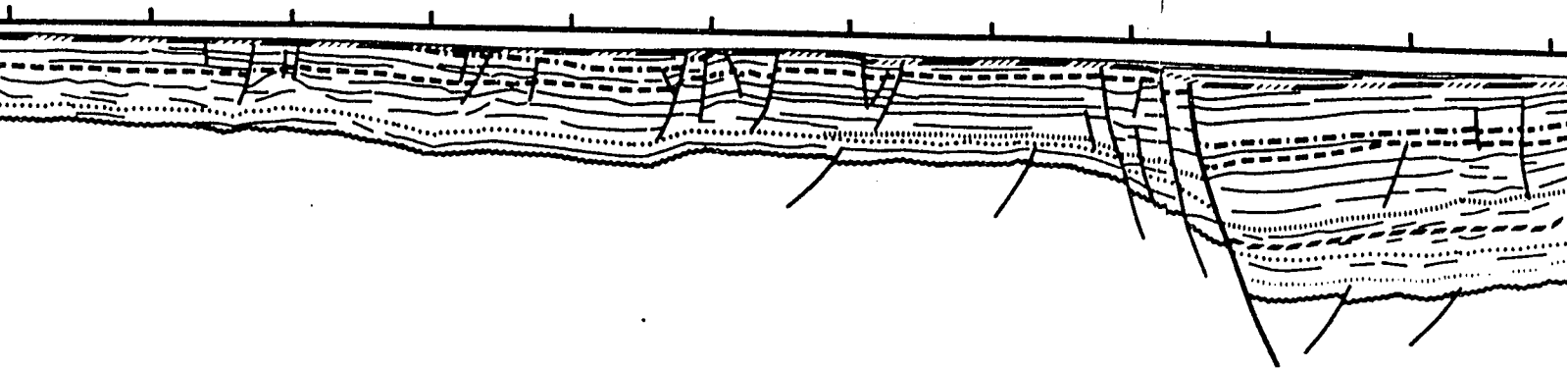






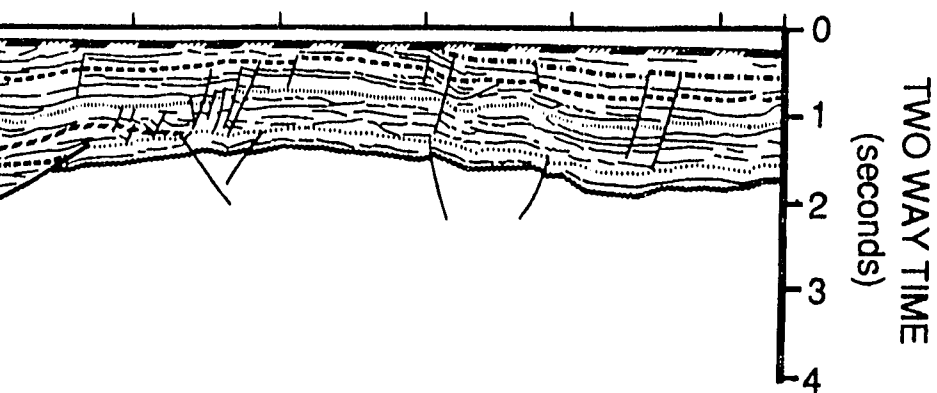
ODP 684





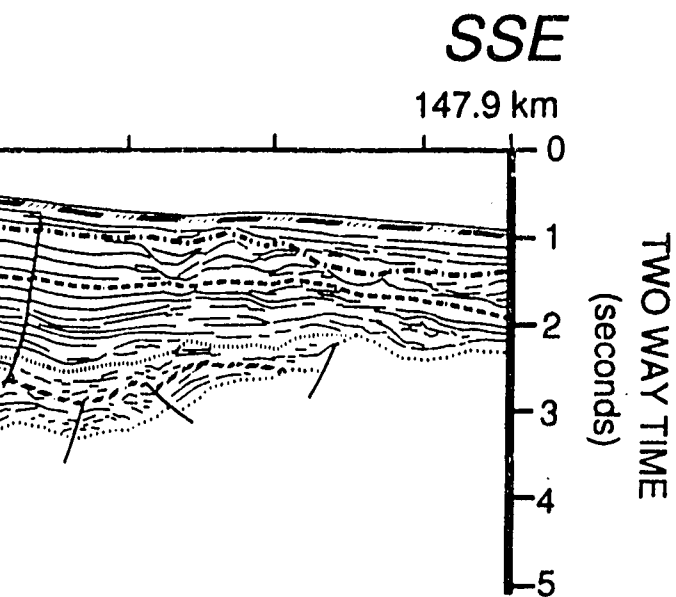
SSE

155 km

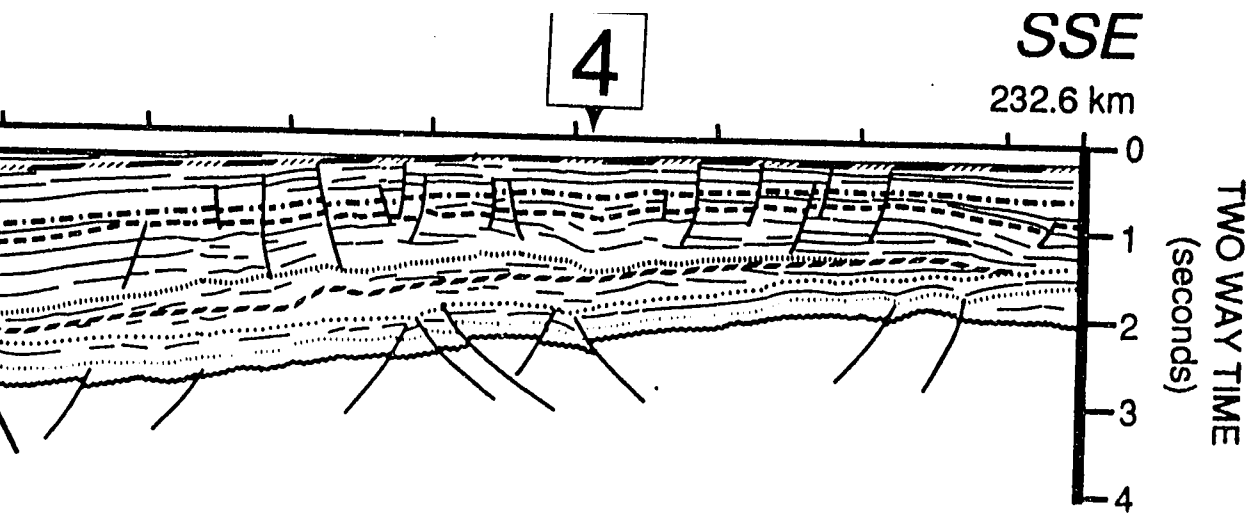


LINE DRAW
FOREARC

NORTH CEN



PANEL



THE DRAWING OF SEISMIC PROFILES
 REARC REGION OFFSHORE PERU
 WITH CENTRAL PART OF STUDY AREA

PANEL 2 - STRIKE LINES

PK

Pre-Cretaceous Basement

SCALE

0

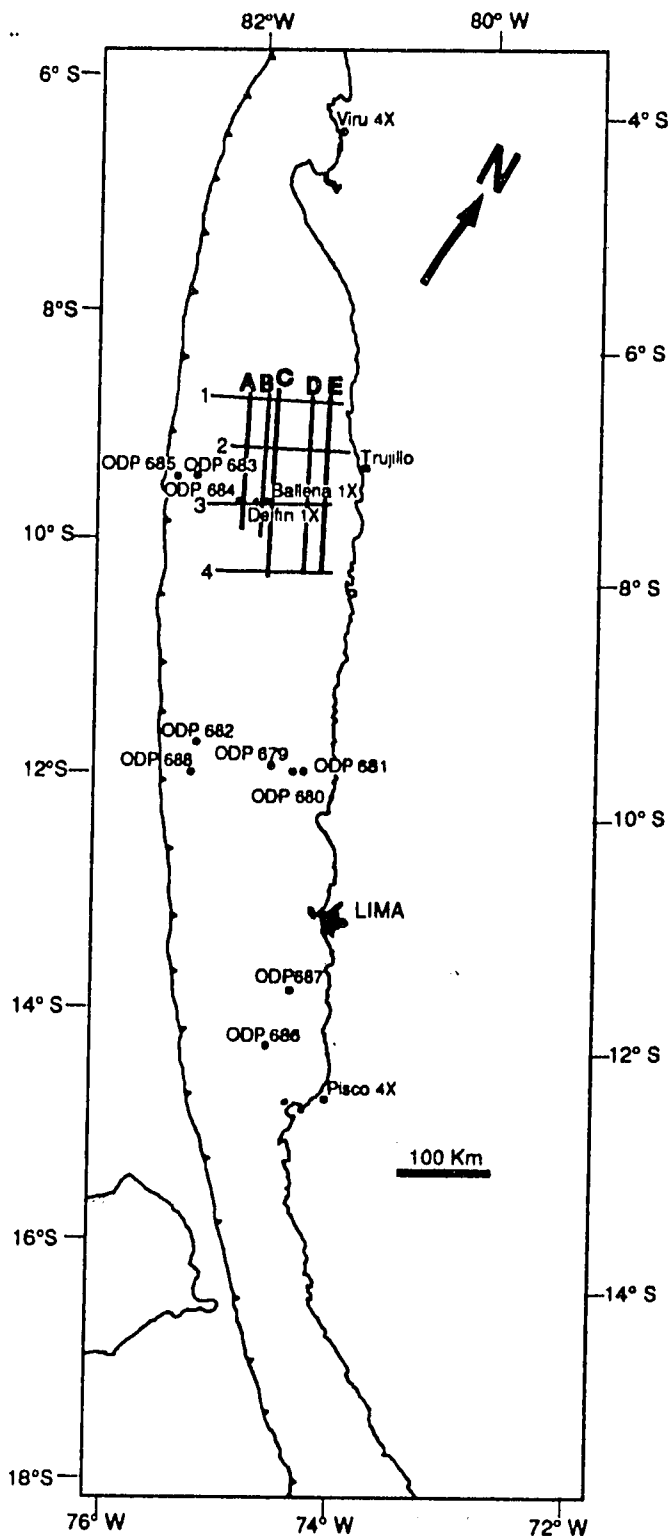
20 km

TWO WAY TIME

PROFILES
PERU

STUDY AREA

PROFILES



PLEASE NOTE:

Oversize maps and charts are filmed in sections in the following manner:

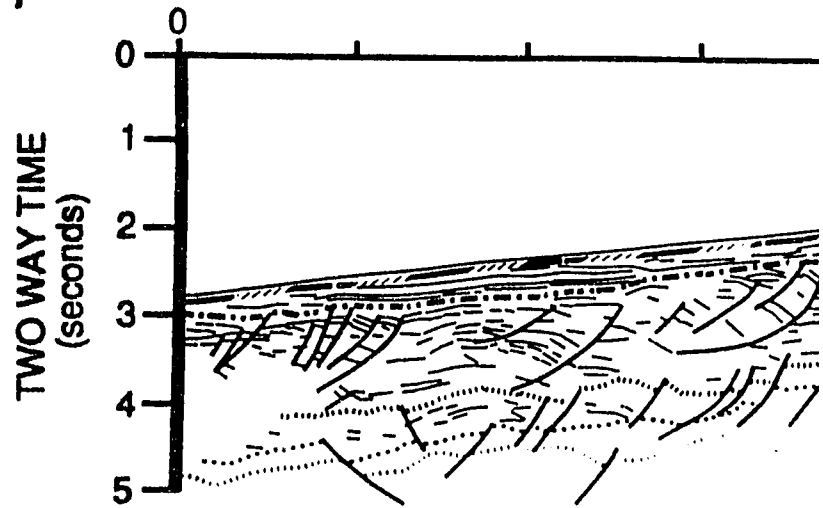
LEFT TO RIGHT, TOP TO BOTTOM, WITH SMALL OVERLAPS

The following map or chart has been refilmed in its entirety at the end of this dissertation (not available on microfiche). A xerographic reproduction has been provided for paper copies and is inserted into the inside of the back cover.

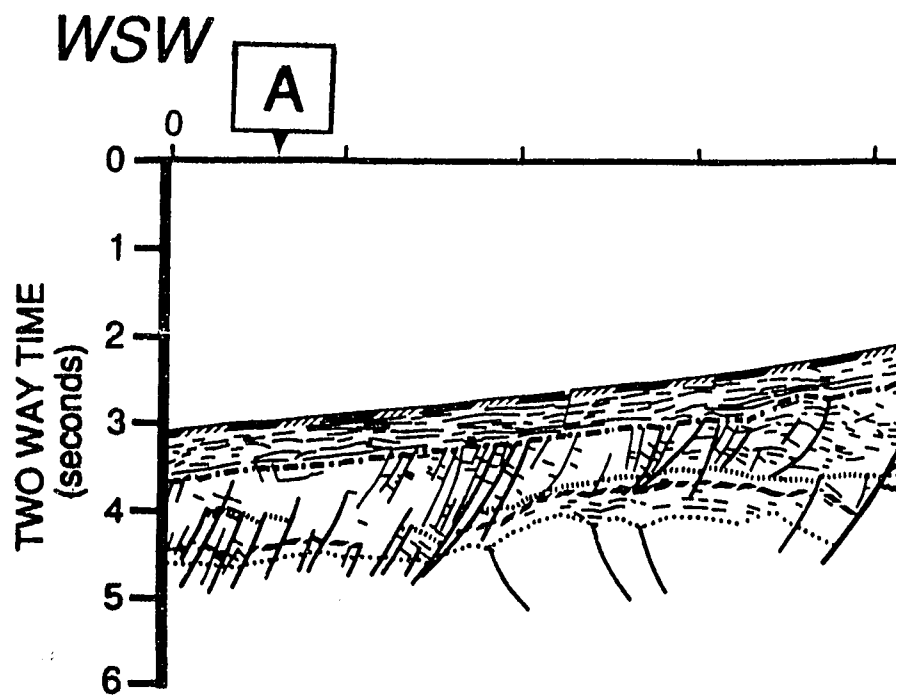
Black and white photographic prints (17" x 23") are available for an additional charge.

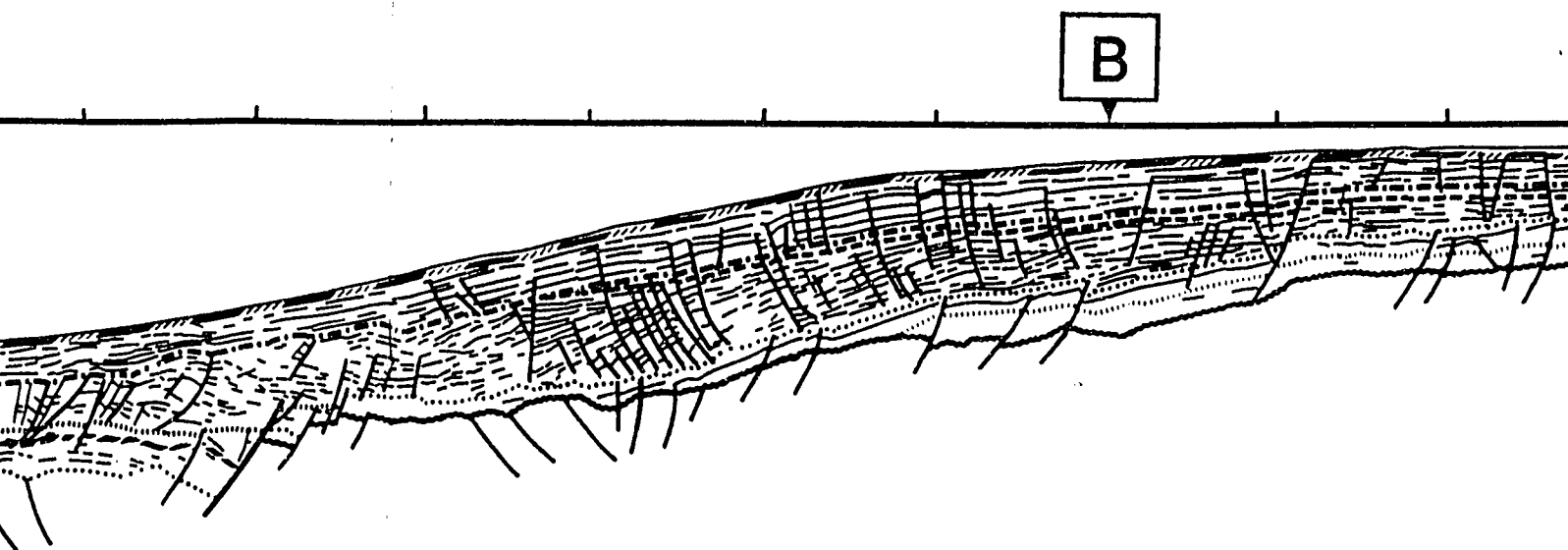
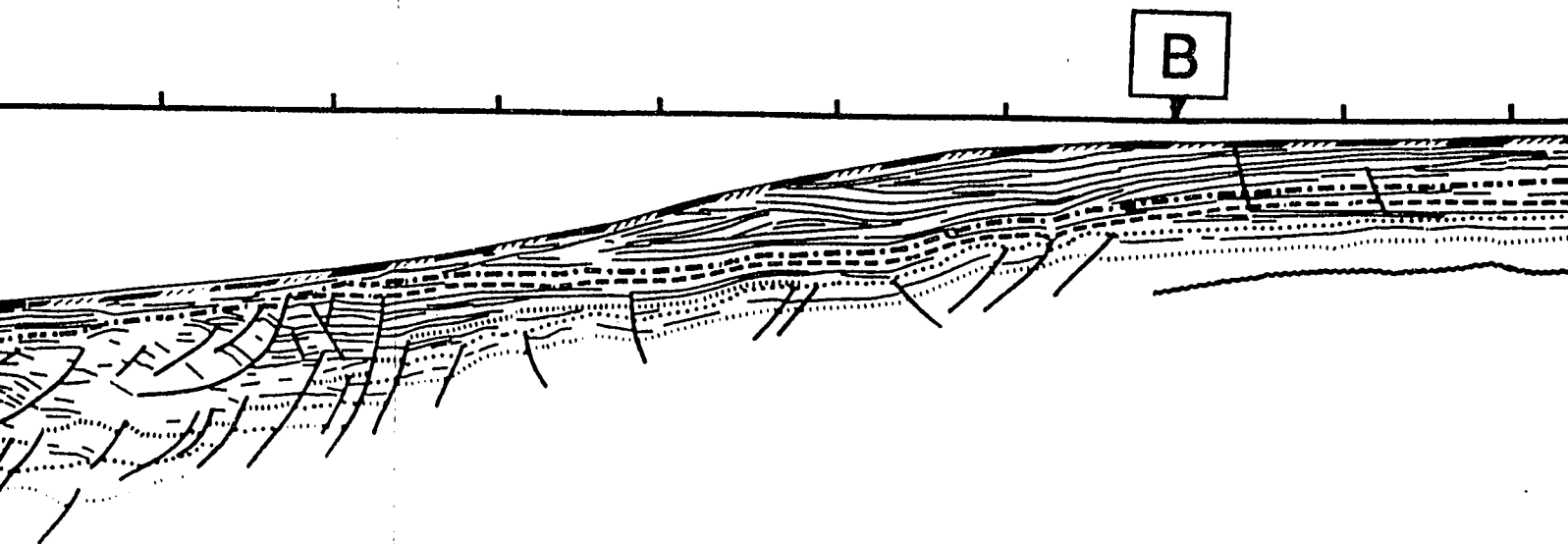
UMI

Profile 1 WSW

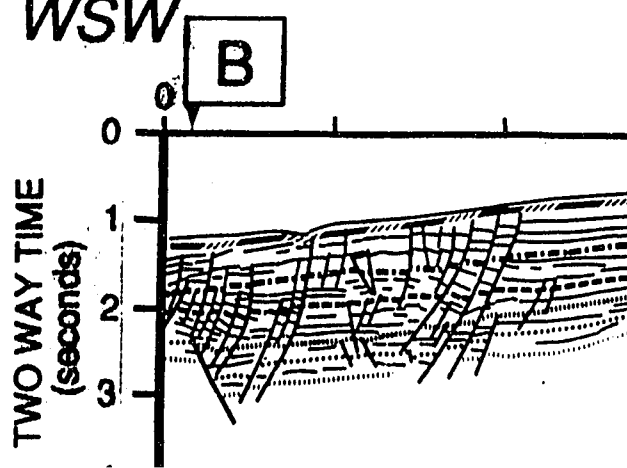


Profile 2 WSW





Profile 3 WSW



TWO WAY TIME
(seconds)

0

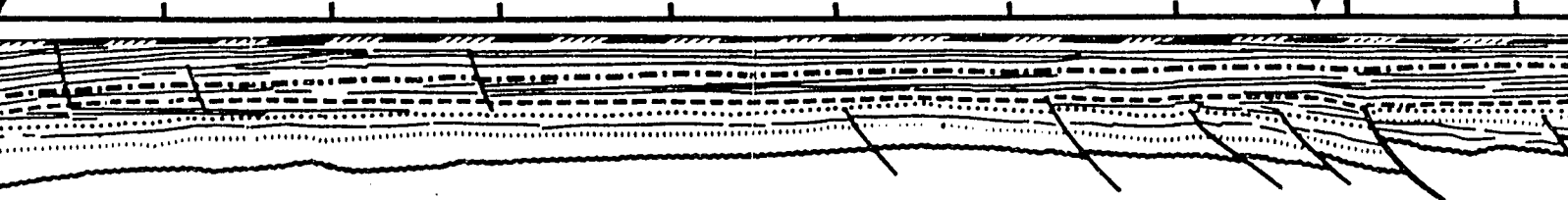
1

2

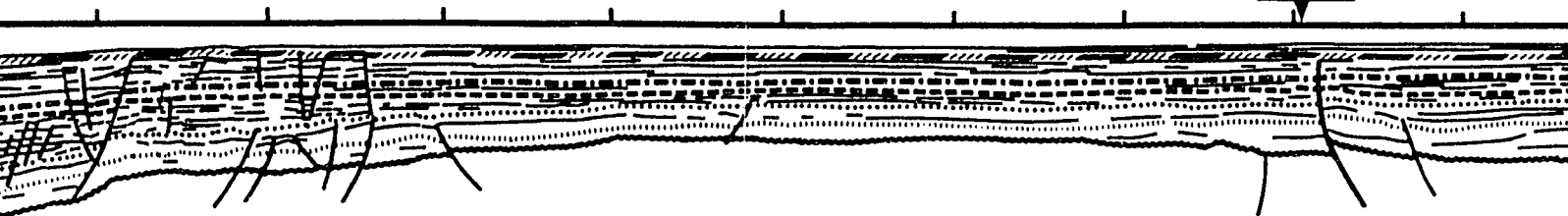
3

B

C

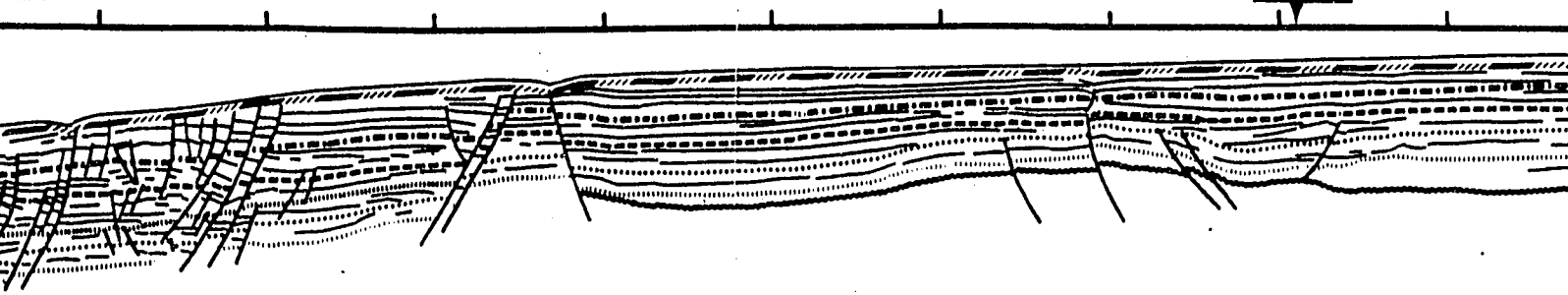


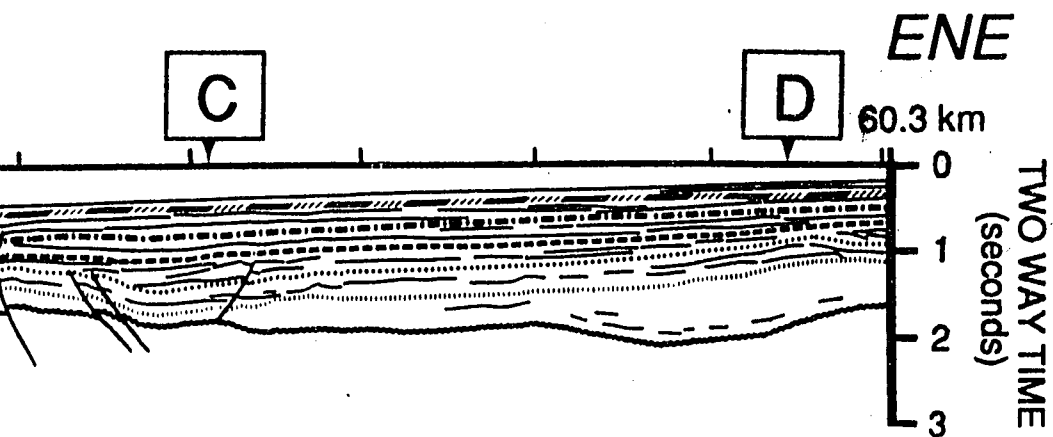
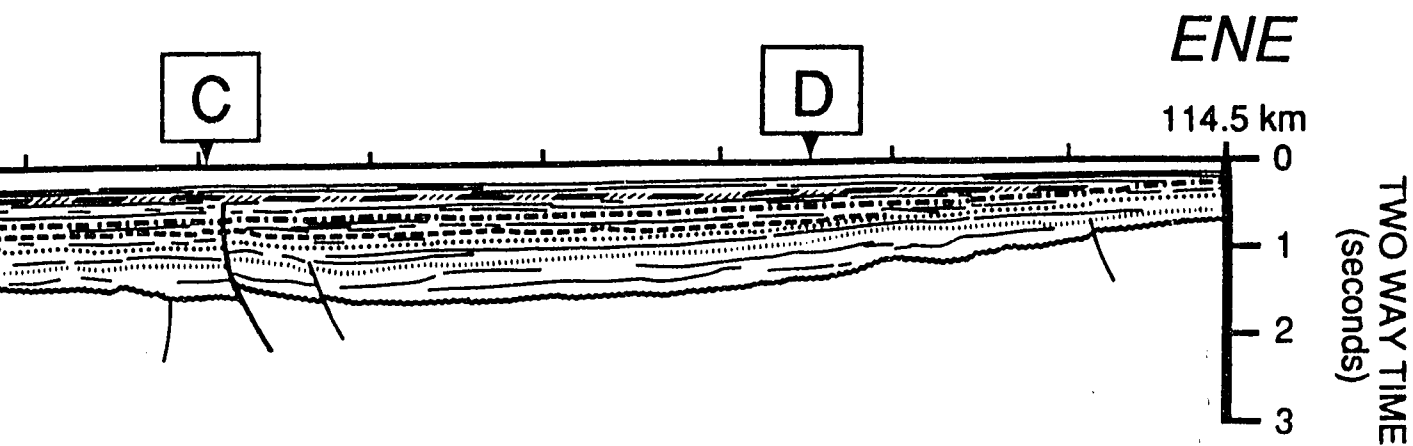
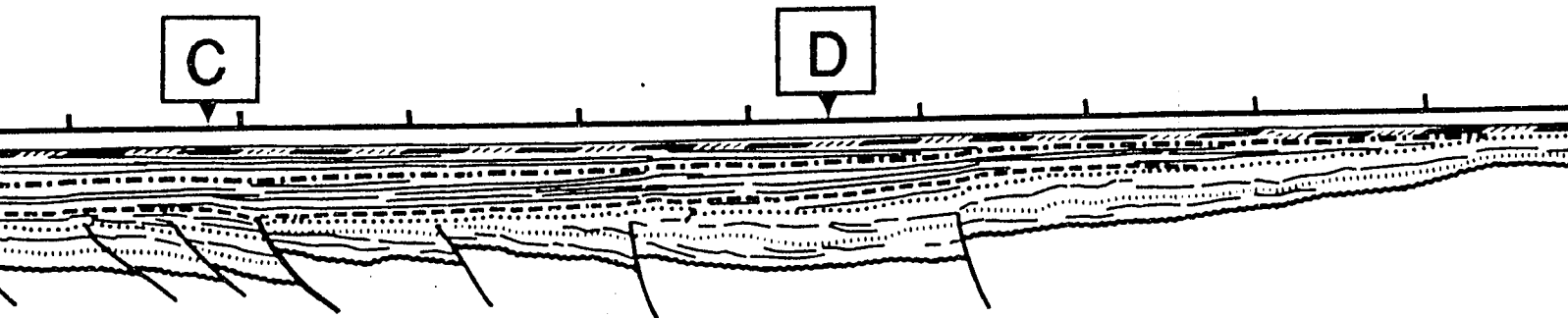
C

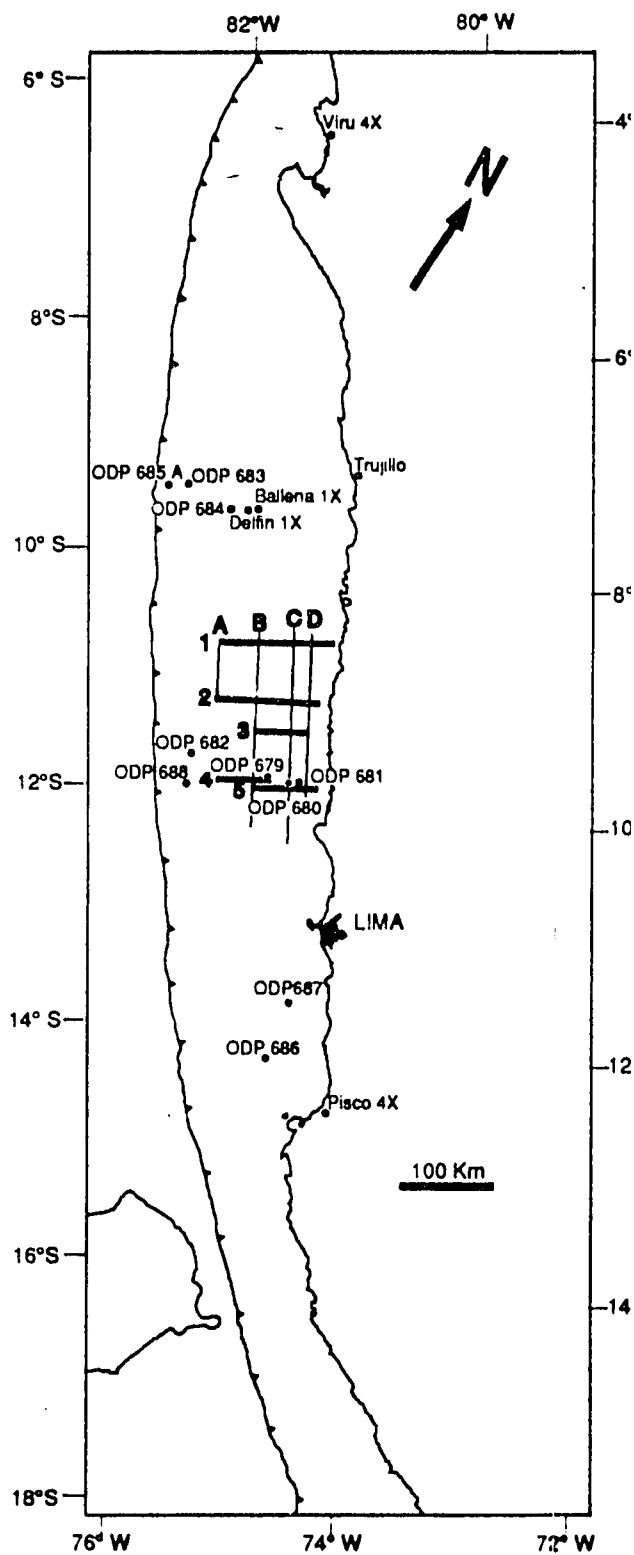
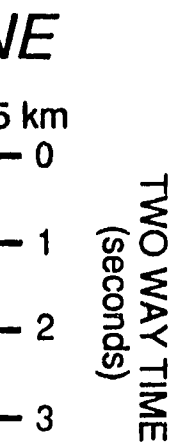
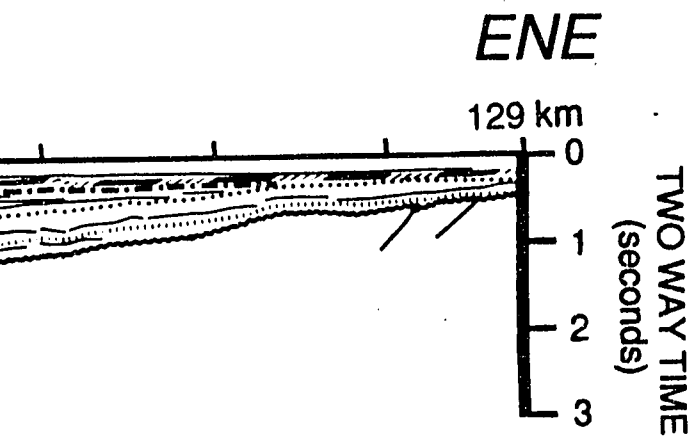


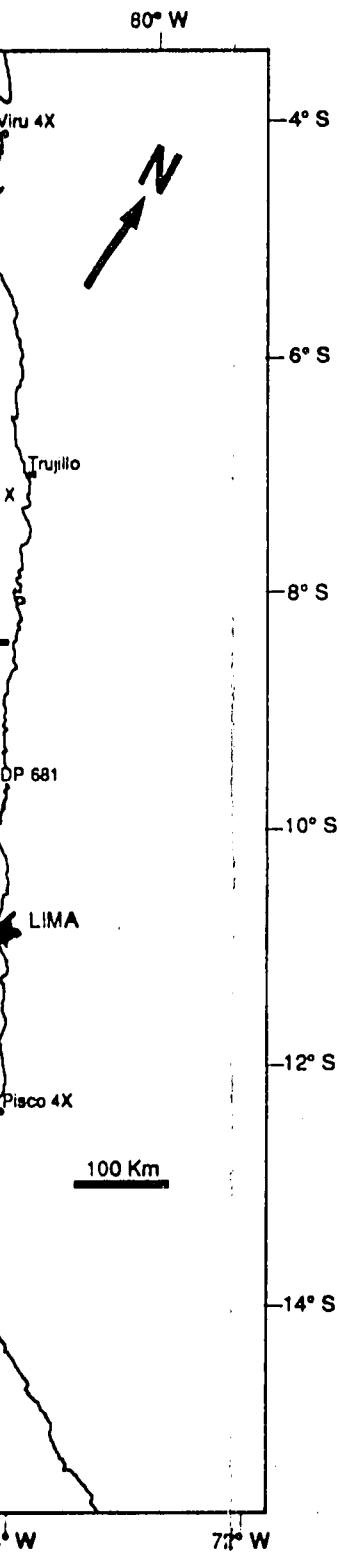
B

C









LINE DRAWING OF SI
FOREARC REGION (

SOUTH CENTRAL PERU

PANE
DIP LIN

L E G E

SEQUENCE A

ING OF SEISMIC PROFILES REGION OFFSHORE PERU

TRAL PART OF STUDY AREA

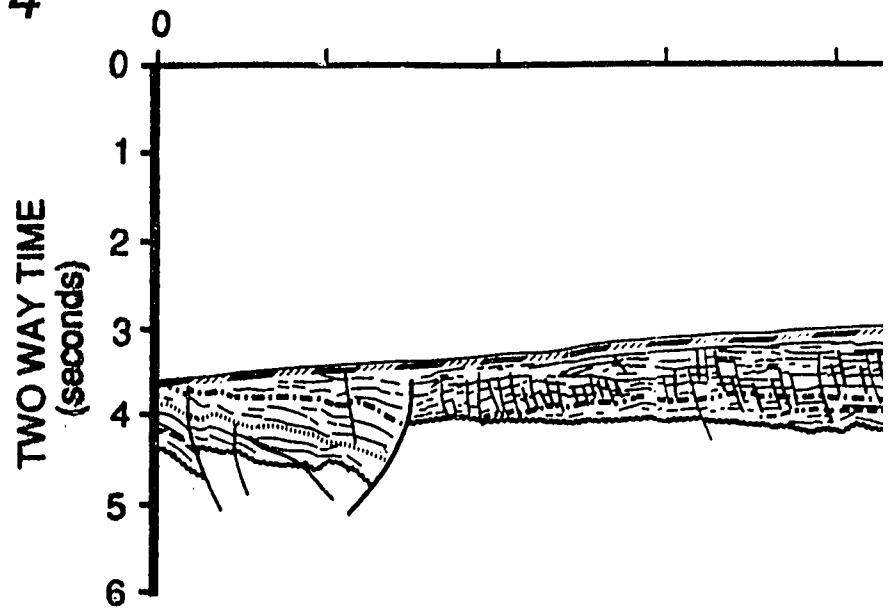
PANEL 3 ***DIP LINES***

L E G E N D

SEQUENCE AGE



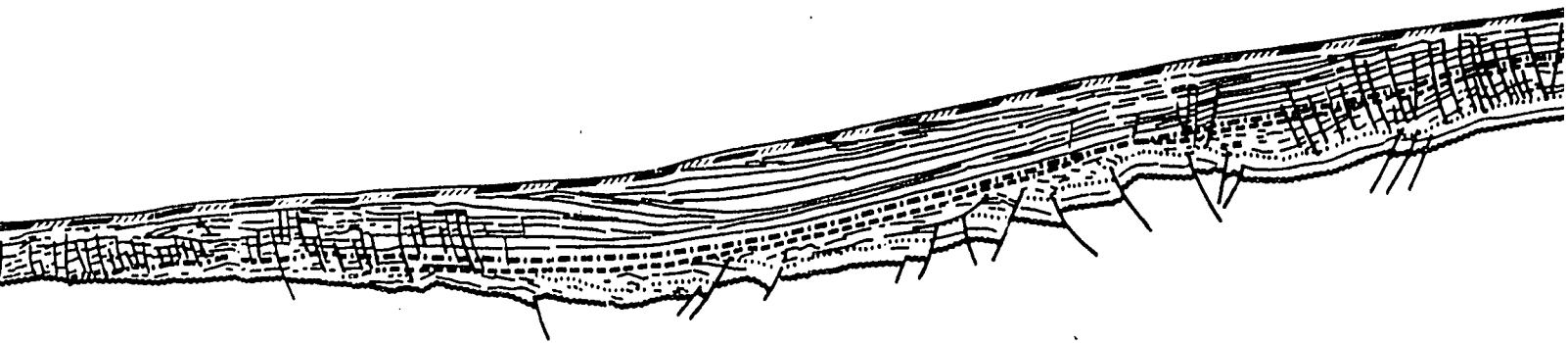
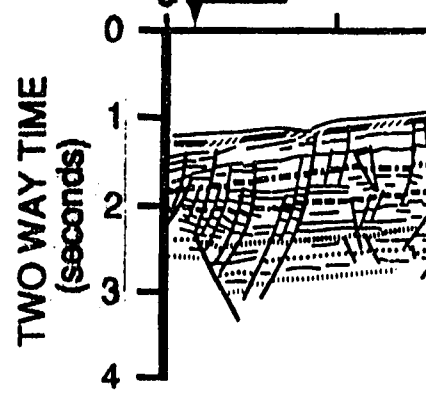
Profile 4 WSW



Profile 3

WSW

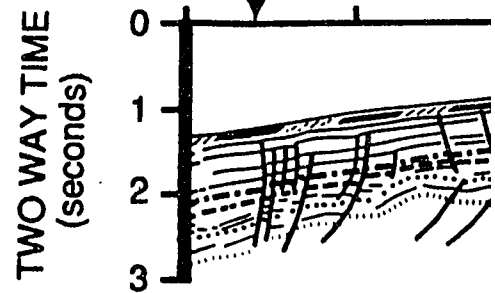
B

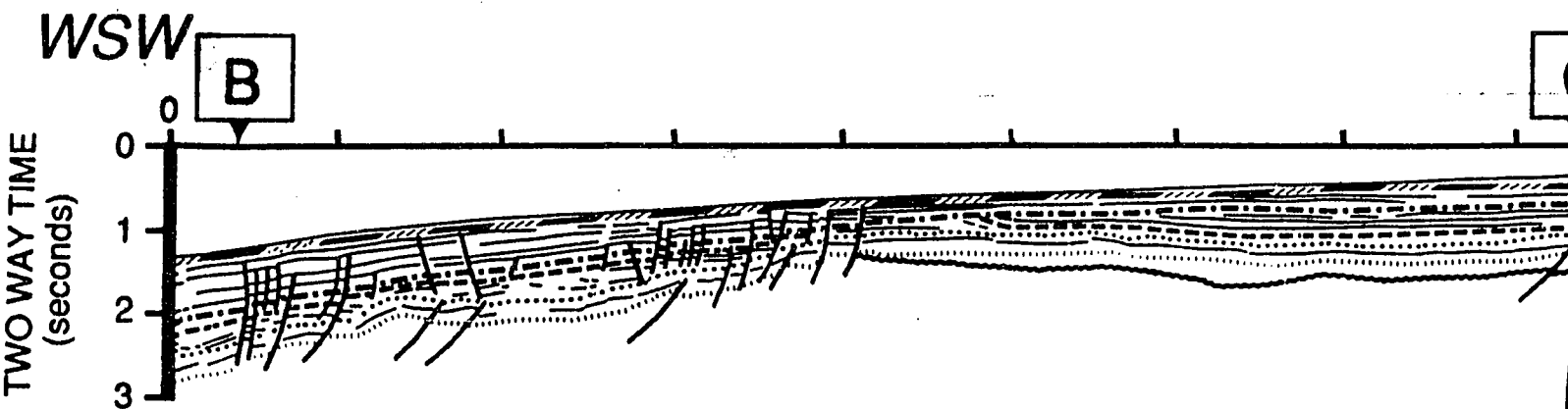
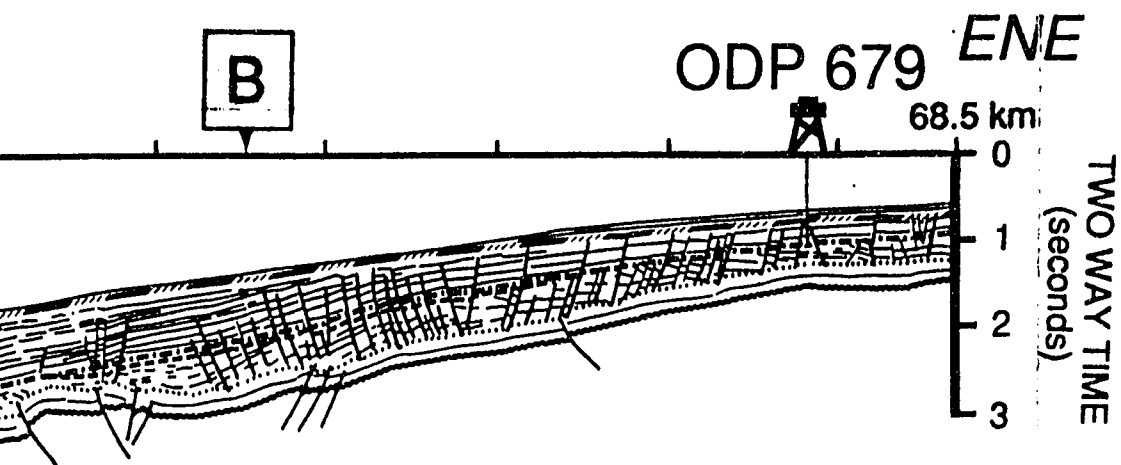
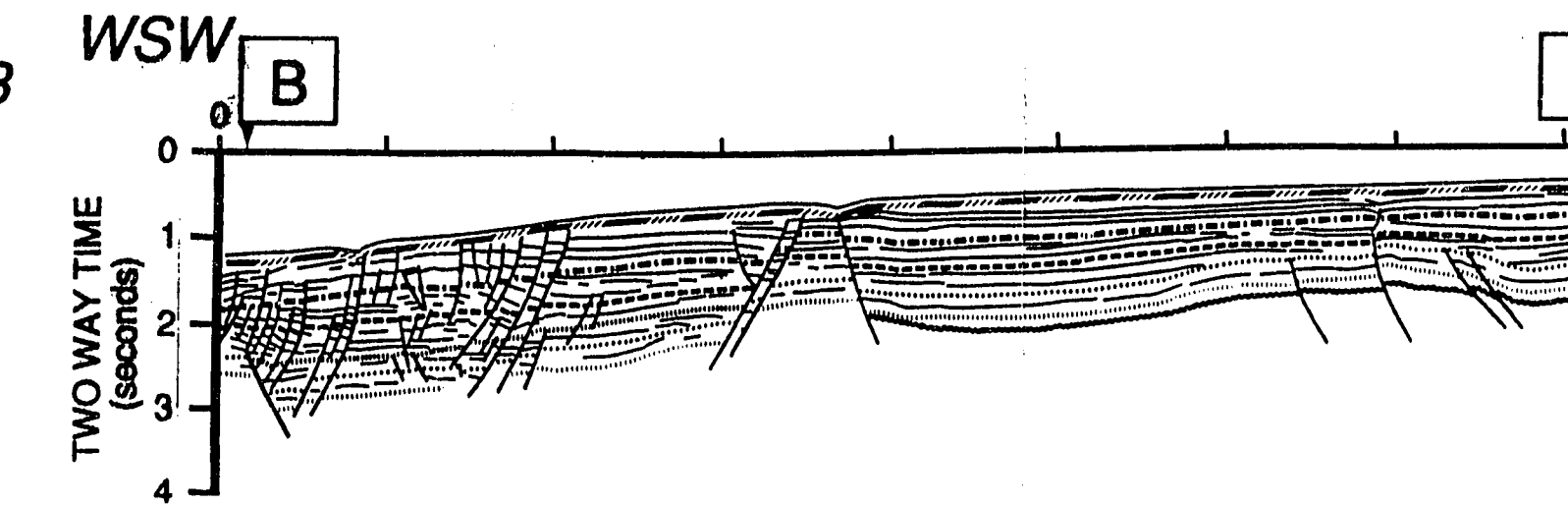


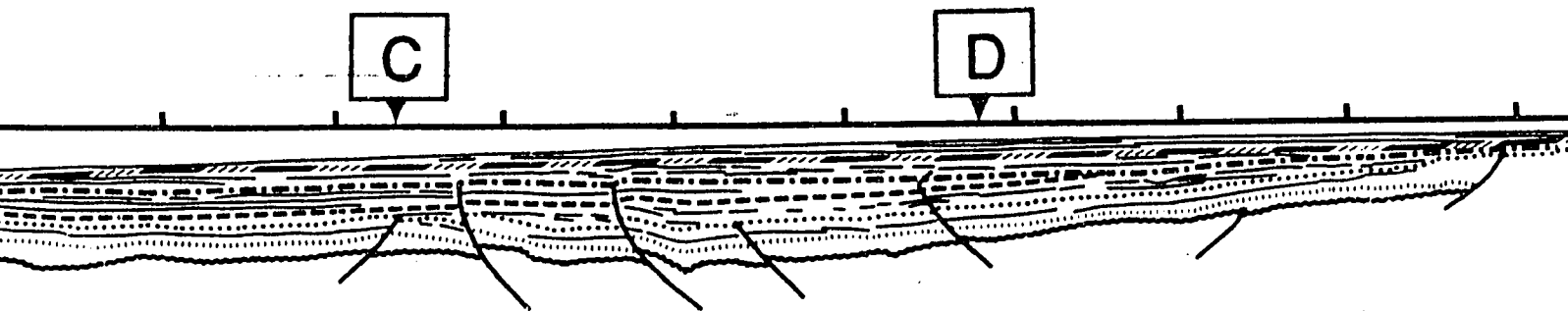
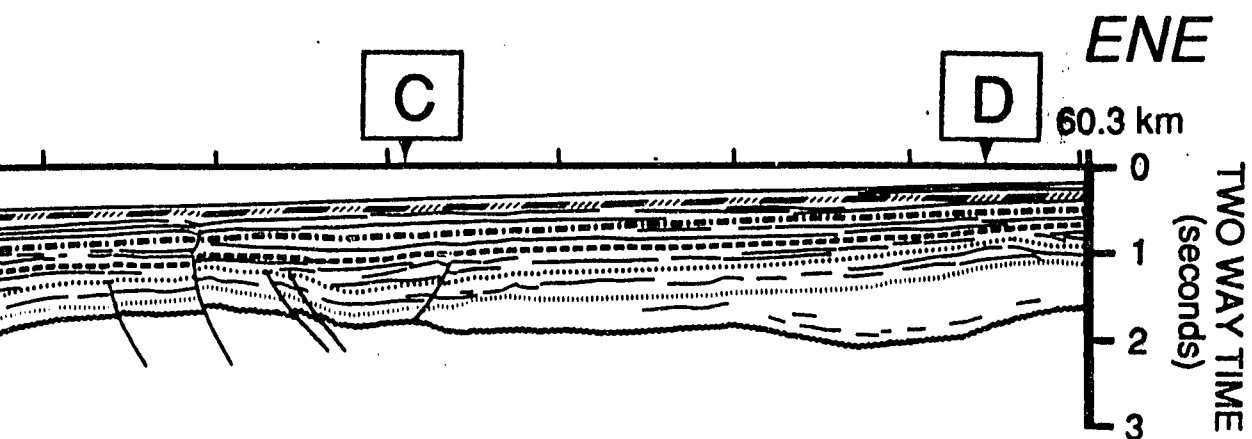
Profile 5

WSW

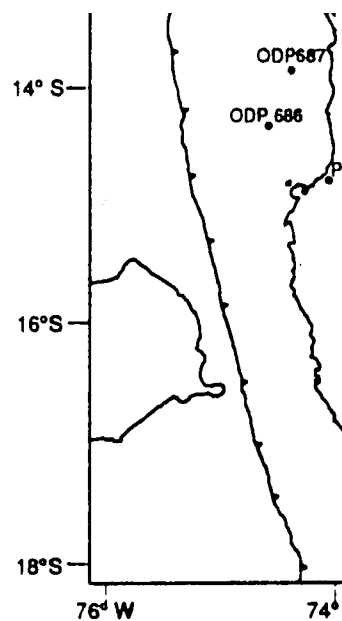
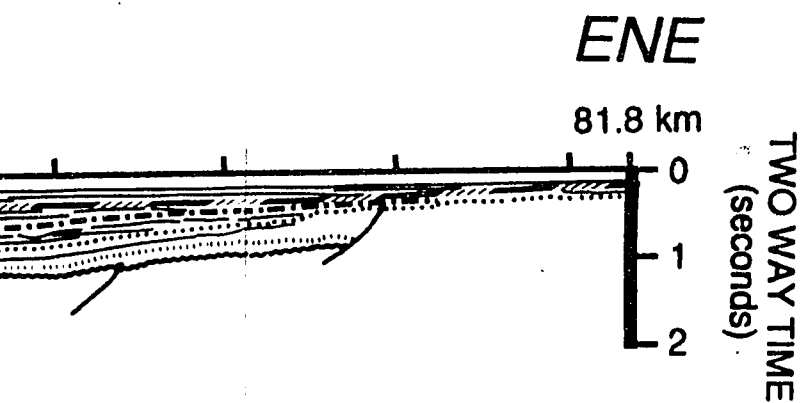
B

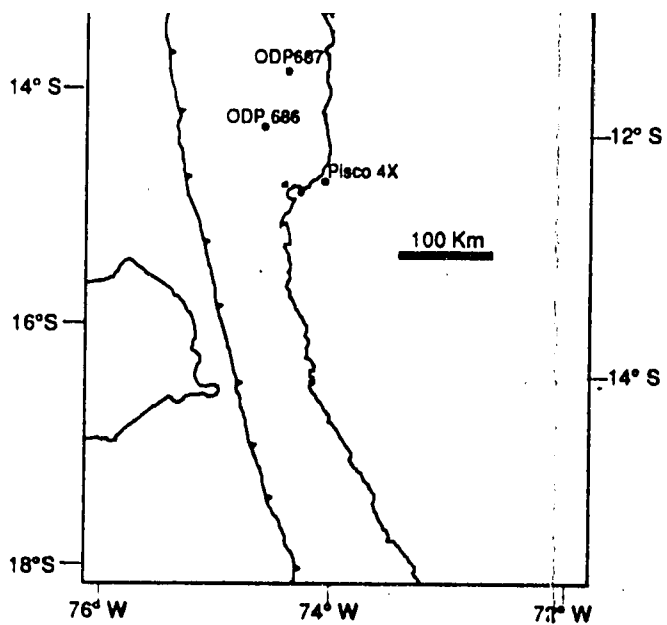






NE
m
TWO WAY TIME
(seconds)





S C A L E

20 km

S E



L E G E N D

SEQUENCE A G E

Q	Quaternary
P	Upper Miocene - Pliocene
M 3	Upper Miocene
M 2	Middle - Lower Miocene
M 1	Lower Miocene
E-O	Uppermost middle Eocene to Oligocene
E 3	Middle Eocene
E 2	Middle Eocene
E 1	Middle Eocene
E ₀	Lower ? - Middle Eocene
K	Cretaceous ?
PK	Pre-Cretaceous Basement

L E G E N D

SEQUENCE A G E

Q	Quaternary
P	Upper Miocene - Pliocene
M 3	Upper Miocene
M 2	Middle - Lower Miocene
M 1	Lower Miocene
E-O	Uppermost middle Eocene to Oligocene
E 3	Middle Eocene
E 2	Middle Eocene
E 1	Middle Eocene
E 0	Lower ? - Middle Eocene
K	Cretaceous ?
PK	Pre-Cretaceous Basement

PLEASE NOTE:

Oversize maps and charts are filmed in sections in the following manner:

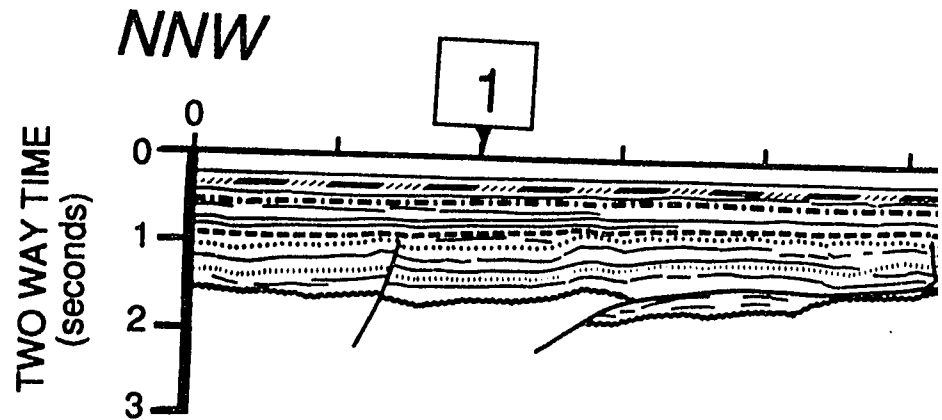
LEFT TO RIGHT, TOP TO BOTTOM, WITH SMALL OVERLAPS

The following map or chart has been refilmed in its entirety at the end of this dissertation (not available on microfiche). A xerographic reproduction has been provided for paper copies and is inserted into the inside of the back cover.

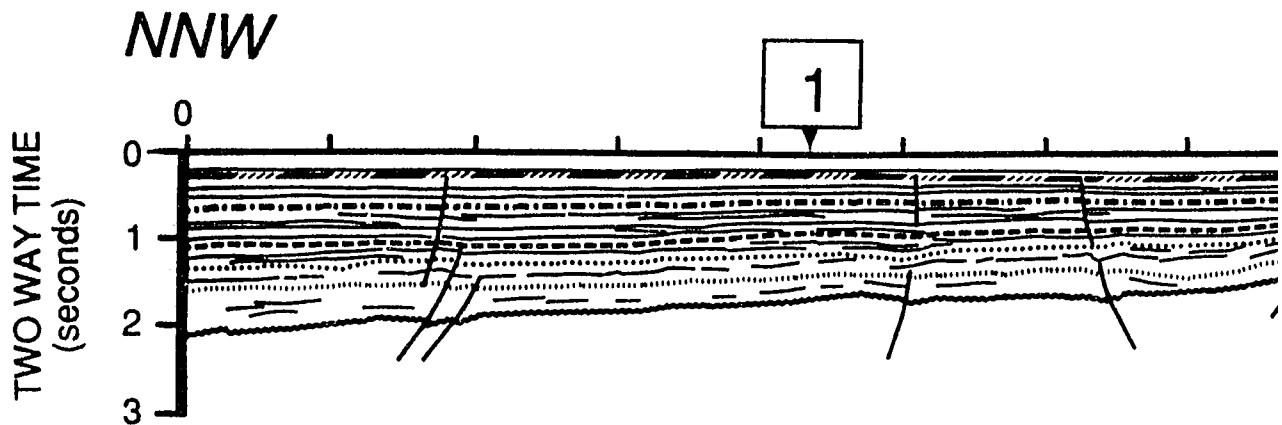
Black and white photographic prints (17" x 23") are available for an additional charge.

UMI

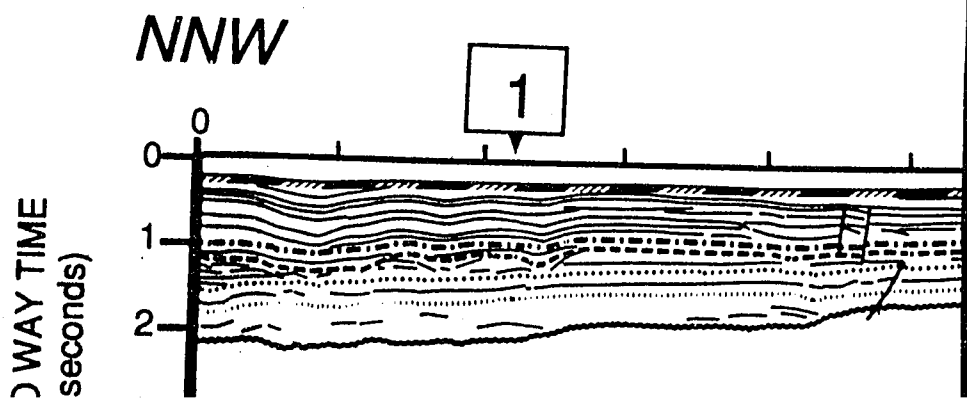
Profile D

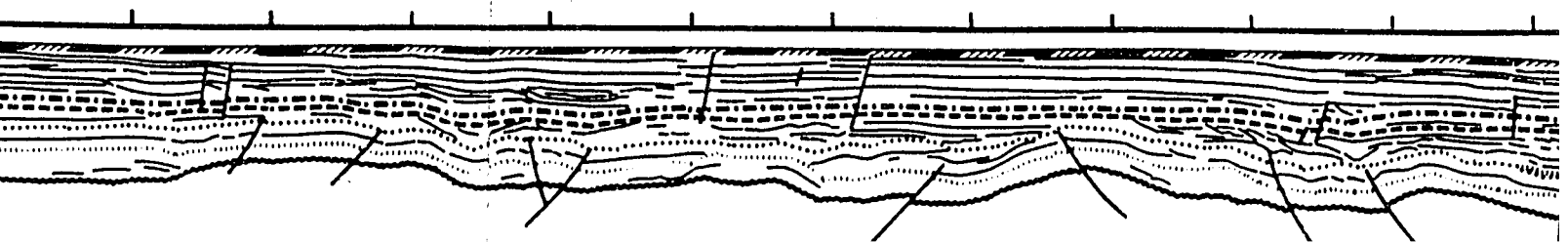
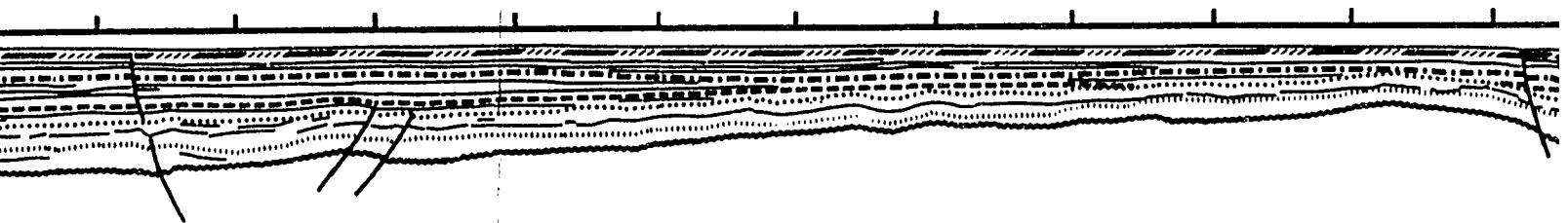
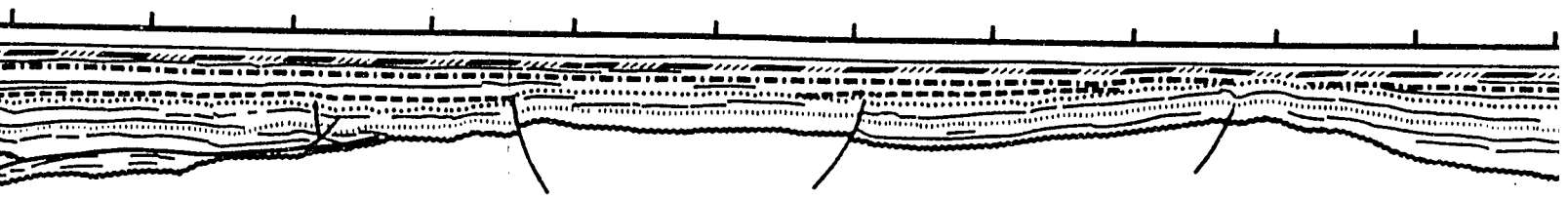


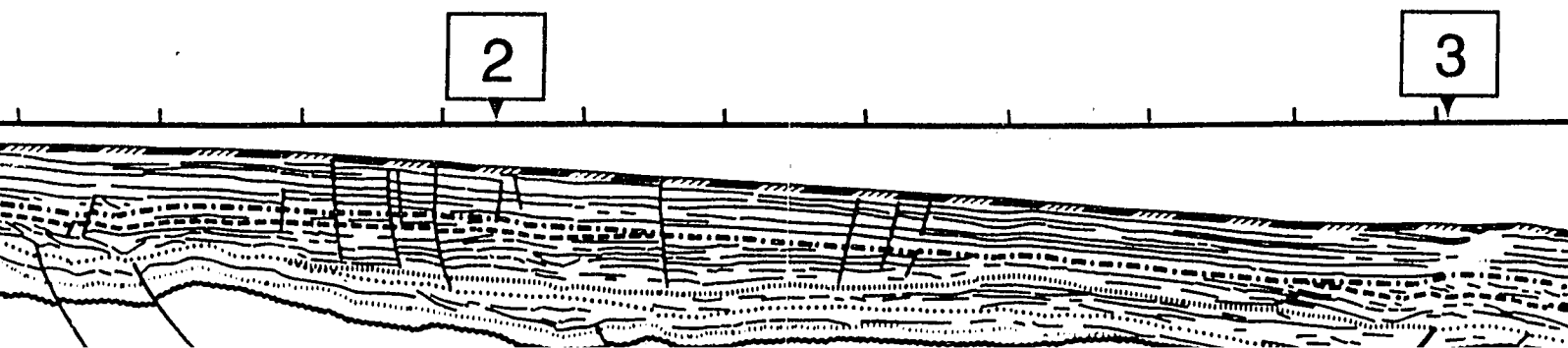
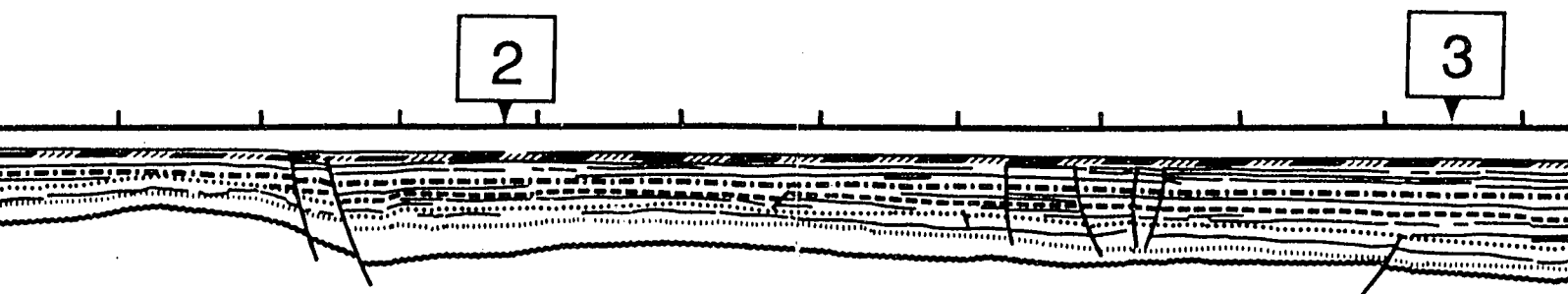
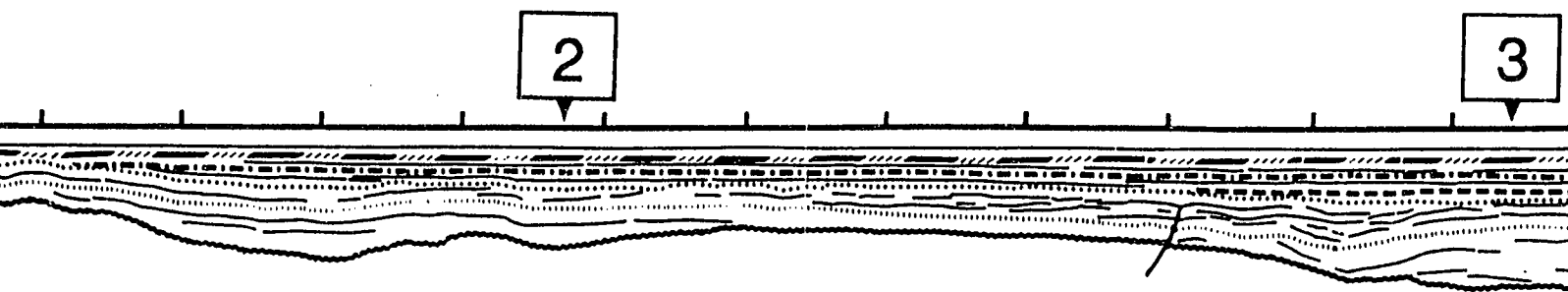
Profile C

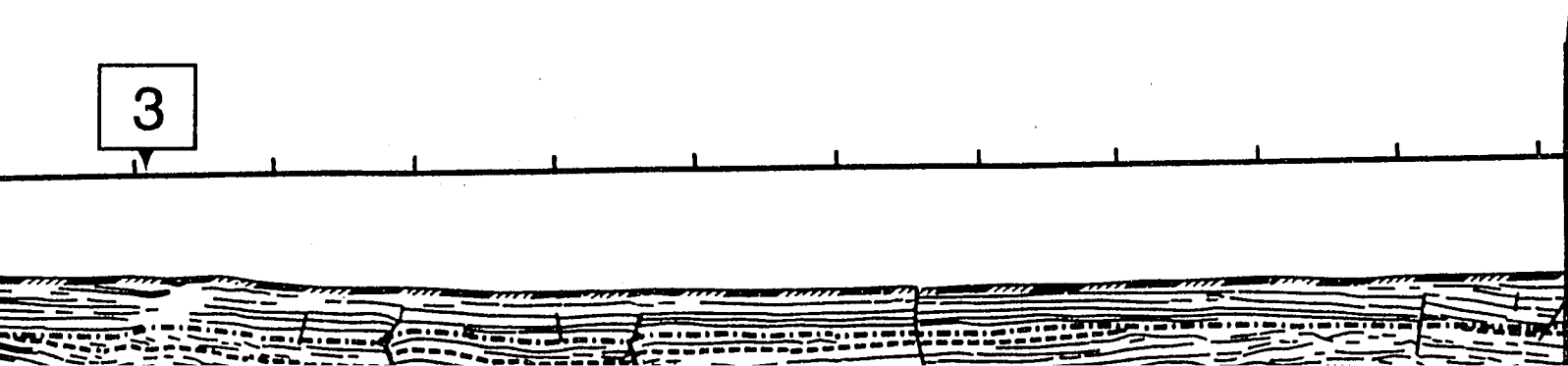
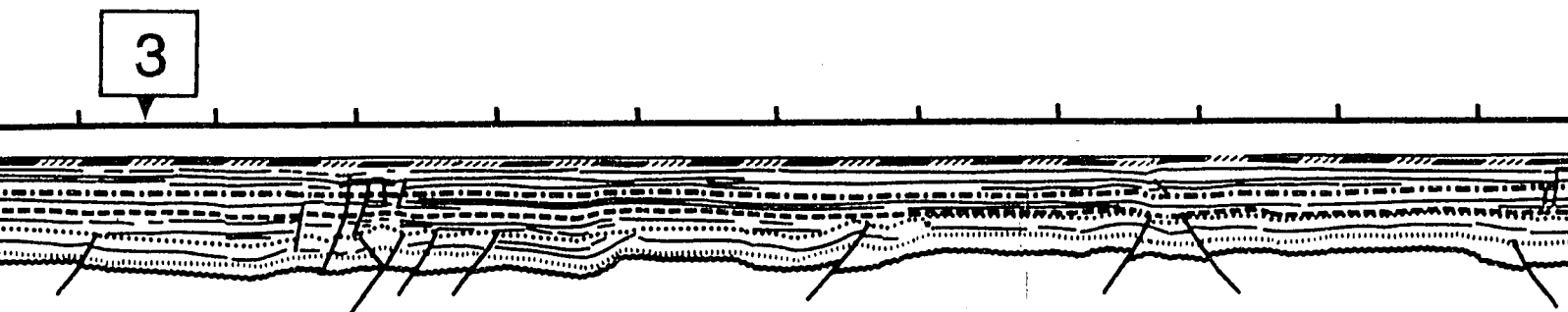
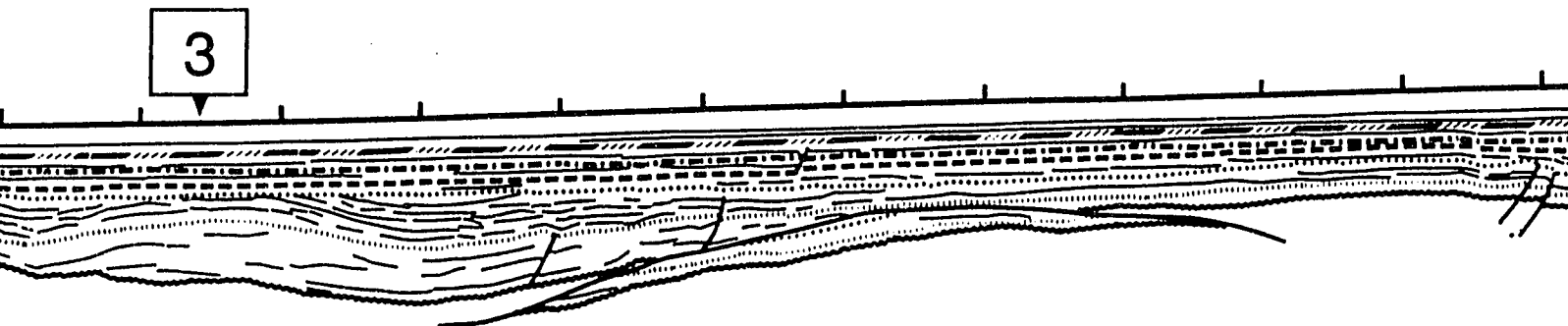


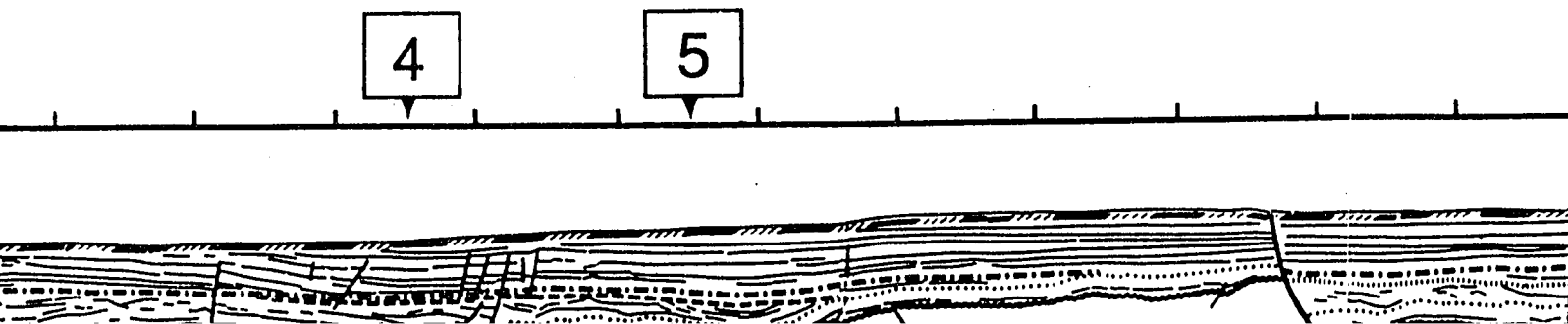
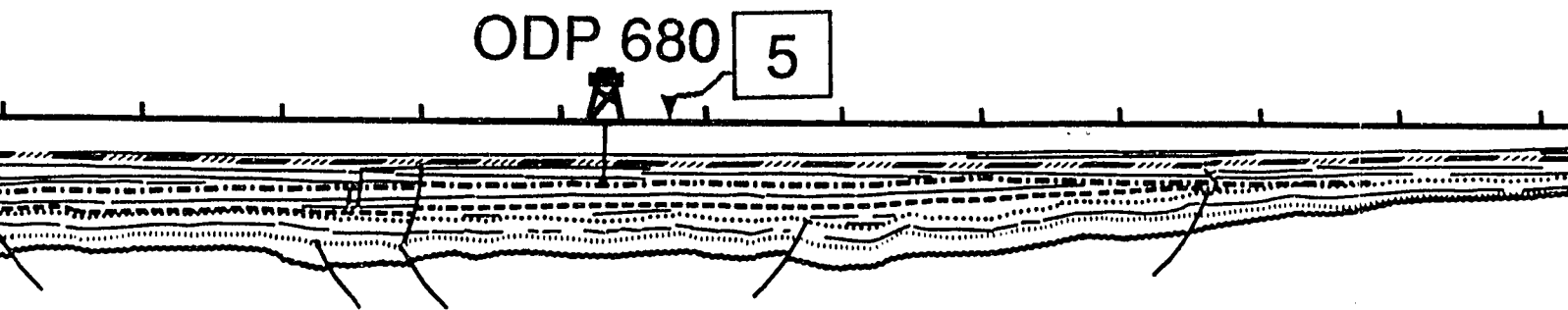
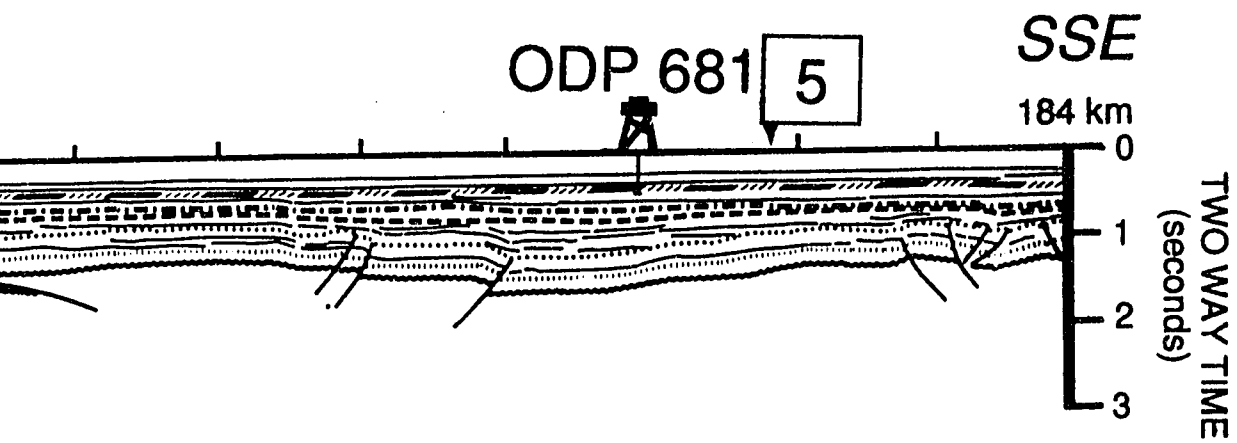
Profile B



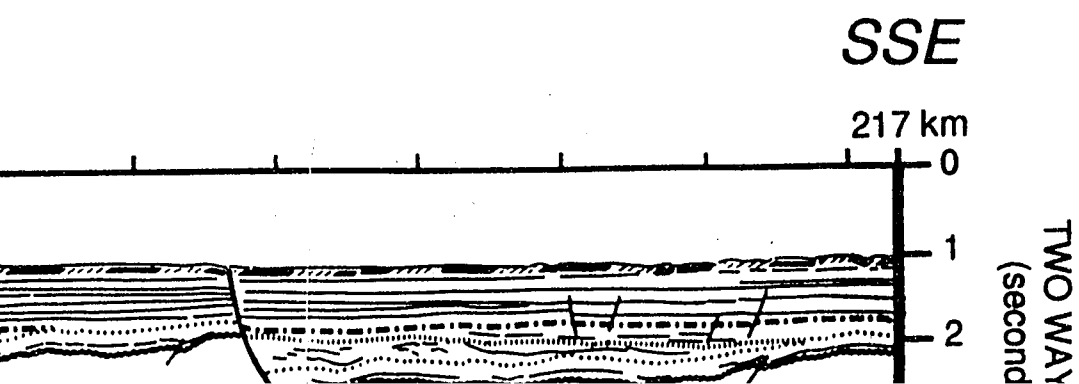
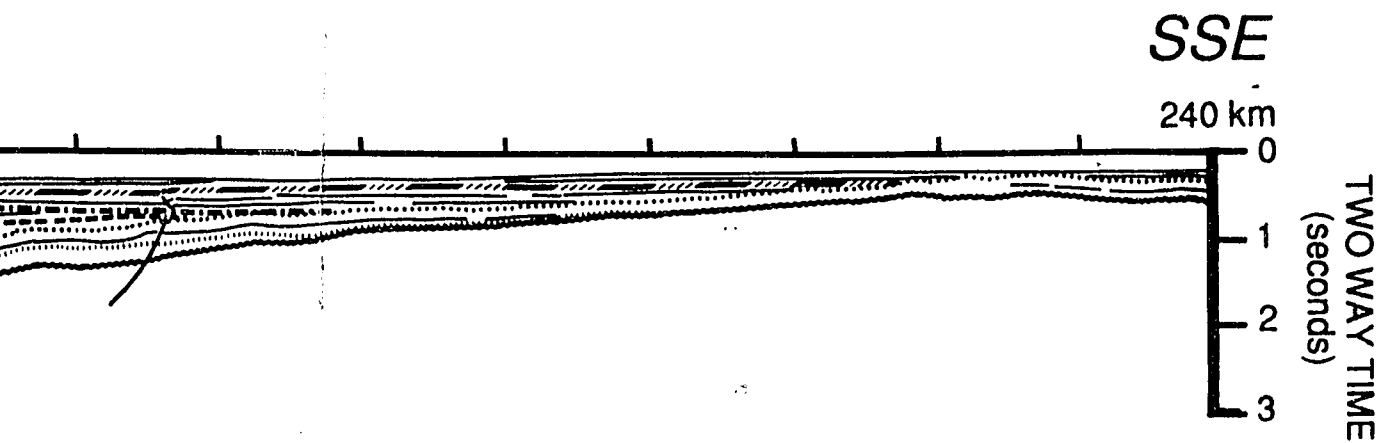








SE
4 km
0
1
2
3
TWO WAY TIME
(seconds)



SE

40 km

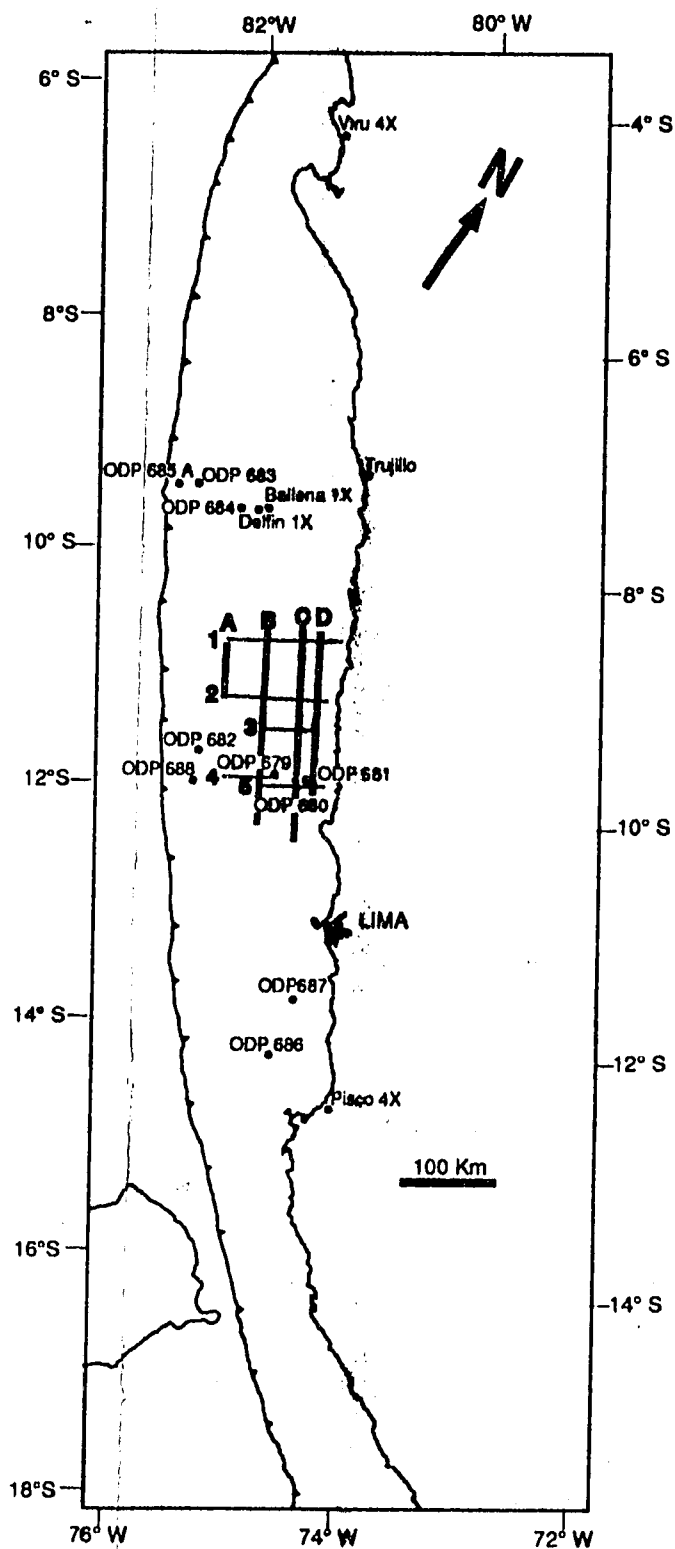
0

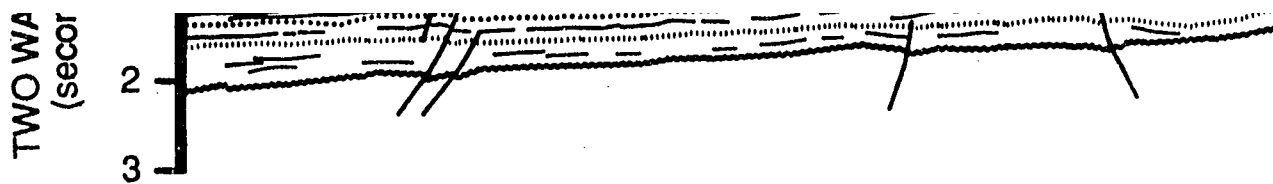
1

2

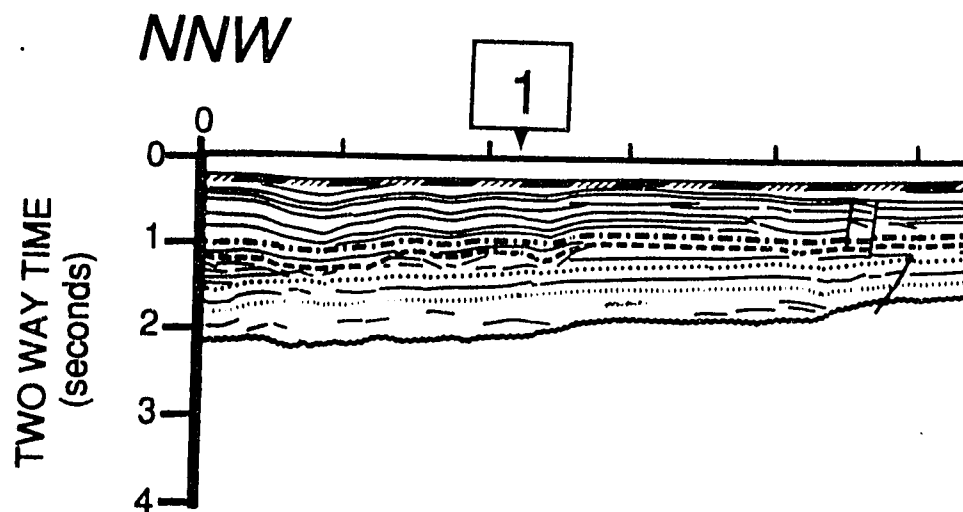
3

TWO WAY TIME
(seconds)

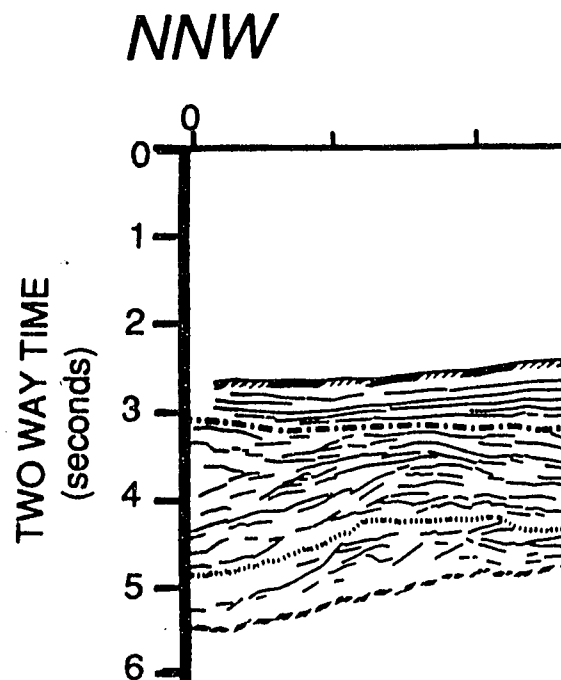


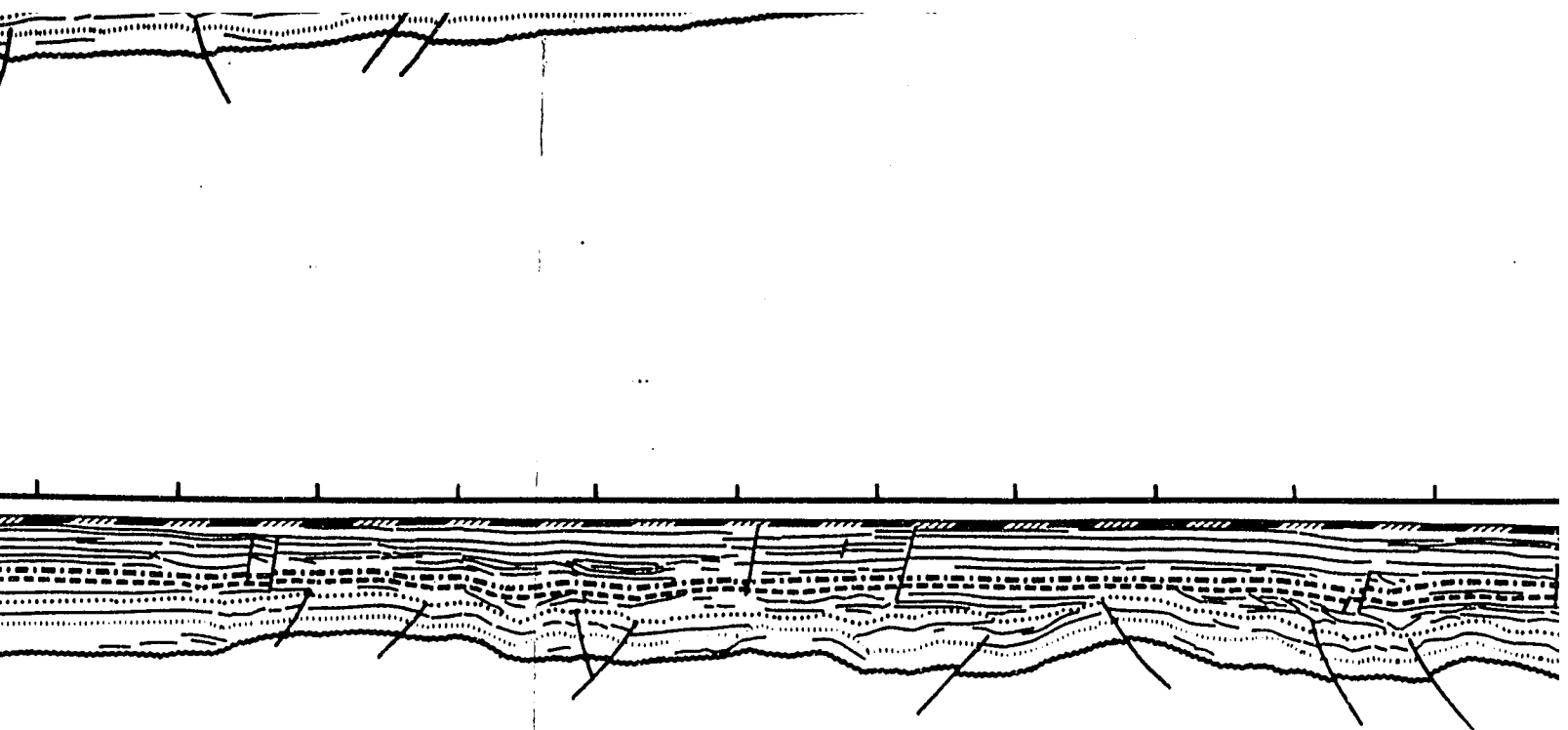


Profile B

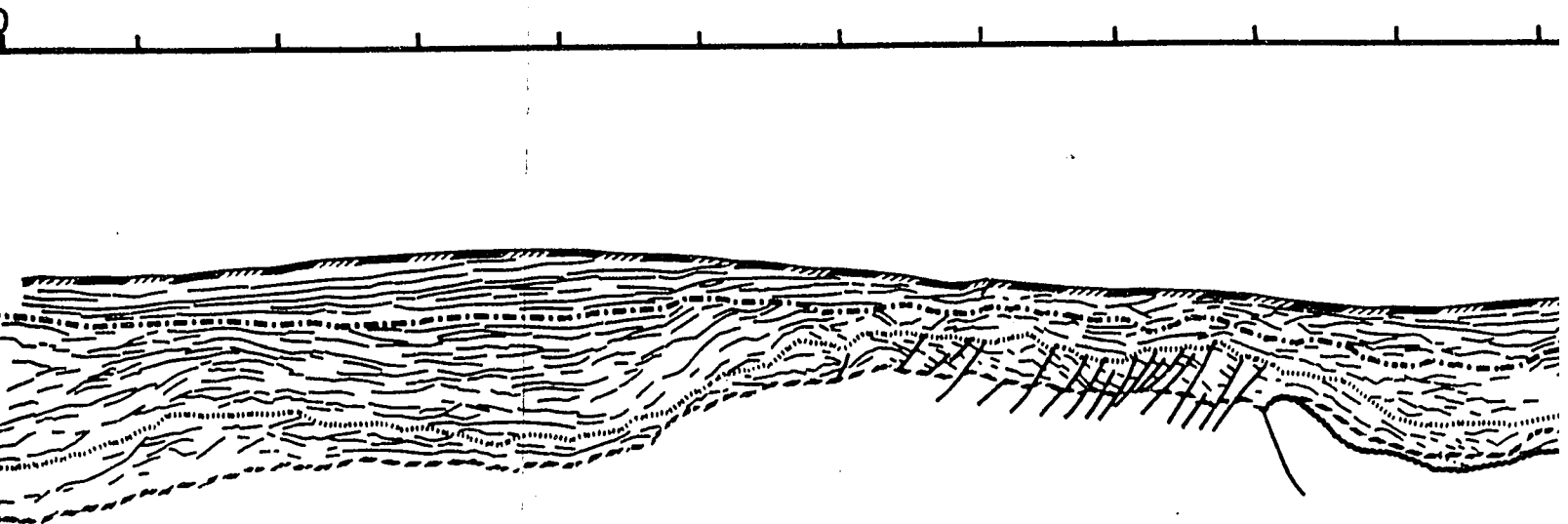


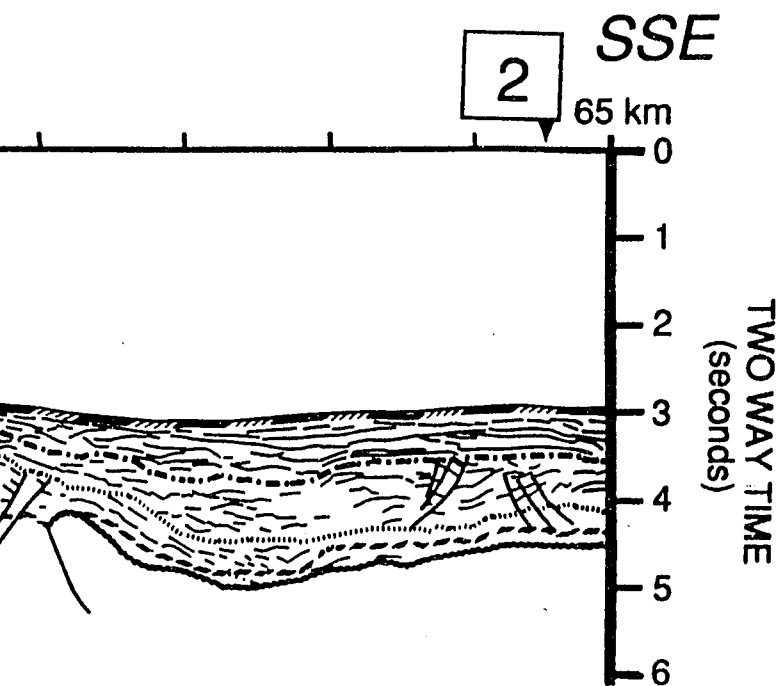
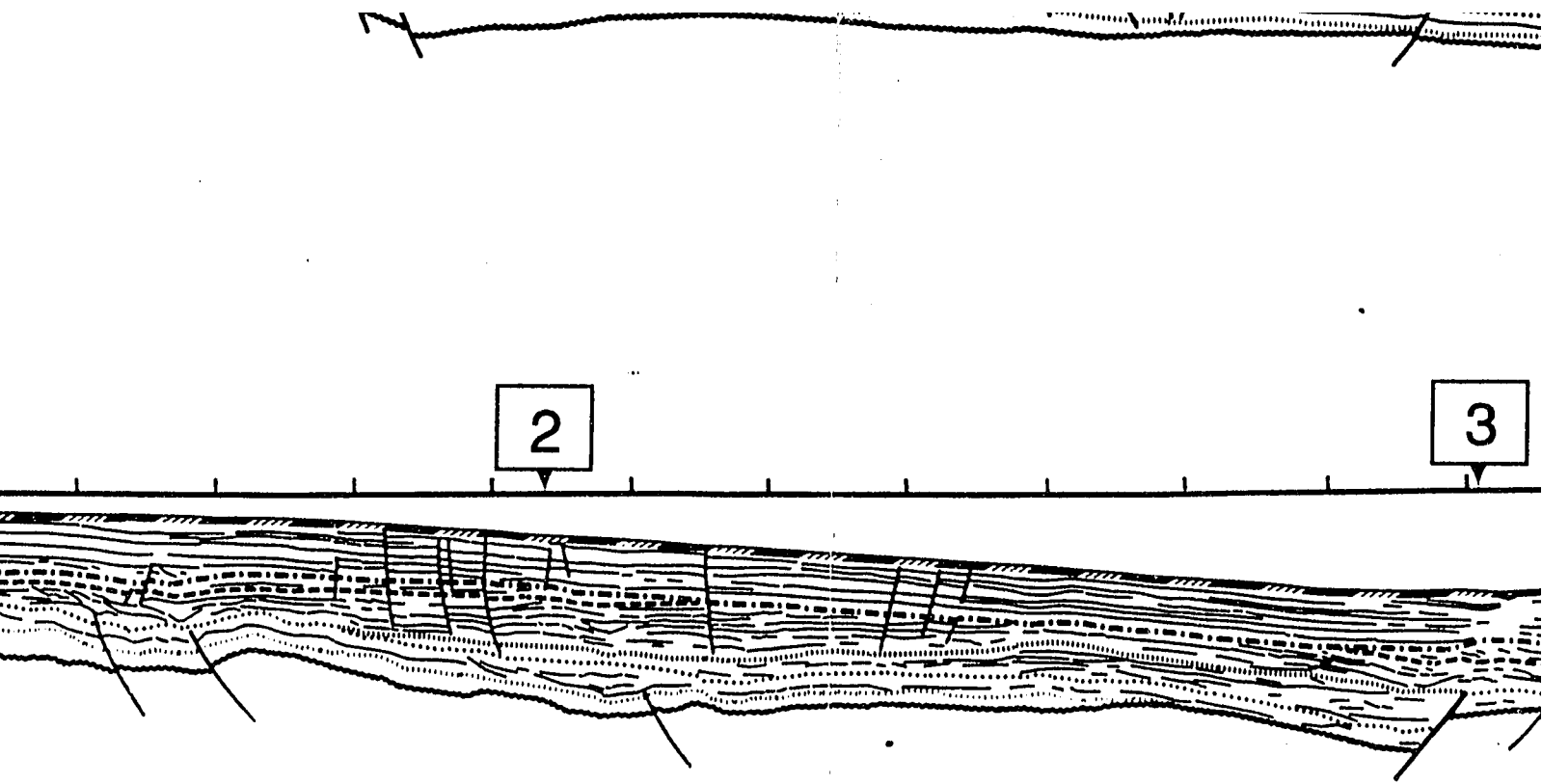
Profile A

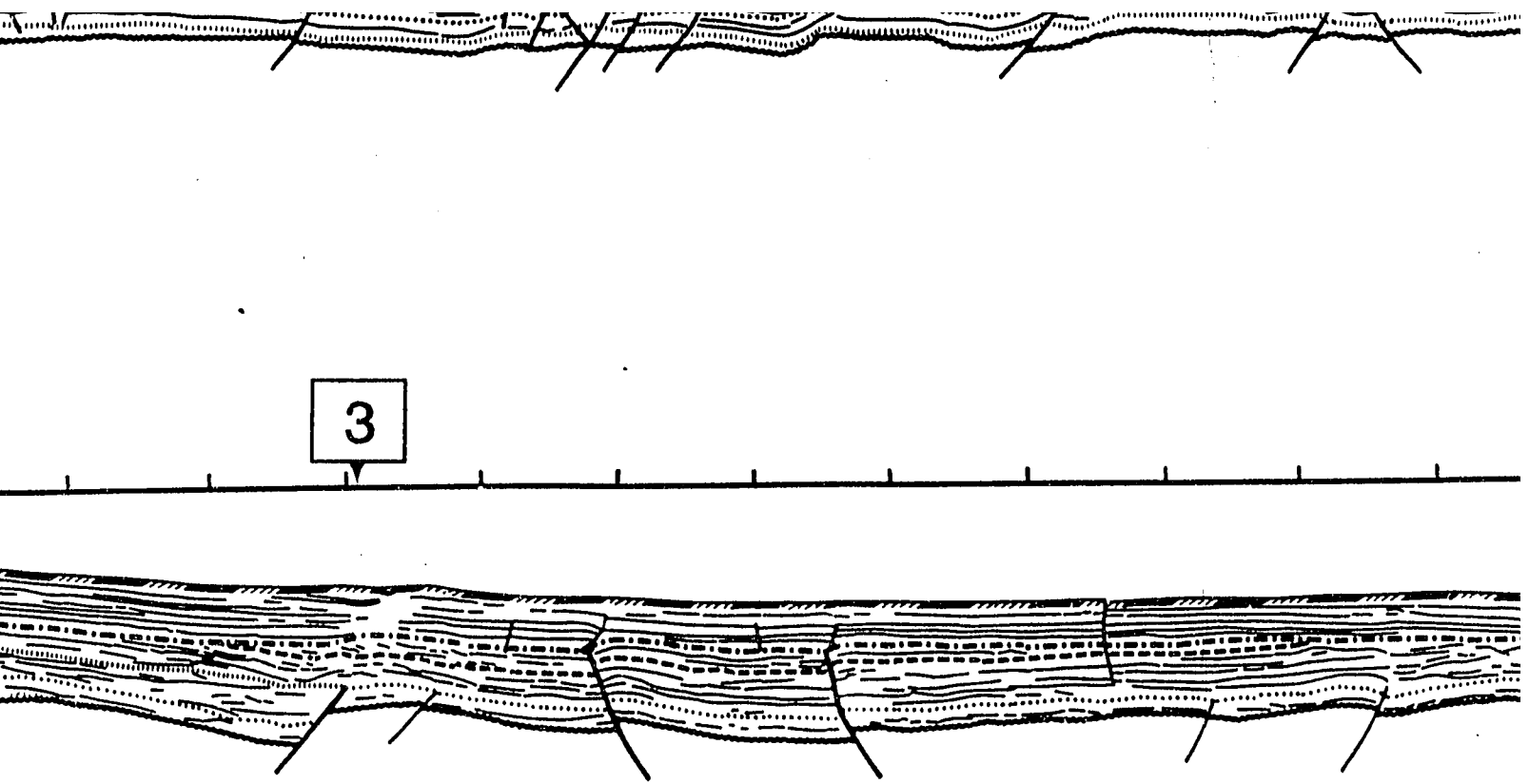




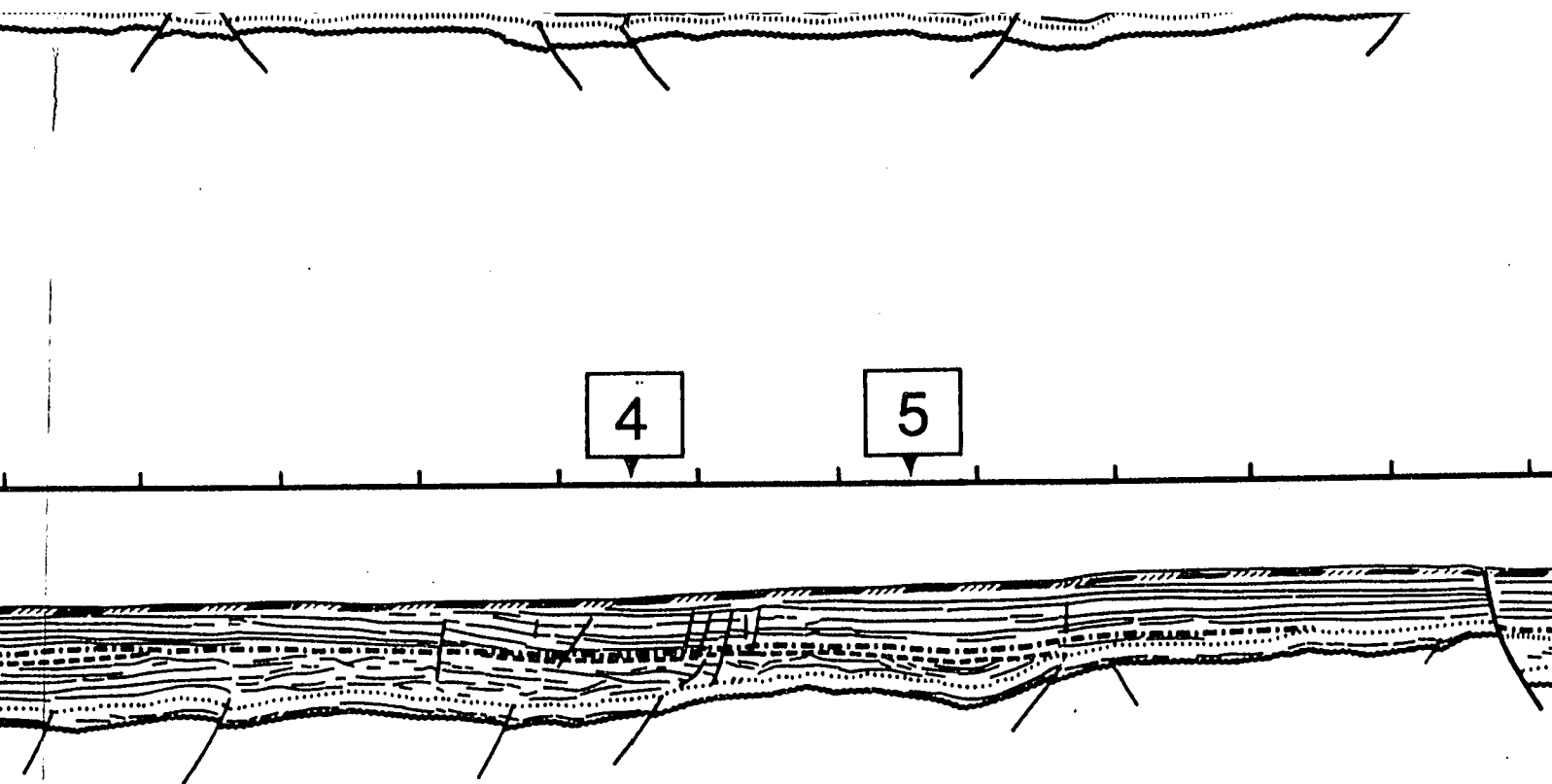
VW







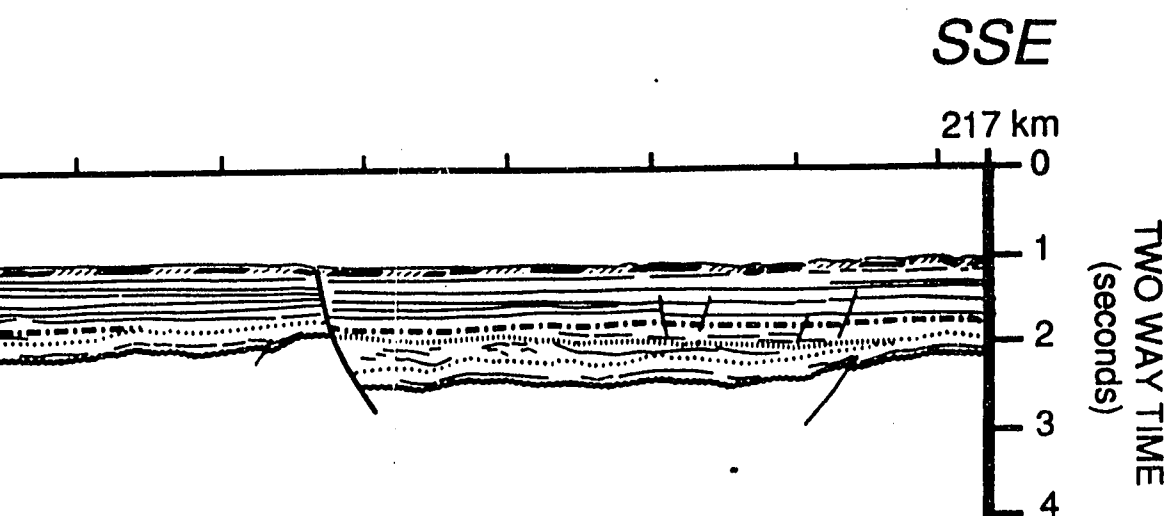
LINE DRAWING OF SEISMIC
FOREARC REGION OFFS
SOUTH CENTRAL PART OF



SEISMIC PROFILES
ON OFFSHORE PERU

PART OF STUDY AREA

WAY TIME
(seconds)
2
3

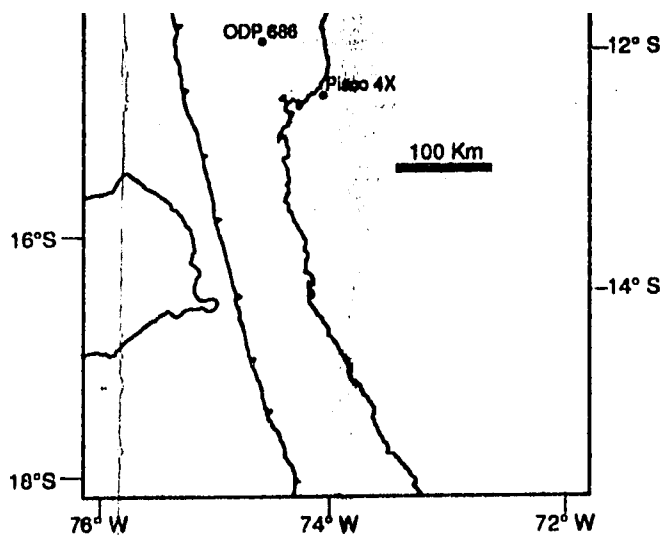


PANEL 4 STRIKE LINES



0 WAY TIME
(seconds)

1
2
3



L E G E N D **SEQUENCE A G E**

Q	Quaternary
P	Upper Miocene - Pliocene
M 3	Upper Miocene
M 2	Middle - Lower Miocene
M 1	Lower Miocene
E-O	Uppermost middle Eocene to Oligocene
E 3	Middle Eocene
E 2	Middle Eocene
E 1	Middle Eocene
E₀	Lower ? - Middle Eocene
K	Cretaceous ?
PK	Pre-Cretaceous Basement

PLEASE NOTE:

Oversize maps and charts are filmed in sections in the following manner:

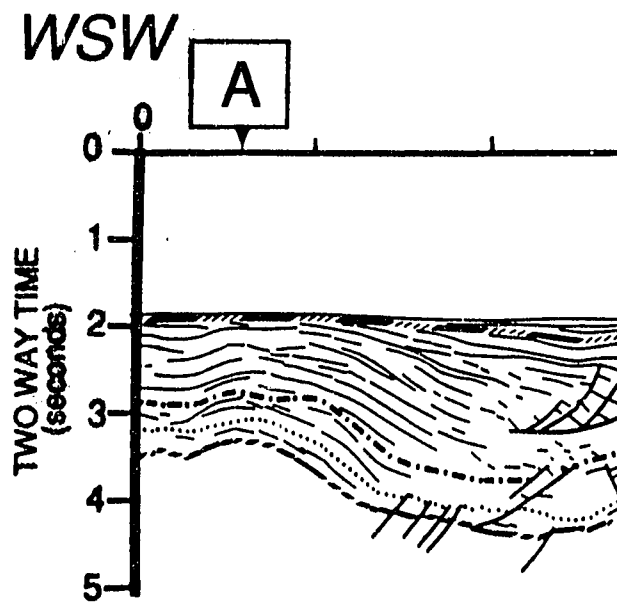
LEFT TO RIGHT, TOP TO BOTTOM, WITH SMALL OVERLAPS

The following map or chart has been refilmed in its entirety at the end of this dissertation (not available on microfiche). A xerographic reproduction has been provided for paper copies and is inserted into the inside of the back cover.

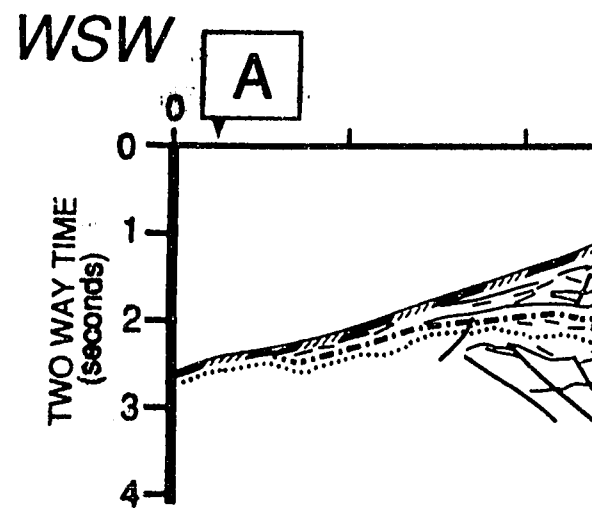
Black and white photographic prints (17" x 23") are available for an additional charge.

UMI

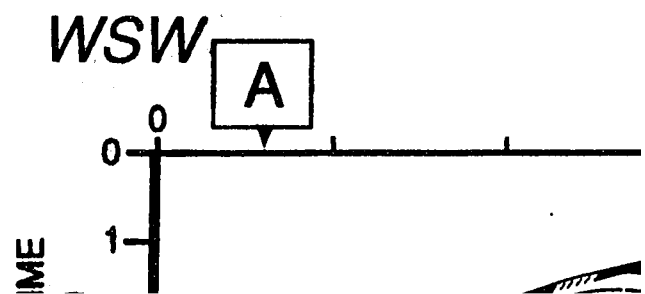
Profile 1

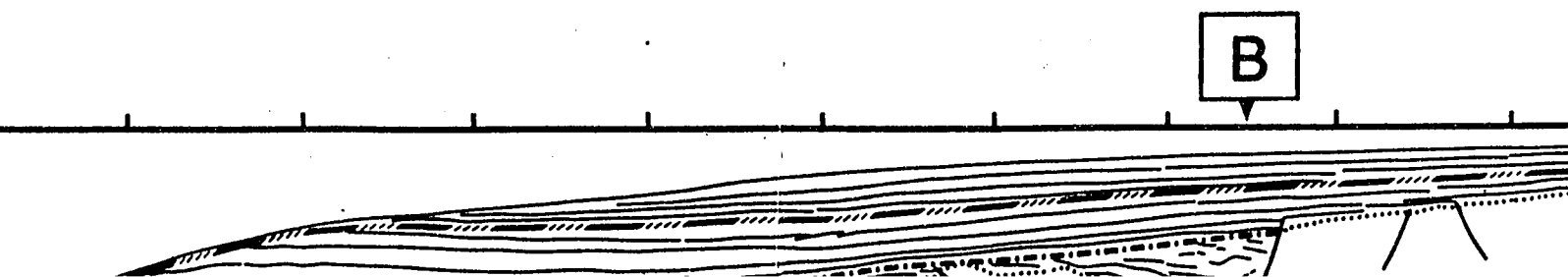
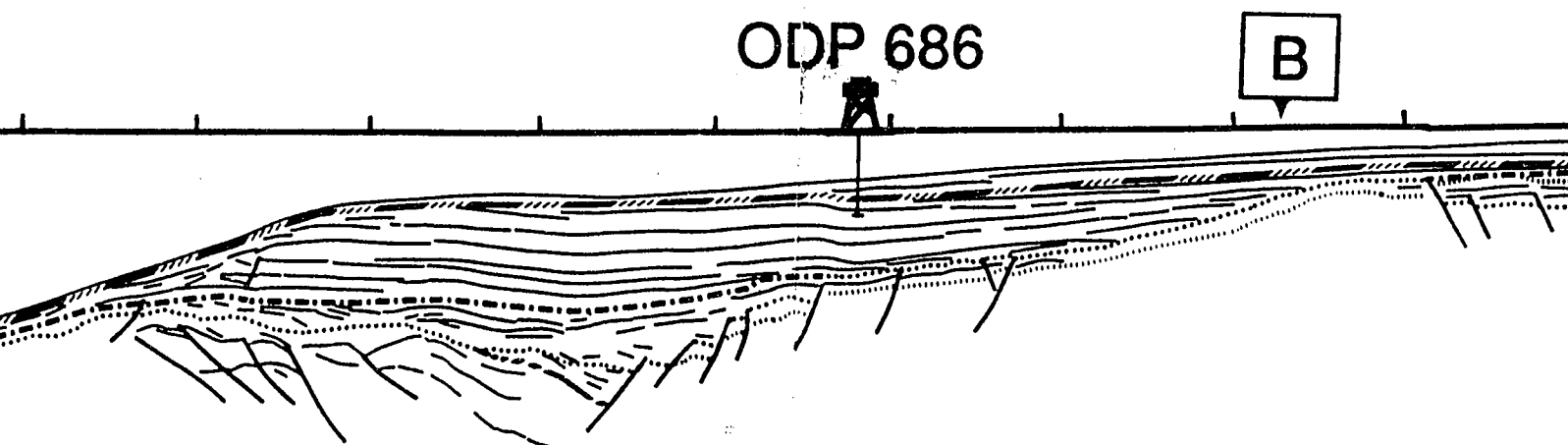
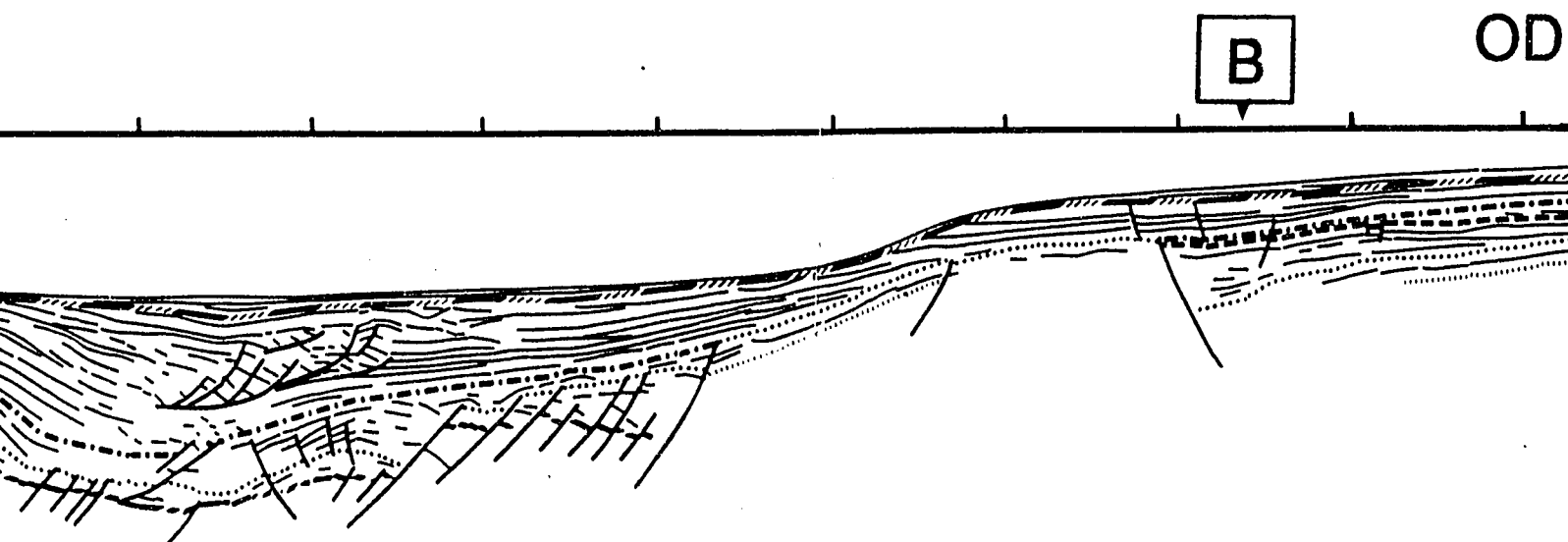


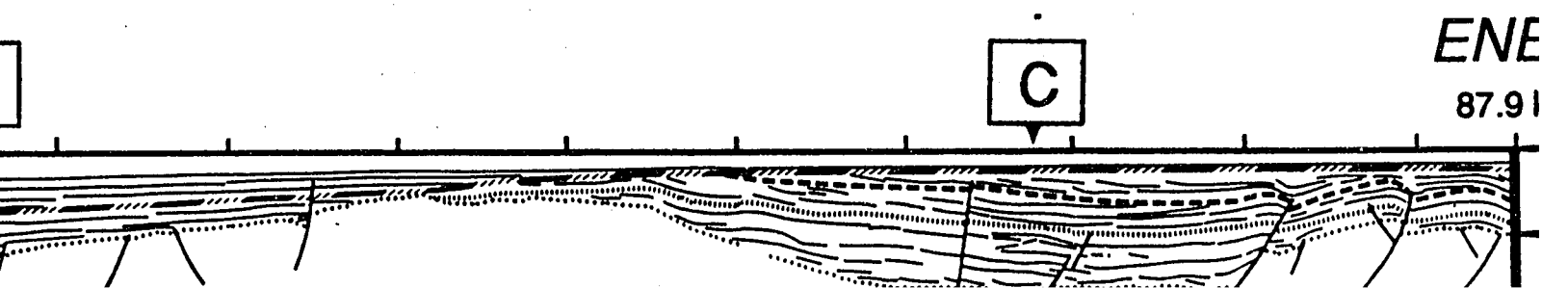
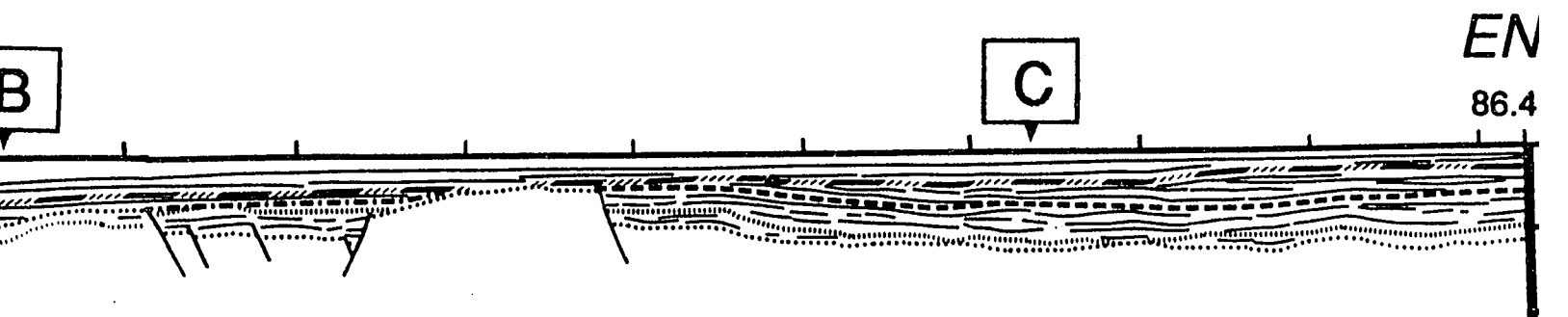
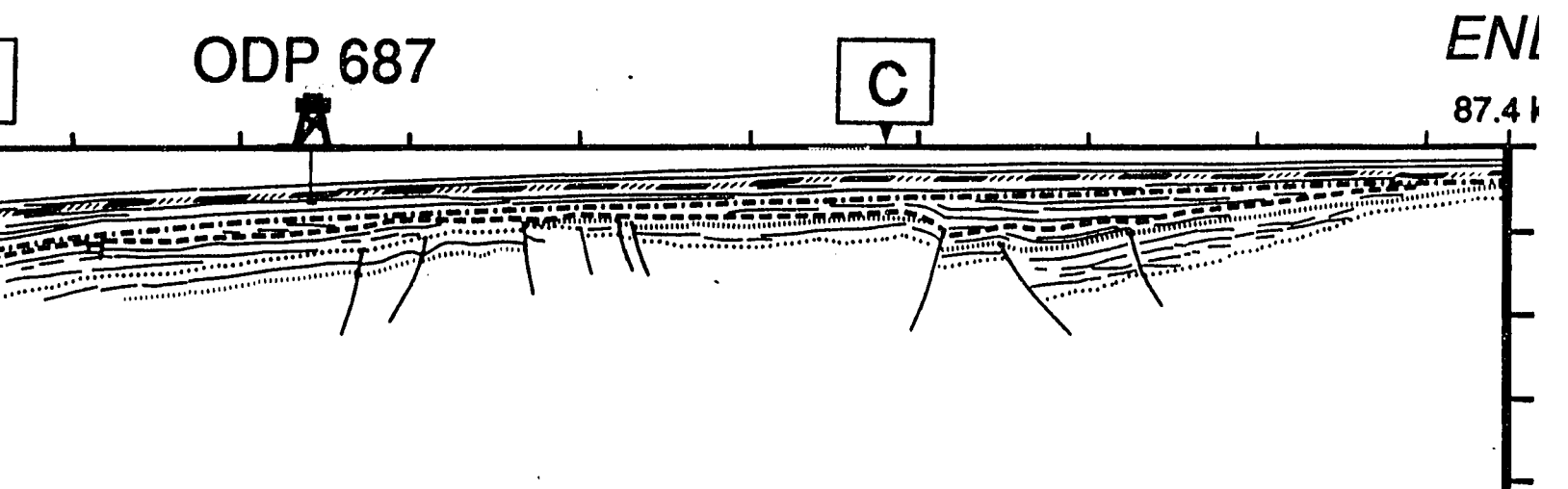
Profile 2



Profile 3







ENE

87.4 km

0
1
2
3
4

TWO WAY TIME
(seconds)

ENE

86.4 km

0
1
2

TWO WAY TIME
(seconds)

ENE

87.9 km

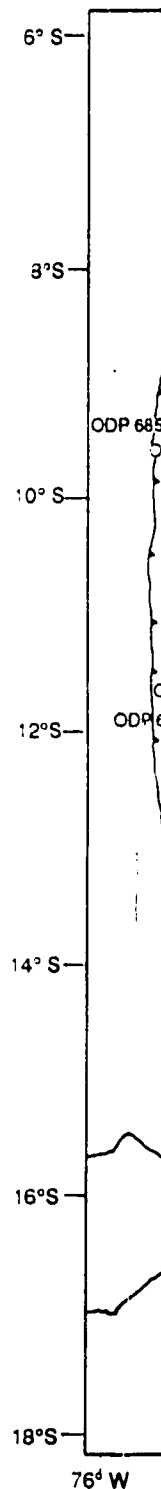
0
1

TWO WAY TIME
(seconds)

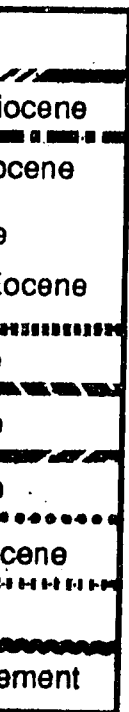
L E G E N D **SEQUENCE A G E**

Q	Quaternary
P	Upper Miocene - Pliocene
M 2	Middle - Lower Miocene
M 1	Lower Miocene
E-O	Uppermost middle Eocene to Oligocene
E 3	Middle Eocene
E 2	Middle Eocene
E 1	Middle Eocene
E₀	Lower ? - Middle Eocene
K	Cretaceous ?
PK	Pre-Cretaceous Basement

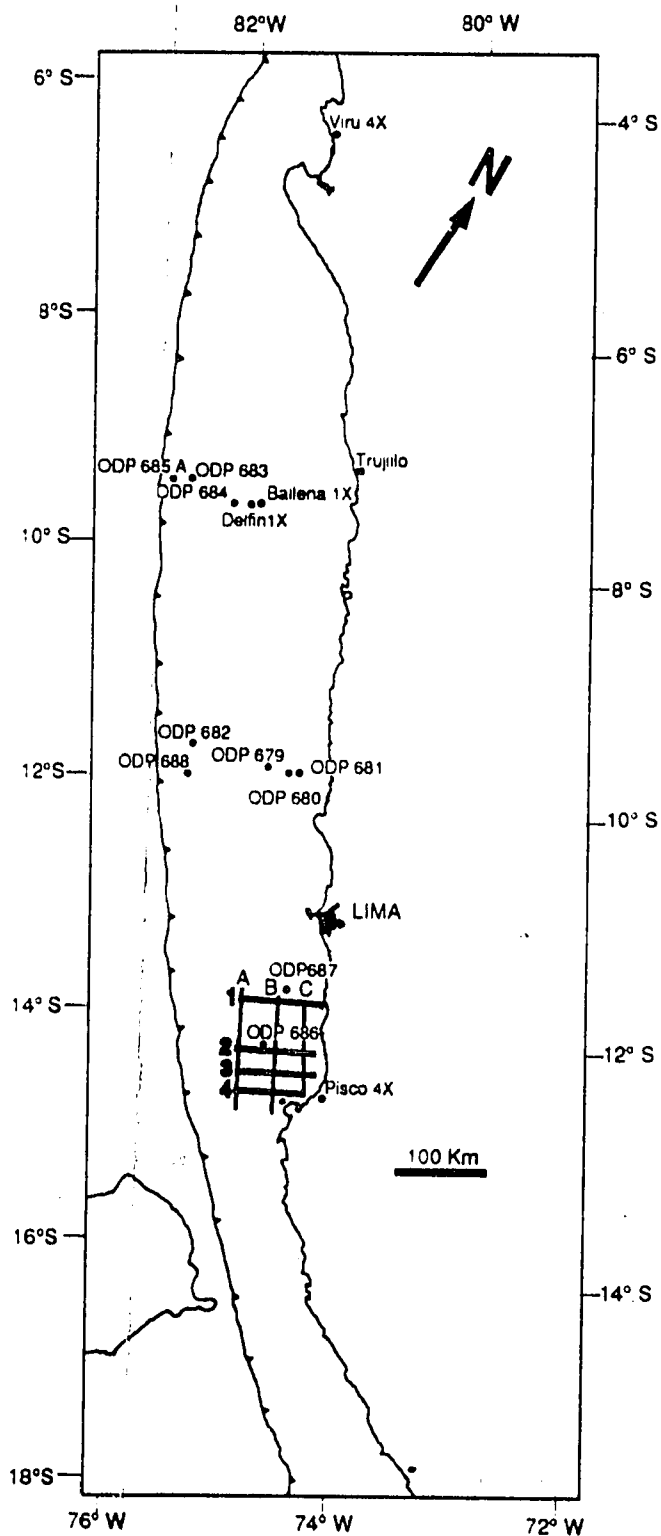
The upper Miocene M3 sequence was not deposited in this area.. Sequences M2, M1 and E-O are not differentiated.

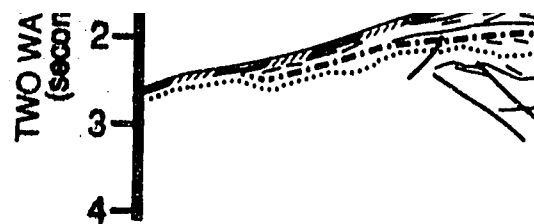


D
E

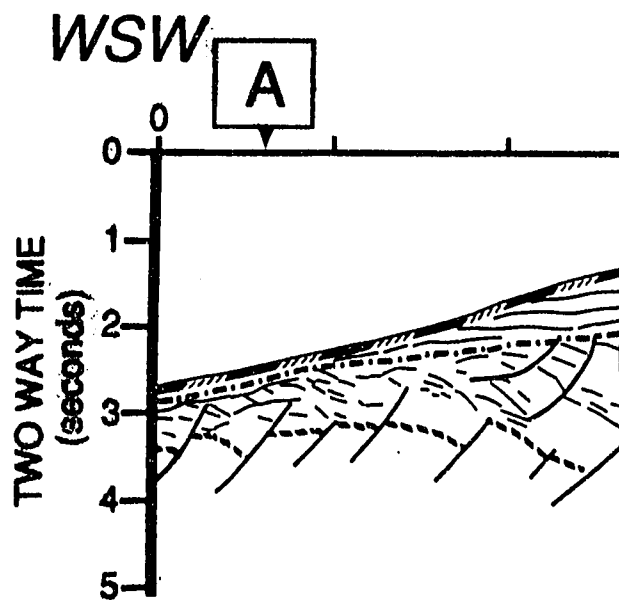


not depo-
and E-O

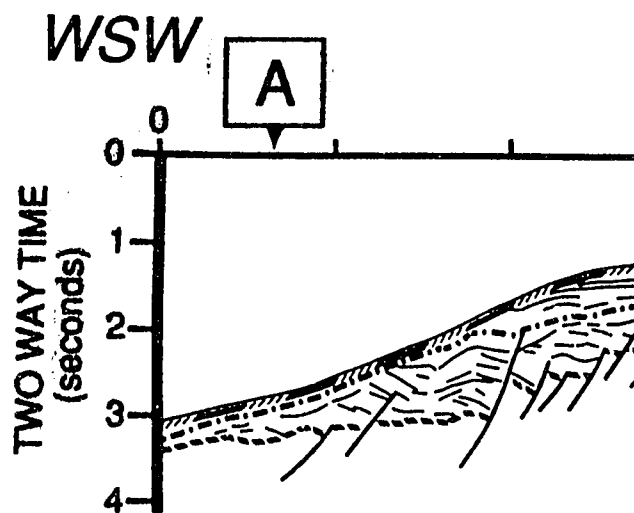


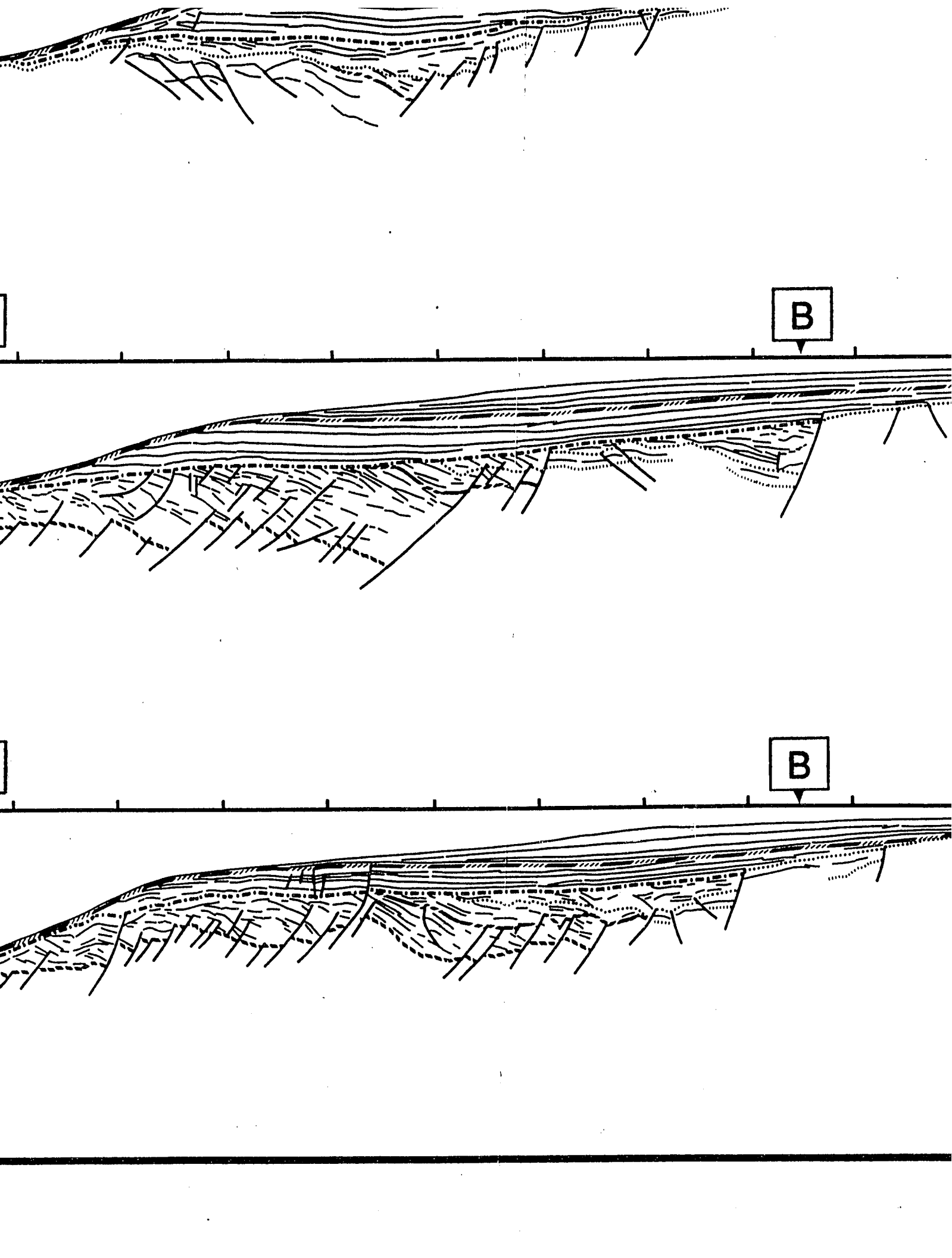


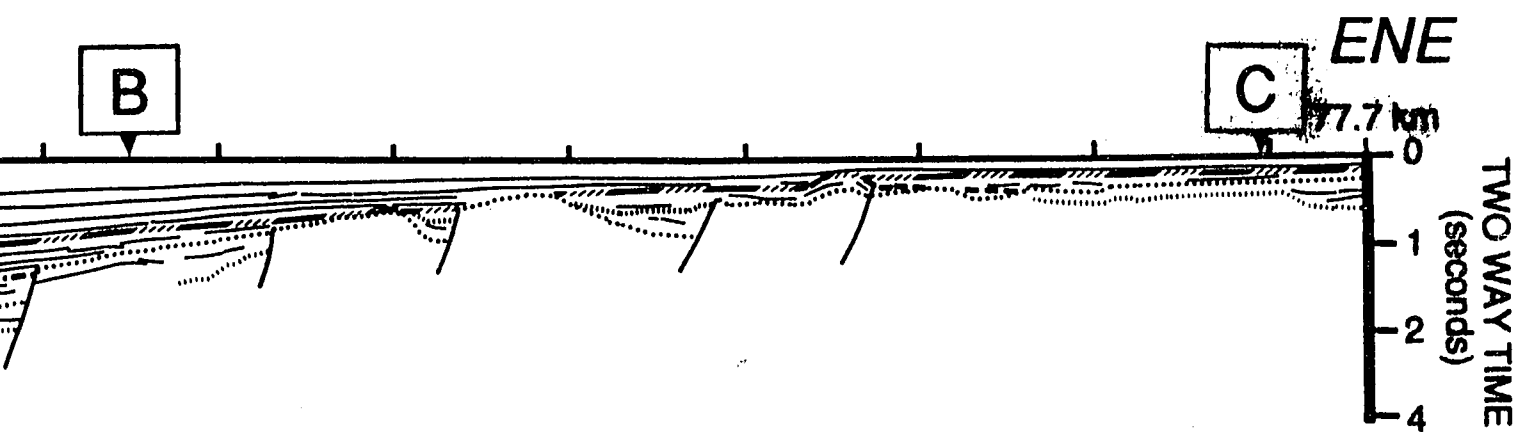
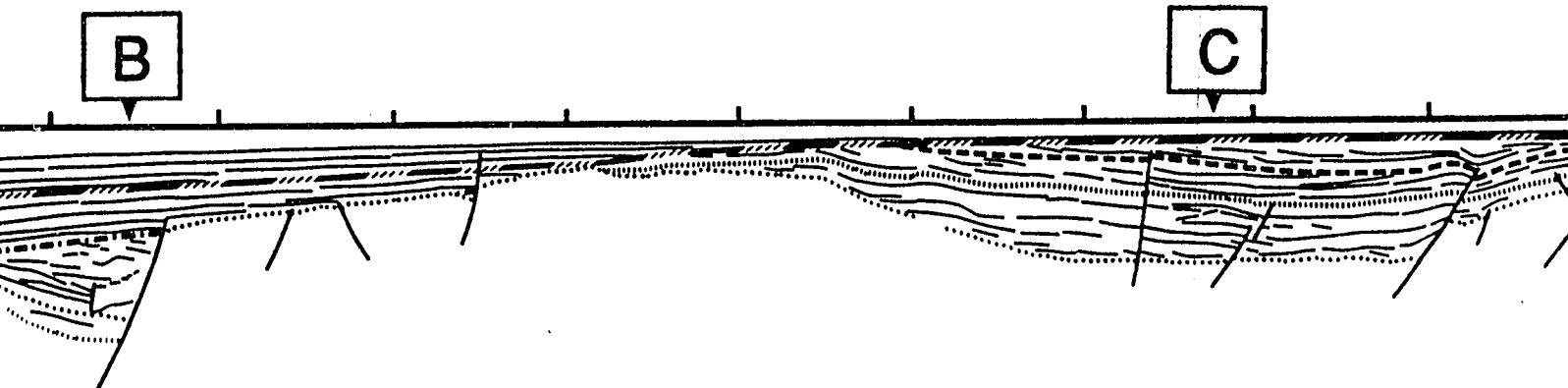
Profile 3

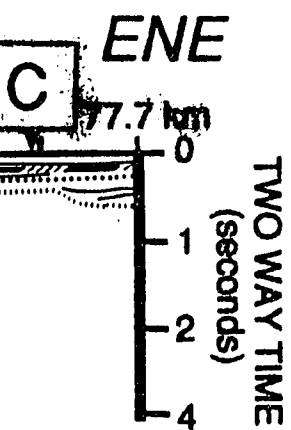
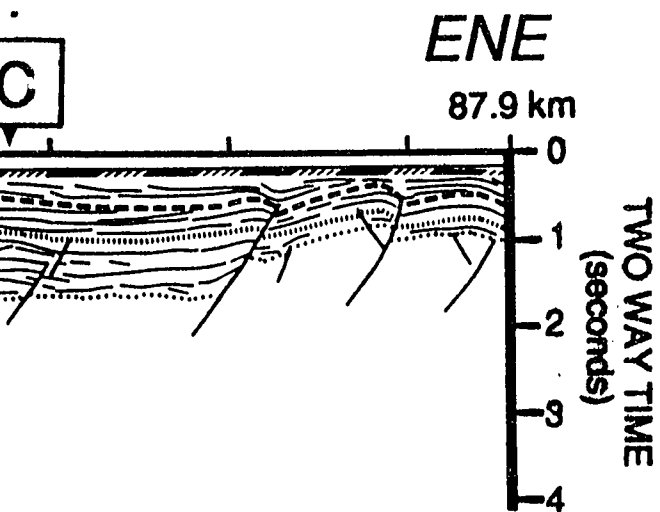


Profile 4









LIN
FO

Sc

E 3	Middle Eocene
E 2	Middle Eocene
E 1	Middle Eocene
E ₀	Lower ? - Middle Eocene
K	Cretaceous ?
PK	Pre-Cretaceous Basement

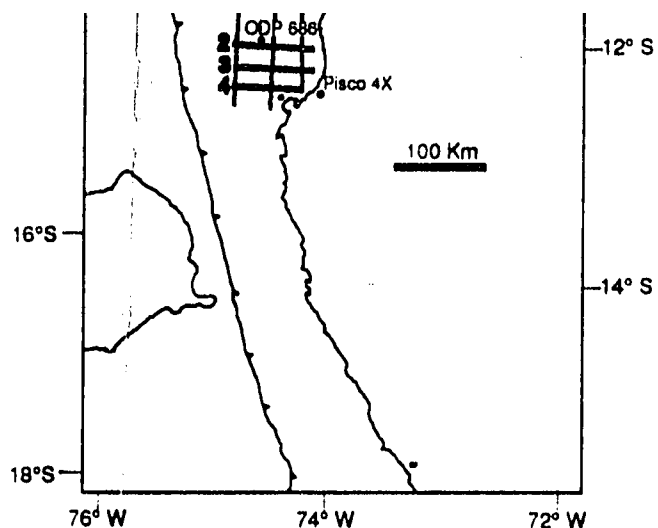
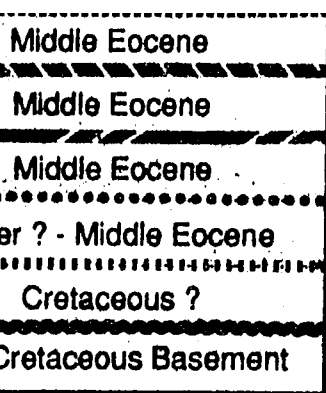
The upper Miocene M3 sequence was not deposited in this area.. Sequences M2, M1 and E-O are not differentiated.

LINE DRAWING OF SEISMIC P FOREARC REGION OFFSHORE

SOUTHERN PART OF STUDY

20 km

*PANEL 5
DIP LINES*

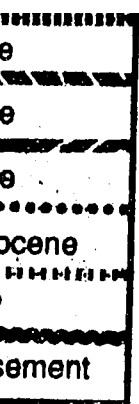


sequence was not dependent on the sequences M2, M1 and E-O

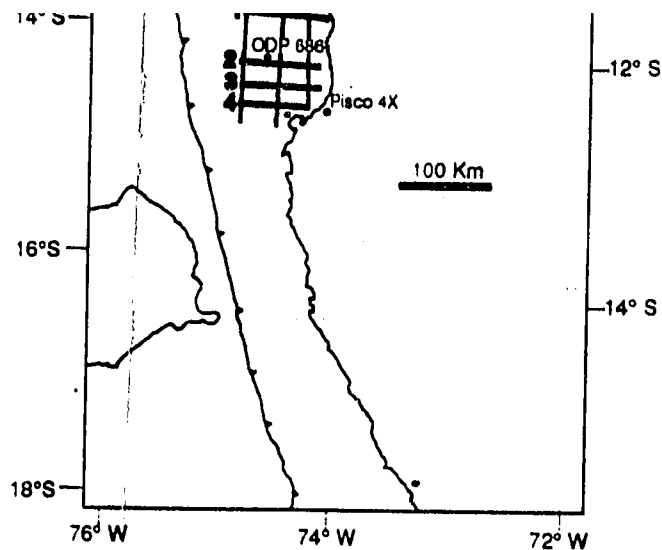
OF SEISMIC PROFILES ON OFFSHORE PERU

PART OF STUDY AREA

*NEL 5
LINES*



not depo-
and E-O



EISMIC PROFILES OFFSHORE PERU

STUDY AREA

*L 5
ES*

PLEASE NOTE:

Oversize maps and charts are filmed in sections in the following manner:

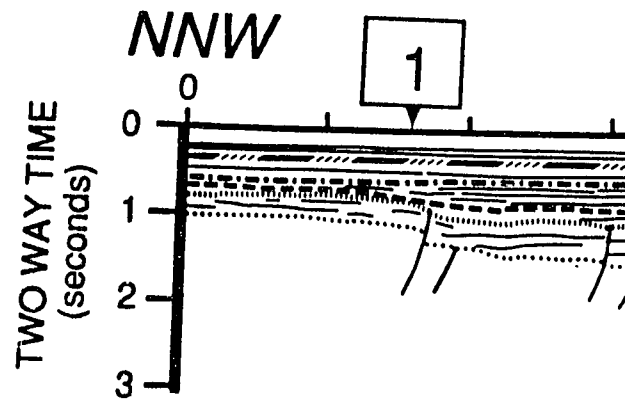
LEFT TO RIGHT, TOP TO BOTTOM, WITH SMALL OVERLAPS

The following map or chart has been refilmed in its entirety at the end of this dissertation (not available on microfiche). A xerographic reproduction has been provided for paper copies and is inserted into the inside of the back cover.

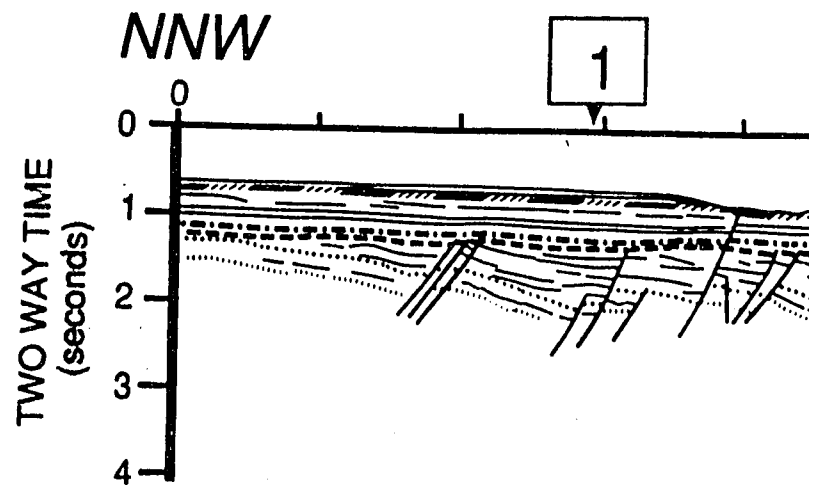
Black and white photographic prints (17" x 23") are available for an additional charge.

UMI

Profile C

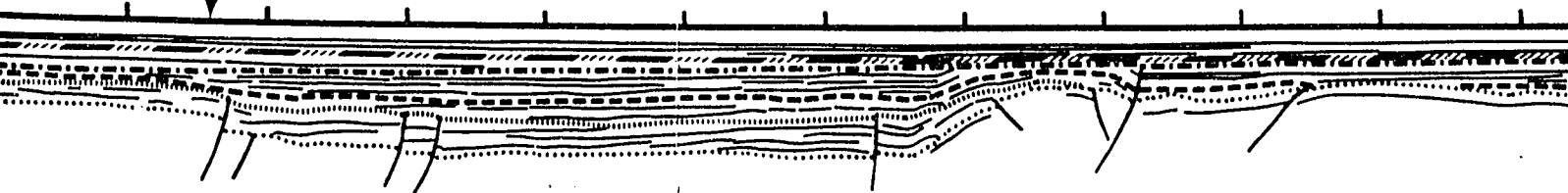


Profile B

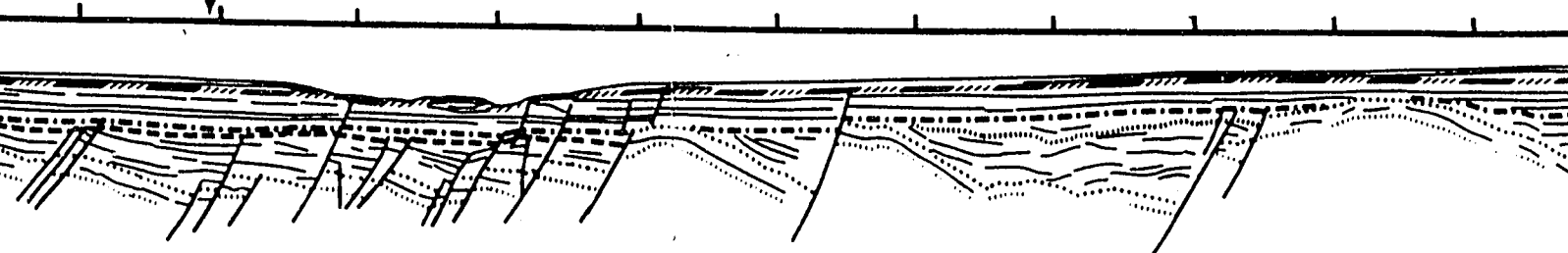


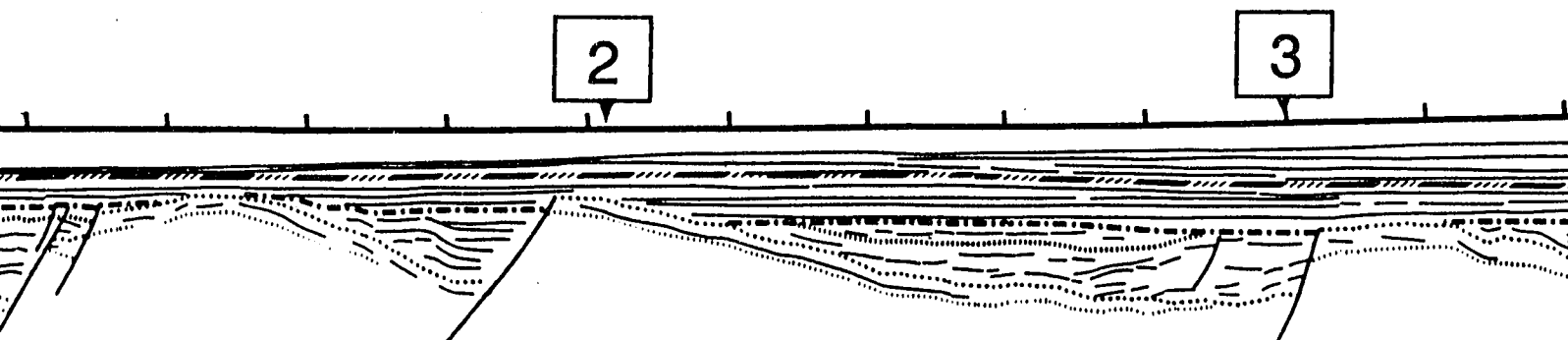
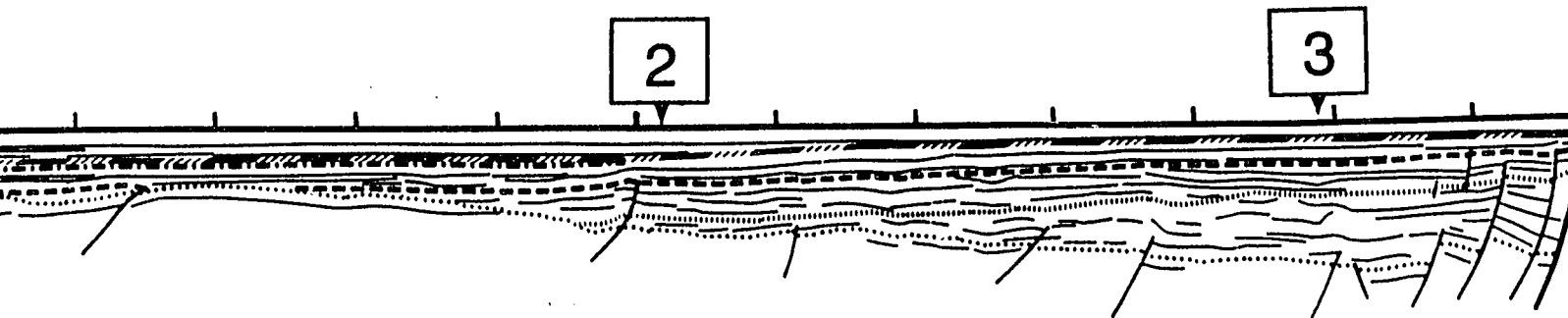
NW

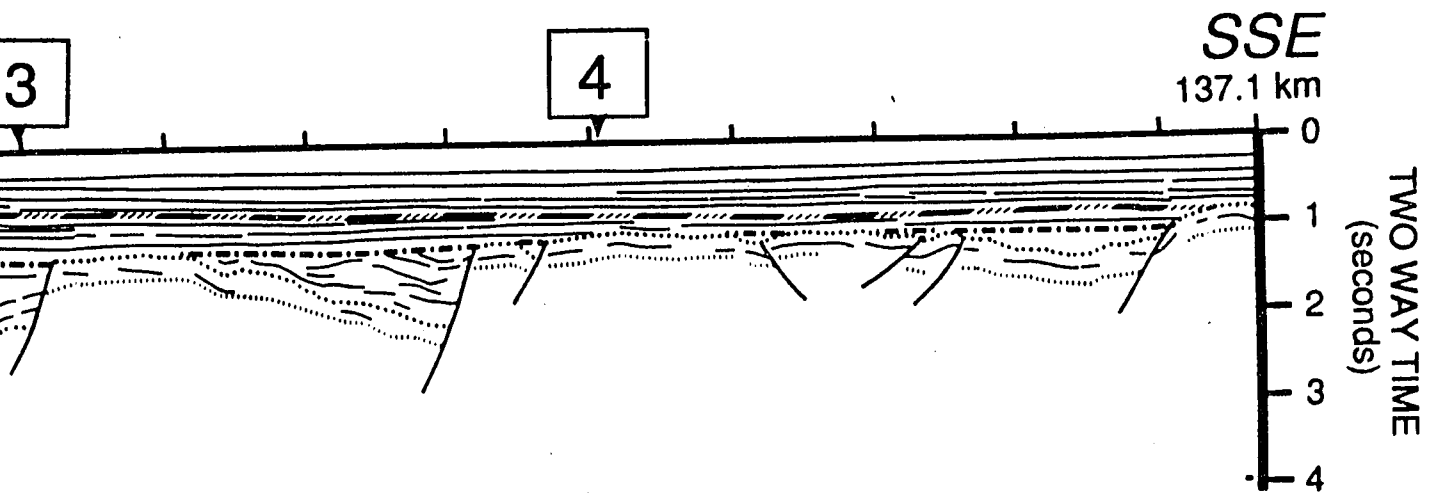
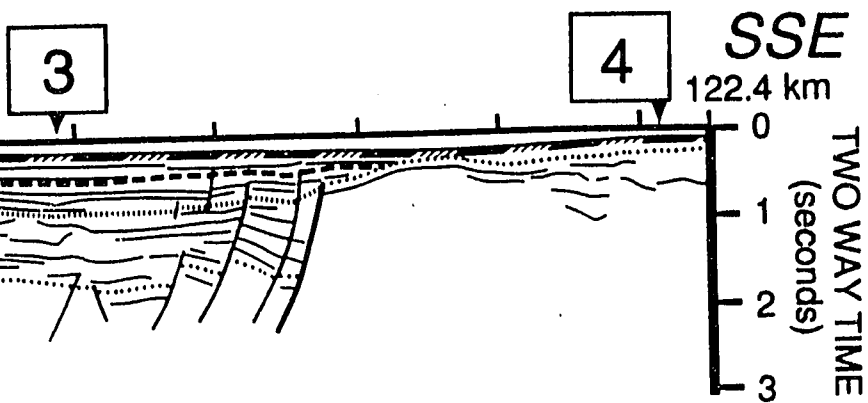
1



1



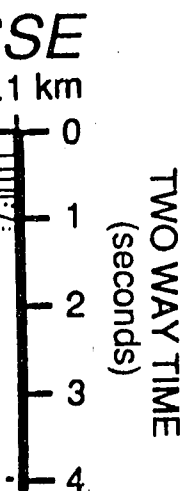




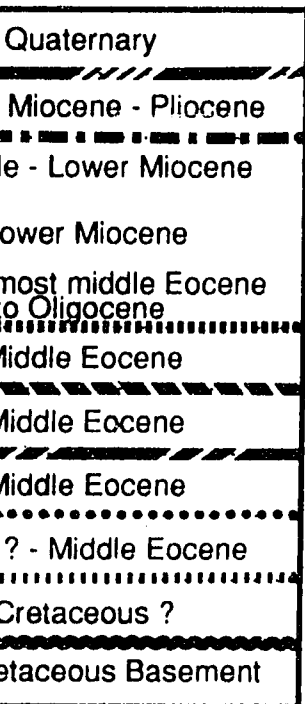
L E G E N D **SEQUENCE A G E**

Q	Quaternary
P	Upper Miocene - Pliocene
M 2	Middle - Lower Miocene
M 1	Lower Miocene
E-O	Uppermost middle Eocene to Oligocene
E 3	Middle Eocene
E 2	Middle Eocene
E 1	Middle Eocene
E₀	Lower ? - Middle Eocene
K	Cretaceous ?
PK	Pre-Cretaceous Basement

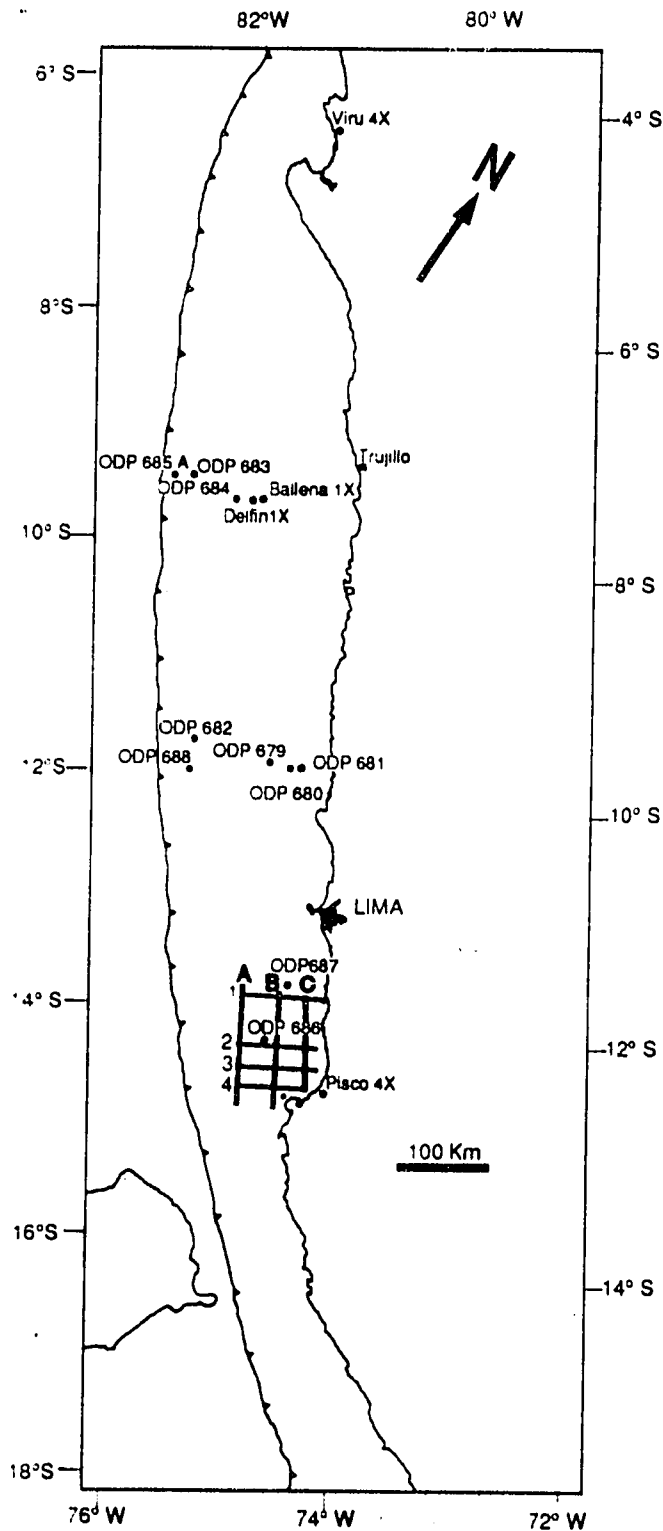
The upper Miocene M3 sequence was not deposited in this area.. Sequences M2, M1 and E-O are not differentiated.



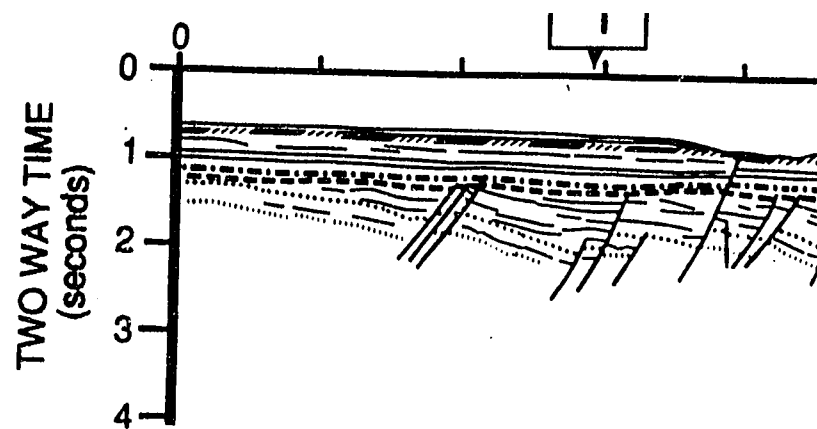
E N D **A G E**



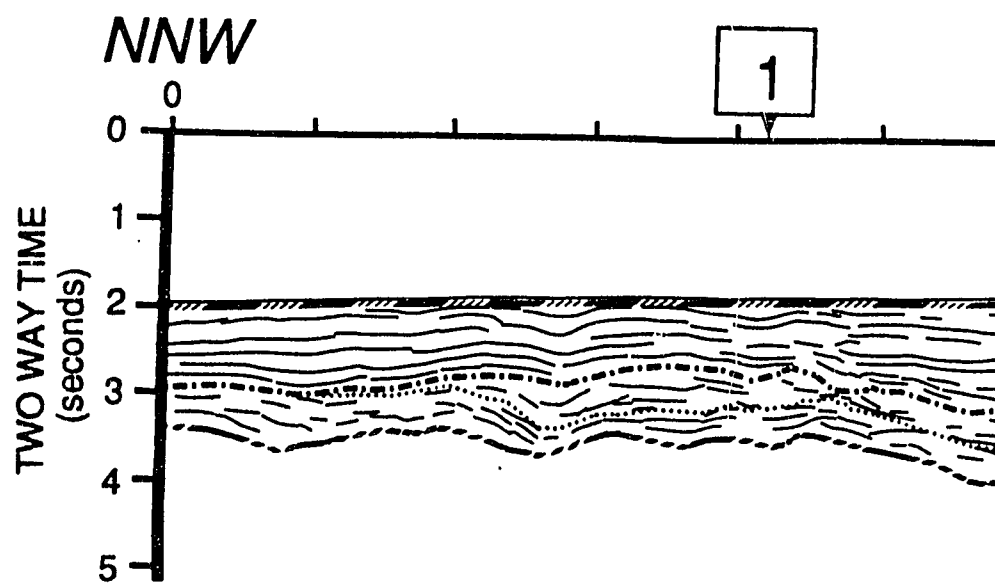
sequence was not deposited
between M2, M1 and E-O



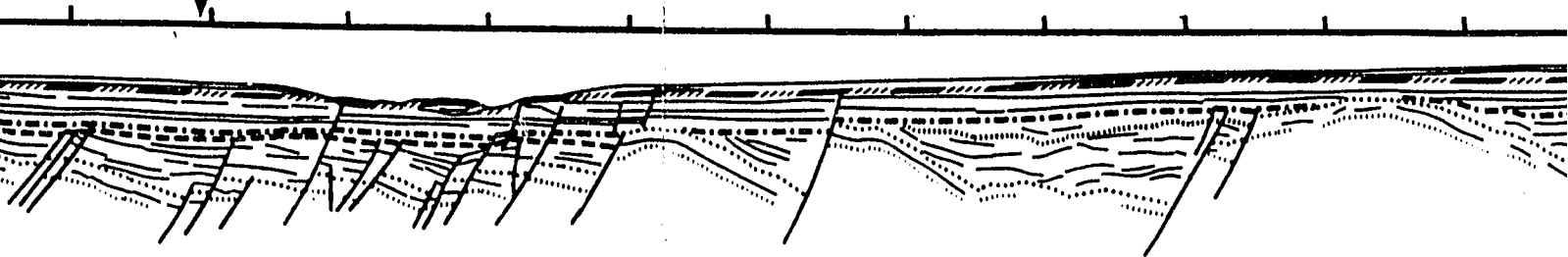
20 km



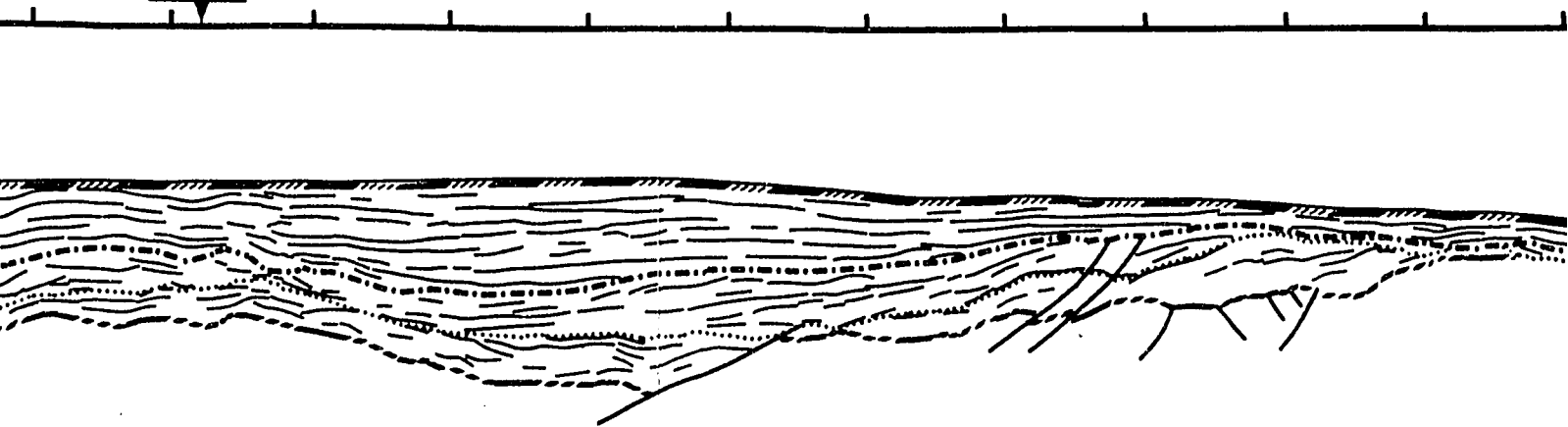
Profile A

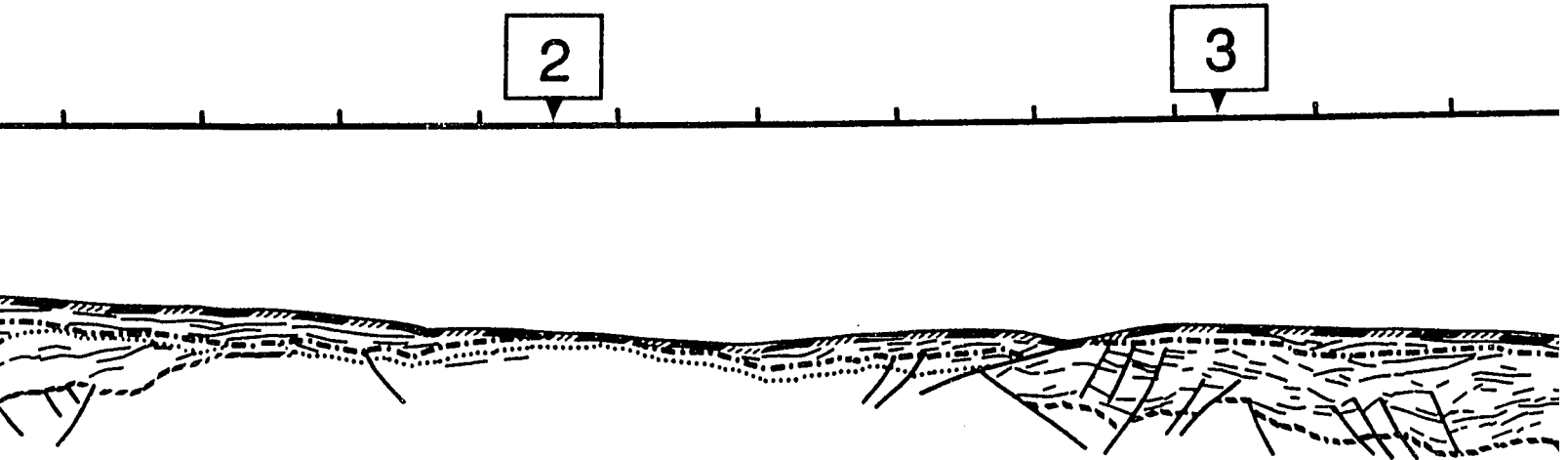
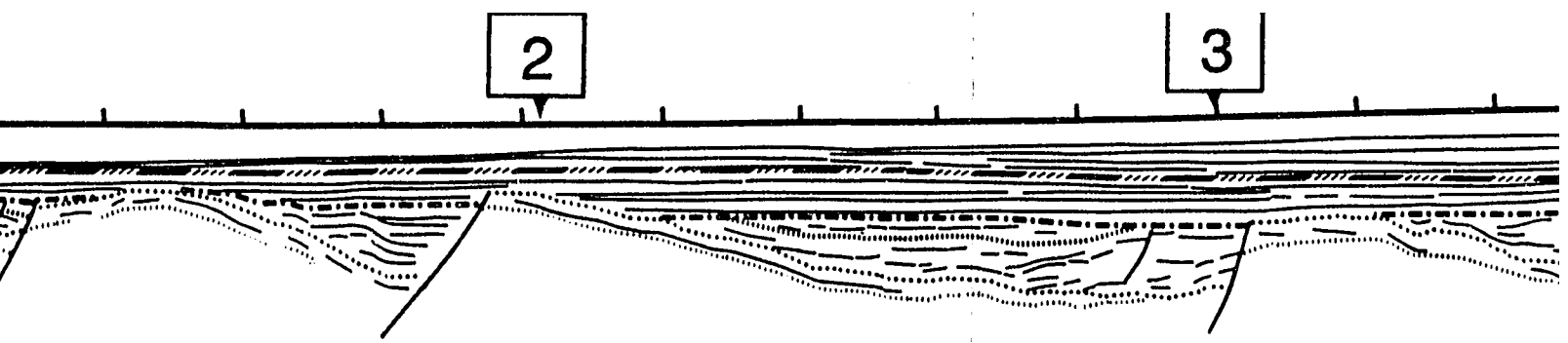


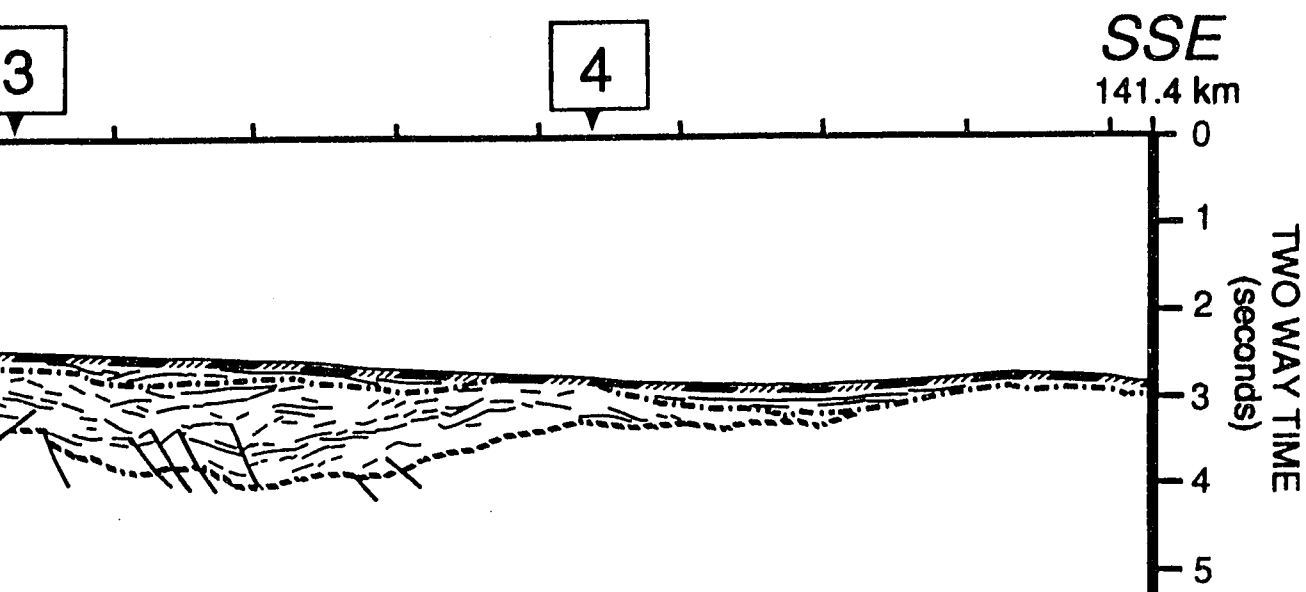
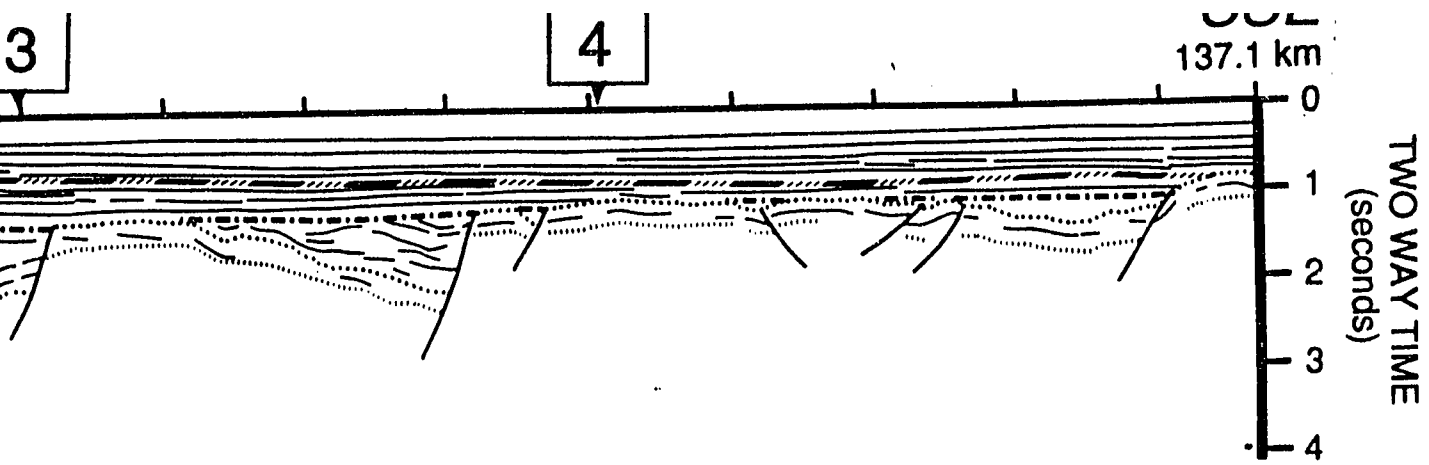
1

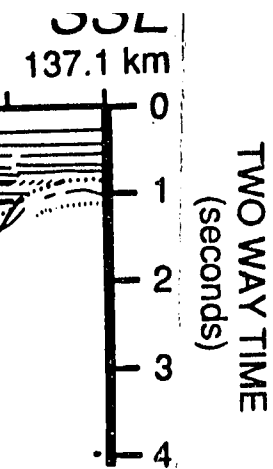


1



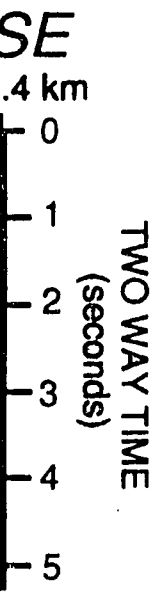






PK Pre-Cretaceous Basement

The upper Miocene M3 sequence was not deposited in this area.. Sequences M2, M1 and E- are not differentiated.



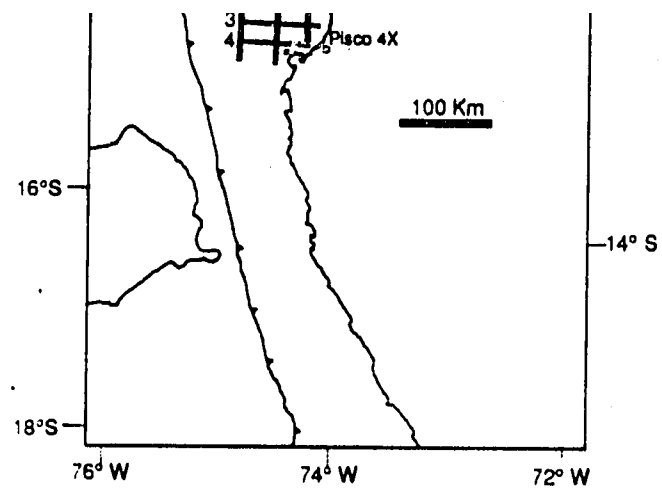
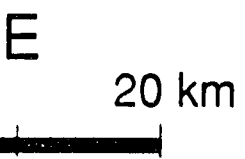
LINE DRAWING OF FOREARC REGION

SOUTHERN PART

*P A I
STRIK*

olaceous Basement

sequence was not deposited
sequences M2, M1 and E-O



VIEWING OF SEISMIC PROFILES REGION OFFSHORE PERU

N PART OF STUDY AREA

PANEL 6
STRIKE LINES

PLEASE NOTE:

Oversize maps and charts are filmed in sections in the following manner:

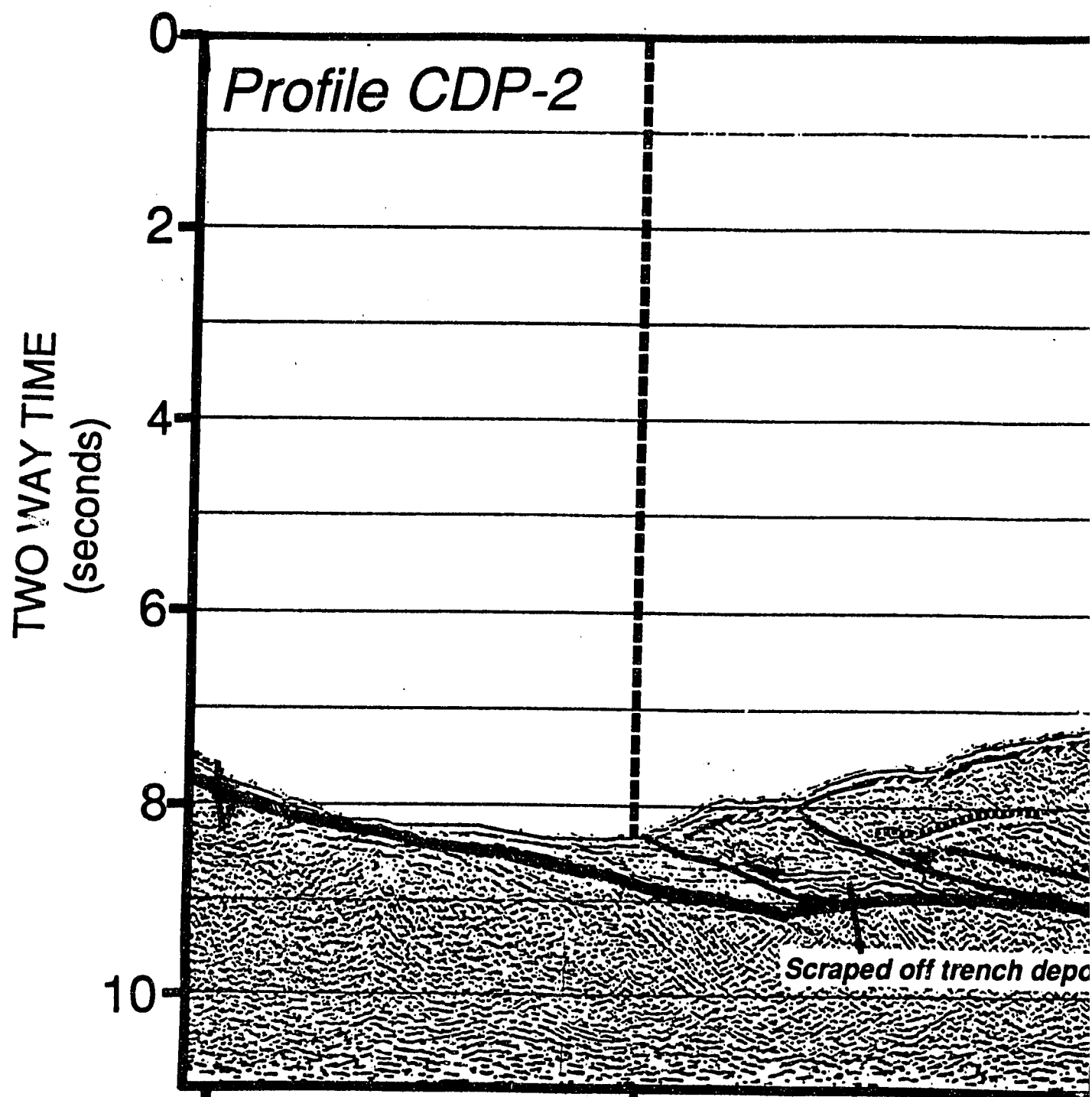
LEFT TO RIGHT, TOP TO BOTTOM, WITH SMALL OVERLAPS

The following map or chart has been refilmed in its entirety at the end of this dissertation (not available on microfiche). A xerographic reproduction has been provided for paper copies and is inserted into the inside of the back cover.

Black and white photographic prints (17" x 23") are available for an additional charge.

UMI

SW

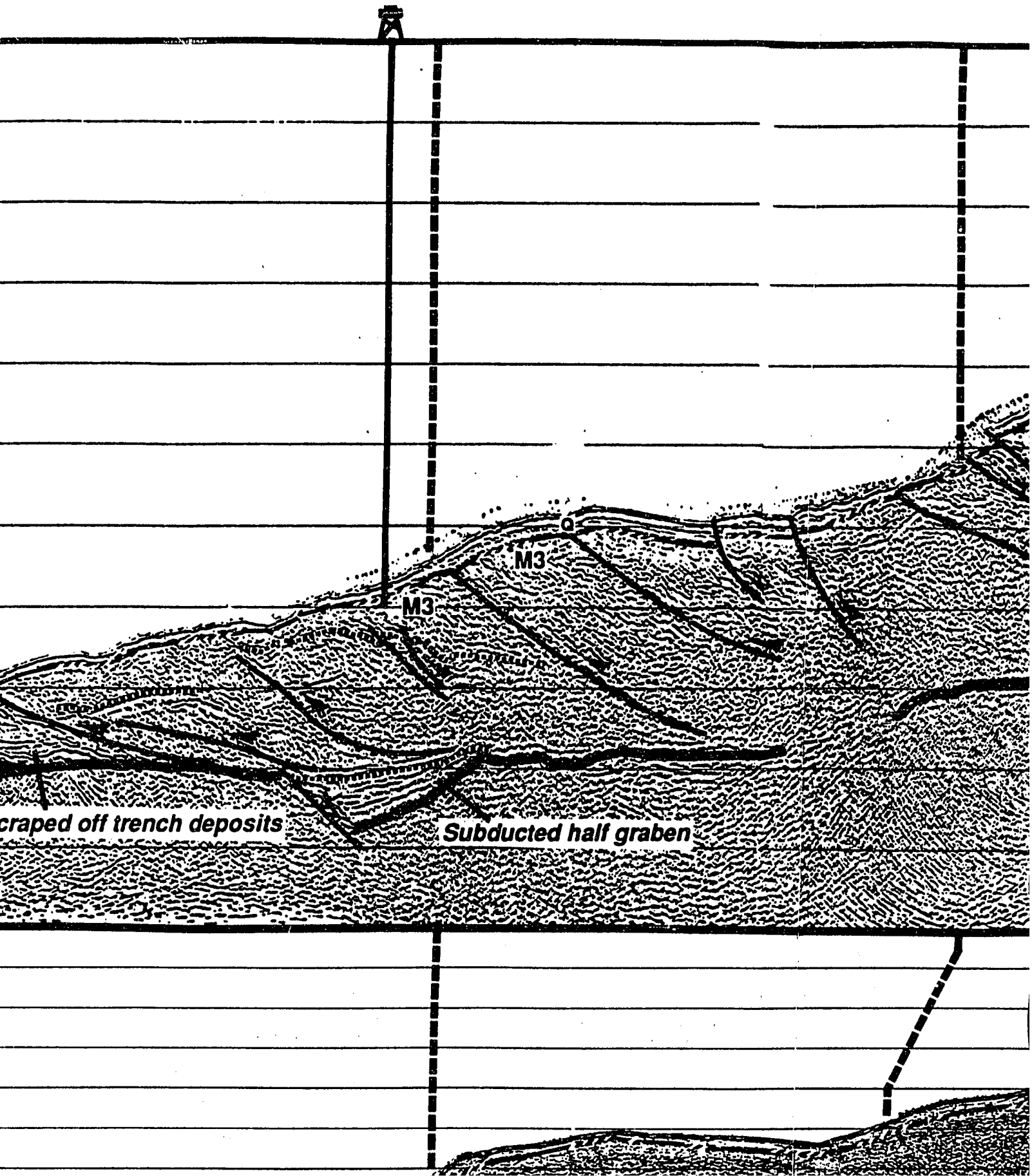


Profile PERU 5

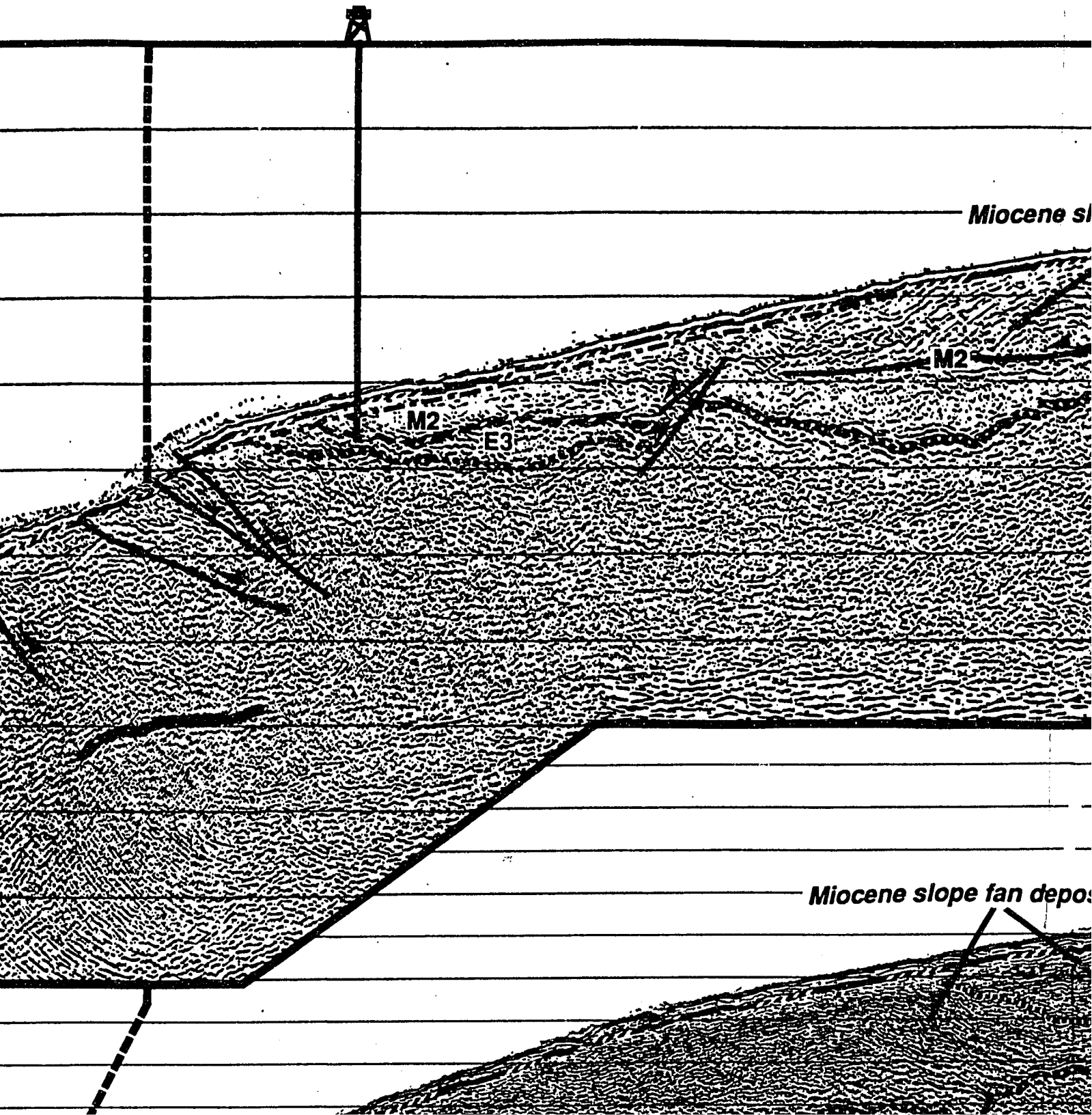
TIME

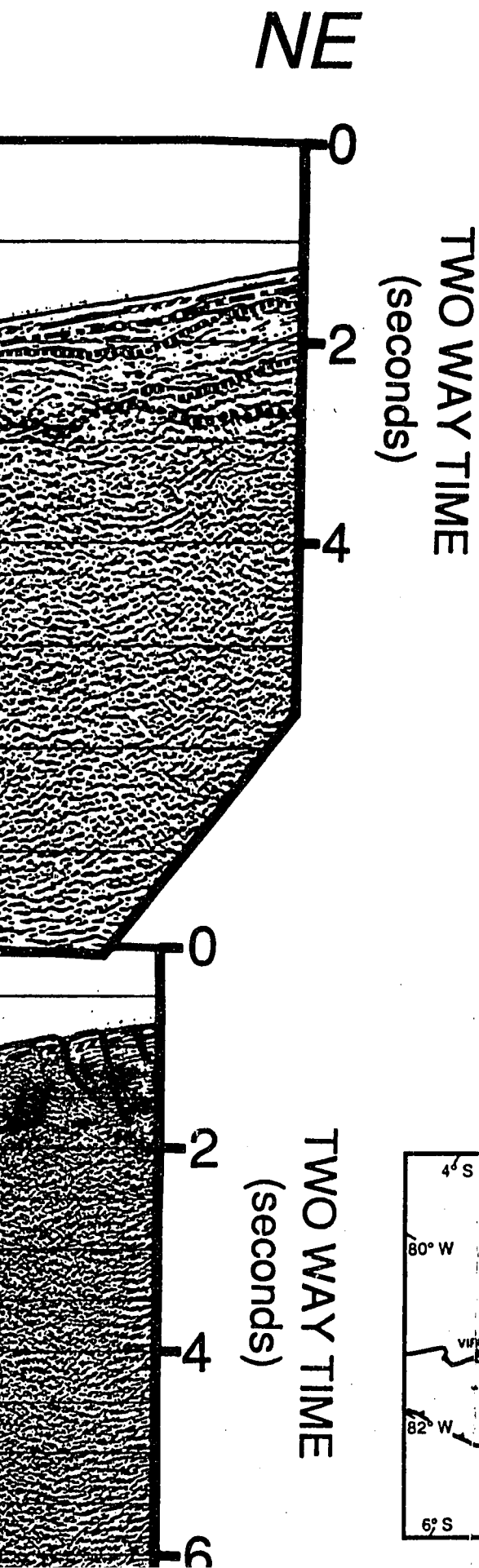
4

ODP 685



ODP 683





ACCRETIONARY TRENCH LOCATED WEST OF THE FOREARC REGION

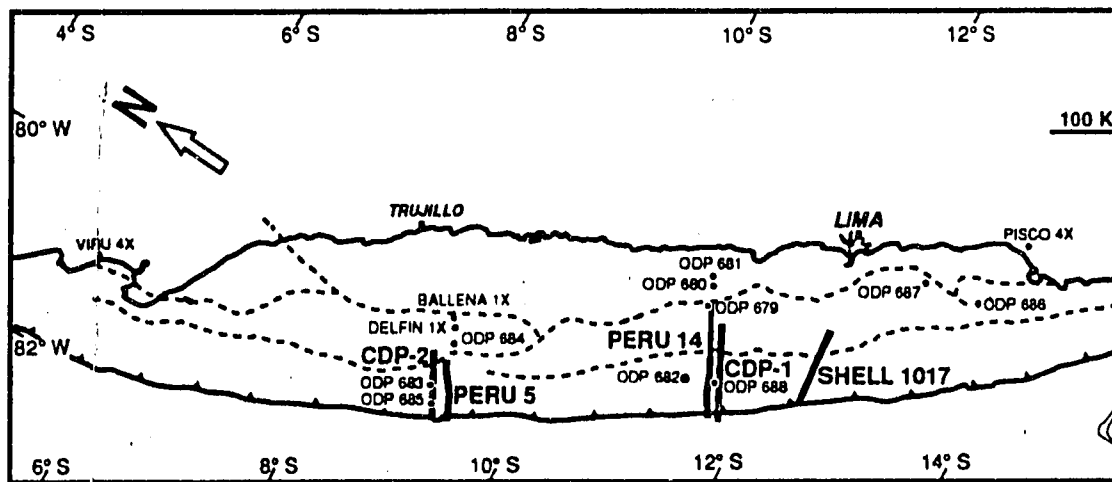
OCEANIC CRUST

UNCONFORMITY

HYDRATE REFLECTOR

NORMAL FAULT

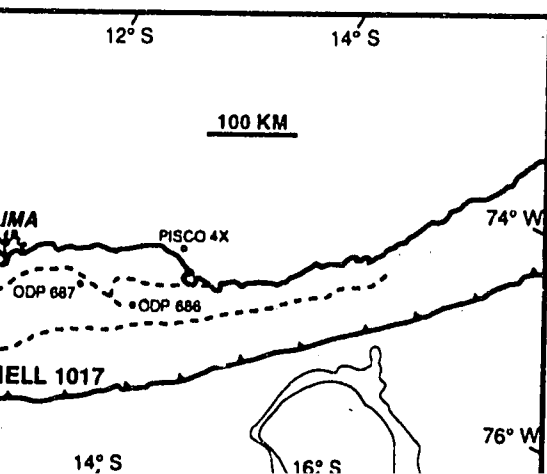
REVERSE FAULT



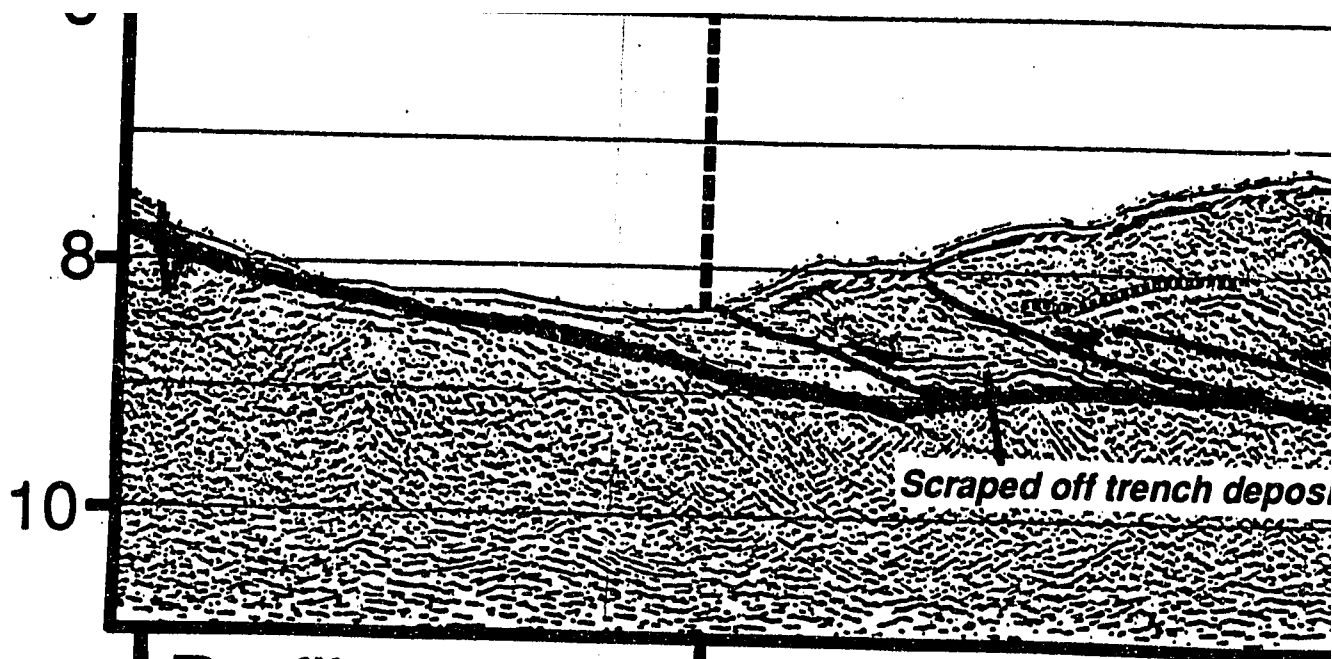
PANEL 7 **RETIONARY ZONE- SLOPE ZONE** **ST OF THE TRUJILLO AND LIMA BASINS** **ARC REGION OFFSHORE PERU**

L E G E N D **SEQUENCE A G E**

Q	QUATERNARY
P	UPPER MIOCENE -PLIOCENE
M 3	UPPER MIOCENE
M 2	MIDDLE - LOWER MIOCENE
E 3	MIDDLE EOCENE
E₀	LOWER ? - MIDDLE EOCENE
	PRE-CENOZOIC BASEMENT

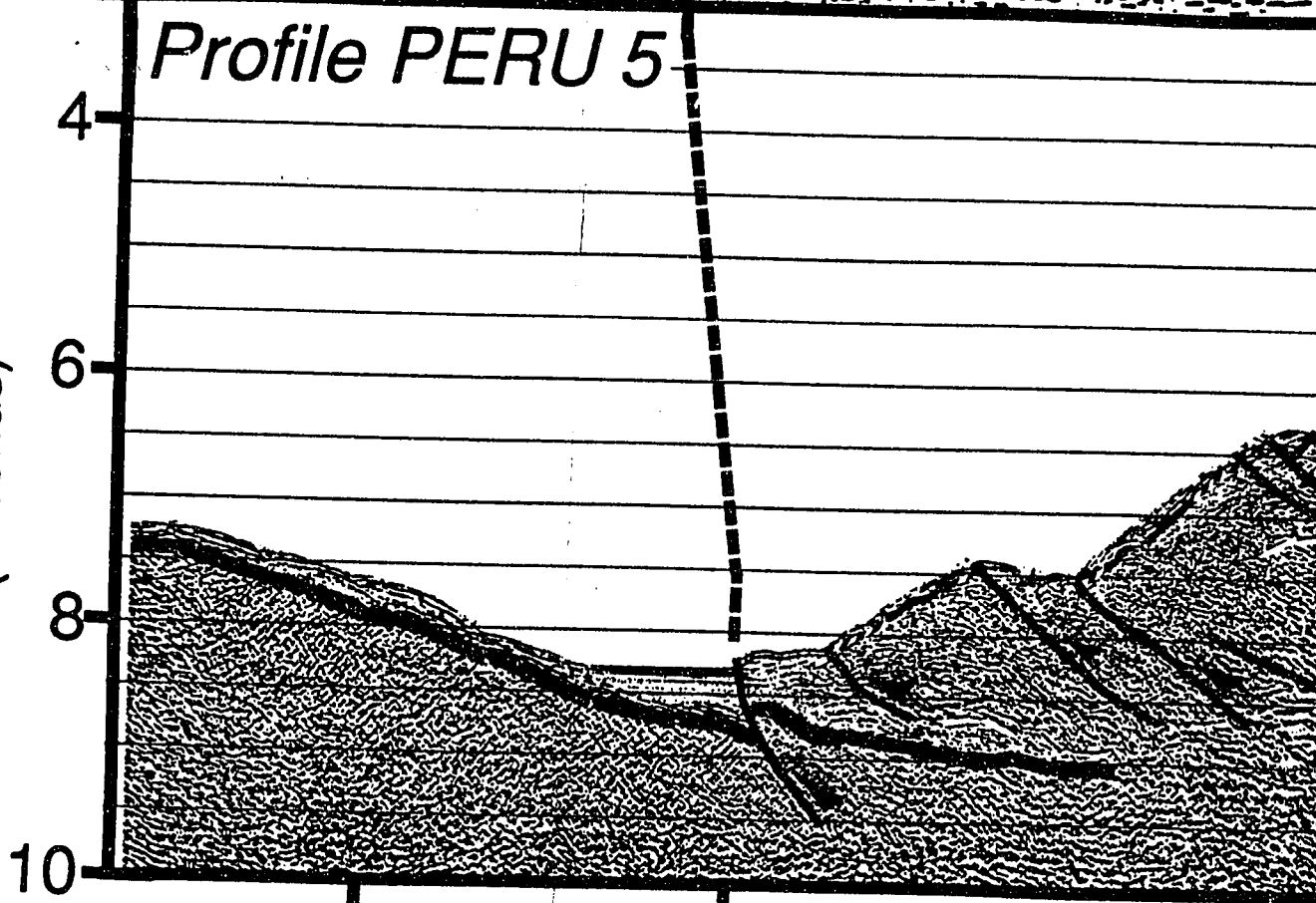


T



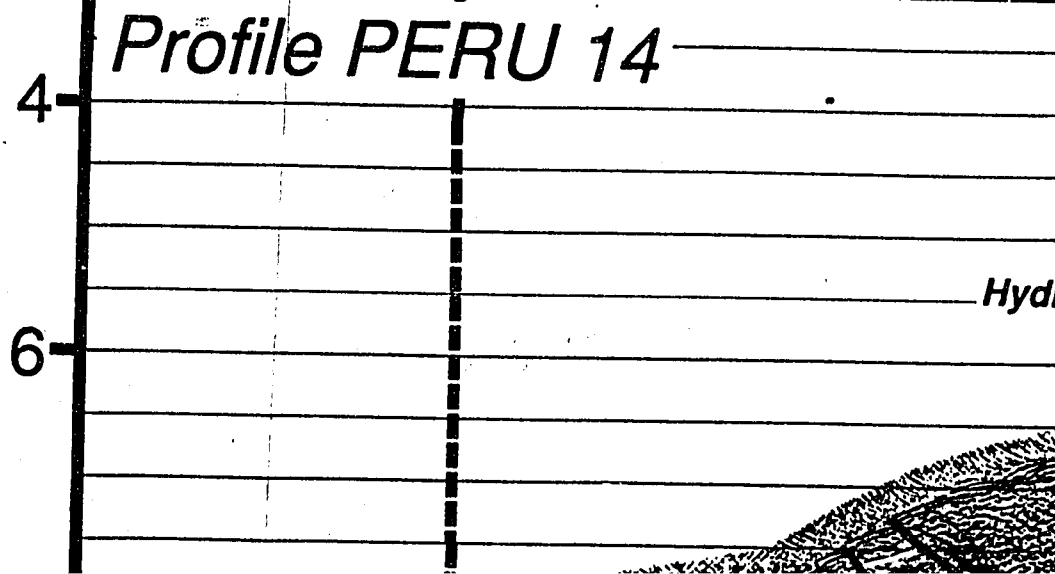
Profile PERU 5

TWO WAY TIME
(seconds)



Profile PERU 14

TWO WAY TIME
(seconds)

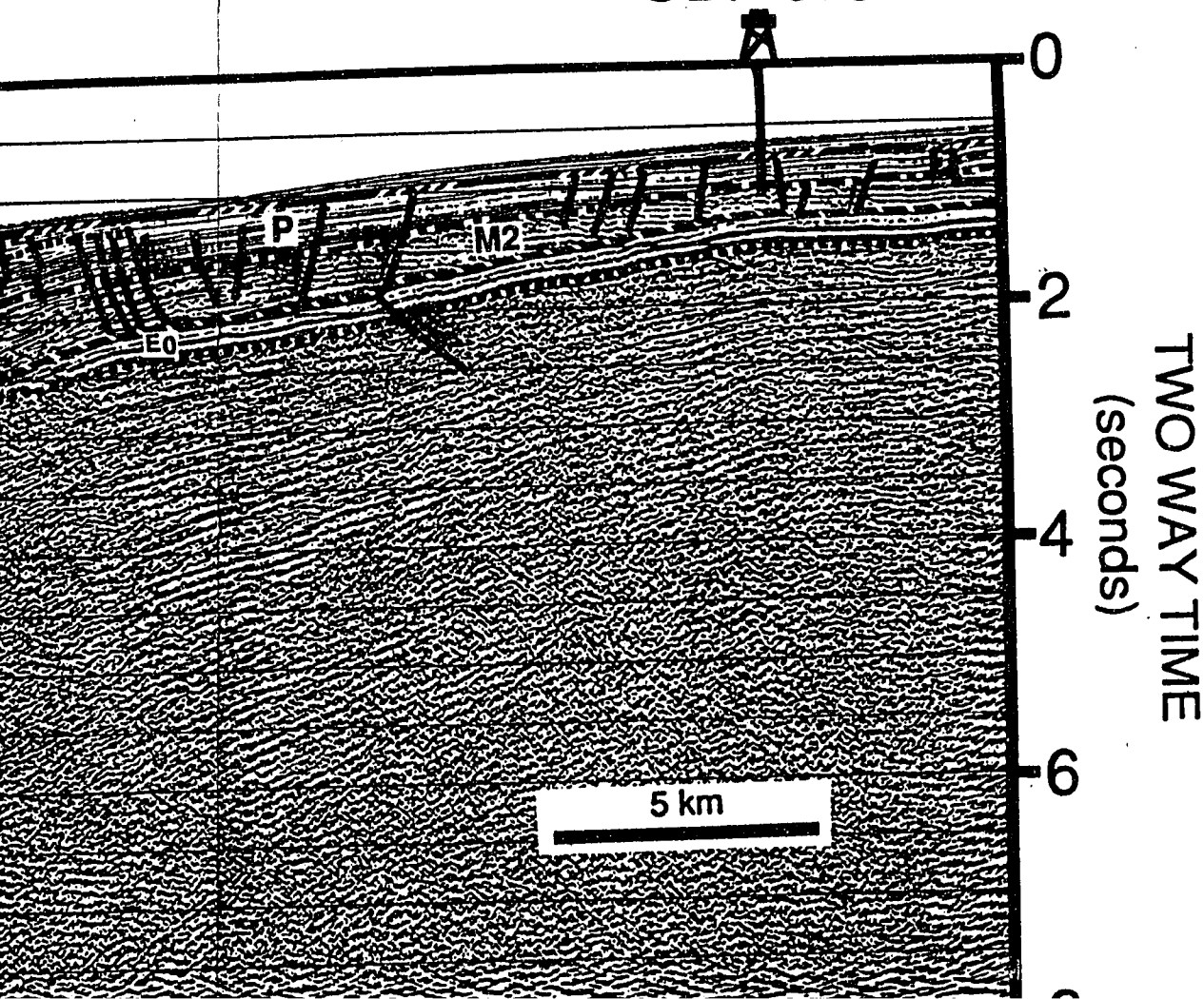


E₀

LOWER ? - MIDDLE EOCENE

PRE-CENOZOIC BASEMENT

ODP 679



TWO WAY TIME
(seconds)

0
2
4
6

Profile CDP-1

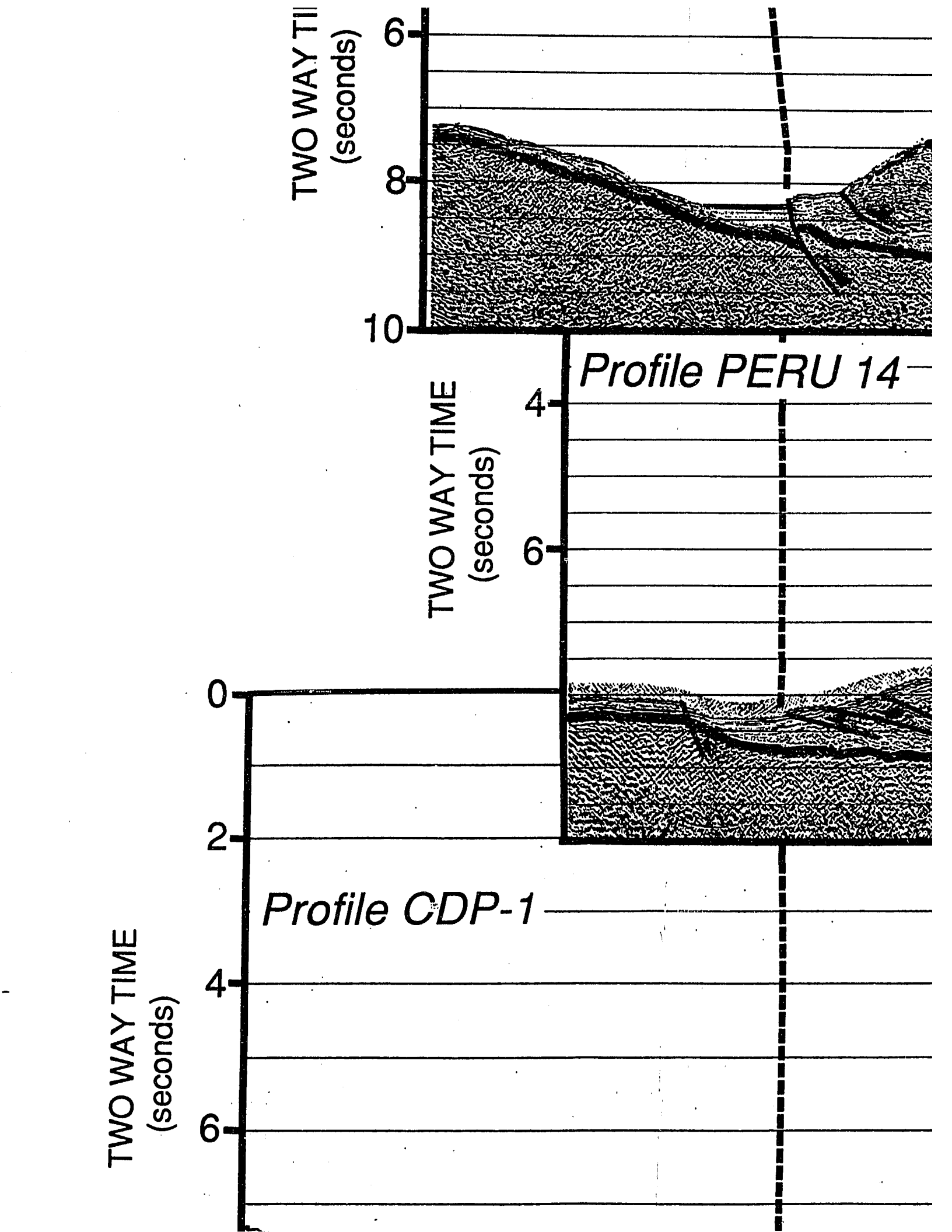
TWO WAY TIME
(seconds)

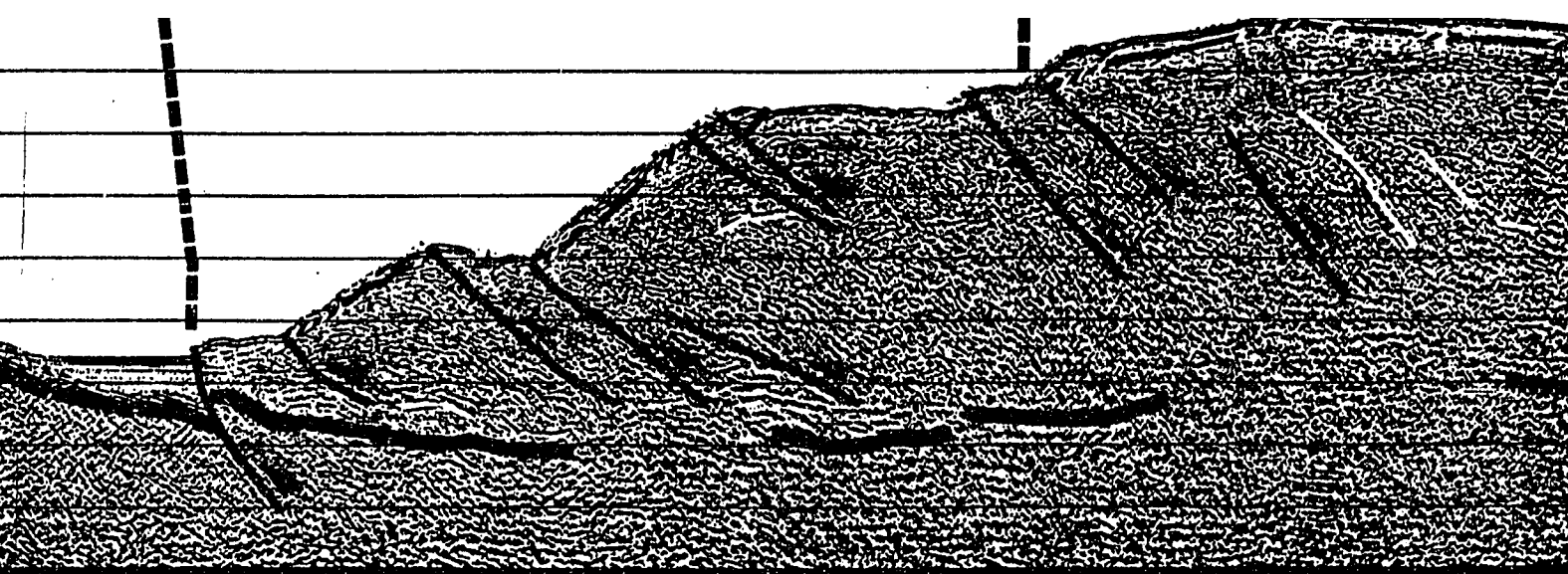
4
6

Profile PERU 14

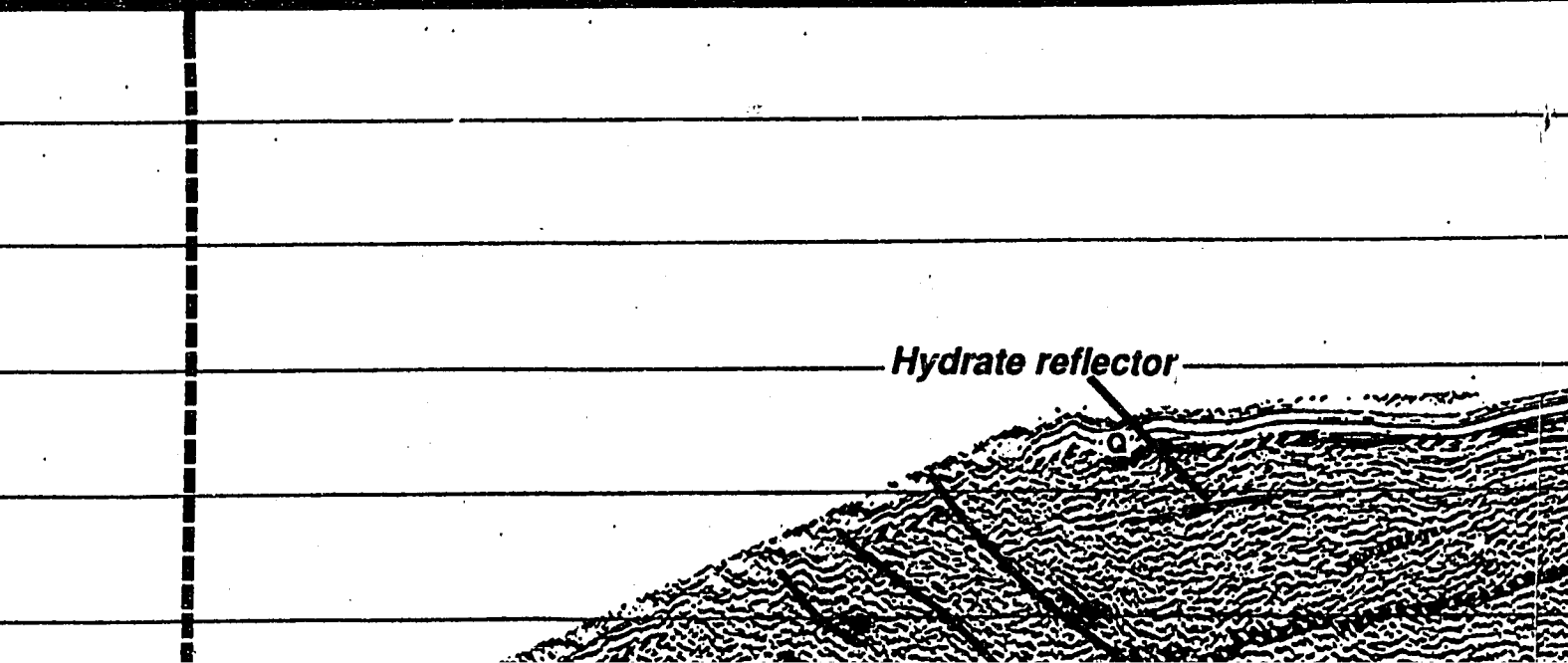
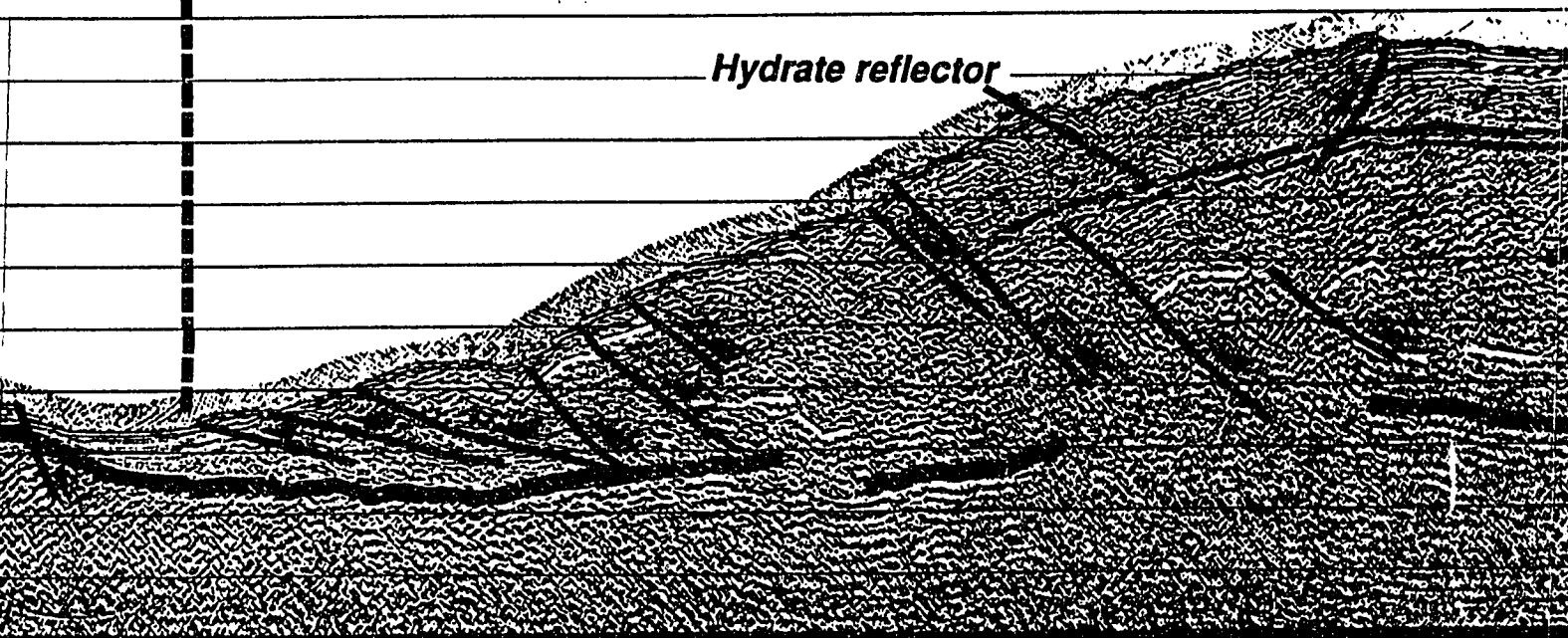
TWO WAY TIME
(seconds)

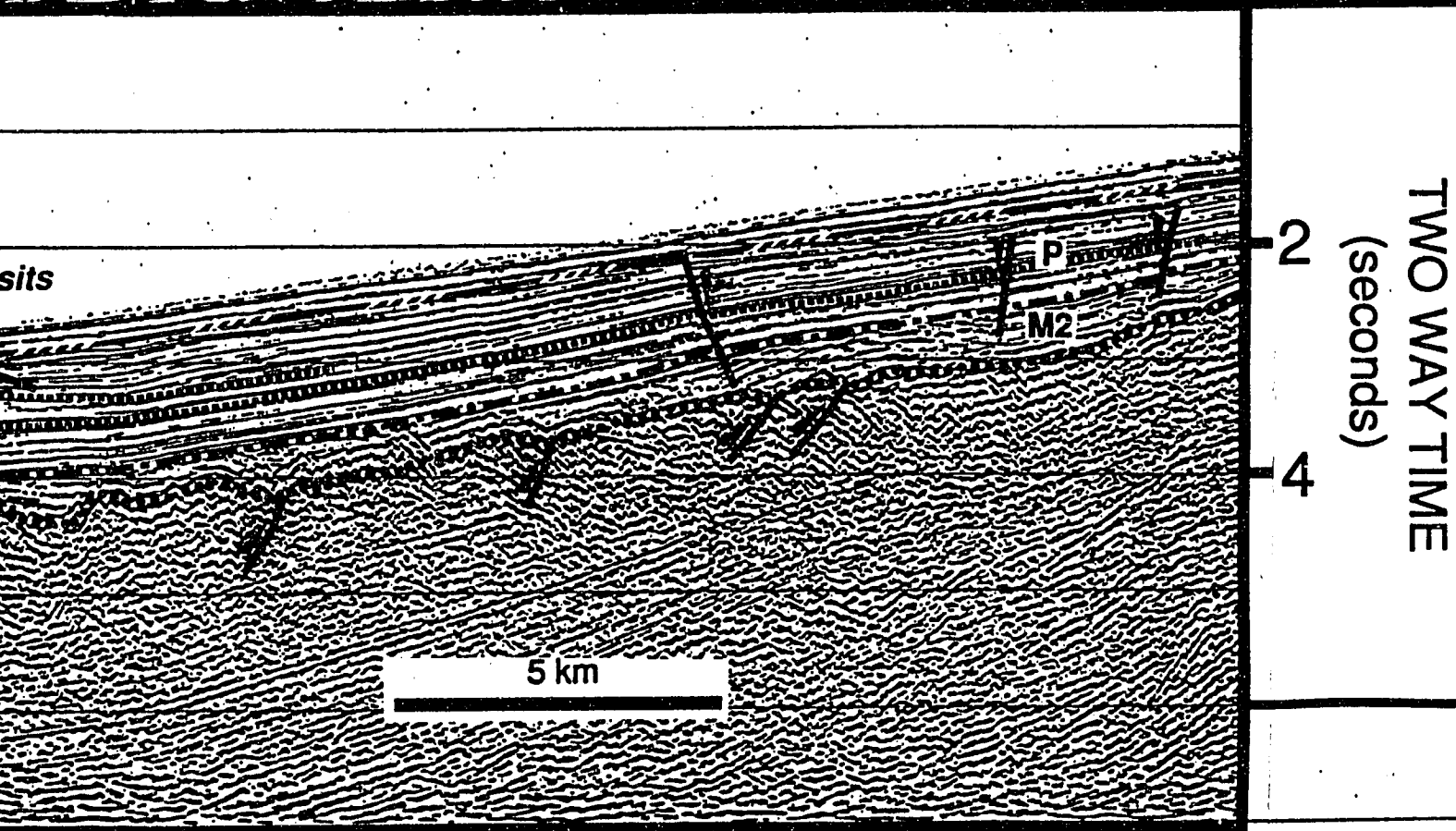
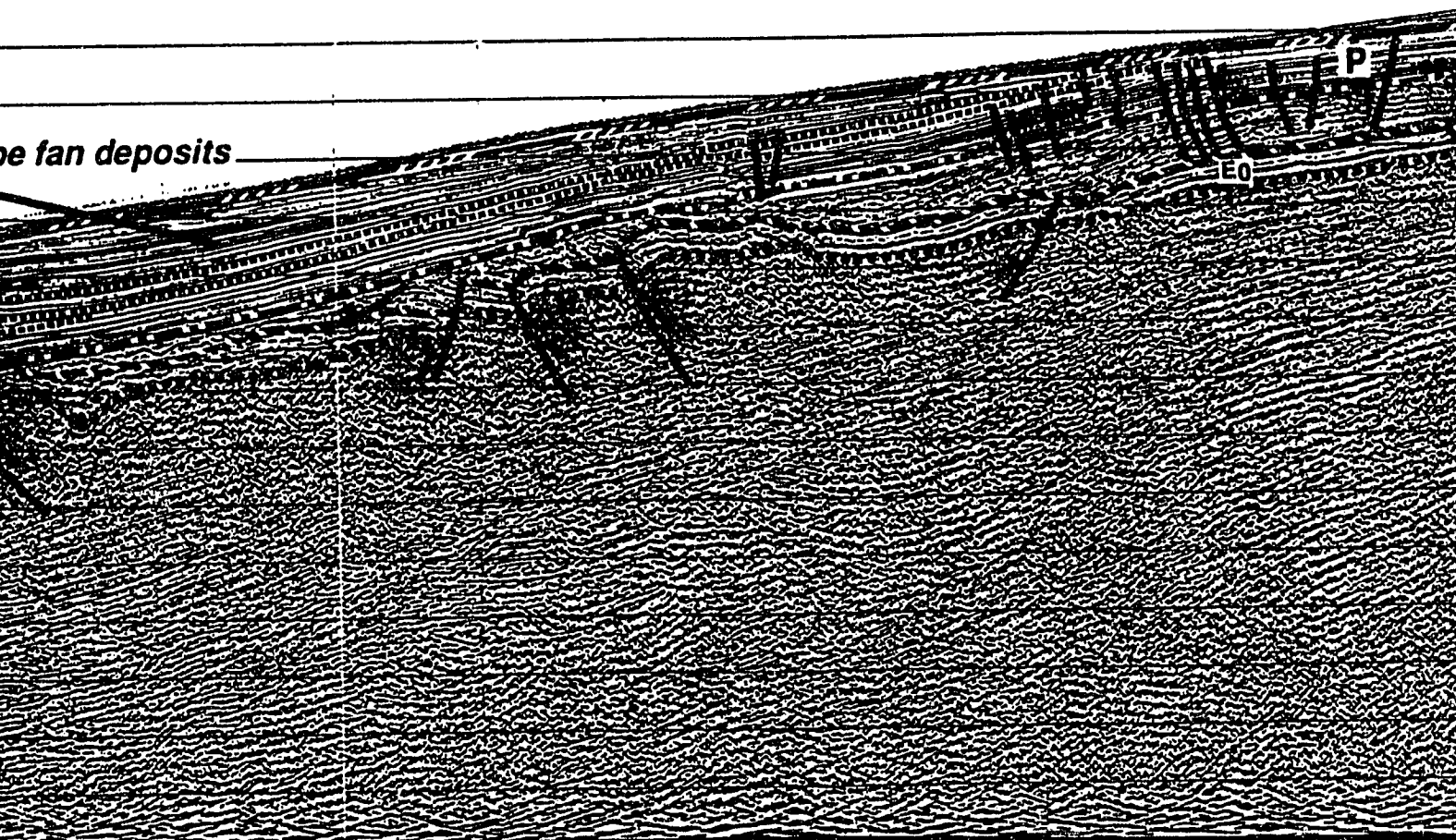
6
8
10



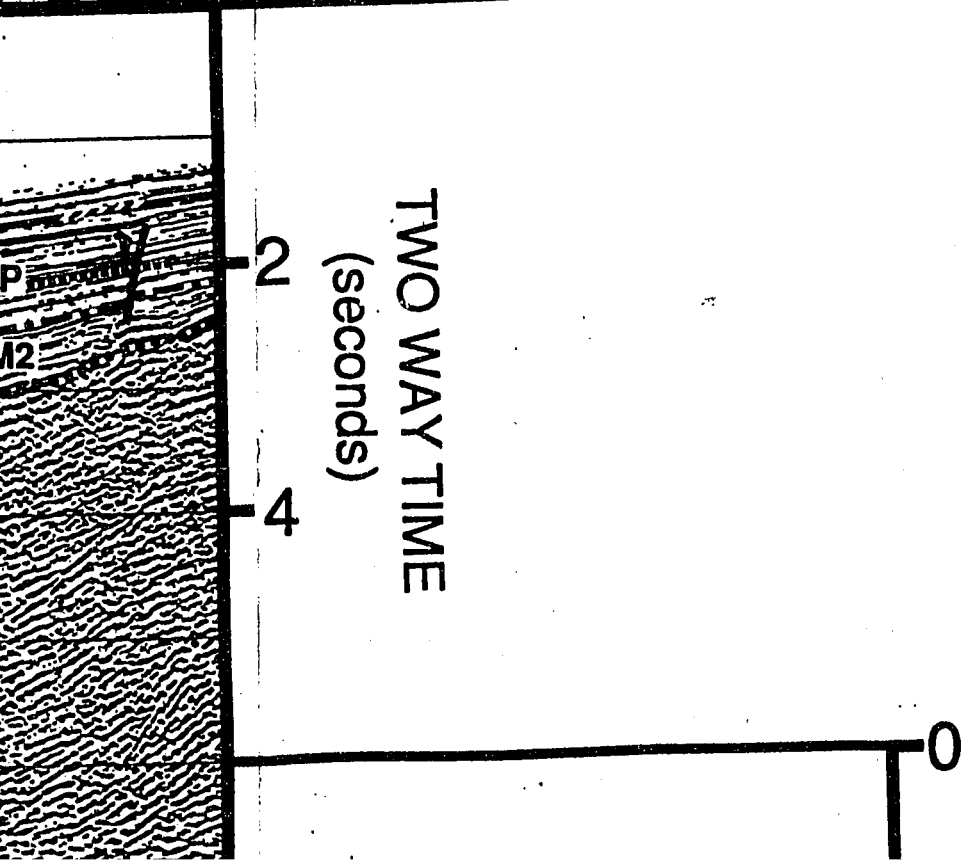
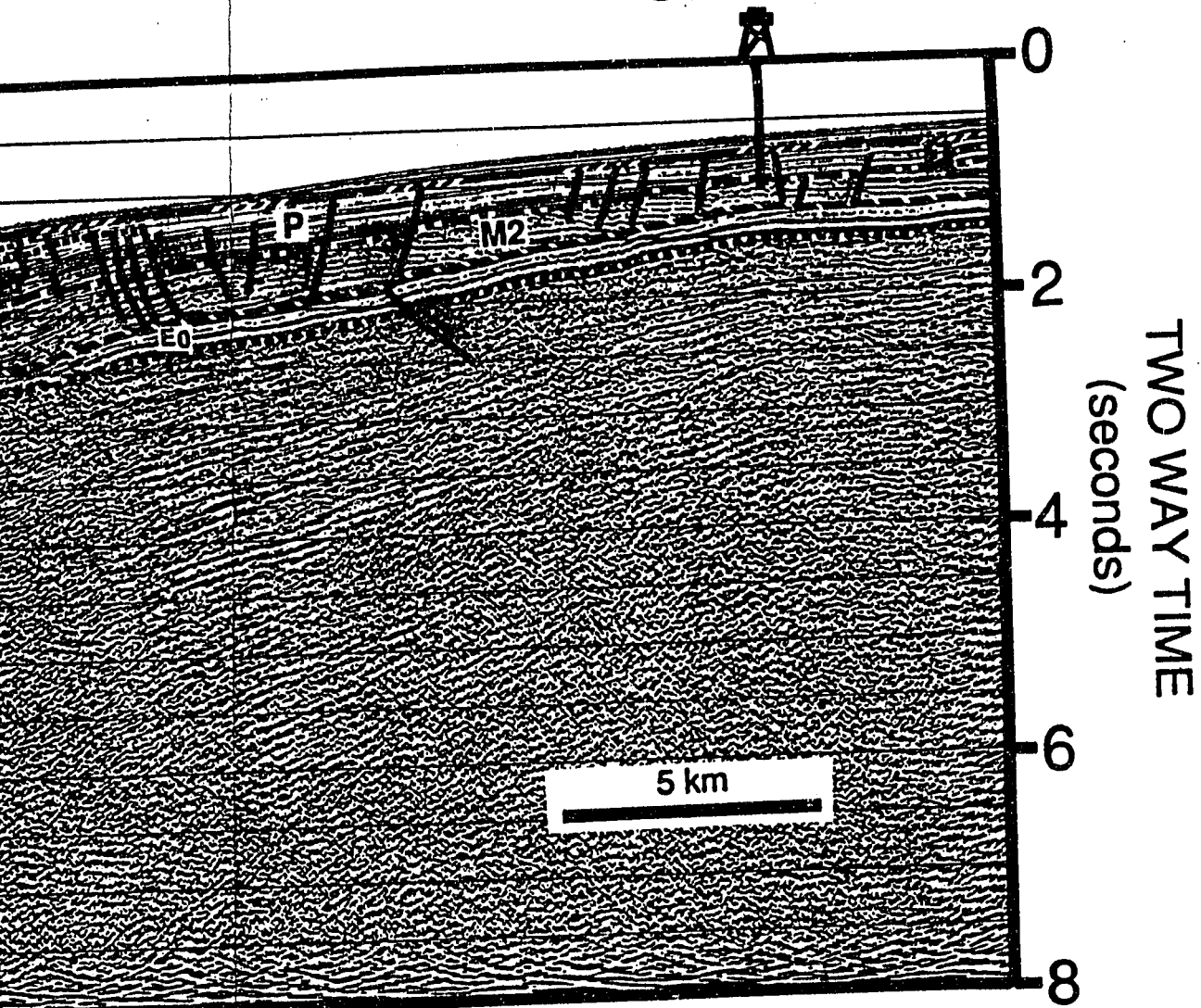


le PERU 14





ODP 679



TWO WAY TIME
(seconds)

Profile CDP-1

4

6

8

10

TWO WAY TIME
(seconds)

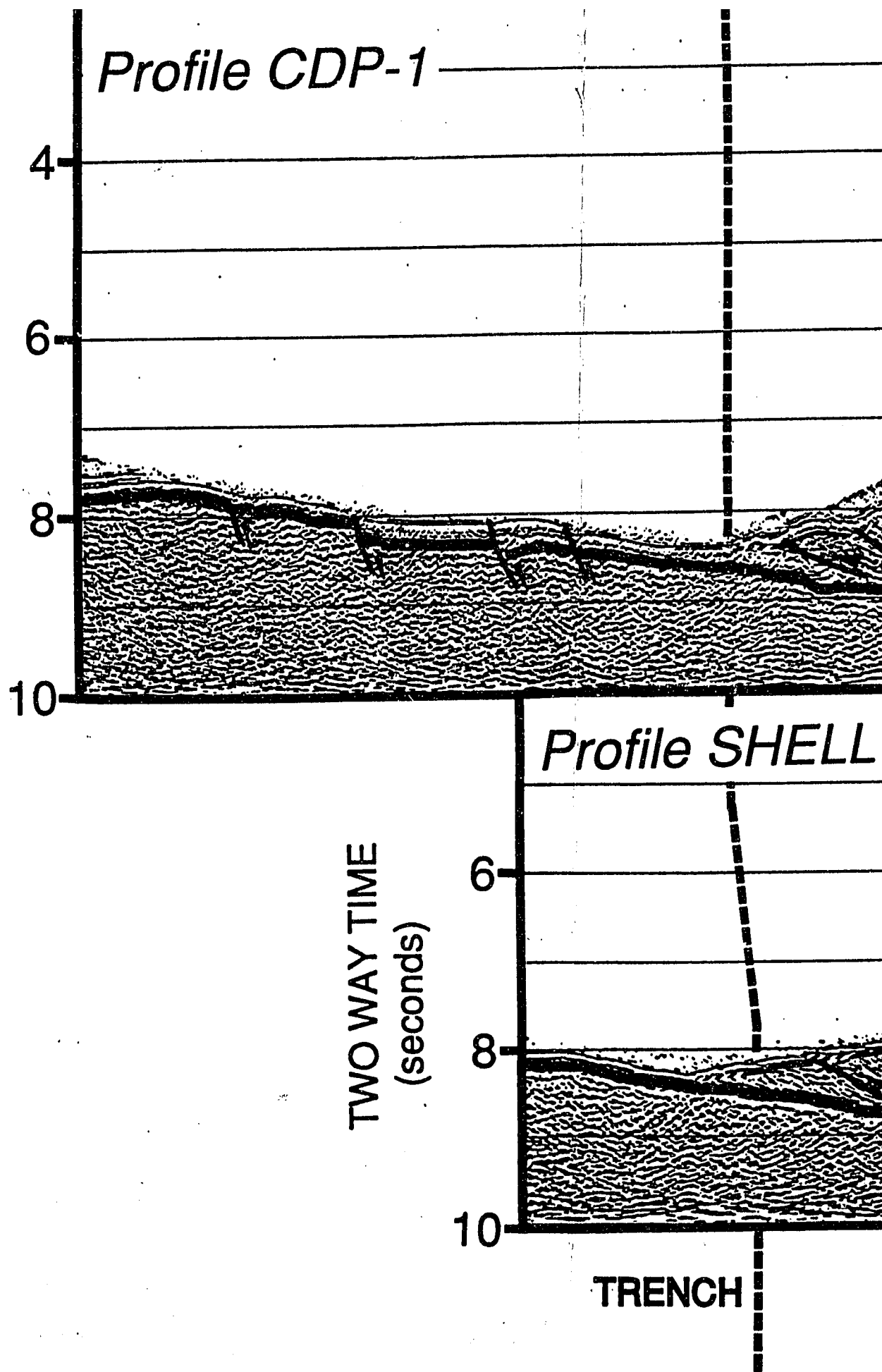
Profile SHELL

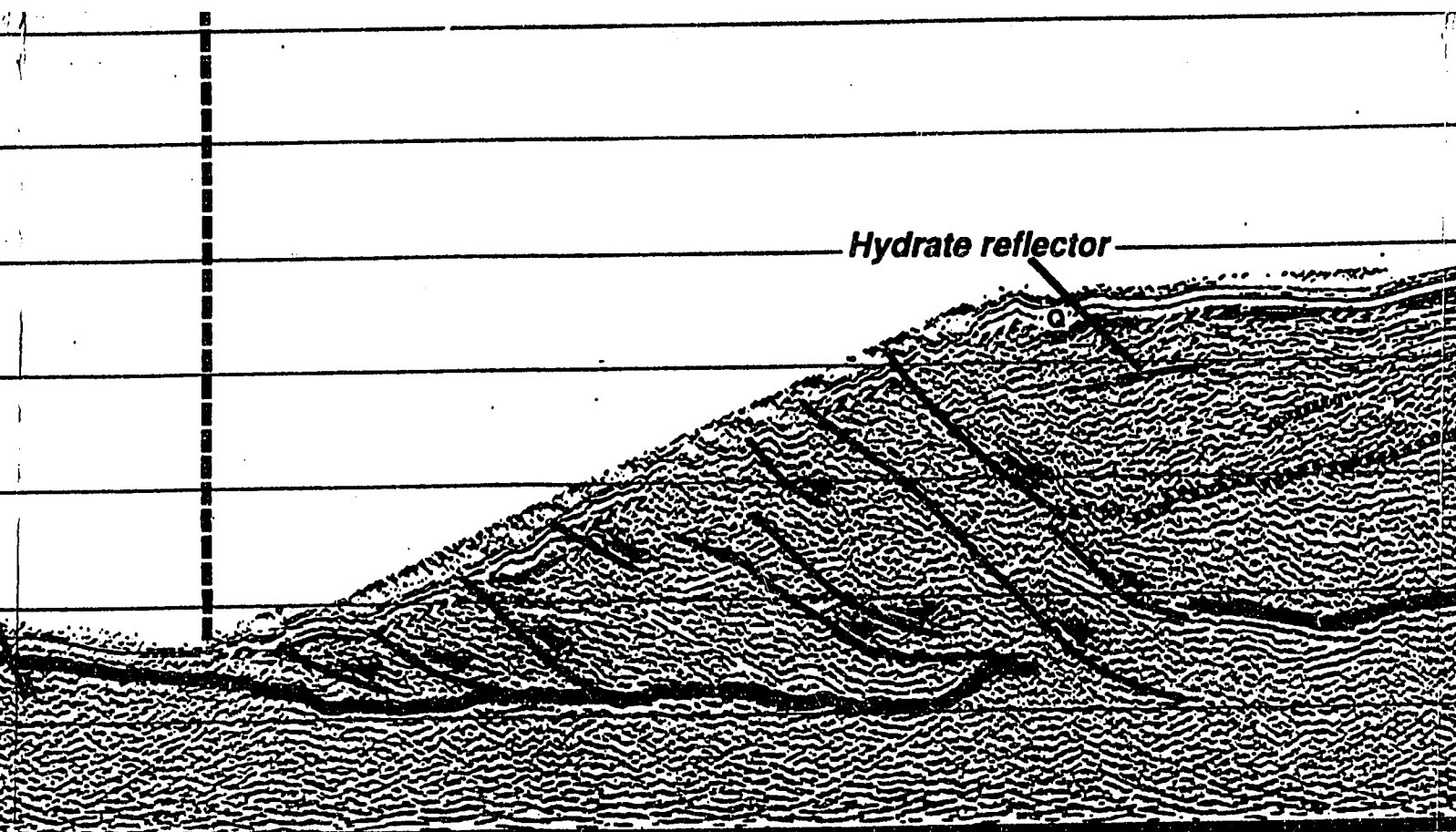
6

8

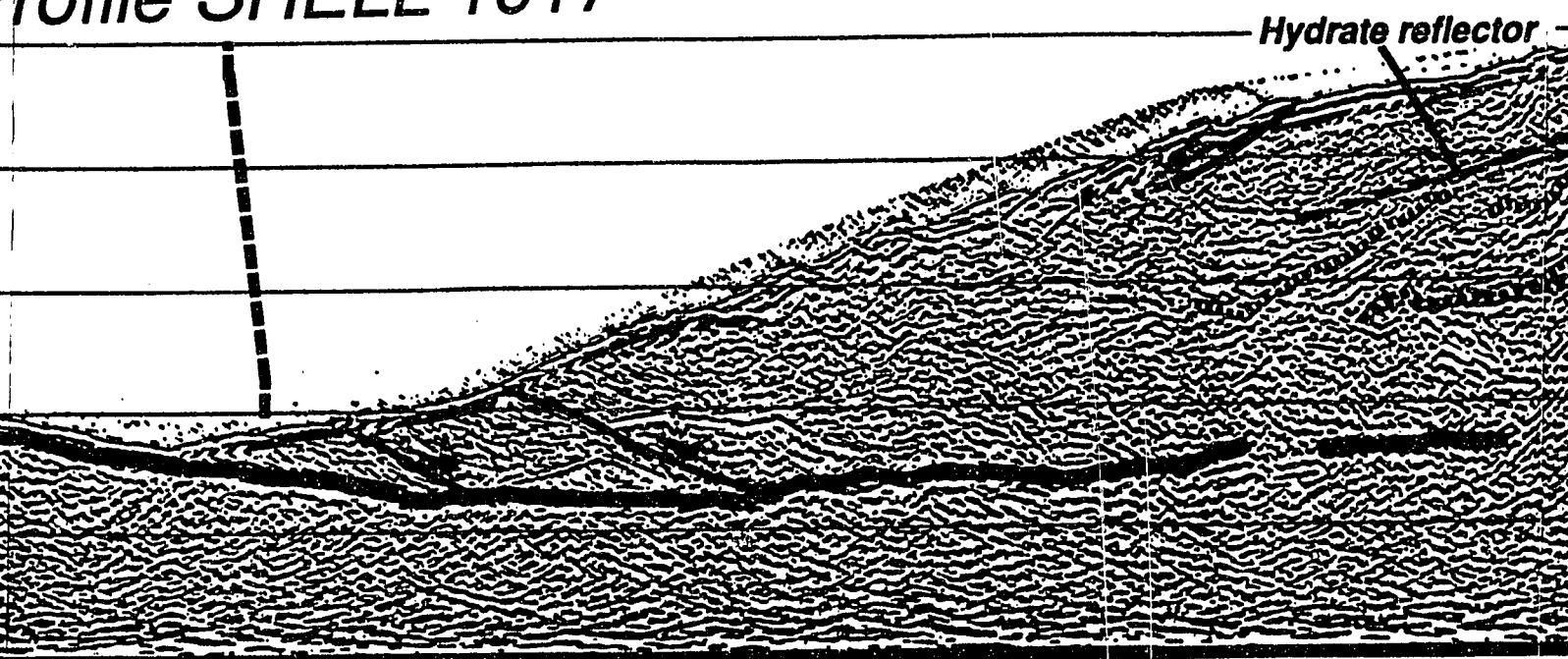
10

TRENCH



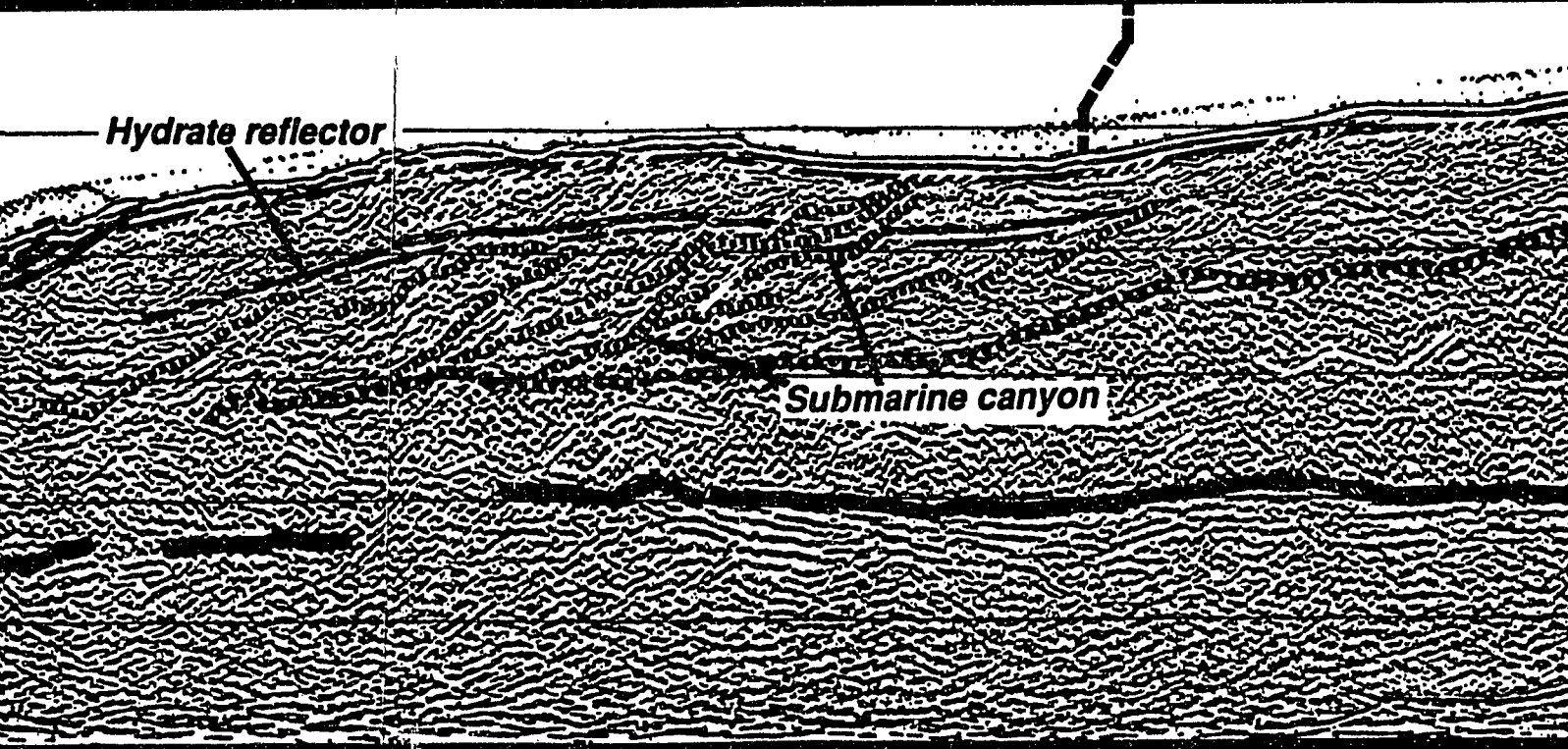
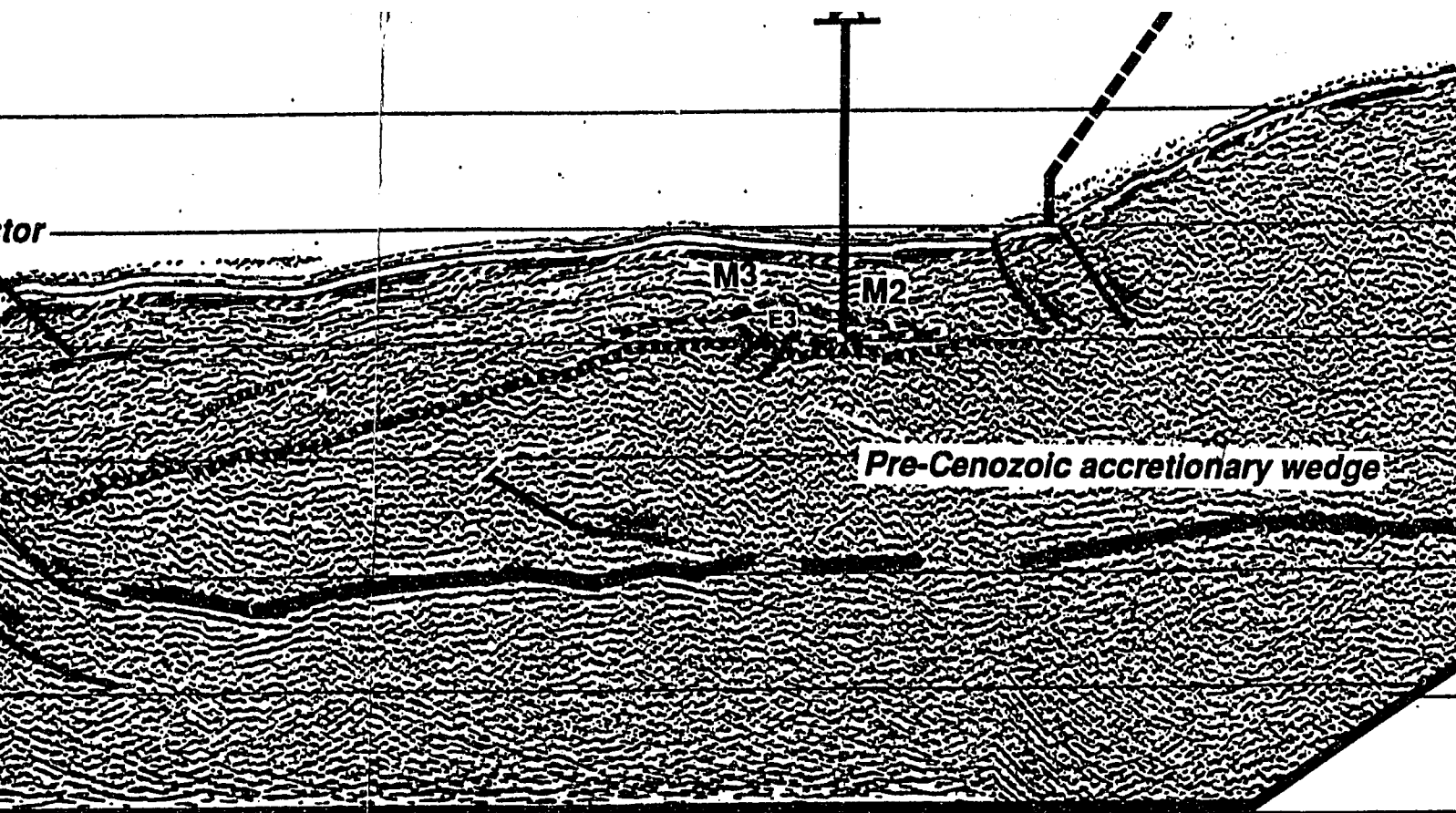


Profile SHELL 1017

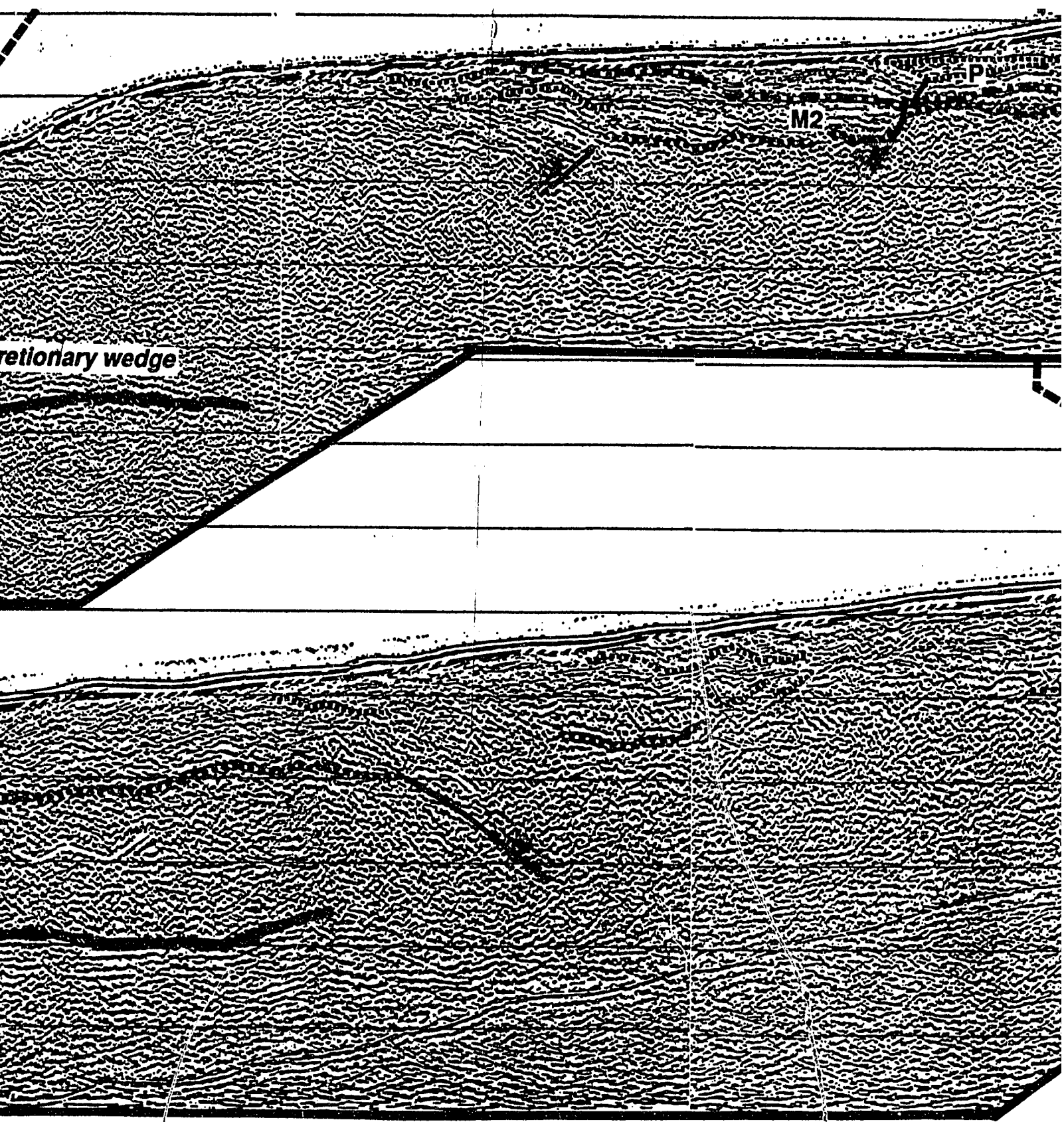


TRENCH

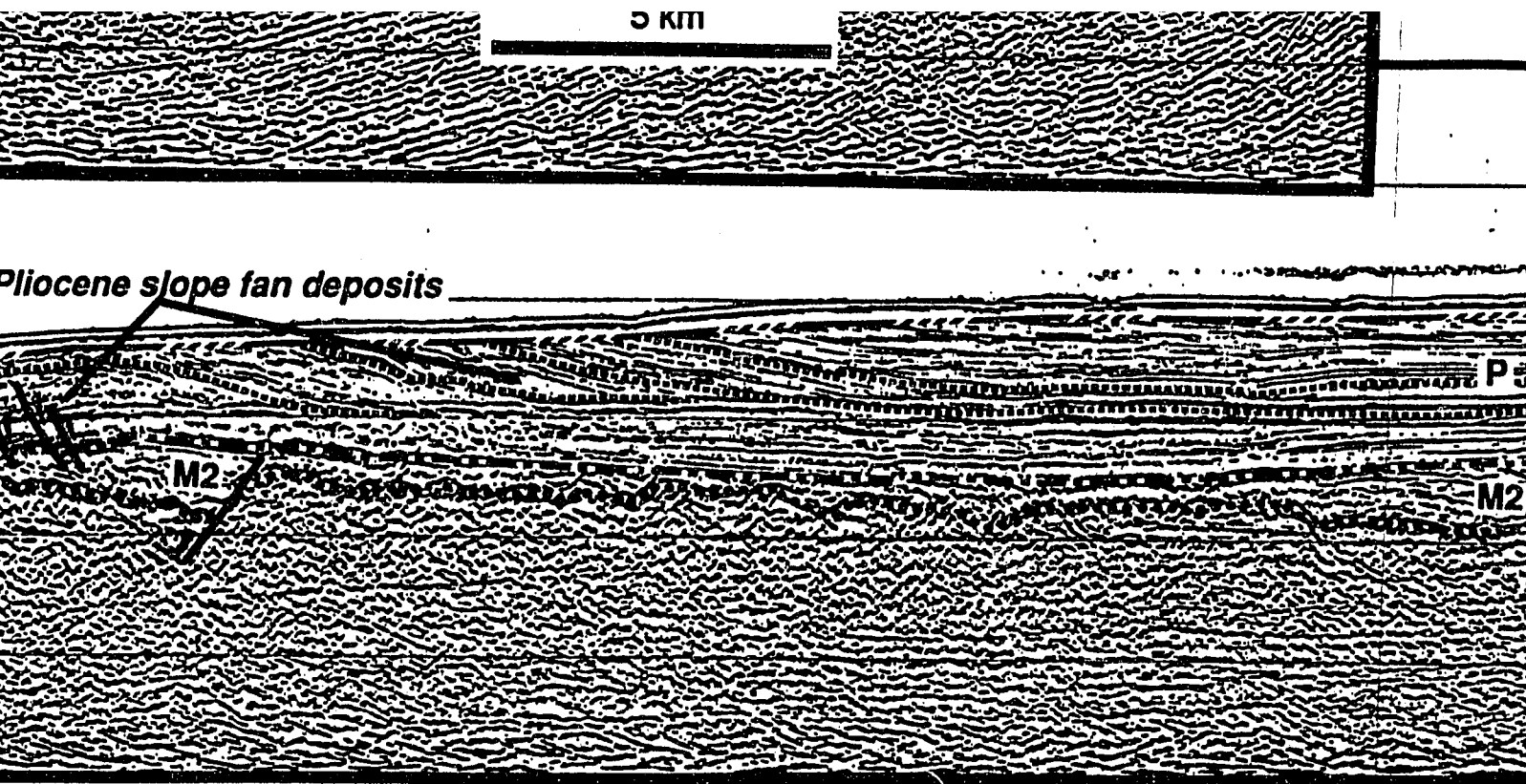
LOWER SLOPE



OWER SLOPE



MIDDLE SLOPE



UPPER SLOPE

TWO WAY TIME
(seconds)

